

TOWARDS THE DEVELOPMENT OF A UNIVERSAL INFLUENZA VACCINE: INVESTIGATING VIRAL-VECTORED VACCINE-INDUCED HETEROSUBTYPIC IMMUNE RESPONSES TO INFLUENZA A

Thesis submitted for the degree of Doctor of Philosophy

Trinity Term 2015

Claire M. Tully

St Edmund Hall

Word count: ~40,000 words

(Excluding appendices, bibliography, diagrams and tables)

Declaration

I hereby declare that the work contained in this thesis is my own and that no part of my thesis has been accepted or is currently being submitted for any degree, diploma or certificate or other qualification in this University or elsewhere. To the best of my knowledge and belief, it contains no material previously published or produced by another party, except where due acknowledgement is made in the text.

Signed, 

Claire Maria Tully

Dated: **18th September 2015**

Dedication

To the memory of my father

BRIAN ‘CHARLIE’ TULLY

January 14, 1956 – July 5, 2012

I Miss You, Everyday

Towards the Development of a Universal Influenza Vaccine: Investigating Viral-Vectored Vaccine-Induced Heterosubtypic Immune Responses to Influenza A

Thesis submitted for the degree of Doctor of Philosophy, Trinity Term 2015

Claire M. Tully, St Edmund Hall, University of Oxford

Abstract

Influenza A viruses pose a continual threat to global society and are responsible for considerable morbidity and mortality on an annual basis. Existing seasonal vaccines must be regularly reformulated to match circulating strains and do not protect against pandemic viruses. A universal influenza vaccine capable of protecting against both seasonal and pandemic strains is a major goal of vaccine developers. In recent years there has been considerable interest in broadly neutralising antibodies that target the stem region of haemagglutinin (HA). Work in this thesis reports the design and production of several tools designed to measure anti-stem responses, namely, two recombinant chimeric HA proteins and a phage display library. In addition the development of three novel viral-vectored vaccines aimed at inducing anti-stem responses and the investigation of their immunogenicity is described. This thesis also examines the cellular events associated with the development of antibody responses in response to viral-vectored vaccination and reports on the immunogenicity of multivalent, multi-antigen viral-vectored vaccination against influenza in work towards the development of a universal influenza A vaccine.

Acknowledgements

I'd like to thank my supervisors Prof Sarah Gilbert and Dr Teresa (Tess) Lambe. In particular Tess for her mentorship, friendship and unwavering sense of humour, without which, I'm almost certain I would not have survived!

I'd like to thank those members, past and present, of the Jenner Institute who helped in some way, shape or form over the last few years. In particular Prof Adrian Hill, Caitlin Mullarkey, Susan Morris, Nick Edwards, Craig Thompson, Matt Dicks, Marta Ulaszewska, Becky Hilson, Senthil Chinnakannan, Vincent Pavot, Naif Alharbi, Alex Lindsay-Perez, Melissa Kapulu, Daria Nikolaeva, Beatrice Ondondo, Anita Gola, Alex Spencer, Louisa Rose, Rhys Hamon, Jake Matthews, Ali Turner, Simon Draper, Lee Li, Sultan Abduljawad, Tina Ahmed, Ahmed Salman, Christos Krastev and Paulo Bettencourt. I'd also like to thank the laboratory support and staff at the FGF.

I am especially grateful for my support network at St Edmund Hall – Prof Stuart Ferguson and Dr Robert Wilkins – thank you for your advice and guidance. I would also like to thank Prof Keith Gull, Prof Fiona Powrie, the Medical Sciences Division and the Wellcome Trust for allowing me the opportunity to carry out the work presented in this thesis.

I cannot forget my friends, both near and far. Thank you for listening, whether you had a clue about what I was talking about, or not! Knowing you were there when I've needed you will not be forgotten. The same goes to my future mother-in-law, Nic. Thank you, thank you, THANK YOU for getting me

through this! To my youngest brother Peter – you are the voice of reason. I'm proud of how well you are doing! You have inspired and encouraged me to keep going more than you know.

And lastly, but certainly not least, thank you to my best friend and partner in crime, Kelsey Jones. My 'other half'.

Here's to the future!

Table of Contents

DECLARATION ..... **ii**
DEDICATION ..... **iii**
ABSTRACT ..... **v**
ACKNOWLEDGEMENTS ..... **vi**
TABLE OF CONTENTS ..... **ix**
LIST OF FIGURES ..... **xix**
LIST OF TABLES ..... **xxiii**
ABBREVIATIONS ..... **xxv**

1. Introduction **1**

Part I
1.1. Influenza Through the Ages **2**
1.2. The Global Impact of Influenza **5**
1.3. Current Strategies Against Influenza **9**

Part II
1.4. The Biology of Influenza A **11**
1.4.1. Structure 12
1.4.2. Infectious Cycle 15
1.5. Pathogenesis of Influenza A **17**
1.5.1. Tropism 17
1.5.2. Evolution 18
1.5.3. Pathology 19
1.6. Immune Responses to Influenza A **21**
1.6.1. Innate Immunity Against Influenza A 21
1.6.2. Adaptive Immunity Against Influenza A 27
1.6.3. Heterosubtypic Immunity Against Influenza A 38
1.6.4. Mouse Models 40

Part III

1.7. Currently Licensed Vaccines Against Influenza A 41

1.7.1. Antigenic Matching 42

1.7.2. Manufacturing Limitations 43

1.7.3. Variable Efficacy 44

1.8. Next Generation Vaccines 47

1.8.1. Novel Vaccine Platforms 47

1.8.2. Novel Vaccine Targets 49

1.9. Correlates of Protection 54

Part IV

1.10. Viral-Vectored Vaccines 56

1.10.1. Adenoviral-Vectors 57

1.10.2. MVA 61

1.11. Thesis Aims 65

1.12. Thesis Outline 66

2. Materials and Methods 67

2.1. Materials 68

2.1.1. Labware and Equipment 68

2.1.2. Reagents 72

2.1.3. Solutions 81

2.1.4. Bacterial Growth Media 82

2.1.5. Cell Culture Media 83

2.1.6. Cell Lines 84

2.1.7. Viral-Vectored Vaccines 85

2.2. General Molecular Biology Methods 87

2.2.1. Bacterial Transformation 87

2.2.1.1. Heat-Shock 87

2.2.1.2. Electroporation 87

2.2.2. Glycerol Stock Preparation 88

2.2.3. Plasmid DNA Purification 88
2.2.4. Bacterial Artificial Chromosome Purification 88
2.2.5. High Fidelity Polymerase Chain Reaction. 89
2.2.6. Site-Directed Mutagenesis 90
2.2.7. Colony PCR Screening 90
2.2.8. DNA Sequencing 91
2.2.9. DNA Restriction Digest 91
2.2.10. Agarose Gel Electrophoresis 92
2.2.11. Phenol Chloroform DNA Extraction 92
2.2.12. Ethanol Precipitation of DNA 93
2.2.13. DNA Ligation 94
2.2.14. TOPO® Blunt-End Cloning 95
2.2.15. In-Fusion® HD Cloning 96

2.3. Construction of a T7 Phage Display Library 97
2.3.1. Production of T7 Clones 97
2.3.1.1. T7 in vitro Packaging and Plaque Assay 98
2.3.1.2. T7 Titration 98
2.3.1.3. T7 Amplification and Purification 98

2.4. Viral Vector Production 100
2.4.1. Recombinant Adenovirus Generation 100
2.4.1.1. Restriction Cloning of Adenovirus Shuttle Vector 100
2.4.1.2. Generation of Recombinant Adenovirus Vectors Using Gateway Technology™ 101
2.4.1.3. ChAdOx1 NP+M1 102
2.4.1.4. ChAdOx1-H7 102
2.4.2. Recombinant MVA Generation 103
2.4.2.1. Restriction Cloning of MVA Shuttle Vector 103
2.4.2.2. MVA-NP+M1 104
2.4.2.3. MVA-NP+M1-HA 104

2.5. Cell Culture Techniques 105
2.5.1. Cell Line Subculture 105

2.5.1.1. Suspension Cell Lines 105
2.5.1.2. Adherent Cell Lines 105
2.5.2. Determination of Cell Viability and Density 105
2.5.3. Resuscitation of Frozen Cells 106
2.5.4. Cryopreservation of Cells 106

2.6. Recombinant Protein Production 108
2.6.1. Adaptation of FreeStyle™ 293-F cells to Expi293™ expression medium 108
2.6.2. Protein Production in HEK 293 Cells 109
2.6.2.1. Expression Vector 109
2.6.2.2. Transient Transfection 109
2.6.2.3. Polyhistidine-Tagged Protein Purification 110
2.6.3. Polyacrylamide Gel Electrophoresis (PAGE) 111
2.6.4. Coomassie Blue Staining 112
2.6.5. Western Blot 112

2.7. Animal Procedures 113
2.7.1. Animals 113
2.7.2. Anaesthesia 113
2.7.3. Immunisation 113
2.7.4. Blood Collection 114
2.7.4.1. Tail Vein Bleed 114
2.7.4.2. Cardiac Puncture 114
2.7.5. Splenocyte Isolation and Preparation 114
2.7.6. Bone Marrow Isolation and Preparation 115

2.8. Immunological Techniques 116
2.8.1. Standardised Whole IgG Enzyme-Linked Immunosorbent Assay (ELISA) 116
2.8.2. Antibody Biopanning Using a T7 Phage Display Library 117
2.8.3. Pseudotype Neutralisation Assay 117
2.8.4. Interferon-Gamma Enzyme-Linked ImmunoSpot (ELISpot) Assay 118

2.8.5. IgG Antibody Secreting Cell ELISpot Assay 119
2.8.6. Memory B Cell IgG ELISpot Assay 120
2.8.7. Cell Surface Marker Staining 120

2.9. Statistics 123

3. Production and Characterisation of Recombinant Haemagglutinin..... 125
3.1. Background 126
3.2. Specific Methods 130
3.3. Results 131
3.3.1. Recombinant HA Construct Design 131
3.3.1.1. H1HA 137
3.3.1.2. H7HA 137
3.3.1.3. cH9/H1 137
3.3.1.4. cH16/H1 138
3.3.1.5. ΔStem-H1HA 138
3.3.1.6. Headless-H1HA 138
3.3.1.7. H1HA-Stem 138
3.3.2. Recombinant HA Expression Analysis 141
3.3.3. Purification of Recombinant HA. 145
3.3.4. Analysis of Group 1 Recombinant HA Stem Structural Integrity by ELISA 148
3.4. Discussion 153
3.5. Chapter Summary 158

4. Development and Optimisation of Phage Display Methods to Epitope Map Antibody Responses to Haemagglutinin 159
4.1. Background 160
4.2. Specific Methods 164
4.3. Results 165
4.3.1. Generation of Recombinant T7 Phage Expressing HA Epitopes 165
4.3.2. Optimisation of a Novel Panning Strategy 168

4.3.2.1. Wash Buffer Optimisation 168
4.3.2.2. Investigation of a Blocking Agent 174
4.3.2.3. Determination of Assay Detection Limits 176
4.3.3. Assessment of Antibody Epitope Profiles in Vaccinated Individuals Over 50 180
4.4. Discussion 186
4.5. Chapter Summary 189

5. Investigation of Circulating T Follicular Helper Cells as Correlates of Immunity to Influenza A 191
5.1. Background 193
5.2. Specific Methods 201
5.3. Results 203
5.3.1. Investigation of Circulating CD4+ T Cell Populations Following Influenza Vaccination 203
5.3.1.1. CXCR5+CD4+ T Cell Populations 203
5.3.1.2. CXCR5-CD4+ T Cell Populations 211
5.3.2. Investigation of Circulating Memory CD4+ T Cell Populations Following Influenza Vaccination. 215
5.3.2.1. CD45RO+CXCR5+CD4+ T Cell Populations 215
5.3.2.2. CD45RO+CXCR5-CD4+ T Cell Populations 223
5.3.3. Relationship Between Circulating TFH-like Cell Populations and Antibody Responses Following Influenza Vaccination 227
5.4. Discussion 229
5.5. Chapter Summary 234

6. Investigation of Antibody Responses Induced by Novel Viral-Vectored Vaccines Expressing Haemagglutinin Stem Constructs 235
6.1. Background 236
6.2. Specific Methods 244
6.3. Results 246
6.3.1. Immunogen Design 246
6.3.1.1. H1HA-Stem 246
6.3.1.2. H1HA-Stem+TM 247

6.3.1.3. cH16/H1 247
6.3.2. Viral Vector Production 250
6.3.3. Anti-Stem Antibody Responses Following DNA-ChAdOx1-MVA Sequential Prime-Boost Vaccination 251
6.3.4. Anti-Trimerisation Domain Responses Following DNA-ChAdOx1-MVA Sequential Prime-Boost Vaccination 258
6.3.5. Anti-Stem Antibody Responses Following AdHu5-MVA Prime-Boost Vaccination 261
6.3.6. Anti-Trimerisation Domain Responses Following AdHu5-MVA Prime-Boost Vaccination 270
6.4. Discussion 274
6.5. Chapter Summary 277

7. Investigation of B and T Cell Responses Induced by Novel Viral Vectors Expressing HA, NP and M1 279
7.1. Background 281
7.2. Specific Methods 286
7.3. Results 290
7.3.1. Immunogenicity of Novel Bivalent Poxviral-Vectored Vaccines Expressing NP+M1 and HA 290
7.3.1.1. MVA-NP+M1-H5 290
7.3.1.1.1. Antibody Responses Against H5HA 290
7.3.1.1.2. T cell Responses Against NP+M1 294
7.3.1.2. MVA-NP+M1-H7 297
7.3.1.2.1. Antibody Responses Against H7HA 297
7.3.1.2.2. T Cell Responses Against NP+M1 303
7.3.2. Immunogenicity of a Mixture of Simian Adenoviral-Vectored Vaccines Expressing NP+M1 or H7HA 307
7.3.2.1. Antibody Responses Against H7HA 307
7.3.2.2. T cell Responses Against NP+M1 312
7.3.3. Investigation of a Prime Boost Regimen Incorporating Poxviral Vectors and Simian Adenoviral Vectors Expressing NP+M1 and H7HA 315

7.3.3.1. Antibody Responses Against H7HA Following ChAdOx1-MVA Immunisation.....316
7.3.3.1.1. ELISA.....316
7.3.3.1.2. H7 Pseudotype Virus Neutralisation.....324
7.3.3.1.3. B Cell Memory Responses Following ChAdOx1-MVA Immunisation.....328
7.3.3.1.3.1. Long-Lived Plasma Cells.....328
7.3.3.1.3.2. Memory B Cells.....333
7.3.3.2. T Cell Responses Following ChAdOx1-MVA Immunisation.....337
7.3.3.2.1. NP+M1.....334
7.3.3.2.2. H7HA.....338
7.4. Discussion.....346
7.5. Chapter Summary.....352

8. Discussion.....353

APPENDICES……367

I. Protocol J004b: Transfection of HEK293 or 293TREx cells with Adenoviral DNA and viral rescue 368
II. Protocol J004c: Preparation of premaster seed stock of virus 374
III. Protocol J004d: Testing infection of a 6 well plate using premaster seed stock virus 379
IV. Protocol J004e: Preparation of Master Seed Virus (MSV) of adenovirus 385
V. Protocol J004f: Cell lysis and benzonase treatment of cell/adenovirus suspension 392
VI. Protocol J005: Adenovirus purification using discontinuous and isopycnic CsCl gradients 396
VII. Protocol J104: Adenovirus Titre Immunoassay 406
VIII. Protocol J176: Recombination of either MVA or FP9 with shuttle vector using Effectene Transfection reagent 416
IX. Protocol J131: 96-well plate MoFlo sort of CEF infected with recombinant poxviruses 421
X. Protocol J016: Infection of CEF with recombinant MVA after cell sorting 428
XI. Protocol J018: Purification of recombinant Poxvirus by plaque picking in 6 well plates 432
XII. Protocol J019a: Bulking up and purifying poxviruses 437
XIII. Protocol J019b: Preparation of a poxvirus master seed virus 441
XIV. Protocol J019c: Purification of poxvirus master seed virus stock using a sucrose cushion 445
XV. Protocol J082: Poxvirus titration using CEF in 6-well plates 450
XVI. Primers used in the production of recombinant haemagglutinin constructs 458
XVII. Sequence of pCMV/R expression vector 459
XVIII. Protein expression and purification analysis 462
XIX. Primers used in the construction of T7 phage display library 470
XX. Correlations between CD4+ T cell populations and antibody responses following influenza vaccination 472
XXI. Sequence of Headless vaccine antigen 473

BIBLIOGRAPHY……475

List of Figures

Figure 1.1 Diagrammatic representation of influenza A 14

Figure 1.2 Innate sensing of influenza A infection 26

Figure 1.3 Adaptive immune responses to influenza A infection in mice 39

Figure 3.1 Phylogenetic tree of influenza A HAs..... 140

Figure 3.2 Expression of recombinant H1HA in FreeStyle™ 293-F cells .. 142

Figure 3.3 Expression of Headless-H1HA in FreeStyle™ 293-F cells 143

Figure 3.4 Purification of recombinant HA constructs 146

Figure 3.5 ELISA of Group 1 HA constructs using mAb C179..... 149

Figure 4.1 Distribution of antigenic regions of HA displayed on T7 166

Figure 4.2 Comparison of detergent Tween® 20 with Triton™ X-100 170

Figure 4.3 Influence of PBS/Triton™ X-100 wash buffer concentrations on non-specific binding 172

Figure 4.4 Determination of optimum wash step number 173

Figure 4.5 Phage pre-incubation with casein 175

Figure 4.6 Titration of mAb using S-tag and HA epitope-decorated phage clones..... 177

Figure 4.7 Distribution of HA peptides recognised by vaccinated adult sera identified by panning with H1N1 PDL 182

Figure 5.1 Circulating memory TFH cell subsets 198

Figure 5.2 Circulating TFH-like cell subsets as defined in this study 199

Figure 5.3 Anti-TIV antibody responses induced by vaccination 200

Figure 5.4 Gating strategy for the analysis of circulating CXCR5+CD4+ T cell subsets..... 204

Figure 5.5 CXCR5 expression within the circulating CD4+ T cell population between vaccine groups 206

Figure 5.6 Proportion of TFH1-like, TFH2-like and TFH17-like subsets in the CXCR5+CD4+ population between vaccine groups and subset expression of PD-1 208

Figure 5.7 Percentage of CXCR5-CD4+ subsets differentially expressing CXCR3, CCR6 and PD-1 between vaccine groups.....212

Figure 5.8 Gating strategy for the analysis of circulating memory CXCR5+CD4+ T cell subsets 216

Figure 5.9 CXCR5 expression within the circulating memory CD4+ T cell population between vaccine groups 218

Figure 5.10 Proportion of TFH1-like, TFH2-like and TFH17-like subsets in the memory CXCR5+CD4+ population between vaccine groups and subset expression of PD-1 220

Figure 5.11 Percentage of memory CXCR5-CD4+ subsets differentially expressing CXCR3, CCR6 and PD-1 between vaccine groups 224

Figure 6.1 HA-specific antibody responses generated by viral vectors expressing Headless multi-antigen MVA-vectored vaccination.....241

Figure 6.2 Stem-specific antibody responses generated by heterologous DNA-ChAdOx1-MVA prime-boost vaccination 255

Figure 6.3 Antibody responses against the T4 fibritin foldon trimerisation domain generated by heterologous DNA-ChAdOx1-MVA prime-boost vaccination.....259

Figure 6.4 Stem-specific antibody responses generated by heterologous AdHu5-MVA prime-boost vaccination.....264

Figure 6.5 Comparison of stem-specific antibody responses generated by heterologous DNA-ChAdOx1-MVA and AdHu5-MVA prime-boost vaccination 267

Figure 6.6 Antibody responses against the T4 fibritin foldon trimerisation domain generated by heterologous AdHu5-MVA prime-boost vaccination..... 271

Figure 7.1 HA-specific antibody responses generated by MVA-NP+M1-H5 292

Figure 7.2 T cell responses following MVA-NP+M1-H5 vaccination 295

Figure 7.3 HA-specific antibody responses generated by MVA-NP+M1-H7 300

Figure 7.4 T cell responses following MVA-NP+M1-H7 vaccination 305

Figure 7.5 HA-specific antibody responses generated by multi-antigen ChAdOx1-vectored vaccination 309

Figure 7.6 T cell responses following multi-antigen ChAdOx1-vectored vaccination 313

Figure 7.7 HA-specific antibody responses generated by heterologous multi-antigen ChAdOx1-MVA viral-vectored vaccination 319

Figure 7.8 HA-specific antibody responses generated by heterologous multi-antigen ChAdOx1-MVA viral-vectored vaccination 321

Figure 7.9 IgG+ long-lived plasma cell responses following ChAdOx1 – MVA immunization 330

Figure 7.10 IgG+ memory B cell responses following ChAdOx1 – MVA immunization 334

Figure 7.11 T cell responses against NP+M1 following heterologous multi-antigen ChAdOx1-MVA viral-vector vaccination.....338
Figure 7.12 T cell responses following heterologous multi-antigen ChAdOx1-MVA viral-vector vaccination 343

List of Tables

Table 2.1 Equipment and consumables used in this study 68

Table 2.2 List of reagents used in this study 72

Table 2.3 Description of solutions used in this study..... 81

Table 2.4 Description of bacterial growth media used in this study..... 82

Table 2.5 Description of cell culture media used in this study..... 83

Table 2.6 Description of the viral-vectored vaccines used in this study 85

Table 2.7 Cell surface marker staining for TFH-like cells 121

Table 3.1 Recombinant HA sequences cloned into pCMV/R 133

Table 4.1 HA epitope sequences displayed on T7 167

Table 4.2 Phage clone distribution following affinity selection by vaccinated sera 183

Table 4.3 Correlations between phage clone distribution and antibody responses 184

Table 6.1 HA immunogen sequences 248

Table 6.2 Immunisation schedule for the induction of anti-stem antibodies by DNA-ChAdOx1-MVA vaccination..... 252

Table 6.3 Immunisation schedule for the induction of anti-stem antibodies by AdHu5-MVA vaccination 263

Table 7.1 Immunisation regimen for delivery of NP+M1 and H7HA by MVA-vectored vaccine 299

Table 7.2 Immunisation schedule for delivery of NP+M1 and H7HA by heterologous prime boost ChAdOx1-MVA viral-vectored vaccination 318

Table 7.3 IC50 antibody titers against H7 and H3 pseudotyped lentiviruses following heterologous multi-antigen ChAdOx1-MVA vectored vaccination.....

.....326

Abbreviations

aa	Amino acids
Ab	Antibody
ACK	Ammonium chloride potassium
Ad	Adenovirus
ADCC	Antibody-dependent cell-mediated cytotoxicity
AdHu	Human adenovirus
ALP	Alkanine phosphatase
APC	Antigen presenting cell
ARDS	Acute respiratory distress syndrome
ASC	Antibody secreting cell
BAC	Bacterial artificial chromosome
BCIP	5-bromo-4-chloro-3-indolyl-phosphate
Bcl-6	B cell lymphoma 6
BCR	B cell receptor
BLIMP-1	B lymphocyte-induced maturation protein-1
BM	Bone marrow
bnAb	Broadly neutralising antibody
bnStAbs	Broadly neutralising anti-stem antibodies
BSA	Bovine serum albumin
CAR	Coxsackievirus and adenovirus receptor
CCL	Chemokine (C-C motif) ligand
CD	Cluster of differentiation
CEF	Chick embryo fibroblasts
CFPS	Cell-free protein synthesis

CGN	*cis*-Golgi network
ChAd	Chimpanzee adenovirus
CIP	Calf intestinal phosphatase
CMV	Cytomegalovirus
CVA	Chorioallantois vaccinia virus Ankara
CXCL	C-X-C motif chemokine ligand
DC	Dendritic cell
DMEM	Dulbecco's Modified Eagle's Medium
DMSO	Dimethyl sulfoxide
DNA	Deoxyribonucleic acid
DOG	2-deoxy-galactose
dsRNA	Double-stranded RNA
DTT	Dithiothreitol
EDTA	Ethylenediaminetetraacetic acid
ELISA	Enzyme-linked immunosorbent assay
ELISpot	Enzyme-linked immunoSpot assay
EMA	European Medicines Agency
Env	HIV-1 envelope glycoprotein
ER	Endoplasmic reticulum
ERGIC	ER-Golgi intermediate compartment
Fab	Fragment antigen-binding
FACS	Fluorescence-activated cell sorting
FasL	Fas ligand
FasR	Fas receptor
Fc	Fragment crystallisable region of an antibody

FcR	Fc receptor
FCS	Foetal calf serum
FDA	Food and Drug Administration
Gal	Galactose
Gc	Golgi complex
GC	Germinal Centre
GFP	Green fluorescent protein
GFPDL	Genome fragment phage display library
GI	Gastrointestinal
GISN	Global Influenza Surveillance Network
GISRS	Global Influenza Surveillance and Response System
GMP	Good manufacturing practice
GMR	Geometric mean ratio
GMT	Geometric mean titer
HA	Haemagglutinin
HAI	Haemagglutination inhibition assay
HCDR	Heavy-chain complementary determining region
HEK	Human embryonic kidney
HI	Haemagglutination inhibition
HIV	Human immunodeficiency virus
HPAI	High pathogenic avian influenza
IAV	Influenza A virus
iBALT	Inducible bronchus-associated lymphoid tissue
IBV	Influenza B virus
IC_{50}	Half maximal inhibitory concentration

ICOS	Inducible T-cell costimulator
IFA	Incomplete Freund's adjuvant
IFN	Interferon
Ig	Immunoglobulin
IIV	Inactivated influenza vaccine
IL	Interleukin
im	Intramuscularly
IMDM	Iscove's modified Dulbecco's medium
IRF	Interferon-regulatory factors
ISG	IFN-stimulated gene
LAIV	Live attenuated influenza vaccine
LB	Lysogeny broth
LLPC	Long-lived plasma cell
LN	Lymph node
LPAI	Low pathogenic avian influenza
LPS	Lipopolysaccharide
M1	Matrix protein 1
M2	Matrix protein 2
M2e	Extracellular domain of M2
M42	M2–related protein encoded by codons from position 145 to 740
МФ	Macrophage
mAb	Monoclonal antibody
MAVS	Mitochondrial antiviral signaling protein
mBC	Memory B cell

MEM	Modified Eagle's Medium
MDCK	Madin-Darby canine kidney
MDV	Master donor virus
MHC	Major histocompatibility complex
MN	Microneutralisation
MVA	Modified vaccinia Ankara
MyD88	Myeloid differentiation factor 88
NA	Neuraminidase
NALT	Nasopharynx-associated lymphoid tissue
NBT	Nitro blue tetrazolium
NDV	Newcastle disease virus
NEB	New England Biolabs
NEP	Nuclear export protein
NFκB	Nuclear factor-κB
NK	Natural killer cell
NKT	Natural killer T cell
NLR	Nucleotide-binding domain and leucine-rich-repeat-containing receptor
NLRP3	NLR family, pyrin domain containing 3
NOS2	Nitric oxide synthase 2
NP	Nucleoprotein
NS1	Non-structural protein 1
NS2	Non-structural protein 2
NS3	Non-structural protein 3
OAS	Original antigenic sin

OD	Optical density
ORF	Open reading frame
Ova	Ovalbumin
PA	Polymerase acidic protein
PAGE	Polyacrylamide gel electrophoresis
PAMP	Pathogen-associated molecular pattern
PB1	Polymerase basic protein 1
PB1-F2	Alternative reading frame of the PB1 gene (segment 2)
PB2	Polymerase basic protein 2
PBMC	Peripheral blood mononuclear cells
PBS	Phosphate buffered saline
PCR	Polymerase chain reaction
PD-1	Programmed cell death protein 1
pDC	Plasmacytoid dendritic cell
PDL	Phage display library
PEB	Phage extraction buffer
PEG	Polyethylene glycol
PEI	Polyethylenimine
PES	Polyethersulfone
PIP	Pandemic Influenza preparedness
pNPP	p-nitrophenyl phosphate
ppNT	Pseudotype particle neutralisation
PRR	Pathogen recognition receptor
RBC	Red blood cell
RBD	Receptor binding domain

RCT	Randomised controlled trial
REU	Relative ELISA units
RIG-I	Retinoic acid inducible gene-I
RIPK3	Receptor-interacting protein kinase 3
RLR	RIG-I-like receptor
RLU	Relative luminescence units
RNA	Ribonucleic acid
SA	Sialic acid
SAα2,3Gal	α -2,3-galactose-linked SA
SAα2,6Gal	α -2,6-galactose-linked SA
scFv	Single-chain variable fragment
SD	Standard deviation
SDS	Sodium dodecyl sulphate
SFU	Spot-forming unit
SLO	Secondary lymphoid organs
SOC	Super optimal culture
SPR	Surface plasmon resonance
SSP	Short synthetic peptide
TAE	Tris-acetate-EDTA
TB	Tuberculosis
T_C	Cytotoxic T lymphocyte
TCR	T cell receptor
TE	Tris-EDTA
T_{FH}	T follicular helper
$T_{FH}1$	T follicular helper cell Type 1

$T_{FH}2$	T follicular helper cell Type 2
$T_{FH}17$	T follicular helper cell Type 17
T_{FR}	Regulatory T follicular helper
TGN	*trans*-Golgi network
T_H	T helper
T_H1	T helper cell Type 1
T_H2	T helper cell Type 2
TIR	Toll–IL-1-resistence
TIV	Trivalent inactivated vaccine
TK	Thymidine kinase
TLR	Toll-like receptor
TNF	Tumour necrosis factor
TNFR	Tumour necrosis factor receptor
tPA	Tissue plasminogen activator
T_{REG}	Regulatory T cell
TRIF	TIR domain-containing adaptor protein inducing IFNβ
VACV	Vaccinia virus
VARV	Variola virus
VE	Vaccine efficacy
VH	Variable heavy
VLP	Virus-like particle
vRNP	Viral ribonucleoprotein
WHO	World Health Organisation

Chapter 1

Introduction

Part I

1.1. Influenza Through the Ages

Influenza viruses* are among the oldest and most common causes of acute respiratory tract infections worldwide. Records of epidemic febrile coughing similar to present-day influenza date back to ancient times and are recorded in the classical literatures of Greece and other civilisations. Notably the famous Plague of Athens in 430 BC advanced in multiple waves reminiscent of modern day pandemics and an influenza-like epidemic was recorded in the writings of Hippocrates in 412 BC [1,2]. Similar descriptions of contagion litter historical records of the Middle Ages [2]. Indeed a specific word, 'creatan' (sic) creatachán meaning weak, emaciated creature, was coined in Ireland in the fourteenth century to describe infection with a particular epidemic respiratory illness that shared features of influenza [3].

The term 'influenza' itself dates to the fourteenth century although it did not come into common usage for another 400 years [3,4]. It was first used in Italy to describe unusual natural events believed to 'influence' disease epidemics which killed elderly and less-fit individuals [3-5]. Similar epidemics of febrile coughing during the fifteenth century were also noted in France to preferentially kill the elderly, as well as young children, and in some cases, induce spontaneous abortion [3]. Of course, identifying the agents of disease

* Influenza viruses are classified into three types, A, B and C. Where 'influenza' is referred to in this thesis, this should be taken to refer to influenza A, unless specified otherwise.

outbreaks, particularly from older lay publications, is relatively speculative without molecular evidence, and scholars remain divided over the precise timing of the first report of an unequivocal influenza pandemic [2]. However, the first contemporary convincing reports of influenza epidemics are believed to have appeared during the seventeenth century [6,7]. Indeed a case description of an epidemic in Dublin during the winter of 1693 is considered the earliest scientific report of a genuine influenza epidemic [2,5,7].

Classical features, such as the rate and breadth of onslaught, increased mortality of the elderly, young children, the infirm or pregnant women, a noted increase in burials and symptoms of fever, coughing and malaise, provide strong collective evidence in support of historical pandemics. One of the earliest accounts of a possible pandemic from the ninth century describes a fever and cough that 'spread like the plague' from Italy across Europe, hinting at the unmistakable explosive spread of modern-day influenza [8]. Later more informative reports from 1173-74, 1293, 1323, and 1386-87, have also been put forward as candidates for the first pandemic on record [2,3,9,10]. Although there remains a degree of uncertainty, the present consensus is that the first definitive record of an influenza pandemic was made during the sixteenth century [3,11]. The first of three in the 1500s, the pandemic of 1510 marked the beginning of a new pandemic era.

In the past 300 years the world has experienced at least 13 pandemics, averaging every 40 years or so [3]. Among these was one of the most catastrophic events ever recorded in medical history [3]. Notoriously referred to

as ‘the greatest medical holocaust in history’, the 1918 Spanish Flu pandemic was the single most lethal outbreak of any disease recorded in history, killing an estimated 50 million people in two years [2,4]. Almost a century since it emerged, these figures serve as a stark reminder of the threat posed by pandemic influenza viruses.

1.2. The Global Impact of Influenza

Seasonal influenza viruses are among the most common causes of acute respiratory illness worldwide. Globally it is estimated that between 5-10% of adults and 20-30% of children become infected in any given season [12]. The circulation period for influenza falls during the winter months for each hemisphere, typically May through to September in the south, and between November and April north of the equator [13,14]. In the tropics, seasonality is less pronounced. Some regions have significant influenza activity all year round while epidemics in other areas transmit predominantly during the rainy seasons [15].

Infections with seasonal influenza place a significant burden on society in terms of excess morbidity and mortality, hospitalisations and economic losses. Of the vast numbers infected each season, approximately 3-5 million develop severe illness and up to 500,000 die [12]. The risk of developing severe complications from seasonal viruses is highest among the elderly, very young children under six months, pregnant women and those with chronic underlying health conditions such as respiratory or cardiac disease, diabetes or immunosuppression [16-24]. Respiratory tract complications such as viral pneumonitis and secondary bacterial pneumonia are the most common complications of influenza but in very rare cases viral myocarditis (infection of the heart muscle) and meningoencephalitis have been reported [25]. Neonates born to influenza-infected mothers are also at risk of preterm birth and low

birth weight [26,27]. Indeed the risk of hospitalisation or death among patients with underlying chronic conditions is more than 30-fold greater [25].

As well as placing a considerable strain on hospitals and health-care providers, the economic costs of seasonal influenza infections are enormous. A previous study based on the 2003 population in the U.S estimated the total economic burden of annual influenza epidemics due to life-years lost, medical costs and loss of earnings amounts to $87.1 billion annually [28]. Similarly in the UK it has been reported that 7.6 million working days are lost every year due to influenza, costing the economy £1.35 billion [29]. Less information is available about the impact of epidemics in less-developed countries, although influenza severity can be affected by infections and co-morbidities more common in these countries [30]. Furthermore, as health care in less-developed nations is frequently inadequate and under-resourced, the overall burden of influenza may be disproportionately higher, which is likely to be particularly damaging to these countries' economies.

In addition to seasonal infections, emerging pandemic influenza viruses present a serious and continued threat to global society. Pandemic influenza viruses have consistently higher attack rates and are typically associated with a higher number of mortalities compared to seasonal strains **[31].** There is also always a risk that a novel pandemic virus may be inherently more virulent than circulating strains, which, upon exposure to an immunologically naïve population, can spark a public health crisis. We increasingly live in a global society whereby people, and therefore these viruses, can travel the globe in a matter of days. The fact that influenza viruses are airborne and frequently

follow a pattern of infectivity preceding notable symptoms can make containment in the event of a highly pathogenic pandemic virus extremely challenging and is particularly concerning for public health agencies.

Influenza viruses are remarkably promiscuous and are known to infect at least twenty species of mammals [32]. These include a large number avian species, such as waterfowl and poultry, in addition to pigs, dogs, horses, cats, bats, various marine mammals such as seals and whales and more exotic creatures including giant pandas, camels and anteaters [32,33]. The vast diversity of animals that are naturally infected by influenza represents an enormous natural viral reservoir. In particular, avian species are susceptible to almost every subtype known, which they unwittingly disseminate globally via their migratory pathways.[34] In wild birds infection typically presents as low pathogenic avian influenza (LPAI) however, specific subtypes, notably H5 and H7 (Influenza A viruses (IAV) are subtyped based on the antigenicity of the major surface glycoproteins, haemagglutinin (HA) and neuraminidase (NA); to date, eighteen subtypes of HA (H1-H18) and eleven different NA (N1-N11) have been identified [35,36]) are known to evolve into highly pathogenic avian influenza (HPAI) viruses causing aggressive disease (system infection owing to changes in HA cleavability by ubiquitous host furin-like proteases) and mortality among poultry populations with considerable economic impact [37] . Furthermore, in the past influenza viruses infecting birds and pigs have crossed the species barrier into humans, sometimes with severe clinical consequences [38-40]. Although to date such zoonosis have been limited to direct contact with infected animals or very close family

contact, there remains a risk that one such virus may mutate to transmit among human populations with a potentially devastating outcome.

1.3. Current Strategies Against Influenza

Measures to prevent and control infection with influenza can be divided into two broad categories: pharmacological interventions, such as vaccines and antiviral drugs, or, non-pharmacological public health strategies, such as individual behavioural interventions to reduce viral spread, and containment in the event of a serious pandemic. At present vaccination is the primary means of protecting individuals and communities against influenza. In the UK vaccination against seasonal influenza is currently recommended on an annual basis for people over the age of 65, pregnant women, specific clinical risk groups as defined in the Green Book such as those with chronic respiratory or heart disease, and children aged 2-4 years [41,42]. However the efficacy of seasonal influenza vaccines varies among populations and is also dependent on how closely the strains included in vaccines match those circulating in a given season [43]. Influenza viruses are continually evolving, which necessitates year-to-year adjustment of seasonal vaccine formulations on the basis of epidemiological surveillance [12].

In 1947 the World Health Organisation (WHO) established an international network of influenza centres and laboratories to rapidly identify and track outbreaks of seasonal and pandemic influenza [44]. This information was used to make recommendations on the composition of seasonal vaccines and to generate vaccine seed strains which were provided gratuitously to vaccine manufacturers [44,45]. Today this network is known as the Global Influenza Surveillance and Response System (GISRS) (formerly the Global Influenza Surveillance Network (GISN)) and it remains a crucial to co-ordinating global

influenza preparedness and response activities [46]. The network currently encompasses six WHO collaborating centers and four WHO essential regulatory laboratories, and is supported by 142 institutions across 112 WHO Member States [46]. Following the emergence of H5N1, the GISRS adopted the Pandemic Influenza Preparedness (PIP) Framework [47]. The PIP Framework aims to improve transparency and sharing information via the GISRS and ultimately increase access to pandemic influenza vaccines [47].

In addition to tracking seasonal strains, GISRS surveillance also monitors influenza specimens for the emergence of drug resistant genes. Antiviral drugs such as adamantanes and neuraminidase inhibitors are frequently used for post exposure prophylaxis following confirmed source contact, particularly if exposure has been to a virulent strain or there is an underlying clinical risk. During the 2009 pandemic, neuraminidase inhibitors such as oseltamivir (Tamiflu®) were reported to accelerate the time to clinical symptom alleviation in infected adults and reduce the number of secondary infections within affected households [48,49]. Since then, an analysis by the Cochrane Database has challenged their effectiveness [50]. The UK government has currently stockpiled Tamiflu® and Relenza® to the value of £560 million. [50,51]

Part II

1.4. The Biology of Influenza A

Influenza viruses belong to the *Orthomyxoviridae* family of viruses, which is comprised of the six genera: influenza, A, B and C, thogotovirus, isavirus and quaranjavirus [35]. Viruses belonging to this family are characterised by a segmented, negative sense, single-stranded ribonucleic acid (RNA) genome [35]. The three genera of influenza differ in their host range and pathogenicity and are grouped on the basis of antigenic differences in the core proteins, nucleoprotein (NP) and matrix protein 1 (M1) [35]. Influenza A and C are known to infect several species, while influenza B viruses (IBV) are limited to mainly human hosts [32]. However, influenza A and B viruses share greater protein homology suggesting influenza C viruses diverged earlier than the other two types [32].

Influenza A viruses (IAV) are subtyped based on the antigenicity of the major surface glycoproteins, HA and NA [35]. To date, eighteen subtypes of HA (H1-H18) and eleven different NA (N1-N11) have been identified [36]. All known subtypes of IAV circulate in birds, with the exception of H17N10 and H18N11, which have recently been identified in bats [36,52,53]. Only three subtypes, H1, H2 and H3, are known to circulate in man and of these, only H1 and H3 subtypes are currently in circulation [36]. Although H5 and H7 subtypes in particular have been know to sporadically infect humans and although

transmission of these among humans is not sustained there is a grave risk any one such virus may be a precursor to the next pandemic.

1.4.1. Structure

The genome of IAV is made up of eight segments which encode a total of seventeen known proteins (Fig. 1.1) [35]. These are haemagglutinin (HA), neuraminidase (NA), NP, M1, M2, the three viral polymerase subunits, polymerase basic protein 1 (PB1), PB2 and polymerase acidic protein (PA), non-structural protein 1 (NS1), nuclear export protein (NEP; also known as NS2) and several more recently identified viral accessory proteins, PB1-F2, PB1-N40, PA-X, PA-N155, PA-N182, M42 and NS3 [54-59]. A hypothetical protein, NEG8 open reading frame (ORF), has been predicted but its existence has yet to be proven [60,61].

HA and NA are the two major virion surface proteins [62,63]. HA functions in viral attachment and entry to host cells via sialic acid residues, whereas NA facilitates budding of new viral particles from the host cells by cleavage of sialic acid [64,65]. The third surface exposed protein, the ion channel M2, spans the viral membrane and can be functionally replaced by the newly discovered protein M42 [66,67]. The three viral polymerase subunits, PB1, PB2 and PA, and the structural protein NP encapsidate the viral genome into helical viral ribonucleoprotein (vRNP) complexes [35]. vRNPs are connected to each other and the viral envelope by M1, which dissociates upon acidification of the viral core via M2 [68,69]. NEP, in addition to M1, functions in the export of vRNPs into the cytoplasm [68,70,71].

IAV also expresses a number of proteins with immune modulating functions. NS1 is a multifunctional protein, which can inhibit the host interferon (IFN) response through several distinct mechanisms [72]. PB1-F2 exerts a pro-apoptotic effect on immune cells and is associated with enhanced virulence [73]. Indeed the balance of expression between PB1-F2 and PB1 is thought to be maintained by PB1-N40 [67]. Interestingly expression of PA-X actually decreases viral pathogenicity [74,75]. The role of other accessory proteins remains less well defined. NS3 is thought to be associated with adaptation of IAVs to murine hosts but this has not yet been confirmed [67]. In addition the functions of PA-N155 and PA-N182 remain unknown [67].

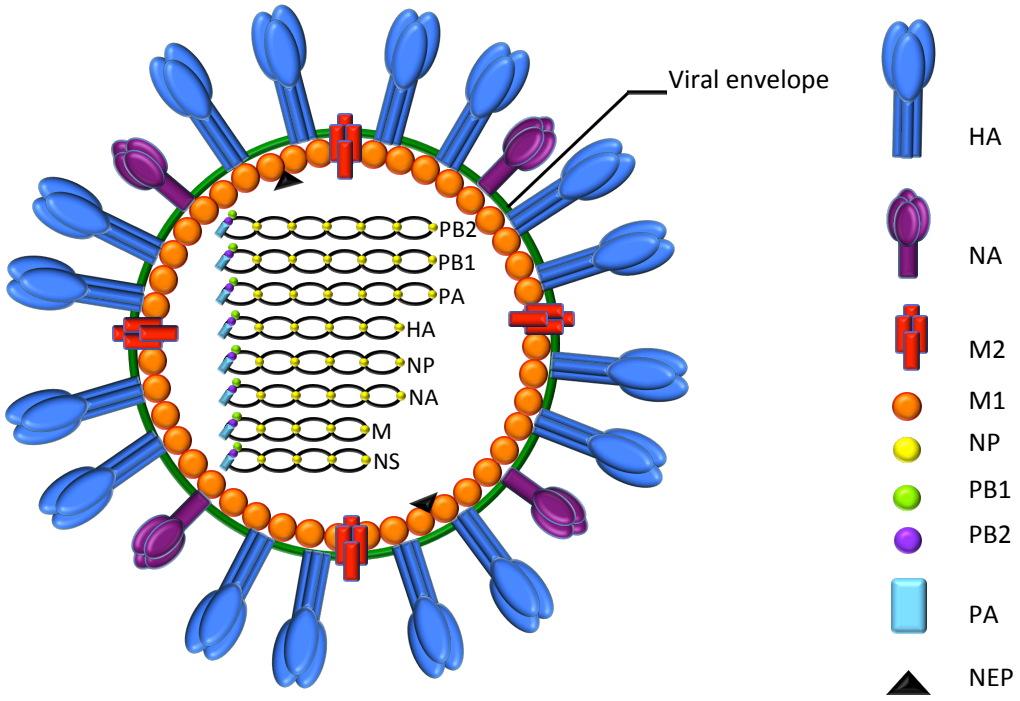


Figure 1.1 Diagrammatic representation of influenza A

Haemagglutinin (HA) is the major virion surface protein. Neuraminidase (NA) and matrix protein 2 (M2) are also surface exposed and embedded in a host-derived viral envelope. Each genomic segment of influenza associates with nucleoprotein (NP) and the three viral polymerase proteins, polymerase basic protein 1 (PB1), polymerase basic protein 2 (PB2) and polymerase acidic protein (PA), which form viral ribonucleoprotein particles (vRNP). Matrix protein 1 (M1) forms a rigid layer beneath the viral envelope and also associates with the viral ribonucleoprotein (vRNP). Nuclear export protein (NEP) mediates export of vRNPs and recruits M1 to the vRNP complex. Influenza viruses are pleomorphic forming spherical virions between 80-120nm in diameter, as well as filamentous forms approximately 100nm in diameter and over 20μm in length [76].

1.4.2. Infectious Cycle

The virus life cycle begins with the attachment of virus particles to the host cell surface via the interaction of HA and sialic acid. Sialic acids (SAs) are a diverse family of monosaccharides that can be found terminally attached to *N*- and *O*-linked glycans on the surfaces of cells and secreted glycoproteins [77]. Their diversity is determined by the variety of different α linkages and substitutions that can be made to the nine carbon atom backbone common to all species [77]. Particular linkages and modifications can be tissue-specific or developmentally regulated [77]. IAVs typically attach to host cells displaying α -2,3-galactose-linked (SAα2,3Gal) or α -2,6-galactose-linked (SAα2,6Gal) SA moieties, depending on the particular subtype.

Viral docking (receptor-mediated attachment of a virus to a cell) on to SA enables the virus to be taken into the cell via receptor-mediated endocytosis, which can be clathrin-dependent or –independent [78,79]. Upon exposure to the low pH within the endosome, HA undergoes a structural rearrangement in order to facilitate insertion of the viral fusion peptide into the endosomal membrane and mediate fusion of the viral and endosomal membranes [80]. In addition, the low pH opens the M2 ion channel, which results in the acidification of the viral core and uncoating of vRNP complexes prior to cytoplasmic release [81]. These then translocate to the cell nucleus and are transcribed and replicated by an RNA-dependent viral RNA polymerase [82]. Viral proteins necessary for transcription and replication are transported to the nucleus and newly synthesised vRNPs are transported to the cytoplasm by NEP and M1. The viral envelope proteins HA, NA and M2 are localised to

the lumen of the rough endoplasmic reticulum (ER) and are transported to the cell membrane via the *trans*-Golgi network (TGN). M1 bound to the cytoplasmic tails of HA and NA is thought to assist in the formation of virus particles by recruiting vRNPs and M2, which alters the membrane curvature at the bud site causing membrane scission and virion release [83,84]. During this process HA is cleaved into mature HA by cellular proteases; a prerequisite for future viral infectivity [85].

1.5. Pathogenesis of Influenza A

1.5.1. Tropism

HA has an important role in determining host tropism and pathogenicity. For example human isolates preferentially bind SAα2,6Gal in contrast to avian isolates which typically bind SAα2,3Gal [86]. SAα2,6Gal moieties are extensively expressed in the human upper respiratory epithelia, although a very minor population of SAα2,3Gal exists in the lower tract [87]. Zoonotic infection of humans with avian isolates is believed to be closely associated with the ability of HA to switch preference from SAα2,3Gal to SAα2,6Gal. Interestingly, a recent paper demonstrated the ability of SAα2,3Gal-tropic viruses to switch preference to long-chain SAα2,6Gal moieties, which predominate on the ferret nasopharyngeal surface and are present in human soft palate tissue [88]. Indeed a number of animals including pigs, guinea fowl, pheasants, turkeys express both receptors and have been proposed as 'mixing vessels' for the generation of novel viruses [89]. However sporadic direct transmissions of avian isolates to humans that replicate efficiently in cells of the lower respiratory tract causing severe disease have also been observed [90-92]. Interestingly, some viruses, including the 2009 H1N1 pandemic strain demonstrate a dual specificity for both SA variants and can infect cells of the upper and lower respiratory tracts [93]. Furthermore SAα2,3Gal is present in the gastrointestinal (GI) tract and some H5N1 infections have been reported as GI infections rather than respiratory, following the consumption of raw poultry blood from infected birds [94].

In addition the cleavage site of any given HA variant is typically recognised by a particular set of trypsin-like enzymes that are limited to specific cells or organs, or, contains a polybasic cleavage site and can be cleaved by subtilisin-like endoproteases expressed almost ubiquitously in the TGN [95]. Viruses with a polybasic cleavage site are generally considered highly pathogenic on account of their ability to replicate throughout a host and spread systemically [95].

1.5.2. Evolution

IAVs evolve by means of two major mechanisms: antigenic drift and antigenic shift. Antigenic drift refers to the gradual evolution of viral strains due to point mutations accrued as a result of the viral RNA polymerase, which lacks proofreading activity [96]. Mutations typically arise within antigenic epitopes of the virion surface proteins HA and NA, resulting in subtle immune-escape variants. This process is responsible for seasonal drift variants within IAVs and IBVs and is the reason seasonal vaccines must be annually updated. In particular HA mutations enable immune-escape, while mutations in the NA can potentially confer drug resistance.

Antigenic shift is a much more dangerous phenomenon and only occurs in IAVs. It results in a major antigenic change and the generation of a novel strain against which the human population may be immunologically naïve. Antigenic shift occurs as a result of the reassortment of viral gene segments between different viruses during a co-infection event [96]. This can occur between IAVs of human and zoonotic origin and has the potential to generate

a novel pandemic virus. In circumstances where there is no pre-existing immunity, emerging pandemic viruses can spread rapidly and if particularly virulent, can have devastating consequences.

1.5.3. Pathology

IAVs cause acute respiratory disease characterised by the sudden onset of high fever, chills, cough, headache, myalgia and fatigue [41]. Highly contagious, transmission typically occurs via exposure to droplets or aerosolised secretions from an infected individual [41]. The incubation period of influenza is usually between 1-3 days and the infectious period precedes notable symptoms [97]. Symptom severity can vary greatly among individuals although uncomplicated influenza is usually self-limiting and resolves within approximately 7 days [97]. The most severe pulmonary form of influenza is primary influenza viral pneumonia [98]. Secondary bacterial pneumonia can also complicate infections [98]. Indeed pneumonia and acute respiratory distress syndrome (ARDS) account for the majority of severe illness and mortality during influenza pandemics [99].

Severe complications following infection such as extensive pulmonary oedema, ARDS and multi-organ failure have been attributed to acute hypercytokinaemia (a potentially fatal abnormal immune overreaction involving positive feedback between cytokines and immune cells) and massive tissue infiltration of mononuclear cells [92,100]. Although the mechanism by which IAVs can induce hypercytokinaemia is poorly understood, disease severity has been shown to strongly correlate with

cytokine release; the highest levels of cytokines have been detected in individuals who previously succumbed to disease [101-103]. In particular elevated levels of interleukin 6 (IL-6), interferon gamma (IFNγ) and tumour necrosis factor alpha (TNFα) have been associated with haemophagocytic syndrome, a disorder characterised by uncontrolled proliferation of histiocytes and heamophagocytosis [92]. Haemophagocytic syndrome following influenza infection is associated with multiple organ failure, disease exacerbation and poor prognosis [104,105].

1.6. Immune Responses Against Influenza A

1.6.1. Innate Immunity Against Influenza A

Innate immune defenses represent the first line of protection against invasion by pathogens. They are comprised of several physical barriers, blood proteins and cell types that respond rapidly to the generic recognition of pathogens. Innate immunity against IAV includes barrier mechanisms such the mucous membrane of the upper respiratory tract, the mucocillary apparatus of epithelial cells and lung-resident innate immune cells, such as macrophages (MΦs), dendritic cells (DCs) and natural killer (NK) cells. The primary targets of IAV are the epithelial cells of the respiratory tract but progeny viruses also infect immune cells such as alveolar MΦs. The ease with which a given IAV can replicate within host epithelial cells depends on several factors relating to both host and virus. From a host perspective, the ability to detect infection and initiate responses to restrict viral replication and spread is among the most important determinants of disease outcome.

In humans (and all mammals) IAV infection is first detected by respiratory epithelial cells and myeloid-derived antigen presenting cells (APCs) via the recognition of various pathogen-associated molecular patterns (PAMP) by several pathogen recognition receptors (PRRs). These include receptors from three distinct classes, the Toll-like receptors (TLRs; transmembrane or intracellularly expressed proteins expressed by immune cells, involved largely in initiating inflammatory immune responses), nucleotide-binding domain and leucine-rich-repeat-containing receptors (NLRs; intracellular PRRs that

recognise cytoplasmic PAMP) and retinoic acid inducible gene-I (RIG-I)-like receptors (RLRs; cytoplasmic RNA helicases that are critical for host antiviral responses) [106]. Of the TLRs, TLR2, TLR3, TLR4, TLR7, TLR8, and TLR10 sense IAV infection in humans [107-111]. TLR3, TLR7 and TLR8 are typically localised to endolysosomal compartments within cells, but are also expressed on the apical cell surfaces of epithelial cells in the human respiratory tract [106]. TLR7, which is highly expressed in human plasmacytoid DCs (pDCs), and TLR8, detect infection by recognition of uridine-rich single stranded genomic influenza RNA [112-115]. Although TLR3 is classically associated with sensing dsRNA replicative intermediates, it is thought to recognise a currently unidentified RNA structure during infection with IAV, as IAV dsRNA is quickly destroyed by the activity of the cellular RNA helicase UAP56 [116-118]. Also associated with non-classical ligands during IAV infection are the cell surface expressed TLRs, TLR2 and TLR4. TLR2 and TLR4 are traditionally associated with the recognition of bacterial cell wall components and lipopolysaccharide (LPS) respectively, but during IAV infection are thought to recognise sugar residues on viral HA [107,119-121]. At present, the ligand for TLR10, the only known inhibitory TLR, is currently unknown [122]. In addition to the many mechanisms of recognition IAV PAMP by TLRs, IAV RNA is also detected by the RNA helicase retinoic acid inducible gene-I (RIG-I) [123]. RIG-I responds specifically to 5′-triphosphate viral ssRNA present in the cytosol following replication [123-125]. Infection in mice has also demonstrated recognition of M2-induced disturbances in intracellular ionic concentrations and PB1-F2 fibrils by the NLR family protein NLRP3 inflammasome complex [126,127].

TLR, RIG-I and NLRP3 activation by IAV initiates intracellular signaling cascades, which ultimately converge in the activation of pro-inflammatory cytokines and IFN responses [128]. All TLRs, with the exception of TLR3, which signals through Toll–IL-1-resistence (TIR) domain-containing adaptor protein inducing IFNβ (TRIF), activate a common signaling pathway via myeloid differentiation factor 88 (MyD88), which results in the downstream activation of two important families of transcription factors, nuclear factor-κB (NFκB) and the interferon-regulatory factors (IRFs). Activation of TLR3 by dsRNA also signals via RIPK3 (receptor-interacting protein kinase 3), which induces necrosis and further inflammation [129]. In addition RIG-I activates NFκB through engagement of the mitochondrial antiviral signaling protein (MAVS). Activation of the NLRP3 inflammasome results in caspase 1 activation and the release of the pro-inflammatory cytokines IL-1β (which promotes the infiltration of inflammatory cells from the circulation into extravascular spaces) and IL-18 (which enhances Type 1 T cell (section 1.6.2.3) and NK cell responses, including cytokine production and cytotoxicity[130]).

Activation of type I (IFN-α and IFN-β; anti-viral cytokines) and type III (IFN-λ; an anti-viral cytokine, particularly important at epithelial surfaces) IFNs induces the transcriptional activation of numerous IFN-stimulated genes (ISGs) resulting in the production of potent cytokines and chemokines, such as IL-1β, IL-6, IL-8, TNFα, chemokine (C-C motif) ligand 2 (CCL2), CCL3, CCL4, CCL5 and C-X-C motif chemokine ligand 10 (CXCL10) [111,131-136]. These have an important role in inducing viral resistance in neighbouring

uninfected cells and recruiting MΦs, neutrophils and T cells into infected lung tissue in humans and mice [111,131-136]. IL-1, IL-8, TNFα, and CCL2, CCL3, CCL4, CCL5, CCL20 and CXCL10 are also produced following necrosis and apoptosis of respiratory epithelia and alveolar MΦs respectively [131-135,137].

The products of ISGs can enhance antiviral responses mediated by DCs, NK and $CD8^+$ T cells [138-141]. Signals between immediate effector cells of the innate system and cells of the adaptive response are crucial to driving appropriate T and B cell responses. Signalling via TLRs and RLRs increases the expression of co-stimulatory molecules on APCs such as CD40, CD80, and CD86 [142]. Indeed type I IFNs promote antigen presentation and cross presentation by DCs and further activates DCs in an autocrine manner (cell signaling in which a cell secretes substances, which bind its own receptors) [143,144]. Nitric oxide synthase 2 (NOS2) and TNFα, which are secreted by activated alveolar MΦs, play a key role in regulating the induction of primary $CD8^+$ T cell responses [102,145]. Furthermore interactions with DCs in the draining lymph nodes (LNs) imprints a lung-homing phenotype on activated $CD4^+$ T cells and lung DCs are pivotal for the induction of $CD8^+$ T cell responses [146,147]. Interestingly, type I IFNs can also mediate an anti-inflammatory effect, which can control inflammasome-mediated responses via inhibition of interleukin IL-1, IL-12 and IL-18, and increased production of IL-10 [148-150]. This has been shown to limit IAV-induced immunopathology in mice [151].

In short, IAV infection in mammals is recognised by several overlapping mechanisms, which converge to rapidly trigger anti-viral, pro-inflammatory responses that recruit and condition additional immune effector cells.

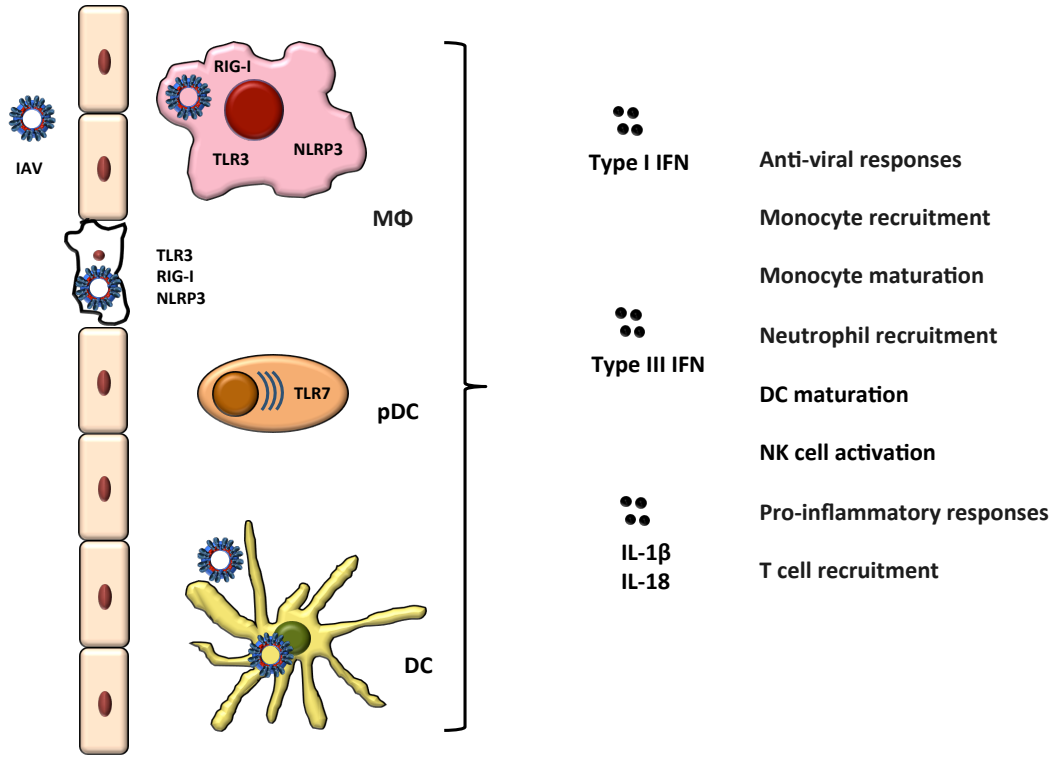


Figure 1.2 Innate sensing of influenza A infection

IAV infection of respiratory tract epithelial cells, MΦs and DCs is sensed by several families of PRRs including TLR3, TLR7 and RIG-I, which results in the downstream activation of Type I and Type III IFN responses. RIG-I, TLR3 and NLRP3 are expressed by epithelial cells and MΦs, and TLR7 is expressed in particular by plasmacytoid DCs. IFNs induce an anti-viral state in neighbouring cells and help to further recruit and activate innate immune effector cells. IAV infection also activates the NLRP3 inflammasome, which contributes to pro-inflammatory responses. DC, dendritic cell; IAV, influenza A infection; IFN, interferon; MΦ, macrophage; NK; natural killer, pDC, plasmacytoid dendritic cell; RIG-I, retinoic acid inducible gene-I; TLR, Toll-like receptor;

1.6.2. Adaptive Immunity Against Influenza A

Adaptive immune responses against IAV are mediated by T and B lymphocytes. Compared to innate immune responses, these responses are much slower to develop following primary infection. However these cells have the capacity to recognise a near-infinite number of antigens with much greater specificity than innate immune cells. Furthermore, following primary responses, a small pool of memory T and B cells survive, which respond with greater speed and magnitude upon subsequent exposures (antigen-specific T cells undergo three phases in the generation of memory cells – clonal expansion in the presence of antigen, contraction by apoptosis following antigen clearance and survival whereby a small number of antigen-specific T cells are maintained for great lengths of time; activated B cells proliferate following antigen stimulation and some develop into memory B cells, most of which are generated with T cell help). Indeed the primary objective of vaccination is to induce potent and long-lasting adaptive immune responses, which will protect against future infections.

1.6.2.1. Humoral Immune Responses Against Influenza A

Naïve B cells that respond to IAV infection typically reside in local LNs draining the upper (cervical LNs) and lower (mediastinal/bronchial LNs) respiratory tract, and are also found dispersed throughout the lung [152]. Following infection, B cells encounter antigen via presentation by APCs such as DCs in the LN or by direct capture of antigen via the B cell receptor (BCR). Local inflammation induced in response to IAV modulates local LNs and induces the formation of tertiary lymphoid structures. This inducible bronchus-

associated lymphoid tissue (iBALT) has distinct B cell follicles and can support B cell proliferation similar to secondary lymph organs (SLOs) (iBALT formation depends on the production of IL-17 by T cells) [153,154].

Once primed, naïve B cells in the respiratory tract differentiate into antibody secreting cells (ASCs) or memory B cells. In mice ASCs are identifiable in the LNs 3 days post infection and by day 7 in the lung [155,156]. Both local and systemic ASCs contribute to serum antibody titers, which can be detected approximately a week post infection in mice (in humans antibodies are first detectable 4-7 days after infection and reach peak titre at approximately 14-21 days) [152,157]. ASCs following infection with IAV in mice reside transiently in the spleen but are maintained long term in the bone marrow (BM) and the lung as long-lived plasma cells (LLPCs) [158,159]. Indeed LLPCs in the lung are present for life [158]. In contrast, memory B cells distribute widely and can be found in the lungs, LNs, BM and the nasopharynx-associated lymphoid tissue (NALT) [160]. The numbers of influenza-specific memory B cells in the lung are far greater than those in the BM [160]. Responses in humans are similar. Challenge studies of infection with seasonal influenza have demonstrated ASCs in the blood peak 7 days post infection [161]. The majority of these undergo apoptosis following clearance of the infection and a small fraction differentiate into LLPCs that survive in the bone marrow from months to years [161,162]. Memory B cells in humans reside in SLOs, although GCs are rarely seen in adult spleen [163].

Following primary IAV infection in mice, ASCs in the lung generate mainly IgG^+ and IgM^+ antibodies, whereas IgA^+ antibodies are predominantly produced by ASCs in the upper respiratory tract [164]. In humans, primary infection generates IgG^+, IgM^+ and IgA^+ antibodies, all of which can be measured in serum [165]. Antibodies are harder to detect in human nasal washes and lung sampling is not practical but challenge studies have shown the presence of predominantly IgA^+ and some IgG^+ antibodies in nasal secretions [165].

IgM^+ antibodies produced by naïve B cells primarily neutralise IAV by activating complement [166]. In contrast, mucosal IgA function primarily to neutralise infectious virions and can act both extra and intracellularly (by preventing cell entry or binding newly synthesised proteins and preventing virus assembly) to protect local epithelial cells from infection [167]. IgG antibodies in humans can transudate into the serous fluid of the respiratory tract from the blood or the lung [168]. In mice both IgG^+ and IgA^+ memory B cells are maintained locally in the respiratory tract and systemically in most tissues for months following infection [160]. In humans IgA^+ memory B cells are preferentially found in the tonsils [169]. In humans memory B cells circulate between SLOs, the blood and the bone marrow.

Antibody responses following natural infection with IAV in humans have been detected against most viral proteins although the majority target the dominant virion surface glycoprotein, HA. Structurally HA is comprised of three identical monomers, each consisting of an antigenically diverse head (HA1) and a

highly conserved stem (HA2) region [63,170-174]. The HA1 region of HA is immunodominant to the HA2 region and the majority of anti-HA1 antibodies induced by infection are strain-specific [170,172-174]. Anti-HA antibodies can provide prophylactic protection and neutralise infectious virions by inhibiting viral attachment (anti-HA1 antibodies) or impeding the structural rearrangement of HA necessary for fusion of the viral and endosomal membranes (anti-HA2 antibodies) [175]. In addition non-neutralising anti-HA antibodies have well-established roles in complement activation, opsonisation enhancement and activation of MΦ and NK cell-mediated antibody-dependent cell-mediated cytotoxicity (ADCC) [176,177]. However, neutralising anti-HA1 antibodies are currently the only universally accepted immune correlate of protection against influenza as a result of early studies which observed higher titers were associated with a lower risk of infection [178,179].

In addition to HA, NA, the second major virion surface protein, and M2, a minor glycoprotein, are also targets of humoral responses. The enzymatic activity of NA is essential for the release of progeny virus and the M2 ion channel protein facilitates unpacking of the viral genome in the endosome [65,66]. Neither anti-NA antibodies or anti-M2 antibodies prevent infection, however they can limit virus spread and reduce replication respectively [65,180]. In addition, both anti-NA and anti-M2 antibodies facilitate ADCC of infected cells and overall contribute to reducing the severity and duration of illness [181,182]. The protective effects of anti-NA and anti-M2 antibodies have both been demonstrated in animal challenge studies, though their roles in human immunity remain incompletely understood [183,184].

In addition to the surface-exposed proteins, infection with IAV also induces antibodies against internal viral proteins including the highly conserved protein NP. Anti-NP antibodies contribute to protection in mice by enhancing viral clearance following challenge [185]. These antibodies are non-neutralising and uniquely rely on T cell involvement to mediate their anti-viral activity, presumably by enhancing DC activation and antigen presentation via Fc (fragment crystallisable region of an antibody) receptor (FcR) engagement on immune complexes [185,186]. Indeed passive transfer of anti-NP antibodies does not protect mice that lack B and T cells but can rescue poor immunity in B cell-deficient mice and is reduced following $CD8^+$ cell depletion [186,187]. Whether or not anti-NP antibodies facilitate ADCC, and what their role is in human immunity, remains to be determined. ADCC has traditionally been measured using chromium-51 release assays, which rely on a target cell line expressing the antigen of interest. However, high background can be a problem with such assays.

1.6.2.1.1. Original Antigenic Sin

In the context of IAV infection, the phenomenon of original antigenic sin (OAS) refers to prior exposure to one strain that leads to a subsequent suboptimal antibody response to novel epitopes in variant strains [188,189]. It has particularly important consequences for vaccine design because humans, unlike animal models frequently used to dissect immune responses to IAV, are not immunologically naïve and have complex individual immunities as a result of a lifetime's exposure. These can clearly impact vaccine-induced responses.

The mechanism of OAS remains incompletely understood. One commonly put forward explanation is that higher frequencies of cross reactive memory B cells with a lower threshold of activation outcompete naïve B cells responding to new epitopes and this ultimately leads to an overall response dominated by antibodies against the 'original' virus [190]. Another hypothesis is that IAV infection of B cells results in antigen presentation by B cells instead of DCs, which may provide suboptimal signals that favour memory responses [191]. One issue with both of these ideas is that in principle they imply B cell responses against highly conserved regions, to which there is pre-existing immunity, should be always boosted. However, as is the case with antibody responses against the highly conserved HA stem region, this does not happen in practice.

Interestingly, OAS has been overcome in sequentially immunised rabbits by administering significantly higher doses of a second virus [192]. Recent modelling of pre-existing immune responses suggests that pre-formed antibodies may mask epitopes such as those on the HA stem and in fact reduce boosting [193]. High doses of antigen could overcome this effect but may not be clinically feasible. However, adjuvants such as MF59 have been reported as being capable of broadening immune responses by inducing potent T follicular helper cell (T_{FH}), which amplify germinal center (GC) B cell responses and further investigation into their use as agents to overcome OAS is warranted [194,195].

1.6.2.2. Cellular Immune Responses Against Influenza A

Infection with IAV induces cellular immune responses from $CD4^+$ and $CD8^+$ T cells. $CD4^+$ T cells function primarily as modulators of the immune system, and are subdivided based on the cytokine profiles that they produce [196]. These cells recognise foreign antigen in the context of major histocompatibility complex (MHC) class II molecules, which are predominantly expressed on professional APCs such as MΦs, DCs and B cells [197]. Activation of naïve $CD4^+$ T cells requires three signals; binding of the peptide:MHC class II to the T cell receptor (TCR):CD4 complex on the T cell, a co-stimulation signal via binding of CD80/CD86 on an activated APC to CD28 on the T cell, and a cytokine signal from the environment, which is necessary to optimally activate differentiation and clonal expansion [197]. Depending on the cytokine milieu induced during the innate response, naïve $CD4^+$ T cells differentiate into one of several effector fates including T_H1, T_H2, T_H17, T_{FH} and T_{REG} cells, and can also exhibit cytolytic activity [196].

$CD4^+$ T cell responses against IAV are broadly systemic and memory $CD4^+$ T cells survive in the lung and spleen of humans and mice [198,199]. In murine models of primary IAV infection, mice lacking $CD8^+$ T cells, $CD4^+$ T cells or B cells, could clear low pathogenic strains [200]. However more pathogenic strains could only be cleared by $CD8^+$ and $CD4^+$ T cells, or B cells and $CD4^+$ T cells together indicating $CD4^+$ T cells alone are not sufficient for viral clearance but have an important role in coordinating and augmenting B and $CD8^+$ T cell responses [200]. However memory $CD4^+$ T cells can direct viral clearance in the absence of B cells or $CD8^+$ T cells [201]. Indeed, in human

influenza challenge studies, memory $CD4^+$ T cell responses are considered the protective correlate *in vivo* [202].

Primary infection of mice with IAV induces $CD4^+$ T cell responses strongly biased towards a T_H1 phenotype [187]. These promote and direct the activation of MΦs and $CD8^+$ T cells by secreting a Type 1 panel of cytokines including IFNγ, TNFα and IL-2 and are essential for the induction of IAV-specific memory $CD8^+$ T cells [187]. T_H1 cytokines also drive IgG2a class switching in mice (IgG1 in humans), which is particularly effective at activating complement, binding Fc receptors and inducing ADCC [203]. Much less is understood about human $CD4^+$ T cell responses to influenza, although memory $CD4^+$ T cell responses have been shown to contribute to protection against disease in a human challenge model [202].

In addition to T_H1 cells, IAV infection in mice also induces responses from $CD4^+$ T regulatory T cells (T_{REG}), which contribute to regulating immune responses. Indeed T_{REG} cells modulate the T_H1 and $CD8^+$ T cell responses induced by infection and also promote influenza-specific T_{FH} responses [204]. T_{FH} cells are $CD4^+$ T cells that function primarily to provide help to B cells by supporting the GC reaction and facilitating affinity maturation and the generation of long-lived memory B cells and plasma cells (Chapter 5). These cells also secrete IFNγ during IAV infection; however, their secretion of IFNγ is not essential for class switching but may enhance it [205]. Indeed class-switching can also be signaled directly by stimulation of TLR9 in B cells [206].

In contrast to $CD4^+$ T cells, $CD8^+$ T cells are primarily cytotoxic and are essential in the clearance of viral infection. $CD8^+$ T cells recognise foreign antigens presented in the context of MHC class I molecules, which enables them to detect infection in all nucleated cells [197]. They are activated by direct recognition of foreign peptide on an activated DC expressing strong co-stimulatory signals (e.g. B7 family and TNFR ligand family), or if the antigen is presented on a DC with weak co-stimulation, this may be overcome by signals provided by an effector $CD4^+$ T cell bound to the same DC [197,207]. Once activated, cytotoxic $CD8^+$ T cells (T_C) migrate to the site of infection and induce apoptosis of infected cells presenting recognised foreign antigens [197]. The lytic activity of T_C is mediated by the release of cytotoxic granules containing serine proteases such as granzyme A and B, and the pore-forming protein, perforin [197]. Perforin permeabilises infected cell membranes, which facilitates delivery of granzymes into the cell and induction of apoptosis [208]. Apoptosis can also be induced in infected cells through interactions of Fas ligand (FasL) on the T_C with Fas receptor (FasR) on a target cell [208]. The major cytokine pattern expressed by activated T_C is similar to T_H1 cells and includes IFNγ, TNFα (TNF-α is a pleiotropic cytokine that can affect APC differentiation and contribute to lung pathology during influenza infection) and TNFβ (TNFβ (also known as lymphotoxin-alpha) is a proinflammatory cytokine that contributes to the development of normal lymphoid architecture during immune responses), which further stimulate antigen presentation and anti-viral activity [209-212]. Following viral clearance, approximately 5-10% of effector T_C survive as long-lived memory cells which reside in lymphoid organs, tissues or continually circulate [213,214]. These cells are capable of rapid

recall responses following re-exposure, the reactivity and affinity of which is determined by the co-stimulatory signals received during the primary response [215].

Murine models of IAV infection have been widely used to characterise T_C responses against influenza. Naïve mice lacking T_C cells demonstrate delayed viral clearance when challenged with influenza virus and have an increased risk of mortality compared to healthy controls [216]. However primed B cell-deficient mice clear infection and are protected following lethal challenge [217]. There is less evidence to support a role for T_C in human infection, although T_C cell responses have been shown to correlate with reduced viral shedding and less severe disease outcomes in the absence of HA-specific antibodies and cross-reactive neutralising antibodies respectively [218,219].

IAV-specific T_C responses are primarily directed against epitopes contained in internal viral proteins such as M1, NP, PA and PB1, which are highly conserved and display a high degree of strain cross-reactivity. These responses are hierarchical and immunodominance patterns can differ substantially between primary and secondary responses [220]. For example primary responses in C57BL/6 mice are dominated by approximately equal numbers of T_C recognising $NP_{366–374}$ and $PA_{224-233}$ [221,222]. Far fewer cells are induced that recognise other known epitopes such as $PB1_{703-711}$, $NS2_{114-121}$, $M1_{128-135}$ or alternatively spliced $PB1\text{-}_{F262-70}$ [223]. In addition, secondary responses are dominated by up to 80% $NP_{366-374}$-specific T_C [220]. Whilst

responses specific for the other five epitopes can still be detected they present at greatly reduced frequencies [220].

The immunodominance patterns observed in secondary responses are influenced by the differential processing and display density of epitopes among different APCs and their capacity to activate naïve and memory $CD8^+$ T cells [224]. During a primary infection, only DCs can activate naïve $CD8^+$ T cells, however memory cells can be activated by other APCs, which vary in number according to anatomical location [224]. This has implications for the rational design of vaccines as the route of vaccination could influence immunodominance patterns depending on which epitopes are preferentially displayed by the APCs, which may vary in number depending on particular anatomical sites. For example there is an abundant pool of APCs in the skin, which are better targeted by intradermal vaccination compared to intramuscular. Furthermore, memory CD8+ T cells are likely to be resident in lung tissue in humans as a result of previous exposure. Vaccination with a single immunodominant epitope is also likely to reduce the breadth of responses in individuals with pre-existing responses. This is important as a lack of broad multi-specific responses to subdominant epitopes may increase the risk of mortality and morbidity [225].

In addition, T cell responses in humans to IAV antigens are influenced by human leukocyte antigen (HLA) polymorphisms. HLA are the most polymorphic human genes and binding of a given peptide within a functional peptide-binding region is restricted to specific HLA alleles [197]. Therefore the

ability of a particular peptide to induce T cell responses depends on that peptide being presented in the context of a particular HLA molecule, which has important consequences for the design of T cell-inducing vaccines [197].

1.6.3. Heterosubtypic Immunity Against Influenza A

Heterosubtypic immunity is defined as immunity induced against a particular strain of IAV that is cross-protective against other subtypes, and can be mediated by T and B cells [226]. It was first reported 50 years ago in mice protected against challenge from the mouse-adapted IAV Jap.305 as a result of previous immunity induced by infection with PR8 [227]. This protection was demonstrated in the absence of neutralising antibodies and thought to be mediated primarily by T cells [227]. However, more recently antibodies have been shown to be capable of providing heterosubtypic protection. Indeed heterosubtypic immunity against IAV is thought to be mediated primarily by T_C cells recognising epitopes of highly conserved internal proteins and B cells producing antibodies that recognise highly conserved epitopes on the virion surface glycoproteins and internal proteins expressed on the surface of infected cells. In addition $CD4^+$ T cells play an important role in modulating heterosubtypic T_C and T cell-dependent B cell responses. The primary objective of new generation ‘universal influenza vaccines’ is the induction of heterosubtypic immune responses.

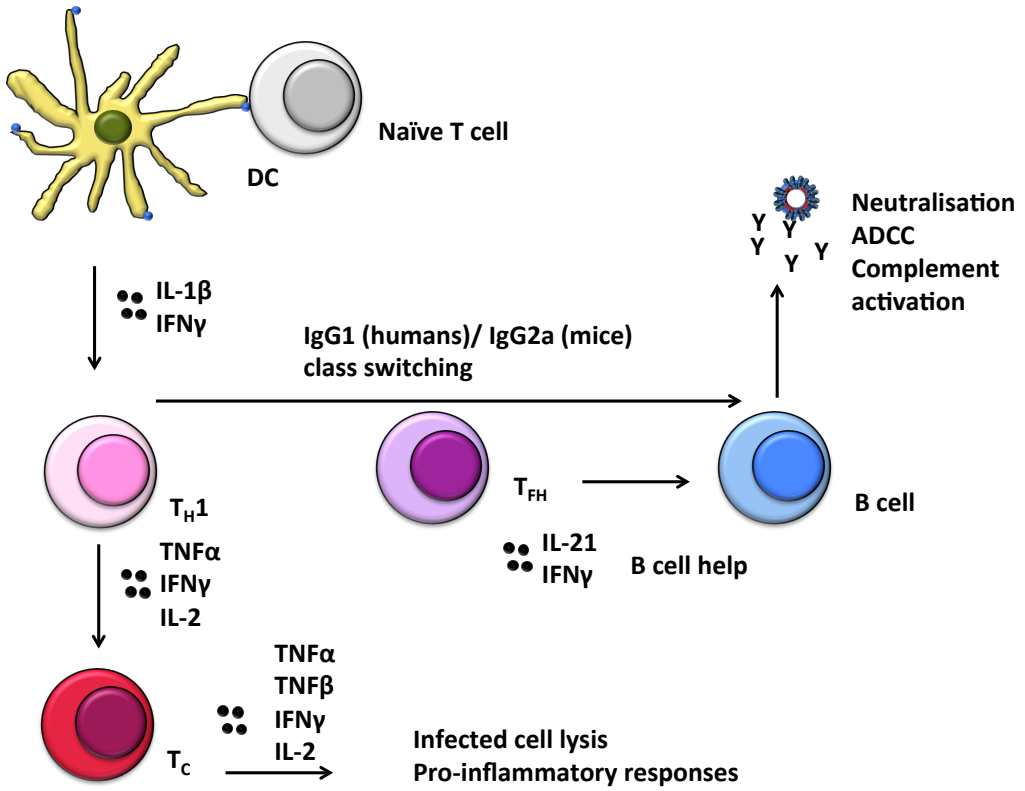


Figure 1.3 Adaptive immune responses to influenza A infection

Following IAV infection naïve $CD4^+$ and $CD8^+$ T cells are primed by activated DCs and develop into effector T_H1 and T_C cells respectively. Effector T_H1 cells secrete pro-inflammatory cytokines such as IFNγ, TNFα and IL-2, which modulate T_C responses and induce antibody class switching (IgG1 in humans, IgG2a in mice). Infection also induces a specialised subset of T helper cells, T_{FH} cells, which regulate B cell immunity. ADCC, antibody-dependent cell-mediated cytotoxicity; DC, dendritic cell; IFN, interferon T_C, Interleukin 2; $CD8^+$ cytotoxic T cell, T_{FH}, T follicular helper cell; IL-2, interleukin-2; T_H1, T helper Type 1 cell; TNF, tumour necrosis factor.

1.6.4. Mouse Models

Mice are the most commonly used animal model of disease in influenza research. They are relatively cheap and convenient to use in terms of husbandry, genetically well studied and easy to manipulate, and there are a wide variety of mouse-specific reagents commercially available to facilitate their use. Furthermore they can be used in large numbers to obtain statistically robust data.

However, there are a number of distinctions between influenza infection in mice and humans. Mice do not develop fever and are unable to cough or sneeze. Their susceptibility to infection depends on the strain of mouse as well as the strain of virus. Wild mice are frequently resistant to infection due to expression of Mx1, a critical anti-viral protein lacking in most laboratory strains [228]. Furthermore, human influenza viruses attach preferentially to SAα2,6Gal moieties abundant in human upper airways. However, SAα2,3Gal, not SAα2,6Gal are abundant in the mouse respiratory tract [229]. Even so, some strains such as the 1918 H1N1 pandemic strain, HPAI H5N1 viruses, certain H7 subtype viruses, some LPAI viruses and the 2009 H1N1 pandemic virus cause disease without prior adaptation [229-233].

The majority of research into influenza uses BALB/c (H-2^d) or C57BL/6 (H-2^b), which differ in their expression of MHC alleles. T cells from C57BL/6 mice preferentially produce T helper Type 1 (T_H1) cytokines (high IFNγ, low IL-4), whereas BALB/c mice favor T_H2 responses (low IFNγ, high IL-4) (section 1.6.2.3) [234].

Part III

1.7. Currently Licensed Vaccines

Vaccination against seasonal influenza was first implemented 70 years ago and to this day remains the cornerstone of influenza prevention [235,236]. Currently licensed seasonal vaccines fall broadly into two classes: inactivated influenza vaccines (IIV) and live-attenuated influenza vaccines (LAIV). The first of these to be developed, IIV, are produced as whole-virion, split-virion or subunit formulations. Whole-virion vaccines are comprised of a crude viral lysate harvested from embryonated chicken eggs and chemically inactivated with formalin or β-propiolactone and phenylmercuric nitrate [237,238]. These vaccines were highly reactogenic, causing fevers, particularly among children, and have been largely replaced by inactivated split-virion or subunit vaccines [239,240]. Split-virion and subunit vaccines are produced by disrupting and purifying virus particles with ether and a detergent such as Triton™ X-100 to remove unnecessary viral components, and in the case of subunit vaccines, are further purified to contain only the virus glycoproteins, HA and NA [240-243]. LAIV are comprised of temperature-sensitive cold-adapted attenuated viruses based on A/AnnArbor/6/60 that are limited to replicating only within the upper respiratory tract (five changes to PB1 (E391, G581 and T661), PB2 (S265) and NP (G34) are responsible for the temperature sensitive and attenuated virus properties) [244]. These have been used widely in Russia since the 1980s but have only been licensed for use in the US and Europe since 2003 and 2012 respectively [245]. Current seasonal vaccine

formulations include three (trivalent) or four (quadrivalent) seasonal influenza virus strains, one from each of the two currently circulating IAV subtypes, H1 and H3, and either one or two strains from the two co-circulating circulating IBV lineages [41]. Pandemic vaccines including those produced and licensed during the 2009 pandemic or against H5N1 are monovalent.

1.7.1. Antigenic Matching

Regardless of vaccine class, all currently licensed vaccines, both inactivated and live-attenuated formulations induce antibodies against HA, the major virion surface protein. Neutralising antibodies reported as haemagglutination inhibition (HI) titers against HA are universally accepted as a major correlate of protection against influenza infection [246-248]. However, antibodies induced by current vaccines are primarily strain-specific and must be continuously updated in order to keep pace with viral escape mutants generated by antigenic drift. In years when vaccine and circulating strains are mismatched, vaccine efficacy ((VE); the percentage reduction in disease in a vaccinated group compared to an unvaccinated group) can be severely compromised [249]. This was first observed within two years of the first licensed influenza vaccine being released when the vaccine completely failed during the winter of 1947 as a result of a new antigenic variant that had spread worldwide [236]. Antigenic drift remains an obstacle; the mid season VE of the 2014/15 vaccine in the UK was estimated at just 3.4% due to antigenic mismatch of the H3N2 circulating virus and the northern hemisphere vaccine strain [250].

1.7.2. Manufacturing Limitations

The redevelopment, remanufacture and retesting of seasonal influenza vaccines is costly and time consuming with the annual production cycle lasting anywhere between 6-9 months [251]. Since the late 1960s, production of IAV vaccine strains has relied on the use of a master donor virus (MDV) derived from A/PuertoRico/8/34 (H1N1), a strain that propagates readily in embryonated chicken eggs [243,252]. A/Ann Arbor/6/60 (H2N2) is used as the MDV in the production of live attenuated cold-adapted vaccines [253]. Generation of vaccine strains that express circulating HA and NA proteins with the other genes from the MDV relies on the natural reassortment properties of IAV viruses [243]. This procedure can potentially generate 256 unique reassortant viruses and selection of the target strain can be a significant bottleneck in the vaccine production cycle. Furthermore, this method depends on and can be limited by a scarcity of embryonated chicken eggs, which is not practical for pandemic situations when chickens may be widely culled and when vaccine production cannot afford to be delayed [252]. Moreover, vaccine strain yields can vary depending on strain pathogenicity. Highly pathogenic avian strains in particular tend to produce much lower viral titers, which can make production targets even harder to reach [254].

Recent advances in the production of seasonal vaccines has been the replacement of eggs by tissue culture cells in the propagation of vaccine strains in addition to a movement towards a more synthetic approach to generating influenza vaccine strains. Cell-based systems using Madin-Darby canine kidney (MDCK) cells (Optaflu®, FLUCELVAX®; Novartis) or Vero cells

derived from the kidney of an African green monkey (Preflucel®; Baxter), have a much shorter lead to production compared to traditional egg-based systems [255]. A move towards producing current vaccine formulations using these technologies could help shorten the production cycle and contribute to increased global production capacity. This would particularly benefit pandemic vaccine production. In addition, cell-based vaccines can be administered to individuals with egg allergies who must currently be excluded from vaccination programmes [41]. These advantages are also afforded by recombinant protein systems, which furthermore do not require the generation of a master seed strain in order to commence production. Indeed, the first recombinant protein-based vaccine (Flublok®; Protein Sciences Corporation) comprised of purified HA protein produced using a baculovirus insect cell expression system (based on the use of recombinant baculoviruses to produce biologically active proteins in cultured insect cells) has a production cycle of just 11 weeks [256].

1.7.3. Variable Efficacy

While a large part of the problem with currently licensed influenza vaccines lies with the technologies and strategies used to produce them, a further issue is VE variability, particularly among populations most at risk. Even when strains are antigenically matched, VE of seasonal IIV has been approximated as 59% in healthy adults aged 18-65 years and is estimated to be even lower in elderly populations for whom vaccination is currently recommended [257]. Furthermore IIV are largely ineffective in children under 2 years of age and repeated IIV vaccination is thought to reduce influenza-

specific T cell responses in this age group [258,259]. Although LAIV have an efficacy of 83% in children aged 6 months to 7 years, this drops to 42% in adults over 60 years and LAIV is currently only recommended for children aged 2-18 years in the UK [41,257].

In order to improve vaccine-induced immune responses, particularly in the elderly, high dose (60μg compared to 15μg standard vaccines) and adjuvanted seasonal vaccines have been licensed in the US (Fluzone® High-Dose; Sanofi Pasteur Inc.) and Europe (FLUAD® (MF59®-Adjuvanted Influenza Vaccine; Novartis)) with some benefit. A recent randomised controlled trial (RCT) demonstrated Fluzone® High-Dose induced significantly higher antibody responses compared to standard dose Fluzone® and was found to be 24.2% more effective in preventing influenza [260]. Observational studies of elderly vaccination with FLUAD® vaccination have estimated this vaccine could provide levels of protection against hospitalisation comparable to non-adjuvanted vaccines in young adults [261]. Adjuvants have also been employed to enhance immune responses to pandemic vaccines. AS03B, a tocopherol based oil in water emulsion an oil-in-water emulsion similar to MF59, is a component of the H1N1 pandemic vaccines Pandemrix® and Arepanrix® (GlaxoSmithKline) and has demonstrated improved immunogenicity compared to non-adjuvanted vaccines [262]. However, Pandemrix® has been associated with narcolepsy onset in children [263,264]. Due to the slightly different purification processes used in the production of split virion vaccines, Pandemrix® contains higher levels of NP than other vaccine formulations [265]. Indeed antibodies to NP

cross-react with human hypocretin receptor 2 and the increased levels of these antibodies induced by vaccination with Pandemrix® has been hypothesised as contributing to the higher incidences of narcolepsy among vaccinees [265]. Narcolepsy also has a strong genetic linkage with the (HLA) DQB1*0602 genotype and this was also observed in persons reactive to Pandemrix® [266].

1.8. Next Generation Vaccines

Manufacturing advances such as synthetic virus generation and cell culture or recombinant protein technologies, in addition to adjuvants and high dose formulations, have contributed and will continue to contribute to improving influenza vaccine availability and efficacy. However, with the exception of recombinant protein vaccines, much of these technologies are still based on IIV or LAIV platforms and target the same antigens. In recent years, influenza vaccine development has moved towards developing novel vaccine platforms and identifying alternative vaccine targets that could potentially provide much broader protection and eliminate the need for annual production cycles.

1.8.1. Novel Vaccine Platforms

Among the most promising platforms in development are DNA-based vaccines, virus-like particles (VLPs) and viral-vectored vaccines. Of these three, DNA-based vaccines, though the least novel, are particularly easy to manipulate and have the advantage of being rapidly scalable [267]. Furthermore they are non-infectious, extremely stable and can be produced at relatively low cost [267]. DNA-based influenza vaccines can induce humoral and cellular immune responses but are less immunogenic than other platforms, particularly in the very young or old [268]. Furthermore vaccination with DNA poses a risk of malignancy and can also induce host autoimmune responses [267]. However, small scale phase I studies have demonstrated DNA-based HA vaccines prime for superior responses compared to protein alone [269]

In comparison however, VLPs are capable of inducing much more potent immune responses, particularly humoral immune responses, most likely on account of their particulate nature and repetitive, high-density display of viral epitopes. Vaccine particles retain a virus-like morphology but do not have a viral core and cannot replicate. They are easily expressed in a variety of cell culture systems and can be readily produced within 12 weeks [270]. Although there have been few trials using influenza VLPs in humans, they appear so far to be safe and immunogenic [271,272].

Of the three platforms, recombinant viral-vectored vaccines are the most advanced [273]. As vaccine delivery vehicles, viral-vectors benefit from their inherent ability to induce pro-inflammatory innate immune responses as a consequence of PRR recognition of viral vector-expressed PAMP. This can augment antigen presentation of vector transgene products and induce potent responses against vaccine antigens. In the past viral vectors have been the platform of choice for the induction of cellular immune responses but they are increasingly being used to induce both humoral and cellular immune responses [274]. There is a small risk that replication incompetent viral vectors could regain the ability to replicate but this would depend on co-infection with replication competent adenoviruses. The likelihood of this happening depends on vaccination route and virus strain. For example replication incompetent adenoviruses are more likely to meet replication competent adenoviruses in the respiratory tract than in a myocyte. However, rare virus species are not likely to ever have the opportunity to co-infect anyway. Among the viral-vectored vaccines in preclinical development are

adeno-associated viral vectors, adenoviral vectors, alphavirus vectors, baculovirus vectors, measles virus vectors, Newcastle disease viral vectors, parainfluenza virus 5 vectors, poxviral vectors and vesicular stomatitis viral vectors [275,276]. The viral vectors used in this study are discussed more thoroughly in Part IV.

1.8.2. Novel Vaccine Targets

Currently licensed influenza vaccines, both seasonal and pandemic, include the virion surface protein HA as the major vaccine antigen. However, the variability of HA and in particular, the immunodominance of the highly mutable regions of HA, make this a rather imperfect antigen choice in its current form. In recent years there has been a movement towards the rational design of influenza vaccines, specifically targeting viral proteins or epitopes that are much more highly conserved, which could potentially provide much broader protection against multiple strains and subtypes, even against emerging pandemic viruses. The induction of such heterosubtypic protection is the aim of these so-called ‘universal influenza vaccines’. To date much of this research has focused on targeting the extracellular domain of M2 (M2e), the stem domain of HA (HA2) and highly conserved internal viral proteins such as NP and M1.

1.8.2.1. M2e

The M2 in channel protein is the least abundant protein on the surface of an influenza virion (20-60 molecules per virion) but it is present at twice the concentration of HA on the surface of infected cells where it is thought to

affect the morphology of budding virions and plays a role in the packaging, assembling and budding of vRNP [66,83,277,278]. Only a small portion of the protein, 23 amino acid residues at the N terminus (M2e), is surface exposed, but this epitope is largely conserved across all IAV subtypes which makes it an attractive vaccine target [279]. The protective capacity of anti-M2e antibodies was first demonstrated in passive transfer experiments in mice [184]. Although anti-M2e antibodies cannot provide sterilising protection, they are thought to protect via ADCC and complement mediated lysis [280]. Anti-M2e antibodies are transient or weak following natural infection, they can be induced by vaccination [281]. However M2e alone is poorly immunogenic and multiple copies, fusion antigens or carriers and adjuvants have been tested as means of boosting immunogenicity [279]. Although vaccines inducing anti-M2e antibodies in mice have demonstrated partial protection against lethal challenge and decreased viral shedding, in pigs, anti-M2e antibodies have been associated with lung pathology and disease exacerbation by an as yet unclear mechanism [282-286]. Human trials of vaccines to induce anti-M2e antibodies have demonstrated safety and immunogenicity but the efficacy of these vaccines and the role anti-M2e antibodies may play in the context of human infection remains unknown [287].

1.8.2.2. HA2

Broadly neutralising anti-stem antibodies (bnStAbs) were first identified in mice over 20 years ago although their importance at the time was largely overlooked [288,289]. However, recent developments in technologies such as phage display have revealed that these antibodies circulate in human sera,

albeit at very low levels, and are capable of neutralising multiple subtypes of IAV [290,291]. Although they represent only a minor component of overall responses to natural infection, such responses were significantly boosted by infection with the 2009 pandemic H1N1 virus (infection with this virus, which had an antigenically distinct HA1 region, predominantly activated broadly cross-reactive memory B cells against the stem that then underwent further affinity maturation) raising the possibility that these antibodies could be boosted to protective levels by vaccination [292-295].

Several approaches have been taken towards developing suitable immunogens capable of inducing bnStAbs, including generating full HA2 constructs that lack the HA1 domain or HA2 fragments, introducing glycosylation sites into the HA1 domain to mask immunodominant epitopes or generating chimeric HA expressing rare HA1 subtypes, which when used in sequential vaccinations can direct immune responses towards the conserved stem region [296-300]. The HA2 domain has been expressed in a native-like conformation in both prokaryotic and eukaryotic systems and has been shown to be capable of inducing immune responses capable of protecting mice from lethal homologous challenge [296,301-303]. In addition vaccination with VLPs expressing HA2 generated broadly reactive antibodies that recognised multiple HA subtypes and also protected against lethal challenge [296]. Chimeric HA have been investigated extensively in several animal models (ferrets for example are more useful than mice in the assessment of symptom reduction and are also able to sneeze, unlike mice) and have successfully induced bnStAbs protective against challenge with either Group 1 or Group 2

viruses (HA subtypes are divided into two major groups, Group 1 and Group 2, on the basis of antigenic properties) (Fig. 3.1) [298,304,305]. These studies have been instrumental in demonstrating a 'proof of principal' that induction of bnStAbs by vaccination is possible. However it is by no means certain that such immunogens will be able to break the immunodominance of antibody responses in influenza-exposed humans or that bnStAbs can be induced by vaccination to levels that will prevent infection, which are also currently unknown.

The production of recombinant HA constructs based on HA2 and the immunogenicity of two novel stem immunogens have been investigated as part of this study and are discussed in detail in Chapters 3 and 6 respectively.

1.8.2.3. NP and M1

Cell-mediated immunity in humans has been shown to correlate with reduced viral shedding and less severe disease outcomes in the absence of HA-specific antibodies and cross-reactive neutralising antibodies respectively [218,219]. However, current IIV do not stimulate these responses and while LAIV primes T cell responses in young children, it does not boost these responses in adults due to the presence of preexisting neutralising antibodies. Until recently, viral proteins that are targeted primarily by cellular responses have been largely overlooked as vaccine antigens compared to major targets of humoral immunity. The internal viral proteins NP and M1 are extensively expressed in virally infected cells and are known targets of naturally induced cellular immune responses. In contrast to traditional vaccine antigens such as

HA, these proteins are highly conserved and have T cell epitopes common among different IAV subtypes, which makes them particularly attractive as vaccine antigens capable of inducing heterosubtypic immune responses. Vaccines capable of inducing or boosting heterosubtypic T cell responses could be particularly useful in pandemic scenarios, especially in the absence of pre-existing antibodies.

To date vaccines expressing NP have been shown to generate cross-reactive T cell responses and protect mice from lethal challenge against multiple IAV subtypes [306-309]. Furthermore, clinical trials of a vaccine expressing a fusion antigen of NP and M1 expressed by MVA (MVA-NP+M1) have demonstrated the vaccine is safe, immunogenic and can reduce viral shedding following challenge [310,311]. Another viral-vectored vaccine ChAdOx1 NP+M1 induced high levels of antigen-specific T cell responses and was safe and immunogenic in humans [312]. This vaccine is currently under investigation in a phase I study to assess the safety and immunogenicity of a heterologous prime-boost regimen using MVA-NP+M1 (NCT01818362). A prime–boost adenovirus-MVA regimen expressing NP+M1 has already demonstrated induction of heterosubtypic immunity in mice [313].

1.9. Correlates of Protection

The 'gold standard' correlate of protection against influenza infection currently used by both the Food and Drug Administration (FDA) of the US and the European Medicines Agency (EMA) for vaccine licensure purposes is the serum haemagglutination-inhibition (HI) titer [248,314-317]. HI titers against a particular strain of influenza are determined by pre-incubating the virus with sera before measuring the ability of the virus to agglutinate red blood cells (RBCs). Inhibition of haemagglutination indicates the presence of neutralising IgG antibodies against HA, specifically the HA1 domain. The association between protection from illness and HI titer was first observed in the 1940s following vaccination with a classic IIV and a HI titer ≥40 has been widely adopted as a correlate for a 50% reduction or more in the risk of influenza infection or disease [179,235]. In a challenge study by Hobson *et al* in the 1970s the 50% protective dose of HI antibody titer was 1/18-1/36 [179].

Unfortunately, there are a number of issues with using HI titers as correlates of protection. Firstly, HI assays are not standardised between labs and as a result of differences in SAα2,3Gal and SAα2,6Gal moieties among animal species, assay results can vary enormously depending on the source of RBCs [318]. Secondly, although numerous studies have demonstrated resistance to influenza infection in persons with pre-exposure HI titers 32 or 40, the cut off point of ≥40 is rather arbitrary and not appropriate for evaluating influenza vaccines in children. Indeed a titer ≥110 is needed to predict the conventional 50% clinical protection rate in children and ≥330 for 80% protection [319]. Furthermore although absolute post-vaccination HI titers

correlate with protection in adults vaccinated with either IIV or LAIV, vaccine failure has been associated with very high HI titers, suggesting that the quality of antibody responses as well as the quantity is important [246]. Thirdly, T cell responses are in fact better correlates of protection in the elderly and may also be a better measure of protective immunity in children receiving LAIV [320,321]. In addition protection induced by LAIV is also likely to be provided through mucosal IgA responses, which are entirely ignored by this assay [322,323]. A fourth point is that although the haemagglutination inhibition assay (HAI) measures neutralising antibodies against HA, this is limited to antibodies that inhibit receptor binding. However, anti-HA antibodies can neutralise infectious virus by several other physiologically relevant mechanisms such as by inhibiting the fusion event by binding the HA2 domain [175]. Antibody functions besides neutralisation such as ADCC can contribute to viral clearance and reduce disease severity and the contribution of these responses against other IAV antigens is missed by this assay.

Clearly correlates of protection depend on vaccine formulation and host factors, such as age and health status, and the one-size-fits-all model currently used to assess pre-licensure vaccines needs to change. In order for research into next generation vaccines targeting novel antigens to progress, new methods are needed and these must be developed with common protocols and standardised reagents in order to reduce inter-laboratory variation, which will accelerate progress towards a universal influenza vaccine.

Part IV

1.10. Viral-Vectored Vaccines

Traditional vaccine technologies such as whole-inactivated, live-attenuated and subunit vaccines have been limited in their ability to induce long-lasting protective immunity against influenza and several other pathogens such as HIV, TB and malaria. Viral vectors, viruses with modified genomes that are no longer pathogenic but can still infect cells and express viral proteins, represent an alternative vaccine antigen delivery platform that has become increasingly popular in recent years. Among the most commonly used viral vectors are human and simian adenoviruses, Newcastle disease virus (NDV), yellow fever virus and several poxviruses such as canarypox, fowlpox, vaccinia virus (VACV) and Modified vaccinia virus Ankara (MVA). As gene delivery vehicles, viral vectors are relatively flexible and can be engineered to express a variety of vaccine antigens, the size of which depends on the particular vector genome [324]. In addition they are relatively straightforward to manipulate, have well-established safety profiles and can be easily scaled and manufactured to good manufacturing practice (GMP) standard [325].

Compared to recombinant protein or DNA vaccines, viral vectors are naturally immunogenic and have an intrinsic adjuvanting capability as a result of virus-induced cell death and the pro-inflammatory environment produced by the expression of viral proteins [324]. Though originally used primarily for their ability to induce potent cellular responses, viral vectors are increasingly being

used to induce humoral responses and are particularly immunogenic when used in heterologous prime-boost regimens [274,310,326]. Factors such as gene promoter strength, viral persistence, route of administration and induction of pro-inflammatory responses, can considerably influence the immunostimulatory capacity of a particular viral-vectored vaccine.

1.10.1. Adenoviral-Vectors

Adenoviruses are non-enveloped, double-stranded DNA viruses that cause mild symptomatic or persistent subclinical infections in several species of vertebrates. First isolated in 1953 from human adenoid-derived cell cultures, more than 60 types of human adenoviruses across seven subgroups (A-G) are currently known [327,328]. In humans, infections are typically associated with respiratory disease in children, however some subtypes are also known to infect the urinary- or gastrointestinal tract and can also cause ocular disease [329]. Adenoviral infections can also result in severe disease among immunocompromised populations [330]. Vaccines against adenovirus serotype 4 and serotype 7 are currently approved for military personnel aged 17-50 years in the U.S. [331]

Several features of adenoviruses make them particularly attractive candidates for the delivery of genetic material into cells and they were originally developed as tools for gene therapy. In particular adenoviruses are genetically stable, have a broad tropism (multiple receptors across several cell types including integrins, coxsackievirus and adenovirus receptor (CAR), heparan sulfate glycosaminoglycans, CD46, CD80, CD86 and sialic acid) and

can grow to high titers *in vitro* and display high levels of transgene expression [332]. The adenoviral genome is also relatively easy to manipulate and traditional vectors have a cloning capacity of up to 8kb [333]. Their use in gene therapy was initially limited on account of the activation of innate immunity and pro-inflammatory responses by adenoviral proteins. An early study using adenoviral vectors resulted in the death of a volunteer as a result of a 'systemic inflammatory response' following adenoviral infection of several organs [334]. However, it is precisely this immunostimulatory potential of adenoviral vectors that makes them attractive candidates for the delivery of vaccine antigens.

The replication cycle of adenovirus is divided into an early and a late phase. The virus genome is comprised of five segments that encode early gene products, E1a, E1b, E2a, E2b, E3, and E4, two delayed early units, IX and IVa2, and a late transcriptional unit that encodes five products, L1–L5 [35]. The early genes are responsible for mainly regulatory proteins while the late phase gene products are mostly involved with capsid assembly. The early gene products of E1, E2 and E4 are essential for viral replication, while the E3 gene products modulate host immune responses [35]. Traditional adenoviral vectors, including all those used in this study, are rendered replication incompetent by deletion of E1 region genes [335]. These vectors are considered safer than replication competent vectors and also benefit from a sustained ability to present antigen on account of the reduced ability of the vector to induce cell death. The E1 region is typically replaced with an expression cassette encoding a gene of interest under the control of a constitutive

promoter, such as the human cytomegalovirus (CMV) immediate/early promoter, and a bovine growth hormone−derived polyadenylation transcription terminator. In order to increase vector capacity for foreign genes, vectors deleted of E1 and E3, or E1 and E4 genes have been developed [336,337]. E4-deleted vectors produce fewer late gene products, which reduces the induction of vector-specific immune responses [338]. Recombinant vector genomes with deletions other than E3 can only be replicated in human cells that express high levels of the deleted transcription unit proteins *in trans.* In theory replication-incompetent adenoviral vectors could recombine with wild type viruses to become replication competent, but as adenoviral-vectored vaccines are typically administered intramuscularly and natural infections occur at mucosal surfaces, it would be an extremely rare event.

The innate adjuvanting capacity of adenoviral vectors is particularly attractive to vaccine developers. Human species C adenovirus serotype 5 vectors (AdHu5) have been extensively characterised and are among the most widely used viral vectors. AdHu5 vectors are known to induce potent $CD8^+$ T cell and antibody transgene-specific responses in several animal models including nonhuman primates [335]. Indeed recombinant adenoviral vectors can efficiently prime and boost T and B cell responses [273]. Upon infection, adenovirus vector transgenes are transcribed endogenously and presented to T cells in the context of MHC class I molecules. However, adenoviral viral vectors also infect and induce the maturation of antigen presenting cells (APCs), which in turn increase cytokine production, which can enhance

antigen-specific responses. For example, adenoviral vectors are known to infect immature DCs, inducing their maturation and expression of the pro-inflammatory cytokine interleukin 12 (IL-12), which enhances antigen presentation and T cell responses [339-341]. Macrophages too can be infected, producing pro-inflammatory cytokines which further amplify immune responses [342]. Even the adenoviral capsid hexon protein is a potent adjuvant for the activation of cellular immune responses against vectored immunogens [343].

Despite demonstration as a highly effective priming agent against several pathogens including influenza, the use of AdHu5 vectors in humans has been greatly limited by widespread pre-existing anti-vector immunity which can neutralise viral vectors and transduced cells before the immune system can be primed against transgene products [336,344,345]. Among the strategies used to overcome this issue is the development of novel adenoviral vectors based on serotypes that are rare or do not circulate in human populations. These have included several species of human adenoviruses belonging to the D (Ad26, Ad28, Ad48 and Ad49) and B (Ad11, Ad35 and Ad50) serotypes and adenoviruses derived from non-human primates [346-348]. Indeed the first non-replicating chimpanzee adenoviral vector (ChAd) was developed over a decade ago [348].

Rare species adenoviral-vectors and ChAds sometimes appear less immunogenic than AdHu5 in animal models, however, this may due to subtle differences in viral receptors among species [349-351]. Interestingly vaccination

with rare species adenoviral vectors induces $CD8^+$ T cells with enhanced memory recall and overall function, especially when used in heterologous prime boost regimens [351-353]. Both rare species adenoviral vectors and ChAds have also been shown to be safe and highly immunogenic in humans [351-353]. Several recombinant ChAds such as ChAd3, ChAd63 and ChAdOx1 have shown robust immunogenicity in phase I clinical trials against pathogens such as Ebola, malaria and influenza [312,354-356]. Experiments describing novel ChAdOx1-vectored influenza vaccines are described in Chapter 7.

1.10.2. MVA

Modified Vaccinia virus Ankara (MVA) is a replication-deficient poxviral vector derived from vaccinia virus (VACV), the poxvirus used as a vaccine to eradicate smallpox [357,358]. Originally generated in an effort to develop a less reactogenic smallpox vaccine, MVA was produced by serial passage of wild-type chorioallantois vaccinia virus Ankara (CVA) through chick embryo fibroblast primary cells (CEF) [357]. During this process six major genomic deletions occurred, resulting in the loss of 26 ORFs, which amounted to approximately 15% of the viral genome [359]. As a result the virus was rendered replication incompetent in the majority of mammalian hosts, with the exception of the Syrian hamster cell line BHK-21 and the rat cell line IEC-6 (the precise molecular basis for the host-range restriction of MVA is still unknown) [360-362]. This newly attenuated strain was renamed MVA and administered to over 120,000 individuals in the 1970s as a vaccine against smallpox [358].

As a smallpox vaccine, MVA induces surprisingly high levels of immunogenicity comparable to replicating VACV [363,364]. However, it was never tested in a smallpox-endemic region and its efficacy against variola virus (VARV) remains unknown. In spite of this, these studies, and many more since, have demonstrated MVA to be safe and well-tolerated in humans, and it is currently stockpiled by the US government as a vaccine against smallpox [358].

Apart from an excellent safety profile, several characteristics of MVA are advantageous as a delivery vehicle for vaccine antigens. As with other members of the *Poxviridae* family, MVA is a large double-stranded DNA virus that replicates within the cytoplasm and as such, poses no risk of recombination into the host cell genome. Generation of recombinant MVA viral vectors is also relatively straightforward using new generation bacterial artificial chromosome (BAC) technology and antigens are easily inserted into well-defined recombination sites such as thymidine kinase (TK) gene locus [365,366]. The large genome size of MVA is particularly attractive for antigen carriage. MVA can stably integrate over 25kb of foreign DNA, which is useful for the expression of sizeable and/or multiple antigens [367]. In addition, transgenes can be placed under the control of early, immediate or late endogenous promoters, or short synthetic promoters (SSP), which can be exploited to target specific arms of the immune system [368]. For example, $CD8^+$ T cell responses against VACV seem to be directed primarily against early gene products [369-372]. The utilisation of immediate/early promoters such as F11 to control transgene expression over the traditional early/late

promoter p7.5 can improve $CD8^+$ T cell responses to transgene products [368]. The exact mechanisms behind this remain unclear but are thought to be contributed to by a 'faster ' immune response and/or the elicitation of a qualitatively different immune response by early professional APCs [373].

The immunostimulatory properties of MVA are a particularly attractive feature of this vector. Classically used for the induction of potent T cell responses, MVA has an intrinsic adjuvanting capacity and can also induce transgene-specific high titer neutralising antibodies [363,374]. Furthermore, MVA can act as an adjuvant augmenting antibody responses when co-administered with seasonal TIV [374]. The immunostimulatory potential of MVA is largely thought to be the result of the loss of several immunomodulatory genes and virulence factors, including type I and type II interferon (IFN) receptors, and CC chemokine receptors [359]. The absence of these genes, which would ordinarily contribute to viral evasion, is thought to enable the induction of stronger innate immune responses. Interestingly $CD8^+$ T cell responses induced by MVA-vectored vaccination are improved following immunisation with full length stable antigen, suggesting antigens expressed by MVA are processed and presented via MHC class I via both the endogenous pathway (where peptide is synthesised in the cytosol) and by cross-presentation (whereby exogenous antigens that are taken into the cell are diverted into the endogenous pathway) [375-377]. In clinical studies, MVA-vectored vaccines have been used safely to boost potent T cell responses against several diseases including TB, influenza, malaria, hepatitis C and Ebola [310,349,353,354,378-380]. Although MVA has been shown to boost and prime potent

cellular transgene responses, it is better at boosting than priming humoral transgene responses [273]. It is speculated that this may be due to the short burst of antigen delivered by MVA, which might be inefficient at priming B cells or because type I IFN and IL-6, both known to be essential for driving plasma cell differentiation, are inhibited by the MVA-expressed interferon resistance gene, E3L [381,382]. At present the heterologous adeno-MVA prime boost regimen is considered the most potent means to induce both T and B cell responses.

1.11. Thesis Aims

- Develop tools capable of assessing humoral immune responses against haemagglutinin and delineating anti-stem antibody responses
- Investigate alternative immune correlates of protection against influenza A
- Work towards developing vaccines capable of inducing heterosubtypic immune responses directed against the stem domain of haemagglutinin
- Work towards developing vaccines capable of simultaneously inducing heterosubtypic cellular and humoral responses against multiple influenza A antigens

1.12. Thesis Outline

- **Chapter 2** provides a description of the materials and methods used throughout the course of this study
- **Chapter 3** describes the design, production, purification and structural characterisation of recombinant haemagglutinin protein constructs which can be used in the assessment antibody responses against haemagglutinin induced by vaccination
- **Chapter 4** describes the design, construction and optimisation of a phage display library and biopanning protocol, which can be used in the assessment antibody responses against haemagglutinin induced by vaccination
- **Chapter 5** investigates circulating T_{FH}-like populations as correlates of immunity against influenza A
- **Chapter 6** investigates the induction of humoral immune responses induced by viral-vectored vaccination of stem immunogens
- **Chapter 7** investigates the induction of humoral and cellular immune responses induced by novel viral-vectored vaccines expressing multiple antigens
- **Chapter 8** summarises the findings of this thesis, draws conclusion and considers future directions

Chapter 2

Materials and Methods

2. Materials and Methods

2.1. Materials

2.1.1. Labware and Equipment

Table 2.1 Equipment and consumables used in this study

Material	Supplier	Cat. No.
0.1cm GenePulser® electroporation cuvette	BioRad	165-2083
0.2µm syringe filter	Sartorius	16534
15mL Corning® centrifuge tubes	Sigma Aldrich	FB55950
50mL Greiner centrifuge tubes	Sigma Aldrich	227261
70µm cell strainers	BD Biosciences	352350
Adhesive PCR seals	Thermo Fisher Scientific	AB-0558
Amicon Ultra-4 centrifugal filter unit with Ultracel-10 membrane	Millipore	UFC801008
Amicon Ultra-15 centrifugal filter unit with Ultracel-10 membrane	Millipore	UFC901008
Armadillo 384-well PCR plate	Thermo Fisher Scientific	AB-2384
BD Plastipak sterile syringe, Leur Slip, (1mL)	Nu-Care Products Limited	M0013
BD Plastipak sterile syringe, Leur Slip, (2mL)	Nu-Care Products Limited	M0185

BD Plastipak sterile syringe, Leur Slip, (5mL)	Nu-Care Products Limited	M2187
BD Plastipak sterile syringe, Leur Slip, (10mL)	Nu-Care Products Limited	M2188
BD Plastipak sterile syringe, Leur Slip, (20mL)	Nu-Care Products Limited	M3086
Corning® rectangular canted neck cell culture flask with vent cap	Thermo Fisher Scientific	Various
Corning® Costar® 6-well tissue culture plates	Sigma Aldrich	CLS3516
Corning® Costar® 12-well tissue culture plates	Sigma Aldrich	CLS3506
Corning® Costar® 24-well tissue culture plates	Sigma Aldrich	CLS3527
Corning® Costar® 48-well tissue culture plates	Sigma Aldrich	CLS3548
Corning® 250 mL centrifuge tubes	Sigma Aldrich	CLS430776
Corning® Costar® reagent reservoirs	Sigma Aldrich	CLS4870
Corning® Costar® Stripette® 2mL	Sigma Aldrich	CLS4486
Corning® Costar® Stripette® 5mL	Sigma Aldrich	CLS4487
Corning® Costar® Stripette® 10mL	Sigma Aldrich	CLS4488
Corning® Costar® Stripette® 25mL	Sigma Aldrich	CLS4489
Corning® Costar® Stripette® 50mL	Sigma Aldrich	CLS4490
Corning® erlenmeyer cell culture flasks	Sigma Aldrich	Various

Disposable haemocytometer	Immune Systems	BVS100
Eppendorf® safe-lock microcentrifuge tubes	Sigma Aldrich	T9661
Falcon 96-well U bottom plate	Fisher Scientific	08-772-17
Freeze 'N Squeeze DNA gel extraction spin columns	BioRad	732-6165
HisTrap™ excel, 5mL	GE Healthcare Life Sciences	17-3712-06
Inoculating loop (irradiated)	VWR International	612-9352
Micro-fine insulin syringe with 29g X 12.7mm needle (1mL)	Nu-Care Products Limited	M4891
Microlance needle (26g X 5/8 inch)	Nu-Care Products Limited	M4300
Microvette tubes (CB300K2E)	Sarstedt	16.444
MultiScreen-IP filter plate, 0.45 µm	Millipore	MAIPS4510
PARAFILM® M	Sigma Aldrich	P7793
Pasteur pipette	Thermo Fisher Scientific	FB55348
Phase lock gel light 1.5 mL	5PRIME	2302800
Nalgene™ Rapid-Flow™ sterile disposable filter units with polyethersulfone (PES) membrane	Thermo Fisher Scientific	569-0020
Nunc Maxisorp® 96-well plates	Thermo Fisher Scientific	DIS-971-030J

Nunc F96 LumiPlate white with lid	Scientific Laboratory Supplies	136101
Petri dishes	Thermo Fisher Scientific	12663575
Slide-A-Lyzer MINI Dialysis Device Kit, 10K MWCO, 0.1mL	Thermo Fisher Scientific	69576
Slide-A-Lyzer dialysis cassettes, 10K MWCO, 30mL	Thermo Fisher Scientific	66830
Spreader microbiological high impact polystyrene L-shaped	Fisher Scientific	12822775
Sterile disposable scalpels	Swann-Morton	05XX

Table 2.1 Equipment and consumables used in this study

2.1.2. Reagents

Table 2.2 List of reagents used in this study

Material	Supplier	Cat. No.
2-deoxy-galactose	Sigma Aldrich	D4407
2-deoxy-D-glucose	Sigma Aldrich	D8375
2-mercaptoethanol	Sigma Aldrich	M6250
2-(*N*-morpholino) ethanesulfonic acid	Sigma Aldrich	76039
2-propanol (isopropanol)	Sigma Aldrich	190764
4-20% Tris-HEPES Gels, 10 X 10cm, 12-well	Thermo Fisher Scientific	25244
4-nitrophenyl phosphate disodium salt hexahydrate (pNPP)	Sigma Aldrich	N2765
6X loading dye	Thermo Fisher Scientific	R0611
10mM dNTP mix	Bioline	BIO-39044
10x Tris/Glycine/SDS	BioRad	161-0732
20X Tris-HEPES-SDS Buffer	Thermo Fisher Scientific	28368
50bp DNA ladder	New England Biolabs	N3236S
50X Tris-acetate-EDTA buffer	Thermo Fisher Scientific	B49
Addavax™	InvivoGen	vac-adx-10
Any kD™ Mini-PROTEAN® TGX™ Gel	BioRad	456-9033

Agar	Sigma Aldrich	A6686
Agarose	Sigma Aldrich	A9539
Alkaline phosphatase donkey anti-mouse IgG (H+L)	Jackson ImmunoResearch	715-056-150
Alkaline phosphatase, calf intestinal (CIP)	New England Biolabs	M0290
Ammonium chloride	Sigma Aldrich	A9434
Ampicillin	Sigma Aldrich	A5354
Antarctic phosphatase	New England Biolabs	M0289S
Anti-human CD183 (BV421)	BD Biosciences	562558
Anti-human CD3 (PE-TR)	Invitrogen	MHCD0317
Anti-human CD4 (APC-H7)	BD Biosciences	560158
Anti-human CD196 (CCR6) (PE)	BD Biosciences	551773
Anti-human CD183 (APC)	BD Biosciences	550967
Anti-human CXCR5 (Alexa Fluor® 488)	BD Biosciences	558112
Anti-human CD279 (PD-1)	BD Biosciences	562516
Anti-human CD45RO (PE-Cy7)	BD Biosciences	337168
Anti-mouse anti-IgG (capture)	Mabtech	3825-3-1000
Anti-mouse IFNγ (mAB AN18)	Mabtech	3321-3-1000
Anti-mouse IFN-γ, biotinylated (mAB R4-6A2)	Mabtech	3321-6-1000
Any kD™ Mini-PROTEAN® TGX™ gel	BioRad	456-9036
AP conjugate substrate kit	BioRad	170-6432

Bacto agar	BD	214010
Benzonase® nuclease	Novagen®	70664-3
Biotaq™ DNA polymerase	Bioline	BIO-21040
Biotinylated detection anti-mouse anti-IgG antibody	Mabtech	3825-6-250
BJ5183 cells	Stratagene	200154
Bovine serum albumin (BSA)	Sigma Aldrich	A9418
Bright-Glo™ luciferase assay system	Promega	E2620
Bromophenol blue	Sigma Aldrich	B0126
Calcium chloride	Sigma Aldrich	21115
Casein in PBS 1% (w/v)	Thermo Fisher Scientific	37582
Chloramphenicol	Sigma Aldrich	C7795
Chloroform	Sigma Aldrich	C2432
Chloroform isoamyl alcohol (24:1)	Sigma Aldrich	25666
Compensation beads	BD Biosciences	552845
Coomassie blue R250	BioRad	161-0400
D-biotin	Sigma Aldrich	B4501
D-galactose	Sigma Aldrich	G0750
D-(+)-glucose	Sigma Aldrich	G5767
Diethanolamine substrate buffer (5X)	Thermo Fisher Scientific	34064
Dimethyl sulfoxide (DMSO)	Sigma Aldrich	D2650

Dithiothreitol (DTT)	Thermo Fisher Scientific	20290
Dulbecco's phosphate buffered saline (PBS)	Sigma Aldrich	D8537
Dulbecco's modified eagle medium (DMEM)	Sigma Aldrich	D6546
EndoFree plasmid mega kit	QIAGEN	12381
Endotoxin-free water	Sigma Aldrich	W3500
Ethanol	Fisher Scientific	BPE2818-500
Ethylenediaminetetraacetic acid (EDTA)	Sigma Aldrich	E7889
Expi293™ expression medium	Life Technologies	A1435101
FastPlasmid mini kit	5PRIME	2300000
Formalin solution, neutral buffered, 10%	Sigma Aldrich	HT501128-4L
FreeStyle™ 293 expression medium	Life Technologies	12338-018
Foetal calf serum (FCS)	Sigma Aldrich	F2442
Gateway® LR Clonase® II enzyme mix	Life Technologies	11791-020
Glacial acetic acid	Sigma Aldrich	1005706
Gene pulsar cuvette 0.2cm	BioRad	165-2089
GeneRuler 1kb DNA ladder	Thermo Fisher Scientific	SM0312
Glycerol	Sigma Aldrich	G5516
Glycine	Sigma Aldrich	G8898
Goat anti-mouse whole IgG alkaline phosphatase conjugate	Sigma Aldrich	A3562

HIV-1 gp140 Protein (group M, subtype CRF07_BC) (His Tag)	Sino Biological Inc	11677-V08H-5
Hydrochloric acid, 37%	Sigma Aldrich	258148
ICOS-biotin	eBioscience	13-9948-82
Imidazole	Sigma Aldrich	I2399
In-Fusion® HD cloning kit	Clontech	638909
Iscove's modified Dulbecco's medium (IMDM)	Life Technologies	12440053
IsoFlo	Oxford Veterinary Services	n/a
Kanamycin	Sigma Aldrich	K0254
KAPA2G Robust HotStart ReadyMix with dye	Kapa Biosystems	KK5704
L-glutamine solution (200mM)	Sigma Aldrich	G7513
L-leucine		
LB agar	Sigma Aldrich	L7025
LB broth	Sigma Aldrich	L7275
LIVE/DEAD® aqua	Life Technologies	L34957
Low molecular weight DNA ladder	New England Biolabs	N3233S
M9 minimal salts	Sigma Aldrich	M6030
M63 minimal salts	USBiological	C6011715

MacConkey agar (Difco)	BD Biosciences	281810
Methanol	Sigma Aldrich	32213
Minimum essential medium eagle alpha modification (αMEM)	Sigma Aldrich	M4526
Monoclonal anti-human influenza A (H1N1, H2N2) (Clone C179)	Clontech	M145
Mouse IFN-γ ELISpot kit (ALP)	Mabtech	3321-2A
NEB 5-alpha competent *E. coli* (High Efficiency)	New England Biolabs	C2987I
Neutral buffered formalin	Sigma Aldrich	HT501128
Ovalbumin (Grade VII)	Sigma Aldrich	A7641
PBS	Sigma Aldrich	D8537
PBS tablets	Life Technologies	KHO0101
Penicillin-Streptomycin	Sigma Aldrich	P0781
Penta·His antibody	QIAGEN	34660
Peptide array A/Anhui/1/2013 (H7N9) haemagglutinin (HA) protein	BEI Resources	NR-44012
Peptide Array A/Shanghai/1/2013 (H7N9) HA protein	BEI Resources	NR-44011
Phenol	Sigma Aldrich	P1037
Phenol chloroform isoamyl alcohol (25:24:1)	Sigma Aldrich	77617
Phusion® high fidelity PCR master mix	New England Biolabs	M0531

Pierce silver stain kit	Thermo Fisher Scientific	24612
Polyethylene glycol (PEG) 8000	Sigma Aldrich	P5413
Polyethylenimine (PEI)	Sigma Aldrich	408727-100ML
Potassium hydrogen carbonate	Sigma Aldrich	237205
ProSieve™ QuadColor™ protein marker, 4.6-300 kDa	Lonza	193837
Proteinase K	QIAGEN	1017738
Q5® site-directed mutagenesis kit	New England Biolabs	E0554S
QIAGEN EndoFree® plasmid kit	QIAGEN	Various
QIAGEN plasmid *plus* kit	QIAGEN	Various
QIAGEN QIAprep® spin miniprep kit	QIAGEN	27104
QIAquick gel extraction kit	QIAGEN	28704
Quick Ligation™ kit	New England Biolabs	M2200S
Recombinant H1 HA protein A/California/04/2009 (H1N1)	BEI Resources	NR-13691
Recombinant H5 HA protein A/Vietnam/1203/2004 (H5N1)	BEI Resources	NR-10510
Recombinant H7 HA protein A/Netherlands/219/2003 (H7N7)	BEI Resources	NR-2633

Restriction endonucleases	New England Biolabs	Various
RPMI-1640	Sigma Aldrich	R0883
S·Tag™ monoclonal antibody	Novagen®	71549-3
SIGMA *FAST*™ BCIP/NBT	Sigma Aldrich	B5655-TAB
Smart Ladder DNA marker	Eurogentec Ltd	MW-1700-10
Sodium acetate buffer solution pH5.2	Sigma Aldrich	S7899
Sodium azide	Sigma Aldrich	S2002
Sodium bicarbonate	Sigma Aldrich	S6014
Sodium carbonate	Sigma Aldrich	223484
Sodium chloride	Sigma Aldrich	S9888
Sodium dodecyl sulphate (SDS)	Sigma Aldrich	L4390
Sodium hydroxide pellets	Sigma Aldrich	221465
Sodium phosphate	Sigma Aldrich	342483
Streptavidin-ALP	Mabtech	3310-8
Streptavidin-PerCP	BD Biosciences	340130
Sucrose	Fluka	84097
Super Optimal Culture (SOC) medium	Life Technologies	1554-034
Swine H1N1 Haemagglutinin Antibody	Aviva Systems Biology	OAPB01365
SYBR Safe in DMSO	Life Technologies	S33102
T4 DNA ligase	New England Biolabs	M0202S
T7 Select 10-3 kit	Millipore	70550

Trans-Blot® Turbo™ mini PVDF transfer packs	BioRad	170-4156
Trans-Blot® Turbo™ midi PVDF transfer packs	BioRad	170-4157
Trizma® HCl buffer solution (pH 7.8)	Sigma Aldrich	T2569
Trizma® HCl buffer solution (pH 8)	Sigma Aldrich	T2564
Triton™ X-100	Sigma Aldrich	X100
Trypan blue	Sigma Aldrich	T8154
TrypLE™ express	Life Technologies	12605010
Tween® 20	Sigma Aldrich	P1379
Water, molecular biology grade	Fisher Scientific	7732-18-5
Zero blunt TOPO® PCR cloning kit	Life Technologies	45-0245

Table 2.2 List of reagents used in this study

2.1.3. Solutions

Table 2.3 Description of solutions used in this study

Buffer	pH	Ingredients
6X sample buffer (laemmli buffer)	6.8	1.5% SDS 10% glycerol 62.5mM Tris-HCl 0.0025% bromophenol blue 2% DTT or 2-mercaptoethanol
Ammonium-chloride-potassium (ACK) lysis buffer	7.2-7.4	0.15M NH_4CL 1mM $KHCO_3$ 0.1mM Na_2EDTA
Coating buffer	7.2-7.4	15mM Na_2CO_3 35mM $NaHCO_3$
Coomassie stain	n/a	0.1% coomassie blue R250 50% methanol 10% glacial acetic acid
Destain solution	n/a	40% methanol 10% glacial acetic acid
Fixing solution	n/a	50% methanol 10% glacial acetic acid
Elution buffer	7.4	20mM Na_3PO_4 0.5M NaCl 500mM imidazole
Equilibration buffer	7.4	20mM Na_3PO_4 0.5M NaCl

FACS buffer	7.4	1% BSA 1mM EDTA 0.1% sodium azide
PBS/T	7.4	1X PBS (0.01M PBS) 0.05% (v/v) Tween® 20
Phage extraction buffer (PEB)	8	20mM Tris-HCl 100mM NaCl 6mM $MgSO_4$
Tris-EDTA (TE)	8	10mM Tris-Cl 1mM EDTA
Wash buffer	7.4	20mM Na_3PO_4 0.5M NaCl 30mM imidazole

Table 2.3 Description of solutions used in this study

2.1.4. Bacterial Growth Media

Table 2.4 Description of bacterial growth media used in this study

Media	**pH**	**Ingredients**
M9LB	7.0-7.1	LB broth/agar supplemented with: 1X M9 salts 20% glucose 0.1M $MgSO_4$

Table 2.4 Description of bacterial growth media used in this study

2.1.5. Cell Culture Media

Table 2.5 Description of cell culture media used in this study

Buffer	pH	Ingredients
Complete αMEM	7.2-7.4	αMEM supplemented with: 2mM L-glutamine 10% FCS 100U/mL penicillin 0.1mg streptomycin
Complete DMEM	7.2-7.4	DMEM supplemented with: 2mM L-glutamine 10% FCS 100U/mL penicillin 0.1mg streptomycin
Complete Iscove's	7.2-7.4	Iscove's supplemented with: 2mM L-glutamine 10% FCS 100U/mL penicillin 0.1mg streptomycin
Expi293™ expression medium	7.2-7.4	No supplements
FreeStyle™ 293 expression medium	7.2-7.4	No supplements

R10	7.2-7.4	RPMI-1640 supplemented with: 2mM L-glutamine 10% FCS 100U/mL penicillin 0.1mg streptomycin

Table 2.5 Description of cell culture media used in this study

2.1.6. Cell Lines

293T/17 cells were received as a gift from Dr Nigel Temperton (Viral Pseudotype Unit, Medway School of Pharmacy, University of Kent) and were maintained in DMEM supplemented with 15% FCS, 100U/mL penicillin and 0.1mg streptomycin.

FreeStyle™ 293-F cells were purchased from Life Technologies and initially cultured in FreeStyle™293 expression medium. They were later adapted and maintained in Expi293™ expression medium.

All cell lines were cultured at 37°C, 5% CO_2.

2.1.7. Viral-Vectored Vaccines

Table 2.6 Description of the viral-vectored vaccines used in this study

Stock number	Vector	Antigen	Promoter
1128	AdHu5	H1HA (A/Texas/05/2009)	CMV immediate/early
1328	AdHu5	Headless-H1HA (A/Texas/05/2009)	CMV immediate/early
1896	AdHu5	H1HA-Stem+TM (A/Texas/05/2009)	CMV immediate/early
1895	AdHu5	H1HA-Stem (A/Texas/05/2009)	CMV immediate/early
Clinical vial	ChAdOx1	NP+M1 (A/Panama/2007/99)	CMV immediate/early
1296, 1308	ChAdOx1	H5HA (A/Vietnam/1203/2004)	CMV immediate/early
1413	ChAdOx1	H7HA (A/Netherlands/219/2003)	CMV immediate/early
1369	ChAdOx1	NP+M1 (A/Panama/2007/99)	CMV immediate/early
1187	MVA	H1HA (A/Texas/05/2009)	mH5 early
1297	MVA	H5HA (A/Vietnam/1203/2004)	P7.5 early/late

1355	MVA	H7HA (A/Netherlands/219/2003)	P7.5 early/late
1181	MVA	Headless-H1HA (A/Texas/05/2009)	mH5 early
1327	MVA	NP+M1 (A/Panama/2007/99)	P7.5 early/late
1388	MVA	NP+M1 (A/Panama/2007/99)	F11 immediate/early
1422	MVA	NP+M1, H5HA (A/Panama/2007/99), (A/Vietnam/1203/2004)	NP+M1: F11 immediate/early, H5HA: p7.5 early/late
1423	MVA	NP+M1, H7HA (A/Panama/2007/99), (A/Netherlands/219/2003)	NP+M1: F11 immediate/early, H7HA: p7.5 early/late

Table 2.6 Description of the viral-vectored vaccines used in this study

2.2. General Molecular Biology Methods

2.2.1. Bacterial Transformation

2.2.1.1. Heat-Shock

50µL NEB 5-alpha competent *E. coli* (High Efficiency) were thawed on ice and mixed with 50-100ng DNA in a 1-5µL volume. Cells were rested on ice for 30min before being heat shocked at 42°C for 30-45s and returned to ice immediately for 5min. 500µL SOC media was added to the cells and they were incubated at 37°C, 220rpm for 1h. 50µL aliquots of serially diluted cells were plated on selective agar plates and incubated at 37°C overnight.

2.2.1.2. Electroporation

A single colony from a fresh plate of the strain to be made electrocompetent (BJ5185, DH10B™) was used to inoculate a 2mL LB starter culture which was incubated for 12-16h overnight at 37°C, 220rpm. The overnight culture was diluted 1:1,000 and used to inoculate a larger volume of LB, which was grown until cells had an optical density (OD) of 0.6 at 600nm (OD_{600}). The culture was cooled on ice for 30min and kept ice cold from this point onwards. Cells were washed three times by centrifugation for 5min at 0°C, 5,000rpm and the pellet was resuspended in 10mL ice-cold water. After the final wash cells were resuspended in 50µL ice-cold water and transferred to a pre-cooled electroporation cuvette (0.1cm) with 50-100ng DNA in a 1-5µL volume. Cells were electroporated at 1.8kV, 25µF, 200Ω using a BioRad GenePulser and returned to ice. 500µL SOC media was added immediately to the cells and they were incubated at 37°C, 220rpm for 1h. 50-100µL

aliquots of serially diluted cells were plated on selective agar plates and incubated at 37°C overnight

2.2.2. Glycerol Stock Preparation

Single isolated colonies were used to inoculate 2mL LB starter cultures which were incubated for 12-16h overnight @ 37°C, 220rpm. 500µL overnight culture was added to 500µL sterile 50% glycerol in a 2 mL screw top tube and mixed gently. The glycerol stock was placed at -80°C for long-term storage. Plasmid DNA was extracted from 1mL of the remaining starter culture using a QIAGEN QIAprep® spin miniprep kit (section 2.2.3) and sent for sequence confirmation (section 2.2.7).

2.2.3. Plasmid DNA Purification

Plasmid DNA was extracted from overnight cultures using QIAGEN QIAprep® spin miniprep kit, QIAGEN plasmid *plus* midi and maxi kits or QIAGEN EndoFree® plasmid maxi and mega kits according to manufacturer's protocol.

2.2.4. Bacterial Artificial Chromosome Purification

Bacterial artificial chromosomal (BAC) DNA was extracted from overnight cultures using the QIAGEN plasmid maxi kit according to the manufacturer's protocol with the exception of using double the recommended volumes of buffers P1, P2 and P3.

2.2.5. High Fidelity Polymerase Chain Reaction

Phusion® high fidelity PCR master mix or Q5® high fidelity DNA polymerase was used to amplify selected gene fragments for cloning and sequencing applications where sequence accuracy was necessary. 50µL reactions were set up as follows:

a) 25µL 2X phusion® HF master mix (1X final conc.)
2.5µL 10mM forward primer (0.5µM final conc.)
2.5µL 10mM reverse primer (0.5µM final conc.)
XµL (1-10ng) template DNA
XµL molecular biology grade H_2O
∑ = 50µL

b) 10µL 5X Q5 reaction buffer (1x final conc.)
1µL 10mM dNTPs (200µM final conc.)
2.5µL 10mM forward primer (0.5µM final conc.)
2.5µL 10mM reverse primer (0.5µM final conc.)
XµL (1-10ng) template DNA
0.5µL Q5® HF DNA polymerase (0.02U/mL)
XµL molecular Biology Grade H_2O
∑ = 50µL

PCR was performed using a BioRad thermal cycler using the following programme:

1x	**Initial denaturation**	**98°C**	**5min**
25-35X	**Denaturation**	**98°C**	**30s**
	Annealing	**55-72°C**	**15-30s**
	Extension	**68-72°C**	**30s/kb**
	Final extension	**72°C**	**5-10min**

Elongation times were calculated according to the length of the amplicon (New England Biolabs (NEB) recommend 15-30s/kb). PCR products were purified using the QIAquick PCR purification kit according to manufacturer's protocol and resuspended in molecular grade water or TE buffer.

2.2.6. Site-Directed Mutagenesis

Site-specific mutagenesis to substitute, insert or delete amino acids was performed using a Q5® Site-Directed Mutagenesis Kit according to manufacturer's instructions. Primers were designed using primer design software at www.NEBaseChanger.neb.com.

2.2.7. Colony PCR Screening

Single bacterial colonies were picked and resuspended in a PCR tube containing 10µL molecular biology grade water. A reference plate was then streaked with the tip. The bacterial suspension was incubated at 98°C for

15min to lyse bacteria. Once cooled, 25µL PCR reactions were set up using KAPA2G Robust HotStart ReadyMix with dye as follows:

12.5µL 2X KAPA2G Robust HotStart ReadyMix	**(1X final conc.)**
1.25µL 10mM forward primer	**(0.5µM final conc.)**
1.25µL 10mM reverse primer	**(0.5µM final conc.)**
2µL template DNA	
3µL molecular biology grade H_2O	

PCR was performed using a BioRad Thermal Cycler as previously described (section 2.2.5) using elongation times of 15s for targets ≤ 1kb or 30-60s/kb for longer fragments.

2.2.8. DNA Sequencing

Samples were sent to Source BioScience (Oxford and Nottingham) for sequencing.

2.2.9. DNA Restriction Digest

Restriction endonucleases were obtained from NEB. Digests were incubated at 37°C for 2h in appropriate enzyme-specific reaction buffer. For standard digests 50µL reactions were set up as follows:

XµL NEB restriction endonuclease	**(10-20U final conc.)**
5µL 10X NEB buffer	**(1X final conc.)**
0.5-1µg template DNA	
XµL molecular biology grade H_2O	
_____	
∑ = 50µL	

Double digests, where applicable, were performed using 10-20U of each enzyme. Following digestion, enzymes were either heat inactivated by incubation at 65-80°C for 20min or removed by spin column purification or phenol-chloroform extraction.

2.2.10. Agarose Gel Electrophoresis

PCR products were separated according to size by 0.7-2% agarose gel electrophoresis (100V, 60min or 120V, 45min) in 1x TAE buffer, stained with SYBR Safe and visualised under a UVP transilluminator. DNA fragment size was estimated by comparison to a DNA ladder. Fragments required for downstream applications were purified using the QIAGEN MiniElute DNA purification kit or BioRad Freeze n' Squeeze DNA gel extraction spin columns according to the manufacturer's protocol.

2.2.11. Phenol Chloroform DNA Extraction

Large DNA molecules or samples unsuitable for purification using the QIAGEN QIAquick PCR purification kit were purified by phenol chloroform extraction. An equal volume of phenol was added to the DNA mixture and

mixed by inversion. The mixture was centrifuged at 13,000g for 10min at room temperature (25°C) in a phase lock gel light tube. The aqueous layer was removed, added to an equal volume of phenol chloroform isoamyl alcohol (25:24:1) and mixed by inversion. The mixture was centrifuged at 13,000g for 10min at room temperature (25°C) in a phase lock gel light tube. The aqueous layer was again removed, added to an equal volume of chloroform isoamyl alcohol (24:1) and mixed by inversion. The mixture was centrifuged at 13,000g for 10min at 4°C in a fresh phase lock gel light tube. The aqueous layer containing the purified DNA was removed and concentrated by ethanol precipitation.

2.2.12. Ethanol Precipitation of DNA

Sodium acetate pH5.2 was added to a solution of DNA making a final concentration of 0.3M. 2.5 times the solution volume of ice-cold 100% ethanol or an equal volume of room temperature isopropanol was added and mixed by inversion. The sample was placed at -80°C for 15min-1h. Precipitated DNA was pelleted by centrifugation at 13,000g for 15min-1h at 4°C. The supernatant was discarded and the pellet was washed 1-3 times in ice-cold 70% ethanol by centrifugation at 13,000g for 15min at 4°C. The supernatant was discarded and the pellet allowed to dry at room temperature before being resuspended in an appropriate volume of molecular grade water or TE buffer. DNA concentration and purity was estimated using a NanoDrop™ 8000 spectrophotometer.

2.2.13. DNA Ligation

T4 DNA ligase or Quick T4 DNA ligase was used to join cohesive or blunt end molecules of double stranded DNA together. Vector to insert ratios were determined using the online NEBio™ calculator (http://www.nebiocalculator.neb.com/#!/). Generally ligations were tested at 1:3, 1:1, and 3:1 vector:insert molar ratios. Standard 10µL reactions were set up as follows:

a) T4 DNA Ligase

1µL 10X T4 DNA ligase buffer	**(1X final conc.)**
XµL vector DNA	**(1X final conc.)**
XµL insert DNA	
0.5µL T4 DNA ligase	**(400U final conc.)**
XµL molecular biology grade H_2O	
_____	
∑ = 10µL	

Reactions were incubated overnight at 16°C and stored at 4°C for up to one week.

Quick ligation 20µL reactions were set up as follows:

b) Quick T4 DNA Ligase

50ng vector DNA	
3-fold molar excess of insert DNA	
+10µL 2X T4 DNA ligase buffer	**(1X final conc.)**
+1µL quick T4 DNA ligase	**(2,000U final conc.)**
∑ = 10µL	

Reactions were incubated at room temperature (25°C) for 5min and stored at -20°C.

2.2.14. TOPO® Blunt-End Cloning

Cloning PCR products into TOPO vectors can assist downstream restriction digest of ligated products and facilitate subcloning. 6µL reactions were set up as follows:

0.4-5µL fresh PCR products
1µL salt solution
1µL pCR®II-Blunt-TOPO®
XµL molecular biology grade H_2O
∑ = 6µL

The reaction was incubated at room temperature for 5-30min and 3µL was transformed into NEB 5-alpha competent *E. coli* (High Efficiency).

2.2.15. In-Fusion® HD Cloning

The In-Fusion® HD cloning kit was used to directionally join fragments of DNA together at any location in a single reaction. The In-Fusion enzyme fuses PCR-generated sequences and linearised vectors by recognising a 5' 15bp sequence at the ends of the PCR fragments which are complimentary to the ends of the vector.10µL reactions were set up as follows:

2µL 5X In-Fusion HD enzyme premix

XµL linearised Vector

XµL purified PCR Fragment

XµL molecular biology grade H_2O

∑ = 10µL

The optimal amount of vector and insert DNA to use in the In-Fusion reaction was calculated using the online In-Fusion® molar ratio calculator (http://www.bioinfo.clontech.com/infusion/molarRatio.do).

2.3. Construction of a T7 Phage Display Library

Phage display is a powerful technique suitable for high throughput identification of high affinity protein-protein or protein-peptide interactions. The T7 Select10-3b vector (Merck Millipore) accommodates peptides or proteins up to 1,200 amino acids in size at mid copy number (5-15 per phage). This system exploits the capacity of the T7 capsid shell to naturally accommodate variation in a region of the 10B capsid protein displayed on the surface of the phage, making it an attractive display vector.

2.3.1. Production of T7 Clones

The T7Select® 10-3 cloning kit includes the T7Select® 10-3 vector as prepared EcoRI/HindIII arms, ready for directional cloning of appropriately prepared inserts. 5µL ligation reactions were set up with 1:3 molar ratios of vector:insert as follows:

0-1.5µL insert	**(0.02-0.06pmol)**
1µL T7Select® vector arms	**(0.5µg;0.02pmol)**
0.5µL 10X ligase buffer	
0.5µL 10mM ATP	**(1mM final conc.)**
0.5µL 100mM DTT	**(10mM final conc.)**
1µL T7 DNA ligase	**(400U final conc.)**
XµL molecular biology grade H_2O	
∑ = 5µL	

Reactions were mixed by gentle pipetting and incubated at 16°C for 16h.

2.3.1.1. T7 in vitro Packaging and Plaque Assay

1µL T7 ligation reactions were added directly to 5µL T7 Packaging Extracts (thawed on ice) for *in vitro* packaging. The reaction was mixed by gentle stirring with a pipette tip, incubated at room temperature for 2h and stopped by addition of 294µL sterile LB.

2.3.1.2. T7 Titration

The number of recombinants generated was determined by plaque assay. Briefly, 200µL BLT5403 *E.coli* cell starter culture was inoculated into 20mL M9LB and incubated for approximately 4 hours at 37°C, 220rpm until reaching an OD_{600} of 1.0. Dilutions of recombinant phage ranging from 10^{-3}-10^{-6} were made with sterile LB. 100µL diluted phage was added to 250µL host cells and 5mL molten top agarose (45-50°C) was added. The phage/cell mixture was immediately plated onto an LB (ampicillin 100µg/mL or carbenicillin 100µg/mL) plate. Plates were incubated at 37°C for 5-6h or overnight at room temperature. Phage titer, described in plaque-forming units (pfu) per unit volume is the number of plaques on the plate times the dilution times 10 (to account for the 0.1 ml of dilution plated).

2.3.1.3. T7 Amplification and Purification

A ratio of $1x10^6$ phage per 10mL cells was distributed as 1mL aliquots into sterile 15mL tubes. 10mL molten top agarose (45-50°C) was added and immediately poured onto LB (ampicillin 100µg/mL or carbenicillin 100µg/mL)

plates and incubated as outlined previously. Phage were eluted by covering each plate with 10mL phage extraction buffer and incubating at 4°C overnight. Amplified phage were harvested by pipetting into sterile tubes. To clarify the lysate 0.5mL chloroform was added and mixed gently by inversion before centrifuging at 3,000rpm. The supernatant was recovered and the process repeated again. 1/10th volume 5M NaCl was added followed by 1/6th volume 50% sterile PEG8000 and the solution was immediately vortexed for 30s. Phage were precipitated on ice overnight at 4°C and pelleted by centrifugation at 9,000rpm for 15min at 4°C. The supernatant was discarded and the pellet air-dried thoroughly before resuspending in 1.2mL 1M NaCl TE buffer. This was further centrifuged at 14,000rpm for 10min and the supernatant diluted to 10mL in phage extraction buffer and filtered through a 0.2µm filter. Titres were determined at 10^{-7}-10^{-10} dilutions as previously described (section 2.3.1.2)

2.4. Viral Vector Production

2.4.1. Recombinant Adenovirus Generation

Traditionally, two methods have been used to generate recombinant adenoviruses – direct ligation of the gene of interest into the adenoviral genome or cloning the gene of interest into a shuttle vector (which can propagate in two different host species) and transferring the gene of interest into the adenovirus genome by homologous recombination in an appropriate adenovirus packaging cell line. As the adenovirus genome is very large (~37kB) the former method is technically very challenging and the latter approach was taken in this study.

2.4.1.1. Restriction Cloning of Adenovirus Shuttle Vector

Antigen DNA sequences (cH16/H1, H1HA-Stem and H1HA-Stem+TM) were synthesised by GeneArt® (Invitrogen) with 5' KpnI and 3' NotI restriction endonuclease sites for subcloning into Invitrogen Gateway® entry vectors. Sequences were synthesised using human-preferred codons and no construct contained the vaccinia virus early gene transcription termination signal 5'-TTTTTNT-3'. Entry clones were excised from existing plasmids by restriction digest (section 2.2.8) and ligated into the pENTR4-Mono entry vector (p2022) previously cut with the same restriction enzymes (section 2.2.12). The pENTR4-Mono vector contains an intron-less non-splicing version of the human cytomegalovirus (CMV) immediate/early promoter and a bovine growth hormone−derived polyadenylation transcription terminator. The ligated product was transformed into NEB 5-alpha competent *E. coli* (section 2.2.1). Single isolated colonies were screened by colony PCR

(section 2.2.6) and positive clones were used to inoculate 2mL starter cultures (50 mg/ml kanamycin) which were incubated for 12-16h overnight @ 37°C, 220rpm. Plasmid DNA was extracted using a QIAGEN QIAprep® Spin miniprep kit (section 2.2.3) and sent for sequencing (section 2.2.7). 500µL was used to make a glycerol stock (section 2.2.2). The glycerol stock of a sequence confirmed clone was used to inoculate 100mL cultures and plasmid DNA was extracted and using a QIAGEN plasmid *plus* midi kit (section 2.2.3).

2.4.1.2. Generation of Recombinant Adenovirus Vectors Using Gateway Technology™

Gateway® cloning technology, used to generate the recombinant adenovirus clones in this study, is based on the site-specific recombination properties of bacteriophage lambda. A proprietary enzyme, Gateway® LR Clonase® II, mediates site-specific recombination between the left (*attL*) and right (*attR*) attachment sites within an entry and destination vector respectively. This directionally inserts vaccine antigens at the E1 locus.

10µL reactions were set up with Gateway® LR Clonase® II, the pENTR4-Mono vector (containing a specific antigen) and the pAd/PL Dest destination vector (p664, containing the adenovirus genome) as follows:

1µL entry vector	**(150ng/µL)**
1µL destination vector	**(150ng/µL)**
6µL TE buffer pH8.0	
2µL Gateway® LR Clonase® II enzyme mix	

Reactions were incubated for 5h or overnight at room temperature and treated with 1µL proteinase K (2 µg/µL) for 10min at 37°C. 3µL of the recombination products was transformed into NEB 5-alpha competent *E. coli* (section 2.2.1). Recombinant colonies were screened by PCR and sent for sequencing (sections 2.2.6, 2.2.3 and 2.2.7). Integrity of the adenovirus backbone was tested by restriction digest (section 2.2.8). Glycerol stocks were used to inoculate 100mL cultures and plasmid DNA was extracted using a QIAGEN Plasmid *Plus* Midi kit (section 2.2.2 and 2.2.3). Extracted shuttle vector DNA was sent to the Jenner Institute Viral Vector Core Facility for production and purification (Appendix I-VII).

2.4.1.3. ChAdOx1 NP+M1

The ChAdOx1 NP+M1 vaccine was previously produced at the Jenner institute [312]. The fusion antigen NP+M1 is inserted at the E1 locus of the ChAdOx1 genome and expression is driven by the human cytomegalovirus (CMV) immediate/early promoter (section 2.1.7).

2.4.1.4. ChAdOx1-H7

The ChAdOx1-H7 vaccine was previously produced at the Jenner institute by Dr Senthil Chinnakannan. The HA antigen, H7HA from

A/Netherlands/219/2003 (H7N7), is inserted at the E1 locus of the ChAdOx1 genome and expression is driven by the human CMV immediate/early promoter (section 2.1.7).

2.4.2. Recombinant MVA Generation

The process of recombinant MVA generation differs from that of adenoviruses. Linearised MVA shuttle DNA can be co-transfected directly into an appropriate cell line with MVA expressing red fluorescent protein (RFP) and the two viruses recombine. Initially Green Fluorescent Protein (GFP) replaces RFP at the TK locus. As GFP in the shuttle vector pMVA-GFP-TD is outside TKL and TKR, selection is transient-dominant. Initially viruses are selected based on GFP expression but in subsequent rounds of purification the recombination event resolves and the GFP is excluded.

2.4.2.1. Restriction Cloning of MVA Shuttle Vector

Antigen DNA sequences (cH16/H1, H1HA-Stem and H1HA-Stem+TM) were synthesised by GeneArt® (Invitrogen) to contain 5' KpnI and 3' NotI restriction endonuclease sites. Sequences were synthesised using human-preferred codons and no construct contained the vaccinia virus early gene transcription termination signal 5'-TTTTTNT-3'. Entry clones were excised from existing plasmids by restriction digest (section 2.2.8) and ligated into the vector backbone of shuttle vector pMVA-GFP-TD (p856) previously cut with the same restriction enzymes and gel extracted (sections 2.2.8, 2.2.9, and 2.2.12).

3µL of the ligation products was transformed into NEB 5-alpha competent *E. coli* (section 2.2.1). Recombinant colonies were screened and sent for sequencing (sections 2.2.6, 2.2.3 and 2.2.7). Glycerol stocks were used to inoculate 100mL cultures and plasmid DNA was extracted and using a QIAGEN Plasmid *Plus* Midi kit (section 2.2.2 and 2.2.3). Extracted shuttle vector DNA was sent to the Jenner Institute Viral Vector Core Facility for production and purification (Appendix VIII-XV).

2.4.2.2. MVA-NP+M1

MVA-NP+M1 was previously produced at the Jenner Institute [310]. The prototype version of this fusion antigen NP+M1 is expressed from the early/late vaccinia P7.5 promoter inserted at the thymidine kinase locus of MVA and consists of the complete sequences of NP and M1 from A/Panama/2007/99 (H3N2) joined by a 7 amino acid linker (section 2.1.7) [310]. A later version produced by Dr Naif Alharbi expresses NP+M1 from the immediate/early vaccinia F11 promoter and inserted at the F11 locus.

2.4.2.3. MVA-NP+M1-HA

The bivalent vaccines MVA-NP+M1-H5 and MVA-NP+M1-H7 were previously produced at the Jenner Institute by Dr Senthil Chinnakannan. In these constructs the fusion antigen NP+M1 is expressed from the immediate/early vaccinia F11 promoter and the HA antigen (H5HA from A/Vietnam/1203/2004 (H5N1) or H7HA from A/Netherlands/219/2003 (H7N7)) is expressed from the early/late vaccinia P7.5 promoter (section 2.1.7).

2.5. Cell Culture Techniques

2.5.1. Cell Line Subculture

2.5.1.1. Suspension Cell Lines

Cell viability and density was firstly estimated (section 2.5.2). Suspension cell lines were subcultured by seeding an appropriate number of cells into fresh pre-warmed media in an erlenmeyer cell culture flask. Cells were incubated at 37°C, 5% CO_2 in an orbital shaker platform rotating at 125 rpm.

2.5.1.2. Adherent Cell Lines

Adherent cell lines were first brought into suspension using TrypLE™ express. Spent medium was removed and the cell monolayer was rinsed with 2mL sterile PBS or TrypLE™ express (trypsin). Dead cells were removed and a volume of TrypLE™ express (1ml per 25cm^2 of flask surface area) was added to the cells and incubated at 37°C for 5min. Detached cells were resuspended in a volume of complete media equal or greater to the volume of TrypLE™ express added, in order to inactivate the trypsin. Cell viability and density was estimated (section 2.5.2) and cells were subcultured by seeding a new flask containing pre-warmed media with the required number of cells. Cells were incubated at 37°C, 5% CO_2.

2.5.2. Determination of Cell Viability and Density

Adherent cell lines were first brought into suspension using TrypLE™ express (2.5.1.2). 20µL cell suspension was removed and mixed with an equal volume of trypan blue. A sample of this was used to fill the counting chamber of a disposable haemocytomer, which was viewed under an inverted phase

contrast microscope using X20 magnification. Full squares were counted and cells on the top and left hand border of squares were included in counts for a particular square. Viable cells appeared bright and non-viable cells stained blue. At least 100 cells were counted per estimation. Concentrations of cells and viability were counted according to the following equations:

$$\text{Cell Count} = \frac{\text{No. of live cells}}{\text{No. of squares counted}} \times 2 \times 10{,}000$$

$$\text{Percentage Viability} = \frac{\text{No. of live cells}}{\text{Total no. of cell counted}} \times 100$$

2.5.3. Resuscitation of Frozen Cells

A frozen vial of cells was thawed rapidly by swirling in a 37°C water bath. The vial was wiped with 70% ethanol before transfer to a laminar flow hood. Vial contents were pipetted drop-wise into 5mL pre-warmed complete growth media appropriate for the cell line. Cell density and viability was estimated using a haemocytometer and trypan blue (section 2.5.2). An appropriate volume of cell suspension was transferred to a flask to achieve the cell seeding density recommended for the cell line. A pre-centrifugation step to remove cryoprotectant was not necessary for the cell lines used in this study.

2.5.4. Cryopreservation of Cells

Cell viability and density was firstly estimated (section 2.5.2). Cells were centrifuged at 1,350rpm for 5min and resuspended in freeze medium (70%

basal medium, 20% FCS, 10% DMSO) at a concentration of $1X10^7$ cells/mL and transferred into cryoprotectant vials. Vials were put in a Mr Frosty and transferred to a -80°C freezer before transfer to liquid nitrogen the following day.

2.6. Recombinant Protein Production

2.6.1. Adaptation of FreeStyle™ 293-F cells to Expi293™ expression medium

A frozen vial of FreeStyle™ 293-F cells was thawed rapidly (section 2.5.1) and transferred to into a 125mL erlenmeyer cell culture flask containing 29mL pre-warmed FreeStyle™ 293 expression medium. Cells were incubated at 37°C, 5% CO_2, 125rpm in an incubator protected from light. 24h post-thaw cell density and viability was monitored using a haemocytometer and trypan blue. Generally if viability was below 60% a new vial was thawed. Cells were subcultured by seeding $0.3X10^6$ cells/mL into fresh pre-warmed FreeStyle™ 293 expression medium and cell density and viability was monitored daily. When the culture reached $>2X10^6$ cells/mL (3-4 days), cells were passaged by seeding $0.6X10^6$ cells/mL into 10mL Expi293™ expression medium and 20mL FreeStyle™ 293 expression medium. When this culture reached $>3X10^6$ cells/mL (3-4 days), cell were passaged by seeding $0.5X10^6$ cells/mL into 20mL Expi293™ expression medium and 10mL FreeStyle™ 293 expression medium. When this culture reached $>3X10^6$ cells/mL (3-4 days), cells were passaged by seeding $0.6X10^6$ cells/mL into 30mL Expi293™ expression medium. Cells were subcultured for two more passages at $0.3X10^6$ cells/mL before cryopreservation (section 2.5.4) or use in transfection (section 2.6.2.1).

2.6.2. Protein Production in HEK 293 Cells

2.6.2.1. Expression Vector

DNA sequences for recombinant proteins (H1HA, H7HA, cH9/H1, cH16/H1, ΔStem-H1HA, Headless-H1HA and H1HA-Stem) were synthesised by GeneArt® (Invitrogen) to contain 5' NotI and 3' KpnI restriction endonuclease sites for cloning into the cytomegalovirus/human T-cell leukaemia virus type 1 repetitive sequence expression vector (pCMV/R), for efficient expression in mammalian cells [383]. All constructs were synthesised using human-preferred codons.

2.6.2.2. Transient Transfection

A frozen vial of Expi293™ expression medium-adapted FreeStyle™ 293-F cells was thawed rapidly and transferred to into a 125mL erlenmeyer cell culture flask containing 29mL pre-warmed Expi293™ expression medium. Cell density and viability was monitored immediately post-thaw using a haemocytometer and trypan blue (section 2.5.2). Cells were incubated at 37°C, 5% CO_2, 125rpm in an incubator protected from light. 24h post-thaw and for 2-4 days thereafter, cell density and viability was monitored. When cells reached a density of ≥1X10^6 cells/mL and were ≥90% viable they were subcultured for two more passages.

24h before transfection, cells were seeded at 1X10^6 cells/mL. Immediately prior to transfection cell density and viability was recorded and a pre-transfection sample taken. A mixture of DNA (66μg per 100mL culture; 5% GFP reporter plasmid) and Expi293™ expression medium (4mL per 100mL

culture) was prepared. Polyethylenimine (PEI; 2µg/mL final concentration) was added drop-wise to the DNA mixture and vortexed well for 1min. DNA complexes were allowed to form by incubation at room temperature for 10min. Cells were transfected by adding the DNA:PEI complexes drop-wise to flasks while swirling, and flasks were immediately returned to the incubator. Cell viability was monitored by microscopy (section 2.5.2) and samples were taken pre-transfection and every 24 hours post-transfection to analyse protein expression by SDS-PAGE (section 2.6.3). Transfection efficiency was estimated by measuring GFP expression using a Leica DM IL microscope.

2.6.2.3. Polyhistidine-Tagged Protein Purification

At 96 hours post transfection or when cell viability dropped below 80% cells were harvested by centrifugation at 1,000g for 10min at 4°C. The supernatant was vacuum-filtered using a Nalgene™ Rapid-Flow™ sterile disposable filter unit with an asymmetric polyethersulfone (PES) membrane and stored on ice thereafter. A proteinase inhibitor cocktail was added and a sample was taken for gel analysis.

Polyhistidine-tagged recombinant proteins were purified by affinity chromatography using a HisTrap™ excel column according to manufacturer's instructions and samples were taken from eluted fractions for gel analysis (section 2.6.3). Fractions containing recombinant protein were pooled and imidazole from the elution buffer was removed by dialysis against 5L PBS for 2h at 4°C with stirring using a Slide-A-Lyzer dialysis cassette. The dialysate

buffer was changed and the sample was dialysed overnight as previously described. The following day the dialysate buffer was removed and the sample dialysed for a further two 2h intervals. The protein sample was removed and filtered though a 0.2µm syringe filter to remove any precipitated protein. The sample was centrifuged at 13,000rpm for 1h at 4°C to further remove any precipitated protein and the supernatant was concentrated using an Amicon Ultra centrifugal filter unit according to manufacturer's instructions. The concentrated protein sample was distributed into clean eppendorfs in 20-50µL aliquots and flash-frozen in liquid nitrogen. Samples were placed at -80°C for long-term storage.

2.6.3. Polyacrylamide Gel Electrophoresis (PAGE)

Samples of cell supernatants for gel analysis were mixed and boiled with 1X sample buffer containing sodium dodecyl sulphate (SDS) and DTT or 2-mercaptoethanol for 5min to denature proteins and reduce disulphide bonds. Cell pellet samples were firstly resuspended in QIAGEN® buffer P2 (500µL/10^7 cells) and freeze-thawed three times before centrifuging at 13,000rpm for 10min at 4°C. Supernatant was removed and boiled with sample buffer as described above. Samples were separated according to size SDS-PAGE using Any kD™ Mini-PROTEAN® TGX™ gels in 1X Tris/Glycine/SDS buffer (200V, 45min). Protein fragments were visualised by coomassie blue (section 2.6.4) or silver staining (2.6.5) and size was estimated by comparison to a ProSieve™ QuadColor™ protein marker (4.6-300 kDa).

2.6.4. Coomassie Blue Staining

Once electrophoresis was complete, SDS-PAGE gels were removed from casts and covered in fixing solution on a rocking platform for 1h. The fixing solution was poured off and the gels rinsed in deionised water. Gels were stained with Coomassie blue stain for 1h on a rocking platform. The gels were washed in deionised water and destained overnight in destain solution.

2.6.5. Western Blot

Proteins separated by SDS-PAGE were transferred to a pre-soaked nitrocellulose transfer membranes from a Trans-Blot® Turbo™ PVDF transfer pack as described in the user manual. Membranes were washed twice for 5min each with PBS on a rocking platform and blocked for 1hr in 3% BSA/PBS. After blocking and between antibody incubations, membranes were washed four times in PBS/T for 5min each and once in PBS for 5min. Primary (anti-his-tag or polyclonal sera; typically 1:1,000) and secondary (alkaline phosphatase donkey anti-mouse IgG (H+L); typically 1:3,000) antibodies were diluted appropriately in 3% BSA/PBS and applied to the membrane for 1h each. Blots were developed by applying a solution of SIGMA *FAST*™ BCIP/NBT (1 tablet per 10mL deionised water). The reaction was stopped by rinsing the blot in deionised water.

2.7. Animal Procedures

2.7.1. Animals

6-10 week-old female BALB/c (H-2^d) mice were obtained from Harlan Laboratories, Oxfordshire and were housed at the Functional Genomics Facility (FGF) under specific pathogen free (SPF) conditions at the Wellcome Trust Centre for Human Genetics. All procedures were performed in accordance with the Animals (Scientific Procedures) Act 1986 under the project licence PPL 30/2889.

2.7.2. Anaesthesia

Prior to vaccination mice were anaesthetised by inhalation 2-3.5% isofluorane delivered in oxygen (2L/min).

2.7.3. Immunisation

Vaccines were administered by intramuscular injection into the adductor muscles of anaesthetised mice using a 26g needle in a total volume of 50µL. MVA vectored vaccines were administered at a dose of $1X10^6$ pfu (Appendix XV), AdHu5 vectored vaccines at $1X10^8$ infectious units (iu) and ChAdOx1 vectored vaccines at either $1X10^8$ or $2.2X10^6$ iu (Appendix VII). Endotoxin-free DNA (section 2.2.3) vaccines were administered at a dose of 50µg per animal. Adjuvanted vaccines made with Addavax™ were formulated in a 1:1 vaccine:adjuvant mixture ratio. A minimum of 8 weeks was left between vaccinations within a single animal.

2.7.4. Blood Collection

2.7.4.1. Tail Vein Bleed

Blood samples from mice in on-going experiments were collected at specific time intervals post-vaccination via the tail vein. Mice were pre-warmed in a heat box at 37°C to ensure blood vessels were adequately dilated. The lateral tail vein was nicked using a scalpel blade while the mouse was held in a restrainer. Blood was collected in microvette tubes (Sarstedt) and left to clot overnight at 4°C before centrifugation at 13,000rpm for 15min, 4°C to separate cells from sera. Sera was stored at -20°C prior to use. No more than 10% of the total blood volume of a mouse was taken on a single occasion and when bleeds were less than one month apart, sample volumes collected were approximately 50µL.

2.7.4.2. Cardiac Puncture

At the end of experiments mice were put under terminal anaesthesia and exsanguinated by inserting a 29g needle syringe into the heart.

Blood was collected into eppendorfs and sera extracted as previously described (section 2.5.4.1)

2.7.5. Splenocyte Isolation and Preparation

Mice were sacrificed by cervical dislocation and spleens were removed by dissection into sterile PBS. Under sterile conditions spleens were crushed and passed through a 70µm cell strainer with 10-15mL PBS. The suspension was centrifuged at 1,350rpm for 5min at room temperature and the supernatant was discarded. The cell pellet was resuspended in 5mL ACK

lysis buffer for a maximum of 5min to remove erythrocytes before being diluted by addition of 25mL PBS. The suspension was centrifuged at 1,350rpm for 5min at room temperature and the supernatant was discarded. Splenocytes were resuspended in 3-5mL complete αMEM and the 'ghost' clump of cellular debris removed. Cells were counted using a CASY counter according to the manufacturer's instructions and adjusted to an appropriate concentration, typically $1X10^7$/mL, in complete αMEM. Prior to further assessment, cells were incubated at 37°C, 5% CO_2.

2.7.6. Bone Marrow Isolation and Preparation

Mice were sacrificed by cervical dislocation and hind limbs were removed by dissection into R10 prior to extraction of bone marrow (BM). Joints were cut to expose the lumen of the femur bones and BM was gently flushed out with 5mL R10 using a 26g needle. The BM suspension was passed through a 70μm cell strainer and centrifuged at 1,350rpm for 5min at room temperature. The supernatant was discarded and cells were processed from this point onwards as previously described (section 2.5.4.4) and resuspended in R10 media.

2.8. Immunological Techniques

2.8.1. Standardised Whole IgG Enzyme-Linked Immunosorbent Assay (ELISA)

Nunc Maxisorp® 96-well plates were coated with 0.1µg recombinant protein per well diluted in coating buffer and incubated overnight at 4°C. Plates were washed six times in PBS/T and blocked with 1% casein in PBS (w/v) for 2h at room temperature or overnight at 4°C and washed as before. These times were kept consistent to either 2h or overnight for all samples within an experiment. A pool of sera containing antibodies against the coating antigen was used to generate a reference standard which was plated in 2-fold dilutions across the plate starting with an initial dilution of 1:100 in PBS/T. Test sera was diluted in PBS/T and added to the plate in duplicate or triplicate (triplicate preferably, depending on sera availability) samples at an appropriate dilution (typically from 1:500 to 1:2,000) along with a positive and negative control (naïve sera). Duplicates greater than 2 standard deviations from the mean were discarded and fresh samples re-assayed. Plates were incubated for 2h at room temperature or overnight at 4°C. They were washed again as previously described and coated with goat anti-mouse whole IgG alkaline phosphatase conjugate (diluted 1:5,000) and each well was incubated with 50µL for 1h at room temperature. Following this step plates were again washed and developed by addition of p-nitrophenyl phosphate (pNPP) diluted in diethanolamine buffer (1mg/mL). Plates were developed until the 5^{th} dilution of the reference standard (1:1,600 dilution) reached an approximate OD_{450} value of 1 using an ELx800 microplate reader. This point was defined as 1 Relative ELISA Unit (REU) and REU of test sera were

calculated from this according to published methods [384]. Only values that fell on the linear portion of the standard curve were accepted. The assay was repeated on samples falling outside of this range, with concentrations adjusted accordingly.

2.8.2. Antibody Biopanning Using a T7 Phage Display Library

Test sera aliquots (50µL) were incubated overnight at 4°C with $1x10^7$ UV-inactivated phage (18h, CL-1000 UV Crosslinker) expressing an irrelevant S-tag (KETAAAKFERQHMDS). The following day nunc maxisorp plates were coated with the neat pre-incubated test sera and left overnight at 4°C. Plates were washed six times in PBS/T and blocked with 200µL 1% casein in PBS (w/v) for 2h at room temperature. To remove low affinity binders the plate was washed six times with PBS/T and incubated with 1% Triton X-100/PBS for 2h at room temperature. This step was repeated twice more and the final wash was left on overnight at 4°C on a shaker. The following day plates were washed ten times with PBS/T and three times with PBS. Bound phage were eluted by incubation with 1% SDS/PBS. Titres were determined at 10^{-1} or 10^{-2} dilutions as outlined previously (section 2.3.1.2).

2.8.3. Pseudotype Neutralisation Assay

All influenza pseudotype lentivirus particles (pp) used in this study were provided by Dr Nigel Temperton (Viral Pseudotype Unit, Medway School of Pharmacy, University of Kent). Starting with an initial 1:40 dilution, test sera was diluted 2-fold in complete DMEM across a Nunc F96 LumiPlate. Pp with an output of 500,000 Relative Luminescence Units (RLU) were incubated

with sera dilutions for 1h at 37°C. Following incubation, $1X10^4$ freshly trypsinised 293T/17 cells were added to each well and the plates were incubated for 48h at 37°C. Luminescence of cell cultures in RLU was evaluated by luminometry using the Bright-Glo™ luciferase assay system. Bright-Glo™ luciferase reagent was added to cells, incubated for 5min at room temperature. Luminescence was measured using a Varioskan™ Flash luminometer. Results were normalised relative to cell-only and pp-only control wells and expressed as the percentage of inhibition of pp entry (neutralisation). The half maximal inhibitory concentration (IC50) (the serum dilution yielding a 50% reduction in luciferase activity) was calculated using GraphPad Prism 6 software.

2.8.4. Interferon-Gamma Enzyme-Linked ImmunoSpot (ELISpot) Assay

MultiScreen-IP filter plates were coated with 0.25µg anti-mouse IFNγ per well in coating buffer and incubated overnight at 4°C. The following day plates were blocked with 200µL complete αMEM for a minimum of 2h at room temperature. Splenocytes were prepared as previously described (section 2.7.5) and resuspended at a concentration of $1X10^7$ cells/mL in complete αMEM. $1x10^6$ cells were plated per well in duplicate samples and diluted 2-fold down the plate. Medium alone was used as a negative control and pools of overlapping peptides (H7HA) or a peptide representing the immunodominant H2-Kd restricted (BALB/c) epitope $NP_{147-158}$ (TYQRTRALV) (within the antigen NP+M1) were added to test wells at a typical final concentration of 2µg/mL. Responses against $NP_{147-158}$ (TYQRTRALV) can be used to gauge the magnitude of MHC class I and MHC class II restricted T

cell responses and may therefore be used to assess if competition with other encoded antigens dampened the magnitude of responses against NP+M1 [385]. Plates were incubated at 37°C, 5% CO_2 for 18-20h. Following peptide stimulation plates were washed six times with PBS and incubated with 0.05µg biotinylated anti-mouse IFN-γ per well for 2h at room temperature. Plates were washed again as previously described and incubated with 0.05µg streptavidin-ALP per well for 1h at room temperature. Following a final wash, spots were developed using AP conjugate substrate kit (BioRad) according to manufacturer's instructions. Plates were dried at room temperature and spots were counted using an AID ELISpot reader. Responses were expressed as spot forming units (SFU) per million splenocytes.

2.8.5. IgG Antibody Secreting Cell ELISPOT Assay

Splenocytes or BM cells were prepared as previously described (sections 2.7.5 and 2.7.6) and resuspended at a concentration of ideally $1X10^7$ cells/mL in complete Iscove's and rested overnight. MultiScreen-IP filter plates were coated with 0.5µg recombinant HA diluted in coating buffer and incubated overnight at 4°C. As a positive control for total IgG secreting cells some wells were coated with anti-mouse anti-IgG. Negative control wells were coated with 0.5µg ovalbumin. The following day plates were blocked with 200µL complete Iscove's for a minimum of 1h at room temperature. $1X10^6$ cells were plated per well and cells were diluted 2-fold down the plate in a total well volume of 200µL. Plates were incubated at 37°C, 5% CO_2 for 5h. Following incubation, plates were washed six times with PBS and

incubated with 1µg per well biotinylated detection anti-mouse anti-IgG antibody for 2h at room temperature. Plates were washed again as previously described and incubated with 0.05µg streptavidin-ALP per well for 1h at room temperature and developed as previously described (section 2.8.4).

2.8.6. Memory B Cell IgG ELISpot Assay

Concavalin A supernatant was prepared in advance from splenocytes isolated from a naïve mouse. Cells were prepared as previously described (section 2.7.4.3) and resuspended at $1.25X10^6$ cells/mL in 2% DMEM. Concavalin A (2.5µg/mL) was added to the flask and they were incubated at 37°C, 5% CO_2 for 48h. The supernatant was harvested and sterile filtered. Aliquots were placed at -80°C for long-term storage.

Splenocytes or BM were prepared as previously described (section 2.8.6) and cultured for 7 days with stimulus mix of 10^6 irradiated naïve splenocytes (1,200 rad), 0.4µg R595 lipopolysaccharide (LPS), and 20µL Concavalin A supernatant per well. After 7 days, cell were harvested and transferred to a pre-coated multiScreen-IP filter plate as before (section 2.8.6). An ex-vivo IgG ELISpot assay for HA-specific and total IgG plasma cells was performed (section 2.8.6).

2.8.7. Cell Surface Marker Staining

The percentage of circulating peripheral T follicular helper-like (T_{FH}-like) cells, in frozen human peripheral blood mononuclear cells (PBMCs) was measured by flow cytometry. Frozen human PBMC samples were thawed (section

2.5.3) and washed twice in pre-warmed R10. Cells were resuspended at 2-3X10^6 cells/mL in R10 and incubated with benzonase® nuclease (10U per mL of cells) for 1h at 37°C. Following benzonase® nuclease treatment, cells were washed in pre-warmed R10 and plated at a concentration of 1X10^6 cells/well in a 96-well U bottom plate. Cell surface marker staining was performed step-wise in a total well volume of 100µL at either 37°C or room temperature (Table 2.7). Cells were centrifuged at 1,800rpm for 5min and washed once in FACS buffer between stains. Following staining cells were washed once in PBS and resuspended in 2% paraformaldehyde (neutral buffered formalin). Fluorescence was measured the following day using an LSRII and analysed with FlowJo software.

Table 2.7 Cell surface marker staining for T_{FH}-like cells

Step	Antibody	Volume per 100µL	Temperature	Time
1	Anti CXCR3-APC	5µL	37°C	10min
	Anti CXCR5-A488	2µL	37°C	10min
2	Anti CD3-PETR	1µL	RT	10min
	Anti CD4-APC-H7	2µL	RT	10min
	Anti CD45RO-PECy7	2µL	RT	10min
	Anti CCR6-PE	5µL	RT	10min
	Anti PD-1-BV421	1µL	RT	10min
3	LIVEDEAD	0.5µL	RT	10min

Table 2.7 Cell surface marker staining for T_{FH}-like cells

The cell surface marker staining panel for T_{FH}-like cells was developed by Dr Cecilia Chui. All flow cytometry experiments and data analysis were performed by Claire Tully (Chapter 5).

2.9. Statistics

Statistical analysis was performed using GraphPad Prism 6 software. The Shapiro-Wilk test was used to test data sets for normality where appropriate. The medians of groups from normally distributed populations were compared using an unpaired t-test (if equal sample variance) or a Welch's corrected unpaired t-test (if unequal sample variance). A Mann-Whitney U test was used to compare medians between groups from populations that were not normally distributed. A one-way ANOVA (normally distributed) or the Kruskall-Wallis test (not normally distributed) was used to compare the medians of three or more groups. Correlations were determined by Spearman's rank correlation coefficient. P values below 0.05 were considered significant.

Chapter 3

Production and Characterisation of Recombinant Haemagglutinin

3. Production and Characterisation of Recombinant Haemagglutinin

3.1. Background

Haemagglutinin (HA) is the major envelope glycoprotein of influenza. Between 400-500 HA spikes, approximately 13.5nm in length, are uniformly distributed on a single spherical virion – five times more than the second major virion surface protein neuraminidase (NA) [62,63]. Functionally, HA mediates virus binding to sialic acid residues on epithelial tissues and entry into host cells [64].

The structure and function of HA is well understood. HA is a type I integral membrane protein (type I proteins have a single transmembrane region of hydrophobic residues, with the amino terminal side extracellular and the carboxy portion exposed on the cytoplasmic side) which oligomerises post-translationally into a quaternary homotrimeric structure before it inserts into the cell membrane [386,387]. (NA is a type II transmembrane protein - the amino terminal side is exposed on the cytoplasmic side of the membrane and the carboxy portion is extracellular). HA is initially expressed as a ~75kD precursor polypeptide, HA0, which folds spontaneously as it is extruded into the endoplasmic reticulum (ER) of an infected cell [388]. The point at which trimerisation occurs is strain specific and can occur in either the ER, the ER-Golgi intermediate compartment (ERGIC) or the *cis*-Golgi network (CGN) [389-392]. At the plasma membrane, the precursor polypeptide HA0 is cleaved by

host proteases into two disulphide-linked polypeptides, HA1 and HA2, forming mature HA [388]. These polypeptides make up two structurally and functionally distinct domains, a globular head region composed of residues within the HA1 domain and a stem structure consisting of part of HA1 and all of HA2 [63]. The globular head domain contains the receptor binding site and is comprised of five overlapping antigenic sites, two of which are highly variable between closely related strains, Sa and Sb, and three that are more cross-reactive, Ca1, Ca2, and Cb [170,174]. The stem domain contains the highly conserved fusion peptide which mediates fusion of the viral and endosome membranes [393]. Upon entry into the cell the acidic pH of the endosome triggers conformational changes in HA that exposes the hydrophobic fusion peptide. This inserts into the target membrane, fusing the outer monolayers of the viral and target membranes. Cleavage of HA0 is essential to activate the membrane fusion properties of HA, without which, the virus is not infectious [85].

Synthesis of HA is typical of cellular glycoproteins. HA is core glycosylated co-translationally in the ER before it is trafficked via the Golgi complex (Gc) to the cell membrane and incorporated into budding virions [387,394]. As it proceeds through the Gc, HA undergoes extensive post-translational modifications including removal of the N-terminal signal peptide, terminal glycosylation, fatty acylation, trimming of asparagine-linked carbohydrate chains and C-terminal palmitoylation [391,395]. Post-translational modification of HA has important consequences for the infectivity and antigenicity of the virus. For example, HA sialic acid affinity is affected by carbohydrate side-

chains near the receptor binding site and immunodominant antigenic sites can be shielded from host immune responses by the introduction of host-specific oligosaccharide linkages such as glycans [396,397].

The choice of system for expression of recombinant HA can considerably influence protein antigenicity as the size, structure and electrostatic charges of HA glycans varies enormously between cell types [398]. Furthermore HA antigenicity is conformation-dependent. Almost all neutralising antibodies that target HA recognise conformation-specific epitopes, some of which depend on trimerisation for complete antigenicity [399]. For example, the HA1 epitope Ca8, recognised by the monoclonal antibody (mAb) H17-L2, is only apparent after exit from the ER, consistent with this being an epitope defined post-trimerisation [392]. In contrast, the mAb Y8-10C2 recognises an Sa epitope in the ER which is lost following ER exit [392]. However the Sb epitope, Sb9, is recognised by the mAb H28-E23 throughout the secretory pathway, suggesting some epitopes are present in both monomeric and trimeric HA [392]. Ultimately, the nature of post-translation modifications in addition to the trimerisation status of recombinant HA determines protein antigenicity. These factors are important for the manufacture of recombinant HA vaccines but also for the production of reagents suitable to accurately measure responses induced against HA.

In this study I have sought to produce several soluble recombinant HA protein constructs for use in the investigation of vaccine-induced antibody responses.

These proteins were produced primarily for ELISA-based studies to assess total IgG antibody responses to HA, in particular, to HA stem.

3.2. Specific methods

Specific methods for this chapter are found in the methods section 2.6.

3.3. Results

3.3.1. Recombinant HA Construct Design

The majority of the vaccine constructs used in this study were based on either the HA sequence from A/California/07/2009 (H1N1) (a triple-reassortant swine influenza A virus containing genes from avian, human, and swine influenza viruses) (GeneBank: ACQ55359.1) or a consensus HA sequence derived from 123 sequences of European pandemic flu (downloaded on July 12 2009 by Prof Sarah Gilbert). The consensus 2009 H1N1 pandemic HA sequence matches A/Texas/05/2009 (H1N1) (GeneBank: ACR19260.1) and differs by two amino acids to the A/California/07/2009 (H1N1) sequence. Both sequences are identical in the stem region. In order to optimally assess antibody responses induced by these vaccines, recombinant H1HA constructs were based on these sequences (Table 3.1). In addition, recombinant H7HA protein based on the sequence from A/Netherlands/219/2003 (H7N7) (GeneBank: AAR02640.1) was produced in order to assess antibody responses induced by vaccination with vaccine constructs based on the same sequence (Chapter 7). The chimeric constructs cH9/H1 and cH16/H1 were produced in order to assess antibody responses against the stem region of H1 (Chapter 6) (the HA1 regions of H9 and H16 are antigenically distinct from the HA1 region of H1).

The pCMV/R vector was received as a gift from Dr Gary Nabel (National Institutes of Health Vaccine Research Centre). For all proteins the signal peptide (residues 2-17), transmembrane domain (residues 521-554 (H1); 525-557 (H7)) and cytoplasmic tail (residues 555-566 (H1); 558-569 (H7))

were not expressed. The native leader sequence was replaced with a high expression Kozac translation initiation sequence (GGCCGCACC) followed by a modified human tissue plasminogen activator (tPA) leader sequence (MDAMKRGLCCVLLLCGAVFVSASQEIHARFRRGS) (Table 3.1) [400]. To induce trimerisation and mimic the antigenicity of HA produced during infection, all constructs were engineered with a cleavable bacteriophage T4 fibritin foldon trimerisation domain (YIPEAPRDGQAYVRKDGEWVLLSTFL). A polyhistidine tag (HHHHHH) was inserted at the C-terminus to enable downstream purification and a thrombin cleavage site (LVPRGS) was introduced in front of the foldon domain for downstream removal of non-HA residues (Table 3.1) [401]. Coding sequences were optimised for efficient expression in *Homo sapiens*. The H1HA, H7HA and Headless-H1HA sequences were cloned into pCMV/R by Dr Lynda Coughlan.

Table 3.1 Recombinant HA sequences cloned into pCMV/R

Protein Construct	Sequence
H1HA **(A/California/07/2009)**	*mdamkrglccvlllcgavfvsasqeiharfrrgs*DTLCIGYHA NNSTDTVDTVLEKNVTVTHSVNLLEDKHNGKL CKLRGVAPLHLGKCNIAGWILGNPECESLSTA SSWSYIVETPSSDNGTCYPGDFIDYEELREQL SSVSSFERFEIFPKTSSWPNHDSNKGVTAACP HAGAKSFYKNLIWLVKKGNSYPKLSKSYINDK GKEVLVLWGIHHPSTSADQQSLYQNADAYVF VGSSRYSKKFKPEIAIRPKVRDQEGRMNYYWT LVEPGDKITFEATGNLVVPRYAFAMERNAGSG IIISDTPVHDCNTTCQTPKGAINTSLPFQNIHPIT IGKCPKYVKSTKLRLATGLRNIPSIQSRGLFGAI AGFIEGGWTGMVDGWYGYHHQNEQGSGYAA DLKSTQNAIDEITNKVNSVIEKMNTQFTAVGKE FNHLEKRIENLNKKVDDGFLDIWTYNAELLVLL ENERTLDYHDSNVKNLYEKVRSQLKNNAKEIG NGCFEFYHKCDNTCMESVKNGTYDYPKYSEE AKLNREEIDGV*ISGRLVPRGSPGSGYIPEAPRD* *GQAYVRKDGEWVLLSTFLGHHHHHH*
H7HA **(A/Netherlands/219/2003)**	*mdamkrglccvlllcgavfvsasqeiharfrrgs*DKICLGHH AVSNGTKVNTLTERGVEVVNATETVERTNVPR ICSKGKRTVDLGQCGLLGTITGPPQCDQFLEF SADLIIERREGSDVCYPGKFVNEEALRQILRES GGIDKETMGFTYSGIRTNGTTSACRRSGSSFY AEMKWLLSNTDNAAFPQMTKSYKNTRKDPALI IWGIHHSGSTTEQTKLYGSGNKLITVGSSNYQ QSFVPSPGARPQVNGQSGRIDFHWLILNPNDT VTFSFNGAFIAPDRASFLRGKSMGIQSEVQVD ANCEGDCYHSGGTIISNLPFQNINSRAVGKCP RYVKQESLLLATGMKNVPEIPGRGLFGAIAGFI ENGWEGLIDGWYGFRHQNAQGEGTAADYKS TQSAIDQITGKLNRLIEKTNQQFELIDNEFTEVE RQIGNVINWTRDSMTEVWSYNAELLVAMENQ HTIDLADSEMNKLYERVKRQLRENAEEDGTGC FEIFHKCDDDCMASIRNNTYDHSKYREEAIQN RIQIDPVKLSSGYKDV*ISGRLVPRGSPGSGYIP* *EAPRDGQAYVRKDGEWVLLSTFLGHHHHHH*

cH9/H1 ***(A/California/07/2009)***	*mdamkrglccvlllcgavfvsasqeiharfrrgs*DTLCIGYHA NNSTDTVDTVLEKNVTVTHSVNLLEDKHNGKL C***ATSLGHPLILDTCTIEGLVYGNPSCDLLLGG*** ***REWSYIVERSSAVNGTCYPGNVENLEELRTLF*** ***SSASSYQRIQIFPDTTWNVTYTGTSRACSGSF*** ***YRSMRWLTQKSGFYPVQDAQYTNNRGKSILF*** ***VWGIHHPPTYTEQTNLYIRNDTTTSVTTEDLN*** ***RTFKPVIGPRPLVNGLQGRIDYYWSVLKPGQT*** ***LRVRSNGNLIAPWYGHVLSGGSHGRILKTDL*** ***KGGN***CNTTCQTPKGAINTSLPFQNIHPITIGKC PKYVKSTKLRLATGLRNVPSIQSRGLFGAIAGF IEGGWTGMVDGWYGYHHQNEQGSGYAADLK STQNAIDEITNKVNSVIEKMNTQFTAVGKEFNH LEKRIENLNKKVDDGFLDIWTYNAELLVLLENE RTLDYHDSNVKNLYEKVRSQLKNNAKEIGNGC FEFYHKCDNTCMESVKNGTYDYPKYSEEAKL NREEIDGV*ISGRLVPRGSPGSGYIPEAPRDGQ* *AYVRKDGEWVLLSTFLGHHHHHH*
cH16/H1 ***(A/California/07/2009)***	*mdamkrglccvlllcgavfvsasqeiharfrrgs*DTLCIGYH ANNSTDTVDTVLEKNVTVTHSVNLLEDKHNGK LC***SLNGISPIHLGDCSFEGWIVGNPSCATNINI*** ***REWSYLIEDPNAPNKLCFPGELDNNGELRHL*** ***FSGVNSFSRTELISPNKWGDILDGVTASCRDN*** ***GASSFYRNLVWIVKNKNGKYPVIKGDYNNTT*** ***GRDVLVLWGIHHPDTETTAINLYASKNPYTLV*** ***STKEWSKRYELEIGTRIGDGQRSWMKLYWHL*** ***MRPGERIMFESNGGLIAPRYGYIIEKYGTGRIF*** ***QSGVRMAK***CNTTCQTPKGAINTSLPFQNIHPI TIGKCPKYVKSTKLRLATGLRNIPSIQSRGLFG AIAGFIEGGWTGMVDGWYGYHHQNEQGSGY AADLKSTQNAIDEITNKVNSVIEKMNTQFTAVG KEFNHLEKRIENLNKKVDDGFLDIWTYNAELLV LLENERTLDYHDSNVKNLYEKVRSQLKNNAKE IGNGCFEFYHKCDNTCMESVKNGTYDYPKYS EEAKLNREEIDGV*ISGRLVPRGSPGSGYIPEAP* *RDGQAYVRKDGEWVLLSTFLGHHHHHH*

ΔStem-H1HA ***(A/California/07/2009)***	*mdamkrglccvlllcgavfvsasqeiharfrrgs*DTLCIGYHA NNSTDTVDTVLEKNVTVTHSVNLLEDKHNGKL CKLRGVAPLHLGKCNIAGWILGNPECESLSTA SSWSYIVETPSSDNGTCYPGDFIDYEELREQL SSVSSFERFEIFPKTSSWPNHDSNKGVTAACP HAGAKSFYKNLIWLVKKGNSYPKLSKSYINDK GKEVLVLWGIHHPSTSADQQSLYQNADAYVF VGSSRYSKKFKPEIAIRPKVRDQEGRMNYYWT LVEPGDKITFEATGNLVVPRYAFAMERNAGSG IIISDTPVHDCNTTCQTPKGAINTSLPFQNIHPIT IGKCPKYVKSTKLRLATGLRNIPSIQSRGLFGAI AGFIEGGWTGMVDGWYGYHHQNEQGSGYAA DLKSTQNA***N***D***T***ITNKVNSVIEKMNTQFTAVGK EFNHLEKRIENLNKKVDDGFLDIWTYNAELLVL LENERTLDYHDSNVKNLYEKVRSQLKNNAKEI GNGCFEFYHKCDNTCMESVKNGTYDYPKYSE EAKLNREEIDGV*ISGRLVPRGSPGSGYIPEAPR DGQAYVRKDGEWVLLSTFLGHHHHHH*
Headless-H1HA ***(A/California/07/2009)***	*mdamkrglccvlllcgavfvsasqeiharfrrgs*DTLCIGYHA NNSTDTVDTVLEKNVTVTHSVNLLEDKHNGKL C***GGGG***CNTTCQTPKGAINTSLPFQNIHPITIGK CPKYVKSTKLRLATGLRNIPSIQSRGLFGAIAG FIEGGWTGMVDGWYGYHHQNEQGSGYAADL KSTQNAIDEITNKVNSVIEKMNTQFTAVGKEFN HLEKRIENLNKKVDDGFLDIWTYNAELLVLLEN ERTLDYHDSNVKNLYEKVRSQLKNNAKEIGNG CFEFYHKCDNTCMESVKNGTYDYPKYSEEAK LNREEIDGV*ISGRLVPRGSPGSGYIPEAPRDG QAYVRKDGEWVLLSTFLGHHHHHH*
H1HA-Stem ***(A/Texas/05/2009)***	*mdamkrglccvlllcgavfvsasqeiharfrrgs*DTLCIGYHA NNSTDTVDTVLEKNVTVTHSVNLLEDK***GSGSG*** TSLPFQNIHPITIGK***T***PKYVKSTKLRLATGLRN***V*** PSIQSRGLFGAIAGFIEGGWTGMVDGWYGYH HQNEQGSGYAADLKSTQNAIDEITNKVNSVIEK MNTQ***D***TAVGKEFNH***D***EKRIENLNKKVDD***CC***L DIWTYNAELLVLLENERTLDYHDSNVKNLYEK VRSQLKNNAKEIGNGCFEFYHKCDNTCMESV KNGTYDYPKYSEEAKLNREEIDGV*ISGRLVPR GSPGSGYIPEAPRDGQAYVRKDGEWVLLSTF LGHHHHHH*

Table 3.1 Recombinant HA sequences cloned into pCMV/R

Lower case italics represent the modified tPA leader sequence. ***Bold underlined italic CAPS*** represent residues that differ to the A/California/07/2009 H1HA sequence. *Italic underlined CAPS* represent the C-terminal sequence (thrombin cleavage site, T4 fibritin foldon trimerisation domain and polyhistidine tag).

3.3.1.1. H1HA

Recombinant H1HA protein was based on the sequence from A/California/07/2009 (GeneBank: ACQ55359.1).

3.3.1.2. H7HA

Recombinant H7HA protein (A/Netherlands/219/2003) (GeneBank: AAR02640.1) included a KRRR344 to G mutation at the polybasic cleavage site [400,402]. This produces a trypsin-independent version of mature HA and does not alter the antigenic character of the protein [400,402].

3.3.1.3. cH9/H1

The boundary between the HA stem and globular head is delineated by a disulphide bond between C52 and C277 (H3 numbering; A/Aichi/02/68) of HA1 [296,403]. These two cysteines are highly conserved across HA subtypes [296]. By replacing the intervening sequence of one subtype with that of an antigenically distinct subtype it is possible to generate chimeric HA that can be used to measure antibodies against HA stem if there has been no previous exposure to subtype used in the globular head region of the chimera [294]. This can be screened for by ELISA. cH9/H1 is composed of the HA2 domain of A/California/07/2009 and HA1 residues from a H9 subtype A/Hong Kong/1073/99 (H9N2) (GeneBank: NP859037) which is antigenically distinct from H1 subtypes (Fig. 3.1) [294].

3.3.1.4. cH16/H1

cH16/H1 was designed using the same approach used to produce cH9/H1. cH16/H1 is composed of the HA2 domain of A/California/07/2009 and HA1 residues from a H16 subtype A/black-headed gull/Sweden/5/99 (H16N3) (GeneBank: AAV91217.1), which is antigenically distinct from H1 subtypes (Fig. 3.1).

3.3.1.5. ΔStem-H1HA

The recombinant protein ΔStem-H1HA is a matched stem-mutant version of H1HA (A/California/07/2009) containing an I545N and an E547T mutation derived from pCMV/R-H1HA by site directed mutagenesis (section 2.2.6) [404]. This mutation inserts an N-glycan into helix A of the HA2 domain blocking access of anti-stem antibodies to HA stem.

3.3.1.6. Headless-H1HA

The Headless-H1HA construct is a truncated version of H1HA (A/California/07/2009) in which the globular head is removed by replacing the intervening HA1 residues between C52 and C277 (H3 numbering; A/Aichi/02/68) with a short glycine linker [296].

3.3.1.7. H1HA-Stem

The H1HA-Stem HA construct was previously produced as inclusion bodies using an *E.coli* based cell-free protein synthesis (CFPS) method followed by protein refolding [303]. The construct is a fusion of HA stem and the T4 fibritin foldon trimerisation domain [303]. The globular head domain (residues 60-291;

H3 numbering; A/Aichi/02/68) of A/Texas/05/2009 (H1N1) (GeneBank: ACR19260.1) was replaced with a linker peptide (GSGSG) and newly exposed hydrophobic residues in HA stem were mutated (F164D and L174D) [303]. The number of disulphide bonds in each monomer was reduced from 4 to 2 by mutating C77 to T and deleting two polypeptide regions containing hydrophobic residues (H38 to C43 and C49 to N61) [303]. Cysteines were introduced at G188C-F189C to favour bonds between monomers [303].

Figure 3.1 Phylogenetic tree of influenza A HAs

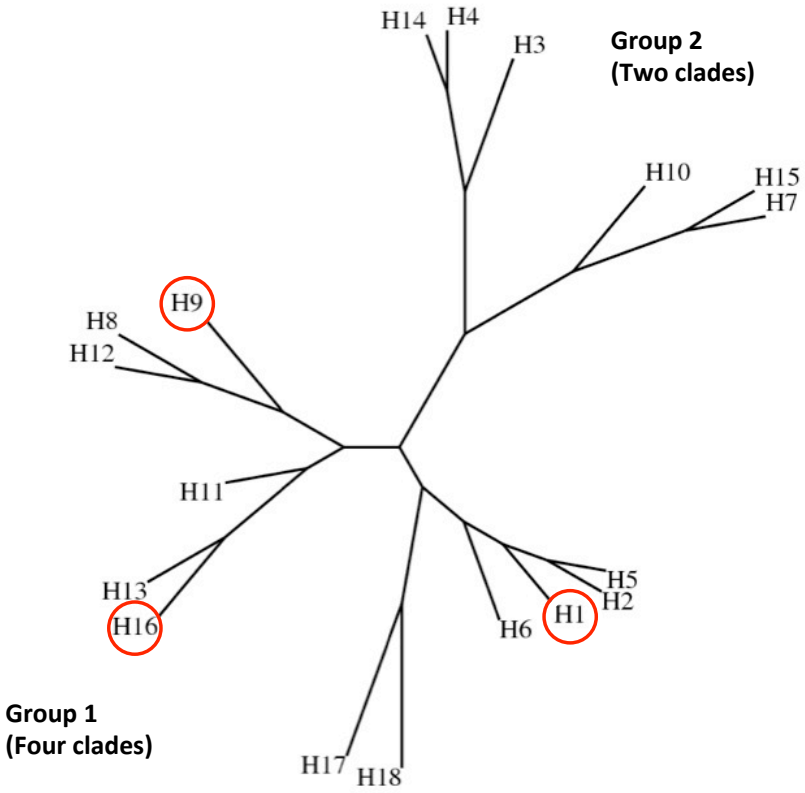


Figure 3.1 Phylogenetic tree of influenza A HAs

HA subtypes are divided into two major groups, Group 1 and Group 2, on the basis of antigenic properties. Group 1 HA are further subdivided into four clades (H9, H8 and H12; H11, H13 and H16; H17 and H18; H6, H1, H2 and H5) and Group 2 HA are subdivided into two clades (H14, H4 and H3; H10, H15, H7). H1, H9 and H16 are circled in red. The tree was drawn using Phylogeny.fr [405,406].

3.3.2. Recombinant HA Expression Analysis

Recombinant HA constructs were expressed using suspension-adapted FreeStyle™ 293-F cells derived from the HEK-293 cell line (section 2.6.2.2). These cells were adapted to Expi293™ expression medium to enable rapid high-density transient mammalian protein expression. Using this system protein can be harvested as quickly as 48 hours and volumetric yields are typically higher than traditional culture systems.

Samples were collected at 24h intervals up to a maximum of 4 days post-transfection for expression analysis by SDS-PAGE and Western blot (section 2.6.3 and 2.6.5). SDS-PAGE separates denatured proteins (coated in a uniform negative charge by SDS) according to their molecular weight, based on their differential rates of migration through a gel in an electrical field. Western blots can be used to detect specific proteins in complex mixtures using labelled antibodies.

Samples of cell supernatant and pellet were examined for accumulation of correctly-folded soluble or misfolded insoluble protein products respectively. The constructs H1HA, H7HA, cH9/H1, cH16/H1, ΔStem-H1HA and H1HA-Stem were expressed by FreeStyle™ 293-F cells and accumulated as soluble proteins in the cell supernatant. A representative example of H1HA expression is shown (Fig. 3.2). The stem construct Headless-H1HA did not express in the soluble fraction (Fig. 3.3).

Figure 3.2 Expression of recombinant H1HA in FreeStyle™ 293-F cells

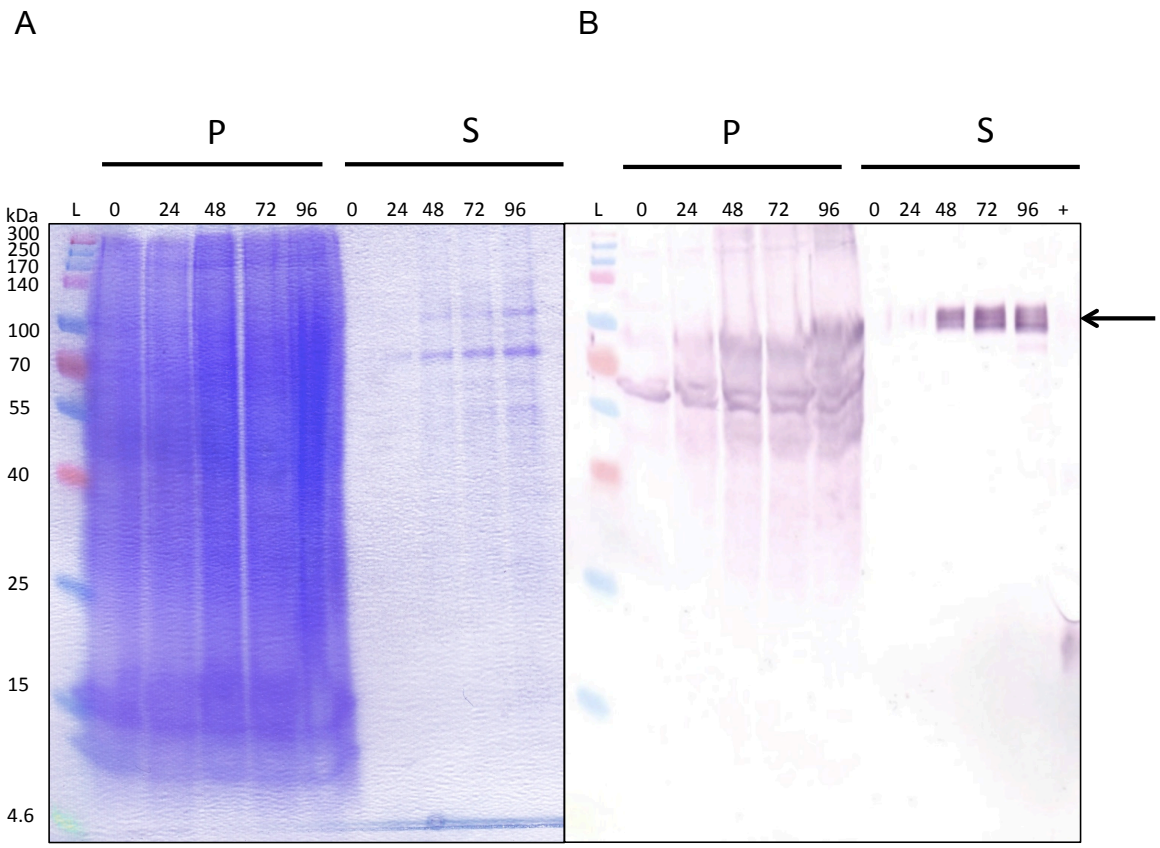


Figure 3.2 Expression of recombinant H1HA in FreeStyle™ 293-F cells

Cell pellet and supernatant samples were collected just before transfection (0 hours) and every 24 hours up to 96 hours post transfection, and examined for protein expression by (A) reducing SDS-PAGE and (B) Western blot using a monoclonal anti-his antibody for detection. Molecular mass in kilodaltons is shown to the left. The apparent molecular mass of a H1HA monomer is ~90 kDa (indicated by arrow). L= molecular weight standard, P = pellet, S = supernatant, + = positive polyhistidine-tagged control.

Figure 3.3 Expression of Headless-H1HA in FreeStyle™ 293-F cells

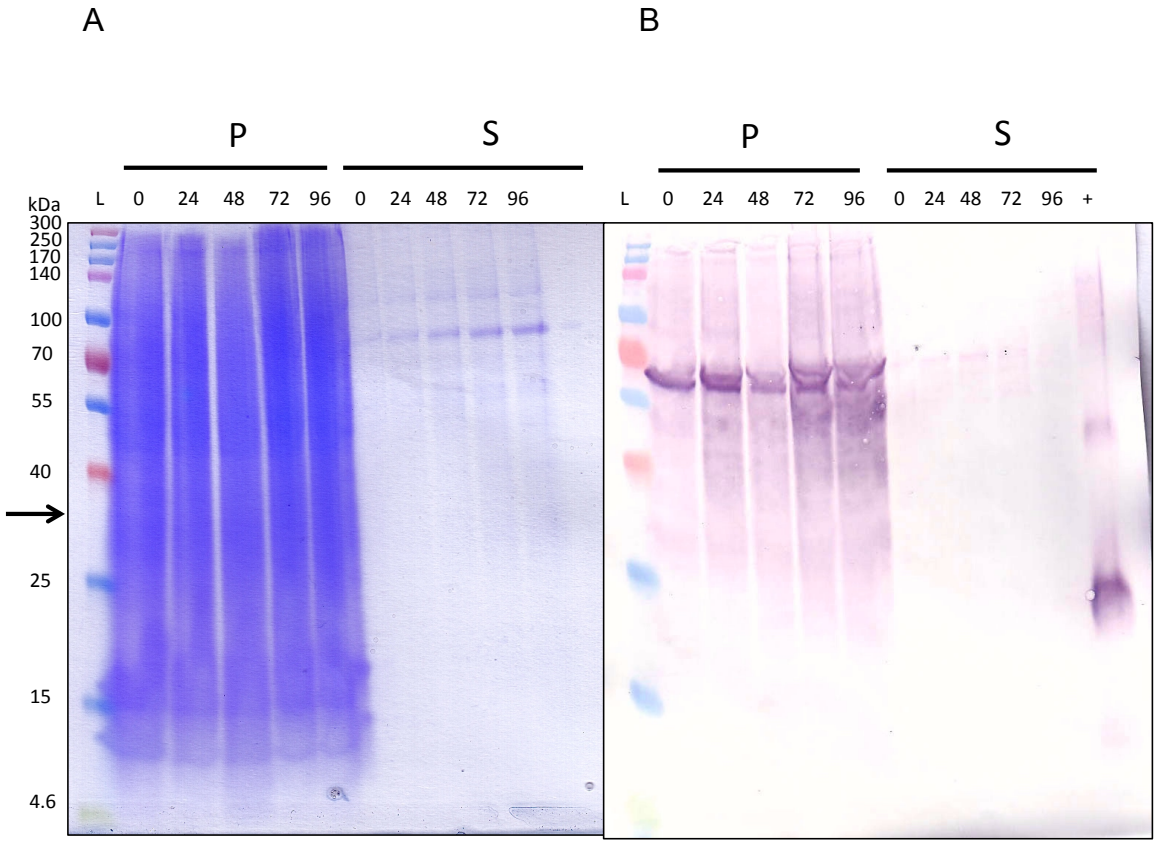


Figure 3.3 Expression of Headless-H1HA in FreeStyle™ 293-F cells

Cell pellet and supernatant samples were collected before transfection (0 hours) and every 24 hours up to 96 hours post transfection, and examined for protein expression by (A) reducing SDS-PAGE and (B) Western blot using a monoclonal anti-his antibody for detection. Molecular mass in kilodaltons is shown to the left. The expected molecular mass of an unglycosylated Headless-H1HA monomer is ~36kDa (indicated by arrow). L= molecular weight standard, P = pellet, S = supernatant, + = positive polyhistidine-tagged control.

Key findings:

H1HA, H7HA, cH9/H1, cH16/H1, ΔStem-H1HA and H1HA-Stem were expressed by FreeStyle™ 293-F cells and accumulated as soluble proteins in the cell supernatant. Headless-H1HA was not expressed in the soluble fraction.

3.3.3. Purification of Recombinant HA

Soluble polyhistidine-tagged recombinant HA was purified by metal ion affinity chromatography (section 2.6.2.3). Eluted fractions were analysed for the presence of protein by SDS-PAGE and Western Blot (Fig. 3.4) (sections 2.6.3 and 2.6.5). Fractions with recombinant HA present were pooled and concentrated (section 2.6.2.3). The maximum recoverable yield of recombinant HA for all constructs was achieved 96h post-transfection, after which cell viability declined below 80%. Recombinant HA yields ranged from 0.7-7.5mg per 250mL culture (2.8-37.5mg/L). Yields varied depending on the construct expressed and were slightly better than reports of HA expression using baculovirus (0.7-20mg/L) expression systems but lower than yields obtained using yeast (13-60mg/L) [407-410]. These systems are discussed in the final chapter discussion (section 3.4).

Figure 3.4 Purification of recombinant HA constructs

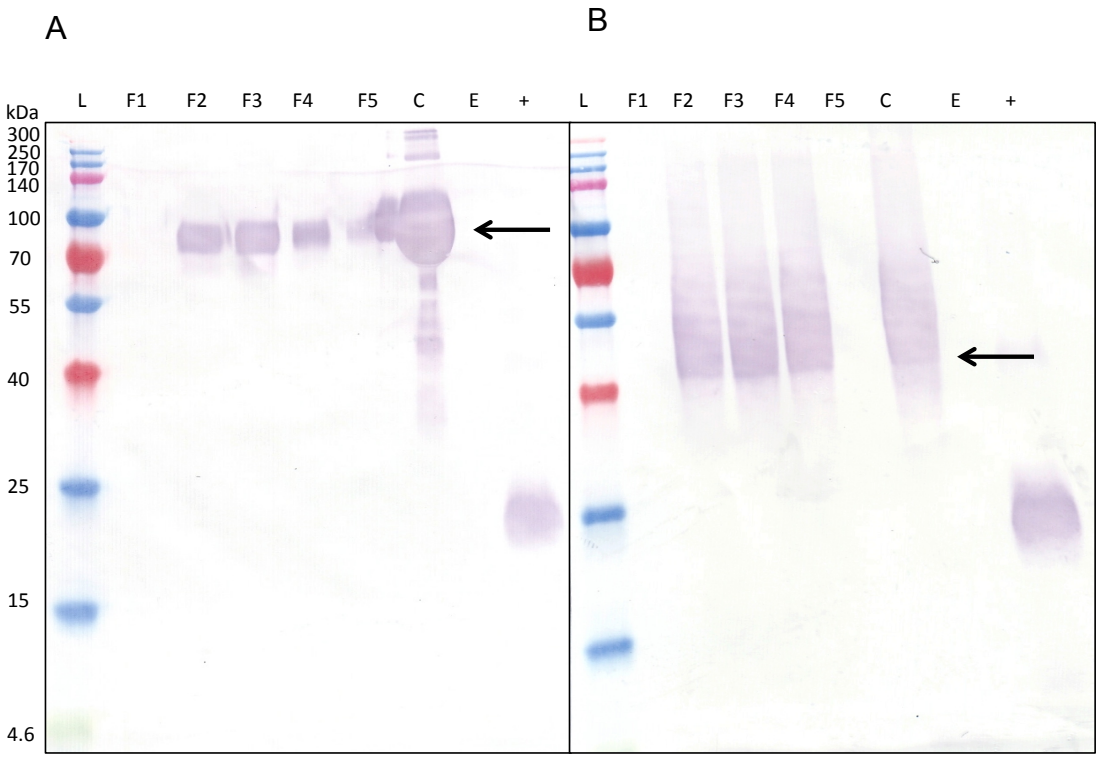


Figure 3.4 Purification of recombinant HA constructs

Eluted column fractions (F1-F5) were examined for (A) H1HA and (B) H1HA-Stem expression by Western blot using a monoclonal anti-his antibody for detection. Molecular mass in kilodaltons is shown to the left. The apparent molecular masses of a H1HA monomer is (~90 kDa) and a H1HA-Stem monomer (~40kDa) are indicated by arrows. L= molecular weight standard, F1-F5 = fractions 1 - 5, C = concentrated protein sample, E = Amicon Ultra centrifugal filter unit eluent, + = positive polyhistidine-tagged control.

Key findings:

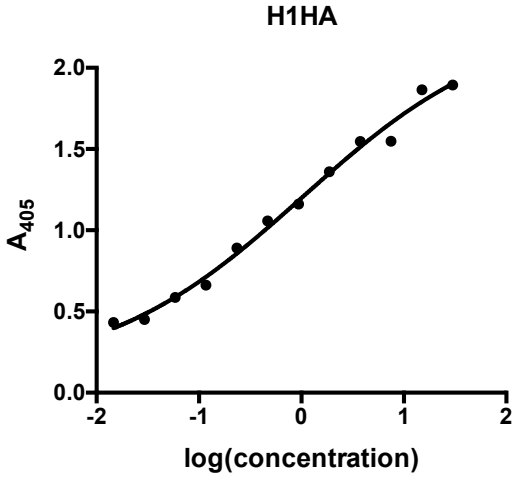
H1HA, H7HA, cH9/H1, cH16/H1, ΔStem-H1HA and H1HA-Stem were purified by metal ion affinity chromatography. Yields varied for individual constructs.

3.3.4. Analysis of Group 1 Recombinant HA Stem Structural Integrity by ELISA

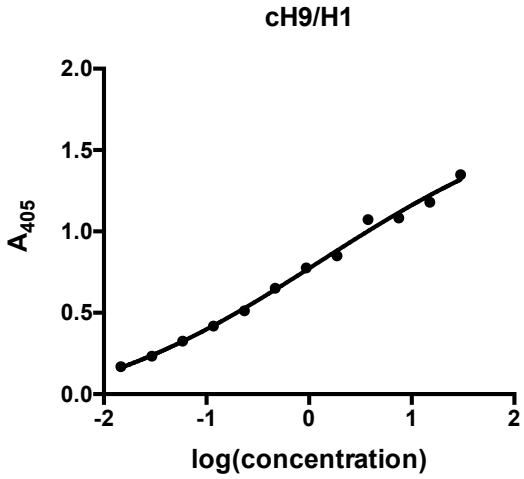
The antigenic conformation of the HA2 domain of purified H1HA, cH9/H1, cH16/H1, ΔStem-H1HA and H1HA-Stem was investigated by ELISA using a mouse mAb (section 2.8.1) (Fig. 3.5). Plates were coated with 5μg/mL recombinant protein in duplicate. C179 was plated in 2-fold dilutions across the plate starting with an initial concentration of 30μg/mL. C179 is a neutralising antibody that recognises an epitope in the stem of multiple Group 1 HAs, which is conformation dependent [411,412]. It has previously been reported to bind exclusively to soluble trimerised HAs [413]. The Group 2 HA, H7HA, does not contain the epitope recognised by C179 and was used as a negative control. Results indicated that the C179 epitope was intact in H1HA, cH9/H1 and cH16/H1 demonstrating correct folding of the stem in these constructs (Fig. 3.5). The stem mutant ΔStem-H1HA was not recognised indicating the glycosylation site introduced in helix A blocked epitope recognition (Fig. 3.5). H1HA-Stem was noted to largely precipitate during purification and recovered samples were not recognised by C179, suggesting this protein was not stable (Fig. 3.5).

Figure 3.5 ELISA of Group 1 HA constructs using mAb C179

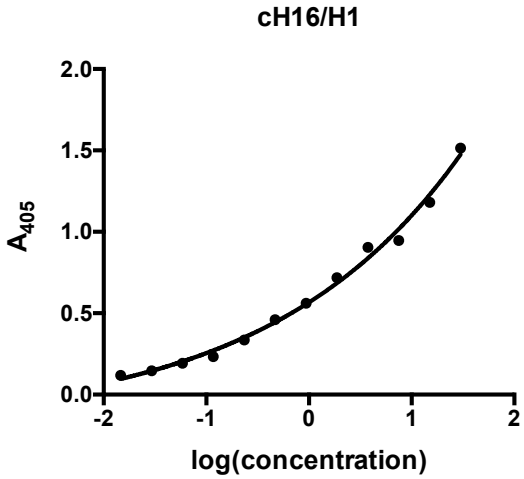
A



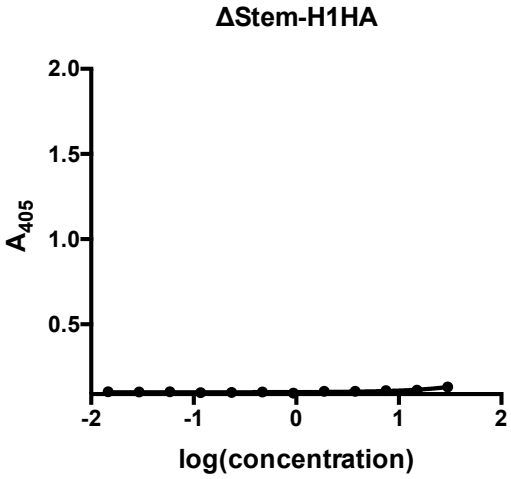
B



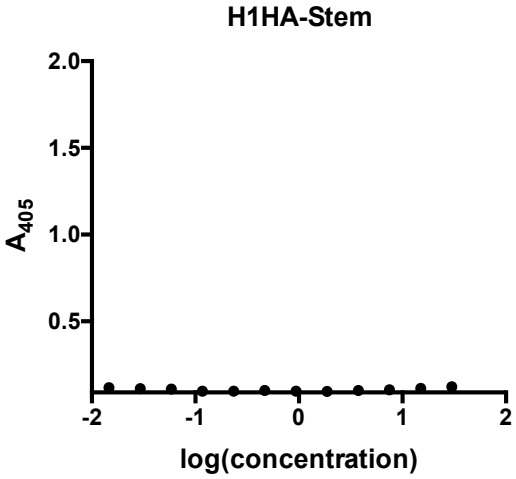
C



D


ΔStem-H1HA
2.0
1.5
1.0
0.5
A405
-2
-1
0
1
2
log(concentration)

E


H1HA-Stem
2.0
1.5
1.0
0.5
A405
-2
-1
0
1
2
log(concentration)

F

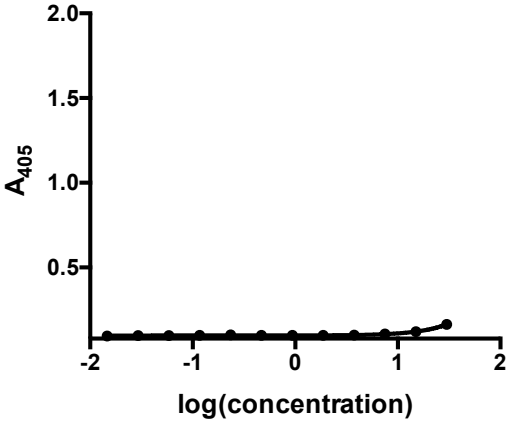

H7HA
2.0
1.5
1.0
0.5
A405
-2
-1
0
1
2
log(concentration)

Figure 3.5 ELISA of Group 1 HA constructs using mAb C179

Stem immunogenicity of constructs with a Group 1 stem was evaluated by measuring binding of the stem-reactive mAb C179 to each of the six recombinant HA constructs purified, H1HA, cH9/H1, cH16/H1, ΔStem-H1HA, H1HA-Stem and H7HA, by ELISA (5μg/mL). Samples were measured in duplicate. Recombinant H7HA does not contain the epitope recognised by C179 and was used as a negative control. The constructs ΔStem-H1HA and H1HA-Stem were not recognised due to masking of the epitope by glycosylation and protein misfolding respectively.

Key findings:

H1HA, cH9/H1, and cH16/H1 were recognised by the stem reactive monoclonal antibody, C179, suggesting the stem regions of these proteins were correctly folded. ΔStem-H1HA was not recognised indicating the glycosylation site to block the binding of stem antibodies was in place. H1HA-Stem was not recognised suggesting this protein did not fold correctly. H7HA does not contain the C179 epitope and was not recognised.

3.4. Discussion

This chapter describes a HEK-293 suspension cell-based method of protein synthesis that can be used in the production of soluble wild type and chimeric HA. This expression system provides a straight-forward, cost-effective, scalable means of producing correctly folded, trimerised, stable recombinant HA in milligram quantities which can be used to assess vaccine-induced responses to HA.

Recombinant HA production was first described two decades ago in E.coli and eukaryotic systems such as yeast and insect cells [414-416]. Bacteria are the most rapid and least expensive of all expression systems but the proteins they produce are rarely secreted, usually do not fold correctly and lack eukaryotic post-translational modifications. Both yeast and insect expression systems are capable of producing secreted and intracellular proteins but are unable to produce the characteristic N-linked glycan structures typical of mammalian proteins. Mammalian cells, though capable of producing the most authentic post-translational modifications for human recombinant proteins, are generally more expensive and can be difficult to scale up.

Today, commercially available soluble recombinant HA is widely produced using baculovirus-insect cell expression systems that provide complex eukaryotic protein processing factors and are capable of the high capacity expression levels seen in prokaryotic systems (Abcam®, BEI Resources, Sino Biological Inc). Advances in the ease of baculovirus recombinant engineering and the availability of bacmids in addition to the cost-effectiveness of the

continuous, semi-automated process utilised for large-scale production has made this an attractive system for biotech companies. Furthermore, as baculovirus vectors are non-pathogenic to mammals, they do not face the same regulatory hurdles as human cell lines used for the production of recombinant therapeutic protein. However, production of 'authentic' protein is extremely favourable for vaccination studies and in the investigation of immune responses by techniques such as ELISA.

I have found some commercially available HA formulations to be inconsistent in terms of quality of composition and structural stability. As measured by ELISA, commercially available recombinant HA frequently lacks an intact HA stem. It is likely these reagents consist of a mixture of HA oligomers and monomers. The structural constraints on soluble HA, that ensure it is transported from the ER to the cell membrane, are less stringent than those for membrane-bound HA [417]. Unlike membrane-bound HA which is targeted for degradation when oligomerised incorrectly, soluble HA can be secreted in varying ratios of monomeric, trimeric or aggregated forms depending on the particular strain of HA [417].

Furthermore detection of low frequency antibodies, such as those directed against HA stem, is limited by assay sensitivity and can be affected by the degree of post-translational modification of the coating recombinant HA. For example, compared to HA produced by an influenza A infected cell, the glycans added to HA produced in cellular expression systems are not desialylated and consequently have a narrower receptor specificity [418].

Enzymatic cleavage of structurally non-essential N-glycans and sialic acid-containing oligosaccharides increases the receptor-binding affinity of HA [419,420]. N-glycans derived from HEK-293 cells are highly branched and occupy a relatively large volume compared to egg or insect cell systems [398]. Reducing the size of these residues downstream of purification could potentially improve recombinant HA antigenicity by unmasking otherwise hidden epitopes. This has considerable implications for the use of these reagents in vaccination studies or the assessment of immune responses as necessary epitope integrity may not always be maintained.

Ideally, immune responses targeting HA need to be assessed against authentic, post-translationally modified HA that accurately mimics either influenza virus and/or vaccine-derived HA antigenically. Routinely studies in academic laboratories are hampered by the lack of commercially available reagents suitable to measure anti-HA responses. The work in this chapter sought to address this need by establishing an in-house system that could be used to rapidly and reliably produce recombinant HA for the assessment of vaccine-induced responses. Additionally, I sought to investigate if this system could be used to produce constructs based solely on the stem domain.

The stem region of HA has not evolved to trimerise as a domain independent of the globular head. Although the production of a HA stem construct has previously been reported in the literature, it was not possible to reproduce a similar HA stem trimer using the HEK-293 system [296,303]. The absence of the globular head exposes hydrophobic residues that are not stable as surface

epitopes. Despite introducing mutations to remove such residues, adding a stabilising trimerisation domain and introducing cysteines to favour inter-monomer bonds - all of which were previously employed to produce a HA stem construct using an E.coli based CFPS method - it was not possible to produce a similar construct, H1HA-Stem, using the HEK-293 system [303]. Although these mutations facilitate correct folding of HA stem trimer, clearly they only do so in the environment of the refold buffer which contains the detergent Brij35 and a pH higher than the ER, ERGIC or CGN of cells [303,421].

An alternative approach to producing recombinant HA constructs suitable for the detection of anti-stem antibodies, chimeric HA, has been previously reported in the literature [294]. Adapting this design method it was possible to produce a chimeric HA protein, cH9/H1, suitable for the detection of anti-stem antibodies. The wild type and chimeric HAs described in this chapter were produced with a removable trimerisation sequence which has been previously used to overcome the production of unstable monomers and induce trimerisation in crystallisation studies [401]. Trimerisation is the final folding step required for complete epitope antigenicity of HA [399]. The recombinant constructs I have produced are largely trimerised and crucially, have proven to be stable over time as assessed by ELISA. Although it may be possible to separate trimeric HA from the formulations commercially available, this is costly and time-consuming.

ELISA based methods are frequently employed as a fast, sensitive and convenient means to quantitate vaccine-induced immune responses. These

assays depend on the availability of suitable protein antigen against which responses are to be assessed. Indeed, the sensitivity and reproducibility of ELISAs is contingent on the quality of antigen available. ELISA based assays currently used to evaluate vaccine-induced immune responses to HA can measure antibodies directed against either the neutral or acid pH conformations of HA, both of which possess unique antibody binding sites only found at that pH [422,423]. However, epitopes generated during the progressive folding of HA cannot be detected and their relevance remains unknown.

The influenza vaccine field has been frustrated by a paucity of tools to investigate immune correlates of protection and a lack of standardisation in assays commonly used to assess immune responses. Although the ELISA is a mainstay assay in the assessment of vaccine induced immune responses, there remains a need to further develop and fully standardise recombinant HA constructs for the assessment of antibody responses. It should also be noted that although the ELISA is frequently used to quantitate antibody responses, it does not assess antibody functionality. Techniques such as microneutralisation assays, pseudotype lentivirus neutralisation assays, haemagglutination inhibition assays (discussed in Chapters 6 and 7) and of course viral challenge studies are appropriate for the assessment of antibody functionality, particularly in terms of virus neutralisation.

3.5. Chapter Summary

- The Expi293™ expression system is an efficient, reproducible and scalable system that can be used for the production of recombinant full-length, wild type and chimeric HA proteins
- Wild type H1HA protein and chimeric cH9/H1 and cH16/H1 maintain a conformational epitope in the stem region that is recognised by a broadly neutralising monoclonal anti-stem antibody, C179, when expressed with a T4 fibritin foldon trimerisation domain. This suggests the presence of this domain does not alter stem antigenicity to such a degree that broadly neutralising epitopes in the stem are lost
- Chimeric HA expressing an antigenically distinct globular head region can be used to measure anti-stem antibodies in samples that have not been previously exposed to the subtype matching the globular head
- It was not possible to produce the stem only constructs Headless-H1HA or H1HA-Stem as recombinant proteins

Chapter 4

Development and Optimisation of Phage Display Methods to Epitope Map Antibody Responses to Haemagglutinin

4. Development and Optimisation of Phage Display Methods to Epitope Map Antibody Responses to Haemagglutinin

4.1. Background

Phage display is a powerful *in vitro* selection technique frequently employed for high throughput identification of high affinity protein-protein or protein-peptide interactions. Phage display libraries (PDLs) were first developed to search for antibody peptide ligands and eventually evolved to express fully conformational proteins [424-426]. By fusing a gene of interest to that of a phage coat protein, phage particles can be produced that display the gene product and contain the gene of interest. This enables individual phage clones to be isolated by an affinity selection step and later identified by sequencing.

Random peptide or gene-fragment phage display libraries (GFPDL) can be used to identify and map immunologically important epitopes. Increasingly in the influenza vaccine field, phage particles are being used to display viral antigens or antibody fragments, such as the fragment antigen-binding (Fab) region or single-chain fragment variable (scFv) regions, and they have been successfully used to delineate vaccine-induced immune responses [194,427-438]. As discussed in Chapter 3, the importance of using tools that are authentic in their representation of conformationally important epitopes to measure immune responses cannot be overstated. In the case of epitopes displayed

by phage particles, structural integrity can be validated by mAbs sensitive only to the folded conformation [424-426].

The filamentous phage, M13, was first used to develop phage display technology 30 years ago and it remains popular today [424]. As a consequence of its non-lytic life cycle, the purification steps between rounds of selection are straightforward and do not expose display molecules to cellular proteases. However, in order for M13 phage particles to assemble, fusion proteins must be transported into the bacterial periplasm where they are incorporated into phage particles [439,440]. This process is sometimes incompatible with native protein folding [439,440].

In this study I have produced a PDL using the commercially available T7Select® system from Novagen®. The T7Select® system is based on the lytic T7 phage which is not dependent on the secretory mechanism that constrains M13 phage technology. Furthermore T7 replicates more rapidly than M13 and plaques can be visualised within 3 hours at 37°C. Functionally, the T7Select® system exploits the capacity of the T7 capsid shell to naturally accommodate variation in a region of the 10B capsid protein displayed on the surface of the phage. Smaller peptides up to approximately 50 amino acids (aa) in size can be displayed at high copy number (415 per phage) while larger peptides or proteins up to 1,200aa can be expressed at either mid (5-15 per phage) or low (0.1-1 per phage) copy number. This feature is particularly useful for the selection of higher affinity interactions as low-valence phage have reduced

avidity [441]. It also enables larger structures to be displayed on the surface of the phage without unwanted intermolecular interactions.

This PDL described in this chapter is representative of frequently recognised antigenic regions of HA from the H1N1 pandemic strain, A/Texas/05/2009 (section 3.2.1), that have been previously reported in the literature [194]. These epitopes are expressed at mid copy number and, as they cover the sequence length of HA, can map vaccine-induced antibody responses to particular regions of interest. In addition, I have further refined the manufacturer's affinity selection protocol in order to eliminate the labour-intensive and time-consuming need to repeatedly pan phage clones (usually needed to eliminate non-specific binding), which has previously been a considerable hindrance of phage technology in terms of reagent consumption and time.

Finally, I have used this library to define the antibody epitope profiles of healthy volunteers over the age of 50 who were previously vaccinated with seasonal trivalent-inactivated influenza vaccine (TIV) or TIV co-administered with the candidate influenza vaccine, MVA-NP+M1. MVA-NP+M1 is a viral vectored vaccine comprising modified vaccinia virus Ankara (MVA), expressing a fusion protein of influenza A nucleoprotein (NP) and matrix protein 1 (M1) [310]. Co-administration of MVA with TIV has previously demonstrated an adjuvanting capacity and adjuvants have been reported to alter the repertoire of antigenic epitopes recognised [194]. This study has sought to investigate if MVA can shape antibody responses to HA, which

could help guide future design of vaccines to target epitopes that might offer broader protection. The results of this screen are reported herein.

4.2. Specific methods

Methods for the development of the PDL are described in section 2.3. The PDL and optimised panning protocols were then used to qualitatively assess human sera samples for antibodies that recognise HA epitopes (section 4.3.3). These sera samples came from participants in a clinical trial previously published by Antrobus *et al*, the details of which are as follows: [442]

Vaccines used: MVA-NP+M1 (MVA expressing NP and M1 antigens from influenza A/Panama/2007/99 as a single fusion protein, described in section 2.4.2.2). TIV (manufactured by Sanofi Pasteur MSD (Lyon, France): single dose contains 15 µg (each) HA of H1N1 (A/California/7/2009), H3N2 (A/Perth/16/2009), and Influenza B (B/Brisbane/60/2008).)

Participants: Healthy volunteers aged 50 years and older.

Vaccination schedule: Volunteers received either TIV (n=8) or co-administered TIV and MVA-NP+M1 (n=9) (same muscle, injection site 1cm apart, vaccines administered within 5 minutes of each other). The protocol was approved by the UK Medicines and Healthcare products Regulatory Agency and the Regional Ethics Committee, and registered at www.clinicaltrials.gov (NCT00942071).

Samples available: Sera collected 21 days after vaccination. Data on fold change in IgG anti-TIV titres from enrolment to 21 days after vaccination was previously published by Antrobus *et al*. [442]

4.3. Results

4.3.1. Generation of Recombinant T7 Phage Expressing HA Epitopes

The T7 Select10-3b vector accommodates peptides or proteins up to 1,200 amino acids (aa) in size at mid copy number (5-15 per phage). Thirteen overlapping antigenic regions spanning the length of the sequence of HA were used to generate a T7 PDL (Fig. 4.1). These regions were previously identified using an M13 PDL and are recognised frequently by human sera [194]. They were chosen in order to enable antibody responses to be mapped along the length of HA and in particular to delineate antibody responses directed against either the globular head or HA stem [194]. These regions ranged from 16 to 96 aa in length and were representative of H1HA from A/Texas/05/2009 GeneBank: ACR19260.1 (Table 4.1).

Figure 4.1 Distribution of antigenic regions of HA displayed on T7

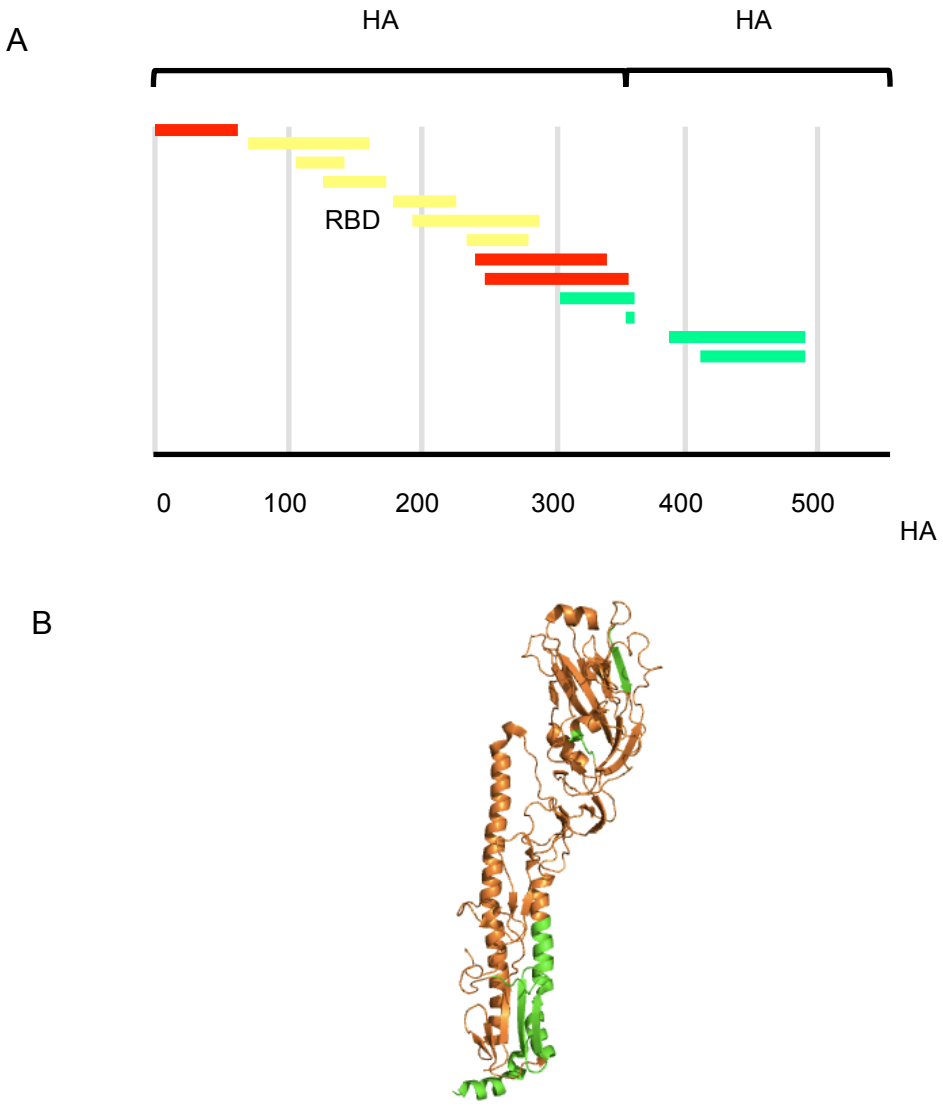


Figure 4.1 Distribution of antigenic regions of HA displayed on T7

Linear representation of antigenic regions based on the HA protein sequence from H1N1 A/Texas/05/2009 GeneBank: ACR19260.1. Red represents antigenic regions within HA1 but not the receptor-binding domain (RBD). Yellow represents regions within the RBD. Green indicates antigenic HA2 regions. (B) Structural representation of antigenic regions mapped to a HA monomer that are displayed (orange) or not displayed (green) by the PDL. RBD = receptor-binding domain.

Table 4.1 HA epitope sequences displayed on T7

Region	Sequence	Peptide sequence
HA1	1-68	MKAILVVLLYTFATANADTLCIGYHANNSTDTVDT VLEKNVTVTHSVNLLEDKHNGKLCKLRGVAPLH
RBD/HA1	75-165	AGWILGNPECESLSTASSWSYIVETSSSDNGTCY PGDFIDYEELREQLSSVSSFERFEIFPKTSSWPN HDSNKGVTAACPHAGAKSFYKNL
RBD/HA1	108-144	YPGDFIDYEELREQLSSVSSFERFEIFPKTSSWP NHD
RBD/HA1	120-175	EQLSSVSSFERFEIFPKTSSWPNHDSNKGVTAAC PHAGAKSFYKNLIWLVKKGNSY
RBD/HA1	182-220	YINDKGKEVLVLWGIHHPSTSADQQSLYQNADAY VFVGS
RBD/HA1	197-286	HHPSTSADQQSLYQNADAYVFVGSSRYSKKFKP EIAIRPKVRDQEGRMNYYWTLVEPGDKITFEATG NLVVPRYAFAMERNAGSGIIISD
HA1	235-281	PKVRDQEGRMNYYWTLVEPGDKITFEATGNLVV PRYAFAMERNAGSG
HA1	239-335	DQEGRMNYYWTLVEPGDKITFEATGNLVVPRYA FAMERNAGSGIIISDTPVHDCNTTCQTPKGAINTS LPFQNIHPITIGKCPKYVKSTKLRLATGL
HA1	239-354	NTTCQTPKGAINTSLPFQNIHPITIGKCPKYVKSTK LRLATGLRNVPSIQSRGLFGAIAGFI
HA2	302-356	AINTSLPFQNIHPITIGKCPKYVKSTKLRLATGLRN VPSIQSRGLFGAIAGFIEG
HA2	341-356	IQSRGLFGAIAGFIEG
HA2	394-489	NKVNSVIEKMNTQFTAVGKEFNHLEKRIENLNKK VDDGFLDIWTYNAELLVLLENERTLDYHDSNVKN LYEKVRSQLKNNAKEIGNGCFEFYHKCD
HA2	410-489	VGKEFNHLEKRIENLNKKVDDGFLDIWTYNAELL VLLENERTLDYHDSNVKNLYEKVRSQLKNNAKEI GNGCFEFYHKCD

4.3.2. Optimisation of a Novel Panning Strategy

Traditional phage display methods rely on sequential rounds of panning to overcome non-specific binding. Typically this involves several consecutive cycles of incubation of a PDL with a target of choice, washing, amplification and reselection of previously bound phage to enrich for true binders. The process is labour-intensive and consumes considerable quantities of test sera – a substantial limitation to using this technology in the assessment of valuable clinical samples. In order to circumvent this issue, I adapted the manufacturers recommended panning protocol. The original protocol advised a minimum of four rounds of panning or until no further increases in the number of phage recovered are observed. I reduced this to a single-screen procedure using a combination of additional extensive wash steps and a blocking agent (sections 4.3.2.1 and 4.3.2.2). The final working protocol is outlined in section 2.8.2.

4.3.2.1. Wash Buffer Optimisation

Three random phage pools expressing different HA epitopes and an S-tag expressing pool were used to investigate the effect of using either Tween® 20 (a polysorbate surfactant with a fatty acid ester moiety and a long polyoxyethylene chain) or Triton™ X-100 (a nonionic surfactant with a hydrophilic polyethylene oxide chain and an aromatic hydrocarbon lipophilic group) to reduce non-specific binding of phage to an anti-S-tag monoclonal antibody. S-tag phage display a 15-residue peptide (KETAAAKFERQHMDS; derived from pancreatic ribonuclease A) recognised by an anti-S-tag mAb and were used as a positive control. The three pools expressing HA epitopes

should not be recognised by the anti-S-tag mAb. The wash conditions that reduced non-specific binding between the phage expressing HA epitopes and the anti-S-tag mAb were deemed optimal.

0.05% PBS/T, a 0.05% (v/v) solution of the detergent Tween® 20 in PBS, is the wash buffer recommended by the T7Select® system. It was reasoned that Triton™ X-100, a similar but stronger non-ionic detergent, might be a more powerful detergent to reduce non-specific binding without denaturing phage surface proteins. Both detergents are mild surfactants that break protein-lipid, lipid-lipid associations, but not protein-protein interactions and are frequently used in the isolation of membrane proteins owing to their ability to retain protein interactors and native and active forms [443].

Phage were washed ten times as per manufacturer's protocol using 0.05% PBS/T or for 2h with either 0.5/1% PBS/T or 0.1/0.5% PBS/Triton™ X-100. Bound phage clones were subsequently eluted and titered (sections 2.8.2 and 2.3.1.2). Fewer non-specific phage were recovered in groups washed with 0.5% PBS/Triton™ X-100 indicating that Triton™ X-100 was preferable to Tween® 20 as a washing agent for the reduction of non-specific binding (Fig. 4.2).

Figure 4.2 Comparison of detergent Tween® 20 with Triton™ X-100

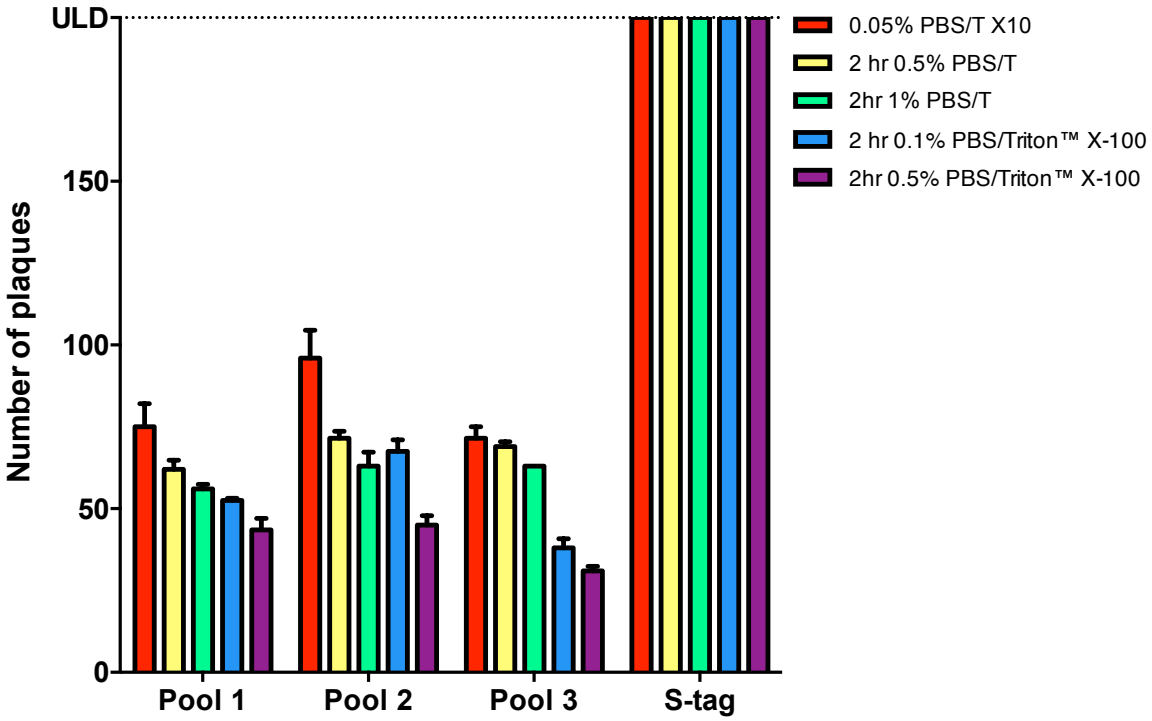


Figure 4.2 Comparison of detergent Tween® 20 with Triton™ X-100

Triton™ X-100 greater reduces non-specific phage binding compared to Tween® 20. Plates were coated with 10µg/mL anti-S-tag mAb and binding of four different phage pools ($1x10^8$ pfu/mL each) was investigated. Plates were washed according to manufacturer's instructions (ten times in 0.05% PBS/T) or for two hours with 0.5% and 1% PBS/T and 0.1% and 0.5% PBS Triton X-100. Bound phage clones were eluted in 1% SDS in PBS and plated at a 10^{-2} dilution. Data are means ± SD. These data are representative of two independent experiments. ULD = upper limit of detection.

Taking forward Triton™ X-100 as the preferred wash agent, further conditions were examined to determine the optimum concentration of PBS/Triton™ X-100 and investigate if increasing the number of wash steps would reduce non-specific binding. As expected, concentrations of Triton™ X-100 above the critical micelle concentration (~0.24mM) did not further reduce non-specific binding however, non-specific binding was further reduced using 1% (v/v) PBS/Triton™ X-100 and this was taken forward as the optimum wash buffer (Fig. 4.3). The number of wash steps was extended and an overnight step included. Increasing the number of wash steps from one to three marginally reduced non-specific binding however the overnight wash made no significant difference and was included in the final protocol as an optional step for convenience (Fig. 4.4).

Figure 4.3 Influence of PBS/Triton™ X-100 wash buffer concentrations on non-specific binding

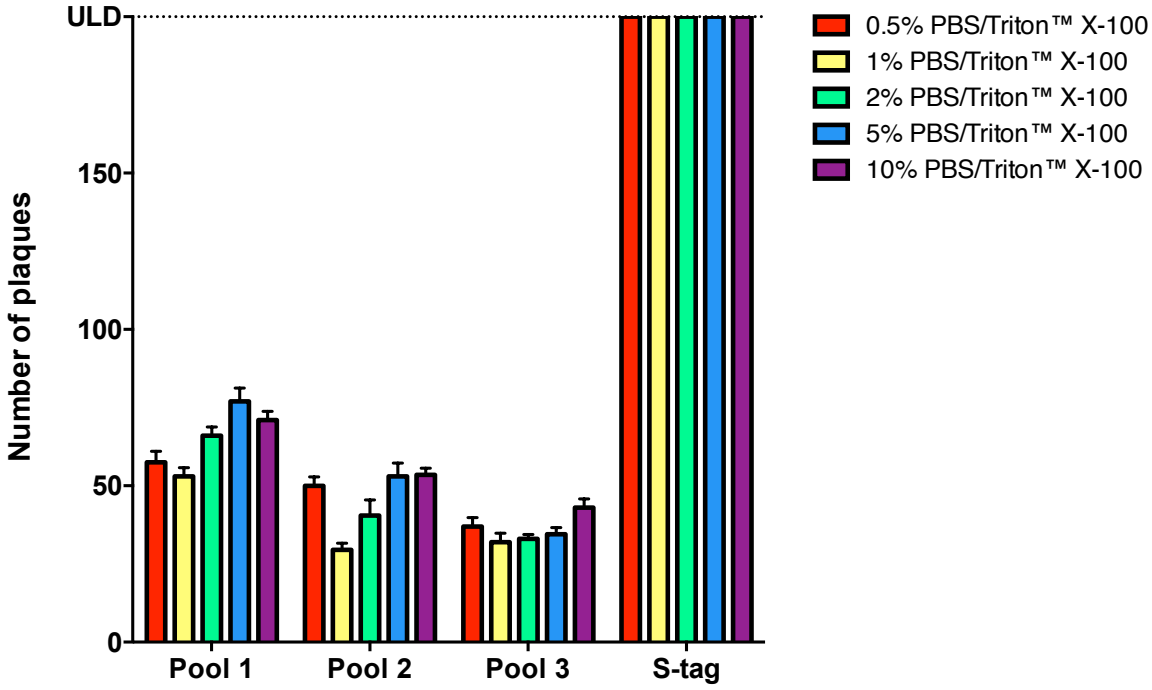


Figure 4.3 Influence of PBS/Triton™ X-100 wash buffer concentrations on non-specific binding

A 1% concentration of Triton™ X-100 in PBS is the optimum detergent concentration to reduce non-specific binding. Plates were coated with 10µg/mL anti-S-tag mAb and binding of four different phage pools ($1x10^8$ pfu/mL each) was investigated. Plates were washed for 2h at room temperature with 0.5-10% PBS/Triton™ X-100. Bound phage clones were eluted in 1% SDS in PBS and plated at a 10^{-2} dilution. Data are means ± SD. These data are representative of two independent experiments. ULD = upper limit of detection.

Figure 4.4 Determination of optimum wash step number

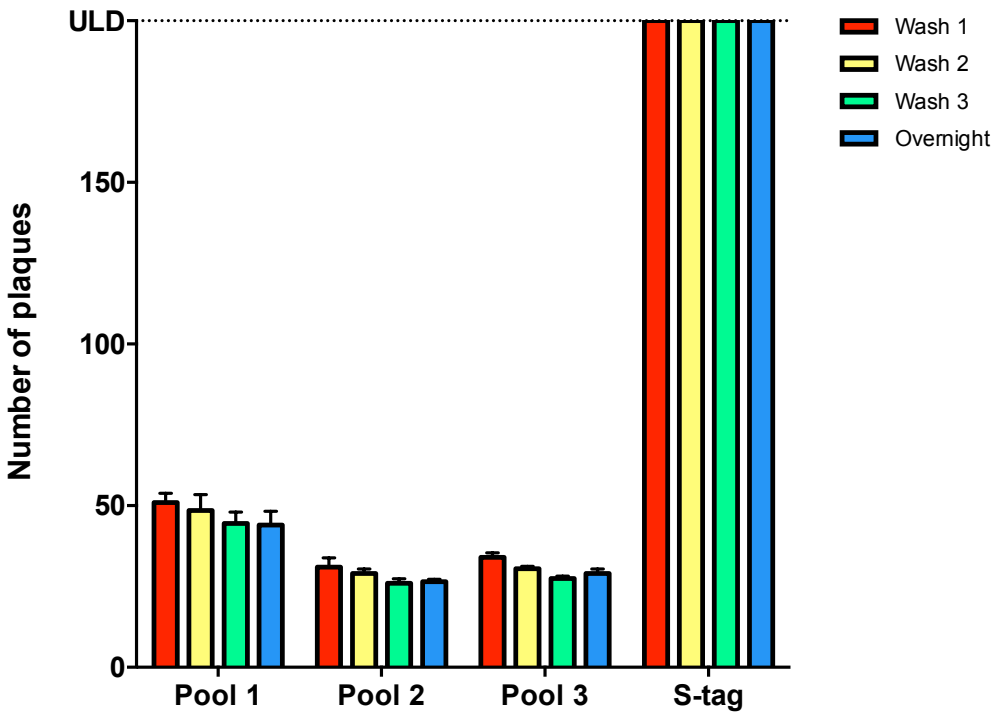


Figure 4.4 Determination of optimum wash step number

Increasing the number of wash steps reduces non-specific binding. Plates were coated with 10µg/mL anti-S-tag mAb and binding of four different phage pools ($1x10^8$ pfu/mL each) was investigated. Plates were washed with 1% PBS/Triton™ X-100 between one and three times for 2h at room temperature and overnight at 4°C on a shaker. Bound phage clones were eluted in 1% SDS in PBS and plated at a 10^{-2} dilution. Data are means ± SD. These data are representative of two independent experiments. ULD = upper limit of detection.

4.3.2.2. Investigation of a Blocking Agent

A solution of 1% casein in PBS, commonly used to block non-specific binding in ELISAs, was used to investigate if non-specific interactions with phage coat proteins could be similarly blocked prior to panning. Results demonstrated pre-incubation of phage clones for 2h at room temperature before incubation with sera almost abrogated non-specific interactions (Fig. 4.5). The final assay protocol was modified to include this step (section 2.8.2).

Figure 4.5 Phage pre-incubation with casein

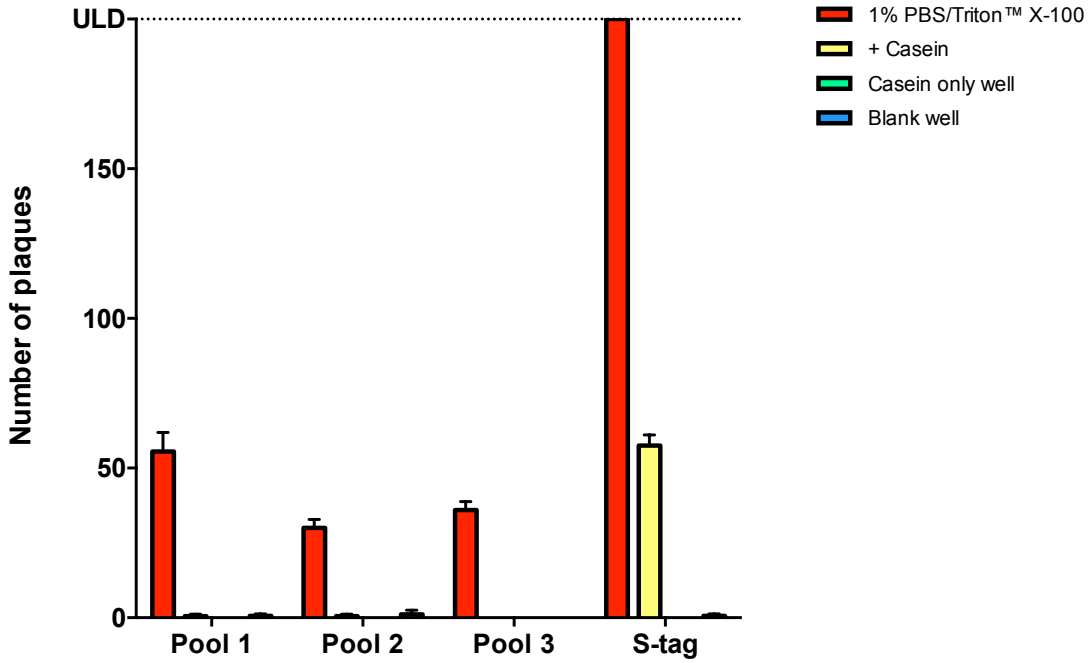


Figure 4.5 Phage pre-incubation with casein

Phage pre-incubation with casein significantly reduces non-specific binding. Phage clones were incubated for 2h in 1% casein in PBS (w/v) (1:1) prior to panning. Plates were washed three times with 1% PBS/Triton™ X-100 for 2h at room temperature and overnight at 4°C on a shaker. Bound phage clones were eluted in 1% SDS in PBS and plated at a 10^{-2} dilution. Data are means ± SD. These data are representative of two independent experiments. ULD = upper limit of detection.

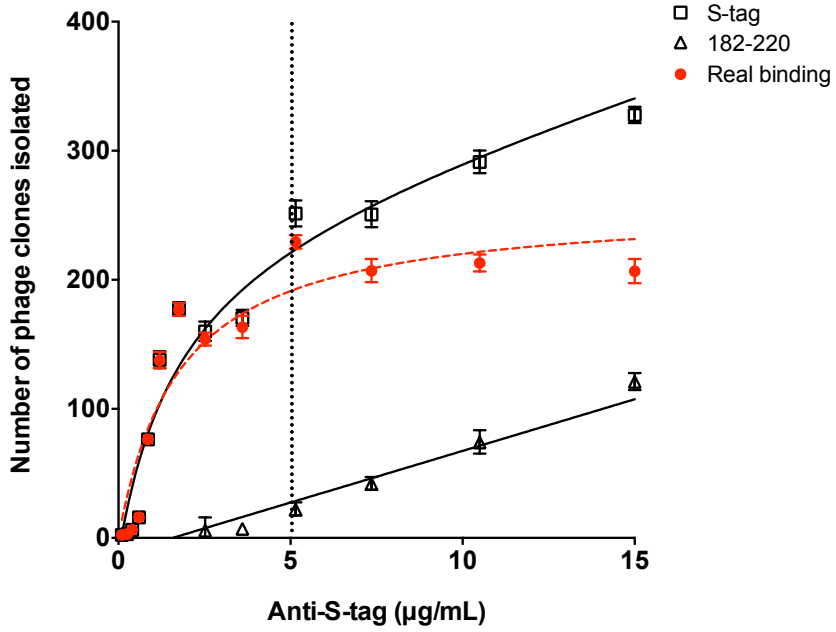
4.3.2.3. Determination of Assay Detection Limits

The final protocol (section 2.8.2) was tested using two mAbs to establish the detection range for this assay. Approximately 0.01% of circulating immunoglobulin (Ig) in the general population has heterosubtypic binding activity to HA stem from Group 1 and Group 2 HA [444]. Between 0.1-1µg can be can be isolated per 100mg intravenous Ig [444]. Assuming normal human sera contains typically 10 mg/mL IgG, I estimated that concentrations of anti-stem Ab above 0.1 µg/ml could be present in vaccinated individuals.

Briefly, S-tag expressing phage clones were titrated against an anti-S-tag mAb (0.1-15µg/mL) capable of detecting as little as 1ng S-tag fusion protein (Fig. 4.6 A). A separate phage clone pool expressing the peptide 182-220 was also titrated against a reciprocal mAb (swine H1N1 haemagglutinin antibody; Aviva Systems Biology) (0.1-20µg/mL) raised against a peptide within this region (Fig. 4.6 B). This mAb had a lower affinity but could be used to detect as little as 10ng peptide (Fig. 4.6 B). Specific binding events were detected between 0.1-5 µg/mL for high affinity antibodies (Fig. 4.6 B). Weaker affinity interactions could not be detected below 0.3µg/mL (Fig. 4.6 B).

Figure 4.6 Titration of mAb using S-tag and HA epitope-decorated phage clones

A



B

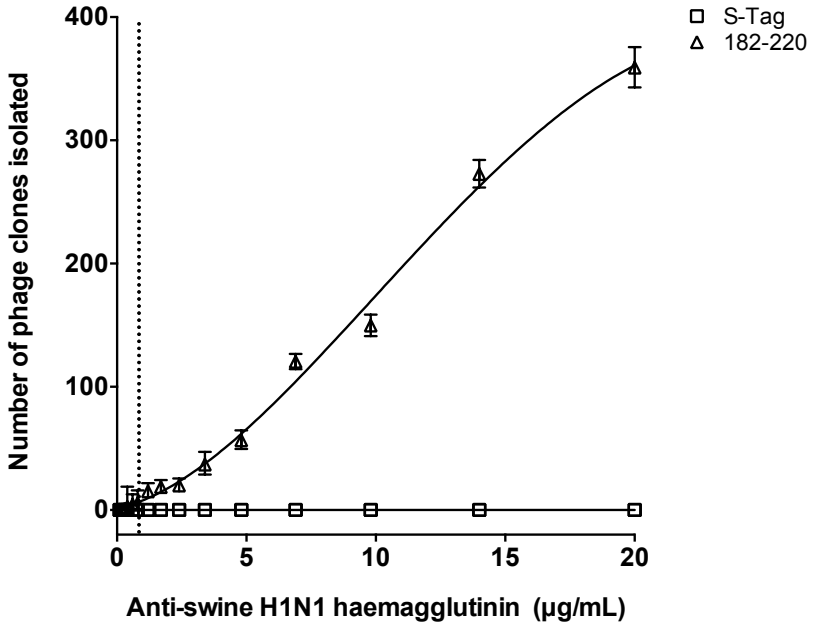


Figure 4.6 Titration of mAb using S-tag and HA epitope-decorated phage clones

(A) S-tag phage clones ($1x10^8$ pfu/mL) were panned against 0.1-15µg/mL anti-S-tag mAb. (B) The epitope recognised by swine H1N1 haemagglutinin antibody is within the sequence 182-220. Phage clones displaying this epitope ($1x10^8$ pfu/mL) were panned against 0.1-20µg/mL swine H1N1 haemagglutinin antibody. A phage pool expressing an irrelevant epitope was included to control for non-specific binding. Specific binding was determined by subtraction. The anti-S-tag mAb did not bind any 182-220 clones. The black dotted line demarcates regions of specific binding. Data are geometric means with 95% confidence interval. These data are representative of three independent experiments.

Key findings:

Optimised conditions for washing in the PDL assay involved use of Triton™ X-100 at 1%. Blocking with casein ameliorated the need for multiple biopanning steps.

4.3.3. Assessment of Antibody Epitope Profiles in Vaccinated Individuals Over 50

The PDL and optimised panning protocols detailed in this chapter were developed to qualitatively assess human sera samples for antibodies that recognise HA epitopes. Serum donors were volunteers aged 50 years and above who participated in a phase I safety clinical trial safety to compare the co-administration of TIV and the candidate influenza vaccine MVA-NP+M1 (n=9) with TIV alone (n=8) [442]. Preclinical studies previously demonstrated MVA-NP+M1 could act as an adjuvant when co-administered with TIV and enhanced antibody responses to HA[374]. The seasonal influenza vaccine administered was a split virion vaccine manufactured by Sanofi Pasteur MSD (Lyon, France). A 0.5mL dose comprised 15µg HA of H1N1 (A/California/07/2009), H3N2 (A/Perth/16/2009), and Influenza B (B/Brisbane/60/2008) [442].

Antibody responses to the HA strains included in the vaccine were previously assessed at baseline and 21-days post-vaccination for haemagglutination-inhibition (HI) capacity [442]. The fold change in the geometric mean titer (GMT) (the geometric mean ratio; GMR) for the H1N1 strain more than doubled between samples at day 0 and day 21 in both groups (GMR, control group = 4, GMR, co-administration group = 10.5) [442]. Sera collected 21 days after vaccination were screened by phage display to assess the specificity of anti-HA antibodies.

Following vaccination with seasonal influenza alone, a total of 329 phage clones (representative of three individual experiments) were captured by immune sera, of which 278 mapped to HA1 and 51 to HA2. Sera from the co-administration group bound a total of 276 phage clones of which 227 mapped to HA1 and 49 mapped to HA2. In each arm, sera predominantly bound HA epitopes in the HA1 region spanning the RBD and a similar number of HA2 clones were isolated from both groups (Fig. 4.7). The ratio of HA1 to HA2 clones was 1.2-fold higher in the control group compared to the group vaccinated with TIV and MVA-NP+M1 (5.56 and 4.63 respectively) (Table 4.2). These ratios are much higher compared to those reported in adults vaccinated with non-adjuvanted (HA1/HA2=0.175) or MF59® adjuvanted (HA1/HA2=1.543) subunit H1N1 vaccines [194].

No correlation was observed between the number of HA1 clones, HA2 clones or total clone numbers and anti-TIV ELISA titers 21 days post-vaccination for individuals from either group (Table 4.3). Similarly, no correlation was observed between the number of HA1 clones isolated and individual haemagglutination-inhibition (HI) titers against A/California/07/09 measured at the same time point (Table 4.3). As only anti-HA1 antibodies are detected by haemagglutination-inhibition assay (HAI), HA2 clone numbers were omitted from the analysis of HI titers. In both vaccination groups a strong positive correlation ([p=0.0006, r=0.9701;TIV] and [p=0.0001, r=0.9707;TIV and MVA-NP+M1]) was observed between the number of HA1 and HA2 clones detected and the total number of all clones captured.

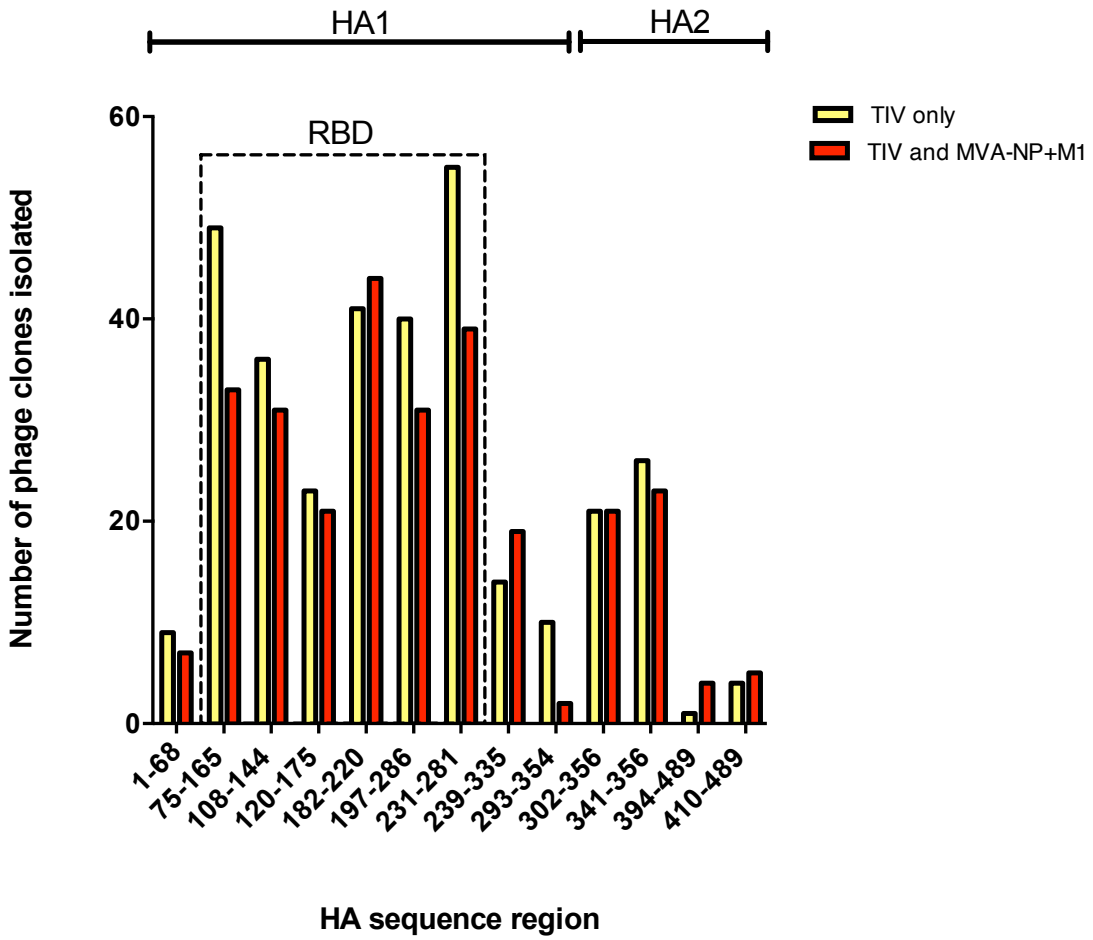


Figure 4.7 Distribution of HA peptides recognised by vaccinated adult sera identified by panning with H1N1 PDL

Amino acid designation is based on the HA protein sequence from H1N1 A/Texas/05/2009 GeneBank: ACR19260.1. Peptides spanning the RBD within HA1 (between positions 131 and 219) are enclosed within the dotted box. These data are representative of three independent experiments. RBD = receptor-binding domain.

Table 4.2 Phage clone distribution following affinity selection by vaccinated sera

Serum sample	Number of eluted phage clones			HA1/HA2
	Total	HA1	HA2	
TIV	329	278	50	5.56
TIV and MVA-NP+M1	276	227	49	4.63

Table 4.3 Correlations between phage clone distribution and antibody responses.

		TIV				TIV + MVA-NP+M1			
Eluted phage clones	Measurement	n	p value	r	Significance	n	p value	r	Significance
HA1 & HA2	Anti-TIV antibodies	8	0.1180	-0.5988	No	9	0.1938	-0.4833	No
HA1	Anti-TIV antibodies	8	0.1710	-0.5476	No	9	0.2626	-0.4100	No
HA2	Anti-TIV antibodies	8	0.0913	-0.6347	No	9	0.2798	-0.3950	No
HA1	Total number of plaques	8	0.0006	0.9701	Yes	9	0.0001	0.9707	Yes
HA2	Total number of plaques	8	0.0012	0.9518	Yes	9	0.0154	0.7899	Yes
HA1	HI titer	8	0.5460	0.2546	No	9	0.9861	0.01271	No

Table 4.3 Correlations between phage clone distribution and antibody responses. The relationships between the total number of phage clones and the number of HA1 or HA2 clones isolated from individuals was assessed against anti-TIV ELISA titers and HI titers, measured against A/California/07/2009, 21 days post-vaccination with TIV or TIV co-administered with MVA-NP+M1. Spearman's rank correlation coefficient (r), two-tailed p values and sample size (n) are shown.

Key findings:

The PDL described in this chapter can be used to map antibody responses against HA to specific epitopes. Vaccination with TIV co-administered with MVA-NP+M1 induces a slightly higher ratio of antibodies recognising the HA2 epitopes in this library among volunteers over 50 years. Higher HA2 and HA1 responses were observed in individuals with higher total plaque numbers overall.

4.4. Discussion

Influenza vaccines remain the primary public heath tool against influenza infection and disease in human populations. The emergence and rapid spread of the 2009 pandemic H1N1 virus underscored the need for more effective, cross-protective vaccines capable of protecting against seasonal and pandemic strains. HA-specific neutralising antibodies have been regarded as the major correlate of protection against infection for the past 70 years [235]. However, the only universally accepted measure of protection used to license influenza vaccines is the haemagglutination-inhibition assay (HAI), an assay that is limited to detecting HA1 responses only [316].

In recent years there has been a growing interest in broadly neutralising heterosubtypic antibodies targeting the conserved HA2 stem region of HA. These antibodies are increasingly being identified in human sera and their induction is a major goal of vaccination [290,295,423,432,445-455]. However, there remains a lack of validated methods to measure anti-stem responses. In this chapter I have described the development and optimisation of a H1N1 PDL to qualitatively assess and delineate antibody responses to HA.

Protective HA-specific neutralising antibodies are typically conformation-sensitive. The HA epitopes represented in this library are assumed to be largely discontinuous and therefore, conformational, (with the exception of the smallest peptide (341-356) which is likely to be linear) on account of their precise and frequent selection by human sera previously tested against a genome fragment PDL [194]. Unfortunately, mAbs, the conventional tools used

to test epitope conformation, were not available to test the epitopes in this library directly. However, as all epitopes were recognised by sera obtained from a phase I clinical trial I have concluded this PDL can be used reliably to qualitatively epitope map antibody responses to HA.

A limitation of the phage display method outlined in this chapter is the lower limit of detection (0.1µg/mL). HA2 antibody responses in particular are known to circulate at extremely low frequencies in the general population, sometimes at levels below the threshold of this assay [444]. Additionally, anti-stem antibodies in pre-clinical samples must also be above this level in order to be detected. Although the assay has been specifically optimised to reduce sera volume requirements, 50µL is required per screen - a relatively large volume to consider for mouse studies.

The H1N1 PDL described in this chapter was used to characterise the antibody responses of individuals from a phase I trial to compare the co-administration of TIV and the candidate influenza vaccine MVA-NP+M1 with TIV alone. MVA-NP+M1 is a viral-vectored vaccine previously shown to have an adjuvanting effect increasing some influenza strain-specific antibody responses when co-administered alongside TIV [442]. MF59® (Novartis) and alum are currently the only adjuvants licensed for seasonal influenza vaccination in Europe and the US, respectively. The co-administration of MF59® with pandemic influenza vaccines has been shown to enhance antibody responses against HA1 [194]. The results in this study indicate that co-administration of MVA-NP+M1 with TIV does not skew antibody responses

towards HA1 anymore than vaccination with TIV alone. Furthermore, although fewer phage clones were isolated by sera from the co-administration group, there was a trend towards greater HA2 responses in these samples. However the strong correlation between total number of responses and the number of responses against HA1 or HA2 in both groups suggests that the higher number of anti-stem responses in some individuals is a consequence of an overall greater state of immune activation induced by non-specific means. A much larger sample size would be needed to further explore these trends.

An interesting question that has not been addressed in this study is what effect MVA-NP+M1 has on the affinity of antibodies generated after vaccination. Acute viral infections such as seasonal influenza A are frequently cleared before high-affinity antibodies can develop. Lower affinity antibodies, in particular low-affinity anti-stem antibodies, have the potential to form pathogenic immune complexes which can enhance viral infection [110,437,456]. MF59® is known to increase antibody affinity when co-administered with pandemic influenza vaccines by inducing early $CD4^+$ T cell responses and increasing the rate of somatic hypermutation [194,457]. The enhancement of HA1-specific antibodies by MF59® is believed to be due to different activation thresholds of naïve HA1 and memory HA2 B cells [194]. It remains to be seen if vaccination with MVA-NP+M1 can significantly augment the production and affinity of HA2 antibodies and this should be investigated in future larger studies using techniques such as surface plasmon resonance (SPR).

4.5. Chapter Summary

- PDLs can be used to delineate antibody responses to specific antigenic regions containing epitopes
- This chapter describes the design and development of a T7 PDL expressing 13 antigenic regions of HA from A/Texas/05/2009, and the optimisation of a novel biopanning protocol
- This library can be used to differentiate antibody responses to the HA1 (globular head) and HA2 (stem) region of HA
- Adjuvants can skew antibody responses towards specific protein domains
- MVA adjuvants antibody responses when co-administered with TIV and induces a higher ratio of HA2 to HA1 antibodies compared to vaccination with TIV alone

Chapter 5

Investigation of Circulating T Follicular Helper-Like Cells as Correlates of Immunity to Influenza

5. Investigation of Circulating T Follicular Helper-Like Cells as Correlates of Immunity to Influenza A

The work described in this chapter was part of a collaboration between Claire Tully, Dr Teresa Lambe and Prof Sarah Gilbert (The Jenner institute, University of Oxford), and Prof Persephone Borrow and Dr Cecilia Chui (Nuffield Department of Medicine, University of Oxford).

The cell surface marker staining panel for T_{FH}-like cells was developed by Dr Cecilia Chui (section 2.8.7). All flow cytometry experiments and data analysis were performed by Claire Tully.

5.1. Background

Currently licensed seasonal influenza vaccines rely primarily on the induction of strain-specific neutralising antibodies for protective efficacy [179]. Indeed the vast majority of current human vaccines against infectious disease mediate protection by way of long-lived humoral memory responses [458]. Yet the precise immunological events that generate protective antibody responses in the context of vaccination remain unclear.

T cell help to B cells is a fundamental feature of adaptive immunity in mammals [459-461]. It is vital for the germinal centre (GC) reaction, which is principally responsible for the generation of high affinity, class-switched antibodies and ultimately, B cell memory [462-464]. In fact, protective vaccine-induced responses are almost always T cell-dependent [465]. For decades Type 2 T helper (T_H2) cells were thought responsible for B cell help due to the prevailing T_H1-T_H2 hypothesis and their ability to produce IL-4, a key mediator of isotype switching and antibody secretion [197]. However, several seminal studies demonstrating humoral responses in mice deficient in key T_H2 genes questioned their involvement [466,467]. T follicular helper (T_{FH}) cells, a distinct $CD4^+$ T cell subset capable of homing to lymphoid follicles and inducing antibody production, were later proposed as specialised helpers of B cells [468-470].

In humans, the T_{FH} cell subset was originally defined by high expression of CXCR5 in lymphoid tissues [468-470]. CXCR5 is a chemokine receptor which enables CXCL13-mediated homing of cells to B cell follicles and GCs in

secondary lymphoid organs (SLO) [470,471]. In addition to CXCR5, T_{FH} cells are also now commonly identified by their expression of inducible T cell co-stimulator (ICOS), programmed cell death protein 1 (PD-1), IL-21 and the transcription factor B cell lymphoma 6 (Bcl-6) [472-476]. Indeed Bcl-6 is considered the 'master regulator' of T_{FH} differentiation and is expressed by activated T_{FH} cells [475,476]. Furthermore, all other T_H subsets express B lymphocyte-induced maturation protein-1 (Blimp-1), an antagonist of Bcl-6 which blocks T_{FH} differentiation [477].

As the field of T_{FH} cell biology has only recently emerged several variations of the definition of a T_{FH} cell currently exist [478]. For the purposes of this study, I have taken *bona fide* T_{FH} cells to be $CD4^+CXCR5^+Bcl\text{-}6^+$ cells within the follicle which may or may not be localised to the GC and function primarily to help B cell responses [478]. Interestingly, a number of studies are beginning to reveal the vast heterogeneity of cells that are capable of migrating to follicles and supporting antigen-specific B cell differentiation within the $CD4^+$ T_H cell subset. In addition to *bona fide* T_{FH} cells, several unconventional T_{FH} subsets have been described in mouse models, such as extrafollicular T_H cells, follicular helper NKT (NKT_{FH}) cells and follicular T regulatory (T_{FR}) cells [479-481]. Even a population of γδ T_{FH} cells has been reported in human blood and SLO tissue [482]. Furthermore, there appears to be overall a large degree of plasticity within T_{FH} populations. For example murine memory T_{FH} cells, have the capacity to differentiate into T_{FH} cells or be recalled into one of the conventional T_H cell compartments [205]. Indeed these cells are able to provide more efficient help than their non-T_{FH} counterparts and they can also

differentiate from canonical memory T cells [483,484]. This flexibility within T_{FH} populations has important consequences for humoral responses. Cytokines typically associated with T_H1, T_H2 and T_H17 T helper subsets can be produced by *bona fide* T_{FH} cells and differentially regulate isotype-switching [205,477,485-487]. While these studies suggest there is a large degree of flexibility within T_{FH} populations the exact molecular details of any inter-subset plasticity remain enigmatic.

In humans approximately 20% of circulating $CD4^+$ memory T cells express $CXCR5^+$ [488,489]. These cells share functional properties with T_{FH} cells and are thought to represent a circulating component of central T_{FH} cell memory. Recently, it has been proposed that circulating memory T_{FH} cells can be divided into nine subsets comprising efficient ($T_{FH}2$ or $T_{FH}17$) or non-efficient ($T_{FH}1$) helpers on the basis of ICOS, PD-1, CCR7, CXCR3 and CCR6 expression (Fig. 5.1) [490]. $T_{FH}1$ cells ($CXCR3^+CCR6^-$) are considered the least effective providers of B cell help as they lack the capacity to help naïve B cells [490,491]. Of particular relevance for influenza vaccine development, $T_{FH}1$ cells have been shown to be induced following vaccination with seasonal trivalent split-virus influenza vaccine and their appearance has been shown to correlate with an increase in pre-existing antibody titers but not primary B cell responses [491]. Seasonal influenza vaccine efficacy is notoriously poor even when vaccines are strain-matched and it is plausible this may be in part due to the induction of the qualitatively poorer $T_{FH}1$ cell subset that is unable to help naïve B cells.

Vaccination strategies that induce cells capable of providing robust help to B cell effector function and are capable of priming naïve B cells could be particularly useful for the development of vaccines aimed at children with no pre-existing immunity or novel pandemic strains. While as yet, no studies have been reported in the literature describing the induction of efficient $T_{FH}2$ ($CXCR3^-CCR6^-$) or $T_{FH}17$ ($CXCR3^-CCR6^+$) cells following vaccination against influenza, a study of HIV-infected individuals has demonstrated a greater frequency of highly functional memory $T_{FH}2$ or $T_{FH}17$ cells in individuals capable of producing broadly neutralising antibodies (bnAbs) [492]. Most anti-HIV bnAbs are highly somatically mutated and have undergone extensive affinity maturation in the GC requiring considerable functional T_{FH} cell help [493,494]. Although bnAbs against the stem domain of HA appear to evolve with relatively fewer somatic mutations than bnAbs against HIV, functional T_{FH} help is critical for their generation and selectively targeting the most efficient T_{FH} cell subsets with vaccines could augment the development of such responses [495].

Characterising the T_{FH} cell subsets that appear in the blood post-vaccination might also be a useful predictor of subsequent humoral responses and vaccine efficacy. To date, two studies have reported distinct populations of circulating T_H cells differing in their expression of CXCR5 which have functional properties similar to T_{FH} cells and are useful predictors of antibody responses following vaccination [491,496]. On the basis of these reports I have investigated the phenotypic profile of circulating T_{FH}-like cells (defined in this study as subsets of $CD4^+$ T cells differing in their expression of CXCR5,

CXCR3 and CCR6) induced in healthy volunteers over the age of 50 who were previously vaccinated with TIV or TIV co-administered with the candidate influenza vaccine, MVA-NP+M1 (Fig. 5.2). MVA-NP+M1 is a viral-vectored vaccine comprising modified vaccinia virus Ankara (MVA), expressing a fusion protein of influenza A nucleoprotein (NP) and matrix protein 1 (M1) [310]. Initial investigation of vaccine-induced antibody responses within these samples by a former student at the Jenner Institute indicated a trend towards a higher median fold increase in antibody responses against TIV in the co-administration arm post-vaccination (Fig. 5.3) [442]. As vaccination with TIV alters the composition of the $CXCR5^{+}CD4^{+}$ T cell subset in the blood and is associated with the induction of non-efficient B cell helpers, I hypothesised that the differences observed in antibody titers in the co-administration arm may be due to subtle variations of T_{FH}-like cell subsets induced following vaccination. The results of this study are reported herein.

Figure 5.1 Circulating memory T_{FH} cell subsets

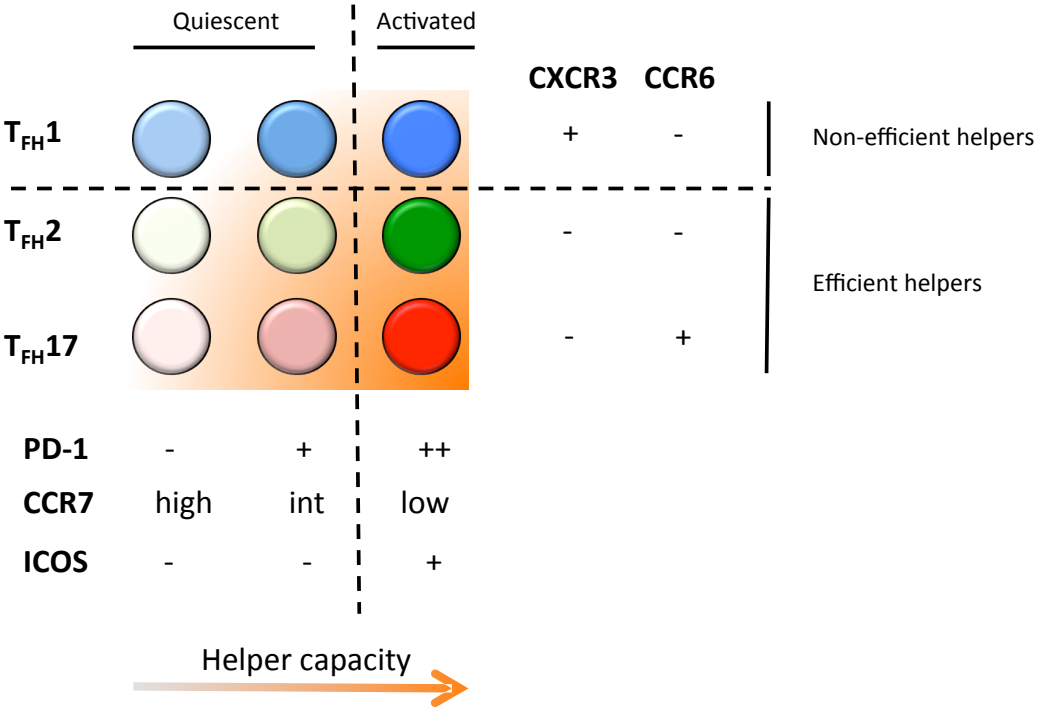


Figure 5.1 Circulating memory T_{FH} cell subsets

Human memory T_{FH} cells in the blood can be divided phenotypically into nine subsets. CXCR3 and CCR6 delineate efficient ($T_{FH}2$ and $T_{FH}17$) from inefficient ($T_{FH}1$) B cell helpers. ICOS expression determines the activation state of the cells. Quiescent populations are described by PD-1 and CCR7 expression. Background colour intensity indicates helper capacity. This figure has been adapted from Schmitt *et al* [490]

Figure 5.2 Circulating T_{FH}-like cell subsets as defined in this study

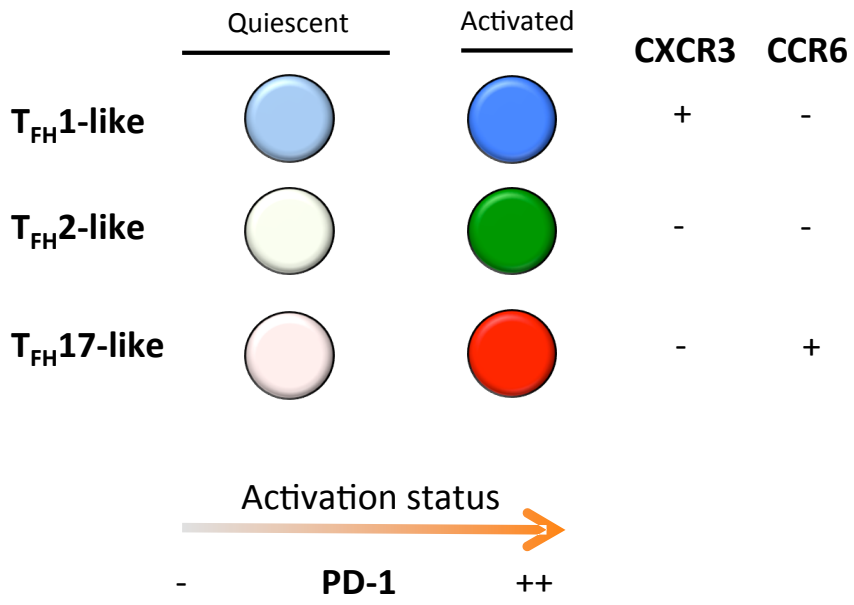


Figure 5.2 Circulating T_{FH}-like cell subsets as defined in this study

CXCR3 and CCR6 can be used to delineate efficient ($T_{FH}2$ and $T_{FH}17$) from inefficient ($T_{FH}1$) B cell helpers (Bcl-6^+, IL-21^+ $CD4^+$ T cells). In this study these markers were used to define populations of circulating $CD4^+CXCR5^+$ and $CD4^+CXCR5^-$ T cells as $T_{FH}1$-like, $T_{FH}2$-like or $T_{FH}17$-like. $CXCR5^+$ and $CXCR5^-$ populations were examined as both have been reported in the literature to correlate with antibody responses following influenza vaccination. Activated cells were defined as those with high relative PD-1 expression.

Figure 5.3 Anti-TIV antibody responses induced by vaccination

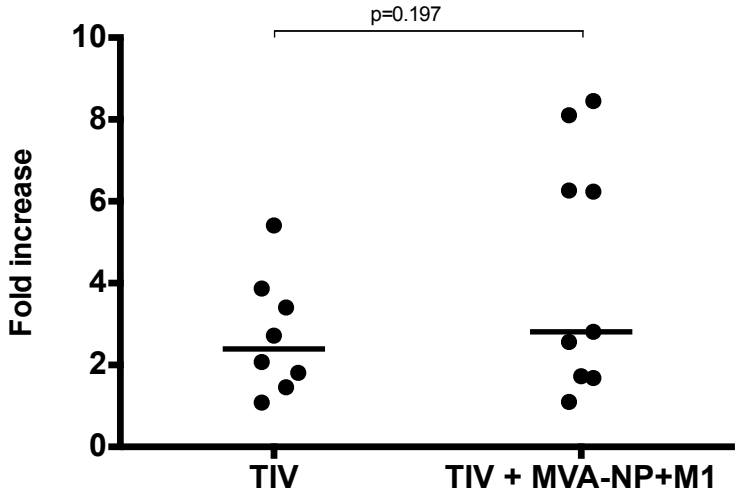


Figure 5.3 Anti-TIV antibody responses induced by vaccination [442]

Fold change in total serum IgG titers against TIV was measured by standardised ELISA using TIV antigen as the coating antigen and reported in relative ELISA units. Individual values and group medians are shown. The data in this graph has been previously published by Caitlin Mullarkey (DPhil, 2013) [442].

5.2. Specific Methods

Vaccines used: MVA-NP+M1 (MVA expressing NP and M1 antigens from influenza A/Panama/2007/99 as a single fusion protein, described in section 2.4.2.2). TIV (manufactured by Sanofi Pasteur MSD (Lyon, France): single dose contains 15 µg (each) HA of H1N1 (A/California/7/2009), H3N2 (A/Perth/16/2009), and Influenza B (B/Brisbane/60/2008).)

Participants: Healthy volunteers aged 50 years and older

Vaccination schedule: Volunteers received either TIV (n=8) or co-administered TIV and MVA-NP+M1 (n=9) (same muscle, injection site 1cm apart, vaccines administered within 5 minutes of each other). The protocol was approved by the UK Medicines and Healthcare products Regulatory Agency and the Regional Ethics Committee, and registered at www.clinicaltrials.gov (NCT00942071).

Samples available: Cryopreserved PBMCs collected 7 days after vaccination (n=8 from each group). Data on fold change in IgG anti-TIV titres from enrolment to 21 days after vaccination (used as a regression partner in section 5.3.3) was previously published by Antrobus *et al* [442].

Methods used: Methods for cell surface staining are described in section 2.8.7. Briefly, Frozen PBMCs were thawed, washed twice, resuspended at 2-3X10^6 cells/mL in R10 and incubated with benzonase® nuclease (10U per mL of cells) for 1h at 37°C. Treated cells were washed and plated at a

concentration of $1X10^6$ cells/well in a 96-well plate. Cell surface marker staining was performed step-wise (i.e. one stain after the other) in a total well volume of 100µL for 10 minutes at either 37°C or room temperature as per Table 2.7. Cells were washed in FACS buffer between stains. Following staining cells were washed resuspended in 2% paraformaldehyde. Fluorescence was measured the following day using an LSRII and analysed with FlowJo software. Reagents (antibodies) are listed in Table 2.2.

Gating strategies are described in the relevant section. Briefly, $T_{FH}1$-like cells were considered to be $CXCR3^+$ $CCR6^-$; $T_{FH}2$-like cells were $CXCR3^-$ $CCR6^-$; $T_{FH}17$-like cells were $CXCR3^-$ $CCR6^+$. Relatively high PD-1 expression was used as an activation marker, and $CD45RO^+$ T cells were memory cells.

5.3. Results

5.3.1. Investigation of Circulating $CD4^+$ T Cell Populations Following Influenza Vaccination

PBMC donors were volunteers aged 50 and older who participated in a phase I safety clinical trial to compare the co-administration of TIV and the candidate influenza vaccine MVA-NP+M1 (n=8) with TIV alone (n=8) (samples from this trial were also described in section 4.2.3) [442]. At the time point investigated in this study (day 7 post-vaccination), PBMCs were not available from one volunteer in the co-administration group.

5.3.1.1. $CXCR5^+CD4^+$ T Cell Populations

Circulating $CXCR5^+CXCR3^+ICOS^+$ T_H cell populations 7 days post influenza vaccination have previously been reported to correlate with the fold increase of global antibody titers at day 28 [491]. So too, have circulating $CXCR5^-ICOS^+IL\text{-}21^+$ T_H cell populations (HI antibody titers and T cells examined at 21 days post-vaccination) [496]. Therefore in this study both $CXCR5^+$ and $CXCR5^-$ populations were assessed at day 7 based on the availability of suitable PBMC samples. Unfortunately day 0 samples were not available for baseline comparison.

There was no significant difference between the median percentage of $CD4^+$ T cells expressing CXCR5 in the blood one week following vaccination with either TIV or TIV co-administered with MVA-NP+M1 (Fig. 5.5; the gating strategy is shown in Fig. 5.4).

Figure 5.4 Gating strategy for the analysis of circulating CXCR5$^+$CD4$^+$ T cell subsets

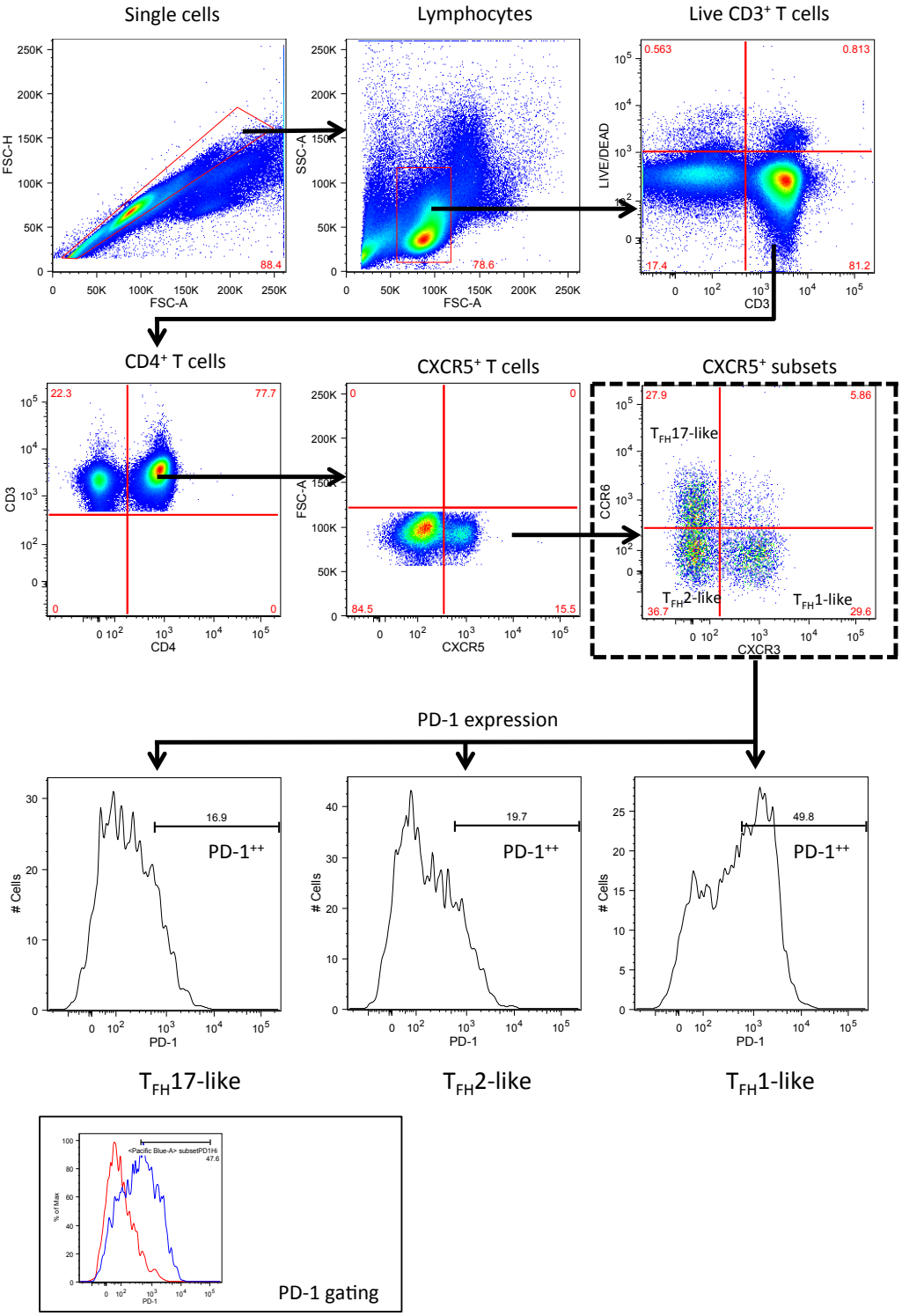
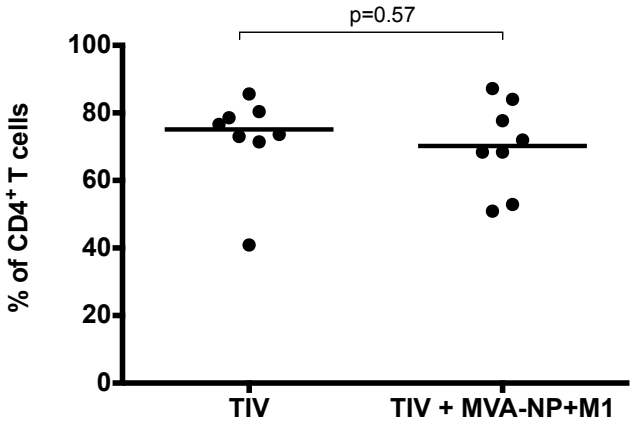


Figure 5.4 Gating strategy for the analysis of circulating $CXCR5^+CD4^+$ T cell subsets

Whole PBMC were gated on single cells and lymphocytes before gating on live $CD3^+$ cells (top row). $CD4^+$ $CD3^+$ lymphocytes were gated as either $CXCR5^+$ or $CXCR5^-$ (middle row) and further gated on CXCR3 and CCR6 expression to identify $T_{FH}1$-like, $T_{FH}2$-like and $T_{FH}17$-like subsets (bottom row). Activated cells were defined as those with high relative PD-1 expression ($PD\text{-}1^{++}$, bottom row). The lower boundary of the $PD\text{-}1^{++}$ gate was defined after visual inspection of the summated data, placing it to achieve 0.5% +ve in the lowest-expressing individual.

Figure 5.5 CXCR5 expression within the circulating CD4$^+$ T cell population between vaccine groups

A



B

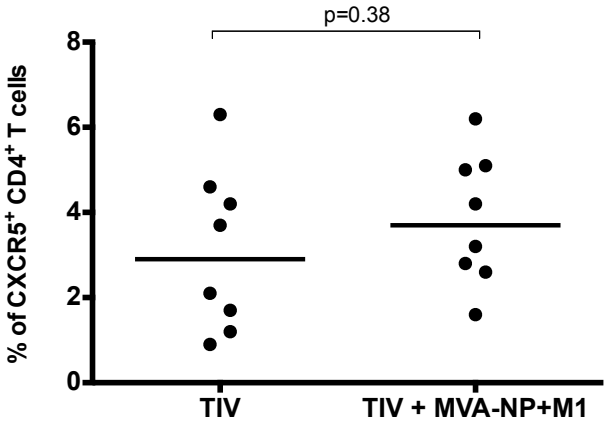


Figure 5.5 CXCR5 expression within the circulating CD4$^+$ T cell population between vaccine groups

(A) Percentage of circulating CD3$^+$ cells expressing CD4 (B) Percentage of total circulating CD4$^+$ T cells expressing CXCR5. Individual values and group medians are shown. No significant differences were observed between groups for either dataset (Mann Whitney).

Investigation of total $CXCR5^{+}CD4^{+}$ T cells indicated no significant differences between the median percentages of circulating $T_{FH}1$-like ($CXCR3^{+}CCR6^{-}$) subsets between groups, although there was a trend towards an increased percentage of high relative PD-1 expressing cells in the co-administration group indicating higher levels of cell activation in volunteers vaccinated with TIV and MVA-NP+M1 (Fig. 5.6 A & B).

No significant differences were observed between median percentages of circulating $T_{FH}2$-like ($CXCR3^{-}CCR6^{-}$) or $T_{FH}17$-like ($CXCR3^{-}CCR6^{+}$) subsets between groups (Fig. 5.6 C & E). There were no differences in the percentage of high relative PD-1 expressing cells between groups within the $T_{FH}2$-like population, although there was a trend towards higher activation of $T_{FH}17$-like cells (defined by percentage high relative PD-1 expression) in individuals receiving MVA-NP+M1 (Fig. 5.6 D & F).

Figure 5.6 Proportion of $T_{FH}1$-like, $T_{FH}2$-like and $T_{FH}17$-like subsets in the $CXCR5^+CD4^+$ population between vaccine groups and subset expression of PD-1

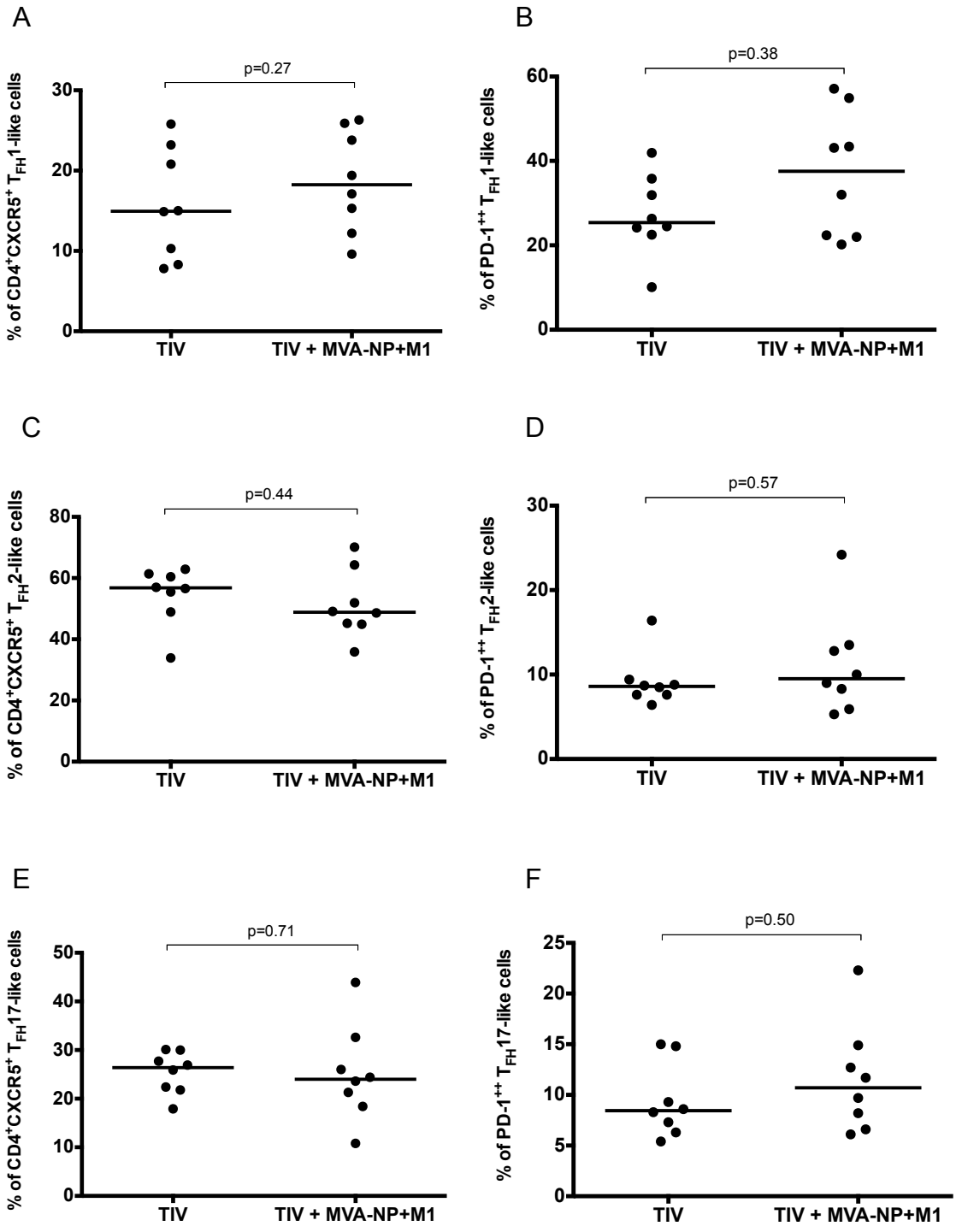


Figure 5.6 Proportion of T_{FH}1-like, T_{FH}2-like and T_{FH}17-like subsets in the $CXCR5^+CD4^+$ population between vaccine groups and subset expression of PD-1

Percentage of blood $CXCR5^+CD4^+$ T cells that are (A) T_{FH}1-like; $CXCR3^+CCR6^-$ (C) T_{FH}2-like; $CXCR3^-CCR6^-$ (E) T_{FH}17-like; $CXCR3^-CCR6^+$. Percentage of (B) T_{FH}1-like (D) T_{FH}2-like and (F) T_{FH}17-like cells with high relative expression of PD-1. Individual values and group medians are shown. No significant differences were observed between groups for all datasets (Mann Whitney).

Key findings:

Comparing between groups vaccinated with TIV versus TIV and MVA-NP+M1, there was no difference in the percentage of circulating $CD4^+$ T cells expressing CXCR5 one week following vaccination. There was also no difference in the proportion of $CD4^+$ T cells having $CXCR5^+$ $T_{FH}1$-like ($CXCR3^+CCR6^-$), CXCR5+ $T_{FH}2$-like ($CXCR3^-CCR6^-$) or CXCR5+ $T_{FH}17$-like ($CXCR3^-CCR6^+$) phenotypes. There were non-statistically significant increases in the proportion of $CXCR5^+$ $T_{FH}1$-like, and $CXCR5^+$ $T_{FH}17$-like cells that had an activated phenotype ($PD\text{-}1^{++}$) in the co-administration group, compared to the TIV alone group.

5.3.1.2. $CXCR5^{-}CD4^{+}$ T Cell Populations

There were no significant differences between the median percentages of circulating $T_{FH}1$-like subsets between groups within the $CXCR5^{-}CD4^{+}$ population although there was a trend towards a higher percentage in the co-administration arm, similar to the $CXCR5^{+}$ population (Fig. 5.7 A). A significantly higher percentage of these cells expressed higher relative levels of PD-1 in volunteers who received TIV and MVA-NP+M1 indicating recent cell activation ($p=0.04$) (Fig. 5.7 B).

No significant differences were observed between median cell percentages for either $T_{FH}2$-like or $T_{FH}17$-like subsets between groups within the $CXCR5^{-}CD4^{+}$ population although there was a trend towards a higher number of $T_{FH}2$-like cells in the group receiving TIV alone (Fig. 5.7 C & E). There were no differences in the percentage of cells with high relative PD-1 expression among $T_{FH}2$-like or $T_{FH}17$-like between the groups (Fig. 5.7 D & F).

Figure 5.7 Percentage of $CXCR5^{-}CD4^{+}$ subsets differentially expressing CXCR3, CCR6 and PD-1 between vaccine groups

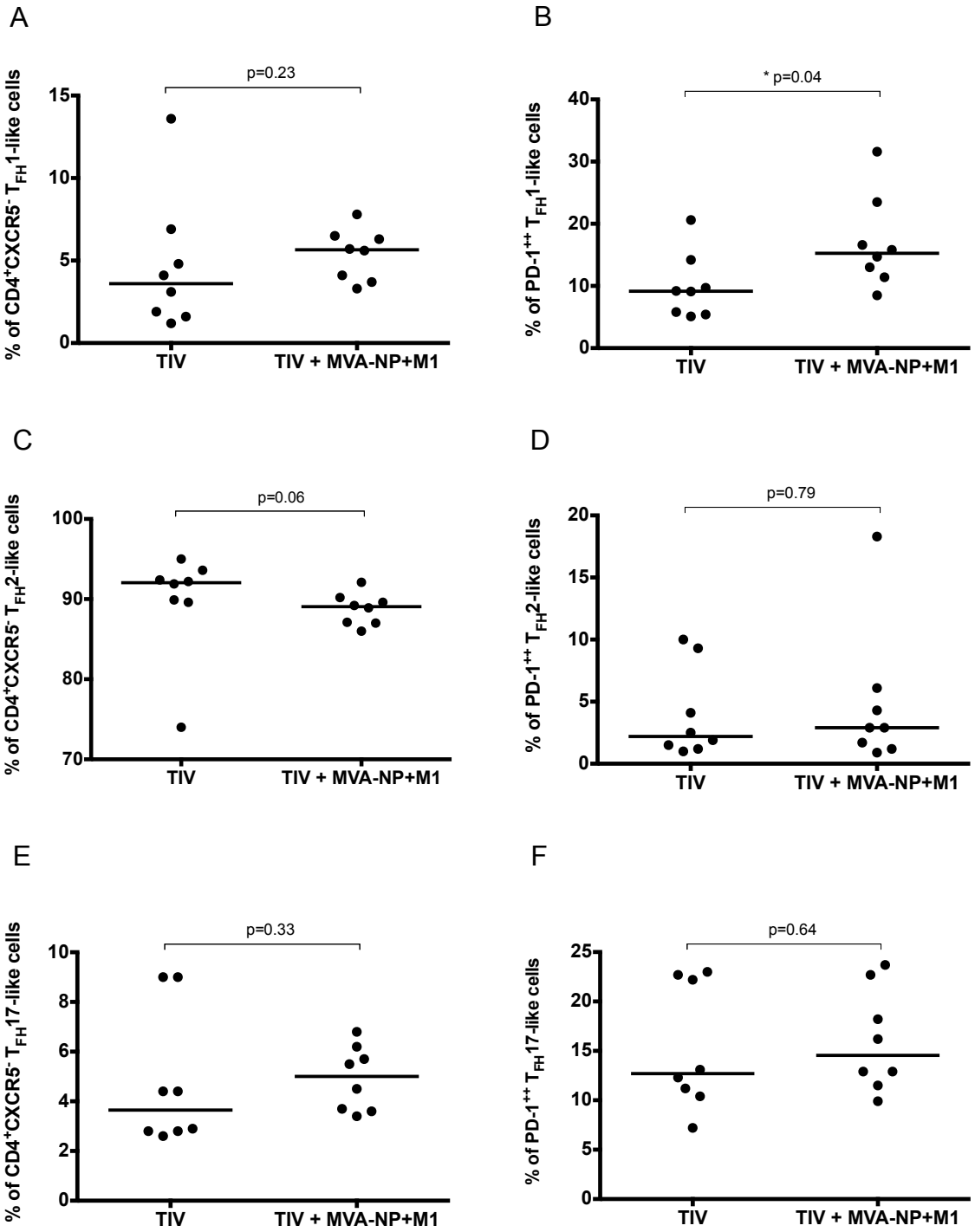


Figure 5.7 Percentage of $CXCR5^{-}CD4^{+}$ subsets differentially expressing CXCR3, CCR6 and PD-1 between vaccine groups

Percentage of blood $CXCR5^{-}CD4^{+}$ T cells that are (A) $T_{FH}1$-like (C) $T_{FH}2$-like and (E) $T_{FH}17$-like. Percentage of (B) $T_{FH}1$-like (D) $T_{FH}2$-like and (F) $T_{FH}17$-like with high relative expression of PD-1. Individual values and group medians are shown. Relative PD-1 expression was significantly higher in the $T_{FH}1$-like population in the co-administration group. No significant differences were observed between groups for all other datasets (Mann Whitney).

Key findings:

Comparing between groups vaccinated with TIV versus TIV and MVA-NP+M1, there were no differences in the proportion of circulating $CD4^+$ T cells having $CXCR5^-$ $T_{FH}1$-like ($CXCR3^+CCR6^-$), CXCR5- $T_{FH}2$-like ($CXCR3^-CCR6^-$) or CXCR5- $T_{FH}17$-like ($CXCR3^-CCR6^+$) phenotypes one week following vaccination. Circulating CXCR5- $T_{FH}1$-like $CD4^+$ T cells more commonly had an activated phenotype following vaccination with TIV and MVA-NP+M1 compared to TIV alone.

5.3.2. Investigation of Circulating Memory $CD4^+$ T Cell Populations Following Influenza Vaccination

5.3.2.1. $CD45RO^+CXCR5^+CD4^+$ T Cell Populations

As the volunteers in this study were over 50 and would have memory responses as a result of a lifetime of exposure to influenza A viruses, I sought to investigate further the $CXCR5^+$ and $CXCR5^-$ populations that were specifically within the memory T_H subset. This was done by gating on CD45RO (CD45RO is an isoform of CD45 expressed on memory T cells, CD45RA is the isoform located on naïve T cells).

Initial investigation demonstrated there were no significant differences between the median percentages of circulating memory $CD4^+$ T cells or $CXCR5^+CD4^+$ memory T cells between groups one week following vaccination with either TIV or TIV co-administered with MVA-NP+M1 (Fig. 5.9; the gating strategy is shown in Fig. 5.8).

Figure 5.8 Gating strategy for the analysis of circulating memory CXCR5^{+}CD4^{+} T cell subsets

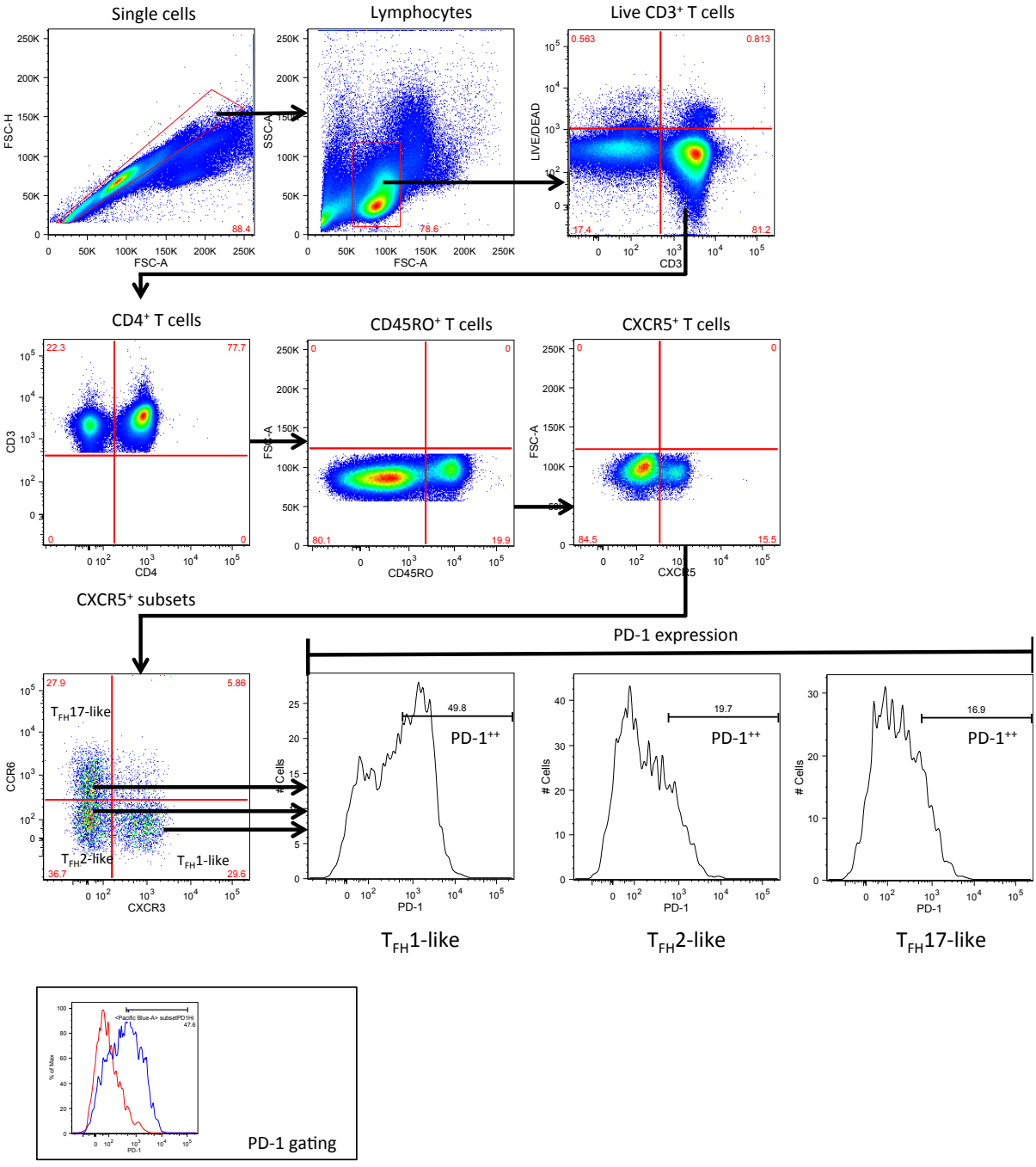


Figure 5.8 Gating strategy for the analysis of circulating memory $CXCR5^{+}CD4^{+}$ T cell subsets

Whole PBMC were gated on single cells and lymphocytes before gating on live $CD3^{+}$ cells (top row). $CD4^{+}$ $CD3^{+}$ lymphocytes were gated on CD45RO followed by CXCR5 (middle row). $CXCR5^{+}$ and $CXCR5^{-}$ populations were further gated on CXCR3 and CCR6 expression to identify memory $T_{FH}1$-like, $T_{FH}2$-like and $T_{FH}17$-like subsets (bottom row). Activated cells were defined as those with high relative PD-1 expression ($PD\text{-}1^{++}$, bottom row). The lower boundary of the $PD\text{-}1^{++}$ gate was defined after visual inspection of the summated data, placing it to achieve 0.5% +ve in the lowest-expressing individual.

Figure 5.9 CXCR5 expression within the circulating memory CD4$^+$ T cell population between vaccine groups

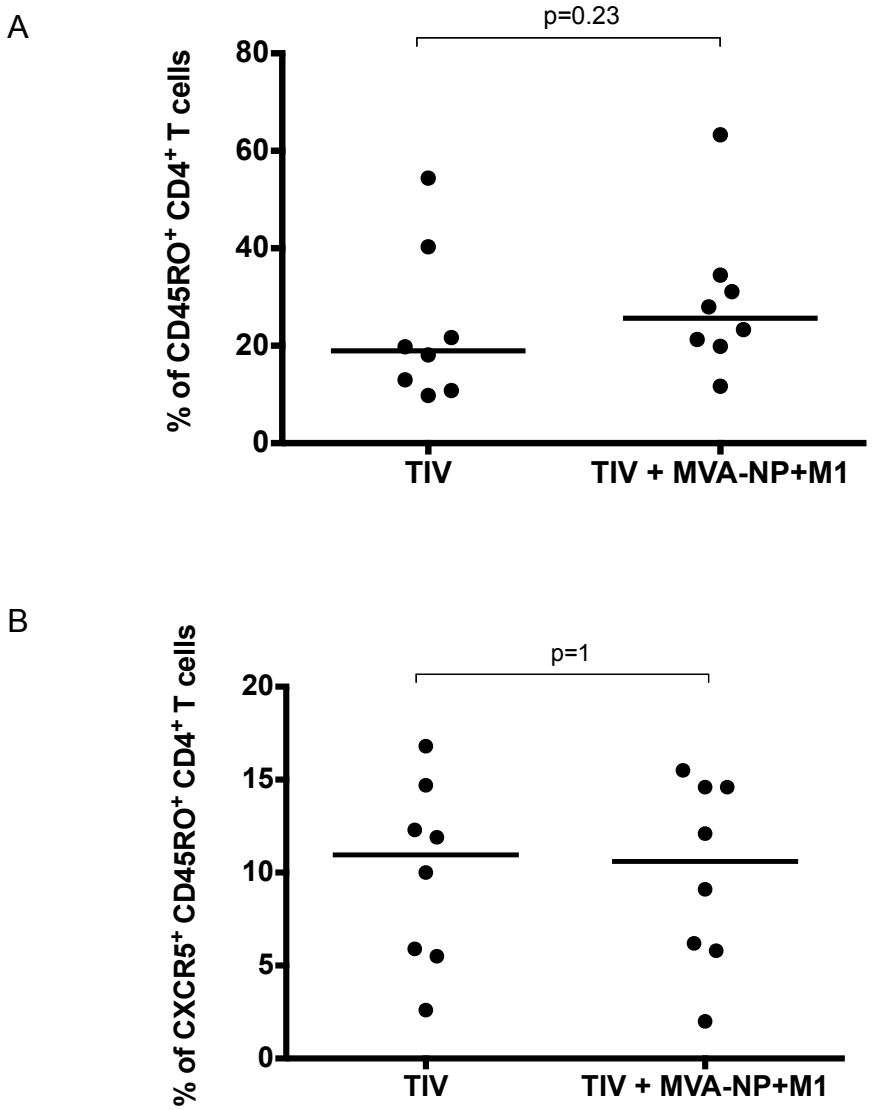


Figure 5.9 CXCR5 expression within the circulating memory CD4$^+$ T cell population between vaccine groups

(A) Percentage of circulating $CD3^+CD4^+$ cells expressing CD45RO (B) Percentage of total circulating $CD45RO^+CD4^+$ T cells expressing CXCR5. Individual values and group medians are shown. No significant differences were observed between groups for all datasets (Mann Whitney).

Analysis of total $CD45RO^{+}CXCR5^{+}CD4^{+}$ T cells indicated no significant differences between the median percentages of circulating memory $T_{FH}1$-like cells between groups, although there was a trend towards a higher median percentage in the co-administration arm (Fig. 5.10 A). In addition, there was a trend towards a greater percentage of high relative PD-1 expression in these cells although this difference was not significant (Fig. 5.10 B).

No significant differences were observed between groups for either the $T_{FH}2$-like or $T_{FH}17$-like memory subsets and there were no differences between percentages of high relative PD-1 expression among these cell populations either (Fig. 5.10 C-F).

Figure 5.10 Proportion of $T_{FH}1$-like, $T_{FH}2$-like and $T_{FH}17$-like subsets in the memory $CXCR5^+CD4^+$ population between vaccine groups and subset expression of PD-1

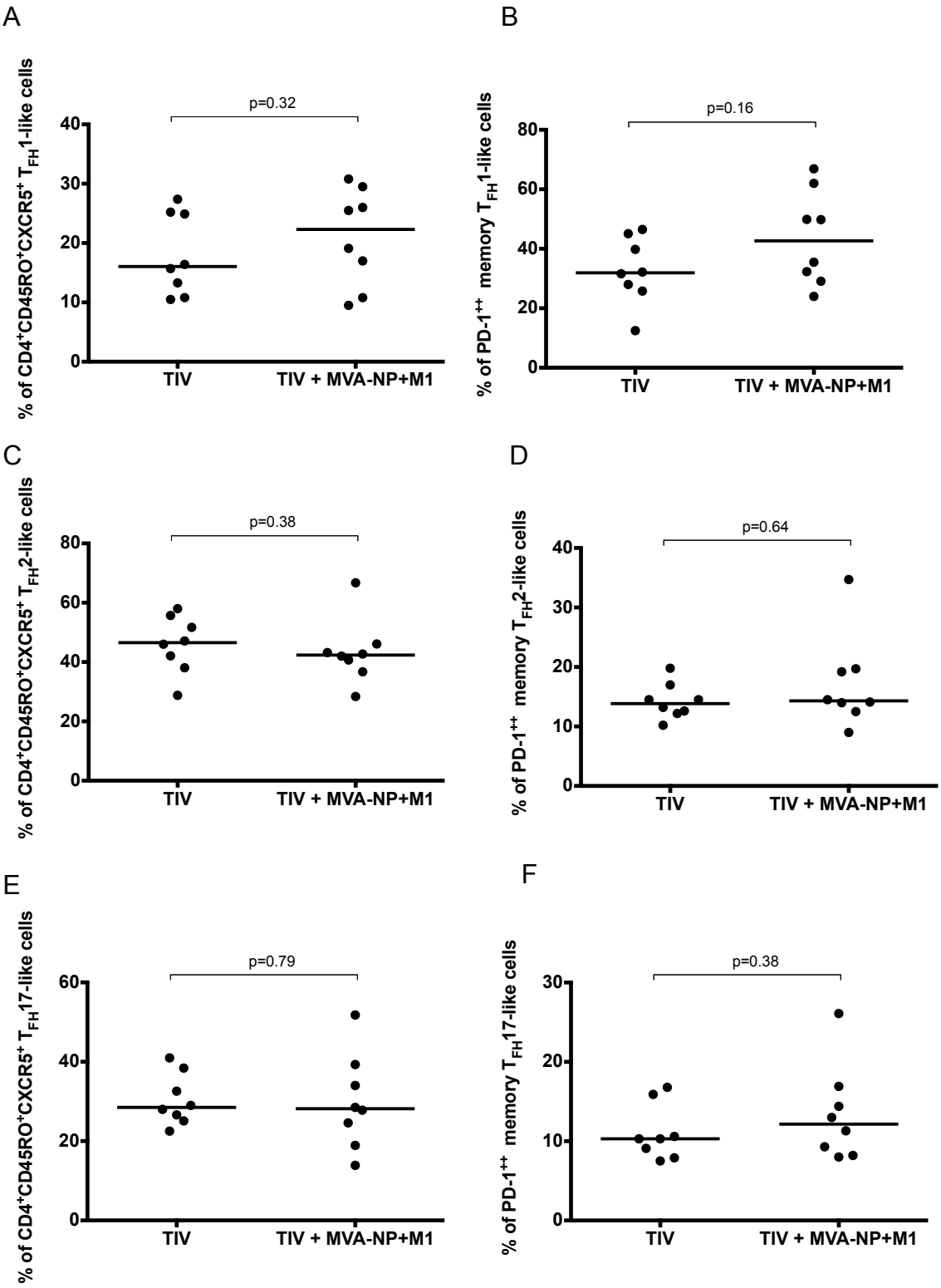


Figure 5.10 Proportion of T_{FH}1-like, T_{FH}2-like and T_{FH}17-like subsets in the memory $CXCR5^+CD4^+$ population between vaccine groups and subset expression of PD-1

Percentage of blood $CD45RO^+CXCR5^-CD4^+$ T cells that are (A) T_{FH}1-like (C) T_{FH}2-like (E) T_{FH}17-like. Percentage of (B) T_{FH}1-like (D) T_{FH}2-like and (F) T_{FH}17-like cells with high relative expression of PD-1. Individual values and group medians are shown. No significant differences were observed between groups for either dataset (Mann Whitney).

Key findings:

Comparing between groups vaccinated with TIV versus TIV and MVA-NP+M1, there was no difference in the percentage of circulating $CD4^+$ T cells expressing CD45RO or co-expressing CD45RO and CXCR5 one week following vaccination. There was also no difference in the proportion of $CD4^+$ $CD45RO^+$ T cells having $CXCR5^+$ $T_{FH}1$-like ($CXCR3^+CCR6^-$), $CXCR5^+$ $T_{FH}2$-like ($CXCR3^-CCR6^-$) or $CXCR5^+$ $T_{FH}17$-like ($CXCR3^-CCR6^+$) phenotypes. There was a non-statistically significant increase in the proportion of $CD45RO^+$ $CXCR5^+$ $T_{FH}1$-like cells that had an activated phenotype ($PD\text{-}1^{++}$) in the co-administration group, compared to the TIV alone group.

5.3.2.2. $CD45RO^{+}CXCR5^{-}CD4^{+}$ T Cell Populations

No significant differences were found between the median percentages of $T_{FH}1$-like, $T_{FH}2$-like or $T_{FH}17$-like subsets within the $CD45RO^{+}CXCR5^{-}CD4^{+}$ population between vaccination groups, although there was a trend towards a higher percentage of $T_{FH}1$-like subsets in the co-administration arm, similar to the $CXCR5^{+}$ memory population (Fig. 5.11 A, C & E). Within the $T_{FH}1$-like subset a greater percentage of cells expressed relatively high levels of PD-1, however this difference was not significant (Fig. 5.11 B). No differences in the percentage of high relative expression of PD-1 were seen in the $T_{FH}2$-like and $T_{FH}17$-like populations between groups (Fig. 5.11 D & F).

Figure 5.11 Percentage of memory CXCR5$^-$CD4$^+$ subsets differentially expressing CXCR3, CCR6 and PD-1 between vaccine groups

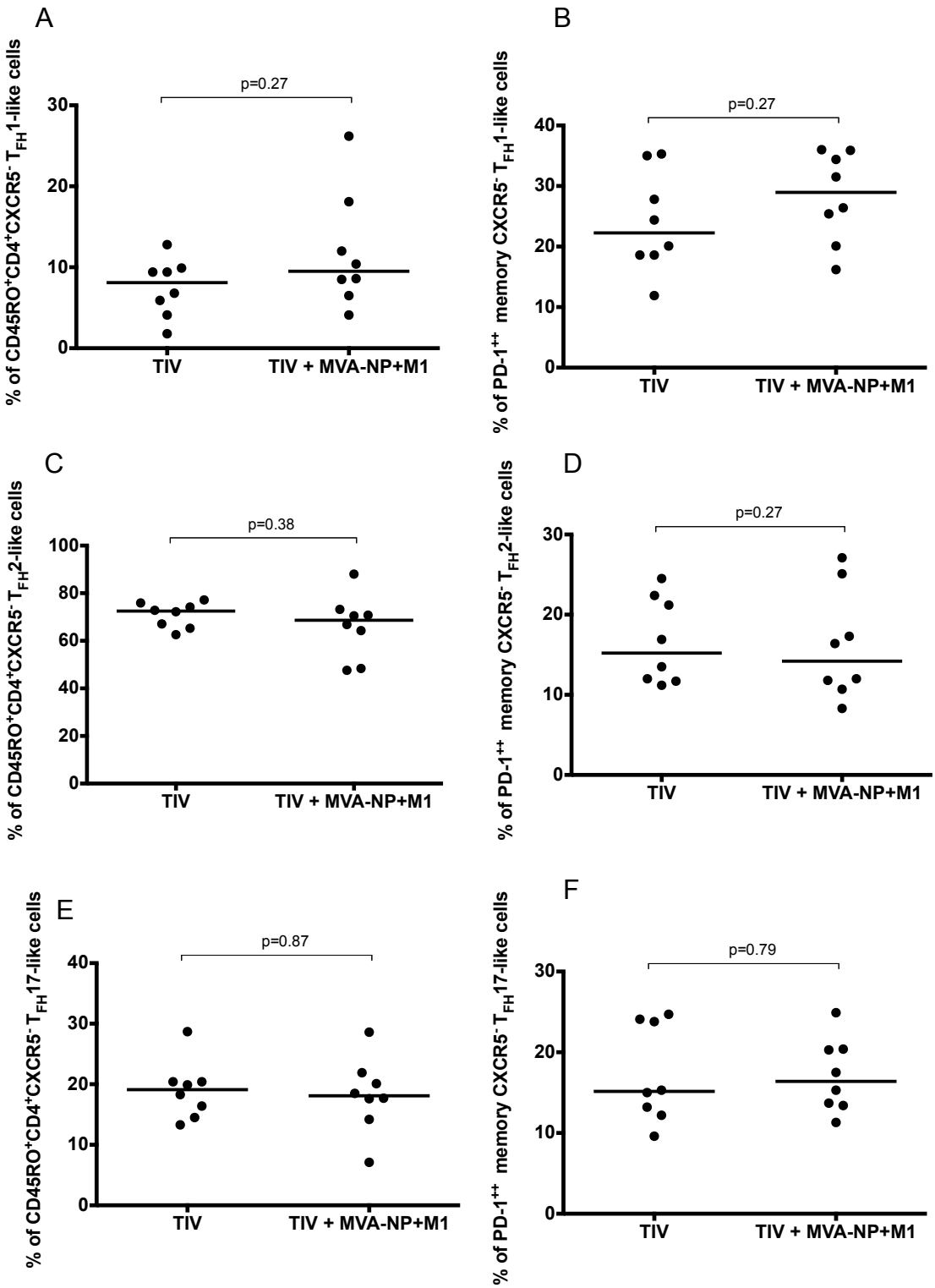


Figure 5.11 Percentage of memory CXCR5$^-$CD4$^+$ subsets differentially expressing CXCR3, CCR6 and PD-1 between vaccine groups

Percentage of blood CD45RO$^+$CXCR5$^-$CD4$^+$ T cells that are (A) T_{FH}1-like (C) T_{FH}2-like (E) T_{FH}17-like. Percentage of (B) T_{FH}1-like (D) T_{FH}2-like and (F) T_{FH}17-like cells with high relative expression of PD-1. Individual values and group medians are shown. No significant differences were observed between groups for all datasets (Mann Whitney).

Key findings:

Comparing between groups vaccinated with TIV versus TIV and MVA-NP+M1, there were no differences in the proportion of circulating $CD4^+$ $CD45RO^+$ T cells having $CXCR5^-$ $T_{FH}1$-like ($CXCR3^+CCR6^-$), $CXCR5^-$ $T_{FH}2$-like ($CXCR3^-CCR6^-$) or $CXCR5^-$ $T_{FH}17$-like ($CXCR3^-CCR6^+$) phenotypes one week following vaccination. There was a non-statistically significant elevation in the proportion of circulating $CXCR5^-$ $T_{FH}1$-like $CD4^+$ $CD45RO^+$ that had an activated phenotype following vaccination with TIV and MVA-NP+M1 compared to TIV alone.

5.3.3. Relationship Between Circulating T_{FH}-like Cell Populations and Antibody Responses Following Influenza Vaccination

The fold change in anti-TIV antibodies measured at baseline (day 0) and day 21 for each individual was used to investigate if the differences in $CD4^+$ T cell populations observed between groups 7 days post-vaccination correlated with the difference in antibody fold change previously reported [442]. All $CD4^+$ and memory $CD4^+$ subpopulations previously described (sections 5.2.1.1, 5.2.1.2, 5.2.2.1, and 5.2.2.2) were assessed. Of the twenty-seven populations investigated, no correlation was seen with the fold increase in anti-TIV antibody responses (Spearman's rank correlation with Bonferroni correction (Appendix XX).

Key findings:

There was no correlation between fold increase in anti-TIV IgG responses and any previously defined subset of T_{FH}-like cells

5.4. Discussion

One of the greatest obstacles to developing superior influenza vaccines is the lack of a definitive correlate of protection against which novel vaccines can be systematically assessed. The current gold standard, a HI titer over 40, is not applicable to children and does not take immune responses other than neutralising antibodies against the HA1 domain of HA into account. T_{FH} cells provide help to B cells and have a direct mechanistic relationship with the development of humoral immune responses, which suggests they may be useful predictors of vaccine-induced antibody outcome. However, in the clinical trial setting, biomarker sampling should be minimally invasive and the localisation of T_{FH} cells to secondary lymph organs contraindicates their routine sampling, which is necessary in the assessment of responses over time.

Bloodletting is a relatively risk-free, ethically justifiable procedure frequently used to acquire samples for the investigation of vaccine-induced immune responses. Populations of circulating T_{FH} cell counterparts have been shown to correlate with humoral immune responses to influenza A [491,496]. However our understanding of the role of these populations in vaccine-induced immunity is still in its infancy. Some of the commonly used markers to identify T_{FH} cells and T_{FH}-like cells, such as CXCR5, PD-1 and ICOS, are transiently expressed markers of activation which can make their identification at different time points technically challenging [497-499]. Furthermore, CXCR5 and ICOS expression is age-related and differs between the elderly and young adults [500]. Indeed two recent studies have presented both

$CXCR5^+CXCR3^+ICOS^+$ and $CXCR5^-ICOS^+IL\text{-}21^+$ subpopulations of circulating T_{FH} cells as predictors of vaccine-induced antibody responses at different time points [491,496].

On the basis of a previously observed trend towards enhanced antibody titers observed in individuals vaccinated with TIV co-administered with MVA-NP+M1 compared to TIV alone, I investigated whether antibody titers correlated with any of several peripheral blood $CD4^+$ T_{FH}-like cell populations differing in their expression of CD45RO, CXCR5, CXCR3 and CCR6. In this study I defined T_{FH}-like cells to be subsets of $CD4^+$ T cells differing in their expression of CXCR5, CXCR3 and CCR6. Volunteers were from a small phase I study and I assessed 8 samples from each arm for between-population differences in T_{FH}-like cell counts induced 7 days post-vaccination using a flow cytometry staining panel developed by a collaborator, Dr Cecilia Chui, which was similar to the method described by Bentibibel *et al* [491]. I observed a trend towards a higher percentage of $CXCR3^+CCR6^-$ cells in both memory and naïve $CXCR5^+$ populations in the co-administration group. Within these populations, there was also a trend towards a greater percentage of high relative PD-1 expression suggesting a higher number of recently activated memory and naïve $T_{FH}1$-like cells in individuals vaccinated with TIV and MVA-NP+M1. Interestingly, the same trends were observed within the naïve and memory $CXCR5^-CD4^+$ T cell populations and there was a significantly higher percentage of activated $CXCR3^+CCR6^-$ within the $CXCR5^-CD4^+$ population. However, the staining panel used in this study does not assess the functionality of these cells and future experiments should aim

investigate Bcl-6 and IL-21 expression in order to further dissect if these cells are circulating *bona fide* T_{FH} cells. This is particularly important considering the known transient expression of CXCR5 and PD-1 and the lack of ICOS staining in this panel.

Manipulating the induction of specific T_{FH} cell subsets by vaccination with specific adjuvants has the potential to differentially shape humoral responses. Both $CXCR5^+$ and $CXCR5^-$ $T_{FH}1$ cells are unable to activate naïve B cells and $CXCR5^+$ $T_{FH}1$ cells are also incapable of activating memory B cells (mBCs) [489]. In contrast, $CXCR5^+$ $T_{FH}2$ cells and $T_{FH}17$ cells can induce naïve B cells to secrete IgM, IgG, IgA, and in the case of $T_{FH}2$ cells, IgE. However $CXCR5^-$ $T_{FH}2$ cells induce only small amounts of IgM and IgE and $CXCR5^-$ $T_{FH}17$ cells are incapable of activating naïve B cells [489]. In terms of vaccine targets, the induction of $CXCR5^+$ $T_{FH}2$ or $T_{FH}17$ is desirable for strong IgG responses.

The results in this study suggest that vaccinating with a combination of TIV and MVA-NP+M1 induces a population with $T_{FH}1$-like characteristics similar to those previously reported after vaccination with TIV alone, but that an increased number of these cells are induced and activated. This may be the result of pathogen-associated molecular pattern (PAMP)-mediated adjuvanting effects of MVA, which is driven by bystander activation of DCs rather than direct infection of cells [501].

While these results are interesting it is important to remember that they are based on a small number of volunteers and should be regarded as

preliminary. Further investigations are needed to establish whether or not the trends observed here are consistent. Furthermore, analysis of high responders (those with high levels of relatively activated $T_{FH}1$-like cells) vversus low responders should be considered in order to increase statistical power for comparative work. In addition, sampling baseline and time points earlier than day 7 is warranted in order to account and control for baseline variation.

The discovery of broadly neutralising influenza antibodies capable of providing heterosubtypic protection has incentivised the pursuit of their induction through rational vaccine design. Most of these antibodies are encoded by the heavy-chain variable region *VH1-69* gene and bind the stem region of HA through highly conserved heavy chain complementary determining region (HCDR) residues [432,445]. In addition, a portion of these antibodies has characteristics indicative of a high degree of affinity maturation in GCs, albeit to not as great an extent as some of the bnAbs identified in the HIV field [502]. However, bnAbs against the stem domain of HA carry more mutations than antibodies generated against the immunodominant head region [502]. Indeed genealogical examination of the somatic mutations required for the human monoclonal antibody F16 to bind group 2 HA has indicated these are acquired progressively [290]. Considering as much as 6% of all B cell express VH1-69, there is a potentially large B cell repertoire capable of producing broadly neutralising heterosubtypic antibody responses that is not being efficiently induced by current vaccination strategies [503]. As T_{FH} cells are necessary for the GC reaction, the development of broadly neutralising

anti-stem antibodies may depend on or could be enhanced by the induction of appropriate T_{FH} cell subsets. Future co-administration studies using adjuvants such as alum or incomplete Freund's adjuvant (IFA), both of which classically skew immune responses towards a T_H2 phenotype, could provide some very interesting answers. At the time of writing this thesis no studies describing the role of alum or IFA on the induction of T_{FH} cells have been published.

5.5. Chapter Summary

- T_{FH} cells are important regulators of B cell responses
- The induction of antibody responses following vaccination with seasonal TIV correlates with the appearance of $T_{FH}1$ cells 7 days post-vaccination [491]
- $T_{FH}1$ cells are associated with the reactivation of memory B cells but are unable to activate naïve B cells
- A $T_{FH}1$-like population appears to be induced following vaccination with TIV co-administered with MVA-NP+M1
- The induction of more efficient T_{FH} cell responses could potentially augment responses against novel epitopes or aid the production of broadly neutralising antibodies, which tend to be highly somatically mutated.

Chapter 6

Investigation of Antibody Responses Induced by Novel Viral-Vectored Vaccines Targeting Haemagglutinin Stem

6. Investigation of Antibody Responses Induced by Novel Viral-Vectored Vaccines Targeting Haemagglutinin Stem

6.1. Background

Infection with seasonal influenza A viruses (IAV) is one of the foremost causes of morbidity and mortality worldwide. Global annual attack rates are estimated between 5-10% in adults and up to 30% in paediatric populations [12]. Cumulatively, this amounts to between 3 to 5 million cases of severe illness and up to 500,000 deaths each year [500]. In addition to frequent seasonal epidemics, genetic reassortment of IAVs can engender pandemics. Although historically such events are relatively uncommon, their emergence is unpredictable and can have potentially devastating consequences. The 1918 Spanish Flu pandemic killed an estimated 50-100 million people and serves as a stark reminder of the threat novel emerging viruses pose to immunologically naïve populations [504].

Vaccination remains the principle means of protecting against IAV infection and disease complications [505,506]. Currently licensed vaccines are comprised of three (trivalent) or four (quadrivalent) components representative of two IAV subtypes, H1N1 and H3N2, and either one or both influenza B lineages (B/Yamagata (3 clades) and B/Victoria (6 clades)) respectively [507,508]. These vaccines offer protection against seasonal strains but their efficacy is

dependent on matching the vaccine strains with the circulating strains of a particular season, which can be difficult to predict months in advance [509]. In order to keep pace with continually evolving IAVs, seasonal vaccines must be regularly updated according to epidemiological surveillance data and mismatch frequently occurs. Indeed, efficacy of the seasonal vaccine administered during the 2014/15 season in the UK was estimated as just 3.4% mid season due to antigenic mismatch of the H3N2 circulating virus and the respective 2014/15 northern hemisphere vaccine strain [250].

Current seasonal vaccines induce protection against IAV infection primarily by inducing neutralising antibody responses against the major virion surface glycoprotein, haemagglutinin (HA). HA is synthesised as an immature polypeptide (HA0) which is cleaved into two disulphide-linked units, HA1 and HA2, in order for the virus to be infectious (Chapter 3) [85]. Structurally, it is composed of three identical monomers, each comprised of a highly variable immunodominant globular head region (HA1) containing the sialic acid binding site, and a highly conserved stem region (HA2) containing the fusion peptide, which mediates binding of the viral and endosomal membranes (Chapter 3) [63,170-174]. Accumulation of mutations in the globular head drives the evolution of antigenically distinct strains resistant to antibody neutralisation, which necessitates the continual reformulation of seasonal vaccines.

At present the induction of neutralising antibodies against the five major antigenic sites (Sa, Sb, Ca1, Ca2 and Cb) within the globular head, as

determined by haemagglutination inhibition assay (HAI), is the only universally accepted correlate of protection against IAV [178,179,510,511]. However, antibodies against HA neutralise virions by several other physiologically relevant mechanisms besides receptor-binding inhibition [175]. Some of these, such as the inhibition of virion release by cross-linking newly formed virions to each other and the cell membrane, and the inhibition of immature HA0 cleavage into mature HA1 and HA2, rely on anti-HA1 antibodies [175]. However, inhibition of viral and endosome membrane fusion is mediated by antibodies directed against the HA stem and these are not detected by HAI [175]. Furthermore, due to the complex conformational changes required to mediate fusion, mutations in the stem are rare, which potentially makes this region a more appropriate vaccine target than the globular head [80].

Despite being discovered over 20 years ago, anti-stem antibodies have until recently, been largely overlooked [288,289]. In the past few years studies using combinatorial phage display libraries have demonstrated these antibodies are in fact widely prevalent in H5N1-exposed and seasonal influenza vaccinees, which has led to a renaissance of interest in this area [447,448]. Since then, a wealth of stem-reactive human monoclonal antibodies (mAbs), with remarkably broad neutralising reactivity against several subtypes of IAV, have been described. While the majority of these broadly-neutralising anti-stem antibodies (bnStAbs) are reactive within either Group 1 (CR6261, F10, CR9114) or Group 2 HA (CR8020, CR8043), at least two (F16 and 3I14) are capable of neutralising HA subtypes across both groups and one, CR9114,

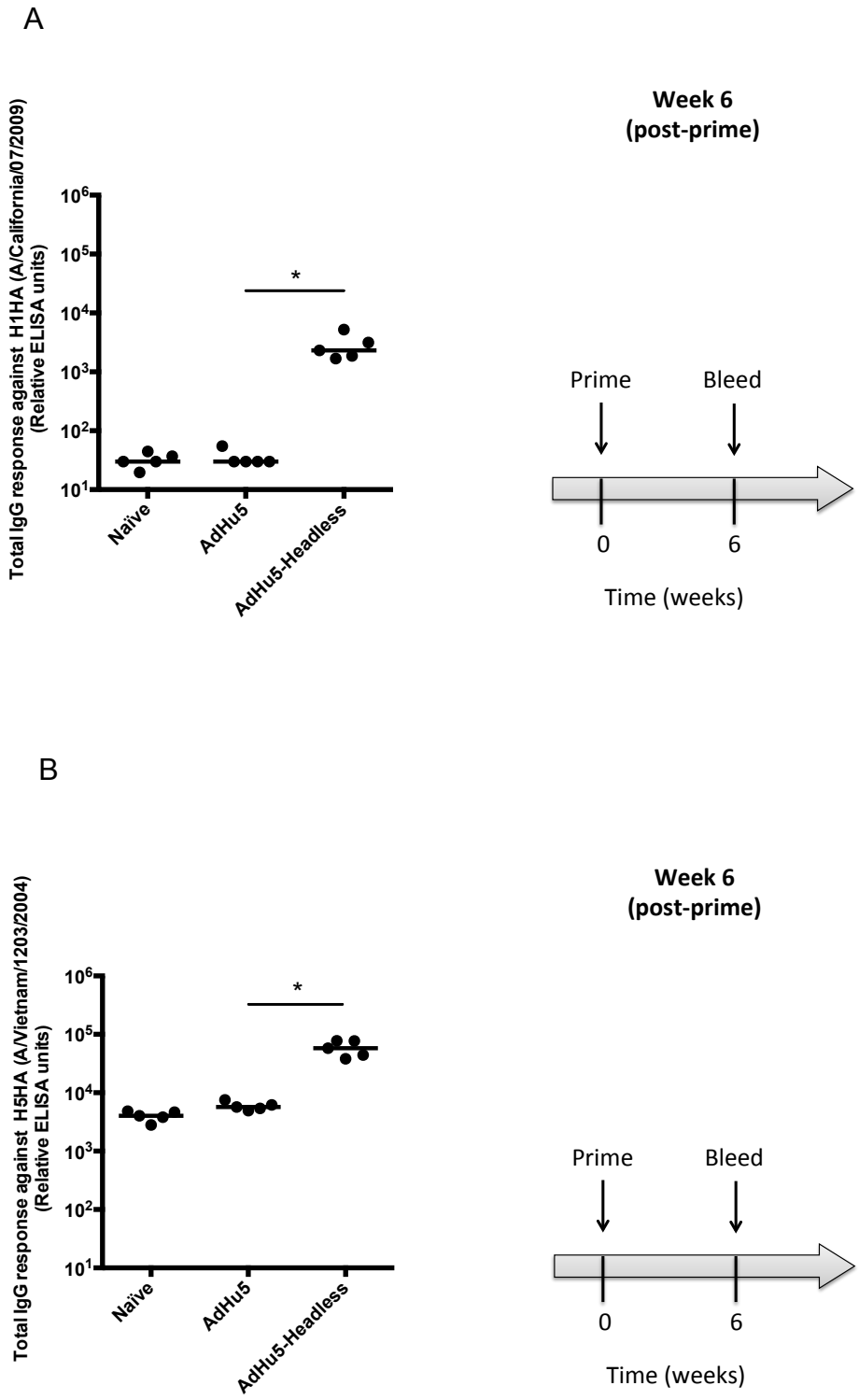
has also demonstrated protection against influenza B viruses [290,432,445-447,449,512,513]. Strikingly all of these human bnStAbs have demonstrated *in vivo* protection against lethal challenge in animal models [290,432,446,449,512,513]. Furthermore, a dominant bnStAb response was induced in individuals exposed to the 2009 pandemic virus, which has greatly incentivised the pursuit of their induction through rational vaccine design [294,423,452]. Indeed promising research has recently demonstrated bnStAbs induced following vaccination with a H5N1 vaccine in humans conferred protection to mice against challenge with a cH9/1N3 virus in passive-transfer experiments [514].

Induction of bnStAbs by vaccination could potentially provide much broader protection against seasonal and even pandemic strains, negating the need to constantly renew seasonal vaccines. The development of so-called 'universal influenza vaccines' aimed at eliciting such responses is the focus of much current research. To date, several approaches have been taken to develop a suitable HA-based immunogen that can direct immune responses towards the stem region, including removing, replacing or shielding the immunodominant globular head [296,300,304,305,515,516]. In particular, studies using chimeric HA in animal models have provided a proof of principle that successive immunisations with a variable head domain can selectively boost bnStAbs [304,305,515,516]. However, whether or not vaccination with such immunogens will be able to overcome pre-existing cross-reactive immunodominant anti-HA1 responses in humans with prior influenza exposure remains to be tested.

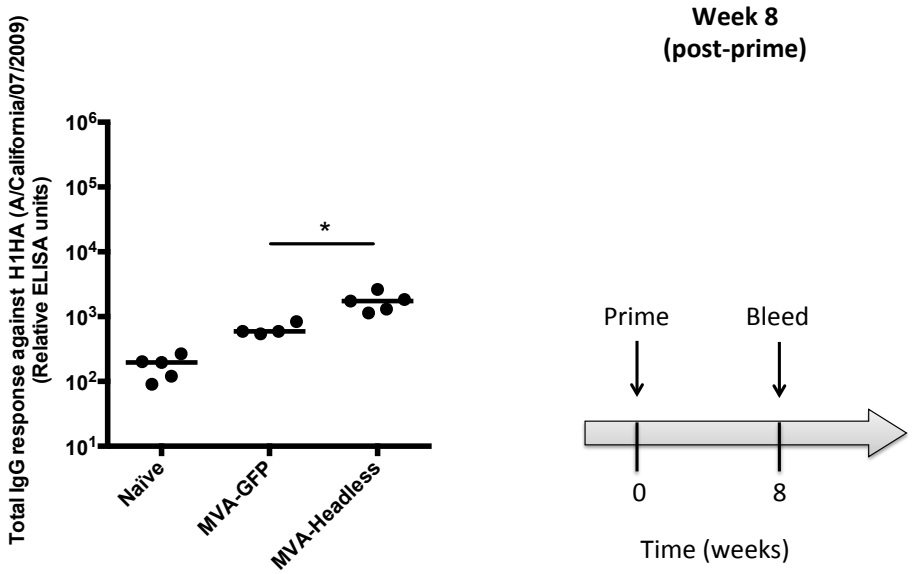
An alternative approach to using modified full-length HA immunogens is to use stem-only constructs. However, as the stem region has not evolved to exist independently of the globular head, stabilising such immunogens has proven difficult, though not impossible. Stem only constructs have been produced in a native-like conformation in both prokaryotic and eukaryotic systems and have induced immune responses capable of protecting mice from lethal homologous challenge [296,301-303]. Vaccination with 'mini-HA' stem trimers and trimeric HA-stem immunogens attached to multivalent ferritin nanoparticles (HA-SS-np) have demonstrated heterosubtypic protection in mice against H5N1 and partial protection in monkeys (mini-HA) and ferrets (HA-SS-np) [517,518]. Pilot data generated here at the Jenner Institute using a viral-vectored construct lacking the globular head region based on the 2009 H1N1 strain (A/Texas/05/2009) (Headless) similarly induced cross-reactive antibody responses against H1 and H5 HA (Fig. 6.1). However, responses were not improved by boosting with MVA-Headless (Fig. 6.1).

In this chapter I have investigated the ability of three novel viral-vector-expressed HA immunogens based on the sequence of A/Texas/05/2009 (H1N1) to induce antibodies against the stem region of HA. Two of these immunogens are stem-only constructs and a third is a chimera of the globular head from A/black-headed gull/Sweden/5/99 (H16N3) and the stem of A/Texas/05/2009 (H1N1). These vaccines have been compared to the original Headless construct and tested in the context of heterologous prime boost regimens with the aim of inducing high titer stem-reactive antibodies. The results of this study are reported herein.

Figure 6.1 HA-specific antibody responses generated by viral vectors expressing Headless multi-antigen MVA-vectored vaccination



C


Total IgG response against H1HA (A/California/07/2009) (Relative ELISA units)
10^6
10^5
10^4
10^3
10^2
10^1
*
Naïve
MVA-GFP
MVA-Headless
Week 8
(post-prime)
Prime
Bleed
0
8
Time (weeks)

D

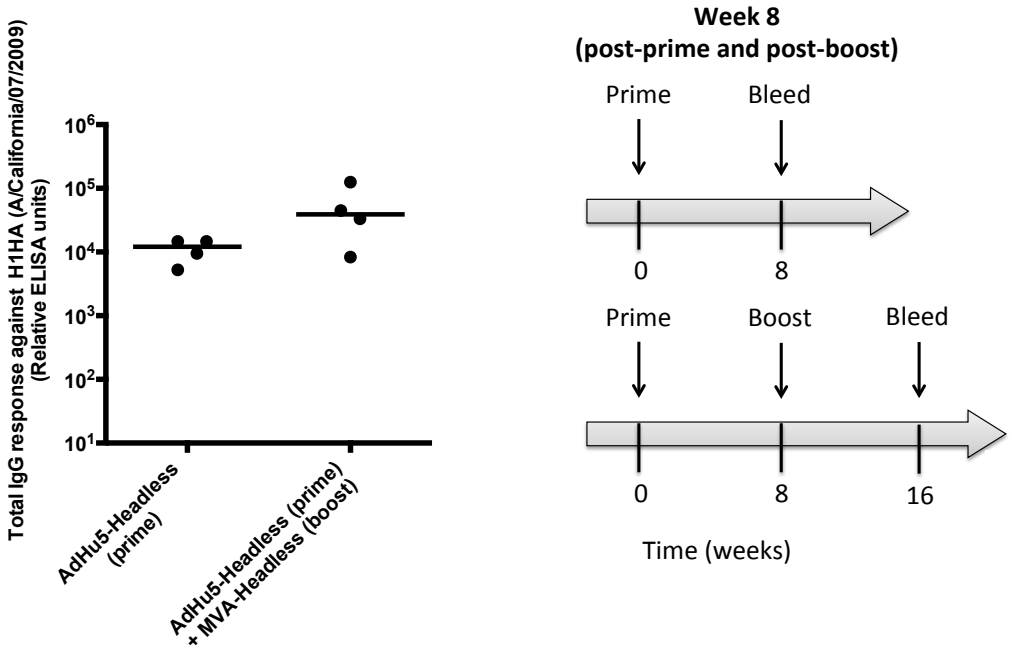

Total IgG response against H1HA (A/California/07/2009) (Relative ELISA units)
10^6
10^5
10^4
10^3
10^2
10^1
AdHu5-Headless (prime)
AdHu5-Headless (prime) + MVA-Headless (boost)
Week 8
(post-prime and post-boost)
Prime
Bleed
0
8
Prime
Boost
Bleed
0
8
16
Time (weeks)

Figure 6.1 HA-specific antibody responses generated by viral vectors expressing Headless multi-antigen MVA-vectored vaccination

6-8 week old BALB/c mice (n=4-5) were immunised i.m. with (A & B) $1x10^8$ iu AdHu5 or $1x10^8$ iu AdHu5-Headless, (C) $1x10^6$ pfu MVA-GFP or $1x10^6$ pfu MVA-Headless or (D) $7x10^8$ iu AdHu5-Headless or $7x10^8$ iu AdHu5-Headless followed by a boosting vaccination 8 weeks later with $1x10^7$ pfu MVA-Headless. Total IgG responses against (A, C & D) recombinant H1HA (A/California/07/2009; H1N1) or (B) recombinant H5HA (A/Vietnam/1203/2004; H5N1) were assayed by standardised ELISA at (A & B) 6 weeks post-vaccination or (C & D) 8 weeks post-vaccination (post-final vaccination in D). Naïve controls are unvaccinated mice. Individual values and group medians are shown. *$p \leq 0.05$ by Mann Whitney. Dr Teresa Lambe and Prof Sarah Gilbert designed the Headless antigen and vaccination regimens. ELISA data for (D) was provided by Dr Teresa Lambe.

6.2. Specific methods

Vaccines used: This chapter describes evaluation of prime-boost vaccination strategies in two separate experiments. A compendium of the vaccines used is found in Table 2.6. In section 6.3.3, mice were vaccinated with DNA plasmids expressing Headless (HA lacking globular head domain but including native leader sequence and transmembrane (TM) domain from H1N1 A/Texas/05/2009 (sequence in appendix XXI), H1HA-Stem (details in 6.3.1.1), H1HA-Stem+TM (transmembrane) (details in 6.3.1.2) and cH16/H1 (details in 6.3.1.3) constructs or GFP (control), or with H1HA protein control (A/California/07/2009). Mice were boosted with ChAdOx1-H5 (A/Vietnam/1203/2004; previously produced in the Jenner Institute) and MVA-H1 (A/Texas/05/2009; previously produced in the Jenner Institute) as described in Table 6.2. In section 6.3.5, mice were vaccinated with AdHu5 viral vectors expressing Headless, H1HA-Stem, H1HA-Stem+TM, or GFP (control), or with H1HA protein control (A/California/07/2009). They were boosted with MVA-H1. Viral vector production is described in 6.3.2.

Subjects: 6-10 week-old female BALB/c (H-2^d) mice (n=4 to 6 as described in the text).

Samples collected: Bleed time points (for storage of serum) are shown in Figures 6.2 and 6.4.

Methods used: Vaccine design and production is described in sections 6.3.1 and 6.3.2, with further details in the methods section 2.4. IgG antibody

responses against cH9/H1 (used to measure Group 1 HA-stem-specific responses as described in section 6.3.3; coated with 0.1µg recombinant protein per well) were evaluated by ELISA as described in section 2.8.1. Responses against the trimerisation domain were evaluated (6.3.4 and 6.3.6) by measuring responses to recombinant HIV-1 envelope glycoprotein (Env; an irrelevant antigen) fused to the T4 fibritin foldon trimerisation domain (Sino Biological Inc) by ELISA (section 2.8.1) (0.1µg protein per well).

6.3. Results

6.3.1. Immunogen Design

The H1 vaccine immunogens designed as part of this study are based on a consensus HA sequence derived from 123 sequences of European pandemic flu (downloaded on 12th July 2009 by Prof Sarah Gilbert). The consensus 2009 H1N1 pandemic HA sequence matches A/Texas/05/2009 (H1N1) (GeneBank: ACR19260.1). The Headless antigen is also based on this sequence and includes the native leader sequence and transmembrane domain (Appendix XXI).

6.3.1.1. H1HA-Stem

H1HA-Stem (Stem) is a fusion of the HA stem domain of H1HA (A/Texas/05/2009) and a T4 fibritin foldon trimerisation domain (section 3.2.1.7). The trimerisation domain replaces the native transmembrane domain and is commonly used to encourage correct folding of recombinant HA (Chapter 3) [303]. The majority of the globular head domain (residues 60-291; H3 numbering; A/Aichi/02/68) of A/Texas/05/2009 (H1N1) (GeneBank: ACR19260.1) has been replaced with a linker peptide (GSGSG). Hydrophobic residues in the stem exposed upon deletion of the globular head have been mutated to encourage native folding (F164 to D and L174 to D) [303]. The number of disulphide bonds in each monomer was reduced from 4 to 2 by mutating C77 to T and deleting two polypeptide regions containing hydrophobic residues (H38 to C43 and C49 to N61) [303]. Cysteines were also introduced at G188 and F189 and at residues A302 and K306 within the trimerisation domain to favour bonds between monomers [303]. In this construct

the native leader sequence has been replaced with a modified leader sequence from the human tissue plasminogen activator (tPA) [400]. Inclusion of a human tPA leader sequence in malaria vaccine constructs has previously demonstrated significantly higher antibody titers most likely due to increased efficiency of antigen secretion and/or expression [519].

6.3.1.2. H1HA-Stem+TM

The H1HA-Stem+TM immunogen (Stem+TM) is based on the H1HA-Stem immunogen but also includes the native TM domain in addition to the trimerisation domain. Full length H1HA constructs expressing a TM domain have been previously reported as inducing superior humoral immune responses in mice compared to constructs lacking a transmembrane domain (Caitlin Mullarkey, DPhil).

6.3.1.3. cH16/H1

The cH16/H1 immunogen has been previously described (section 3.1.2.4). The vaccine construct did not include the polyhistidine tag.

Table 6.1 HA immunogen sequences

Vaccine Construct	Sequence
H1HA-Stem	***mdamkrglccvlllcgavfvsasqeiharfrrgs***DTLCI GYHANNSTDTVDTVLEKNVTVTHSVNLLED KGSGSGTSLPFQNIHPITIGKTPKYVKSTKLR LATGLRNVPSIQSRGLFGAIAGFIEGGWTG MVDGWYGYHHQNEQGSGYAADLKSTQNAI DEITNKVNSVIEKMNTQDTAVGKEFNHDEK RIENLNKKVDDCCLDIWTYNAELLVLLENER TLDYHDSNVKNLYEKVRSQLKNNAKEIGNG CFEFYHKCDNTCMESVKNGTYDYPKYSEE AKLNREEIDGVGSGSGSGSG***YIPEAPRDGQ CYVRCDGEWVLLSTFLG***
H1HA-Stem+TM	***mdamkrglccvlllcgavfvsasqeiharfrrgs***DTLCI GYHANNSTDTVDTVLEKNVTVTHSVNLLED KGSGSGTSLPFQNIHPITIGKTPKYVKSTKLR LATGLRNVPSIQSRGLFGAIAGFIEGGWTG MVDGWYGYHHQNEQGSGYAADLKSTQNAI DEITNKVNSVIEKMNTQDTAVGKEFNHDEK RIENLNKKVDDCCLDIWTYNAELLVLLENER TLDYHDSNVKNLYEKVRSQLKNNAKEIGNG CFEFYHKCDNTCMESVKNGTYDYPKYSEE AKLNREEIDGVGSGSGSGSG***YIPEAPRDGQ CYVRCDGEWVLLSTFLG***GSGSGSG***KLEST RIYQILAIYSTVASSLVLVVSLGAISFWMCS NGSLQCRICI***
cH16/H1	***mdamkrglccvlllcgavfvsasqeiharfrrgs***DTLCI GYHANNSTDTVDTVLEKNVTVTHSVNLLED KHNGKLCSLNGISPIHLGDCSFEGWIVGNPS CATNINIREWSYLIEDPNAPNKLCFPGELDN NGELRHLFSGVNSFSRTELISPNKWGDILD GVTASCRDNGASSFYRNLVWIVKNKNGKY PVIKGDYNNTTGRDVLVLWGIHHPDTETTAI NLYASKNPYTLVSTKEWSKRYELEIGTRIGD GQRSWMKLYWHLMRPGERIMFESNGGLIA PRYGYIIEKYGTGRIFQSGVRMAKCNTTCQT PKGAINTSLPFQNIHPITIGKCPKYVKSTKLR LATGLRNIPSIQSRGLFGAIAGFIEGGWTGM VDGWYGYHHQNEQGSGYAADLKSTQNAID EITNKVNSVIEKMNTQFTAVGKEFNHLEKRI ENLNKKVDDGFLDIWTYNAELLVLLENERTL DYHDSNVKNLYEKVRSQLKNNAKEIGNGCF EFYHKCDNTCMESVKNGTYDYPKYSEEAKL NREEIDGVISGRLVPRGSPGSG***YIPEAPRD GQAYVRKDGEWVLLSTFLG***

Table 6.1 HA immunogen sequences

Bold lower case italics represent the modified tPA leader sequences. ***Bold italic CAPS*** represent the transmembrane domain and cytosolic residues. ***Bold italic underlined CAPS*** represent the T4 fibritin foldon trimerisation domain.

6.3.2. Viral Vector Production

DNA sequences for H1HA-Stem, H1HA-Stem+TM and cH16/H1 were synthesised by GeneArt® (Invitrogen) and subcloned into Invitrogen Gateway® entry vectors prior to generation of recombinant human adenovirus serotype 5 vectors (section 2.4.1.1 and 2.4.1.2). The same sequences were also cloned into MVA shuttle vectors (section 2.1.2.1). Purified shuttle vector DNA was sent to the Jenner Institute Viral Vector Core Facility for viral vector production and purification (Appendix I-XV). With the exception of AdHu5-cH16/H1, all viral-vectored vaccines were successfully produced. Haemagglutins are known to be toxic and as this particular construct lacked a transmembrane domain it is possible production of cH16/H1 inhibited viral propagation as the beginnings of cytopathic effect was initially observed but no virus was propagated (Rhys Hamon Vector Core, Jenner Institute, personal communication).

6.3.3. Anti-Stem Antibody Responses Following DNA-ChAdOx1-MVA Sequential Prime-Boost Vaccination

The timeline for production of AdHu5 and MVA viral vectors expressing H1HA-Stem, H1HA-Stem+TM and cH16/H1 was estimated to be between 6-14 weeks. In the interim vaccinations priming mice with DNA plasmids expressing these constructs were set up to assess the induction of stem-specific immunity. Additional viral vectors expressing the Group 1 HA, H5 (A/Vietnam/1203/2004; H5N1), which has a stem sequence similarity of 81.53% to H1 (A/Texas/05/2009; H1N1) and an immunologically distinct globular head, or full-length H1 (A/Texas/05/2009; H1N1), were administered at 4 and 12 weeks post DNA prime respectively, in order to boost responses towards the conserved stem domain.

6-8 week old BALB/c mice (n=4-6) were immunised i.m. according to the vaccination regimen outlined in Table 6.2. Mice were vaccinated with 10μg recombinant H1HA protein (A/California/07/2009), representative of a high dose (per kg body mass) of currently licensed vaccines in humans (which typically contain 15μg of recombinant HA per vaccine strain) for comparison. Total IgG responses against recombinant cH9/H1 were assayed by standardised ELISA at 2 weeks after each vaccination and 8 weeks following the final vaccination (Fig. 6.2). cH9/H1 is composed of the HA2 domain of A/California/07/2009, which is identical to HA2 of A/Texas/05/2009, and HA1 residues from a H9 subtype A/Hong Kong/1073/99 (H9N2) (GeneBank: NP859037), which is antigenically distinct to H1, H5 and H16 (Chapter 3) [294]. This can be used to measure Group 1 HA stem-specific responses.

Table 6.2 Immunisation schedule for the induction of anti-stem antibodies by DNA-ChAdOx1-MVA vaccination

Time (weeks)	0	4	12
Group	**Prime**	**Boost**	**Boost**
A	H1HA protein	-	-
B	-	ChAdOx1-H5	MVA-H1
C	DNA-GFP	ChAdOx1-H5	MVA-H1
D	DNA-Headless	ChAdOx1-H5	MVA-H1
E	DNA-H1HA-Stem	ChAdOx1-H5	MVA-H1
F	DNA-H1HA-Stem+TM	ChAdOx1-H5	MVA-H1
G	DNA-cH16/H1	ChAdOx1-H5	MVA-H1

Table 6.2 Immunisation schedule for the induction of anti-stem antibodies by DNA-ChAdOx1-MVA vaccination

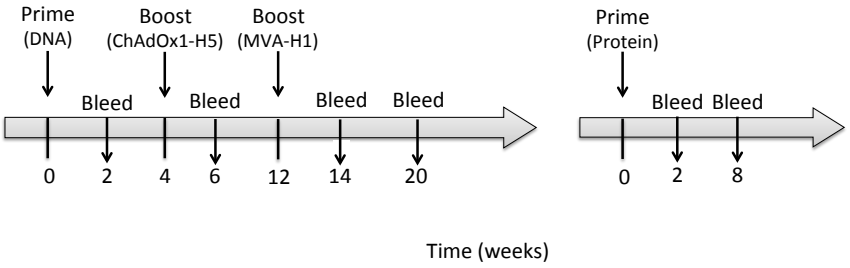
Five groups of BALB/c mice (n=6) were immunised i.m with 50µg plasmid DNA expressing one of four immunogens designed to induce anti-stem antibodies, Headless, H1HA-Stem, H1HA-Stem+TM or cH16/H1, or with a control plasmid expressing GFP. A control group was not primed with DNA. Another group of mice (n=4) received 10µg recombinant H1HA protein (A/California/07/2009). All groups except mice primed with protein were boosted at 4 weeks with $1x10^8$ iu ChAdOx1-H5 and at 12 weeks with $1x10^6$pfu MVA-H1.

There were no significant differences between mice immunised with DNA-Headless, DNA-H1HA-Stem, DNA-H1HA-Stem+TM, DNA-cH16/H1 or 10μg recombinant H1HA protein at 2 weeks following the first vaccination (p=0.1820) (Fig. 6.2A). However mice vaccinated with DNA-H1HA-Stem+TM had significantly higher anti-stem antibody responses compared to control mice receiving DNA-GFP at this time point (*p=0.0173 by Mann Whitney) (Fig. 6.2 A). At 2 weeks following the boost with ChAdOx1-H5, there were no significant differences between groups primed with DNA-Headless, DNA-H1HA-Stem, DNA-H1HA-Stem+TM, DNA-cH16/H1 and the control group primed with GFP (Fig. 6.2 B). Similarly, at 2 weeks post the second boost with MVA-H1 there were no significant differences between groups primed with DNA-Headless, DNA-H1HA-Stem, DNA-H1HA-Stem+TM, DNA-cH16/H1 and the control group primed with GFP (Fig. 6.2 C). However, mice primed with DNA-Headless had significantly higher antibody responses compared to mice primed with GFP (*p=0.0411 by Mann Whitney) at this time point (Fig. 6.2 C).

At the final time point, 8 weeks following vaccination with MVA-H1, mice primed with DNA-Headless and DNA-H1HA-Stem+TM had significantly higher responses compared to mice primed with GFP (both *p=0.0411), however there were no significant differences between groups primed with DNA-Headless, DNA-H1HA-Stem, DNA-H1HA-Stem+TM and DNA-cH16/H1 (Fig. 6.2 D). In addition mice primed with DNA-Headless, DNA-H1HA-Stem, DNA-H1HA-Stem+TM and DNA-cH16/H1 all had significantly higher responses at 8 weeks following final vaccination compared to sera taken from

mice 8 weeks following vaccination with 10μg recombinant H1HA protein alone (*p=0.0148 by ANOVA) (Fig. 6.2 D). However, there were no significant differences between mice primed with 10μg recombinant H1HA protein and naïve (unvaccinated) BALB/c sera 8 weeks post immunisation (Fig. 6.2 D). In addition there were no significant differences between mice primed with GFP or mice vaccinated with ChAdOx1-H5 and MVA-H1 only at all time points. Taken together these results suggest that vaccination with DNA-vectored HA-based immunogens that include a transmembrane domain can prime marginally better anti-stem antibody responses compared to constructs that lack a transmembrane domain and overall these responses are significantly better compared to vaccination with protein alone.

Figure 6.2 Stem-specific antibody responses generated by heterologous DNA-ChAdOx1-MVA prime-boost vaccination



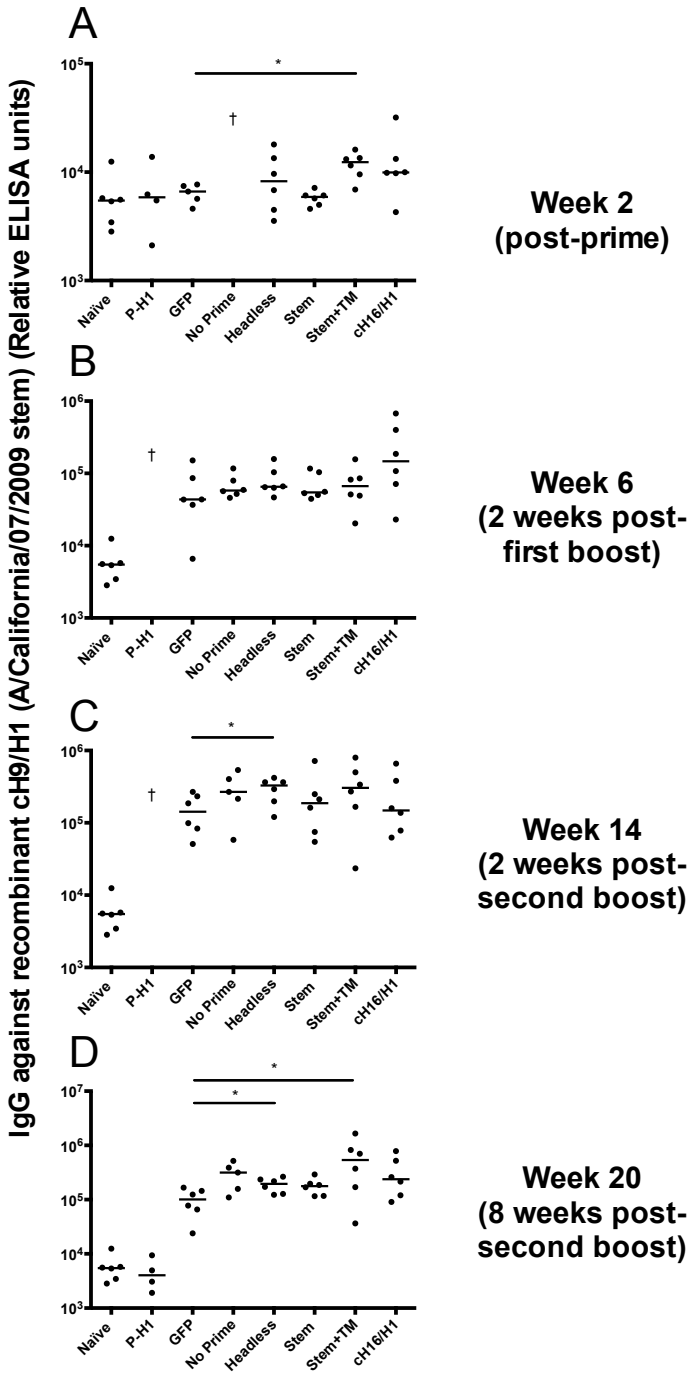


Figure 6.2 Stem-specific antibody responses generated by heterologous DNA-ChAdOx1-MVA prime-boost vaccination

6-8 week old BALB/c mice (n=4-6) were immunised i.m. according to the vaccination regimen in Table 6.2. Total IgG responses against recombinant cH9/H1 were assayed by standardised ELISA at (A) 2 weeks post-prime, (B) 2 weeks post ChAdOx1-H5 boost, (C) 2 weeks post MVA-H1 boost and (D) at 8 weeks post MVA-H1 boost. Responses in mice vaccinated with 10μg recombinant H1HA protein alone (P-H1) at (A) 2 weeks and (D) 8 weeks post-vaccination are shown for comparison. Naïve controls are unvaccinated mice. The abbreviation 'P-H1' indicates recombinant H1HA protein (A/California/07/2009). Individual values and group medians are shown. *p≤0.05 by Mann Whitney. † indicates data not available for this time point.

Key findings:

DNA plasmids expressing HA-based immunogens that include a transmembrane domain prime for anti-stem antibody responses when compared to a GFP-expressing control. This experiment did not reveal significant differences between any of the HA-primed regimens at any time point, but differences between the groups (i.e. putative effect sizes) appear small and the experiment may have lacked statistical power to do so. Heterologous prime-boost regimens were more efficient in generating anti-stem IgG responses than vaccination with HA protein.

6.3.4. Anti-Trimerisation Domain Responses Following DNA-ChAdOx1-MVA Sequential Prime-Boost Vaccination

Total IgG responses were also measured against recombinant HIV-1 envelope glycoprotein (Env) fused to the T4 fibritin foldon trimerisation domain in order to estimate responses to the trimerisation domain included in the H1HA-Stem, H1HA-Stem+TM, cH16/H1 constructs and the cH9/H1 test antigen used in ELISAs (Fig. 6.3). This has previously been reported as being highly immunogenic [520]. Samples were pooled for each group and assessed at all time points. No samples had titers outside of the 95% confidence interval of the geometric mean of background responses measured in naïve BALB/c sera (Fig. 6.3). These results suggest that antibody responses induced against the trimerisation domain by DNA-H1HA-Stem, DNA-H1HA-Stem+TM and DNA-cH16/H1 were negligible (Fig. 6.3).

Figure 6.3 Antibody responses against the T4 fibritin foldon trimerisation domain generated by heterologous DNA-ChAdOx1-MVA prime-boost vaccination

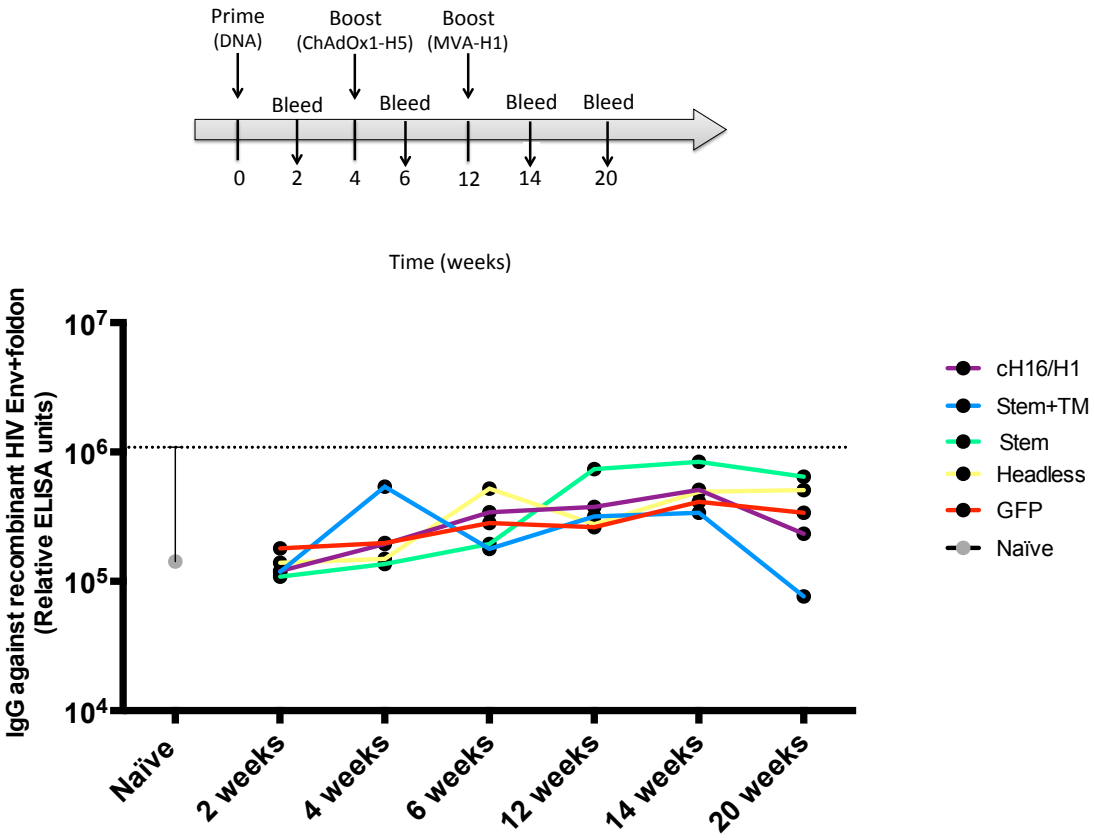


Figure 6.3 Antibody responses against the T4 fibritin foldon trimerisation domain generated by heterologous DNA-ChAdOx1-MVA prime-boost vaccination

6-8 week old BALB/c mice (n=4-6) were immunised i.m. according to the vaccination regimen in Table 6.2. Total IgG responses against recombinant HIV-1 envelope glycoprotein fused to a T4 fibritin foldon trimerisation domain were assayed by standardised ELISA at all time points. Data are pooled samples at each time point. Geometric mean and standard deviation of four replicate naïve (unvaccinated) samples are shown. The dotted line represents the upper boundary of the 95% confidence interval.

Key findings:

Antibody responses induced against the trimerisation domain by the HA-based constructs was negligible.

6.3.5. Anti-Stem Antibody Responses Following AdHu5-MVA Prime-Boost Vaccination

6-8 week old BALB/c mice (n=6) were immunised i.m. according to the vaccination regimen outlined in Table 6.3. Total IgG responses against recombinant cH9/H1 were assayed by standardised ELISA at 2 weeks and 8 weeks after each vaccination (Fig. 6.4). At 2 weeks post-prime mice vaccinated with AdHu5-Headless, AdHu5-H1HA-Stem and AdHu5-H1HA-Stem+TM had significantly higher antibody responses compared to control mice vaccinated with AdHu5-GFP (****p<0.0001 by ANOVA) (Fig. 6.4 A). In addition, mice primed with AdHu5-Headless had significantly higher responses compared to mice who received AdHu5-H1HA-Stem or AdHu5-H1HA-Stem+TM at the same time point (**p=0.0012 by ANOVA). Anti-stem IgG antibodies were significantly higher in mice primed with AdHu5-Headless at 8 weeks post-prime compared to groups receiving AdHu5-H1HA-Stem (**p=0.0015 by ANOVA), but they were not significantly boosted following vaccination with MVA-H1 (Fig. 6.4 B & C). In contrast anti-stem antibody titers were significantly boosted in mice primed with AdHu5-H1HA-Stem and AdHu5-H1HA-Stem+TM (**p=0.0022 for both) (Fig. 6.4 C). However no significant differences were observed between mice primed with AdHu5-Headless, AdHu5-H1HA-Stem or AdHu5-H1HA-Stem+TM at either 2 or 8 weeks post-boost (Fig. 6.4 C & D). Mice primed with AdHu5-Headless, AdHu5-H1HA-Stem or AdHu5-H1HA-Stem+TM had significantly higher responses compared to mice vaccinated with 10μg recombinant H1HA protein alone at all time points (***p=0.0003 by ANOVA). There were no significant differences between mice primed with recombinant H1HA protein

and naïve sera from unvaccinated mice at all time points suggesting anti-stem responses are not induced following vaccination with protein alone.

Table 6.3 Immunisation schedule for the induction of anti-stem antibodies by AdHu5-MVA prime-boost vaccination

Time (weeks)	0	8
Group	**Prime**	**Boost**
A	H1HA protein	**-**
B	AdHu5-GFP	MVA-H1
C	AdHu5-Headless	MVA-H1
D	AdHu5-Stem	MVA-H1
E	AdHu5-Stem+TM	MVA-H1

Table 6.3 Immunisation schedule for the induction of anti-stem antibodies by AdHu5-MVA prime-boost vaccination

Four groups of BALB/c mice (n=6) were immunised i.m with $1x10^8$ iu AdHu5 expressing one of Headless, H1HA-Stem, H1HA-Stem+TM or GFP. Another group of mice (n=4) received 10μg recombinant H1HA protein (A/California/07/2009). All groups except mice primed with protein received a boosting vaccination of $1x10^6$pfu MVA-H1 at 8 weeks.

Figure 6.4 Stem-specific antibody responses generated by heterologous AdHu5-MVA prime-boost vaccination

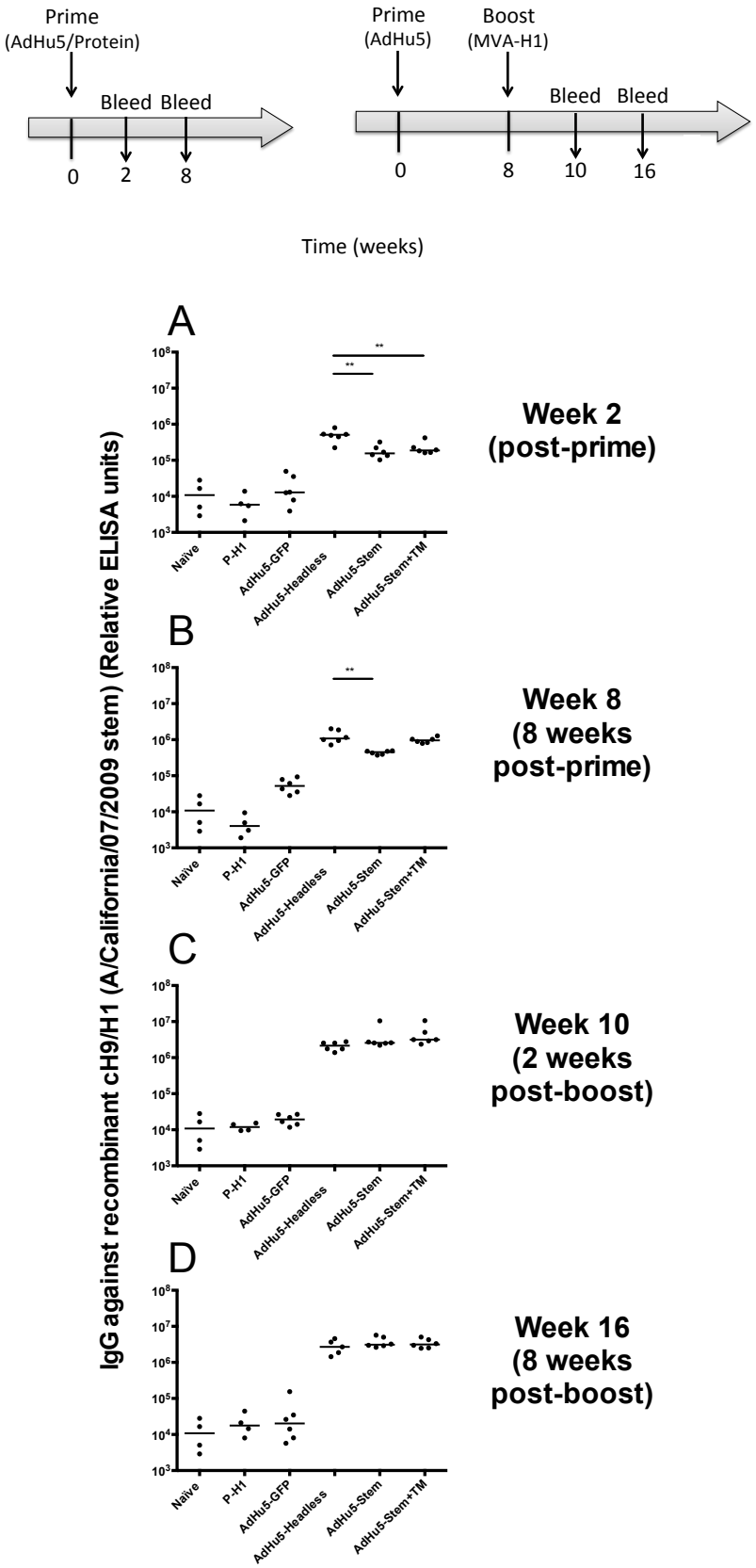
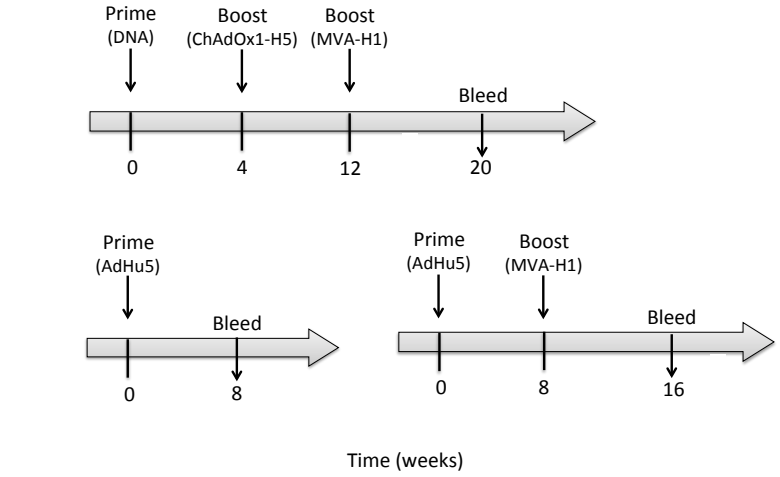


Figure 6.4 Stem-specific antibody responses generated by heterologous AdHu5-MVA prime-boost vaccination

6-8 week old BALB/c mice (n=4-6) were immunised i.m. according to the vaccination regimen in Table 6.3 (A-D). Total IgG responses against recombinant cH9/H1 were assayed by standardised ELISA at (A) 2 weeks post-prime, (B) 8 weeks post-prime (C) 2 weeks post MVA-H1 boost and (D) at 8 weeks post MVA-H1 boost. Responses in mice vaccinated with 10μg recombinant H1HA protein alone (P-H1) at (A) 2 weeks and (D) 8 weeks post-vaccination are shown for comparison. Naïve controls are unvaccinated mice. The abbreviation 'P-H1' indicates recombinant H1HA protein (A/California/07/2009). Individual values and group medians are shown. **p≤0.01 by one-way ANOVA, assuming Gaussian distribution with Dunnett post-test comparing mean responses to the AdHu5-Headless prime regimen.

Compared to the DNA-ChAdOx1-MVA regimen, anti-stem IgG titers were significantly higher in all groups primed with AdHu5 at 8 weeks post the boost with MVA-H1 (Fig. 6.5). Interestingly responses at 8 weeks following a single vaccination with AdHu5-Headless and AdHu5-H1HA-Stem were also significantly higher compared to responses at 8 weeks post-final vaccination with the DNA-ChAdOx1-MVA regimen (**p=0.0022 for both), however there were no significant differences between mice vaccinated with DNA-ChAdOx1-MVA-H1HA-Stem+TM and AdHu5-H1HA-Stem+TM at the same time point, (which seems to be largely the result of better boosting of the H1HA-Stem+TM construct in the DNA-ChAdOx1-MVA regimen compared to Headless and H1HA-Stem) (p=0.0931) (Fig. 6.5). Collectively these results indicate vaccination with AdHu5 alone is superior to a sequential prime boost regimen with DNA-ChAdOx1-MVA at inducing anti-stem responses but overall there are no significant differences between antibody response magnitude induced by heterologous Ad-MVA prime-boost vaccination using Headless, H1HA-Stem or H1HA-Stem+TM antigens.

Figure 6.5 Comparison of stem-specific antibody responses generated by heterologous DNA-ChAdOx1-MVA and AdHu5-MVA prime-boost vaccination



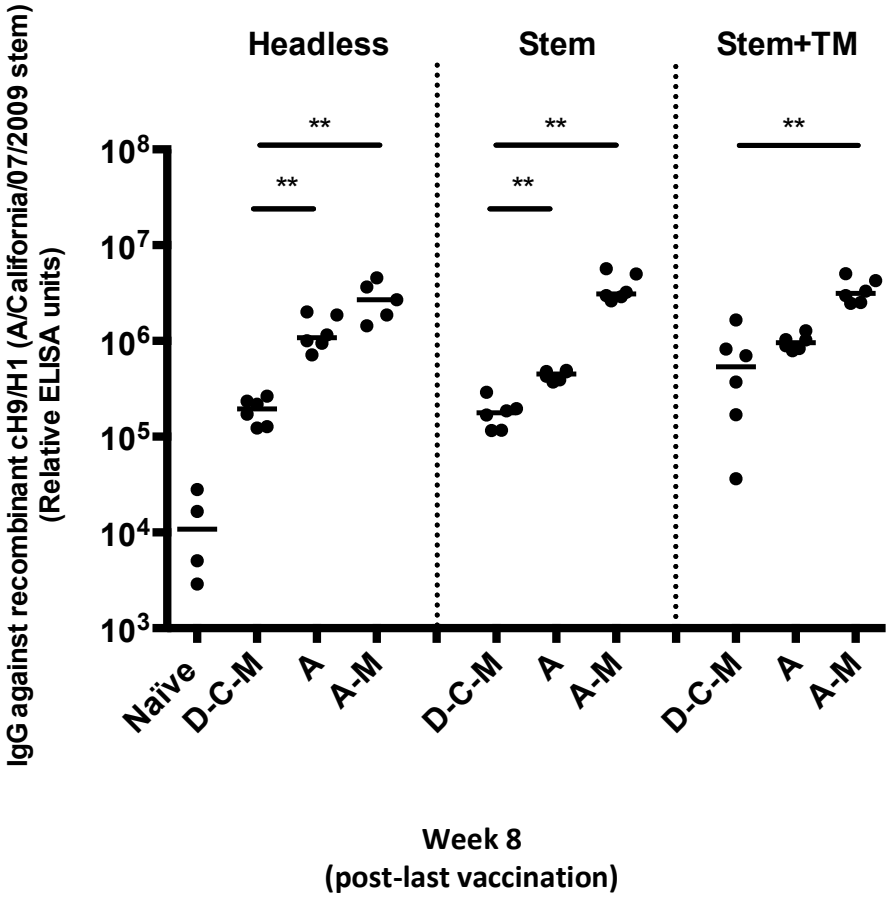


Figure 6.5 Comparison of stem-specific antibody responses generated by heterologous DNA-ChAdOx1-MVA and AdHu5-MVA prime-boost vaccination

6-8 week old BALB/c mice (n=6) were immunised i.m. according to the vaccination regimens in Tables 6.2 and 6.3. Total IgG responses against recombinant cH9/H1 were assayed by standardised ELISA at 8 weeks following the vaccinations listed on the x-axis. Naïve controls (n=4) are unvaccinated mice. The abbreviations 'A', 'C', 'D' and 'M' are used in place of 'AdHu5', 'ChAdOx1', 'DNA' and 'MVA' respectively. A dash is used to indicate separate sequential vaccinations. Individual values and group medians are shown. **p≤0.01 by Mann Whitney.

Key findings:

AdHu5 virally-vectored vaccines that express HA-based immunogens prime for anti-stem antibody responses when compared to a GFP-expressing control. Prior to an MVA-H1 boost, the AdHu5-Headless construct generated the greatest antibody response, but after the boost there was no difference between the different HA-based constructs (because responses in the Headless group were not boosted whereas responses in the other two groups were). AdHu-MVA prime boost regimens were more effective than DNA-ChAdOx1-MVA regimens in generating anti-stem IgG antibodies.

6.3.6. Anti-Trimerisation Domain Responses Following AdHu5-MVA Prime-Boost Vaccination

Total IgG responses against the T4 fibritin foldon trimerisation domain for each group were also measured by standardised ELISA at all time points using recombinant HIV-1 envelope glycoprotein fused to the T4 fibritin foldon trimerisation domain (Fig. 6.6). Mice vaccinated with AdHu5-H1HA-Stem+TM had detectable titers outside of the 95% confidence interval of the geometric mean of background responses measured in naïve BALB/c sera at both time points following the boost with MVA-H1. This suggests antibody responses are induced against the trimerisation domain following viral-vector delivery of constructs expressing this domain but the magnitude of these responses depends on factors other than the gene delivery vehicle (Fig. 6.5).

Figure 6.6 Antibody responses against the T4 fibritin foldon trimerisation domain generated by heterologous AdHu5-MVA prime-boost vaccination

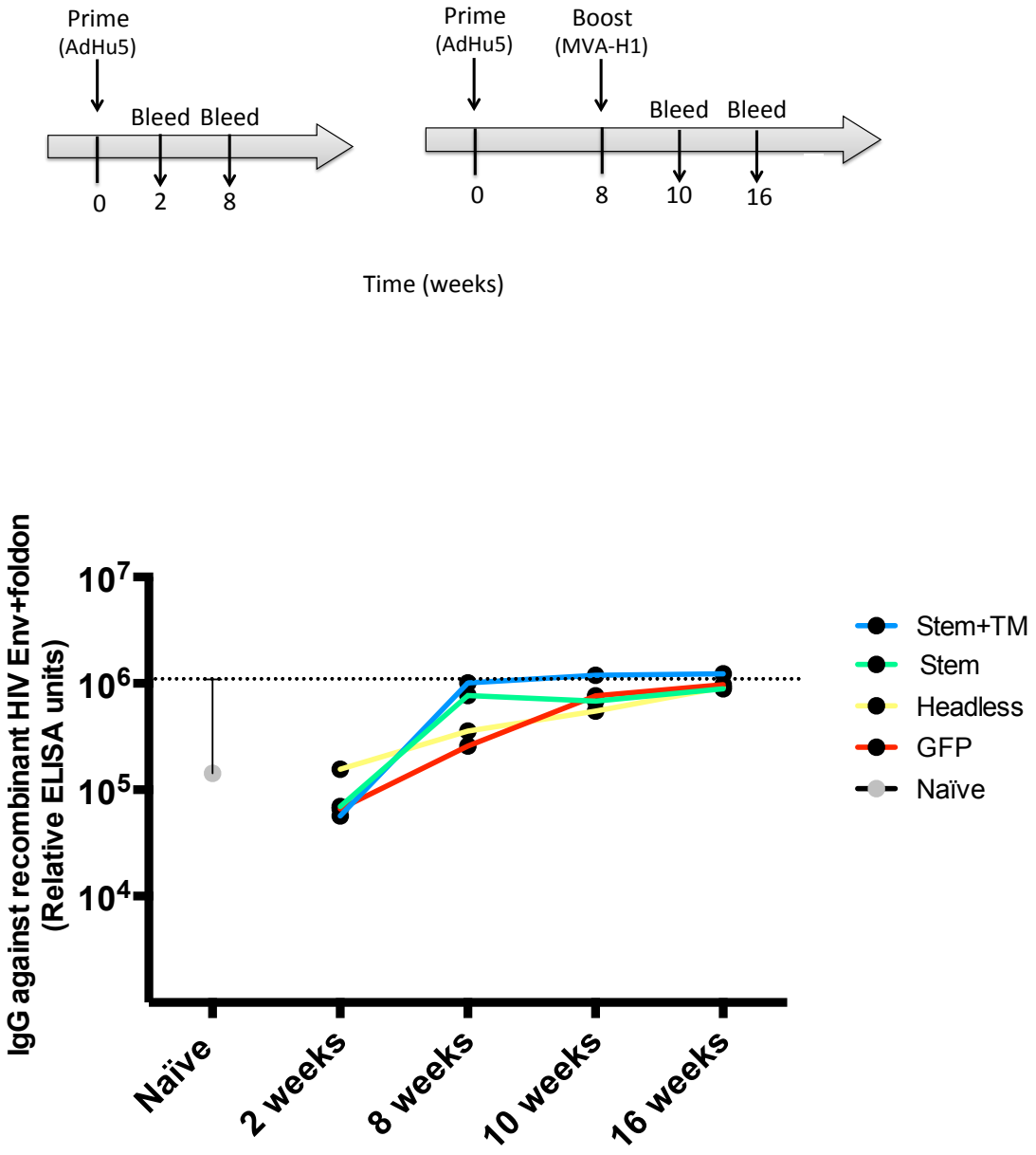


Figure 6.6 Antibody responses against the T4 fibritin foldon trimerisation domain generated by heterologous AdHu5-MVA prime-boost vaccination

6-8 week old BALB/c mice (n=6) were immunised i.m. according to the vaccination regimen in Table 6.3. Total IgG responses against recombinant HIV-1 envelope glycoprotein fused to a T4 fibritin foldon trimerisation domain were assayed by standardised ELISA at all time points. Data are pooled samples at each time point. Geometric mean and standard deviation of four replicate naïve samples are shown. The dotted line represents the upper boundary of the 95% confidence interval.

Key findings:

Antibody responses induced against the trimerisation domain by the AdHu5HA-based constructs were (just) detectable for one of the vaccines, and should be controlled for in future studies.

6.4. Discussion

BnStAbs have the potential to provide protection against infection with seasonal and pandemic strains of IAV. Unsurprisingly, there is considerable interest in developing immunogens capable of inducing these responses, with view to developing universal influenza vaccines. The present study has investigated the ability of three novel vaccine constructs to induce anti-stem antibodies in mice by means of DNA and virally-vectored vaccination regimens in comparison to a first-generation stem immunogen, Headless. Anti-stem IgG serum responses were assessed using a recombinant chimeric HA, cH9/H1, designed to specifically measure antibodies against the stem region of Group 1 HAs (Chapter 3). (Exposure to H9 subtypes in humans has been reported, albeit rarely, and the H16 subtype may prove a potentially better tool for human studies where results could be confounded by pre-existing antibodies against the globular head domain of H9 [521]. This can be controlled for and is discussed further in the final discussion of this thesis).

In line with published studies assessing vaccine delivery vectors, priming with AdHu5 was significantly more immunogenic compared to DNA. Boosting with ChAdOx1 and MVA did not compensate for this. Antibody titers observed at the end points of each experiment suggest that the novel immunogens H1HA-Stem, H1HA-Stem+TM and cH16/H1 are capable of inducing responses comparable to Headless, at least in the case of a DNA prime for cH16/H1, and in both DNA and AdHu5 priming regimens for H1HA-Stem and H1HA-Stem+TM. The addition of the TM domain did not alter end-titer responses induced by H1HA-Stem however the lack of a TM domain in

cH16/H1 may have prohibited the production of AdHu5 vectors expressing this antigen as a result of HA-induced toxicity. Although the immunogenicity of the constructs expressed by MVA could not be tested due to time constraints, it is possible the presence of the TM domain on H1HA-Stem+TM could induce higher antibody titers. MVA-vectored vaccine preparations expressing native HA including a TM domain contain remnants of cell membrane with embedded HA, the amount of which depends on the purification methods used during production (Dr Vincent Pavot, personal communication). This constitutes additional antigen not accountable by pfu, which could affect antibody response magnitude. Further studies investigating boosting with MVA-H1HA-Stem, MVA-H1HA-Stem+TM and MVA-cH16/H1 are warranted to assess this.

An important finding from this study is that although anti-stem responses primed by Headless were not boosted by MVA-H1, antibodies induced by H1HA-Stem and H1HA-Stem+TM were significantly boosted. Although it has not been verified, the ability of H1HA-Stem and H1HA-Stem+TM to induce responses that are subsequently boosted by native H1HA could be because more native-like epitopes are preserved in these immunogens as a result of addition of the trimerisation domain. Recent research in the HIV field has demonstrated that a stable native-like trimerised glycoprotein immunogen can induce neutralising antibodies against higher resistance viruses compared to unstable antigens, which tend to induce responses against more sensitive variants [522]. These more sensitive viruses are neutralised by recognition of linear epitopes, whereas more resistant viruses are recognised by

conformational epitopes, some of which overlap with epitopes recognised by bnAbs isolated from HIV-infected individuals, which display a high degree of somatic hypermutation [522]. This suggests that, at least in the case of HIV, inducing a more cross-reactive response cannot be achieved simply by increasing the titer of responses against linear epitopes and that native-like trimers may represent a more promising starting point for developing vaccines aimed at inducing bnAbs [522]. Considering all of the bnStAbs discovered to date in the influenza field recognise conformational epitopes, it seems likely this will hold true for influenza. Furthermore, non-neutralising anti-stem antibodies have been associated with the formation of immune complexes and enhanced respiratory disease in pigs [437]. In addition infection of adults with the 2009 H1N1 influenza virus was associated with immune complex–mediated disease caused by high titers of low-avidity non-neutralising antibodies and complement activation in the respiratory tract [110]. Although non-neutralising anti-stem antibodies can augment viral clearance via ADCC, this contribution is unlikely to balance the cost of immune-complex mediated pathology [523]. It is therefore paramount that vaccines aimed at eliciting anti-stem antibodies against IAV induce predominantly functionally neutralising antibodies. At present, work is underway to produce a chimeric pseudotyped lentivirus capable of measuring neutralising anti-stem antibodies against Group 1 HA (George Carnell, personal communication). Future studies using this will be useful to assess the functionality of the antibody responses induced by the vaccine constructs described in this chapter.

6.5. Chapter Summary

- Broadly neutralising anti-stem antibodies (bnStAbs) could potentially protect against multiple strains of seasonal and pandemic IAV
- This chapter assess the ability of three novel vaccine constructs, H1HA-Stem, H1HA-Stem+TM and cH16/H1, to induce anti-stem antibody responses
- H1HA-Stem, H1HA-Stem+TM and cH16/H1 are capable of inducing anti-stem antibody responses comparable to Headless
- Only responses primed by AdHu5-expressed H1HA-Stem and H1HA-Stem+TM are boosted by vaccination with MVA-H1HA

Chapter 7

Investigation of B and T Cell Responses Induced by Novel Viral Vectors Expressing HA, NP and M1

7. Investigation of B and T Cell Responses Induced by Novel Viral Vectors Expressing HA, NP and M1

Part of the data described in this chapter (specifically, Figure 7.2) has been peer-reviewed and published:

Enhancing cellular immunogenicity of MVA-vectored vaccines by utilizing the F11L endogenous promoter.

Alharbi NK, Spencer AJ, Salman AM, Tully CM, Chinnakannan SK, Lambe T, Yamaguchi Y, Morris SJ, Orubu T, Draper SJ, Hill AV, Gilbert SC.

Vaccine. 2016 Jan 2;34(1):49-55.

7.1. Background

Sterilising immunity against influenza A virus (IAV) is antibody-mediated. All currently licensed seasonal influenza vaccines, whether inactivated or live attenuated, induce neutralising antibodies that protect against infection by preventing haemagglutinin (HA) -mediated virus entry into respiratory tract epithelia [524,525]. However, IAVs are notoriously adept at reinventing themselves and continuously evolve to escape host immunity by generating antigenically distinct escape mutants. Although humoral immune responses induced following infection or vaccination are frequently potent they are predominantly strain-specific and this unfortunately means they are redundant against newly-emerging heterologous strains [526]. Such antibody-escape variants can originate by one of two means; either as a result of subtle point mutations arising from the inherently error-prone viral RNA polymerase, a process known as antigenic drift, or, from a genetic recombination event, antigenic shift, whereby, whole genome segments are exchanged between distinct viruses co-infecting a single cell. This latter circumstance is particularly high-risk and can spawn an entirely novel, potentially pandemic, virus.

In contrast, cellular immune responses target predominantly internal viral proteins and frequently recognise epitopes that are highly conserved across different subtypes of influenza A, making them important mediators of heterosubtypic immunity. In particular, the contribution of $CD8^+$ cytotoxic T lymphocytes (T_C) has been recognised for almost 40 years. Upon infection these cells are activated in secondary lymph organs and recruited to the site

of infection where they play an important role in limiting virus spread. Foreign antigen presentation in the context of MHC class I molecules stimulates the production of cytolytic mediators such as perforin and granzyme, which in turn induce apoptosis in influenza-infected cells [527]. While substantially less is understood about the role of $CD4^+$ T helper (T_H) cells during influenza infection, these cells have been classically associated with the promotion of effective antibody responses and the precise mechanisms by which they contribute to the development of influenza-specific antibodies is a rapidly evolving area of research (Chapter 5). Animal models in particular have been instrumental in delineating the role of T_C cells against influenza. Naïve mice lacking T_C cells have an increased risk of mortality and demonstrate delayed viral clearance when challenged with influenza virus compared to healthy controls [216]. Yet B cell-deficient mice previously primed against influenza can still clear an infection and remain protected from death following a lethal challenge, despite their lack of B cells [217]. While there is substantially less evidence supporting the role of T_C cells in human immunity to influenza, a seminal challenge study demonstrated that high levels of T_C cells correlated with reduced viral shedding in the absence of HA-specific antibodies and more recently, higher levels of these cells were shown to correlate with less severe disease outcomes during the 2009 pandemic in the absence of cross-reactive neutralising antibodies [218,219]. These data suggest that vaccination strategies to induce anti-influenza T cell responses in human populations have the potential to reduce influenza-associated morbidity and mortality by boosting naturally induced heterosubtypic T cell responses and such responses could be particularly important against pandemic viruses.

Mounting evidence suggests it will take a multi-angle approach targeting more than one antigen and engaging several arms of the immune system in order to stimulate protective responses against mercurial pathogens such as influenza, malaria and HIV. In the area of vaccine development, replication-deficient viral-vectored vaccines remain an unparalleled technology in the induction of strong cellular immune responses [273]. Heterologous prime-boost regimens using adenoviral (Ad) vectors and modified vaccinia virus Ankara (MVA) have shown particular promise for maximising T cell responses against a range of infectious diseases including influenza [326,528-531]. More recently however, viral-vectored vaccines have been further extended as a platform to induce both humoral and cellular immune responses [274]. Notably, heterologous Ad-MVA regimens incorporating the blood stage malaria antigens, *Plasmodium falciparum* merozoite surface protein 1 (MSP1) or apical membrane antigen 1 (AMA1), have been used to simultaneously induce antibody and T cell responses and, in the case of MSP1, have achieved humoral responses equivalent to, or better than, candidate protein only vaccines [519,529,532,533]. In these experiments mice received a mixture of two antigens, each delivered by an individual viral vector [534]. New generation multivalent viral vectors, such as described in this chapter, could provide a dose-sparing alternative (in terms of vector). However, delivery of more than one antigen by vaccination can result in antigenic competition [534]. While the mechanisms mediating this phenomenon remain unclear, interference between B and T cell responses following vaccination with bivalent viral-vectors should be investigated on a per-antigen basis [534].

Viral-vectored vaccines against influenza A have already shown promise as platforms to induce synergistic immune responses. MVA-NP+M1 is a candidate influenza viral-vectored vaccine comprising modified vaccinia virus Ankara (MVA), expressing a fusion protein of nucleoprotein (NP) and matrix protein 1 (M1) [310]. The vaccine antigen consists of the complete sequences of NP and M1 from A/Panama/2007/99 (H3N2) joined by a 7 amino acid linker (NP and M1 sequences have >98% sequence homology to A/Switzerland/9715293/2013, the currently circulating H3N2 strain recommended for the 2015/16 Northern hemisphere vaccine) [310]. This vaccine is designed to boost pre-existing T cell responses in adults with pre-existing immunity to IAV but could also be used to prime responses in young children. Indeed MVA-NP+M1 has an excellent safety profile in humans, is immunogenic and capable of providing a protective effect against influenza challenge [310,311]. As a first step towards inducing simultaneous B and T cell responses against influenza A, co-administration of MVA-NP+M1 with seasonal trivalent-inactivated influenza vaccine (TIV) was previously investigated at the Jenner Institute [374,442]. This approach was successful in both human and animal models and induced T cell responses against conserved internal antigens whilst enhancing antibody responses against influenza A surface proteins [442]. However, a major disadvantage of co-administering MVA-NP+M1 with TIV as a clinically viable vaccination strategy is that ultimately, this regimen relies on sufficient stocks of seasonal vaccine. Indeed one of the primary hurdles faced by the current production system of influenza vaccines is the time lag in the production of adequate supplies of seasonal vaccines which also makes this system completely unreliable in

pandemic situations. At present the majority of seasonal vaccines produced rely on the availability of fertilised chicken eggs [240,535]. However, production of viral-vectored vaccines is not restricted by egg supply. Furthermore, both adenovirus and MVA-vectored vaccines can be grown to high titers and purified by relatively straightforward methods [536]. Although a viral-vectored vaccine only regimen expressing HA would also depend on correct antigenic matching of vaccine and circulating strains, manufacture times would be quicker meaning in the event of mismatch, production could be switched to the new strain with less risk of vaccine stock shortfalls.

In this chapter I have explored the ability of a novel bivalent viral-vectored vaccine and simian viral-vectored vaccines to simultaneously induce B and T cell responses against the influenza A antigens HA, NP and M1. I have taken forward the most promising of these regimens and investigated vaccine immunogenicity when used in a heterologous ChAd-MVA prime-boost regimen with the over-arching aim of inducing maximum T and B cell responses. The results of this study are reported herein.

7.2. Specific methods

This chapter describes results from five separate experimental protocols

Protocol 1 (H5):

Vaccines used:

MVA-H5 (single antigen vector expressing H5 from A/Vietnam/1203/2004); MVA-NP+M1-H5 (bivalent, with NP+M1 expressed from the F11 promoter, and H5 (same strain) from P7.5, see section 2.4.2.3)

Sample availability/utilisation:

Serum 2 weeks post-vaccination:

Responses against recombinant H5HA protein (A/Vietnam/1203/2004; BEI resources) measured by ELISA (section 2.8.1. and 7.3.1.1.1)

Protocol 2 (different promoters):

Vaccines used:

MVA-NP+M1 (expressed from P7.5); MVA-NP+M1 (expressed from F11); MVA-NP+M1-H5 (bivalent, as above); MVA-GFP (control)

Sample availability/utilisation:

Splenocytes 2 weeks post-vaccination:

T cell responses against the $NP_{147-158}$ (TYQRTRALV) epitope were measured by IFN-γ ELISpot (section 2.7.5, 2.8.4 and 7.3.1.1.2)

Protocol 3 (H7):

Vaccines used:

MVA-NP+M1 (P7.5); MVA-NP+M1 (F11); MVA-NP+M1-H7 (bivalent, with NP+M1 expressed from the F11 promoter, and H7 (from A/Netherlands/219/2003) from P7.5, see section 2.4.2.3); MVA-H7 (same strain). See Table 7.1.

Sample availability/utilisation:

Serum 2 and 8 weeks post-vaccination:

Total serum IgG responses against recombinant H7HA protein A/Netherlands/219/2003 were measured at all time points (section 2.8.1. and 7.3.1.2.1)

Splenocytes 2 weeks post-vaccination:

T cell responses against the $NP_{147-158}$ (TYQRTRALV) epitope were measured by IFN-γ ELISpot (section 2.7.5, 2.8.4 and 7.3.1.2.2)

Protocol 4 (ChAdOx1 prime):

Vaccines used:

ChAdOx1 NP+M1 (see section 2.4.1.3); ChAdOx1-H7 (A/Netherlands/219/2003, see section 2.4.1.4); Recombinant H7HA (same strain). ChAdOx1 vaccines were administered simultaneously, either mixed or in separate limbs.

Sample availability/utilisation:

Serum 2 and 8 weeks post-vaccination:

Total serum IgG responses against recombinant H7HA protein (A/Netherlands/219/2003) (section 2.8.1. and 7.3.2.1).

Splenocytes 2 weeks post-vaccination:

T cell responses against the $NP_{147-158}$ (TYQRTRALV) epitope (sections 2.7.5 and 2.8.4) (section 2.7.5, 2.8.4 and 7.3.2.2)

Protocol 5 (prime-boost):

Vaccines used:

Prime with ChAdOx1 NP+M1; ChAdOx1-H7; or both ChAdOx1 vaccines simultaneously (separate limbs). Boost with MVA-NP+M1-H7 (bivalent). Schedule outlined in Table 7.2.

Sample availability/utilisation:

Serum 2 and 8 weeks post each vaccination and at 26 weeks:

Total serum IgG responses against recombinant H7HA protein were measured (section 2.8.1. and 7.3.3.1.1).

Serum 8 weeks post-boost:

Breadth of anti-HA antibody functionality assessed by pseudotype neutralisation assay (section 2.8.3 and 7.3.3.1.2).

Bone marrow (BM) cells and splenocytes at 26 weeks:

Total IgG^+ ASCs, H7HA-specific ASCs (representative of LLPCs) and mBC-derived ASCs were assessed by ELISpot (section 2.7.5, 2.7.6, 2.8.5, 2.8.6 and 7.3.3.1.3).

Splenocytes 2 weeks post-prime and 2 weeks post-boost:

T cell responses against the $NP_{147-158}$ (TYQRTRALV) epitope, and against H7HA from two different peptide pools (one representative of H7HA from A/Netherlands/219/2003 and another representative of regions of sequence diversity in A/Anhui/1/2013 and A/Shanghai/1/2013) were measured (section 2.7.5, 2.7.6, 2.8.5, 2.8.6 and 7.3.3.2.2)

Subjects: 6-10 week-old female BALB/c ($H\text{-}2^d$) mice (numbers as described in the text).

Methods used: Standardised ELISA techniques are described in section 2.8.1. The ELISpot assays used in this chapter are described in 2.8.4, 2.8.5, and 2.8.6. The pseudotype neutralisation assay is described in 2.8.3

7.3. Results

7.3.1. Immunogenicity of Novel Bivalent Poxviral-Vectored Vaccines Expressing NP+M1 and HA

7.3.1.1. MVA-NP+M1-H5

7.3.1.1.1. Antibody Responses Against H5HA

In order to examine if the humoral immune responses induced by bivalent MVA vectors expressing the T cell-inducing fusion antigen NP+M1 and a second antigen, HA, were comparable to those induced by single antigen vectors, a preliminary experiment was set up to investigate antibody responses induced by MVA-H5 and MVA-NP+M1-H5. The bivalent vectored-vaccine, MVA-NP+M1-H5, was previously produced by Dr Senthil Chinnakannan (section 2.4.2.3). The H5HA antigen was chosen as a random representative of Group 1 HA. BALB/c mice (n=5) were immunised intramuscularly (i.m.) with $1x10^6$ plaque-forming units (pfu) MVA-H5, a single antigen vector expressing the Group I HA, H5HA (A/Vietnam/1203/2004; H5N1), or, MVA-NP+M1-H5, a bivalent vaccine expressing the same H5HA antigen in addition to the T cell fusion antigen, NP+M1. Serum was collected at 2 weeks post-vaccination and total serum IgG responses were measured by ELISA against recombinant H5HA protein (A/Vietnam/1203/2004; BEI resources).

Antibody responses were significantly higher compared to unvaccinated naïve mice for both MVA-H5 and MVA-NP+M1-H5 (**p=0.009 for both). No significant differences in antibody responses were observed between mice receiving MVA-H5 or MVA-NP+M1-H5 (p=0.69) (Fig. 7.1). This indicates that

co-expression of NP+M1 in the bivalent vectored-vaccine did not interfere with the generation of specific humoral responses against H5HA.

Figure 7.1 HA-specific antibody responses generated by MVA-NP+M1-H5

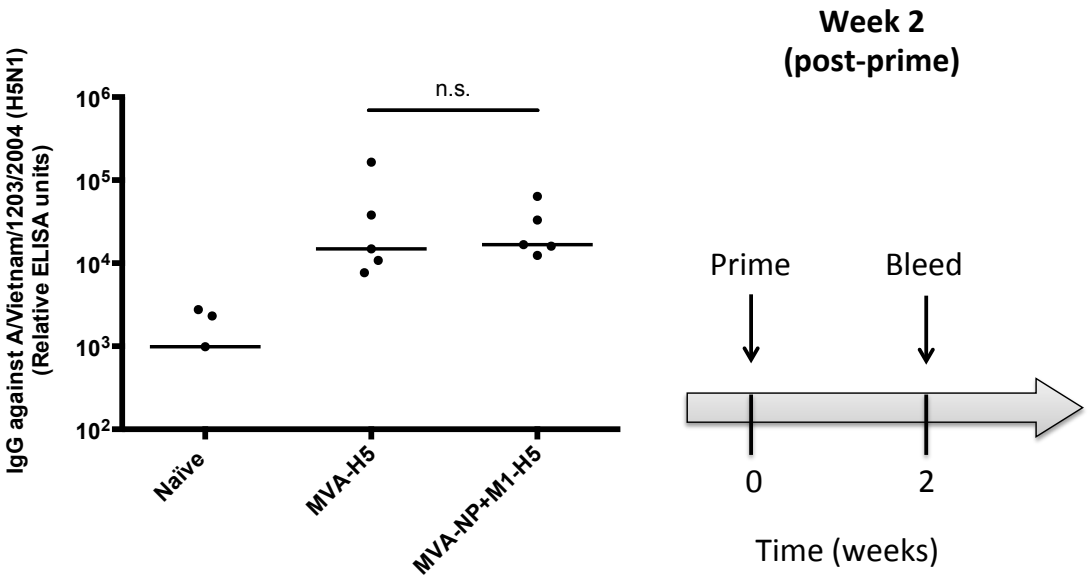


Figure 7.1 HA-specific antibody responses generated by MVA-NP+M1-H5

6-8 week old BALB/c mice (n=5) were immunised i.m. with $1x10^6$ pfu MVA-H5 or $1x10^6$ pfu MVA-NP+M1-H5. Total IgG responses against recombinant H5HA (A/Vietnam/1203/2004; H5N1) were assayed by standardised ELISA at 2 weeks post-vaccination. Naïve controls are unvaccinated mice. Two data points in the naïve group have not been plotted as they were below the limit of detection. Individual values and group medians are shown. n.s. = not significant. These data are representative of two independent experiments.

Key findings:

Co-expression of H5 and NP+M1 in a bivalent vector did not compromise generation of anti-H5 IgG antibodies in this system.

7.3.1.1.2. T cell Responses Against NP+M1

To date all clinical data published on MVA-NP+M1 has been based on the prototype vaccine that expresses NP+M1 under control of the early/late vaccinia promoter P7.5 (section 2.1.7). However, new-generation bivalent constructs control NP+M1 expression using the early vaccinia promoter F11, (as enhanced immunogenicity has previously been observed using this promoter) while HA expression is driven by P7.5 [368]. In order to assess the effect of this different promoter in addition to the presence of a second (irrelevant) vaccinating antigen (in this case H5) on T cell responses, BALB/c mice (n=5) were immunised with $1x10^6$ pfu MVA-NP+M1 (P7.5), MVA-NP+M1 (F11) or MVA-NP+M1-H5 (with F11 expressing NP+M1). Splenocytes were isolated 2 weeks post-vaccination and T cell responses were measured by *ex vivo* IFN-γ ELISpot against the immunodominant BALB/c epitope in NP, $NP_{147-158}$ (TYQRTRALV) (sections 2.7.5 and 2.8.4).

Following vaccination with the bivalent vaccine, MVA-NP+M1-H5 (F11), T cell responses in mice (median spot-forming units per million splenocytes (SFU)=206) were significantly higher (****p<0.0001) compared to mice vaccinated with MVA-NP+M1 (P7.5) (median SFU=60) (Fig. 7.2). Similarly, significantly higher T cell responses were observed following vaccination with MVA-NP+M1 (F11) (median SFU=162) compared to MVA-NP+M1 (P7.5) (median SFU=60) (**p=0.0002) (Fig. 7.2). Differences between T cell responses generated by vaccination with the bivalent MVA-NP+M1-H5 (F11) vaccine compared to MVA-NP+M1 (F11) were not significant.

Figure 7.2 T cell responses following MVA-NP+M1-H5 vaccination

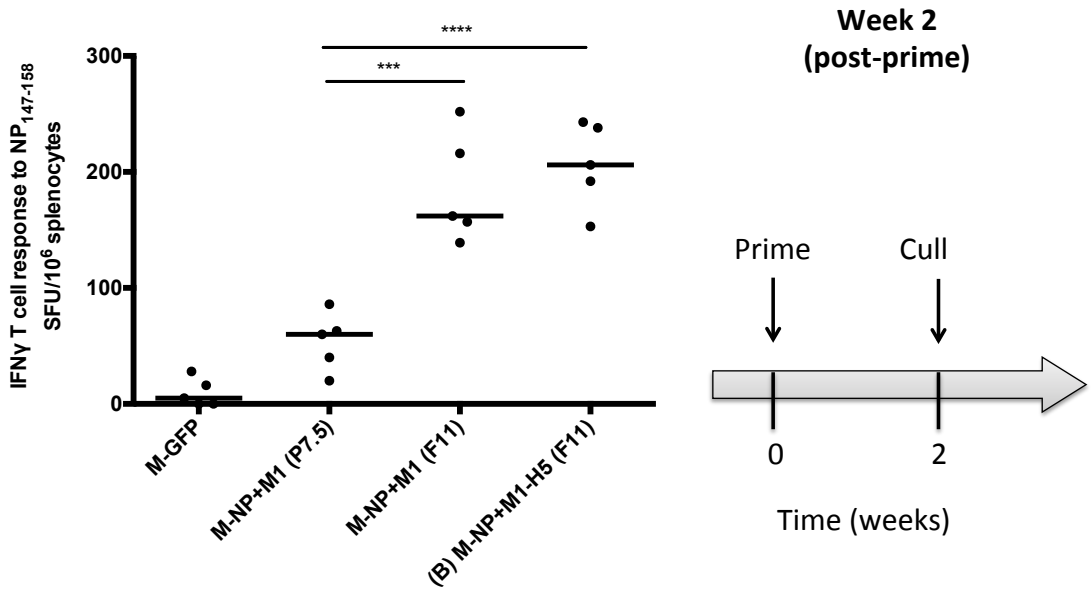


Figure 7.2 T cell responses following MVA-NP+M1-H5 vaccination

IFNγ ELISpot *ex vivo* T cell responses to NP+M1 in 6-8 week old BALB/c mice (n=5) immunised i.m. with $1x10^6$ pfu MVA-GFP, MVA-NP+M1 (P7.5), MVA-NP+M1 (F11) or MVA-NP+M1-H5 (F11). The promoter (F11 or P7.5) controlling expression of NP+M1 in each construct is shown in brackets. The abbreviation 'B' represents 'bivalent'. Individual values and group medians are shown. ***p≤0.001, ****p≤0.0001 by one-way ANOVA, assuming Gaussian distribution with Dunnett post-test comparing mean responses to vaccination with MVA-NP+M1 (P7.5).

Key findings:

NP-specific T cell induction was more effective when NP+M1 was expressed under the F11 promoter, compared to the P7.5, promoter. Addition of H5 in the bivalent construct did not significantly reduce this NP-specific response.

7.3.1.2. MVA-NP+M1-H7

7.3.1.2.1. Antibody Responses Against H7HA

As the immunogenicity of HA can vary greatly depending on subtype, humoral responses induced by vaccination with MVA-NP+M1-H7, a second bivalent construct expressing the Group 2 HA, (A/Netherlands/219/2003; H7N7), in addition to NP+M1, was also investigated. BALB/c mice (n=5-10) were immunised i.m. against H7HA and/or NP+M1 according to the immunisation regimes in Table 7.1. As an extension, mice were also co-administered vaccines into separate limbs as this has previously been shown to minimise T cell interference whilst maintaining B cell responses [534]. Serum was collected at 2 and 8 weeks post-vaccination. Total serum IgG responses at all time points were measured against recombinant H7HA protein A/Netherlands/219/2003 (sections 2.6 and 3.2.1) (Fig. 7.3 A & B).

Mice immunised with MVA-NP+M1-H7 had the highest median H7HA-specific IgG antibodies at 2 weeks post-vaccination compared to all other groups (Fig. 7.3 A). These responses were significantly higher compared to vaccination with 10μg recombinant H7HA alone (***p=0.0001) or by co-administration of MVA-H7 and MVA-NP+M1 administered in separate limbs (**p=0.002, line not drawn on graph for clarity) (Fig. 7.3 A). There were no significant differences in H7HA-specific IgG responses between groups receiving MVA-NP+M1-H7 or a mixture of MVA-H7 and MVA-NP+M1, although responses after MVA-NP+M1-H7 were marginally better compared to the vaccination with MVA-H7 alone (*p=0.015, line not drawn on graph for clarity) (Fig. 7.3 A). Furthermore these responses were maintained and mice vaccinated with

MVA-NP+M1-H7 had higher median responses compared to all other groups 8 weeks post-vaccination (Fig. 7.3 B). These responses were also significantly higher compared to vaccination with recombinant 10μg H7HA alone (*p=0.0427) (Fig. 7.3 B). Overall, groups vaccinated with viral vectors had higher H7-specific IgG responses compared to vaccination with recombinant H7HA protein only. These results demonstrate that the novel bivalent vaccine MVA-NP+M1-H7 induces superior H7HA-specific IgG responses compared to protein and these responses are not diminished by the presence of NP+M1 in a bivalent vaccine. As the fold-increase in antibody titers against the H7HA antigen was greater than H5HA in vaccinated compared to naïve animals (presumably due to an intrinsic ability of H7 peptides to bind MHC molecules in BALB/c mice better than H5 peptides), this antigen was taken forward for later experiments. It is important to note, however, that H7 epitopes have been identified that are identical to human proteins and can contribute to reduced humoral responses against H7HA in humans [537].

Table 7.1 Immunisation regimen for delivery of NP+M1 and H7HA by MVA-vectored vaccine

Group	Vaccine	Antigen promoter
A	H7HA protein	-
B	MVA-NP+M1	P7.5
C	MVA-NP+M1	F11
D	MVA-H7	P7.5
E	MVA-NP+M1-H7	F11 (NP+M1), P7.5 (H7)
F	MVA-NP+M1 and MVA-H7 (mixture)	P7.5 (both)
G	MVA-NP+M1 (right limb) & MVA-H7 (left limb)	P7.5 (both)

Table 7.1 Immunisation regimen for delivery of NP+M1 and H7HA by MVA-vectored vaccine

Six groups of BALB/c mice (n=5-10) were immunised i.m with $1x10^6$ pfu MVA-vectored vectors ($1x10^6$ pfu of each vaccine in the case of Groups F and G) expressing H7HA and/or NP+M1 either alone, as a mixture or by co-administration into separate limbs. Another group of mice (n=4) received 10μg recombinant H7HA protein (A/Netherlands/219/2003). Antigen expression in MVA-vectored vaccines is controlled by promoters. P7.5 is an early/late vaccinia promoter. F11 is an early vaccinia promoter.

Figure 7.3 HA-specific antibody responses generated by MVA-NP+M1-H7

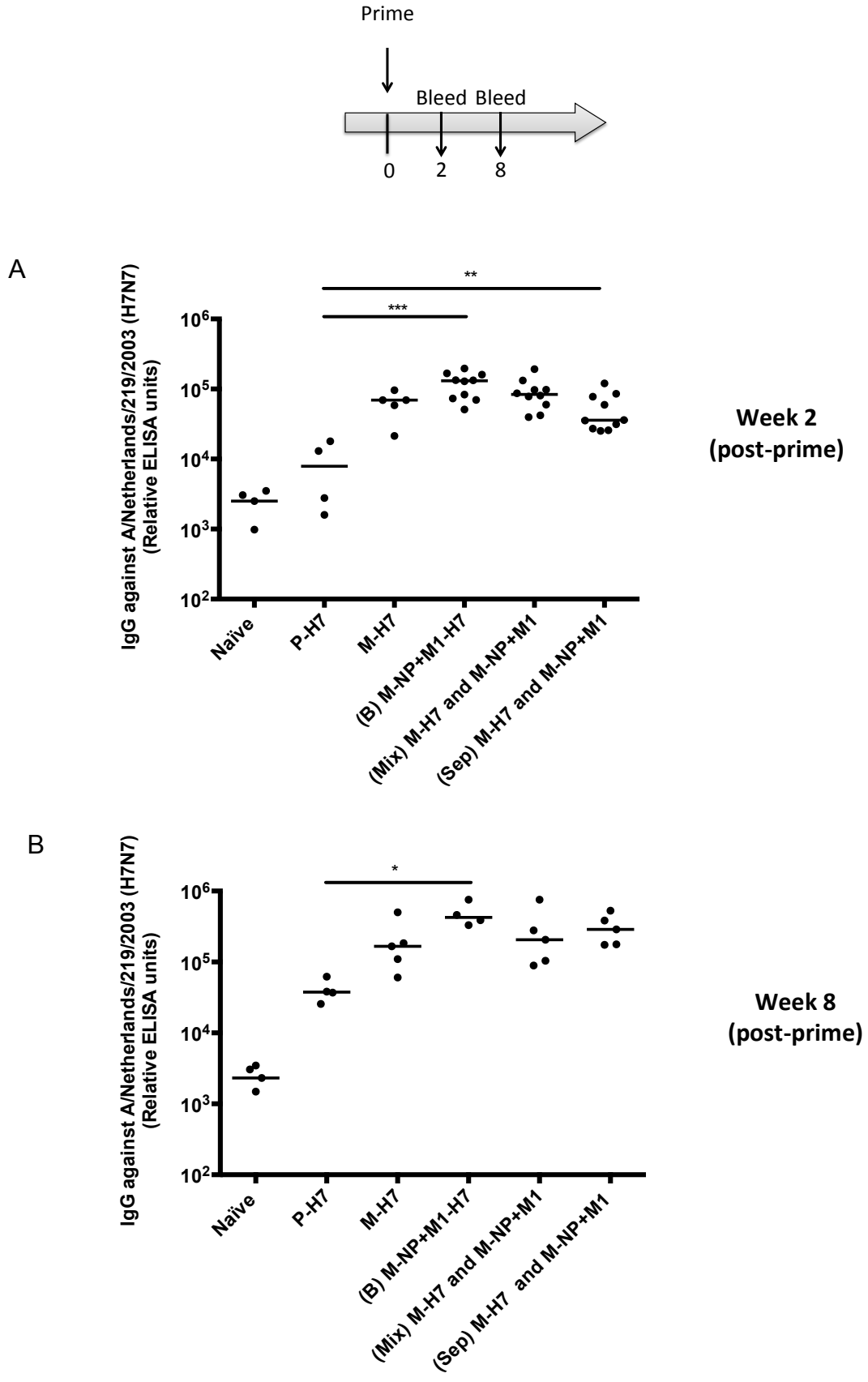


Figure 7.3 HA-specific antibody responses generated by MVA-NP+M1-H7

6-8 week old BALB/c mice (n=5-10) were immunised i.m. according to the vaccination regimen in Table 7.1. Total IgG responses against recombinant H7HA (A/Netherlands/219/2003; H7N7) were assayed by standardised ELISA at (A) 2 and (B) 8 weeks post-vaccination. (A) The group receiving the bivalent construct, and that receiving vaccines in separate limbs, had significantly greater titres than the protein group, as shown. In all other pairwise comparisons (not shown) the only other groups that were significantly different from each other were MVA-NP+M1-H7 versus MVA-NP+M1 and MVA-H7 (separate limbs) (**p=0.002), and MVA-NP+M1-H7 versus MVA-H7 (*p=0.015). Naïve controls are unvaccinated mice. One data point in each naïve group has not been plotted because it was below the limit of detection. The abbreviation 'P-H7' indicates recombinant H7HA protein (A/Netherlands/219/2003). 'M' is used in place of 'MVA' and 'B', 'Mix' and 'Sep stand for 'bivalent', 'mixture' and 'separate vaccines' respectively. Individual values and group medians are shown. *p≤0.05 **p≤0.005, ***p≤0.001 by one-way ANOVA, assuming Gaussian distribution with Dunnett post-test comparing mean responses to the protein only regimen. These data are representative of two independent experiments.

Key findings:

H7-expressing MVA virally-vectored vaccines generated a stronger H7-specific IgG antibody response than vaccination with H7 protein alone. A bivalent MVA construct expressing H7 and NP+M1 was more effective than monovalent vaccines, singly or in combination.

7.3.1.2.2. T Cell Responses Against NP+M1

The phenomenon of antigenic competition among T cells has previously been observed following a co-administration heterologous prime boost regimen using MVA vectors at the boost expressing single pre-erythrocytic or blood-stage *Plasmodium falciparum* antigens [534]. However, it was not observed following an adenovirus prime [534]. The authors of this study hypothesised that MVA infected cells from the boosting vaccination are more rapidly eliminated by $CD8^+$ T cells primed after the first vaccination but they did not investigate if competition occurred following an MVA prime [534]. In order to assess if T cell interference following multi-antigen MVA vaccination could be a vector-related phenomenon, BALB/c mice were vaccinated according to the regimen in Table 7.1. Splenocytes were isolated 2 weeks post-vaccination for examination of responses against NP+M1. T cell responses were measured by *ex vivo* IFN-γ ELISpot against the immunodominant BALB/c epitope in NP, $NP_{147-158}$ (TYQRTRALV) (sections 2.7.5 and 2.8.4). There were no significant differences between T cell responses generated by vaccination with MVA-NP+M1 (P7.5) alone (median SFU=31) compared to vaccination with either a mixture of MVA-NP+M1 (P7.5) and MVA-H7 (median SFU=34) or by co-administration of MVA-H7 and MVA-NP+M1 (P7.5) into separate limbs (median SFU=60) (Fig. 7.4). However responses following vaccination with MVA-NP+M1 (F11) (median SFU=160) or the bivalent vaccine MVA-NP+M1-H7 (F11) (median SFU=192) were significantly higher compared to vaccination with MVA-NP+M1 (P7.5) (**p<0.01 and ***p<0001. respectively) suggesting the strong early F11 promoter is better for the induction of potent T cell responses than the early/late P7.5 promoter (Fig. 7.4). Collectively

these results indicate that T cell responses are not reduced following a priming vaccination of MVA-vectored vaccines against H7HA and/or NP+M1 in BALB/c mice and that the novel bivalent vaccine MVA-NP+M1-H7 (F11) elicits potent T cell responses comparable to those induced by vaccination with MVA-NP+M1 (F11) (Fig. 7.4).

Figure 7.4 T cell responses following MVA-NP+M1-H7 vaccination

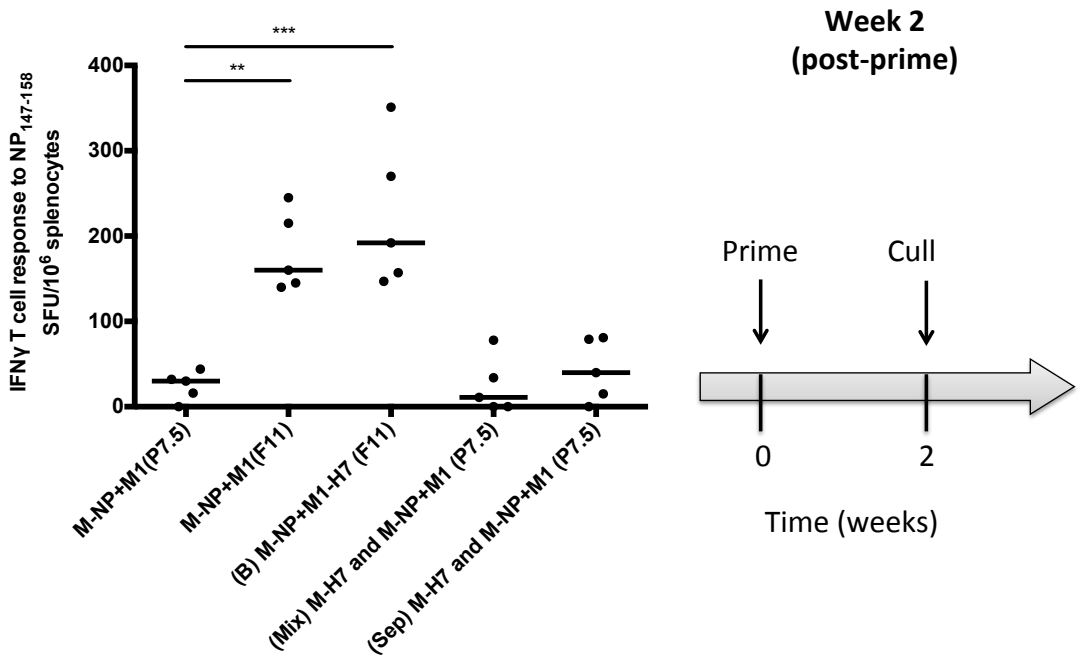


Figure 7.4 T cell responses following MVA-NP+M1-H7 vaccination

IFNγ ELISpot *ex vivo* T cell responses to NP+M1 in 6-8 week old BALB/c mice (n=5) immunised i.m. according to the vaccination regimen in Table 7.1. The promoter (F11 or P7.5) controlling expression of NP+M1 in relevant constructs is shown in brackets. The abbreviation 'M' is used in place of 'MVA'. 'B', 'Mix' and 'Sep' stand for 'bivalent', 'mixture' and 'separate vaccines' respectively. Individual values and group medians are shown. **p≤0.01, ***p≤0.001 by one-way ANOVA, assuming Gaussian distribution with Dunnett post-test comparing mean responses to vaccination with MVA-NP+M1 (P7.5).

Key findings:

Further to section 7.3.1.1.2, there was no evidence that including H7 as an antigen in a bivalent MVA construct with NP+M1 was associated with reduced induction of NP-specific IFNγ-secreting T cells.

7.3.2. Immunogenicity of a Mixture of Simian Adenoviral-Vectored Vaccines Expressing NP+M1 or H7HA

The simian adenovirus vectored-vaccine, ChAdOx1 NP+M1, is currently in clinical development as a novel T cell-inducing vaccine against influenza A [312]. This vaccine is safe and immunogenic in humans and induces T cell responses comparable to those following vaccination with MVA-NP+M1 [312]. However, the ability of this vector to induce humoral immune responses against influenza has not yet been investigated. Furthermore, unlike common human adenovirus serotypes, chimpanzee adenovirus vectors are not limited by pre-existing anti-vector responses so are more clinically relevant (although the number of doses that can be given before anti-vector responses in humans become problematic remains to be determined). For these reasons the ChAdOx1 vector was chosen in this study to investigate responses generated by multi-antigen vaccination against the influenza A antigens HA, NP and M1, and as a bivalent vector was not available, a mixture of monovalent vaccines was used.

7.3.2.1. Antibody Responses Against H7HA

BALB/c mice were immunised using ChAdOx1 vectors against H7HA or the fusion antigen NP+M1, or both, either as a mixture or by administration into separate limbs. Serum was collected at 2 and 8 weeks post-vaccination. Total serum IgG responses at all time points were measured against recombinant H7HA protein A/Netherlands/219/2003 (sections 2.6 and 3.2.1) (Fig. 7.5).

There were no significant differences between the median H7HA-specific IgG antibodies at two weeks post-vaccination between the groups vaccinated with ChAdOx1-H7 alone or ChAdOx1-H7 and ChAdOx1 NP+M1 either as a mixture or individually into separate limbs (Fig. 7.5 A). All responses induced by vaccination with ChAdOx1-vectored vaccines were significantly higher compared to vaccination with 10μg recombinant H7HA (**p≤0.01) (Fig. 7.5 A). Vaccination responses were followed to 8 weeks post-vaccination (Fig. 7.5 B). No significant differences were observed at 8 weeks between mice receiving ChAdOx1-vectored vaccines, however, these responses were significantly higher than mice receiving 10μg recombinant H7HA (**p≤0.01) (Fig. 7.5 B). These results demonstrate that vaccination with ChAdOx1-vectored vaccines expressing H7HA induce superior immune responses compared to protein and these responses are maintained in multi-antigen vaccination regimens.

Figure 7.5 HA-specific antibody responses generated by multi-antigen ChAdOx1-vectored vaccination

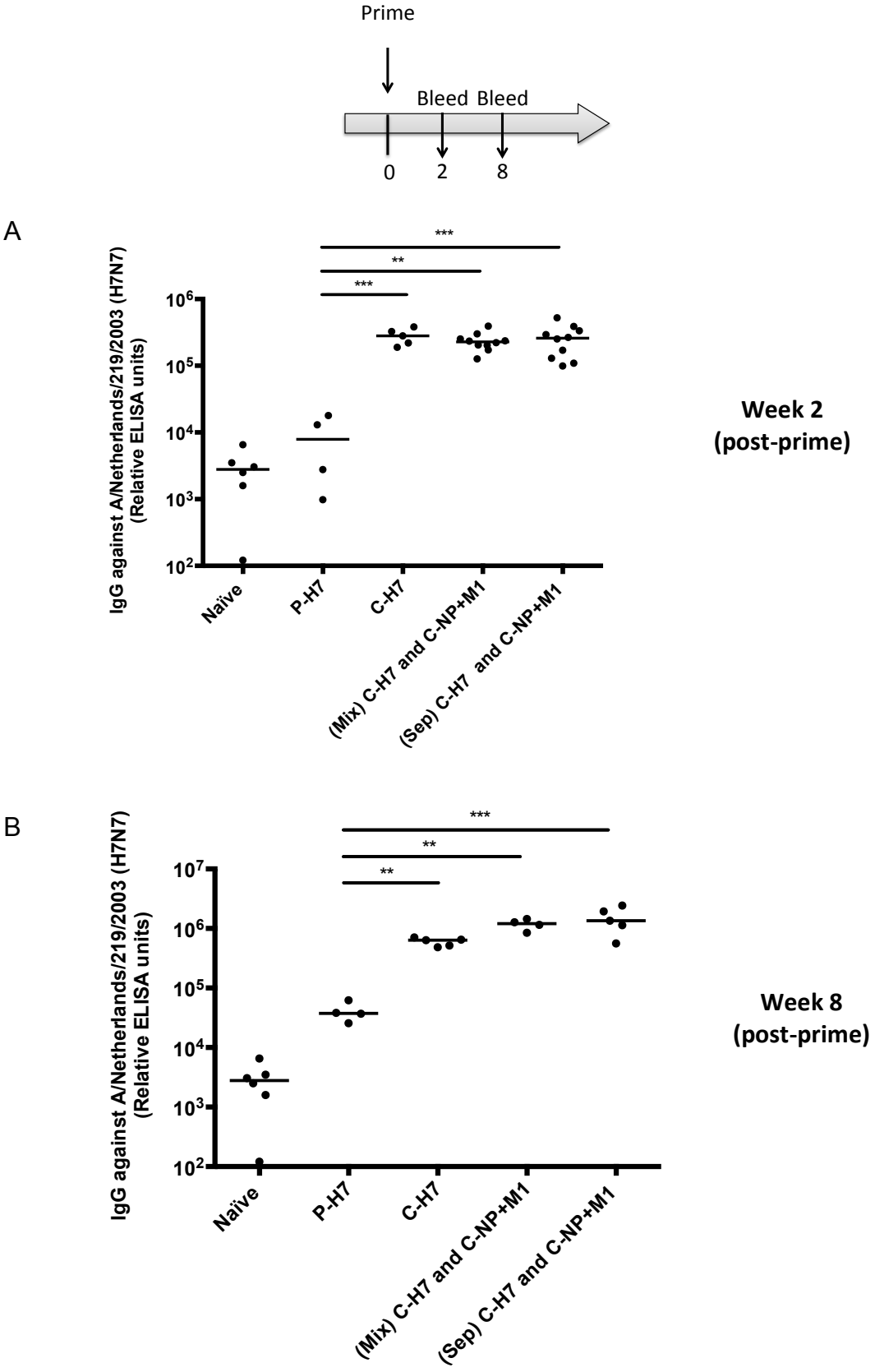


Figure 7.5 HA-specific antibody responses generated by multi-antigen ChAdOx1-vectored vaccination

6-8 week old BALB/c mice (n=5-10) were immunised i.m. with ChAdOx1-vectored vaccines expressing H7HA ($1x10^8$ iu) or NP+M1 ($2.2X10^6$ iu) either singly, as a mixture or by co-administration into separate limbs. Another group of mice (n=4) received 10μg recombinant H7HA protein (A/Netherlands/219/2003). Total IgG responses against recombinant H7HA (A/Netherlands/219/2003; H7N7) were assayed by standardised ELISA at (A) 2 and (B) 8 weeks post-vaccination. Naïve controls are unvaccinated mice. The abbreviation 'P-H7' indicates recombinant H7HA protein (A/Netherlands/219/2003). 'C' is used in place of 'ChAdOx1'. 'Mix' and 'Sep' stand for 'mixture' and 'separate vaccines' respectively. Individual values and group medians are shown. **p≤0.01, ***p≤0.001 by one-way ANOVA assuming Gaussian distribution with Dunnett post-test comparing mean responses to the protein only regimen. These data are representative of two independent experiments.

Key Findings:

Vaccination with a ChAdOx1-vectored vaccine expressing H7 induced greater H7-specific IgG antibody titres than vaccination with H7 protein alone. Vaccination alongside ChAdOx1 NP+M1 did not impact on antibody generation.

7.3.2.2. T Cell Responses Against NP+M1

BALB/c mice were immunised as before (section 7.3.2.1) and splenocytes were isolated 2 weeks post-vaccination in order to assess T cell responses against NP+M1. T cell responses were measured by *ex vivo* IFN-γ ELISpot against the immunodominant BALB/c epitope in NP, $NP_{147-158}$ (TYQRTRALV) (sections 2.7.5 and 2.8.4). Mice vaccinated with ChAdOx1 NP+M1 (median SFU=515) had significantly higher responses compared to mice that received either a mixture of ChAdOx1 NP+M1 and ChAdOx1-H7 (median SFU=73) or ChAdOx1 NP+M1 and ChAdOx1-H7 administered into separate limbs (median SFU=226) (***$p \leq 0.001$) (Fig. 7.6). A trend towards higher T cell responses was observed when the vaccines were administered in separate limbs compared to a single shot mixture of both, however this difference was not significant (Fig. 7.6). Together these results demonstrate T cell responses against NP+M1 are reduced following a priming vaccination of ChAdOx1-vectored vaccines against H7HA and NP+M1. Furthermore, given that vaccination against NP+M1 and H7HA using MVA-vectored vaccines did not significantly reduce T cell responses, these results suggest that the phenomenon of antigenic interference is not simply antigen-dependent but can be influenced by the properties of viral vectors (e.g. ChAdOx1 vectors have prolonged transgene expression compared to MVA).

Figure 7.6 T cell responses following multi-antigen ChAdOx1-vectored vaccination

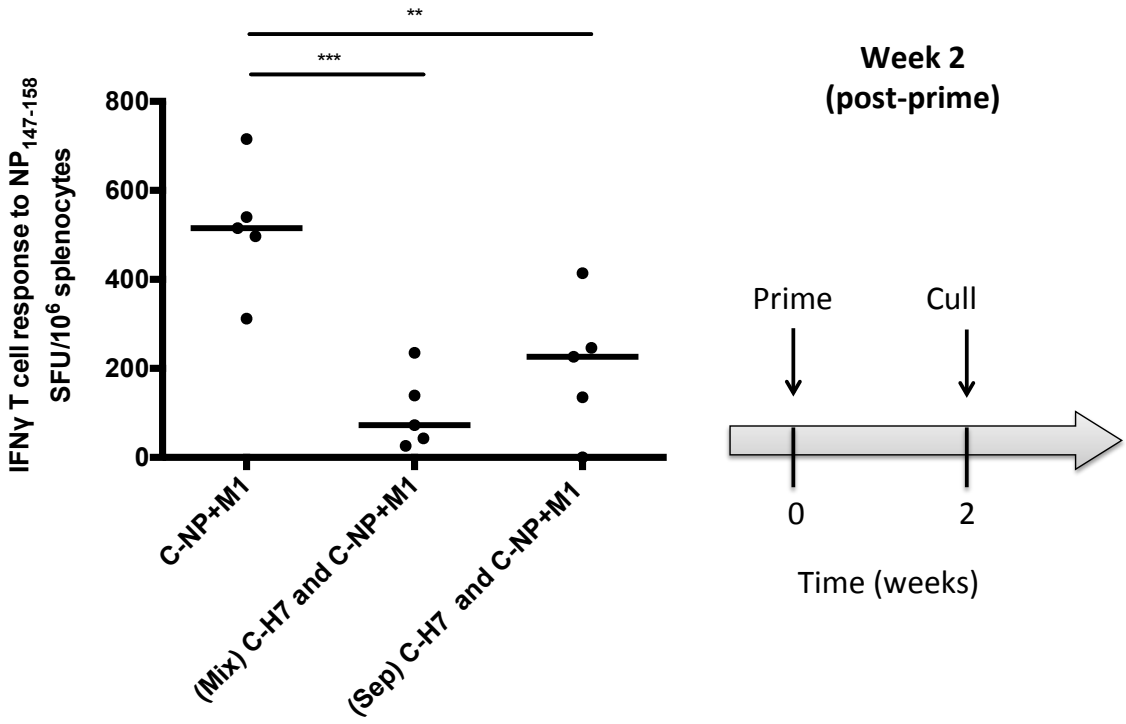


Figure 7.6 T cell responses following multi-antigen ChAdOx1-vectored vaccination

IFNγ ELISpot *ex vivo* T cell responses to NP+M1 in 6-8 week old BALB/c mice (n=5) immunised i.m. with ChAdOx1-vectored vaccines expressing H7HA ($1x10^8$ iu) or NP+M1 ($2.2X10^6$ iu) either singly, as a mixture (Mix) or by co-administration into separate limbs (Sep). The abbreviation 'C' is used in place of 'ChAdOx1'. 'Mix' and 'Sep' stand for 'mixture' and 'separate vaccines' respectively. Individual values and group medians are shown. **p≤0.01, ***p≤0.001 by one-way ANOVA, assuming Gaussian distribution with Dunnett post-test comparing mean responses to vaccination with ChAdOx1 NP+M1.

Key findings:

Induction of NP-specific IFNγ-secreting T cells was reduced when ChAdOx1-H7 vaccines were administered alongside ChAdOx-NP+M1. This finding contrasts with similar experiments using MVA virally vectored vaccines (e.g. Figure 7.4), suggesting that the phenomenon of antigenic interference may be influenced by the properties of viral vectors

7.3.3. Investigation of a Prime-Boost Regimen Incorporating Poxviral Vectors and Simian Adenoviral Vectors Expressing NP+M1 and H7HA

Building on the results outlined in sections 7.3.1 and 7.3.2, the most promising vaccine combinations capable of inducing both B and T cell responses were brought forward to assess their immunogenicity in the context of a heterologous prime boost regimen. Adenovirus-MVA prime boost regimens are currently one of the leading strategies to induce potent T cell responses against vaccinating antigens [538]. Given both the MVA and ChAdOx1 viral-vectored priming regimens previously described were capable of inducing humoral immune responses superior to those induced by protein only, and, these responses against H7HA were not negatively impacted by the presence of NP+M1, those priming vaccines least likely to exhibit antigenic interference of T cell responses against NP+M1 were taken forward.

7.3.3.1. Antibody Responses Against H7HA Following ChAdOx1 – MVA Immunisation

7.3.3.1.1. ELISA

As adenoviral vectors have a greater ability to induce antibody responses compared to poxvirus vectors and can simultaneously induce more potent T cell responses, ChAdOx1-vectored vaccines were used to prime responses [538]. BALB/c mice (n=18) received a priming vaccination of either ChAdOx1 NP+M1, ChAdOx1-H7 or both, administered separately into opposite limbs as outlined in Table 7.2. Serum was collected at 2 and 8 weeks post each vaccination and responses were followed for 26 weeks. Total serum IgG responses at all time points were measured against recombinant H7HA protein A/Netherlands/219/2003 (sections 2.6 and 3.2.1) (Fig. 7.7).

Mice primed with ChAdOx1-H7 or ChAdOx1-H7 and ChAdOx-NP+M1 had significantly higher total IgG against H7HA at all time points compared to vaccination with either protein alone or with ChAdOx1 NP+M1 followed by MVA-NP+M1-H7 (***p≤0.001 for all comparisons) (Fig. 7.7). Mice primed with ChAdOx1-H7 and ChAdOx1 NP+M1 also demonstrated the highest median peak antibody response at 8 weeks post-boost and these responses were significantly higher compared to mice primed with ChAdOx1-H7 alone (**p=0.004) (Fig. 7.7). Peak responses were observed at 8 weeks post-boost in mice primed with ChAdOx1-H7 and ChAdOx1 NP+M1, or ChAdOx1-H7 alone, and at 2 weeks post-vaccination with MVA-NP+M1-H7 in mice primed with ChAdOx1 NP+M1 (Fig. 7.7). However the peak response for mice vaccinated with protein only was at 10 weeks post-vaccination (Fig. 7.7).

Antibody responses persisted for at least 26 weeks post-vaccination in all groups (Fig. 7.7). No significant differences were seen between mice primed with ChAdOx1-H7 and ChAdOx1 NP+M1, or ChAdOx1-H7 alone for all other time points (Fig. 7.7). As expected, no antibody responses against H7HA were detected in mice primed with ChAdOx1 NP+M1 until 2 weeks following the MVA-NP+M1-H7 boost (Fig. 7.7). These responses after the second vaccination were comparable to the protein only regimen.

Interestingly, antibody responses from mice primed with ChAdOx1 NP+M1 were significantly lower compared to mice receiving MVA-NP+M1-H7 alone, 2 weeks post-boost (****$p<0.0001$) (Fig. 7.8), meaning that prior exposure to ChAdOx1 NP+M1 appeared to abrogate antibody responses to MVA-NP+M1-H7. It is unclear why this is but it may be due to antigenic competition due to prolonged transgene expression by ChAdOx1 NP+M1. The effect was not sustained, since 8 weeks after MVA-NP+M1-H7 the groups' antibody titers were equivalent (Fig. 7.8).

Taken together these results indicate superior humoral immune responses against H7HA are generated by heterologous ChAd-MVA prime boost regimens that deliver a H7HA prime and these responses are not impeded by co-priming against the T cell antigen, NP+M1.

Table 7.2 Immunisation schedule for delivery of NP+M1 and H7HA by heterologous prime boost ChAdOx1-MVA viral-vectored vaccination

Time (weeks)	**0**	**8**
Group	**Prime**	**Boost**
A	H7HA protein	-
B	ChAdOx1 NP+M1	MVA-NP+M1-H7
C	ChAdOx1-H7	MVA-NP+M1-H7
D	ChAdOx1 NP+M1 (right limb) ChAdOx1-H7 (left limb)	MVA-NP+M1-H7

Table 7.2 Immunisation schedule for delivery of NP+M1 and H7HA by heterologous prime boost ChAdOx1-MVA viral-vectored vaccination

Three groups of BALB/c mice (n=6-18) were immunised i.m with ChAdOx1-vectored vaccines expressing H7HA ($1x10^8$ iu) or NP+M1 ($2.2X10^6$ iu), or both, by co-administration into separate limbs. Another group of mice (n=4) received 10µg recombinant H7HA protein (A/Netherlands/219/2003). All groups except mice primed with protein were boosted at 8 weeks with $1x10^6$ pfu MVA-NP+M1-H7.

Figure 7.7 HA-specific antibody responses generated by heterologous multi-antigen ChAdOx1-MVA viral-vectored vaccination

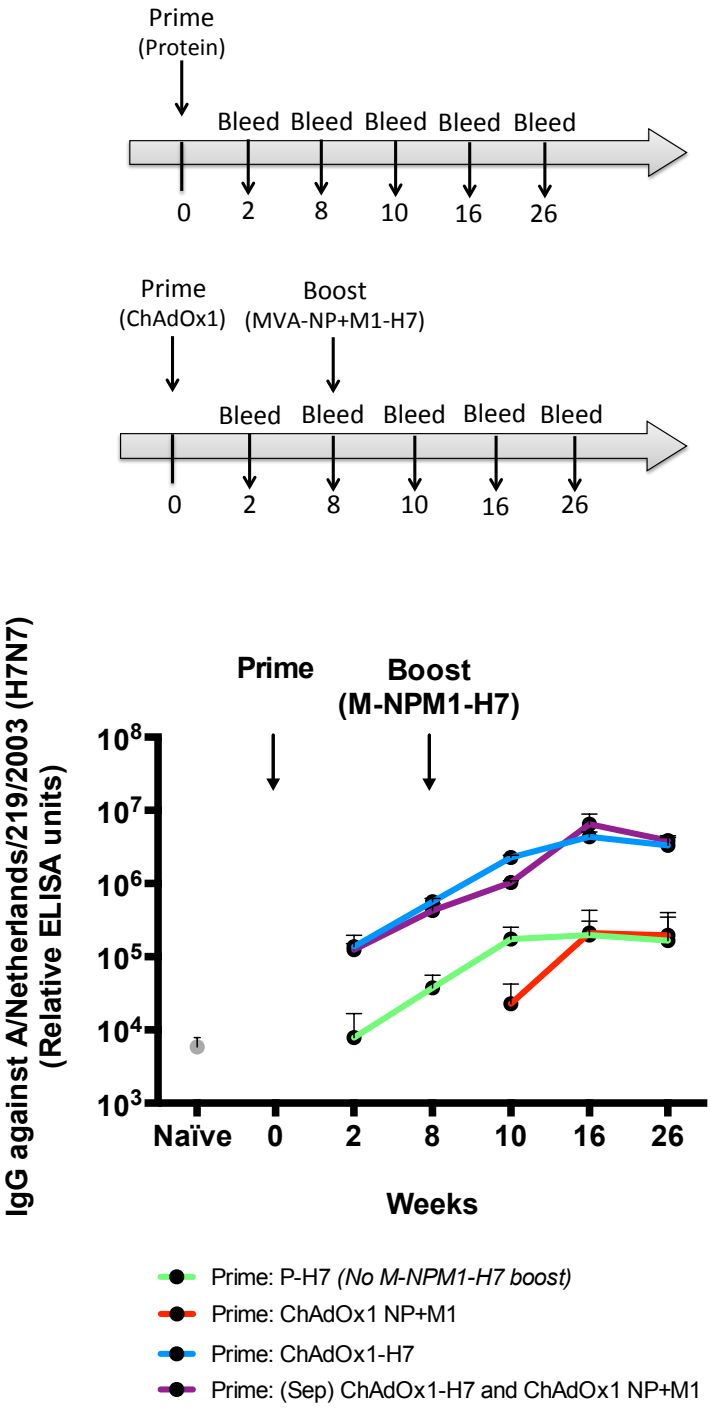


Figure 7.7 HA-specific antibody responses generated by heterologous multi-antigen ChAdOx1-MVA viral-vectored vaccination

6-8 week old BALB/c mice (n=6-18) were immunised i.m. according to the vaccination regimen in Table 7.2. Total IgG responses against recombinant H7HA (A/Netherlands/219/2003; H7N7) were assayed by standardised ELISA at all time points. Both ChAdOx1-H7 containing regimens were significantly higher than either the P-H7 and ChAdOx1 NP+M1-only regimens at all time points (**p<0.01). There were no statistically significant differences between the two ChAdOx1-H7 containing regimens, except at week 16 (8 weeks after the boost), when the mixed regimen was highest (**p=0.004). Prior to the boost, the antibody titers for the ChAdOx1 NP+M1-primed regimen were equivalent to naïve, unvaccinated mice. Naïve controls are unvaccinated mice. The abbreviation 'P-H7' indicates recombinant H7HA protein (A/Netherlands/219/2003), 'C', is used in place of 'ChAdOx1', 'Sep' stands for separate vaccines and 'M', is used in place of 'MVA'. Data are medians with interquartile range. These data are representative of two independent experiments.

Figure 7.8 HA-specific antibody responses generated by heterologous multi-antigen ChAdOx1-MVA viral-vectored vaccination

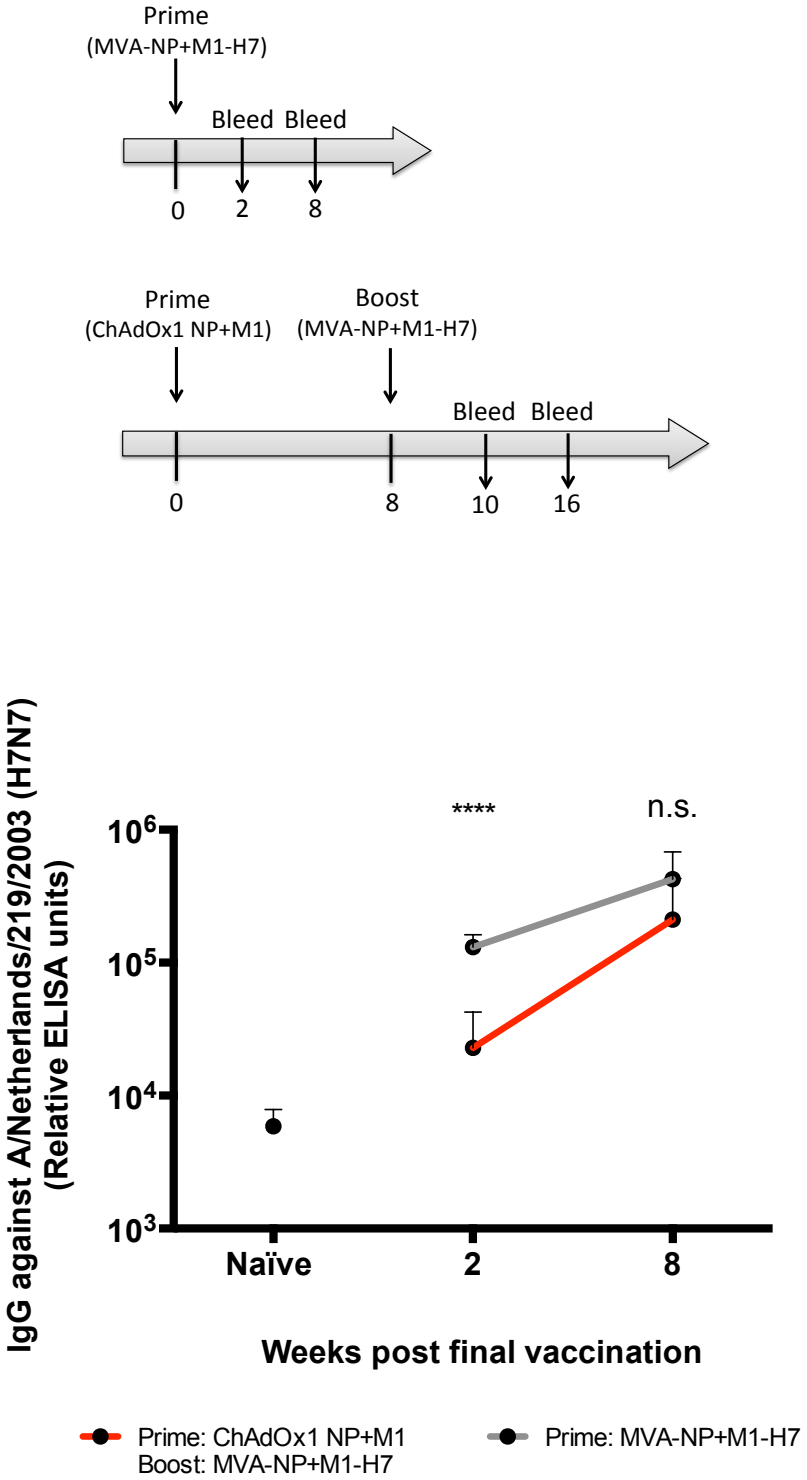


Figure 7.8 HA-specific antibody responses generated by heterologous multi-antigen ChAdOx1-MVA viral-vectored vaccination

6-8 week old BALB/c mice (n=6-18) were immunised i.m. with $2.2X10^6$ iu. ChAdOx1 NP+M1 and boosted with $1x10^6$ pfu MVA-NP+M1-H7. Or mice were vaccinated with a single shot of $1x10^6$ pfu MVA-NP+M1-H7. Total IgG responses against recombinant H7HA (A/Netherlands/219/2003; H7N7) were assayed by standardised ELISA at 2 and 8 weeks post-vaccination (final vaccination in the case of the prime-boost). Naïve controls are unvaccinated mice. Data are medians with interquartile range. ****p≤0.0001 by Mann Whitney.

Key findings:

Mice primed with ChAdOx1-H7 or ChAdOx1-H7 and ChAdOx1 NP+M1, and boosted with MVA-NP+M1-H7, had significantly higher total IgG against H7HA at all time points compared to vaccination with either protein alone or with ChAdOx1 NP+M1 followed by MVA-NP+M1-H7. The dual prime regimen gave significantly higher IgG titres than ChAdOx1-H7 alone at one time point, but overall the results between the two groups were similar.

7.3.3.1.2. H7 Pseudotype Virus Neutralisation

Replication incompetent pseudotype lentiviruses expressing HA are increasingly being employed in neutralisation assays to assess antibody functionality as a safer alternative to wild-type influenza A virus [539]. In addition to being substantially less hazardous, particle neutralisation assays (ppNT) using pseudotype lentiviruses expressing HA can detect heterosubtypic antibodies against the stem domain of HA, unlike the traditional haemagglutination-inhibition (HAI) assay, which only measures responses against the globular head [294,298,540]. Furthermore these particles can be engineered to display HA but not the second virion surface protein neuraminidase (NA). This avoids the potentially confounding effect of anti-NA antibodies when assessing influenza-exposed samples from humans or animal challenge models and is advantageous compared to traditional microneutralisation (MN) assays.

In order to assess the breadth of anti-HA antibody functionality induced by vaccination with a heterologous ChAd-MVA prime-boost regimen delivering NP+M1 and H7HA, sera taken 8 weeks following the boost vaccination with MVA-NP+M1-H7 was tested against pseudotyped lentiviruses expressing group 2 HA molecules. Two strains of H7HA pseudotypes were tested, A/chicken/Italy/1082/1999 (H7N1), a low pathogenic avian influenza (LPAI) strain closely related to the vaccine immunogen A/Netherlands/219/2003 (H7N7), and A/Shanghai/2/2013 (H7N9), the novel LPAI first identified in humans in 2013 (Table 7.3). A third pseudotype expressing a different Group 2 subtype, H3HA from A/Udorn/307/1972 (H3N2), was also used to

investigate if the ChAd-MVA prime-boost regimen delivering NP+M1 and H7HA could also induce heterosubtypic antibody responses against other subtypes (Table 7.3). All assays included a negative control of a pool of naïve BALB/c sera that did not show any neutralisation.

Pooled sera from mice primed with ChAdOx1-H7 or ChAdOx1-H7 and ChAdOx1 NP+M1 completely neutralised both H7 pseudotypes at all serum dilutions tested (Table 7.3). In addition, IC_{50} values (the concentration of antibody that neutralises 50% of virus) from mice primed with ChAdOx1 NP+M1 and boosted with MVA-NP+M1-H7 were higher compared to mice vaccinated with protein alone, although these values were lower compared to sera from mice primed with ChAdOx1-H7 or ChAdOx1-H7 and ChAdOx1 NP+M1for each H7 pseudotype (Table 7.3). IC_{50} values against A/Udorn/307/1972 (H3N2) were comparable between all groups vaccinated with viral vectors but lower in the control group vaccinated with protein alone (Table7.3). Collectively these results indicate that viral-vectored vaccinating regimens provide better heterosubtypic protection compared to protein alone and antibody functionality is not diminished by the delivery of a second vaccine against the T cell antigen NP+M1, during the priming vaccination (Table 7.3).

Table 7.3 IC_{50} antibody titers against H7 and H3 pseudotyped lentiviruses following heterologous multi-antigen ChAdOx1-MVA viral-vectored vaccination

	% amino acid sequence identity to A/Netherlands/219/2003		Group IC_{50} titers			
Pseudotype subtype	HA	HA2	C-NP+M1	C-H7	C-NP+M1 and C-H7	H7 protein
A/chicken/Italy/1082/1999	98.4	98.6	2560-5120	>5120	>5120	1280-2560
A/Shanghai/2/2013	96.1	97.3	1280-2560	>5120	>5120	640-1280
A/Udorn/307/1972	47.8	64.3	320-640	320-640	320-640	160-320

Table 7.3 IC_{50} antibody titers against H7 and H3 pseudotyped lentiviruses following heterologous multi-antigen ChAdOx1-MVA viral-vectored vaccination

6-8 week old BALB/c mice (n=6-18) were immunised i.m. according to the vaccination regimen in Table 7.2. Pooled sera from each group was tested against two antigenically distinct H7HA-expressing pseudotypes and a third H3HA virus. 'C' is used in place of 'ChAdOx1'. The IC_{50} titer is the reciprocal of the serum dilution that results in 50% inhibition of virus entry. IC_{50} values were reported as titer ranges from <40 to >5120 (<40 = lower cut off, >5120 = upper cut off).

Key Findings:

Mice primed with ChAdOx1-H7 or ChAdOx1-H7 and ChAdOx1 NP+M1, and boosted with MVA-NP+M1-H7, had comparable neutralisation activity against both H7 pseudotyped viruses, and the H3 pseudotype. These responses were greater compared to mice primed with ChAdOx1 NP+M1 or mice vaccinated with H7 protein only.

7.3.3.1.3. B Cell Memory Responses Following ChAdOx1 – MVA Immunisation

Long-lived humoral immunity is principally mediated by two B cell subsets - long-lived plasma cells, which continuously secrete large quantities of antibodies to maintain constitutive humoral immunity, and, memory B cells (mBCs), which drive rapid recall responses upon antigen re-exposure and enable further antibody diversification. LLPCs develop in secondary lymph organs (SLO) but predominantly reside long-term in the bone marrow (BM) [541,542]. mBCs on the other hand are largely spleen-resident (in mice) [543]. In order to further understand the basis of the humoral responses against HA observed following heterologous prime-boost ChAd-MVA viral-vectored vaccination and to investigate response longevity, the number of IgG^+ H7HA-specific (A/Netherlands/219/2003 (H7N7)) LLPCs and mBCs was assessed after a time period sufficient for the development of memory responses. 18 weeks following the boosting vaccination BALB/c mice (n=6) were sacrificed and BM cells and splenocytes were isolated (sections 2.7.5 and 2.7.6).

7.3.3.1.3.1. Long-Lived Plasma Cells

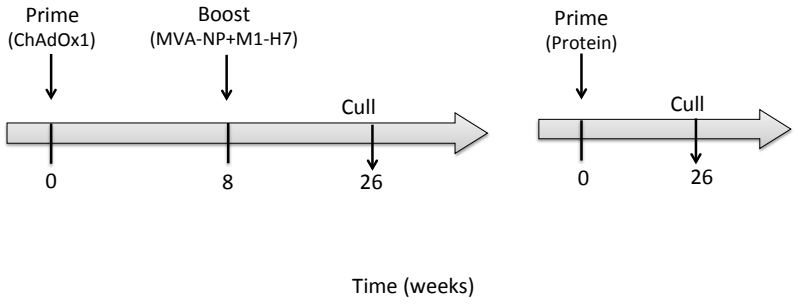
Total IgG^+ ASCs and H7HA-specific ASCs representative of LLPCs were measured by IgG ASC ELISpot assay (section 2.8.5) (Fig. 7.9).

Elevated numbers of H7HA-specific LLPCs were detected in the BM of all immunised groups compared to naïve BALB/c mice (***$p<0.001$ for all comparisons) (Fig. 7.9 A). There were no significant differences between the number of H7HA-specific LLPCs detected in mice primed with ChAdOx1-H7

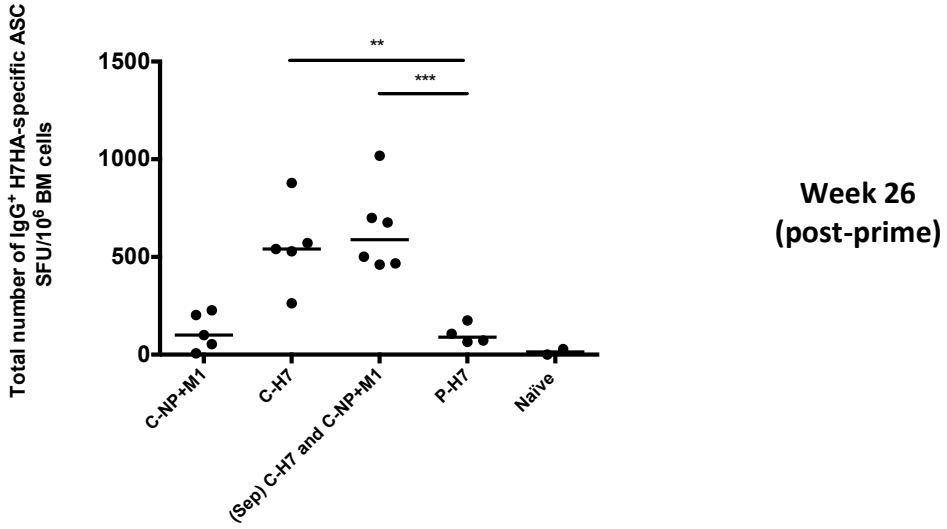
(median SFU=541) only or ChAdOx1-H7 and ChAdOx1 NP+M1 (median SFU=589) (Fig. 7.9 A). However the number of H7HA-specific LLPCs detected in mice primed with ChAdOx1-H7 only or ChAdOx1-H7 and ChAdOx1 NP+M1 were significantly higher compared to mice primed with ChAdOx1 NP+M1 (median SFU=100) or protein alone (median SFU=89) (Fig. 7.9 A).

There were no significant differences between the total number of IgG^+ LLPCs between groups immunised with viral vectors, however the total number of IgG^+ LLPCs was significantly higher in mice primed with ChAdOx1 NP+M1 (median SFU=3880) compared to mice receiving a single shot of H7HA protein (median SFU=2302) (Fig. 7.9 B). These results demonstrate vaccination with viral-vectored vaccines expressing H7HA and NP+M1 induce significantly higher numbers of LLPCs which maintain high levels of H7HA-specific functional antibody titers in the serum up to 18 weeks post-vaccination and these responses are not competitively disadvantaged by the delivery of a second vaccine against the T cell antigen NP+M1, during the priming vaccination.

Figure 7.9 IgG$^+$ long-lived plasma cell responses following ChAdOx1 – MVA immunisation



A



B

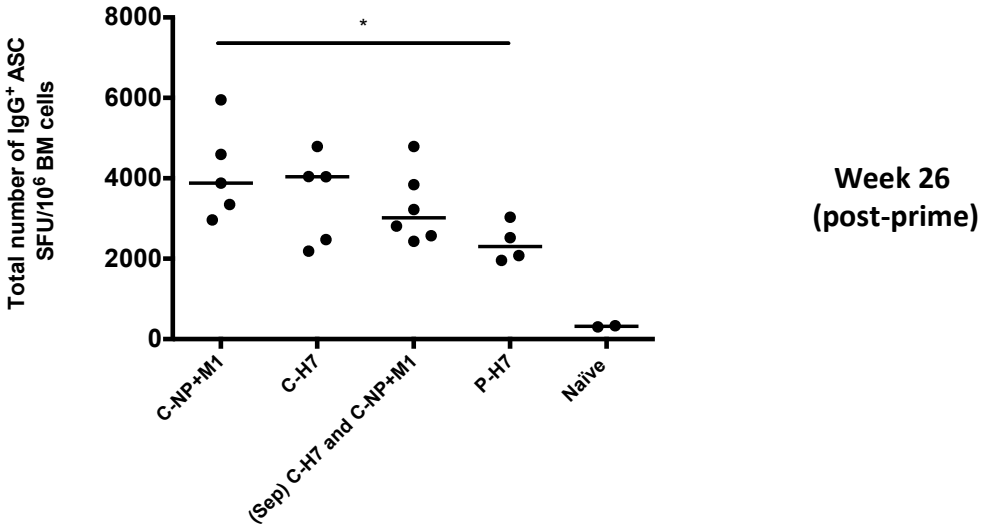


Figure 7.9 IgG$^+$ long-lived plasma cell responses following ChAdOx1 – MVA immunisation

IgG ASC ELISpot *ex vivo* responses to H7HA (A/Netherlands/219/2003) in BALB/c mice (n=4-6) immunised i.m. according to the vaccination regimen in Table 7.2. The numbers of (A) H7HA-specific (A/Netherlands/219/2003) IgG$^+$ and (B) total IgG+ ASCs in the bone marrow were determined. Note that in (A) all vaccinated groups had significantly elevated numbers of ASCs compared to naïve (unvaccinated) mice (**p<0.001). In (B) both ChAdOx1-H7 containing regimens also has significantly elevated numbers compared to ChAdOx1 NP+M1 (p<0.001). Naïve controls are unvaccinated mice. The abbreviation 'P-H7' indicates recombinant H7HA protein (A/Netherlands/219/2003) and 'C', is used in place of 'ChAdOx1'. 'Sep' indicates the vaccines were administered into separate limbs. Individual values and group medians are shown. *p≤0.05 **p≤0.01 ***p≤0.001 by one-way ANOVA, assuming Gaussian distribution with Dunnett post-test comparing mean responses to vaccination with recombinant H7HA protein.

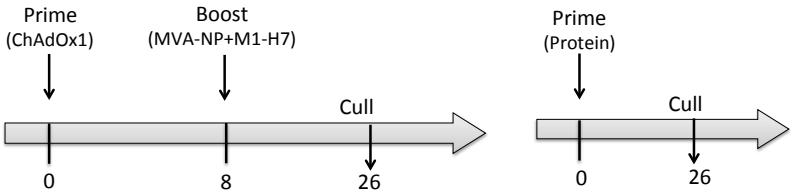
Key findings:

The number of H7HA-specific LLPCs detected in mice primed with ChAdOx1-H7 only or ChAdOx1-H7 and ChAdOx1 NP+M1 were significantly higher compared to mice primed with ChAdOx1 NP+M1 or protein alone.

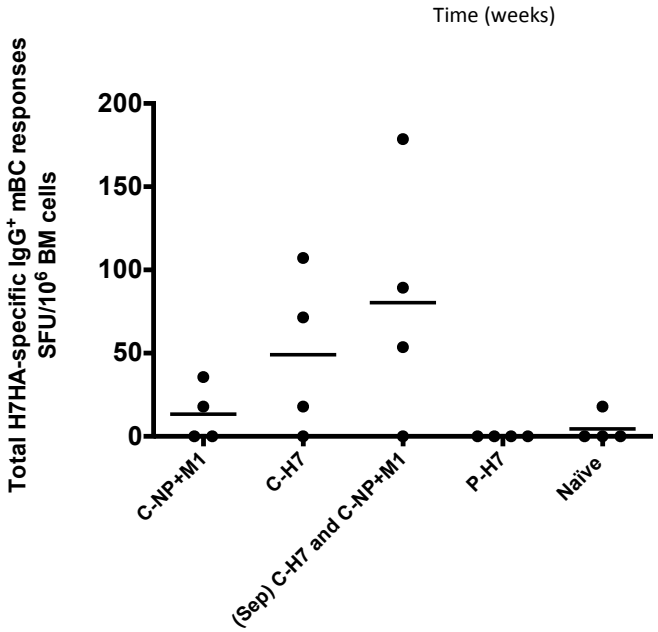
7.3.3.1.3.2. Memory B Cells

mBC ELISpots were performed on isolated splenocytes in order to assess the number of mBC-derived ASCs post-vaccination. Non-specific responses were measured against ovalbumin (Ova) and subtracted from responses against H7HA. A very small number of H7HA-specific mBC-derived ASCs were detected in groups vaccinated with viral-vectors (after subtraction of non-specific responses: ChAdOx1 NP+M1 prime, median SFU=9.2; ChAdOx1-H7 prime, median SFU=71.4; ChAdOx1 NP+M1 and ChAdOx1-H7 prime, median SFU=53.6) (Fig. 7.10 A). No ASCs were detected in the spleens of mice vaccinated with recombinant H7HA only (Fig. 7.10 A). There were no differences in the total number of IgG^+ mBC-derived ASCs between vaccination groups (Fig. 7.10 B). These findings suggest the humoral immune memory against H7HA induced by heterologous ChAd-MVA viral-vectored vaccination is largely the result of LLPCs and this regimen induces relatively small numbers of mBCs.

Figure 7.10 IgG$^+$ memory B cell responses following ChAdOx1 – MVA immunisation

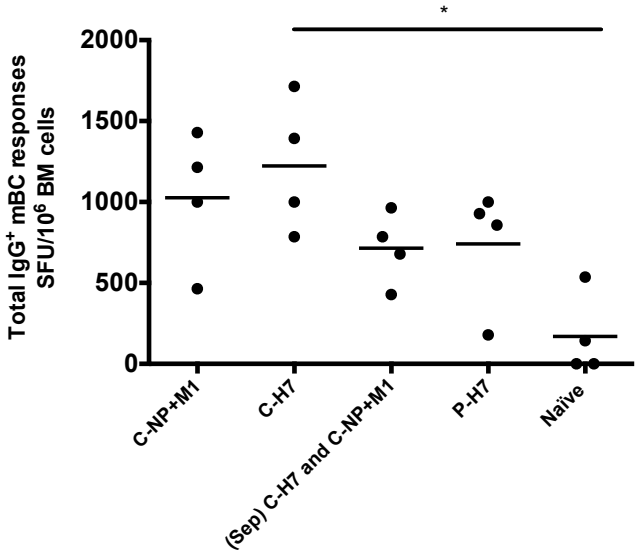


A



Week 26 (post-prime)

B



Week 26 (post-prime)

Figure 7.10 IgG$^+$ memory B cell responses following ChAdOx1 – MVA immunisation

Memory B cell-derived IgG ASC ELISpot *ex vivo* responses to H7HA (A/Netherlands/219/2003) in BALB/c mice (n=4) immunised i.m. according to the vaccination regimen in Table 7.2. The numbers of (A) H7HA-specific (A/Netherlands/219/2003) IgG+ and (B) total IgG$^+$ ASCs in the spleen 18 weeks post-boost with MVA-NP+M1-H7 were determined. Naïve controls are unvaccinated mice. The abbreviation 'P-H7' indicates recombinant H7HA protein (A/Netherlands/219/2003) and 'C', is used in place of 'ChAdOx1'. 'Sep' indicates the vaccines were administered into separate limbs. Individual values and group medians are shown. *p≤0.05 by one-way ANOVA, assuming Gaussian distribution with Dunnett post-test comparing mean responses to naïve unvaccinated mice.

Key findings:

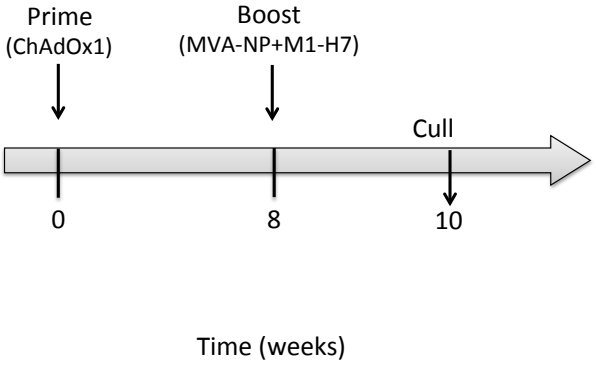
A very small number of H7HA-specific mBC-derived ASCs were detected in groups vaccinated with viral-vectors. The rank of groups mirrored results for LLPCs, and while they were not significantly different, this may have been due to a lack of statistical power.

7.3.3.2. T Cell Responses Following ChAdOx1 – MVA Immunisation

7.3.3.2.1. NP+M1

BALB/c mice (n=6) were immunised according to the regimen outlined in Table 7.2. Splenic PBMCs were isolated 2 weeks post-prime and 2 weeks post-boost in order to assess T cell responses against NP+M1 and H7HA. T cell responses against NP+M1 were measured by *ex vivo* IFN-γ ELISpot against the immunodominant BALB/c epitope in NP, $NP_{147-158}$ (TYQRTRALV) (sections 2.7.5 and 2.8.4). In line with previous results there were significantly higher T cell responses from mice primed with ChAdOx1 NP+M1 (median SFU= 526) compared to mice that received ChAdOx1 NP+M1 and ChAdOx1-H7 (median SFU=200) (Fig. 7.9). No responses were seen from mice vaccinated with ChAdOx1-H7 after the prime. Following the boost, T cell responses against NP+M1 were higher in all groups (Fig. 7.9). In mice that were primed with ChAdOx1 NP+M1, T cell responses were boosted over 5-fold (median SFU=2773) (Fig. 7.5). These responses were significantly higher compared to mice primed with ChAdOx1 NP+M1 and ChAdOx1-H7 (median SFU=967) or mice primed with ChAdOx1-H7 (median SFU=18). Interestingly mice primed with ChAdOx1-H7 had lower T cell responses to NP+M1 following vaccination with MVA-NP+M1-H7 compared to mice receiving MVA-NP+M1-H7 alone (median SFU=192) (section 7.3.2.2.). These results demonstrate that vaccination with either ChAdOx1 NP+M1 or co-administration of ChAdOx1 NP+M1 and ChAdOx1-H7 followed by immunisation with MVA-NP+M1-H7 induces potent T cell responses against NP+M1 and these responses are improved by administering ChAdOx1 NP+M1 and ChAdOx1-H7 into separate limbs

Figure 7.11 T cell responses against NP+M1 following heterologous multi-antigen ChAdOx1-MVA viral-vector vaccination



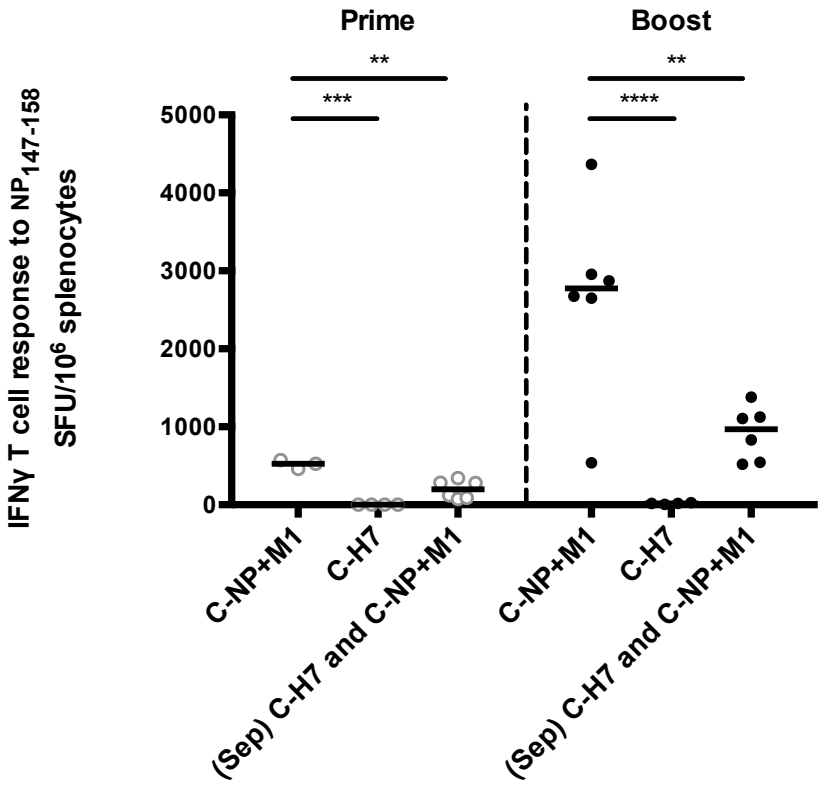


Figure 7.11 T cell responses against NP+M1 following heterologous multi-antigen ChAdOx1-MVA viral-vector vaccination

IFNγ ELISpot *ex vivo* T cell responses to NP+M1 in 6-8 week old BALB/c mice (n=6) immunised i.m. according to the vaccination regimen in Table 7.2. The abbreviation 'C' is used in place of 'ChAdOx1' and 'Sep' indicates the vaccines were administered into separate limbs. Individual values and group medians are shown. *p≤0.05, **p≤0.01, ***p≤0.001, ****p≤0.0001 by one-way ANOVA, assuming Gaussian distribution with Dunnett post-test comparing mean responses to vaccination with ChAdOx1 NP+M1.

Key findings:

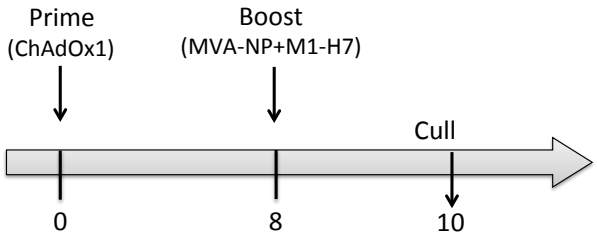
Vaccination with ChAdOx1 NP+M1, either alone or co-administered with ChAdOx1-H7, followed by boosting immunisation with MVA-NP+M1-H7, induces higher T cell responses against NP+M1 compared to mice primed with ChAdOx1-H7.

7.3.3.2.2. H7HA

BALB/c mice (n=6) were immunised as before (section 7.3.4.2.1). T cell responses against H7HA were measured by *ex vivo* IFN-γ ELISpot against two different H7HA peptide pools, one representative of H7HA from A/Netherlands/219/2003 (H7N7) and another representative of regions of amino acid sequence diversity in the HA of A/Anhui/1/2013 (H7N9) and A/Shanghai/1/2013 (H7N9) (sections 2.7.5 and 2.8.4). As expected, mice primed with ChAdOx1 NP+M1 had no detectable H7HA-specific T cell responses 2 weeks post-vaccination (Fig. 7.12 A & B). Indeed T cell responses in these mice against either set of H7HA peptide pools were significantly lower after the MVA-NP+M1-H7 boost compared to groups receiving a ChAdOx1-H7 prime (median SFU=48 (Netherlands); median SFU=12 (Anhui/Shanghai)) (Fig. 7.12 A & B). Interestingly, unlike the reduced responses observed when assessing T cell responses against NP+M1, there were no significant differences between the H7HA-specific T cell responses against either H7HA peptide pool 2 weeks post-prime between mice vaccinated with ChAdOx1-H7 (median SFU=321 (Netherlands); median SFU=16 (Anhui/Shanghai)) or ChAdOx1-H7 co-administered with ChAdOx1 NP+M1 (median SFU=259 (Netherlands); median SFU=6 (Anhui/Shanghai)) (Fig. 7.12 A & B). Furthermore T cell responses against both H7HA peptide pools following the MVA-NP+M1-H7 boost were only marginally better in mice primed with ChAdOx1-H7 (median SFU=935 (Netherlands); median SFU=60 (Anhui/Shanghai)) compared to mice that received ChAdOx1-H7 co-administered with ChAdOx1 NP+M1 (median SFU=429 (Netherlands); median SFU=20 (Anhui/Shanghai)) (Fig. 7.12 A & B). Collectively these

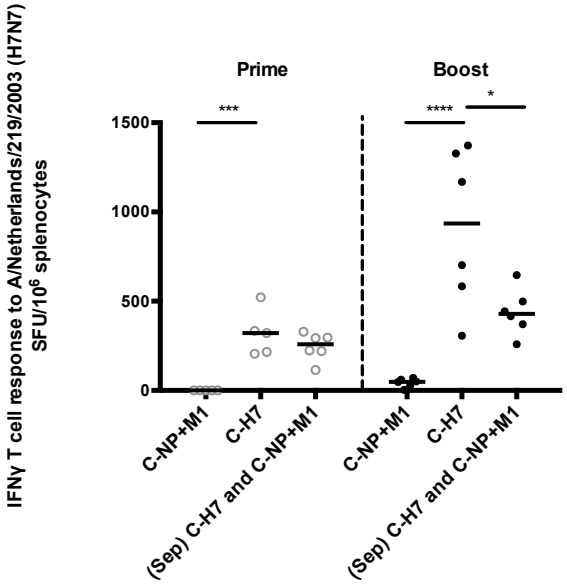
results demonstrate that vaccination with either ChAdOx1-H7 or co-administration of ChAdOx1 NP+M1 and ChAdOx1-H7 followed by immunisation with MVA-NP+M1-H7 induces heterosubtypic T cell responses against H7HA and the reduction in T cell responses following administering ChAdOx1 NP+M1 with ChAdOx1-H7 is relatively small.

Figure 7.12 T cell responses following heterologous multi-antigen ChAdOx1-MVA viral-vector vaccination



Time (weeks)

A



B

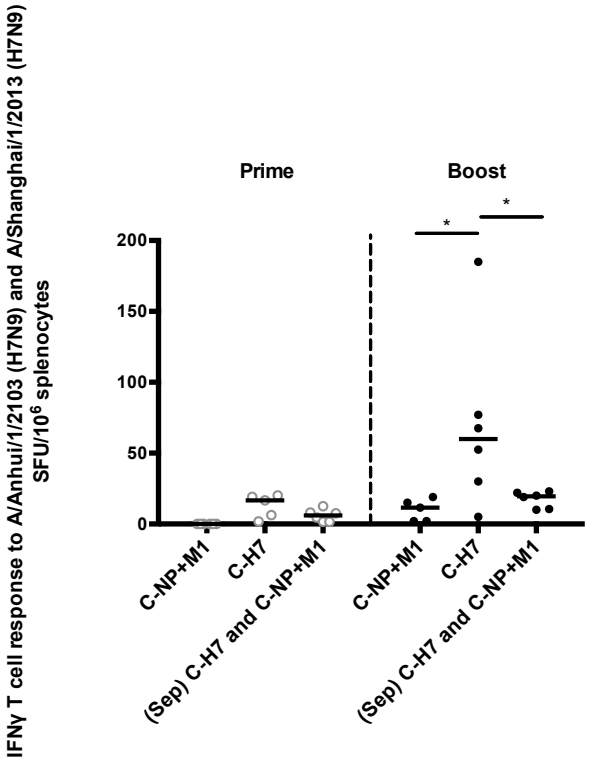


Figure 7.12 T cell responses following heterologous multi-antigen ChAdOx1-MVA viral-vector vaccination

IFNγ ELISpot *ex vivo* T cell responses to (A) H7HA (A/Netherlands/219/2003; H7N7) or (B) H7HA (A/Anhui/1/2013 & A/Shanghai/1/2013; H7N9) in 6-8 week old BALB/c mice (n=5-6) immunised i.m. according to the vaccination regimen in Table 7.2. The abbreviation 'C' is used in place of 'ChAdOx1' and 'Sep' indicates the vaccines were administered into separate limbs Individual values and group medians are shown. *p≤0.05, ***p≤0.001, ****p≤0.0001 by one-way ANOVA, assuming Gaussian distribution with Dunnett post-test comparing mean responses to vaccination with ChAdOx1-H7.

Key findings:

Vaccination with ChAdOx1-H7, either alone or co-administered with ChAdOx1 NP+M1, followed by boosting immunisation with MVA-NP+M1-H7, induces heterosubtypic T cell responses against H7HA. In general, co-administration of ChAdOx1-based vaccines leads to reduced responses against either vaccine target, although this effect is relatively small.

7.4. Discussion

Seasonal influenza A infections cause significant morbidity and mortality worldwide and remain a major issue for public health. Furthermore, emerging novel zoonotic IAVs pose a serious and persistent pandemic threat. For the past 70 years vaccination has been the primary defence strategy against influenza A [506,544,545]. However traditional inactivated influenza vaccines (IIVs) do not induce broad-spectrum immunity and live attenuated influenza vaccine (LAIV) efficacy, may be limited in individuals with pre-existing humoral responses [546-548]. Recent strategies to increase influenza virus preparedness have shifted towards developing so-called 'universal' vaccines capable of providing heterosubtypic protection against several subtypes of IAV. Whilst both B and T cells can mediate heterosubtypic immune responses, inducing antibodies against the stem domain of HA has been the focus of much of the research aimed at developing universal influenza vaccines. This has been largely incentivised by the increased prevalence of anti-stem antibodies observed in populations following the 2009 pandemic (Chapter 6) [288,290,291,432,444-449,451,454,512,549,550]. However, little is known about the potential impact targeting conserved epitopes in the HA stem by widespread vaccination could have on viral evolution and caution must be exercised when targeting a pathogen as mutable as IAV. Multipronged approaches, targeting several antigens via B and T cell responses could severely limit the generation of viral escape mutants compared to monovalent vaccines, particularly if responses can be directed against highly conserved epitopes essential to viral fitness.

In the present study I have investigated the ability of novel ChAd and MVA-vectored vaccines to simultaneously induce B and T cell responses against the influenza A antigens, HA and NP+M1. Viral-vectored vaccines are increasingly being used as platforms for the induction of humoral responses in addition to strong cellular immunity. Influenza A vaccines stimulating cellular immune responses have previously demonstrated efficacy in animal models and indeed, humans [307,311,551-553]. The aim of this study was to induce the highest level of heterosubtypic and homologous immune responses by targeting the conserved internal viral antigens NP+M1 in addition to the major virion surface protein, HA.

These results demonstrate vaccination with novel bivalent MVA-vectored vaccines elicit potent T cell responses against NP+M1 whilst simultaneously inducing strong antibodies, and this result holds for different subtypes of HA. Furthermore, T cell responses against NP+M1 were significantly higher than responses induced by the first generation of clinically investigated MVA-vectored vaccines, a promising result for future clinical works [310,442]. In addition I investigated immune responses against HA and NP+M1 delivered by ChAd-vectored vaccines. Delivery of multiple antigens by a single vector is preferable to monovalent vaccines for a number of reasons. However, at the time of this study only monovalent ChOx1-vectored vaccines were available for preclinical investigation. In order to deliver both HA and NP+M1 in a single vaccination, vaccines were mixed or delivered into separate limbs. Using these vectors, significant T cell competition was observed. This was in agreement with reports of antigenic competition in studies of DNA vaccine

plasmids in mixtures but contrasted previous co-administration studies in the malaria field, which reported T cell responses of similar magnitude to two vaccinating antigens following an adenovirus prime [534,554]. While the exact mechanisms of antigenic interference following vaccination remain unknown, this phenomenon is thought to be influenced by spatial constraints on $CD8^+$ T cells, including limited access to antigenic epitopes on antigen presenting cells (APC) or co-stimulatory molecules [555,556]. In support of this hypothesis, and as has been previously reported in the literature, T cell responses were improved by administering the vaccines into separate limbs. However, this does not fully explain why antigenic competition was not observed following the delivery of NP+M1 and HA by the bivalent MVA-vectored vaccine, which, was also inconsistent with the idea that antigenic-competition is simply an antigen-dependant phenomenon. However, as distinct promoters drove the expression of NP+M1 and HA in the bivalent vaccine, and F11 controls early expression whereas P7.5 is early/late, this supports the idea that differences between the expression times of antigens may contribute to the enhanced T cell responses observed. In fact very early expression of T cell stimulating antigens by MVA has previously demonstrated higher T cell responses and even reversal of immunodominance hierarchies [557]. However, in the malaria vaccine co-administration study, both antigens were expressed concurrently as in the ChAd-vectored vaccines used in this study, indicating other factors, which may or may not pertain to specific viral vectors, can influence this phenomenon. As the aim of this study was not to investigate the mechanisms of antigenic competition observed but instead to determine the most appropriate vaccination regimen to induce optimal B and T cell responses,

this was not further investigated. However, future studies examining responses induced by co-administration of monovalent MVA-vectored vaccines expressing different antigens under the control of matched promoters may shed light on the situation. It should also be noted that responses against NP+M1 in this study were measured against the immunodominant H2-Kd restricted (BALB/c) epitope $NP_{147-158}$ (TYQRTRALV), which can be used to gauge the magnitude of MHC class I and MHC class II restricted T cell responses (and may therefore be used to assess if competition with other encoded antigens dampened the magnitude of responses against NP+M1) [385]. However this peptide does not measure the breadth of responses across NP or M1-specific responses and future studies that seek to further delineate these aspects of the T cell responses observed in this study are advised to use pools of overlapping peptides.

Heterologous prime-boost antigen delivery strategies, in particular those that boost with MVA, have an excellent track record of inducing potent T cell responses. Therefore I sought to investigate if vaccination with MVA-NP+M1-H7 could overcome the T cell competition observed following co-administration of ChAdOx1-vectored vaccines whilst simultaneously boosting humoral responses against H7HA. Promisingly, boosting with MVA-NP+M1-H7 significantly enhanced T cell responses against NP+M1 and H7HA, regardless of whether antigenic competition was observed following a priming vaccination. Although boosting of responses did not overcome the suppressive effects of co-administration entirely, T cell responses against NP+M1 and H7HA were significantly improved.

The boosting ability of MVA, to enhance B cell responses following vaccination against Ebola with a ChAd vector, ChAd3, has recently been reported (Ewer et al, manuscript submitted). In agreement with this finding, the heterologous ChAd-MVA vaccination regimen described here boosted H7HA-specific serum IgG responses by a factor of ten in mice primed with ChAdOx1-vectored vaccines. Whilst high titer IgG antibodies are frequently assessed as an indicator of protective immune responses, an important consideration for influenza vaccine developers is the functionality of antibodies induced by vaccination. High titer non-neutralising antibodies against IAV have been previously associated with poorer clinical outcomes in humans [530]. Encouragingly, the two strains of H7-pseudotyped viruses used to assess responses were neutralised at all serum dilutions tested in mice primed with both antigens. Furthermore, this sera also demonstrated the ability to neutralise a heterosubtypic H3HA-pseudotyped virus, albeit less potently. This is an important finding in light of the pandemic threat posed by currently circulating avian H7 viruses. Furthermore, these humoral responses were maintained for up to 18 weeks post-vaccination. Indeed the highest numbers of H7HA-specific LLPCs and mBCs were induced in mice primed with both antigens. However, the findings from this study also suggest that humoral immune memory against H7HA induced by heterologous ChAd-MVA viral-vectored vaccination is largely the result of LLPCs rather than mBCs. The induction of mBCs is important for the generation of high affinity antibodies upon subsequent exposures to the same or slightly divergent strains. These cells are responsible for the generation of hypersomatically mutated high affinity antibodies in addition to replenishing the LLPC pool.

Future studies are needed to investigate the mechanisms behind why the humoral responses induced by the viral-vectored vaccine regimens reported in this study have not greatly stimulated production of these cells.

In summary, I have shown that vaccination against HA, NP and M1 during priming and boosting vaccinations via ChAd-MVA viral vectors induces potent heterosubtypic and homologous T and B cell responses. Whilst T cell competition is observed upon co-administration of monovalent ChAdOx-1 vectored vaccines, this effect is reduced by vaccination at different sites. Importantly, strong humoral immune responses, which are neutralising and long lasting, are induced against HA regardless of whether or not at second antigen was deliver during the prime. Whilst this study has characterised immune responses *ex vivo*, systemic effects must be taken into consideration when assessing vaccine efficacy. Future studies are needed to assess these vaccines in the context of an influenza challenge models.

7.5. Chapter Summary

- Vaccination with MVA-NP+M1-HA induces antibody responses comparable to vaccination with MVA-HA
- MVA-NP+M1-H7 induces superior T cell responses to vaccination with MVA-NP+M1, where NP+M1 is expressed by F11 in both vaccines
- Vaccination with ChAdOx1-H7 and ChAdOx1 NP+M1, as a mixture, or administered into separate limbs, induces antibody responses comparable to vaccination with ChAdOx1-H7 alone
- T cell competition is observed following vaccination with ChAdOx-NP+M1 when administered with ChAdOx1-H7, but this is reduced by vaccinating into separate sites
- There were no significant differences between antibody responses in groups primed with either ChAdOx1 NP+M1 and ChAdOx1-H7 or ChAdOx1-H7 alone following a boost with MVA-NP+M1-H7
- Priming with ChAdOx1 NP+M1 and ChAdOx1-H7 significantly reduced T cell responses to both NP and H7HA
- Significantly higher numbers of memory B cells were induced in the groups that received HA at prime and boost
- There were no differences in the number of circulating IgG^+ long-lived plasma cells in groups that received one or two antigens at prime
- Heterosubtypic neutralising antibodies induced by groups vaccinated with viral vectors were superior to vaccination with protein alone, regardless of whether one or two antigens were administered during prime

Chapter 8

Discussion

8. Discussion

Since the 1940s, vaccination has been, and continues to be, the cornerstone of public health measures against IAV. Antibody-inducing vaccines that target the major virion surface protein, HA, have dominated this era. Unsurprisingly, classical assays developed to measure such responses, in particular the haemagglutination-inhibition assay (HAI), have remained the principal means by which protection against infection is assessed. Indeed neutralising IgG antibodies against HA, reported as haemagglutination inhibition (HI) titers, are considered the primary immune correlate of protection against IAV by convention and are still used in vaccine licensure processes today. However this one-size-fits-all model of neutralising antibodies against the globular head of HA determining protection is not sufficient for populations such as the elderly and is simply not the only outcome by which vaccines such as LAIV, that also induce T cell responses, should be measured against.

Recombinant HA production to provide substrate for measuring vaccine-induced humoral immunity.

In recent years however, there has been considerable interest in a particular subset of antibodies against HA with broad reactivity and neutralising potential with view to developing universal influenza vaccines potentially capable of protecting against both seasonal and pandemic strains. These antibodies bind the stem region of HA and are not typically induced by current vaccine formulations or specifically measured by traditional assays. In order to progress towards developing vaccines capable of inducing anti-stem antibodies, there has been a need to firstly establish new methods to

accurately detect and measure these responses. Work in this thesis describes the production of soluble recombinant HA proteins using an easily scalable and reproducible mammalian cell-based protein expression system, the Expi293™ expression system. The purpose of producing soluble recombinant HA and establishing this system was to provide suitable reagents to enable the assessment of antibody responses against HA and specifically, HA stem by ELISA, a relatively straightforward and inexpensive assay used routinely in the vaccine development field to assess humoral responses (Chapter 3).

The Expi293™ expression system was successful in producing both wild type, full-length and chimeric HAs, all of which were stabilised by the addition of a T4 fibritin trimerisation domain. Whilst it was not possible to produce the stem domain of HA independently, the stem region of both chimeric proteins, cH9/H1 and cH16/H1, was recognised by the conformation-specific broadly neutralising anti-stem monoclonal antibody, C179, indicating that the addition of an exotic head domain did not broadly alter the conformation of the antigens to such an extent that conformation-dependent neutralising antibodies could not bind. Although the production of stabilised stem-only constructs remains a key goal in terms of vaccine antigen design, chimeric HA provide an authentic substitute for measuring anti-stem antibody responses. Indeed the cH9/H1 produced as part of this study was subsequently used to successfully measure anti-stem antibodies in BABL/c mice induced by vaccination (Chapter 6). In humans however, exposure to H9 subtypes has been reported, albeit rarely, and the H16 subtype may

prove a potentially better tool for human studies where results could be confounded by pre-existing antibodies against the globular head domain of H9 [521]. Although H16 viruses are capable of attaching to human tissues, at the time of writing this thesis no infections have been reported in man, meaning the likelihood of anti-H16 responses being present in human sera are lower for H16 than for H9 [558]. In any event, H9 and H16 responses could easily be controlled for by measuring responses against full-length constructs, reverse chimeras or head only constructs.

The development of a reliable, efficient and reproducible in-house means of producing reagents for the assessment of vaccine-induced immune responses is important, particularly as commercially produced recombinant HAs can vary in stability and lose conformational epitopes in the stem domain, leading to batch-to-batch variation and in worst case scenarios, false negative results. This is presumably because they are not typically produced with a stabilising trimerisation domain and/or routinely tested for stem conformation. Conformational epitope assessment requires monoclonal antibodies that are not readily commercially available, with the exception of C179 and CR6261 at present. Incidentally, these are very expensive and unlikely to appeal to profit-driven commercial producers. In light of the current reproducibility crisis in the biological sciences reported in several leading journals, it is vital to employ reliable and trustworthy methods and reagents in the assessment of clinically relevant disease interventions. Though this study has focused solely on HA, the Expi293™ expression system could be applied

to expression studies of other important influenza proteins with view to also producing these in-house.

Phage display to understand the breadth of vaccine induced antibody responses

In addition to the expression and the production of several recombinant HA proteins, this thesis describes the development of a phage display library (PDL) and subsequent optimisation of a novel biopanning strategy for use in the assessment of vaccine-induced humoral responses against HA (Chapter 4). In contrast to using ELISAs, whereby the amount or relative amount of antibodies directed against an entire domain or region of HA is measured, the phage display library can be used to provide a more detailed assessment of which particular epitopes within a specific protein or protein domain are recognised by antibodies. The particular epitopes chosen for this study were picked on the basis that they spanned the length of the HA molecule and were previously reported to be frequently recognised by circulating IgG antibodies in humans [194]. Inevitably, by selecting only 13 epitopes to display, the library cannot specifically measure every antibody clone generated against HA, but rather it is best used to delineate between the overall extent of 'head versus stem' responses within samples. Furthermore these epitopes are displayed independent of trimerisation and not every epitope has been confirmed to be conformational due to a paucity of reciprocal monoclonal antibodies. However, as all of these epitopes are recognised by human sera, it can be deduced that they are displayed in an antigenic form and therefore relevant for investigating infection or vaccine-induced responses.

The optimisation of a single-step screening protocol also described in Chapter 4, considerably aids the assessment of high-value clinical trial samples and small-volume murine samples, which are often limited in supply. Traditionally, screening with PDLs involves repeated rounds of biopanning, which consumes considerable volumes of test sera. The strategy developed in this study eliminates this issue. In the literature PDLs are increasingly being utilised to delineate antibody responses induced by adjuvanted vaccination regimens and they could similarly be used to investigate if antibody response distribution is differentially affected by the intrinsic adjuvanting properties of individual viral vectors. The library developed was later employed successfully to investigate if co-administration of MVA-NP+M1 with seasonal TIV (which previously demonstrated higher antibody responses compared to vaccination with TIV alone) had an effect on the distribution of antibody responses against either the globular head domain or the stem domain of H1HA in human clinical trial samples (Chapter 4). Results indicated vaccination with TIV co-administered with MVA-NP+M1 induced a slightly higher ratio of antibodies recognising the HA2 epitopes in this library among volunteers over 50 years. Although the library described is representative of epitopes from H1HA (A/Texas/05/2009), additional libraries could be made for any HA strain in order to assess the breadth of responses across HA subtypes. However, protein arrays could provide a similar global picture of the breadth of antibody responses across several subtypes of HA for considerably less cost. A major drawback of phage display is the need for sequencing, which even today remains relatively expensive and adds to the

cost of using this method. An alternative approach, which could bypass the need to sequence, is to develop individual 'libraries' expressing only one epitope. This was attempted during the early stages of development of the library reported here, but it was not possible to maintain pure phage clones over long periods of time and the final library was comprised of a pool of all clones.

T_{FH} cells: Understanding immunologic processes upstream of antibody production

Although technologies such as phage display and the production of stabilised native-like reagents for measuring antibodies against HA contribute to more accurately assessing humoral responses against HA and HA stem in particular, the precise immunological events that lead to the induction of long-lasting protective antibody responses following vaccination remain unclear. Understanding the mechanisms by which naïve B cells and/or memory B cells are differentially activated and expanded will be critical for the design of better influenza vaccines. For example, T follicular helper cells (T_{FH}), a subset of $CD4^+$ T cells, are essential for the generation of memory B cell responses and recent research has indicated a specific population of T_{FH} cells, $T_{FH}1$ cells, appear to be induced following vaccination with traditional seasonal vaccines [491]. Work in this thesis demonstrates that a similar population is primarily induced when seasonal TIV is co-administered with MVA-NP+M1 (Chapter 5). Indeed there were no differences in the proportion of $CD4^+$ T cells or $CD4^+$ $CD45RO^+$ T cells having $CXCR5^+$ $T_{FH}1$-like ($CXCR3^+CCR6^-$) or $CXCR5^-$ $T_{FH}1$-like ($CXCR3^+CCR6^-$) phenotype between groups. In addition

there were non-statistically significant increases in the proportion of $CXCR5^+$ $T_{FH}1$-like, $CXCR5^+$ $T_{FH}17$-like, $CXCR5^-$ $T_{FH}1$-like, $CD45RO^+CXCR5^-$ $T_{FH}1$-like and $CD45RO^+$ $CXCR5^+$ $T_{FH}1$-like CD4+ T cells that had an activated phenotype ($PD\text{-}1^{++}$) in the co-administration group, compared to the TIV alone group.

Understanding the mechanisms by which $T_{FH}1$ or $T_{FH}1$-like cells are induced will be important in guiding future rational vaccine design as this particular subset is thought to be less efficient at activating naïve B cells and is not associated with primary B cell responses. The vast majority of people receiving an influenza vaccine do so on a background of memory B cell responses primarily directed against the immunodominant globular head region of HA and activation of these memory B cells under the direction of $T_{FH}1$ cells results in the induction of plasma cells. Considering memory B cells recognising the conserved stem region of HA are extremely rare, it might be preferable in terms of vaccination, to aim to expand the B cell memory pool by priming naïve B cell responses against stem antigens, which could then be boosted by natural infection, as opposed to trying to boost a very tiny number of cells. At present the amount of circulating anti-stem IgG antibodies required to protect humans against infection is unknown, but it is expected that as a result of the restricted access anti-stem antibodies might have to the membrane proximal region on the closely packed virion surface, this could be many factors higher than the amount of antibodies against the globular head region needed to mediate neutralising activity. One step towards improving B cell responses against novel epitopes that are not

induced by current vaccines is to direct T_{FH} cell responses towards $T_{FH}2$ or $T_{FH}17$ subsets, which are more efficient at priming naïve B cell responses than $T_{FH}1$ cells. Furthermore, if, as is the case with the production of broadly neutralising antibodies (bnAbs) in HIV-infected individuals, the induction of broadly neutralising anti-stem antibodies (bnStAbs) following vaccination against influenza requires a high degree of hypersomatic mutation, then designing vaccines that will support efficient T_{FH} cell responses may better facilitate this. Might this pose a dilemma for viral-vectored vaccines, well established for their induction of strong Type 1 responses? Perhaps. However investigation of co-administration of classical Type 2 adjuvants (e.g. alum) may facilitate a balance of efficient Type 1 and 2 responses, thus preserving the strong cytotoxic T cell responses viral-vectored vaccines are distinguished for whilst favouring more efficient germinal centre reactions.

Assessment of vaccine candidates targeted at generating broadly neutralising immune response against HA

Though research into fine-tuning adaptive immune responses induced by vaccination is clearly warranted, a more immediate issue has been the construction of authentic vaccine antigens. Indeed, the production of a stable, immunogenic and HA stem-based vaccine that displays bnAb epitopes has been the focus of several research groups since the emergence of the 2009 pandemic. The work outlined in this thesis has contributed to this body of research by investigating the ability of three novel stem immunogens and a chimeric HA to induce anti-stem antibody responses in BALB/c mice following viral-vectored vaccination (Chapter 6). Three antigens, Headless, H1HA-

Stem and H1HA-Stem+TM induced comparable IgG^+ anti-stem antibody responses following an AdHu5-MVA prime boost regimen (Chapter 6). The rational design process for the development of stable stem immunogens is largely guided by computer-directed protein modelling, and trial and error. Many constructs, including two described in this thesis (Chapter 6), have sought to address the instability of a truncated HA stem by introducing specific mutations that are predicted to preserve antigenicity among monomers whilst reducing the instability that occurs from the removal of the globular head and exposure of hydrophobic amino acids. In this thesis the inclusion of a trimerisation domain and the native HA transmembrane domain were also investigated as a means of potentially improving antigenicity by contributing to stem stabilisation (Chapter 6). These results show that DNA plasmids expressing HA-based immunogens, which include a transmembrane domain, better prime anti-stem antibody responses compared to controls. However Ad-MVA prime boost regimens are more effective than DNA-ChAdOx1-MVA regimens in generating anti-stem IgG antibodies. Furthermore antibody responses induced against the trimerisation domain by the AdHu5 constructs were (just) detectable (although they were not detectable in the DNA prime regimen) and should be controlled for in future studies.

Interestingly constructs, which have not folded into a native-like stem conformation have still provided some degree of protection to mice challenged with divergent viruses by inducing B and presumably T cell responses [559]. However the provision of conformational broadly neutralising

epitopes is essential for the induction of bnStAbs and it is important that responses induced by stem constructs are in fact neutralising as low affinity, non-neutralising antibodies could mediate immune-complex formation potentially leading to enhanced respiratory disease.

Assessment of vaccine candidates targeted at generating T and B cell responses against HA and NP+M1

The development of conformational stem immunogens is undoubtedly a major step towards the development of a universal influenza vaccine. However, too often history has demonstrated the ability of IAV to escape immune responses and although the stem of HA is functionally restricted and highly conserved, there remains the possibility that even with vaccines that induce high titers of bnStAbs, viral mutants could escape. The greater the number of mutations required to facilitate viral escape, the less likely it is that these will occur simultaneously. It seems therefore prudent that the ultimate universal influenza vaccine should have at least two or more antigenic targets and can induce both arms of the adaptive immune system. The induction of T and B cell responses induced by vaccination with viral-vectored vaccines delivering multiple IAV antigens has been described in this thesis as a first step towards the development of a multivalent universal influenza vaccine. These results demonstrated that co-expression of HA and NP+M1 in a bivalent vector did not compromise generation of anti-HA IgG antibodies and the induction of T cell responses against NP+M1 were significantly higher when this antigen was expressed under control of the F11 promoter compared to the P7.5 promoter used in the prototype vaccine, MVA-NP+M1.

In addition, co-administration of ChAdOx1-vectored vaccines expressing NP+M1 and HA (singly) did not compromise anti-HA IgG responses. However, T cell responses against NP+M1 were significantly impaired. Combining these vaccines in a ChAdOx1-MVA prime boost regimen demonstrated that mice primed with ChAdOx1-HA either with or without ChAdOx1 NP+M1 induced the highest IgG responses against HA. Furthermore these antibodies were functionally neutralising against H7 and H3 pseudotyped lentiviruses and these regimens induced significantly higher LLPCs compared to vaccination with protein alone. Vaccination with ChAdOx1 NP+M1, either alone or co-administered with ChAdOx1-H7, followed by boosting immunisation with MVA-NP+M1-H7, induced higher T cell responses against NP+M1 compared to mice primed with ChAdOx1-H7. Similarly vaccination with ChAdOx1-H7, either alone or co-administered with ChAdOx1 NP+M1, followed by boosting immunisation with MVA-NP+M1-H7, induced higher heterosubtypic T cell responses against H7HA. In general, co-administration of ChAdOx1-based vaccines lead to reduced T cell responses against both antigens, although this effect was relatively small.

Whilst a bivalent MVA-vectored vaccine is already in existence, future works are needed to further develop adenoviral vectors to accommodate more then one transgene. Beyond this, trivalent viral vectors expressing at least two transgene antigens in addition to an expression-displayed antigen could be used to deliver high dose multivalent vaccines. However, such vaccines may come with a price in the form of antigenic competition between immune cells or reactogenicity and future studies will need to investigate this.

Future outlook

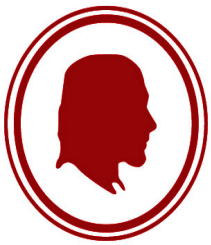
At the time of writing this thesis, reports of two different stabilised HA stem based vaccines emerged simultaneously. One detailed stabilised 'mini-HA' stem trimers produced using an iterative mutational design process to adjust the position of residues at the membrane distal portion of the stem ultimately yielding trimerised antigens with preserved bnStAb epitopes [518]. The second described trimeric HA-stem immunogens stabilised by truncations and linker mutations attached to multivalent ferritin nanoparticles (HA-SS-np) [517]. Both vaccines demonstrated heterosubtypic protection in mice against H5N1 and partial protection in monkeys (mini-HA) and ferrets (HA-SS-np) [517,518]. These constructs could be easily adapted to viral vector platforms and might particularly benefit from expression by new-generation expression-display viral vectors currently in development at the Jenner Institute (Dr Vincent Pavot, personal communication). Particulate vaccine formulations are well known to facilitate antigen entry into antigen-presenting cells (APCs) through passive or active targeting and depot formation, often eliciting superior antibody responses compared to non-particulate analogous vaccines. Compared to HA-SS-np, which delivers 8 trimeric HA spike per nanoparticle, AdHu5 vectors, for example, could deliver ten times as much antigen per particle by fusion of antigen to the minor capsid protein IX (pIX). Furthermore, the intracellular mature virion envelope protein D8 expressed by MVA, which has been previously engineered to express malarial antigens (Dr Vincent Pavot, personal communication), could also be used to display HA stem immunogens. Delivery of antigens with the additional benefit of the adjuvanting properties of viral vectors could assist in achieving the high level

antibody titers believed to be necessary in humans to prevent infection, particularly in the context of a heterologous prime boost regimen. Furthermore, viral vectors can also be used to express additional antigens via the traditional transgene route, delivering a one-two punch.

The work described in this thesis has developed a number of tools to measure heterosubtypic immune responses against influenza, investigated the cellular events associated with the induction of antibody responses induced by viral vectored vaccination, designed and tested several novel vaccine immunogens designed to elicit anti-stem antibodies and explored the immune responses induced following multivalent viral-vectored vaccination. These studies will inform future studies towards the development of a universal influenza A vaccine.

APPENDICES

Appendix I



1.0 Jenner Laboratory Protocol Number J004b

2.0 Version Number 5

3.0 Transfection of HEK293 or 293TREx cells with Adenoviral DNA and viral rescue.

This protocol uses GMO. All users MUST be registered with the University Occupational Health Service as set out in the University's health and safety regulations. Health surveillance is a legal requirement under COSHH.

If you are not currently registered with the Occupational Health Service for work with GMO, or need to check your registration, please contact the ORCRB NDM Personnel team.

4.0 Other documents

MSDS	refer to MSDS for the relevant safety information on the individual reagents: \\Imsnw3_jenner_server\jenner\hill_group\Safety\COSHH assessments\Manufacturers material safety data sheets
R002	Adenovirus
R004	GMO RA appendix
J008	Infecting 293 cells with adenovirus
J011	Passaging 293 cells
J199	Passaging TREx cells
J173	Preparation of template DNA using DNA Releasy
J175	Virus ID and Purity PCR using KAPA 2G robust polymerase
J245	Virus ID and Purity PCR using KAPA Long Range, Hot Start polymerase Ready mix
J252	General working practice in the Virus Room

5.0 Definitions

DMEM	Dulbecco's Modified Eagle's Media
FBS	Foetal Bovine Serum
RNAse	Ribonuclease
DNAse	Deoxyribonuclease
BSA	Bovine serum albumin
CPE	Cytopathic effects

6.0 Objective

To transfect HEK293A or 293TREx cells with recombinant adenoviral plasmid. It is recommended to perform a control transfection with serotype-matched GFP or mCherry-expressing virus at the same time (p2026: pAdc63-GFPTIP-nil; p2108: pAd5-mCherry). This will help to separate problems due to poor transfection efficiency from problems related to virus growth/antigen toxicity. It may also be useful to perform a mock transfection with Lipofectamine alone to enable any toxic effects of the transfection reagent to be observed.
This protocol describes the transfection and also the subsequent passaging of transfected cells. The cells are passaged into larger tissue-culture flasks once or twice as they reach 90% confluency as this maintains the expression of the E1 genes by the cells, such expression is required for virus rescue.
Usually, rescued virus is apparent (by CPE) on day 7 or 8 (i.e ~5 days after subculture into a T75 flask). However, in some instances the virus has only rescued after a further passage into a T175. The important factor is to keep the cell culture healthy and sub-culture when required. We would not routinely continue with a virus longer than 14 days but would attempt a new transfection with freshly prepared plasmid DNA. If this failed we would discuss how to continue with virus requestor.
NOTE: ChAdOX1 grows more slowly than either AdH5 or AdC63 and the culture times given below may need to be adjusted accordingly.

General working practice:

- Do not have more than one virus in the hood at any one time.
- The aliquoted reagents (lysis buffer, CsCl, Storage buffer etc) are for use by everyone. Please note: they are single use - **DO NOT** place opened reagents back on the shelves
- Wipe the hood and equipment thoroughly with Microbicide and then 70% ethanol before use and between handling different viruses.
- Change gloves between viruses (this ensures any trace amounts of virus are completely removed).
- Do not use micropipettes when working with cell culture material. It is difficult to ensure the micropipettes are sterile due to the complexity of their construction. Transfer material to an interim container and then take a small sample. In this protocol we do need to use them but just be aware of the potential problems associated with their use.
- Ensure items placed in the dispo-jar are covered by the Microbicidal solution.
- When finished, empty the dispo-jar. Wipe down the hood with Microbocodal solution and 70% ethanol. Switch off and close the hood. Re-stock any equipment as required.
- Do not put liquid waste into the autoclave bins – pour it into a container, treat with Microbicide if necessary and then dispose of down the sink.

Note:

1) When using 293TREx cells, blasticidin **MUST** be present in the media at all stages to retain the repression of antigen expression. This includes post-transfection culture where the media does not contain Pen/Strep.

2) HEK293A cells and T-REx-293 cells are immortalised lines of primary human embryonic kidney cells transformed by sheared human Ad5 DNA. The cells harbor the E1A and E1B region of the adenoviral genome, that complement, in trans, the deletion of the E1 region in the recombinant adenovirus. The cells constitutively express the adenoviral E1 proteins (E1A and E1B) while they are dividing. When they reach confluency, total protein expression, including E1, is reduced. During their natural lifecycle, adenoviruses express the E1 proteins at all stages (see Fig. 3) and the proteins are therefore extremely important for successful virus rescue. It is therefore important that cells do not reach confluency during routine passage and also that seeding densities in preparation for transfection are suitably low.

Reagents

3 x wells of 6 well plate per transfection being performed of HEK293 or 293TREx cells at ~80% confluency in 2 ml 10% DMEM (for seeding densities see below).

DMEM (high glucose, with pyruvate)
Sigma D6546
OptiMEM (Reduced serum medium, with Glutamine and HEPES, without Phenol red)
Invitrogen 11058-21
TrypLE™ Express
Invitrogen 12605010
Phosphate Buffered Saline (without Ca^{2+} and Mg^{2+})
Sigma D8537
200 mM Glutamine
Sigma G7513
100x Penicillin/Streptomycin solution
(10,000 Units penicillin-G and 10mg strep per ml)
Sigma P0781
Foetal Bovine Serum
Sigma 12103C
Lipofectamine™ 2000 transfection reagent
Invitrogen 11668-019
10 mg/ml Blasticidin S-HCl
Melford Labs B1105

Complete 10% FCS DMEM - without Blasticidin for HEK293A cells,
with blasticidin for 293TREx cells

50 ml FCS	(~10% final conc)
5 ml Pen/strep	(100 U Penicillin, ~0.1 mg strep ml^{-1} final conc)
10 ml L-glutamine	(~4 mM final conc)
250 µl Blasticidin	**(~5ug/ml final conc)**

Complete 10% FCS DMEM without Pen/strep - without Blasticidin for HEK293A cells, with blasticidin for 293TREx cells

50 ml FCS	(~10% final conc)
10 ml L-glutamine	(~4 mM final conc)
250 µl Blasticidin	**(~5ug/ml final conc)**

Lysis buffer (10 mM Tris, 1 mM $MgCl_2$. pH 7.8)

5 ml 1 M Tris-HCl pH 7.8
0.5 ml 1 M $MgCl_2$
Make up to 500 ml with 18.2 MΩ water to 500 ml using a measuring cylinder
Autoclave.

7.0 Equipment

15 ml Falcon Tubes	
50 ml Falcon Tubes	
Class II BioSafety Cabinet	
Microscope DMIL	Leica
Centrifuge	Beckman
2 ml screw-capped tubes	
T25 tissue culture plates	
1.5 ml microcentrifuge tubes (autoclaved)	TREFF
Sterile, serological pipettes	
Sterile filter tips	Rainin

8.0 Method

Day 1 Cell Seeding

The cells are provided by the person performing routine cell culture. It is important to make sure that you request 6 well plates at the relevant densities and also the antibiotic-free media should be used (either completely antibiotic free for HEK293A cells, or D10B-P/S for TREx293 cells.
Invitrogen recommend that cell density is 90-95% for transfection using Liopfectamine2000. However, for adenovirus rescue, the cells need to be dividing (to express E1 proteins and support viral replication)

8.1 Prepare sufficient single wells of 6 well plates for the following:
- 3 x wells of 6 well plate to be transfected with mcherry control DNA
- 3 x wells of 6 well plate to be mock-transfected with Lipofectamine alone
- 3 x wells of 6 well plate for experimental transfection/s.

Day 2 Cell transfection

8.2 Warm an aliquot of OptiMEM for the preparation of DNA-Lipofectamine complexes to ROOM TEMPERATURE – (not 37°C).

8.3 Warm an aliquot of OptiMEM for cell washing/media replacement to 37°C

8.4 Warm 10% FCS DMEM without Pen/strep to 37°C

Note: The adenovirus shuttle plasmid is large (~35 kb) and as such is fragile. Pipette very gently to prevent shearing the DNA.

8.5 Mix lipefectamine gently before use.

8.6 Prepare:

1 x sterile 2 ml screw-capped tube containing 85 µl restriction enzyme mix + 215 µl OptiMEM without serum.

1 x sterile 2 ml screw-capped tube containing 30 µl lipofectamine 2000 + 270 µl OptiMEM without serum.

8.7 Mix tubes gently by flicking.

8.8 Incubate at room temperature for 5 min.

8.9 Mix the contents of the 2 tubes. Add the DNA to the lipofectamine, not vice versa. Flick tubes gently to mix, and incubate at room temperature for at least 20 min (complexes are stable for 6 h at Room Temp).

8.10 Remove the media from the single wells of 6 well plates and add 2 ml of OptiMEM, to each.

8.11 Add the 300 µl of DNA/lipid complexes to the first well of the 6 well plate, 200 µl to the second well of the 6 well plate and the remaining transfection mix to the third well of the 6 well plate and mix by tilting the plate gently to ensure that the transfection mix covers all the cells.

8.12 Place the cells at 37°C, 5% CO_2 for 4 to 6 hours. 293 cells can be left overnight but for T-REX cells the transfection mix **must be removed after 4 to 6 hrs** to prevent toxicity

8.13 Replace the media with 5 ml of antibiotic-free media.

8.14 Place the cells at 37°C, 5% CO_2.

Day 4 Passaging cells to maintain cell viability and promote virus rescue.

8.15 Inspect cells using microscope, they should be confluent and beginning to appear crowded, patches of CPE may be evident. If the virus rescue has been very efficient, it may have destroyed the cell layer in the most concentrated well. The other wells should provide a sample where not all of the monolayer has been destroyed.

8.16 Check for fluorescent protein expression in the control flask to assess transfection efficiency.

8.17 Warm TrypLE Express, 10% FCS DMEM (+ blasticidin) to 37°C. **The cells are fragile at this stage and must be treated very gently.**

8.18 Select the well that contains approximately 50% healthy cells and transfer media (approx. 2 ml) from the single well of 6 well plate to a fresh T75 flask.

8.19 Add a further 12 ml fresh media to the T75.

8.20 Add 3 ml TrypLE Express and place plate at 37°C for approx 2 min to detach cells.

8.21 Add 3 ml D10 to the plate, swirl to ensure all cells are suspended in the media and transfer to the T75 (final media volume in flask should be approx. 20 ml).

8.22 Place at 37°C, 5% CO_2. The cells will take approximately 48 hr to reach confluency and then monitor for the appearance of CPE, this should begin 48-72 hr after cell passage

8.23 Continue with either harvest at day 7-11 or a further round of cell passage. Even if there are no obvious CPE, it is worth storing some material to titrate on a 6 wp in addition to splitting the cells. There is usually some virus present and the titration should allow this to grow out.

Day 7 – 11 Harvesting of adenovirus-infected cells

Cells showing a CPE should detach from the flask with gentle tapping. Transfer cells and media to a sterile, 50 ml tube. Centrifuge (1500 x g, 5 min, RT) to pellet the cells and then aspirate the supernatant to waste. Resuspend the cell pellet in 2 ml lysis buffer. Freeze/thaw x 3 and store at -20°C.This stage is called the transfection stock (TF).

Day 7-11 Passaging cells into T150 if there are no signs of CPE

8.24 Inspect cells using microscope, they should be confluent and beginning to appear crowded.

8.25 Warm TrypLE Express, PBS and 10% FCS DMEM without antibiotics to 37°C. The cells are fragile at this stage and must be treated very gently.

8.26 Transfer media from the T75 to a fresh T150.

8.27 Wash cells carefully with 10 ml PBS (aim fluids along the top of the flask to prevent dislodging the cells).

8.28 Add 5 ml TrypLE Express and place flask at 37°C for approx 2 min to detach cells.

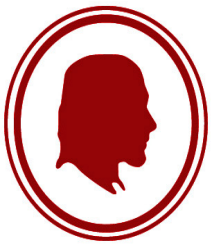
8.29 Add 15 ml 10% FCS DMEM to the flask and transfer to the T150.

8.30 Place at 37°C, 5% CO_2 and monitor for the appearance of CPE, this should begin 48-72 hr after cell passage. It is important to be able to distinguish between gaps between the cells where they have not reached confluency and genuine CPE. The positive control virus should be observed in parallel to clarify cell morphology under the two different conditions.

9.0 Revision History

Version Number	What Changed	Who Changed it	Date changed
1	**First written**	**Ali Turner**	**12.04.12**
2	**Cell seeding densities added**	**Rachel H**	**05.11.12**
4	**Changed to include 3 wells of 6wp, addition of different volumes of the transfection mix to the 3 wells and selection of the well containing 50% viable cells for further work.**	**Ali Turner**	**18.02.14**
5	**General updating – no real changes to protocol**	**Ali Turner**	**04.03.14**

Appendix II



1.0 Jenner Laboratory Protocol Number J004c

2.0 Version Number 5

3.0 Preparation of premaster seed stock of virus.

This protocol uses GMO. All users MUST be registered with the University Occupational Health Service as set out in the University's health and safety regulations. Health surveillance is a legal requirement under COSHH.

If you are not currently registered with the Occupational Health Service for work with GMO, or need to check your registration, please contact the ORCRB NDM Personnel team.

4.0 Other documents

MSDS	refer to MSDS for the relevant safety information on the individual reagents: \\Imsnw3_jenner_server\jenner\hill_group\Safety\COSHH assessments\Manufacturers material safety data sheets
R002	Adenovirus
R004	GMO RA appendix
J008	Infecting 293 cells with adenovirus
J011	Passaging 293 cells
J199	Passaging TREx cells
J252	General working practice in the Virus Room

5.0 Definitions

DMEM	Dulbecco's Modified Eagle's Media
FBS	Foetal Bovine Serum
RNAse	Ribonuclease
DNAse	Deoxyribonuclease
BSA	Bovine serum albumin
CPE	Cytopathic effects

6.0 Objective

To prepare a premaster seed virus stock that can be used to infect a bulk prep. A serial dilution of the transfection stock is used to infect cells in a 6 well plate. In this

way it is possible to harvest a well that is showing complete and uniform CPE at 48 - 72 hours. It is important not to harvest cells before this as the virus will still be in early stages of replication and the yield of infectious units (IU) will be low.
In addition, an excess of the capsid proteins are produced by the adenovirus. These bind to cell surface proteins and cause the cells to detach from the flask and also each other (*in vivo* this is used to create gaps between the cell layer and allow the virus to escape). This is evident by cells floating less than 24 hours after infection. This effect is minimised by pelleting the cells and re-suspending them in lysis buffer so that the proteins are removed with the tissue culture supernatant.
Cell lysis results in the release of proteases from the cells which are able to degrade proteins. Importantly this includes the adenoviral capsid proteins that are required for infectivity. To minimize protease activity, once the cells are lysed ensure that the sample is kept chilled and keep incubations at 37°C as short as possible.

General working practice:

- Do not have more than one virus in the hood at any one time.
- Do not use VVCF cell culture media.
- The aliquoted reagents (lysis buffer, CsCl, Storage buffer etc) are for use by everyone. Please note: they are single use - **DO NOT** place opened reagents back on the shelves
- Wipe the hood and equipment thoroughly with TriGene and then 70% IMS before use and between handling different viruses (to clean the hood, wet some blue roll thoroughly with the cleaning agent and wipe the hood surface, do not spray the hood directly as this is corroding the painted surfaces).
- Change gloves between viruses (this ensures any trace amounts of virus are completely removed).
- Where possible, do not use micropipettes when working with cell culture material. It is difficult to ensure the micropipettes are sterile due to the complexity of their construction. Transfer material to an interim container and then take a small sample. In this protocol we do need to use them but just be aware of the potential problems associated with their use.
- Ensure items placed in the dispo-jar are covered by the TriGene solution.
- When finished, empty the dispo-jar and re-fill with fresh, diluted TriGene solution. Wipe down the hood with TriGene solution and 70% IMS. Switch off and close the hood. Re-stock any equipment as required.
- Do not put liquid waste into the autoclave bins – pour it into a container, treat with TriGene if necessary and then dispose of down the sink.

Note:

3) When using T-REx-293 cells, blasticidin **MUST** be present in the media at all stages to retain the repression of antigen expression. This includes post-transfection culture where the media does not contain Pen/Strep.

4) HEK293A cells and T-REx-293 cells are immortalised lines of primary human embryonic kidney cells transformed by sheared human Ad5 DNA. The cells harbor the E1A and E1B region of the adenoviral genome, that complement, in trans, the deletion of the E1 region in the recombinant adenovirus. The cells constitutively express the adenoviral E1 proteins (E1A and E1B) while they are dividing. When they reach confluency, total protein expression, including E1, is reduced. During their natural lifecycle, adenoviruses express the E1 proteins at all stages (see Fig. 3) and the proteins are therefore extremely important for successful virus rescue. It is therefore important that cells do not reach confluency during routine passage and also that seeding densities in preparation for transfection are suitably low.

7.0 Reagents

DMEM (high glucose, with pyruvate)
Sigma D6546
200 mM Glutamine
Sigma G7513
100x Penicillin/Streptomycin solution
(10,000 Units penicillin-G and 10mg strep per ml)
Sigma P0781
Foetal Bovine Serum
Sigma 12103C
10 mg/ml Blasticidin S-HCl
Melford Labs B1105
18.2 MΩ/cm ultrapure water
Elga
1 M Tris-HCl pH 7.8
Sigma T2569
1 M MgCl2
(Sigma) Fluka 63069

Complete 10% FCS DMEM ± Blasticidin

50 ml FCS	(~10% final conc)
5 ml Pen/strep	(100 U Penicillin, ~0.1 mg strep ml-1 final conc)
10 ml L-glutamine	(~4 mM final conc)
250 μl Blasticidin	(~5ug/ml final conc)

Lysis buffer (10 mM Tris, 1 mM MgCl2. pH 7.8)
5 ml 1 M Tris-HCl pH 7.8
0.5 ml 1 M MgCl2
Make up to 500 ml with 18.2 MΩ water to 500 ml using a measuring cylinder
Filter sterilise.

8.0 Equipment

Class II BioSafety Cabinet	Scanlaf Ltd
Microscope	Leica

DMIL
37°C water bath
Benchtop centrifuge
Sterile, serological pipettes
Micropipettes and Sterile filter tips Rainin
Pipette aid
6 well plate

9.0 Method

8.31 Prepare a 6-well plate with either HEK293 or HEK293TREx cells the day before required so that they are 70 – 80% confluent at the time of infection (see J011 and J199).

8.32 Options for source material:

a. Add 500 µl transfection stock cell lysate to the first well and rock plate backward, forwards and side to side to evenly distribute the virus.
b. Add 20 µl previously prepared premaster cell lysate
c. Add 5 µl purified stock

8.33 Take 500 µl of media from the first well, add to the second well and repeat the mixing step.

8.34 Repeat step 9.2.3 for the remaining 4 wells

8.35 Place plate at 37°C, 5% CO_2 for ~**72 hours**.

8.36 Harvest the cells and media from the well that shows uniform CPE using a cell lifter and 2 ml serological pipette, transfer the material into a 15 ml tube.

8.37 Freeze/thaw the sample twice.

8.38 Pellet the cells using the centrifuge (1500 x g, 5 min, RT).

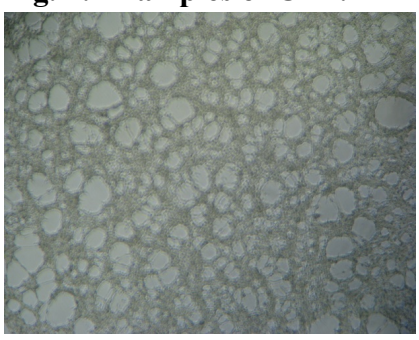
8.39 **Transfer supernatant to a fresh 2 ml screw-capped tube*.**

8.40 Take 50 µl of the material into a 2 ml tube to provide material for test infection.

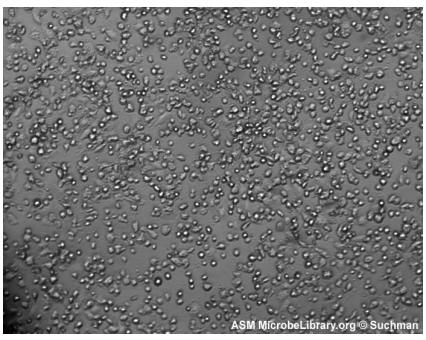
8.41 Freeze all samples.

***This is important to ensure that subsequent steps are performed on a uniform solution. If the cell pellet is not removed, this might sequester virus particles and end up being used to infect either the test infection plate or the HF leading to more IU being added than realised.**

Fig. 1: Examples of CPE.

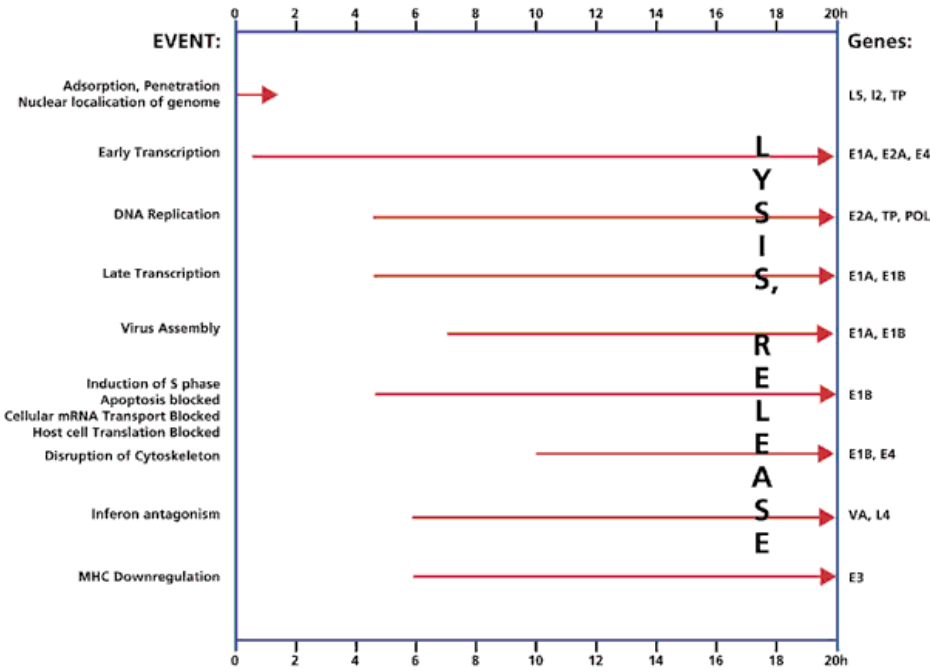


AdC63 and ChAdOX



AdHu5

Fig. 2: Adenoviral life cycle, gene expression



10.0 Revision History

Version Number	What Changed	Who Changed it	Date changed
1	First written	Ali Turner	13.04.12
2	2% media changed to 10% media. Preparation of sample for PCR altered	Ali Turner	17.07.12
3	Step to transfer s/n to fresh tube after harvest and F/T of premaster material from the 6 well plate	Ali Turner	03.09.12
4	Step to remove sample for test infection and pictures of different CPE	Rachel Hossack	14.02.13
5	No longer changing the media at time of infection Infecting with greater volume of TF cell lysate No PCR QC performed at this stage	Ali Turner	22.10.13

Appendix III

1.0 Jenner Laboratory Protocol Number J004d

2.0 Version Number 5

3.0 Testing infection of a 6 well plate using premaster seed stock virus

This protocol uses GMO. All users MUST be registered with the University Occupational Health Service as set out in the University's health and safety regulations. Health surveillance is a legal requirement under COSHH.

If you are not currently registered with the Occupational Health Service for work with GMO, or need to check your registration, please contact the ORCRB NDM Personnel team.

4.0 Other documents

MSDS	refer to MSDS for the relevant safety information on the individual reagents: \\Imsnw3_jenner_server\jenner\hill_group\Safety\COSHH assessments\Manufacturers material safety data sheets
R002	Adenovirus
R004	GMO RA appendix
J008	Infecting 293 cells with adenovirus
J011	Passaging 293 cells
J199	Passaging TREx cells
J252	General working practice in the Virus Room

5.0 Definitions

DMEM	Dulbecco's Modified Eagle's Media
FBS	Foetal Bovine Serum
RNAse	Ribonuclease
DNAse	Deoxyribonuclease
BSA	Bovine serum albumin
CPE	Cytopathic effects

6.0 Objective

To perform a test serial dilution in a 6wp with a sample from the premaster seed stock. Virus growth (CPE) is monitored over 72 hours. This allows us to adjust the amount of premaster seed lysate we use to infect the flasks for MSV.
In this way it should be possible to ensure that the MSV flasks show complete and uniform CPE at 48 -72 hours. It is important not to harvest cells before this as the virus will still be in early stages of replication and the yield of infectious units (IU) will be low.
In addition, an excess of the capsid proteins are produced by the adenovirus. These bind to cell surface proteins and cause the cells to detach from the flask and also each other (*in vivo* this is used to create gaps between the cell layer and allow the virus to escape). This is evident by cells floating less than 24 hours after infection. This effect is minimised by pelleting the cells and resuspending them as they are harvested so that the proteins are removed with the tissue culture supernatant.
This protocol is performed as an alternative to titration of the premaster seed stock virus for which we currently do not have the resources to perform.

General working practice:

- Do not have more than one virus in the hood at any one time.
- The aliquoted reagents (lysis buffer, CsCl, Storage buffer etc) are for use by everyone. Please note: they are single use - **DO NOT** place opened reagents back on the shelves
- Wipe the hood and equipment thoroughly with TriGene and then 70% IMS before use and between handling different viruses (to clean the hood, wet some blue roll thoroughly with the cleaning agent and wipe the hood surface, do not spray the hood directly as this is corroding the painted surfaces).
- Change gloves between viruses (this ensures any trace amounts of virus are completely removed).
- Where possible, do not use micropipettes when working with cell culture material. It is difficult to ensure the micropipettes are sterile due to the complexity of their construction. Transfer material to an interim container and then take a small sample. In this protocol we do need to use them but just be aware of the potential problems associated with their use.
- Ensure items placed in the dispo-jar are covered by the TriGene solution.
- When finished, empty the dispo-jar and re-fill with fresh, diluted TriGene solution. Wipe down the hood with TriGene solution and 70% IMS. Switch off and close the hood. Re-stock any equipment as required.
- Do not put liquid waste into the autoclave bins – pour it into a container, treat with TriGene if necessary and then dispose of down the sink.

Note:

5) It is important that the cells are maintained in the log phase of growth so that the E1 protein expression rates are maximal. The adenovirus requires these proteins for growth. If the cells have reached confluency, then protein expression drops and the virus cannot replicate. The cells must not reach

greater than 80% confluency during culture and especially must not exceed this level prior to being sub-cultured ready for virus infection.

6) HEK293 cells are very loosely adherent – take care when pipetting into flasks and ensure that media is added away from the cell layer.

7) When using T-REx-293 cells, blasticidin **MUST** be present in the media at all stages to retain the repression of antigen expression. This includes post-transfection culture where the media does not contain Pen/Strep.

8) HEK293A cells and T-REx-293 cells are immortalised lines of primary human embryonic kidney cells transformed by sheared human Ad5 DNA. The cells harbor the E1A and E1B region of the adenoviral genome, that complement, in trans, the deletion of the E1 region in the recombinant adenovirus. The cells constitutively express the adenoviral E1 proteins (E1A and E1B) while they are dividing. When they reach confluency, total protein expression, including E1, is reduced. During their natural lifecycle, adenoviruses express the E1 proteins at all stages (see Fig. 3) and the proteins are therefore extremely important for successful virus rescue. It is therefore important that cells do not reach confluency during routine passage and also that seeding densities in preparation for transfection are suitably low.

7.0 Reagents

DMEM (high glucose, with pyruvate)
Sigma D6546
200 mM Glutamine
Sigma G7513
100x Penicillin/Streptomycin solution
(10,000 Units penicillin-G and 10mg strep per ml)
Sigma P0781
Foetal Bovine Serum
Sigma F2442
10 mg/ml Blasticidin S-HCl
Melford Labs B1105
18.2 MΩ/cm ultrapure water
Elga
1 M Tris-HCl pH 7.8
Sigma T2569
1 M $MgCl_2$
(Sigma) Fluka 63069

Complete 10% FCS DMEM ± Blasticidin

50 ml FCS	(~10% final conc)
5 ml Pen/strep	(100 U Penicillin, ~0.1 mg strep ml^{-1} final conc)
10 ml L-glutamine	(~4 mM final conc)
250 µl Blasticidin	**(~5ug/ml final conc)**

Lysis buffer (10 mM Tris, 1 mM $MgCl_2$. pH 7.8)

5 ml 1 M Tris-HCl pH 7.8
0.5 ml 1 M $MgCl_2$
Make up to 500 ml with 18.2 MΩ water to 500 ml using a measuring cylinder
Filter sterilise.

8.0 Equipment

50 ml Falcon Tubes
Class II BioSafety Cabinet Scanlaf Ltd
Microscope Leica DMIL
37°C water bath
Benchtop centrifuge
Sterile, serological pipettes
Micropipettes and Sterile filter tips Rainin
Pipette aid
6 well plate

9.0 Method

8.42 Prepare a 6 well plate of cells 24 hours before use such that the cells are 70 – 80% confluent at the time of infection.
8.43 Number 6 x 2 mL screw cap tubes 1 to 6.
8.44 Transfer relevant volume of D10 media to a 50 ml centrifuge tube.
8.45 Using micropipette transfer 1.5 ml media to first tube and 750 µl media to subsequent tubes.
8.46 Add 30 µl test infection material to the first tube.
8.47 Using the micropipette set to 750 µl, triturate x10. Transfer 750 µl across to the next tube and triturate as previously. Repeat for remaining tube. NOTE: The same pipette tip can be used throughout this dilution as it is not required to be absolutely accurate.
8.48 Add 750 µl of the samples to wells of the 6 well plate (starting with the most dilute first and using the same pipette tip throughout).
8.49 Place cells at 37°C, 5% CO_2.
8.50 Monitor for appearance of CPE over 48-72 hours, use this information to decide on an inoculum volume for bulk virus preparation using the calculation below:

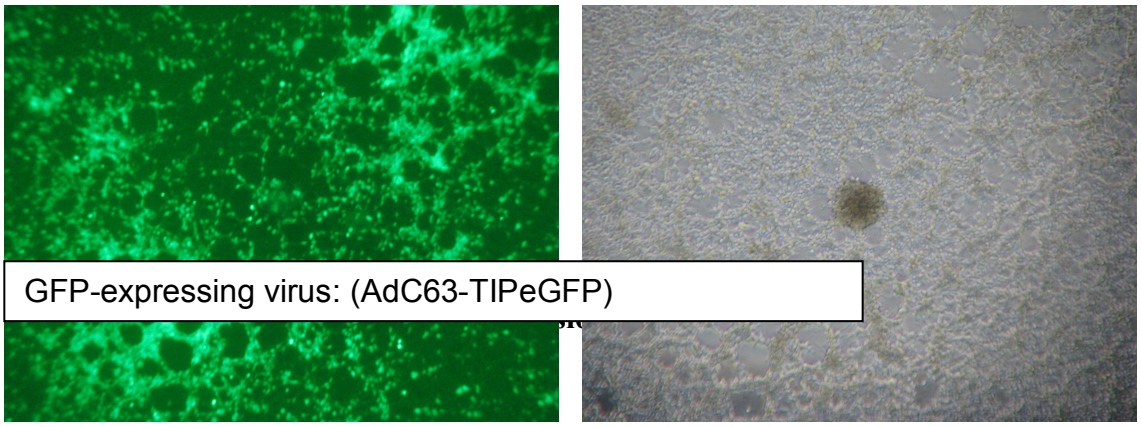
Surface area of 6 well plate	9.5 cm^2
Surface area of T150	150 cm2

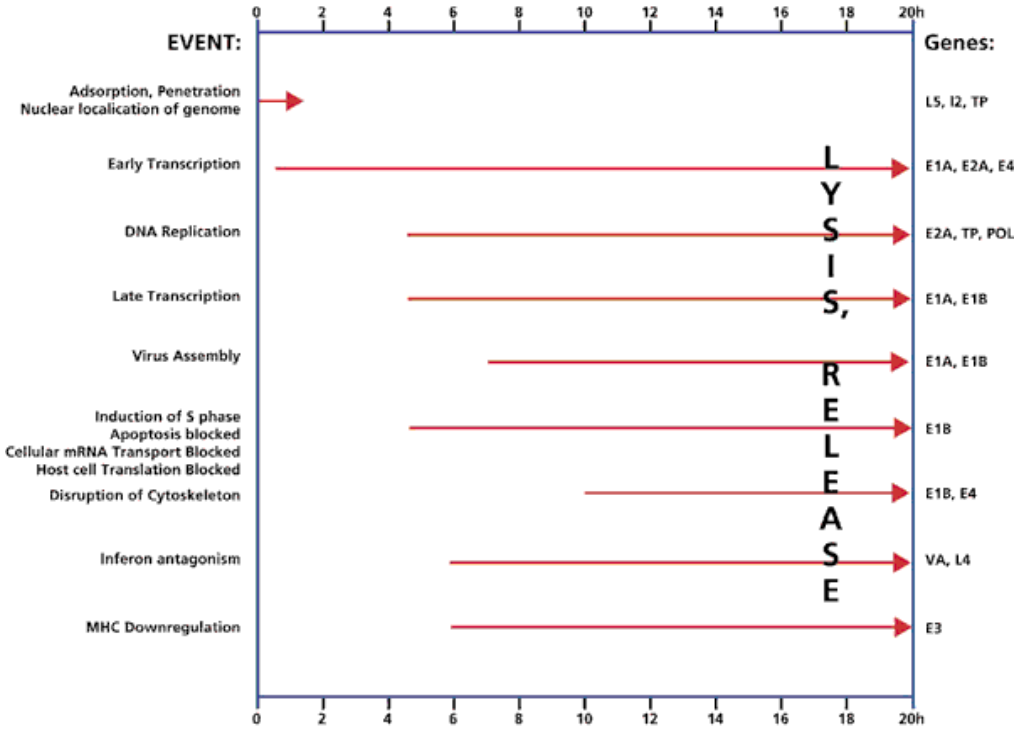
Ratio:~16

Therefore, multiply the volume used to obtain optimal CPE by 16 to calculate the volume required for inoculation of a T150 flask or multiply by 160 to inoculate a hyperflask.

Well #	Amount of virus in well (µL)	Amount of virus to add to a T150 (µL)	Amount of virus to add to a HF (µL)
1	15	240	2400
2	7.5	120	1200
3	3.75	60	600
4	1.88	30	300
5	0.94	15	150
6	0.47	8	75

Fig. 1: Example of CPE





10.0 Revision History

Version Number	What Changed	Who Changed it	Date changed
1	First written	Ali Turner	13.04.12
2	Changed to 6wp titration rather than T150	Ali Turner	26.06.12
3	Changed to use a dilution over a more suitable range	RH	12.11.12
4	Addition of a spin step to pellet cell debris before dilution.	JM	13.06.13
5	Preparation of serial dilution altered to be in 2 ml screw-capped tubes	Ali Turner	17.09.13

Appendix IV



1.0 Jenner Laboratory Protocol Number J004e

2.0 Version Number 4

3.0 Preparation of Master Seed Virus (MSV) of adenovirus

This protocol uses GMO. All users MUST be registered with the University Occupational Health Service as set out in the University's health and safety regulations. Health surveillance is a legal requirement under COSHH.

If you are not currently registered with the Occupational Health Service for work with GMO, or need to check your registration, please contact the ORCRB NDM Personnel team.

4.0 Other documents

MSDS	refer to MSDS for the relevant safety information on the individual reagents: \\Imsnw3_jenner_server\jenner\hill_group\Safety\COSHH assessments\Manufacturers material safety data sheets
R002	Adenovirus
R004	GMO RA appendix
J008	Infecting 293 cells with adenovirus
J011	Passaging 293 cells
J199	Passaging TREx cells
J252	General working practice in the Virus Room
J004f	Cell lysis and benzonase treatment of cell and adenovirus suspension
J004d	Test infection of adenoviral premaster seed stock material

5.0 Definitions

DMEM	Dulbecco's Modified Eagle's Media
FBS	Foetal Bovine Serum
RNAse	Ribonuclease
DNAse	Deoxyribonuclease
BSA	Bovine serum albumin
CPE	Cytopathic effects
IMS	Industrial methylated spirit

IU Infectious units

6.0 Objective

To infect a large batch of 293 cells with premaster cell lysate of a virus that has previously been used in a test infection. This should provide sufficient virus for a standard prep: 5 x 10^{10} to 5 x 10^{11} IU total.
Handling Hyperflasks of cells requires training by an experienced user to prevent the cells being dislodged during media replacement.

General working practice:

- Do not have more than one virus in the hood at any one time.
- The aliquoted reagents (lysis buffer, CsCl, Storage buffer etc) are for use by everyone. Please note: they are single use - **DO NOT** place opened reagents back on the shelves
- Wipe the hood and equipment thoroughly with TriGene and then 70% IMS before use and between handling different viruses (to clean the hood, wet some blue roll thoroughly with the cleaning agent and wipe the hood surface, do not spray the hood directly as this is corroding the painted surfaces).
- Change gloves between viruses (this ensures any trace amounts of virus are completely removed).
- Where possible, do not use micropipettes when working with cell culture material. It is difficult to ensure the micropipettes are sterile due to the complexity of their construction. Transfer material to an interim container and then take a small sample. In this protocol we do need to use them but just be aware of the potential problems associated with their use.
- Ensure items placed in the dispo-jar are covered by the TriGene solution.
- When finished, empty the dispo-jar and re-fill with fresh, diluted TriGene solution. Wipe down the hood with TriGene solution and 70% IMS. Switch off and close the hood. Re-stock any equipment as required.
- Do not put liquid waste into the autoclave bins – pour it into a container, treat with TriGene if necessary and then dispose of down the sink.

Note:

9) It is important that the 293 cells are maintained in the log phase of growth so that the E1 protein expression rates are maximal. The adenovirus requires these proteins for growth. If the cells have reached confluency, then protein expression drops and the virus cannot replicate. The cells must not reach greater than 80% confluency during culture and especially must not exceed this level prior to being sub-cultured ready for virus infection.

10) HEK293 cells are very loosely adherent – take care when pipetting into flasks and ensure that media is added away from the cell layer.

11) When using T-REx-293 cells, blasticidin **MUST** be present in the media at all stages to retain the repression of antigen expression. This includes post-transfection culture where the media does not contain Pen/Strep.

12) HEK293A cells and T-REx-293 cells are immortalised lines of primary human embryonic kidney cells transformed by sheared human Ad5 DNA. The cells harbor the E1A and E1B region of the adenoviral genome, that complement, in trans, the deletion of the E1 region in the recombinant adenovirus. The cells constitutively express the adenoviral E1 proteins (E1A and E1B) while they are dividing. When they reach confluency, total protein expression, including E1, is reduced. During their natural lifecycle, adenoviruses express the E1 proteins at all stages (see Fig. 3) and the proteins are therefore extremely important for successful virus rescue. It is therefore important that cells do not reach confluency during routine passage and also that seeding densities in preparation for transfection are suitably low.

7.0 Reagents

DMEM (high glucose, with pyruvate)
Sigma D6546
200 mM Glutamine
Sigma G7513
100x Penicillin/Streptomycin solution
(10,000 Units penicillin-G and 10mg strep per ml)
Sigma P0781
Foetal Bovine Serum
Sigma F2442
10 mg/ml Blasticidin S-HCl
Melford Labs B1105
18.2 MΩ/cm ultrapure water
Elga
1 M Tris-HCl pH 7.8
Sigma T2569
1 M $MgCl_2$
(Sigma) Fluka 63069

Complete 10% FCS DMEM ± Blasticidin

50 ml FCS	(~10% final conc)
5 ml Pen/strep	(100 U Penicillin, ~0.1 mg strep ml^{-1} final conc)
10 ml L-glutamine	(~4 mM final conc)
250 µl Blasticidin	**(~5ug/ml final conc)**

Lysis buffer (10 mM Tris, 1 mM $MgCl_2$. pH 7.8)
5 ml 1 M Tris-HCl pH 7.8
0.5 ml 1 M $MgCl_2$
Make up to 500 ml with 18.2 MΩ water to 500 ml using a measuring cylinder
Filter sterilise.

8.0 Equipment

50 ml Falcon Tubes

Class II BioSafety Cabinet	Scanlaf Ltd
Microscope DMIL	Leica
37°C water bath	
Benchtop centrifuge	
Sterile, serological pipettes	
Micropipettes and Sterile filter tips	Rainin
Pipette aid	
6 well plate	
Hyperflask M	Appleton Woods
BC390	

9.0 Method

8.51 Prepare a hyperflask of cells the Friday before such that the cells are 70 – 80% confluent at the time of infection.

CELLS ARE SEEDED TO REACH 70-80% CONFLUENCY APPROX 72 hr AFTER SEEDING.
CHECK CELL CONFLUENCY BEFORE INFECTION: ONLY PROCEED IF CELLS ARE 70-80% CONFLUENT.
IF CONFLUENCY IS SLIGHTLY LOWER FIRST THING IN THE MORNING, LEAVE FLASKS UNTIL THE AFTERNOON. DO NOT LEAVE UNTIL THE

8.52 Pre-warm a 500 ml bottle of complete D10 media to 37°C. If necessary, add the required amount of premaster seed stock lysate (as calculated from the test infection) to a 50 mL Falcon tube.

8.53 Using a serological pipette, remove ~15mL of media from the bottle and discard.

8.54 Using a serological pipette, remove ~30mL of media from the bottle and add to the Falcon tube containing the required amount of premaster.

8.55 Mix by gently inverting 10 times. Avoid generating bubbles.

8.56 Add the contents of the Falcon tube to the bottle of media using a serological pipette.

8.57 Mix by gently inverting 10 times.

8.58 Carefully pour the media from the hyperflask into a dispojar.

8.59 Refill the flasks with media containing the premaster cell lysate. This should be done by tilting the flask to about 60° and then angling the bottle of media so that the media is poured into the air dam within the neck. This minimizes the formation of bubbles as well as the washing off of cells.

8.60 Place cells at 37°C, 5% CO_2.

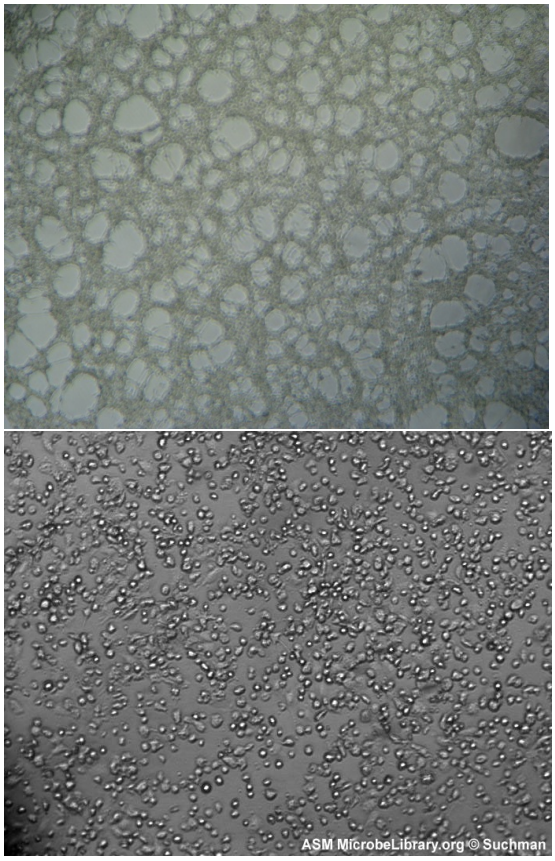
8.61 Monitor for appearance of CPE over 24-72 hours.

DO NOT HARVEST HYPERFLASKS EARLIER THAN 48 hr. IF EXTENSIVE CPE HAS DEVELOPED PRIOR TO THIS, EITHER CULTURE CELLS UNTIL 48 hr AND RE-CHECK HF OR DISCARD HF AND REPEAT INFECTION USING A SMALLER INOCULUM.
We have tried harvesting at 24hr several times when CPE has looked well developed but yield was too low when banded

8.62 Harvest the infected cells when they show optimal CPE (see note above).

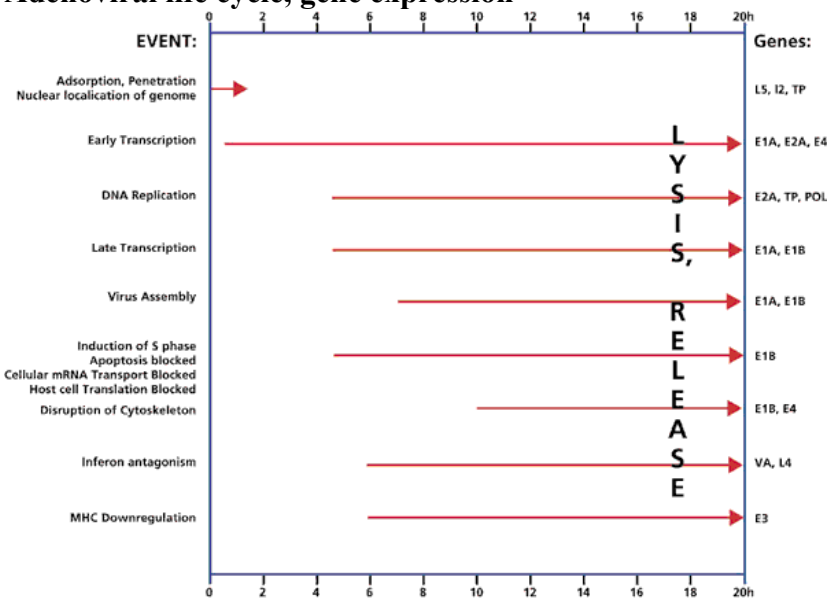
a. Dislodge the cells by tapping the side of the hyperflask
b. Carefully pour the media and cells into two 250 ml PP centrifuge bottles. Clean carefully around the necks of the HF with 70% ethanol to minimize risk of contamination while pouring. Fill 250 ml PP centrifuge bottles to the mark on the shoulder of the bottle – do not try to transfer all of the media at this stage.
c. Pellet cells (1500 x g, 5 min, 4°C) in the benchtop centrifuge
d. Aspirate supernatant to waste.
e. Refill the hyperflask with 500 mL PBS (with Ca and Mg) and tap the side of the flask to dislodge any remaining cells.
f. Pour the PBS into the centrifuge bottles containing the cell pellet. Fill 250 ml PP centrifuge bottles to the mark on the shoulder of the bottle – do not try to transfer all of the media/PBS. Discard remaining media/PBS in the HF.
g. Centrifuge (1500 x g, 5 min, 4°C).
h. Aspirate supernatant to waste.
i. Resuspend cells in 15 mL lysis buffer.
j. Transfer material to a 50 ml centrifuge tube.
k. Proceed with protocol J004f (material can be stored at -20°C at this stage).

Fig. 1: Examples of CPE.



AdC63 and ChAdOX **AdHu5**

Adenoviral life cycle, gene expression



Cell confluency

For optimum virus growth, the cells must be actively dividing. Cells seeded on Friday for use 72 hr later are fine for virus production. The problem with seeding cells any lower is that as they divide they form “islands” of cells where the central regions have been 100% confluent (will start to pile up on top of each other) and will have slowed down in growth. These cells are then non-

optimal for virus propagation and therefore you will have lost some of the capacity for production.

10.0 Revision History

Version Number	What Changed	Who Changed it	Date changed
1	First written	Ali Turner	13.04.12
2	Notes added about cell confluency levels and time of HF harvest	Ali	21.09.12
3	Inclusion of initial dilution of premaster and wash of HF with PBS	Rachel Hossack	06.11.12
4	Pictures updated. Decanting media technique further elaborated.	Rachel Hossack	05.05.13

Appendix V

1.0 Jenner Laboratory Protocol Number J004f

2.0 Version Number 4

3.0 Cell lysis and benzonase treatment of cell/adenovirus suspension

This protocol uses GMO. All users MUST be registered with the University Occupational Health Service as set out in the University's health and safety regulations. Health surveillance is a legal requirement under COSHH.

If you are not currently registered with the Occupational Health Service for work with GMO, or need to check your registration, please contact the ORCRB NDM Personnel team.

4.0 Other documents

MSDS	refer to MSDS for the relevant safety information on the individual reagents: \\lmsnw3_jenner_server\jenner\hill_group\Safety\COSHH assessments\Manufacturers material safety data sheets
R002	Adenovirus
R004	GMO RA appendix
J004 Appendix	Benzonse manufacturer's product sheet
J252	General working practice in the Virus Room

5.0 Definitions

DNA Deoxyribonucleic acid

6.0 Objective

Adenoviral production in 293 cell lines involves the harvest of the cells and the virus particles they contain. Current methods mean that we do not harvest the virus that has been released into the tissue culture supernatant.
The virus particles are released from the cells by physical fracture (freeze/thaw) and then separation from cell debris. Purification occurs in two stages: low speed (1500 x g) centrifugation to pellet cell debris followed by ultracentrifugation and banding of the virus using two different methods of CsCl gradient.

Cell lysis results in the release of proteases from the cells which are able to degrade proteins. Importantly this includes the adenoviral capsid proteins that are required for infectivity. To minimize protease activity, once the cells are lysed ensure that the sample is kept chilled and keep incubations at 37°C as short as possible: when thawing the sample, mix at regular intervals to ensure this happens as quickly as possible.

In this protocol, benzonase is used for two functions:
To reduce sample viscosity due to the release of DNA during cell lysis and to reduce clumping of adenovirus due to DNA binding: nucleic acids can adhere to cells and viral particles causing aggregation and alteration in particle size/charge. Removal of contaminating nucleic acids will prevent this interference.

To reduce the concentration of nucleic acids as required for recombinant biologicals for therapeutic use. During purification performed at the Jenner Institute, the contaminating nucleic acids are firstly hydrolysed and then removed from the virus suspension by further downstream purification.

Benzonase is an endonuclease that works to reduce all contaminating, free nucleic acids to oligonucleotides of between 3 to 5 bases in length.

Note concerning incubation time for benzonase treatment of harvested, infected HEK293/HEK293 TREx cells:

The optimum incubation temperature for benzonase is 37°C. However, as a compromise between virus stability and enzyme activity, the incubation is performed at RT.

General working practice:

- Do not have more than one virus in the hood at any one time.
- Do not use VVCF cell culture media.
- The aliquoted reagents (lysis buffer, CsCl, Storage buffer etc) are for use by everyone. Please note: they are single use - **DO NOT** place opened reagents back on the shelves
- Wipe the hood and equipment thoroughly with TriGene and then 70% IMS before use and between handling different viruses (to clean the hood, wet some blue roll thoroughly with the cleaning agent and wipe the hood surface, do not spray the hood directly as this is corroding the painted surfaces).
- Change gloves between viruses (this ensures any trace amounts of virus are completely removed).
- Where possible, do not use micropipettes when working with cell culture material. It is difficult to ensure the micropipettes are sterile due to the complexity of their construction. Transfer material to an interim container and then take a small sample. In this protocol we do need to use them but just be aware of the potential problems associated with their use.

- Ensure items placed in the dispo-jar are covered by the TriGene solution.
- When finished, empty the dispo-jar and re-fill with fresh, diluted TriGene solution. Wipe down the hood with TriGene solution and 70% IMS. Switch off and close the hood. Re-stock any equipment as required.
- Do not put liquid waste into the autoclave bins – pour it into a container, treat with TriGene if necessary and then dispose of down the sink.

7.0 Reagents

18.2 MΩ/cm ultrapure water Elga
1 M Tris-HCl pH 7.8 Sigma T2569
1 M $MgCl_2$ Sigma) Fluka 63069
25U/µl BENZONASE, PURITY > 99% 100KUN Merck 70664-100KUN

Lysis buffer (10 mM Tris, 1 mM $MgCl_2$. pH 7.8)

5 ml 1 M Tris-HCl pH 7.8
0.5 ml 1 M $MgCl_2$
Make up to 500 ml with 18.2 MΩ water to 500 ml using a measuring cylinder
Filter sterilise.

8.0 Equipment

50 ml Falcon Tubes
Class II BioSafety Cabinet Scanlaf

37°C water bath
Dry ice
Benchtop centrifuge
Sterile, serological pipettes
Micropipettes and Sterile filter tips Rainin
Pipette aid
Rotary mixer

9.0 Method

8.63 For each hyperflask or 5 x T150 preparation of virus: resuspend the cell pellets in a total volume of 15 mL lysis buffer.
8.64 Freeze by placing on in an IMS/dry ice bath.

The protocol may be stopped at any point after a freezing step by storing the resuspended cell pellet at

-20°C.

8.65 Thaw the pellet (30°C water bath). Repeat the freeze thaw (IMS/dry ice bath and 30°C water bath) a further two times.

Whilst thawing leave at 30°C for the shortest time possible, mix during incubation.

After the final thaw, add **500 U of Benzonase per 1 ml of cell lysate (i.e. 20 µl / 1 ml).**

8.66 Mix thoroughly by gently inverting tube 10 times.

8.67 Place tube in rotary mixer

8.68 Incubate for 1 hour at RT.

8.69 Centrifuge at 1500 x g for 5 minutes at 4°C.

8.70 Use immediately.

10.0 Revision History

Version Number	What Changed	Who Changed it	Date changed
1	First written	Ali Turner	13.04.12
2	Change of benzonase concentration due to reagent swapping for cheaper bulk reagent. Also use of mixer	Ali Turner	23.06.12
3	Change to lysis procedure – 3 x F/T before benzonase treatment	Rachel Hossack	06.11.12
4	Benzonase quantity doubled	Ali Turner	

Appendix VI



1.0 Jenner Laboratory Protocol Number: J005

2.0 Version Number 13

3.0 Title: Adenovirus purification using discontinuous and isopycnic CsCl gradients

This protocol uses GMO. All users MUST be registered with the University Occupational Health Service as set out in the University's health and safety regulations. Health surveillance is a legal requirement under COSHH.

If you are not currently registered with the Occupational Health Service for work with GMO, or need to check your registration, please contact the ORCRB NDM Personnel team.

4.0 Other documents

MSDS reagents: refer to MSDS for the relevant safety information on the individual

\\Imsnw3_jenner_server\jenner\hill_group\Safety\COSHH assessments\Manufacturers material safety data sheets

R002 Adenovirus
R004 GMO RA appendix

J008 Infecting 293 cells with adenovirus
J011 Passaging 293 cells
J104 Adenovirus Titre Immunoassay
J005 App I Annotated images of CsCl centrifugation steps for troubleshooting.

5.0 Definitions

Ad Adenovirus
CsCl Caesium chloride

CPE Cytopathic effect
PBS Phosphate buffered saline
HF Hyperflasks

6.0 Objective

The purification of recombinant adenovirus by two different methods of density centrifugation using Caesium chloride solutions as solvents. The first step involves a form of rate zonal centrifugation whereby the component particles are separated in a manner based upon mass (larger particles will sediment faster). The second centrifugation step is isopycnic centrifugation whereby the particles are separated according to density.
This method describes purification of recombinant adenovirus from a single hyperflask – scale up or down as necessary.
Note concerning incubation time for benzonase treatment of harvested, infected 293 cells:

The optimum incubation temperature for benzonase is 37°C. However, as a compromise between virus stability and enzyme activity, the incubation is performed at RT.

Note about CsCl solutions

In January 2011 we had an issue with bands not forming on two separate viruses, one on first banding and one on second banding (lab book VC27 5th Jan 2001; Production records VC261 And VC296). The virus that failed the first banding – one tube was correct and the other had a diffuse band where the empty and complete capsids should have banded. Both tubes were pooled and the viruses banded perfectly during the overnight centrifugation. The second virus banded perfectly during the 2 hr spin but was diffuse after the overnight centrifugation. To solve this issue, 1) the centrifuge was cleaned thoroughly and all of the o-rings and gaskets were greased. 2) Nicky suggested that she has previously seen CsCl settling out during prolonged storage and as a consequence loaded CsCl of incorrect density.
The virus that didn't band on the overnight centrifugation step was re-banded o/n with thoroughly mixed CsCl and worked perfectly.
Therefore – ensure all CsCl solutions are thoroughly mixed both prior to aliquoting and prior to adding to centrifugation tubes.

General virus handling:

- Ensure only one virus is handled at any one time in the hood.
- Wipe hood thoroughly with Trigene solution between viruses and change gloves.
- Soak forceps in 10% Trigene solution for 10 mins after use with each virus as these come into very close contact with the virus preparations. Use a fresh pair of forceps if more than one virus is being purified simultaneously. Ensure that the virus is not exposed to Trigene.

This protocol should not be performed without prior training as some of the procedures are complex and demonstration of the techniques is required.

7.0 Reagents

Hyperflasks containing adenovirus-infected HEK293A or TREx293 cells.
Cells should be showing a cytopathic effect CPE (round grapelike clusters), but the majority should still be attached to the flask.
18.2 MΩ water
1M Trizma-HCl pH7.8
Sigma T-2569-100ml
Caesium Chloride Sigma
203025
PBS containing Ca & Mg PAA
H15-001
1M $MgCl_2$ Sigma
63069-100ML
Sucrose* Fluka
84097
*it is important that this material is low in endotoxins, do not substitute this supplier

Solution preparation:

Pre-rinse Duran bottles with 18 MΩ-water. Add solids to a Duran bottle and add some 18.2 MΩ-water, then add liquids. Add a clean magnetic stir bar and place on a stir plate until solids have dissolved. Transfer to a volumetric flask and top up with water.
Filter sterilise the solution into 500 ml sterile tissue culture bottles.

For each new solution record lot number of Trizma base and Sucrose used.

1.25 g/ml density CsCl (density = 1.25 g/mL = 1.98 M) in 10 mM Tris pH 7.8.

166.89 g CsCl
5 ml 1 M Tris pH 7.8
Add 18.2 MΩ water to 500 ml using volumetric flask
Filter sterilise.

1.35 g/ml density CsCl (density = 1.35 g/mL = 2.78 M) in 10 mM Tris pH 7.8.

233.65 g CsCl
5 ml 1 M Tris pH 7.8
18.2 MΩ water to 500 ml using volumetric flask.

Filter sterilise.

Lysis buffer (10 mM Tris, 1 mM $MgCl_2$. pH 7.8)

5 ml 1 M Tris-HCl pH 7.8
0.5 ml 1 M $MgCl_2$
Make up to 500 ml with 18.2 MΩ water to 500 ml using a measuring cylinder
Filter sterilise.

Storage buffer (10 mM Tris, 7.5% w/v sucrose. pH 7.8)

Weigh 75 g sucrose and transfer to a 1 litre measuring cylinder.
Add 18.2 MΩ water up to ~800 ml.
Add 10 ml 1 M Tris-HCl pH 7.8
Seal top of measuring cylinder with parafilm and invert cylinder repeatedly until sucrose has full dissolved.
Adjust volume to 1000 ml.
Filter sterilise and store either at 4°C in the virus lab or on the shelf in mol biol.

8.0 Equipment

Class II BioSafety Cabinet Scanlaf Mars
Benchtop Centrifuge Beckman Coulter Allegra X-12R
CO_2 incubator RS Biotech Galaxy R
37°C water bath Grant SUB6
Microscope Leica DMIL
IMS Fisher M/4400/17
Corning conical tubes, 250 ml PP Centrifuge tube, plug seal cap Fisher CFT-900-021Y
Bottle-top filters Fisher TKV-238-050Y
Volumetric flasks
500 ml and 1 l sterile Duran bottles
5 ml syringes Fisher SZR-150-170T19G
Needles nu-care products M1500
Ultraclear centrifuge tubes 14.0 ml Beckman Coulter 344060
Dialysis cassettes 3-12 ml & 0.5-3ml Thermo-Fisher 66453 & 66455
Slide-A-Lyzer Buoys for 3-12 ml and 0.5-3 ml dialysis cassettes 66432 & 66430
250 ml polypropylene bottles

Dry ice in suitable container
Beckman ultracentrifuge Beckman
Coulter Optima L-80 XP
SW40Ti rotor & buckets Beckman
Coulter
Balance
Forceps
Tube holder

9.0 Method

Check that the ultracentrifuge buckets are clean, place buckets in the biological safety cabinet and spray with 70% IMS to sterilise. Wipe off excess IMS with blue roll and allow the remaining liquid to evaporate whilst the samples are prepared.

If preparing two viruses at the same time ensure that they are kept completely separate and that tubes containing different viruses are NEVER open at the same time in the hood. Wipe down all surfaces carefully between handling different viruses and change gloves.

9.1 Mix aliquots of CsCl thoroughly before use.

9.2 Set up the relevant number (3 tubes per hyperflask) of Caesium Chloride gradients in 14 ml Beckman Ultraclear tubes.

9.2.1 Add 3.5 ml 1.25 g/ml CsCl solution to the tubes using a pipette.

9.2.2 Take up 10 ml of 1.35 g/ml CsCl solution into a 10 ml pipette and use this to underlay the 1.25 g/ml CsCl solution with 3.5 ml 1.35 g/ml CsCl solution. Pipette very slowly and only add 3.5ml

Ensure that the interface between the two solutions is visible.

This is absolutely crucial to this centrifugation method as the interface remains intact during centrifugation and is the limit to which the adenovirus migrates.

9.3 Add the cell lysate supernatant evenly to each tube containing CsCl gradients. Take care not to disturb the interface whilst adding the sample. This can be avoided by adding the sample slowly down the side of the tube. Top up the tubes if required with lysis buffer. It is important to fill the tubes to within 2mm of the top to prevent tube failure.

9.4 Place centrifuge tubes in the buckets for the SW40 Ti rotor and balance them to within 0.1g of each other.

9.5 Centrifuge for 2 hours at **110 000 x g** @ 4˚C. (This is shown as 109388 x g when entered into the display).

NOTE: use all 6 buckets correctly sealed and mounted in the rotor

9.6 Once the centrifuge run is complete, remove rotor from the ultracentrifuge, transfer the buckets to the holder and move to the biological safety cabinet.

9.7 Unscrew the bucket lids and remove the tubes using forceps.

9.8 Place the tube in a clamp stand above an empty beaker (this should be treated with a biocide after use).

9.9 Two virus bands should be visible close to the centre of the tube; the upper band is incomplete virus and the lower band intact virus (see Fig. 1).

9.10 Decide how many tubes are required for the second centrifugation step:

This is based on experience. The major concern is that placing too much virus in each tube will lead to aggregation of the virus particles.

9.11 Set up the second caesium gradients in 14 ml Beckman ultraclear tubes:
Mix aliquots of CsCl thoroughly before use.

Using 10 ml serological pipettes, add 6 ml of 1.35 g/ml CsCl to each tube

9.12 Using a 19G needle and 5 ml syringe pierce the tube from the first centrifugation step approximately 5 mm below the band by gently twisting and pushing the needle through the wall of the tube. *Be careful not to hold your other hand on the other side of the tube whilst doing this for risk of injury.*

9.13 Once the needle is inside the tube gently pull on the syringe with the bevel pointing upwards to extract the lower band.

9.14 Discard the used centrifuge tube into the beaker.

9.15 Repeat for all tubes. The same needle and syringe can be used, however care should be taken not to apply pressure to the plunger of the syringe whilst piercing the tube.

9.16 Divide the virus supernatant between the tubes set up for the second centrifugation step. Top up the tubes if required with lysis buffer. It is important to fill the tubes to within 2 mm of the top to prevent tube failure.

9.17 Place the tubes in the buckets for the SW40 Ti rotor. Balance the tubes to within 0.1g of each other with lysis buffer and centrifuge at **160000 x g for 18-19 hr** (i.e. overnight). (This is shown as 159005 x g when entered into the display).

9.18 Once the centrifuge run has finished, remove rotor from the centrifuge, transfer the buckets to the holder and move to the biological safety cabinet.

9.19 Remove the centrifuge tube using forceps and place in the retort clamp. Two bands may be visible. However, the upper band may not

be present if the virus added onto the 2nd gradient was very pure. Remove the lower band using a 19G needle and 5 ml syringe. This can be placed safely to one side to be directly loaded into the dialysis cassette.

At this stage, mark a dialysis cassette with the name of the virus and pre-wet with pre-chilled storage buffer.

9.20 Discard the used centrifuge tubes into the beaker of Trigene.
9.21 Add the purified virus band to a dialysis cassette using a needle and syringe:
- 9.21.1 Transfer the wetted dialysis cassette to the hood.
- 9.21.2 Insert cassette into the buoy to function as a holder.
- 9.21.3 Place a needle on a 5 ml syringe and insert the needle so that just the bevel of the needle in inside the cassette. Insert a small amount of air to the cassette so that it is slightly inflated which makes it easier to add the virus without piercing the membrane.
- 9.21.4 Add virus solution
- 9.21.5 Tilt cassette and remove air such that the cassette is full with no air bubble.

9.22 Place the cassette back into the beaker of 500 ml of cold storage buffer, cover with foil and place on a magnetic stir plate. Dialyse for 90 minutes changing the buffer every 30 mins.
9.23 Remove virus from dialysis cassette, tilting the cassette ensure all of the solution is removed, and aliquot.

Ensure there are at least 10 x 10 μl aliquots for QC
Label virus clearly with stock number. Store at -80°C.
Enter in the File Maker Pro Virus database the details and location of the new virus.

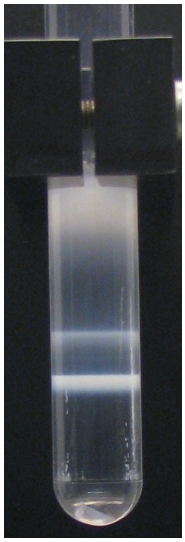


Fig. 1. Discontinuous gradient centrifugation of adenovirus preparation.

Viral banding pattern typically formed following 2 hr centrifugation step. Lower band is correctly formed adenovirus. Upper band contains viral capsids lacking DNA

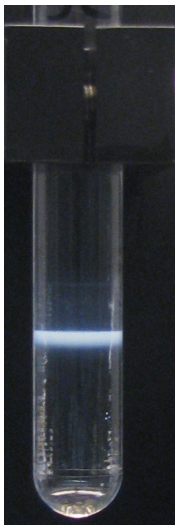


Fig. 2. Isopycnic centrifugation of adenovirus preparation.

Viral banding pattern typically formed following 16 hr centrifugation step.

Band contains correctly formed adenovirus.

10.0 Revision History

Version Number	What Changed	Who Changed it	Date changed
2	Amount of Benzonase added	Nicky Green	
2	2nd gradient preparation, dilution of band from first gradient and only using heavy CsCl	Nicky Green	
3	Amount of Benzonase added	Nicky Green	
3	Dialysis step added between bandings 2 x 2 step gradients	Nicky Green	
4	Buffer recipes to include ready-made stocks of Tris buffer and $MgCl_2$. Removal of dialysis step between bandings. Second, optimised, isopycnic centrifugation procedure added instead of step gradient.	Ali turner	
5	Modified for new ultracentrifuge	Nicky Green	
6	Slight modifications to format. Addition of note about preparing two viruses at the same time.	Ali Turner	
7	Changed to single HF	Ali	
8	Centrifugation speeds corrected – RCF is entered as RCF (max) from rotor tables	Ali	
9	Note about CsCl settling and relevant change to protocol	Ali	07.01.11
10	Method clarification and images added	Ali	07.03.11
11	OH statement added	S. Morri	7.04.11
12	Removal of part of methods already covered in protocol J004. Replace	R.Hossack	06.11.12

	Microsol with Trigene.		
13	**Underlaying of gradients clarified. Pictures replaced. Displayed speed added.**	**R. Hossack**	**30.05.13**
14	**Change in centrifuge spin time at step 9.17**	**Louisa Rose**	**20.08.13**

The effect of osmolality on biological particles requires special consideration. The osmolality of most mammalian fluids is 290-300 mOsm.4 This is the osmolality of balanced salt solutions (e.g., 0.85-0.9% NaCl) and most common media. High osmolality solutions not only remove water from the interior of membrane bound particles, they also remove water bound to macromolecules like DNA. Loss of water from cells will reduce their size and increase their density, thereby affecting their buoyancy and r te of sedimentation. The osmotic effect on cells and macromolecules may be reversible, though it is a possible source of error that should be avoided. Over the years, a variety of different compounds have been developed as density gradient media in order to enhance the separation process and to overcome osmolality and viscosity problems. There are five main classes of density gradient medium:

- Polyhydric (sugar) alcohols
- Polysaccharides
- Inorganic salts
- Iodinated compounds
- Colloidal silica

Ionic gradient media, comprised of concentrated heavy metal salts, are almost exclusively used for isopycnic separations of nucleic acids. Cesium chloride and cesium sulfate are the most widely used heavy metal salts with gradient densities of up to 1.91 g/cm3. Other useful salts include sodium iodide, sodium bromide and the rubidium salts. The steepness and shape of the ionic density gradient formed depends on the centrifugal force and type of rotor respectively. Ionic gradient media are highly ionic and non-viscous with high osmolarities. It should be kept in mind that the density of the sample is highly dependent on the sample's hydration, which in turn depends on the dehydration power of the ionic gradient media

Note: When considering biological particles, it is important to remember that the osmolality of the medium can significantly alter the size and apparent buoyant density of membrane-bound particles. A high external osmolality will cause membranebound particles to shrink while a low osmolality in the medium will cause the particles to swell.
Fig. 2 shows that particles centrifuged in gradients of Percoll under physiological conditions (280 to 320 mOsm/kg H_2O) have much lower apparent buoyant densities than in sucrose or metrizamide (see also Table 1, page 18).

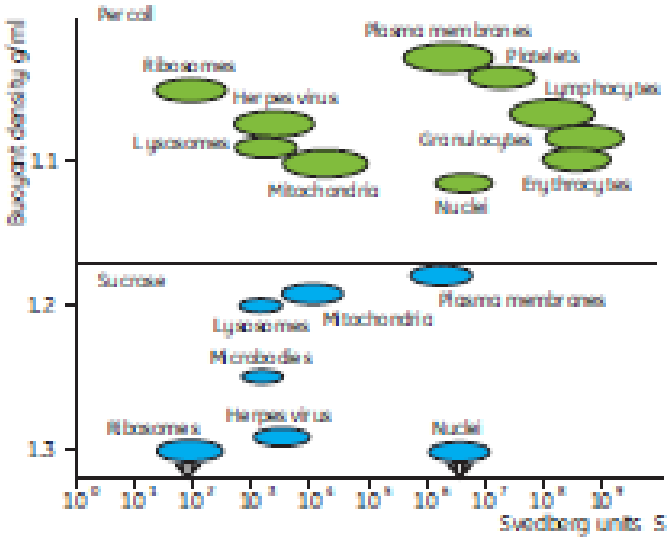
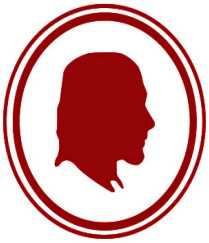


Fig 2. Approximate sedimentation rates and isopycnic banding densities of particles in a rat liver homogenate, herpes virus and human blood cells in gradients of Percoll (green) compared with sucrose gradients (blue). Svedberg units = sedimentation coefficient, $1S = 10^{-13}$ s. (27, reproduced by kind permission of the authors and publisher).

Appendix VII



1.0 Jenner Laboratory Protocol Number J104

2.0 Version Number 12

3.0 Adenovirus Titre Immunoassay

This protocol uses GMOs. All users MUST be registered with the University Occupational Health Service as set out in the University's health and safety regulations. Health surveillance is a legal requirement under COSHH.

If you are not currently registered with the Occupational Health Service for work with GMO or need to check your registration, please contact the ORCRB NDM Personnel team.

4.0 Notes:

This assay is very susceptible to cell loss from the monolayers during the immunostaining protocol. It also appears to be sensitive to edge effect both during cell culture and staining. Specifically:
HEK293 cells are only loosely adherent. We use coated plates to try and overcome this but the monolayers are still relatively fragile.

Take care with pipetting throughout the protocol (cell culture and staining)

When flicking the plates during staining, flick once only.

Edge effect during cell culture

- Evaporation from the edge wells and particularly the corner wells can negatively affect cell health in these wells (see note in appendix)
- If the volume is too low, the meniscus that forms can both concentrate un-adhered calls to the edges and leave those cells in the centre of the wells with insufficient media covering them.
- Use the Nunc square boxes with damp blotting paper to provide a constant high humidity atmosphere.

Edge effect during staining.

- When plates are transferred between different temperatures the edges will alter temperature much more rapidly than the centre wells. It is

important to allow the entire plate to reach the same temperature at each step.

- Avoid stacking plates as those in the centre will be at very different temperatures to the outer plates.
- Ensure incubation times are long enough to bring the plate to uniform temperature.

5.0 Other documents

MSDS refer to MSDS for the relevant safety information on the individual reagents:

\\Imsnw3_jenner_server\jenner\hill_group\Safety\COSHH assessments\Manufacturers material safety data sheets

R002 adenovirus

\\Imsnw3_jenner_server\jenner\hill_group\Safety\GMO RA\R002 adenovirus.doc

R004 GMO RA appendix

C030 Culture of primary cells and cell lines including freezing and reviving
C024 Use of penicillin for tissue culture by sensitised individuals
C066 Use of antibiotics for selection of cells

NOTE: DAB IS CONSIDERED A POSSIBLE CARCINOGEN – see MSDS.

Waste should be washed down the sink with copious amounts of water.

Safety glasses must be worn when washing 96-well plates during the staining process. There is a risk that eye splashes may occur when flicking the fluid from the plates into the sink.

J011 Passaging 293 cells

6.0 Definitions

FCS	Foetal calf serum
MVA	Modified vaccinia Ankara
DMEM	Dulbecco's modified Eagle's media

7.0 Objective

To calculate the infectious viral titre by visualizing Immunostained infectious cells.

8.0 Reagents

DMEM D6546	Sigma
Pen/Strep	Sigma
Glutamine	Sigma

FCS F2442	Sigma
Trypan blue stain T8154	Sigma
TrypLE Express I2605	Invitrogen
Sterile water W3500	Sigma
Methanol 32213	Sigma
PBS (without Ca^{2+} and Mg^{2+}) D8537	Sigma
D-PBS (Dulbecco's Phosphate-Buffered Saline (D-PBS), Powder (for 10 litres) 21600-069	Invitrogen
BSA (≥98% (agarose gel electrophoresis), lyophilised powder) A7906	Sigma
1000x Primary anti-Hexon Antibody 10901	Cambridge Bioscience
1x Secondary Antibody HRP conjugated. 10902	Cambridge Bioscience
ImmPACT DAB SK-4105	Vector Labs
Poly-L-Lysine hydro-bromide P1399-25mg	Sigma
Pre-Sept tablets	

9.0 Equipment

Class II BioSafety Cabinet Mars	Scanlaf
CO_2 incubator Galaxy R	RS Biotech
37°C water bath SUB6	Grant
Microscope DMIL	Leica
Disposable haemocytometer	
96-well flat-bottomed tissue culture plate	
Repeater pipette	
Aspirator	
Sterile 1.5 ml microcentrifuge tubes	
Vortex	
Squeezy bottle containing D-PBS	
p200 8 well multichannel pipette	
p300 8 well multichannel pipette	

NOTE: the multichannel pipettes require the use of particular pipette tips to function correctly

10.0 Method

Preparation of reagents:

Poly-L-Lysine working solution (100 μg/ml)

Supplied in 25 mg vials (1 vial is sufficient for approx 50 x 96-well plates).
Reconstitute powder and transfer to a sterile 500 ml Nalgene bottle. Make up to **250 ml** with sterile water (100 μg/ml final concentration).
Filter sterilise (0.2 μm filter) into a sterile Nalgene bottle.
Store at 4°C
Allow 5 ml (50 μl/well) for each 96-well plate to be coated.

D-PBS containing 1% BSA

Each plate requires ~20 ml of D-PBS containing 1% BSA for use in blocking and for dilution of antibodies during immunostaining on day 4.
Aliquots of D-PBS with BSA can be prepared and stored at -20°C, to be thawed out on the day of use. Otherwise, make up on the day by adding 0.2 g BSA to 20 ml D-PBS for each plate.

Complete 10% FCS DMEM+Blasticidin

500 ml DMEM

50 ml ml FCS	(10% final conc)
5 ml Pen/strep	(100 U Penicillin, 0.1 mg strep ml^{-1} final conc)
10 ml L-glutamine	(4 mM final conc)
250 μl Blasticidin	**(5ug/ml final conc)**

Day 1

10.1 Coating of 96-well plates with poly-L-lysine

10.1.1 Coat plates with Poly-L-Lysine at 100 ug/ml, 50 μl per well (use the repeater multi-channel pipette.

10.1.2 Leave for 30 minutes at room temperature.

10.1.3 Flick the poly-L-lysine solution out of the plate and into the sandwich box in the TC hood.

10.1.4 Use a repeater multi-channel pipette to add 100 μl of sterile water to each well

10.1.5 Flick the water out of the plate and into the sandwich box placed in the TC hood.

10.1.6 Repeat water wash a further two times

10.1.7 Leave plates to dry in the TC hood with the lids off for approx 2-3 hours

10.1.8 Plates can be prepared in advance and stored at 4°C.

10.2 Plating cells – viruses are usually titred on Trex cells irrespective of the cell line used for production

10.2.1 Cells should be counted by a glass haemocytometer.

10.2.2 The density of cells should be standardised to a concentration of 8.8 x 10e5 per ml.

10.2.3 50 µl of cells seeded per well (44000 cells per well) -5 ml per plate.

10.2.4 Place plates in the Nunc square box with some damp blotting paper underneath to provide a constant, high humidity environment.

10.2.5 Incubate plates overnight in 37°C, 5% CO_2 incubator

Day 2

10.3 Preparation of serial dilution of virus.

10.3.1 Remove four 10 µl aliquots of purified virus from the -80°C freezer and thaw at RT.

10.3.2 Label sufficient sterile 1.5 ml microcentrifuge tubes for the dilutions shown below, in quadruplicate for each virus.

10.3.3 Ensure that you use good pipetting technique as described in J212 to make sure we achieve data of the highest quality possible.

10.3.4 Add the required volume of 10% FCS DMEM (+ blasticidin) to each tube.

10.3.5 Take 5 µl of sample from the stock tube and add to the first tube of the series. Important: add the 5 µl to the side of the tube – do not immerse the pipette tip into the media as this is likely to transfer extra virus that is coated to the outside of the pipette tip.

10.3.6 Continue to prepare the dilution series as shown in the table above. **N.B. vortex every preparation of the new dilution for 3 seconds and change pipette tips for every dilution.**



	Virus stock	10^{-2}	10^{-4}	10^{-6}	10^{-7}	10^{-8}	10^{-9}
Virus (µl)	Stock	5	5	5	50	50	50
10% DMEM (µl)	-	495	495	495	450	450	450

10.4 Infection of cells with serial dilution of virus

10.4.1 Using the multichannel aspirating pipette, aspirate media from 96 well plates prepared the previous day- take care not to damage the cell monolayer with the pipette tips. You will need to touch the well bases but just take as much care as possible.

10.4.2 Carefully, so as not to damage the cell layer, add 50 µl of each dilution per well to the side wall of the well – use the ??? pipette with 3 x 50 µl repeats

10.4.3 Place plates in the Nunc square tray with damp blotting paper in the base to provide a constant, high humidity environment.

10.4.4 Incubate plates overnight in 37°C, 5% CO_2 incubator

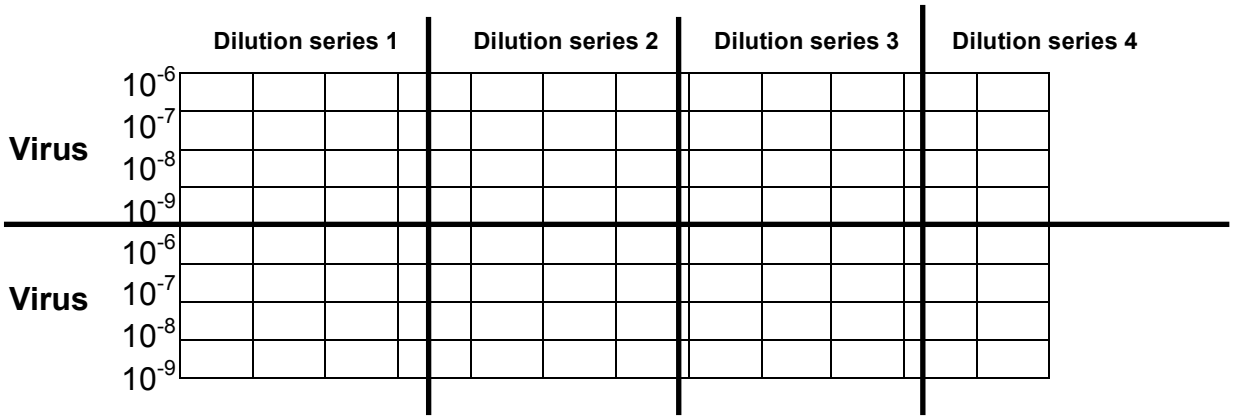


Fig. 1: 96-well plate layout.

Day 3

10.5 Addition of media to wells to ensure cell health.

10.5.1 Using a multichannel pipette, add 50 µl of 10% DMEM + blasticidin to each well of the plates

10.5.2 Incubate plates overnight in 37°C, 5% CO_2 incubator

10.5.3 Place methanol in freezer at -20°C for use on day 4

Day 4

10.6 Fixing cells - work should commence exactly 48 hours after infection with virus.

10.6.1 Using multichannel aspirator, aspirate media from 96 well plate, one plate at a time.

10.6.2 Take care not to damage the cell monolayer with the pipette.

10.6.3 Very gently, using a multichannel pipette, add 100 µl of pre-chilled methanol (from step 9.5.3) to all wells.

10.6.4 Incubate plates at -20°C in virus lab for at least 20 minutes.

NOTE: Protocol can be stopped and plates stored at -20°C until required.

10.7 Immunostaining – wear safety glasses

10.7.1 Wash plates 3 times with D-PBS. (Immerse plates in D-PBS in a sandwich box and flick into the sink. Do not use plate washer as it will disrupt cells.)

10.7.2 Block for 2 hours at RT with 100 µl of PBS with 1% BSA at room temperature – do not stack plates. Alternatively, block overnight at 4°C.

10.7.3 Remove blocking solution by flicking in sink.

10.7.4 Dilute primary antibody 1:1000 in D-PBS+1%BSA (5 µl in 5 ml per plate) + an additional 2.5 µl in 2.5 ml to allow for the multi-step dispenser to pick up sufficient volume.
10.7.5 Add 50 µl of 1 x anti-Hexon antibody solution to each well using the BIOHIT e1200 multidispenser pitpette and BIOHIT filter tips.
10.7.6 Incubate for 1 hour at room temperature – do not stack plates.
10.7.7 Gently wash the fixed cells 3 times in D-PBS as previously.
10.7.8 Dilute secondary antibody 1:1000 in D-PBS+1%BSA (5 µl in 5 ml per plate) + an additional 2.5 µl in 2.5 ml to allow for the multi-step dispenser to pick up sufficient volume.
10.7.9 Add 50 µl of 1 x Secondary antibody solution (HRP-conjugated) to each well using the BIOHIT e1200 multidispenser pitpette and BIOHIT filter tips.
10.7.10 Incubate for 1 hour at room temperature – do not stack plates.
10.7.11 Gently wash the fixed cells 5 times in D-PBS
10.7.12 Add 50 µl of freshly prepared DAB solution to each well using the BIOHIT e1200 multidispenser pitpette and BIOHIT filter tips.
10.7.13 Incubate for at least 10 minutes or until brown dots start to appear.
10.7.14 Remove DAB by flicking in the sink and wash plate twice in tap water.
10.7.15 If the plate is to be read using a conventional microscope: add more tap water and leave the wells wet. Plates can then be stored in the fridge but must be kept in the dark.

If using the Elispot plate reader, place the plates upside down on a piece of blueroll and leave to dry out for 2 hours before counting. Plates can be left open and upside down on blue roll overnight at RT but must be in a box protected from light.

10.8 Counting

10.8.1 Count the positive stained cells (brown). **NOTE:** if the plates have been developed outside the virus lab, they must not be taken back in for counting; an alternative microscope must be used. Count the dilution which contains between 20 and 100 brown cells in each replicate.

Alternatively, the AID Elispot reader (near to the PCR machine in Immunology) can be used:

10.8.2 Cut a piece of white paper or card to fit underneath the plate. Place this in the Elispot reader and put the plate on top.
10.8.3 Turn on the Elispot reader and log into the computer using standard Novell login credentials.
10.8.4 Place plate in the holder. We traditionally place dilution series 1 to the left.

10.8.5 Locate the program 'Eli' in the C:/Elispot4.osr folder. Create a desktop shortcut for future use. Open the program and press the login button:

The computer brings up an error message : layout file "does not exist". Press OK

Username = vector

Password = vector

10.8.6 Tools > Count Settings > Ad Immuno > OK.

10.8.7 Click the icon to open a new document

10.8.8 Tools > Stage > Calibrate Stage.

When a window opens, click the 'A1' button under the 'Calibrate these wells' heading. Using te arrows at the right of the screen, adjust the position and size of the circle so that it fits just inside well A1. Repeat for wells A12 and H12, and press OK.

10.8.9 Press the 'Go' icon to read and count the plate. Click on one of the well images to view it. If the pictures is not clear, adjust the camera settings using Tools > Camera settings. If it is difficult to focus with the camera, check that the plates are dry.

If the reader is marking parts of the well that do not contain a brown dot:

Tools > Count Settings > Ad Immuno > edit. Increase the intensity threshold and recount the plate. **NOTE:** It is better to miss some dots than to count extra spots, as it is easy to add spots later.

10.8.10 Open each image sequentially and add spots that the reader has missed by clicking the 'Add spots' (target) icon and then clicking on the brown cells. Only edit wells with 20 – 200 spots. Note which dilution series is counted in each case.

10.8.11 When finished, click Save As:

S:/Vector Core Facility/Image Files/Titration Images. This will create a folder containing the well images, along with a notepad document showing the final counts.

10.8.12 When finished, click the 'Eject' icon to remove the plate.

10.8.13 Enter counts into the 'Immuno Counts' tab of the Adenovirus Production Chart on S:/Virus Production Records. The spreadsheet should calculate the titre automatically, using the formula:

"average number of spots" x *"serial dilution"* x *"dilution factor"* = *"x"* iu/ml

e.g. if counts of 36 and 40 are obtained at the 10^{-7} dilution:

$\underline{(36+40)} = 38 \times (1 \times 10^{7}) \times 20 = 7.6 \times 10^{9}$ iu/ml

NOTE: Check that the 'Average per Well' cell is selecting the appropriate values in its formula.

10.8.14 Input the titre into the appropriate tab of the spreadsheet (Either 'Stock Maintenance' or 'New Adenoviruses').

10.8.15 Calculate the P to I ratio by dividing the viral particles per ml (from spec reading) by the IU/ml from titration.

P:I values above 100 are usually considered too high for AdCh63 viruses, whilst values above 50 are usually too high for AdHu5 viruses. In this case, consider repeating the hyperflask infection and purification process.

NOTE: Some plates have been observed with odd wells that contain pink media before titration feeding at 24h.p.i. (media is usually turning a yellow colour at this point). The reason for cell death in these wells is not yet known, but it may be the result of microsol contamination. **Jake Matthews, 18.11.10.**

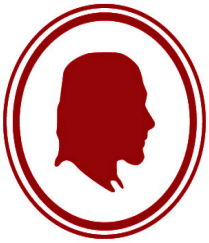
11.0 Revision History

Version Number	What Changed	Who Changed it	Date changed
V01		**FC**	
V02	**Correction to primary Antibody data as it is not HRP conjugated**	**FC**	
V02	**Antibody dilution is 1000x!**	**MD**	
V03	**Re-written**	**Ali Turner**	**14.04.10**
V04	**Addition of instruction to wear safety glasses during immunostaining washing steps**	**Ali Turner**	**08.06.10**
V05	**Poly-L-lysine coating method altered**	**Ali Turner**	**15.06.10**
V06	**Dilution of secondary antibody added to method**	**Ali Turner**	**23.08.10**
V07	**D-PBS+BSA section altered. Increased to 4x dilution series, plating 10^{-6}, 10^{-7}, 10^{-8}, 10^{-9}dilutions. Elispot reader method added. Note about dead cells added.**	**Jake Matthews**	**18.11.10**
V08	**Preparation of dilution series altered from microcentrifuge tubes and vortexing to 96 deep-well plate and trituration**	**Ali Turner**	**18.01.11**
V09	**Safety data added**	**S. Morris**	**12.04.11**
V10	**Dilution series changed back to microcentrifuge tubes and vortexing**	**Ali Turner**	**05.03.12**
12	**Added details of multidispenser and to make up sufficient reagent to allow for this**	**Ali Turner**	**04.05.12**

Appendix:

During culture, water and media commonly evaporate from the wells that are closest to the perimeter of the plate, with the outer 36 and corner wells being the most affected. The result is a variation in cell growth across the plate, while any media components, such as salt, can become concentrated to the point where they are harmful to the cells. A volume loss as small as 10% can concentrate media components and metabolites enough to alter cell physiology, consequently impacting on the viability of downstream data, causing heterogeneous or biased results to occur.
If the cells are unhealthy in the outer wells, they are more likely to be lost from the plate during washing.

Appendix VIII



1.0 Jenner Protocol Number: J176

2.0 Version Number: 09

3.0 Title: Recombination of either MVA or FP9 with shuttle vector using Effectene Transfection reagent

This protocol uses GMOs. All users MUST be registered with the University Occupational Health Service as set out in the University's health and safety regulations. Health surveillance is a legal requirement under COSHH.

If you are not currently registered with the Occupational Health Service for work GMOs, or need to check your registration, please contact the ORCRB NDM Personnel team.

Poxvirus production must ALWAYS be performed on CEF
(not DF-1 cell line that may be used for titration).
NOTE: DF-1 cells are not validated for the generation of vaccines for GMP manufacture. Therefore, they most **ONLY** be used for **virus titration** (NOT plaque picking or any stage of bulk up) during routine production. This will prevent any inadvertent misuse of the cells.

4.0 Other documents

J013 CEF Culture
J017 Linearisation of plasmids
J015 Cell sorting following infection-transfection and first screen

MSDS
refer to MSDS for the relevant safety information on the individual reagents:

\\Imsnw3_jenner_server\jenner\hill_group\Safety\COSHH assessments\Manufacturers material safety data sheets

Note: **Trypan blue solution** is a possible **carcinogen** and should be handled using the appropriate PPE

C030 Culturing of primary cells and cell lines including freezing and reviving

C024 Use of penicillin for tissue culture by sensitised individuals

R003 Poxvirus Risk Assessment \\Imsnw3_jenner_server\jenner\hill_group\Safety\GMORA\R003 poxvirus.doc

R004 GM RA appendix

5.0 Definitions

DF1	Doug Foster strain 1 cells
CEF	Chicken Embryo Fibroblasts
DMEM	Dulbecco's Modified Eagles Medium
FCS	Foetal Calf Serum

6.0 Objective

To recombine an FP9 or MVA shuttle vector with FP9-mCherry or MVA-RFP parental virus respectively. This protocol should result in the production of recombinant, GFP positive viruses for subsequent MoFlo sorting.
This protocol refers to the use of linearised plasmid DNA. However, if marker-less virus is being prepared using the transient/dominant selection system, the plasmid should NOT be linearised.
Note: CEF are used for MVA recombination. **When recombining FP9, primary (P0) CEF MUST be used.**

7.0 Equipment/materials

MVA
6-well plates containing ~100% confluent CEF
These are seeded at 1 x 10^6 CEF/well in 2 ml D10 media 24 hours prior to use or 0.5 x 10^6 cells/well 48 hours prior to use.

FP9
6-well plates containing ~100% confluent **PRIMARY** CEF (i.e. non-passaged).
These are seeded at 3 x 10^6 cells/well in 2 ml D10 media. Due to the primary nature of the cells, they adhere to a greater or lesser extent. However, this seeding density, in our hands, results in sufficient levels of infection and transfection and subsequent recombination.

DMEM Sigma
D6546
100x Pen/Strep solution

(10,000 units penicillin-G and 10 mg strep per ml) Sigma
P0781
200 mM Glutamine Sigma
G7513
FCS Sigma
F2442
TrypLE Express Gibco
I2605

Complete 2% FCS DMEM:
500 ml DMEM
10 ml FCS (2% final conc)
5 ml Pen/strep (100 U Penicillin, 0.1 mg strep ml^{-1} final conc)
10 ml L-glutamine (4 mM final conc)

Effectene Transfection Reagent Kit Qiagen
301425
MVA.RFP/FP9-mcherry
1.5 μg of linearised shuttle vector DNA
Class II BioSafety Cabinet Scanlaf
Mars
CO_2 incubator RS Biotech
Galaxy R
37°C water bath Grant
SUB6
Microscope Leica
DMIL
6-well tissue culture plates
Disposable haemocytometer
1.5 ml microcentrifuge tube (heat sterilised)
Aspirator Integra
BioSciences Vacusafe
Sterile 2 ml screw-capped tubes
Cell lifter Fisher
FB55160

8.0 Method

8.1 Day 1:

8.1.1 Seed $1x10^6$ CEF cells (in 2ml D10 media) in a single well of a 6 well plate. One plate is needed for each virus to be made – **multiple recombinations must NOT be performed on the same plate.** When recombining FP9, primary cells must be seeded at 3×10^6 in 2ml in a single well upon arrival from IAH Compton.

8.1.2 Incubate at 37°C with 5% CO_2 overnight.

8.2 Day 2:

8.2.1 Transfer the 6 well plate to the virus lab incubator.

8.2.2 Pre-warm D2 media to 37°C.

8.2.3 Thaw MVA RFP (or FP9-mCherry) - these are stored in a nalgene box in the -80°C freezer in immunology.

8.2.4 Aspirate media from the 6 well plate

8.2.5 Infect cells with FP9-mCherry or MVA-RFP:
Previous recombinations have worked well using 5 x 10^6 total PFU/well (MOI ~ 2.5) with CEF - therefore, infect with 5 x 10^6 total PFU, in 1 ml D2 media. **More than one recombination is typically being prepared at a time and therefore the media is normally in a 50 ml tube. When adding the virus to this tube, do not insert the Gilson pipette into the tube but just "dot" the virus in the upper side of the tube and then mix thoroughly by inverting the tube 10 times.**

8.2.6 Incubate at 37°C; 5% CO_2 for 90 minutes.

8.2.7 Approximately 75 minutes into the above incubation period, begin preparing transfection complexes in a sterile 2 ml tube: 1 µg linearised DNA is added per well. Give the DNA a brief vortex (1 sec) and then flick tube to collect contents towards the base of the tube. DNA used should be high quality plasmid DNA, purified using a Qiagen purification kit.

DNA	Volume of Enhancer	Volume of Buffer EC
1.5 µg	**3 µl**	Make total volume up to **112.5 µl**

8.2.8 Incubate the reaction mix at room temperature for 5 min and pulse centrifuge for a few seconds to remove all droplets from the lid.

8.2.9 Add 37.5 µl of Effectene Transfection reagent to the DNA-Enhancer mixture and vortex for 10 sec, flick tube to collect contents towards the base of the tube.

8.2.10 Incubate at room temperature for 10 min to allow transfection complex formation.

8.2.11 During incubation, aspirate media from the well of CEF to be transfected and replace with 2 ml, fresh, warm DMEM + 2% FCS.

8.2.12 Make final volume of transfection mix up to 0.75 ml using warm DMEM + 2% FCS and triturate gently 10 times to ensure the complexes are thoroughly resuspended.

8.2.13 Add 0.5 ml transfection complex mix to each well and ensure equal distribution by rocking the plate backwards, forwards and side to side.

8.2.14 Incubate 48 hours at 37°C; 5% CO_2.

8.3 Day 4:

8.3.1 Observe fluorescence – GFP positive cells should be visible. Where no GFP fluorescence is seen in the entire well it will be necessary to repeat the recombination.

8.3.2 Harvest cells and media by scraping (using a cell lifter) and transfer to a sterile 2 ml screw-capped tube using **a 2 ml serological pipette.**

8.3.3 Store at -20°C until required.

9.0 Revision History

Version Number	Why it changed/ What Changed	Who Changed it	Date Changed
1	First written	Chris	30.06.10
2	Volumes adjusted to account for the use of only 1 well rather than 2.	Chris	28.07.10
3	To account for both MVA and Fp9 shuttle vectors	Chris	01.10.10
4	Method clarified	Ali	08.12.10
5	OH statement added	S. Morris	19.04.11
6	Method adapted for use of DF-1 cells for MVA	J. Matthews	30.03.12
7	Method clarification	Ali Turner	24.07.12
8	Method clarification	Ali Turner	8.04.13
9	Note to only use CEF for poxvirus production – not DF-1 cells	Ali Turner	18.04.13

Appendix IX



1.0 Jenner Laboratory Protocol Number J131

2.0 Version Number 13

3.0 Title: 96-well plate MoFlo sort of CEF infected with recombinant poxviruses

This protocol uses GMOs. All users MUST be registered with the University Occupational Health Service as set out in the University's health and safety regulations. Health surveillance is a legal requirement under COSHH.

If you are not currently registered with the Occupational Health Service for work GMOs, or need to check your registration, please contact the ORCRB NDM Personnel team.

Poxvirus production must ALWAYS be performed on CEF
(not DF-1 cell line that may be used for titration).
NOTE: DF-1 cells are not validated for the generation of vaccines for GMP manufacture. Therefore, they most **ONLY** be used for **virus titration** (NOT plaque picking or any stage of bulk up) during routine production. This will prevent any inadvertent misuse of the cells.

4.0 Other documents

MSDS refer to MSDS for the relevant safety information on the individual reagents:
\\lmsnw3_jenner_server\jenner\hill_group\Safety\COSHH assessments\Manufacturers material safety data sheets

R003 Poxvirus
C030 Culture of primary cells and cell lines including freezing and reviving
C024 Use of penicillin in tissue culture by sensitised individuals

J176 Recombination of Poxvirus with shuttle vector using Effectene Transfection reagent
J018 Purification of recombinant MVA by plaque picking in 6 well plates
J173 Preparation of template DNA using DNA Releasy
J175 Virus ID and Purity PCR using KAPA2G robust polymerase

5.0 Definitions

DF-1 Doug Foster strain 1 cells
Organ: embryo
Strain: East Lansing Line (ELL-0)
Cell Type: fibroblastspontaneously transformed
FBS Foetal bovine serum
MEM Minimum essential media
RFP Red fluorescent protein.
GFP Green fluorescent protein.
DMEM Dulbecco's modified Eagle's media
CEF Chicken embryonic fibroblasts

6.0 Objective

Purification of fluorescent, recombinant poxviruses can be accelerated by a MoFlo sort whereby infected cells are single-cell sorted into a 96-well plate based on their fluorescence. This method is superior to that of plaque picking as none of the cells surrounding the plaque are co-transferred to the well. The resultant single cells are lysed by sorting them into wells containing sterile water and then CEF added to the wells to permit virus propagation. Wells containing appropriate virus are identified by microscopy and the entire well is harvested, screened by PCR and cell lysates from the relevant well titrated following protocol J018.
This method is performed using CEF cells for both MVA and FP9 viruses. A T150 flask of 100% confluent CEF cells is infected with a small volume of cell lysate harvested from the recombination between Poxvirus and shuttle vector. It is important that the cell culture does not contain a large amount of virus as although the cells are sorted based on fluorescence, if there are virus particles attached to the outside of the cell membrane they will be co-transferred to the wells where they can then replicate.
Routinely we do not prepare control cells as the parameters are saved on the Flow cytometer

7.0 Reagents

CEF
DMEM Sigma D6546
100x Pen/Strep solution
(10,000 units penicillin-G and 10 mg strep per ml) Sigma P0781

200 mM Glutamine	Sigma
G7513	
FBS	*Sigma*
F2442	
TrypLE Express	Gibco
I2605	
Trypan blue stain	Sigma
T8154	
Tissue culture grade water	Sigma
W3500-100ML	

Complete 2% (10%) FCS DMEM:

500 ml DMEM	
10 (50 ml) ml FCS	(2% (10%) final conc)
5 ml Pen/strep	(100 U Penicillin, 0.1 mg strep ml^{-1} final conc)
10 ml L-glutamine	(4 mM final conc)

8.0 Equipment

Class II BioSafety Cabinet	Scanlaf
Mars	
CO_2 incubator	RS Biotech
Galaxy R	
37°C water bath	Grant
SUB6	
haemocytometer	
-80°C freezer	
Individually wrapped reagent reservoir	Starlab
E2310-1010	
Dry ice	
96 well tissue culture plates	Fisher
TKT-520-030T	
Gilson pipettes and filter tips	

9.0 Method

9.1 Day 1:

9.1.1 Seed a 6 well plate with CEF cells at 1 x 10^6 per well for MVA in 10% FBS DMEM for MoFlo controls (2 wells RFP; 2 wells GFP; 2 wells uninfected for MVA) (2 wells mCherry; 2 wells GFP; 2 wells uninfected for FP9).

9.1.2 Prepare one T15 flask per virus

9.1.3 Incubate at 37°C with 5% CO_2 overnight.

9.2 Day 2:

9.2.1 Transfer the *6 well plate* and T150 flasks of cells to virus lab.

9.2.2 Place plate and flasks of cells in incubator (37°C, 5% CO_2) until required.

9.2.3 Freeze/thaw the cell lysate(s) to be MoFlo sorted 3x and vortex for 15 sec.

9.2.4 Aliquot media into Falcon tubes:

3 ml D2 media into each of 3 x 15ml Falcon tubes (for controls)

15 ml D2 media into 50 ml tubes for each test sample.

9.2.5 Control wells are infected at an MOI ~0.001, VVCF have stocks of pre-diluted control viruses to use for this purpose. To prepare controls, add either MVA-RFP and MVA-GFP or FP9- mCherry and FP9-GFP cell lysate to respective 3 ml aliquots of D2 media and vortex for up to 5 seconds. Leave one of the 3 ml aliquots of D2 to add to uninfected controls. Aspirate media from all wells and add 1 ml of each control to each of 2 wells.

9.2.6 To prepare viruses, thoroughly clean cabinet, taking particular care to clean Gilson pipettes, and change gloves. Add 10 µl of test sample cell lysate to 35 ml D2 media and vortex (up to 5 sec).

9.2.7 Aspirate the D10 media from the T150 flask of cells and replace with 35 ml of virus/D2 suspension.

9.2.8 Incubate infected cells for up to 3 days at 37°C with 5% CO_2;

9.3 Day 4/5

9.3.1 Observe the plate/flasks using the fluorescence microscope to check for GFP positive recombinant virus. Also use red fluorescence to check RFP/mCherry is expressing.

9.3.2 Prepare one 96-well plate per virus to be sorted by adding 50 µl sterile water to each well.

9.3.3 Prepare 50ml fresh sterile PBS in 50 ml Falcon tubes – *3 tubes for controls* and separate tubes for each test sample.

9.3.4 Pre-warm the PBS and TrypLE to 37°C.

Preparation of control cells

9.3.5 Aspirate the media from the control plate.

9.3.6 Wash cells once with ~5 ml of PBS.

9.3.7 Add 1 ml of TrypLE per well and incubate at 37°C until 80% of the cells are detached – monitor frequently under microscope.

9.3.8 Add 5 ml PBS to each well then take cells up and down gently and transfer to 50ml Falcon tubes.

9.3.9 Rinse wells with an additional 5 ml PBS and transfer to the 50 ml Falcon tube.

9.3.10 Centrifuge at 190 x g (900 rpm) for 3 minutes at RT.

9.3.11 Aspirate the supernatant.

9.3.12 Resuspend the cells gently by tapping the tube.

9.3.13 Add ~20 ml PBS.

9.3.14 Centrifuge at 190 x g (900 rpm) for 3 minutes at RT.

9.3.15 Aspirate the supernatant (leaving approximately 200ul residual volume) and then flick the tube gently in the liquid to get a single cell suspension.

9.3.16 Place all the samples in a Virus carrying box. (Wipe it with Microsol before use).

9.3.17 Prepare all controls and take them to Drew to set up the MoFlo.

Preparation of experimental cells

9.3.18 Aspirate the media from one T150 flask.

9.3.19 Wash cells once with ~10 ml PBS

9.3.20 Add 10 ml of TrypLE and incubate at 37°C until 80% of the cells are detached – monitor frequently under microscope.

9.3.21 Add 10 ml **PBS** then take cells up and down gently and transfer to 50ml Falcon tubes.

9.3.22 Rinse cells with an additional 10 ml PBS and transfer to the 50 ml Falcon tube.

9.3.23 Centrifuge at 200 x g for 3 minutes at RT.

9.3.24 Aspirate the supernatant.

9.3.25 Resuspend the cells gently by tapping the tube.

9.3.26 Add ~20 ml PBS.

9.3.27 Centrifuge at 200 x g for 3 minutes at RT.

9.3.28 Aspirate the supernatant (leaving approximately 200ul residual volume) and then flick the tube gently in the liquid to get a single cell suspension.

9.3.29 Place the sample in a Virus carrying box. (Wipe it with Microsol before use) and take to Drew for sorting.

9.3.30 96-well plates are returned to the virus room and CEF cells added: 50,000 cells per well in 200 μl 2% DMEM. (5 x 10^6 cells in 20 ml per plate). **NOTE –CELLS MAY BE TRYPSINISED AND COUNTED TOGETHER FOR MULTIPLE PLATES. HOWEVER, THEY MUST NOT BE PLACED IN A SINGLE REAGENT RESERVIOR TO SEED MULTIPLE PLATES AS THE MULTICHANNEL PIPETTE WILL DIP INTO THE 96-WELL PLATES CONTAINING DIFFERENT VIRUSES.**
Alternatively, the 96-well plates can be placed at -20°C and the cells added later.
Place plate in incubator (37°C, 5% CO_2) for 2-4 days until recombinant virus can be observed.

9.3.31 The entire wells containing recombinant virus (as visualised by fluorescence) are harvested. Where possible, at least 5 wells should be harvested in the first instance + the dump well. In cases where MoFlo sorting has previously failed for a particular virus it may be worth harvesting as many candidate wells as possible for PCR screening to maximize the chance of obtaining correct virus.

Wells to be harvested are scraped with a P1000 tip, transferred into a 2 ml Starstedt tube and frozen/thawed x3. 20ul of lysate is taken and added to 30ul DNA RelEasy in a PCR tube and extracted using the 'Tough DNA RelEasy' program (see J173). Samples are screened with reference to J175. The remaining lysate is stored at -20°C in

the virus lab freezer for subsequent plaque purification and amplification.

Appendix I

Use of cytochalisin D to inhibit release of MVA from infected cells.

5 mg/ml Cytochalisin D (ready-made sterile solution)
Sigma C2618-200UL

Working concentration = 1 µM
Mw 507.62
Therefore stock solution 0.01M (10 mM)

0.1mM would be 100X solution (addition of 150 µl to 15 ml D2)

Dilute stock solution to 20 ml in PBS and prepare 160 µl aliquots

10.0 Revision History

Version Number	What Changed	Who Changed it	Date Changed
01	First written	Ali Turner	
02	Infecting T150 flasks with virus instead of 6 well plates	Chris Schultz	
03	Testing of dump well virus by PCR screen	Ali Turner	
04	Made applicable to both MVA and Fp9 sorts	Chris Schultz	
05	Method clarified	Ali Turner	15th December 2010
06	Not recorded		
07	OH statement added	S. morris	19.04.11
08	Note about seeding multiple plates	Ali turner	07.10.11
09	Method adapted for use of DF-1 cells when sorting MVA	J Matthews	30.03.12
10	DF-1 cells for FP9 as well. Method clarified	Ali Turner	19.06.12
11	CEF only – not DF-1 cells + explanatory note	Ali Turner	18.04.13
12	Modified to use PBS only instead of PBS + 2% FBS (step 9.3 onwards)	Jake Matthews	13.05.13
13	Water reagent details added. Control reactions stated as not necessary.	Ali Turner	11.03.15

	Changed to T150 flasks. Centrifugation step altered speed to match new centrifuge		

Appendix X



1.0 Jenner Laboratory Protocol Number: J016

2.0 Version Number: 03

3.0 Title: Infection of CEF with recombinant MVA after cell sorting.

This protocol uses GMOs. All users MUST be registered with the University Occupational Health Service as set out in the University's health and safety regulations. Health surveillance is a legal requirement under COSHH.

If you are not currently registered with the Occupational Health Service for work GMOs, or need to check your registration, please contact the ORCRB NDM Personnel team.

4.0 Other Documents

MSDS refer to MSDS for the relevant safety information on the individual reagents:
\\Imsnw3_jenner_server\jenner\hill_group\Safety\COSHH assessments\Manufacturers material safety data sheets

R003 Poxvirus Risk Assessment
\\Imsnw3_jenner_server\jenner\hill_group\Safety\GMORA\R003 poxvirus.doc

CO30 Culturing primary cell and cell lines including freezing and reviving
C024 Use of penicillin for tissue culture by sensitised individuals

J013 CEF culture
J014 Infection and transfection of CEF with MVA and shuttle vector
J015 Preparation of CEF infected with recombinant MVA for cell sorting
J018 Purification of recombinant MVA by plaque picking in 6 well plates

5.0 Definitions

CEF Chicken embryo fibroblasts
FCS Foetal calf serum
DMEM Dulbecco's modified Eagle's media
MVA Modified vaccinia Ankara

6.0 Objective

To infect CEF with a lysate of previously sorted CEF following infection and transfection with MVA and shuttle vector respectively.
Ensure cells infected with different viruses are handled separately in the biological safety cabinet, wiping the surface down and changing gloves between different viruses.

7.0 Reagents

90% confluent CEF
DMEM Sigma
D6546
100x Pen/Strep solution
(10,000 units penicillin-G and 10 mg strep per ml) Sigma
P0781
200 mM Glutamine Sigma
G7513
FCS Sigma
F2442
MoFlo-sorted viruses
Either snap frozen on day of MoFlo-sort or snap-frozen and stored at -80°C
In-house reagent
2% LMP agarose in dH_20 (heat sterilised) Sigma
A9414
2xMEM without phenol red Gibco
21935
Complete 2% (10%) FCS DMEM:
500 ml DMEM
10 (50 ml) ml FCS (2% (10%) final conc)
5 ml Pen/strep (100 U Penicillin, 0.1 mg strep ml^{-1} final conc)
10 ml L-glutamine (4 mM final conc)

10.0 Equipment

Class II BioSafety Cabinet Scanlaf
Mars
CO_2 incubator RS Biotech
Galaxy R
37°C water bath Grant
SUB6

Microscope Leica
DMIL
6-well tissue culture plates
Disposable haemocytometer
Vortex
Sterile 1.5 ml microcentrifuge tubes

11.0 Method

11.1 Infection

11.1.1 Prepare one 6 well plate of CEF in 10% FCS DMEM per virus required:

Plate cells at 1 x 10^6 CEF in 2 ml per well if required the following day

Plate cells at 0.5 x 10^6 cells in 2 ml per well if required 48 hours later

11.1.2 Incubate (37°C, 5% CO_2) until 90% confluent.

11.1.3 Transfer 6-well plates to virus lab.

11.1.4 Thaw the sorted tubes containing the virus-infected CEF, add 1 ml of 2% FCS DMEM in each tube.

11.1.5 Vortex the tubes (this will bring out all the enclosed viral particles from the cells).

11.1.6 Label sufficient sterile 1.5 ml microcentrifuge tubes for the following dilutions,

		10^{-1}	10^{-2}	10^{-3}	10^{-4}	10^{-5}
Virus (μl)	neat	100	100	100	100	100
2% DMEM (μl)	-	900	900	900	900	900

11.1.7 Add the required volume of 2% FCS DMEM to each microcentrifuge tube.

11.1.8 Thaw the virus (es) to be titrated and add 100 μl of the stock to the first tube of the series. Continue to prepare the dilution series as shown in the table above. **N.B**. **vortex every preparation of the new dilution for 3 seconds and change pipette tips for every dilution.**

11.1.9 Aspirate the media from the first plate.

11.1.10 Pipette the virus-containing medium from the tubes into the relevant wells of the 6 well plates.

11.1.11 Incubate for 1hour (37°C, 5% CO_2).

11.1.12 Proceed with either 9.2 or 9.3

11.2 Agarose Overlay

11.2.1 Heat the 2% Low melting point agarose (solid) in the microwave, to melt (2-3 minutes on high power) and keep it in water bath at 37°C for at least 15 minutes.

11.2.2 Place 4% FCS MEM in 37°C water bath for at least 15 minutes.

11.2.3 Remove the culture medium from the well containing **neat lysate** and transfer to a 2 ml tube – store at -80°C in case there is any problem with the protocol.

11.2.4 Aspirate the media from the remaining wells of the 6 well plates.

11.2.5 Pour 4% FCS MEM into an equal volume of 2% low melting point agarose in 50 ml Falcon tube *(note: add FCS MEM to the agarose to prevent agarose setting in the 50 ml Falcon tube as it is poured).*

11.2.6 Pipette 2 ml of this mixture in the wells of six well plates, as quick as possible to prevent re-solidification of the agarose.

11.2.7 Incubate (37°C, 5% CO_2) for 2-4 days.

11.3 **CMC overlay:**

11.3.1 Mix sufficient D2 media and CMC in a ratio 2/3 D2:1/3 CMC for 2 ml per well required.

11.3.2 Aspirate media containing virus.

11.3.3 Replace with 2 ml D2/CMC overlay per well.

11.3.4 Incubate for 2-4 days

11.4 Checking for recombinant virus production

11.4.1 After two days check the 6-well plates under fluorescence microscope and mark the required virus plaques. Continue as per J018.

8.0 Revision History

Version Number	What Changed	Why it Changed	Who Changed it
01	First written	N/A	A. Turner
02	Various points in method	Updated for CMC overlay	Ali Turner
03	Safety data added	Safety regulations	S. Morris (19.04.11)

Appendix XI

1.0 Jenner Laboratory Protocol Number: J018

2.0 Version Number: 09

3.0 Title: Purification of recombinant Poxvirus by plaque picking in 6 well plates

This protocol uses GMOs. All users MUST be registered with the University Occupational Health Service as set out in the University's health and safety regulations. Health surveillance is a legal requirement under COSHH.

If you are not currently registered with the Occupational Health Service for work GMOs, or need to check your registration, please contact the ORCRB NDM Personnel team.

Poxvirus production must ALWAYS be performed on CEF
(not DF-1 cell line that may be used for titration).
NOTE: DF-1 cells are not validated for the generation of vaccines for GMP manufacture. Therefore, they most **ONLY** be used for **virus titration** (NOT plaque picking or any stage of bulk up) during routine production. This will prevent any inadvertent misuse of the cells.

4.0 Other Documents

MSDS refer to MSDS for the relevant safety information on the individual reagents:
\\Imsnw3_jenner_server\jenner\hill_group\Safety\COSHH assessments\Manufacturers material safetly data sheets

Note: **Trypan blue solution** is a possible **carcinogen** and should be handled using the appropriate PPE

C030 Culturing primary cells and cell lines including freezing and reviving
C024 Use of penicillin for tissue culture by sensitised individuals

R003 Poxvirus Risk Assessment
\\lmsnw3_jenner_server\jenner\hill_group\Safety\GMO RA\R003 poxvirus.doc
J013 CEF culture
J019 Bulking up poxviruses
J020 Jenner poxvirus PCR Document

5.0 Definitions

CEF Chicken embryo fibroblasts
FCS Foetal calf serum
MEM Minimum essential media
RFP Red fluorescent protein.
GFP Green fluorescent protein.
DMEM Dulbecco's modified Eagle's media

6.0 Objective

To purify recombinant poxvirus from parental virus by plaque picking following infection of CEF (MVA) with a serial dilution of plaque lysate. After each round of purification ID, Purity and Flank PCR are performed to screen for the presence of the desired antigen and to check for the presence of parental poxvirus (MVA-RFP or FP9-mcherry). When one round of plaque picking is confirmed as free of parental virus by PCR, a plaque from the next round of plaque picking is used to infect a T175. This T175 is then also screened by ID, Flank and Purity PCR and is used as a premaster for subsequent MSV Infection if found to be correct and pure.

Ensure cells infected with different viruses are handled separately in the biological safety cabinet, wiping the surface down and changing gloves between different vectors.

7.0 Reagents

CEF	Institute for Animal Health, Compton.
DMEM D6546	Sigma
2xMEM without phenol red 21935	Gibco
100x Pen/Strep solution (10,000 units penicillin-G and 10 mg strep per ml) P0781	Sigma
200 mM Glutamine G7513	Sigma
FCS F2442	Sigma
TrypLE Express I2605	Gibco
Trypan blue stain T8154	Sigma

CMC high viscosity BDH#
279294T
10 mM Tris, 140 mM NaCl [pH7.8]
1M Trizma pH 7.8 solution Sigma
T2569
NaCl (BioPerformance Certified, ≥99% (titration), Cell Culture Tested) Sigma
S6191

Complete 2% (10% for FP9) FCS DMEM:
500 ml DMEM
10 (50 ml for FP9) ml FCS (2% (10% for FP9) final conc)
5 ml Pen/strep (100 U Penicillin, 0.1 mg strep ml^{-1} final conc)
10 ml L-glutamine (4 mM final conc)
do not substitute for alternative supplier. This product has been found to be lower in endotoxins levels than those from other suppliers.

12.0 Equipment

Class II BioSafety Cabinet Scanlaf
Mars
CO_2 incubator RS Biotech
Galaxy R
37°C water bath Grant
SUB6
Microscope with objective marker attachment Leica
DMIL
Disposable haemocytometer
-80°C freezer

Dry ice
6 well tissue culture plates Fisher
TKT-520-030T
Gilson pipettes and filter tips

13.0 Method

13.1 Infection of CEF.

13.1.1 Prepare one 6 well plate of CEF per virus plaque to be titrated. Standard procedure is to purify one plaque.
13.1.2 Incubate at 37°C with 5% CO_2 until ~90% confluent.
13.1.3 Transfer the 6 well plates to the virus lab.
13.1.4 Aspirate the media and replace with 1ml fresh, pre-warmed D2.
13.1.5 Infect one well of the 6 well plate with 20 µl of the material to be purified (This will either be lysate that was harvested from the MoFlo sorted 96 wp or a plaque pick from a previous

titration). Tilt the plate side to side and front to back 5 times to ensure mixing (do not move the plate in circles as this forces the virus to the edge of the well).

13.1.6 Take 100 µl from the well that has just been infected and transfer it to the next well using a Gilson with a P200 tip. Tilt the plate as in step 9.1.5 to mix.

13.1.7 Repeat step 9.1.6 four more times to give the following plate layout:

Well 1 ~2x 10^{-2} dilution 1ml D2 + 20µl lysate	**Well 2** ~2x 10^{-3} dilution 1ml D2 + 100µl from well 1	**Well 3** ~2x 10^{-4} dilution 1ml D2 + 100µl from well 2
Well 4 ~2x 10^{-5} dilution 1ml D2 + 100µl from well 3	**Well 5** ~2x 10^{-6} dilution 1ml D2 + 100µl from well 4	**Well 6** ~2x 10^{-7} dilution 1ml D2 + 100µl from well 5

13.1.8 Incubate for 90 ± 30 mins at 37°C with 5% CO_2.

13.1.9 Mix sufficient D2 media and CMC in a ratio 2/3 D2 : 1/3 CMC for 2 ml per well required.

13.1.10 Aspirate media containing virus.

13.1.11 Replace with 2 ml D2/CMC overlay per well.

13.1.12 Incubate for 2-4 days.

13.1.13 Pick plaques as required.

13.2 Plaque picking.

13.2.1 2 ml screw capped tubes containing 100 µl 10 mM Tris pH9.0 are stored in the VVCF drawers in the virus room. These are for the plaques to be picked into. Transfer one to the BSC2.

13.2.2 Using the microscope, identify a well isolated plaque of desired fluorescence/no fluorescence and use the objective cell dotter to mark a ring around the plaque.

13.2.3 Transfer the plate to the BSC2 and use a p1000 pipette and tip to remove the plaque from the monolayer.

13.2.4 Check, using the microscope that the correct region has been harvested.

13.2.5 Place the tubes on dry ice to freeze; thaw in 37°C water bath and vortex very hard.

13.2.6 Repeat freeze, thaw and vortex twice more for each tube. (Virus may be frozen at -20°C for storage).

13.2.7 In the BSC2, harvest well 1 (the well that was infected with the most concentrated lysate) by scraping and transfer to a 2ml tube. Freeze-thaw-vortex three times before taking 20µl for DNA RelEasy extraction and freezing the remainder at -20°C.

Note: After performing titration of first round plaques it is not necessary to harvest the most concentrated well for PCR screening because this is equivalent to the material screened after MoFlo harvest. Harvest of the most concentrated well is necessary after titration of later round plaques.

13.3 Recombinant virus purity

When a plaque passes ID, Flank and Purity PCR 50ul of a subsequent pick is taken and used to infect a T150 as premaster. For example, if plaque 1 (from MoFlo) passes all PCR, this plaque should be titrated and plaque 1.1 picked for premaster infection. See J019 Bulking Up Poxviruses.

After premaster harvest 20ul of premaster lysate should be PCR screened – if this passes it can then be used to infect multiple T150s to produce the MSV.

14.0 Revision History

Version Number	What Changed	Who Changed it	Date changed
01	First written	A.Turner	
02	Altered to contain CMC method variation	A.Turner	
03	Method altered	Ali Turner	
04	Agarose method removed	Ali Turner	15th Dec 2010
05	Safety data added	S. Morris	19.04.11
06	Clarification of which wells should be plated in step 9.2.6.	C.Schultz	06.07.11
07	Method altered. Adapted for use of DF-1 cells for MVA	J Matthews	30.03.12
08	Reduced to picking only 1 plaque/plate	J Matthews	26.07.12
09	Altered to stipulate CEF only and to detail how to plaque pick in the BSC2, not under the microscope	A Turner	11.04.12

Appendix XII



1.0 Jenner Laboratory Protocol Number: J019a

2.0 Version Number: 2

3.0 Title: Bulking up and purifying poxviruses

This protocol uses GMOs. All users MUST be registered with the University Occupational Health Service as set out in the University's health and safety regulations. Health surveillance is a legal requirement under COSHH.
If you are not currently registered with the Occupational Health Service for work GMOs, or need to check your registration, please contact the ORCRB NDM Personnel team.

4.0 Other Documents

MSDS refer to MSDS for the relevant safety information on the individual reagents:
\\Imsnw3_jenner_server\jenner\hill_group\Safety\COSHH assessments\Manufacturers material safety data sheets

Note: **Trypan blue solution** is a possible **carcinogen** and should be handled using the appropriate PPE

Risk assessments covering the use of poxviruses within the Jenner Institute are listed below and can be found in the safety folder on the s: drive or hard copies are available in the office area. These must be read and understood prior to commencing work using these viruses. In addition, the appendix to the GMO RA (R004) documents all of the antigens might be encoded by the poxviruses. These should be read and understood as relevant to the work being undertaken.

GMO RA R003 poxvirus
GMO RA R004 GM RA app
C052 use of sonicator
C030 Culturing primary cells and cell lines including freezing and reviving
J013 CEF culture
J018 plaque picking

J208 preparation of 36% sucrose
J209 preparation of 10mM Tris for MVA production

5.0 Definitions

CEF Chicken embryo fibroblasts
CPE Cytopathic effects
FCS Foetal calf serum
MVA Modified vaccinia Ankara
FP9 a plaque-purified, high passage attenuated, European strain of Fowlpox virus
DMEM Dulbecco's modified Eagle's media
GMO Genetically modified organism
RA Risk assessment

6.0 Objective

Large-scale preparation of MVA/FP9 requires the infection of CEF, the extraction of virus from the cell lysate and crude purification to remove cell debris from the sample. This protocol describes the preparation of a premaster stock of virus.

Ensure cells infected with different viruses are handled separately in the biological safety cabinet, wiping the surface down and changing gloves between different vectors.

7.0 Reagents

CEF
DMEM Sigma
D6546
Pen/Strep Sigma
Glutamine Sigma
PBS (without Ca^{2+} and Mg^{2+}) Sigma
D8537
FBS Sigma
12103C
Trypan blue stain Sigma
T8154
TrypLE Express Gibco
I2605
10 mM Tris [pH9]
10 mM Tris pH9, sterile
From 1M Tris pH 9 stock solution SIGMA
T2819-100ml
36% w/v sucrose solution (in 10mM Tris pH9), (filter sterilised)
It is important that this material is low in endotoxins Fluka
84097

Premaster cell/media lysate
Cells and media from a T150 flask infected with material confirmed free from parental poxvirus by PCR. If this is the first time the virus has been made, the premaster will have been prepared from a plaque pick one round on from a plaque that passed QC PCR (for example plaque 1.1 is usually used if plaque 1 passed QC PCR). If this is a rebulk prep, the premaster is prepared by infection of a CEF T150 with cell lysate from the original premaster.

15.0 Equipment

Class II BioSafety Cabinet Mars	Scanlaf
Benchtop Centrifuge Allegra X-12R	Beckman Coulter
CO_2 incubator Galaxy R	RS Biotech
37°C water bath SUB6	Grant
Microscope DMIL	Leica
Industrial methylated spirit (IMS) M/4400/17	Fischer
2 ml screw cap tubes.	
Disposable haemocytometer	
Sterile transfer pipette (pastette)	
-80°C freezer Scientific U57085	New Brunswick
25 cm cell scrapers	
50ml centrifuge tubes	
Dry ice	

16.0 Method

16.1 Preparing and infecting CEF with virus in T150 flasks (Premaster).

16.1.1 Prepare one T150 flask per virus with CEF cells such that they are 90% confluent at time of infection. One T150 is required for each set of 5 x T150 flasks required.

16.1.2 Incubate (37°C, 5% CO_2) until 90% confluent.

16.1.3 Transfer T150 flask to the virus lab

16.1.4 The source material may either be a plaque pick or a previous premaster cell lysate is performing a re-bulk':

16.1.4.1 Plaque pick: pipette 50 µl of prepared plaque pick (three times freeze, thaw and vortexed) into 15 ml of 2% FCS DMEM in a 15 ml falcon tube and vortex thoroughly.

16.1.4.2 Premaster cell lysate: transfer 50 µl of prepared premaster (thawed and vortexed) into 15 ml of 2% FCS DMEM in a 15 ml falcon tube and vortex

thoroughly.

16.1.5 Aspirate the 10% DMEM and replace with the 2% media containing the virus.

16.1.6 Incubate (37°C, 5% CO_2) and monitor appearance of CPE (~100% infected cells should be evident after approximately 3 days).

16.1.7 Scrape off the virus-infected cells from the T150 flask into 50 ml falcon tubes. *(Cells and supernatant may be frozen for storage at this stage).*

16.1.8 Place the 50 ml falcon tubes with virus infected CEF on dry ice to freeze, thaw in 37°C water bath and vortex very hard.

16.1.9 Repeat freeze/thaw once more before taking a 20ul aliquot and adding to 30ul DNA RelEasy in a PCR tube for DNA extraction. Freeze the remaining lysate and store until needed for MSV infection.

17.0 Revision History

Version Number	What changed and Why it Changed	Who Changed it	Date changed
01	**N/A**	**Ali Turner**	**7th January 2013**

Appendix XIII



1.0 Jenner Laboratory Protocol Number: J019b

2.0 Version Number: 03

3.0 Title: Preparation of a poxvirus master seed virus

This protocol uses GMOs. All users MUST be registered with the University Occupational Health Service as set out in the University's health and safety regulations. Health surveillance is a legal requirement under COSHH.
If you are not currently registered with the Occupational Health Service for work GMOs, or need to check your registration, please contact the ORCRB NDM Personnel team.

4.0 Other Documents

MSDS refer to MSDS for the relevant safety information on the individual reagents:
\\Imsnw3_jenner_server\jenner\hill_group\Safety\COSHH assessments\Manufacturers material safety data sheets

Note: **Trypan blue solution** is a possible **carcinogen** and should be handled using the appropriate PPE

Risk assessments covering the use of poxviruses within the Jenner Institute are listed below and can be found in the safety folder on the s: drive or hard copies are available in the office area. These must be read and understood prior to commencing work using these viruses. In addition, the appendix to the GMO RA (R004) documents all of the antigens might be encoded by the poxviruses. These should be read and understood as relevant to the work being undertaken.

GMO RA R003 poxvirus
GMO RA R004 GM RA app
C052 use of sonicator
C030 Culturing primary cells and cell lines including freezing and reviving
J013 CEF culture

5.0 Definitions

CEF Chicken embryo fibroblasts
CPE Cytopathic effects
FCS Foetal calf serum
MVA Modified vaccinia Ankara
FP9 a plaque-purified, high passage attenuated, European strain of Fowlpox virus
DMEM Dulbecco's modified Eagle's media
GMO Genetically modified organism
RA Risk assessment

6.0 Objective

Large-scale preparation of MVA/FP9 requires the infection of CEF, the extraction of virus from the cell lysate and crude purification to remove cell debris from the sample. This protocol describes the preparation of a premaster stock of virus, infection of CEF with premaster lysate to form a master seed virus prep and purification through a sucrose cushion. Sucrose cushion purification separates the viral particles from the cell lysate. The potency, ID, purity and sterility of the virus are then assayed using standard methods.

General tissue culture/virus handling:

Never pour media or solutions

This is considered bad practice and potentially a route of cell culture contamination. A drop of medium remaining on the vessel's threads after pouring can form a liquid bridge when the cap is replaced forming a route of entry for microorganisms. If pouring cannot be avoided (hyperflasks only), remove any traces of media from the neck with an alcohol-soaked piece of blue roll.

If liquid gets into the threads of media/PBS/TrypLE bottles during use, wipe with an alcohol-soaked piece of blue roll.

Never remove spent supernatant from cells or pellets that are to be retained to waste by pouring.

Pouring should be avoided (see above). Pouring into the waste pots has the potential to 1) splash the microbiocidal agent into the material being retained and inactivate it; 2) cross contaminate the prep with virus material not completely inactivated in the waste pot.

Only handle one virus in the BSC.

Ensure cells infected with different viruses are handled separately in the biological safety cabinet, wiping the surface down and changing gloves between different vectors.

7.0 Reagents

CEF
DMEM Sigma D6546

Pen/Strep	Sigma
Glutamine	Sigma
PBS (without Ca^{2+} and Mg^{2+}) D8537	Sigma
FCS F2442	Sigma
Trypan blue stain T8154	Sigma
TrypLE Express I2605	Gibco
Neubaur haemocytometer	
10 mM Tris, 140 mM NaCl [pH7.8] J209	In house reagent

Premaster cell/media lysate

Cells and media from a T175 flask infected with material confirmed free from parental poxvirus by PCR. If this is the first time the virus has been made, the premaster will have been prepared from a plaque pick one round on from a plaque that passed QC PCR (for example plaque 1.1 is usually used if plaque 1 passed QC PCR). If this is a rebulk, the premaster is prepared by infection of a CEF T175 with cell lysate from the original premaster.

18.0 Equipment

Class II BioSafety Cabinet Mars	Scanlaf
Benchtop Centrifuge Megafuge 40	Heraeus
CO_2 incubator	
37°C water bath SUB6	Grant
Microscope DMIL	Leica
2 ml screw cap tubes.	
Corning conical tubes, 250 ml PP Centrifuge tube, plug seal cap CFT-900-021Y	Fisher
Bottle, Polyallomer, 250 mL, 60 x 120 mm 355627	Beckman Coulter
-80°C freezer Scientific U57085	New Brunswick
25 cm cell scrapers FB55198	Fisher
Storage bottle disposable with plug seal cap sterile TKV-185-030f	Fisher Scientific
50ml centrifuge tubes	
15 ml centrifuge tubes	
Dry ice	

19.0 Method

19.1 Preparing and infecting CEF with virus in 5 x T175 flasks (Master seed virus).

19.1.1 Prepare 5x T175 flasks/virus for a standard prep (adjust if a large prep is to be made).

19.1.2 Incubate (37°C, 5% CO_2) until ~90% confluent.

19.1.3 Thaw premaster cell lysate using water bath *(ensure material is only just thawed – do not leave in waterbath longer than necessary as prolonged incubation >RT will lead to proteolytic degradation of the virus particles).*

19.1.4 Prepare D2 media containing virus lysate by pipetting 140 ml D2 media per 5x T175 flask prep into an empty 250 ml conical tube. **Take 1ml of the premaster lysate and transfer to a 1.5 ml O-ring tube and store this at -80^{0}C as a premaster for future preps – this should be labeled with the stock number of the current prep and the date + operator.** Then add the remaining ~34 ml of the premaster lysate to the 250ml conical tube and mix by inverting bottle gently 5 times *(avoid bubble formation as this will potentially denature proteins on the virus surface and reduce infectivity)*

19.1.5 Aspirate the 10% FCS DMEM from the 5 x T175 flasks and replace with 35 ml of 2% FCS DMEM/virus suspension.

19.1.6 Incubate (37°C, 5% CO_2) until all cells are infected and beginning to show signs of CPE (3-5 days).

19.2 Harvesting virus.

19.2.1 Scrape off the virus-infected cells with the cell scraper and transfer everything, using a 25 ml pipette, into a 250 ml conical bottomed tube.

19.2.2 Balance the tubes and centrifuge them at 700 x g for 10 minutes to pellet cell debris.

19.2.3 Using 25 ml pipettes, transfer the supernatants to autoclaved 250 ml flat-bottom ultracentrifuge tubes and top up to the shoulder of the bottle* with PBS (using 1 x 100 ml bottle per virus) **Retain cell pellet.**

19.2.4 Balance ultracentrifuge tubes by weighing them all and adjusting to the lightest bottle by removing media.

19.2.5 Add 2 ml of 10 mM Tris, 140 mM Nacl [pH7.8] to the pelleted cell debris, resuspend thoroughly and transfer to a fresh 15 ml Falcon tube, rinse the 250 ml conical bottomed tube by adding a further 1 ml 10 mM Tris, 140 mM Nacl [pH7.8] rinsing and transferring to the 15 ml tube.

19.2.6 Top up the total volume of this tube to 5.5 ml.

*** These ultracentrifuge tubes must be filled to the shoulder of the bottle, otherwise the tubes can deform during a spin. If the fluid level is not high enough top up with PBS to the required level.**

Proceed with J019c. Alternatively, materials may be frozen at this stage.

Appendix XIV



1.0 Jenner Laboratory Protocol Number: J019c

2.0 Version Number: 01

3.0 Title: Purification of poxvirus master seed virus stock using a sucrose cushion

This protocol uses GMOs. All users MUST be registered with the University Occupational Health Service as set out in the University's health and safety regulations. Health surveillance is a legal requirement under COSHH.
If you are not currently registered with the Occupational Health Service for work GMOs, or need to check your registration, please contact the ORCRB NDM Personnel team.

4.0 Other Documents

MSDS refer to MSDS for the relevant safety information on the individual reagents:
\\Imsnw3_jenner_server\jenner\hill_group\Safety\COSHH assessments\Manufacturers material safety data sheets

Note: **Trypan blue solution** is a possible **carcinogen** and should be handled using the appropriate PPE

Risk assessments covering the use of poxviruses within the Jenner Institute are listed below and can be found in the safety folder on the s: drive or hard copies are available in the office area. These must be read and understood prior to commencing work using these viruses. In addition, the appendix to the GMO RA (R004) documents all of the antigens might be encoded by the poxviruses. These should be read and understood as relevant to the work being undertaken.

GMO RA R003 poxvirus
GMO RA R004 GM RA app
C052 use of sonicator
C030 Culturing primary cells and cell lines including freezing and reviving
J013 CEF culture

J018 plaque picking
J208 preparation of 36% sucrose
J209 preparation of 10mM Tris for MVA production

5.0 Definitions

CEF Chicken embryo fibroblasts
CPE Cytopathic effects
FCS Foetal calf serum
MVA Modified vaccinia Ankara
FP9 a plaque-purified, high passage attenuated, European strain of Fowlpox virus
DMEM Dulbecco's modified Eagle's media
GMO Genetically modified organism
RA Risk assessment

6.0 Objective

Large-scale preparation of MVA/FP9 requires the infection of CEF, the extraction of virus from the cell lysate and crude purification to remove cell debris from the sample. This protocol describes the purification through a sucrose cushion. Sucrose cushion purification separates the viral particles from the cell lysate. The potency, ID, purity and sterility of the virus are then assayed using standard methods.

Ensure cells infected with different viruses are handled separately in the biological safety cabinet, wiping the surface down and changing gloves between different vectors.

7.0 Reagents

10 mM Tris pH9, sterile
From 1M Tris pH 9 stock solution SIGMA T2819-100ml
36% w/v sucrose solution (in 10mM Tris pH9), (filter sterilised)
It is important that this material is low in endotoxins Fluka 84097

Viral material;
15 ml Falcon tube containing infected cell pellet resuspended in 10 mM Tris buffer
250 ml polyallomer ultracentrifuge bottle containing cleared tissue culture supernatant from 5 x T175 flasks

20.0 Equipment

Class II BioSafety Cabinet Scanlaf Mars
Benchtop Centrifuge Heraeus Magefuge 40

CO_2 incubator Galaxy R	RS Biotech
37°C water bath SUB6	Grant
Industrial methylated spirit (IMS) M/4400/17	Fischer
2 ml screw cap tubes.	
Tube, Thinwall, Ultra-Clear™, 14 ml, 14 x 95 mm *These actually have a max capacity of 13 ml* 344060	Beckman Coulter
Corning conical tubes, 250 ml PP Centrifuge tube, plug seal cap CFT-900-021Y	Fisher
Bottle, Polyallomer, 250 mL, 60 x 120 mm 355627	Beckman Coulter
Cup-horn Sonicator	Sonics and
Materials	
Sterile transfer pipette (pastette)	
-80°C freezer	New Brunswick
Scientific U57085	
15 ml centrifuge tubes	
Dry ice	
Optima L-80 XP Ultracentrifuge	Beckman Coulter
Type 19 fixed-angle centrifuge rotor	Beckman Coulter
SW40 Ti rotor	

21.0 Method

21.1.1 Centrifuge the tubes from J019b step 9.2.3 (33 000 x g, 60 min, 4°C) using ultracentrifuge and Type 19 rotor.

21.1.2 During the 60 min centrifugation, process the cell debris from J019b step 9.2.4.

21.1.3 Freeze the pellets on dry ice, thaw in 37°C water bath and vortex for 10 seconds such that the debris forms a monodisperse suspension.

21.1.4 Repeat freeze/thaw/vortex.

21.1.5 Place samples on dry ice until the ultracentrifuge spin begins to decelerate.

21.1.6 Thaw samples and vortex for 10 seconds.

21.1.7 Sonicate samples for 1 minute, 57 Hz. *(Switch on the sonicator, connect the lower pipe of the tube holder to the cold tap water and drain the upper pipe just in the sink, keep the tube in the holder and push the start button. After finishing disconnect everything and turn the sonicator off).*

21.1.8 Centrifuge the 15 ml tube (700 x g, 5 min).

21.1.9 Aspirate the supernatant from the 250 ml ultracentrifuge bottle.

21.1.10 Add the supernatant from the 15 ml tube to the virus pellet, Resuspend thoroughly and transfer virus suspension to a 15 ml Falcon tube.

21.1.11 This material can be stored at -20°C.
21.1.12 Clean the 250ml flat-bottomed tubes according to step 9.2.17.

21.2 **Purification through 36% w/v sucrose cushion.**

21.2.1 If previously frozen: thaw the impure virus in 37°C water bath and vortex for 10 seconds.
21.2.2 Ensure no clumps are present in the virus suspension – centrifuge samples (1000 x g, 5 min, 4°C)
21.2.3 For each 5 x T175 flask prep, use one ~7.5 ml sucrose cushion.
21.2.4 Prepare the ultracentrifuge buckets by placing in the biological safety cabinet, spray the bucket lids with 70% ethanol and leave to evaporate at the back of the hood. Spray the internal surfaces of buckets of the SW40 rotor with 70% ethanol, turn upside-down to drain and then place inside the virus lab biological safety cabinet to allow residual ethanol to evaporate.
21.2.5 Add 7.5 ml of 36% sucrose (in 10 mM Tris, 140 mM NaCl [pH7.8] to a 13 ml thin-walled ultracentrifuge tube.
21.2.6 Layer the virus solution (max. volume of 5.5 ml for this size centrifuge tube) onto the top of the sucrose, slowly and carefully with a sterile transfer pipette without disturbing the sucrose layer.
21.2.7 If preparing multiple viruses, seal the first tube, wipe down the surfaces and change gloves before loading the second virus.
21.2.8 Place the ultracentrifuge tubes inside the buckets and balance using the balance scale.
21.2.9 Centrifuge at 30 000 x g, 4°C for 2 hours using the Optima L-80 XP Ultracentrifuge. During the centrifuge run prepare the top and side labels for the vials of purified virus – tubes should be fully labeled and placed in the virus lab fridge before the run is finished.
21.2.10 Remove and discard the supernatant carefully using the aspirator – remove the top of the upper layer first to ensure this does not contact the purified pellet at the base of the tube.
21.2.11 Re-suspend the pellet in 10 mM Tris, 140 mM NaCl [pH7.8] in a total volume of 800 µl.
21.2.12 Transfer the virus to a 2 ml screw cap tube.
21.2.13 Wash the centrifuge tube with ~300 µl of 10 mM Tris, 140 mM NaCl [pH7.8] and transfer this to the screw cap tube.
21.2.14 Sonicate the tube (1 min, 57 Hz)
21.2.15 Vortex the tube for 10 sec.
21.2.16 Carefully aliquot the virus into 2ml screw-capped vials:

- **First, transfer 6 x 10 µl into vials and transfer to the -80°C freezer in immunology. These aliquots are used**

for viral titration and PCR.

- **Aliquot 10ul into a single vial and place in the virus lab fridge for sterility testing.**
- **Split the remainder into 200 µl aliquots and place these in the -80°C freezer in immunology. Note the number of aliquots for entry into the virus database.**

21.2.17 Immerse the centrifuge buckets and tubes in a container containing 10% Distel for a maximum of 10 min, rinse thoroughly 4 times with tap water and then 15MΩ Elga water. The centrifuge bottles with plug seal caps should be placed in autoclave bags (unassembled) and sent for autoclaving. **The screw-on lids should NOT be autoclaved.**
Centrifuge buckets are allowed to air-dry – do not put lids on the buckets, leave them loose on the holder to allow and residual water to evaporate.

21.3 Database maintenance

Virus storage (s:Reagent storage info/virus storage/virus stock database)

Account name: user
Password: virus
Add new record and fill in details.

MVA production chart: (S:\VIRUS PRODUCTION RECORDS)

22.0 Revision History

Version Number	What changed and Why it Changed	Who Changed it	Date changed
01	**N/A**	**Ali Turner**	
02	**Method simplified to enable efficient handling of multiple viruses. Tris buffer altered to 10mM Tris, 140mM NaCl, pH7.8**	**Ali Turner**	**24th Feb 2015**

Notes:
MVA IMV and EEV can also be purified using CsCl gradients (IMV and EEV sediment at 1.27 and 1.23 g/ml respectively). However, sucrose cushion is much less expensive.
We perform only a single round of purification through sucrose (a single 36% w/v sucrose centrifugation). This generates a pellet that contains both virus and cell debris.
A further purification step is possible using a sucrose gradient (40%, 36%, 32%, 28% and 24%) that is left for 2.5 hr to diffuse and then overlaid with virus from the first purification step. Centrifugation is performed (19 000 x g, 50 min, 4°C)

Appendix XV



1.0 Jenner Laboratory Protocol Number: J082

2.0 Version Number: 06

3.0 Title: Poxvirus titration using CEF in 6-well plates.

This protocol uses GMOs. All users MUST be registered with the University Occupational Health Service as set out in the University's health and safety regulations. Health surveillance is a legal requirement under COSHH.
If you are not currently registered with the Occupational Health Service for work GMOs, or need to check your registration, please contact the ORCRB NDM Personnel team.

4.0 Other Documents

MSDS refer to MSDS for the relevant safety information on the individual reagents:
\\Imsnw3_jenner_server\jenner\hill_group\Safety\COSHH assessments\Manufacturers material safetly data sheets
R003 Poxvirus Risk Assessment
\\Imsnw3_jenner_server\jenner\hill_group\Safety\GMO RA\R003 poxvirus.doc
J013 CEF culture
J019 Bulking up poxviruses
C009 MVA Immunostaining Titre
C010 MVA X-Gal Liquid Stain Titre
C030 Culturing primary cells and cell lines including freezing and reviving
C024 Use of penicillin for tissue culture by sensitised individuals

5.0 Definitions

CEF Chicken embryonic fibroblasts
FCS foetal calf serum
DMEM Dulbecco's modified Eagle's media
MVA Modified vaccinia Ankara
LMP Low melting point

CMC Carboxymethylcellulose
x-gal 5-bromo-4-chloro-3-indoyl-beta-D-galactoside
DAB 3,3'-Diaminobenzidine

6.0 Objective

To titrate a preparation of recombinant MVA using CEF in 6-well plates. Method is given for screening by microscopy for fluorescent marker- expressing recombinant poxvirus. Each virus preparation should be tested in quadruplicate: Two different CEF preps are used at different passage number (i.e. seed 6-well plates from fresh CEF and the previous week's delivery). Two separate serial dilutions are titrated on each cell batch. A single concentration of a reference virus should be titred at the same time. Therefore, plate one 6-well plate of each cell batch for the virus titration and on a separate plates seed two wells with each cell batch for the reference virus.

7.0 Reagents

1 x 6 well plate containing 90% confluent CEF per virus to be titred

DMEM Sigma
D6546
100x Pen/Strep solution
(10,000 units penicillin-G and 10 mg strep per ml) Sigma
P0781
200 mM Glutamine Sigma
G7513
FCS Sigma
F2442
2 x MEM without phenol red Gibco
21935
2% LMP agarose in dH_20 (heat sterilised) Sigma
A9414
CMC high viscosity BDH#
279294T
0.2% Triton-X 100 in PBS
low gelling temperature agarose (Type VII)
ImmPACT DAB (3,3'-Diaminobenzidine) + Vector Labs
SK-4105
Liquid Chromogen Stain & Diluent
Pre-Sept tablet ASP
SPR25
Primary antibody: Rabbit anti-Vaccinia Virus ISL
126-1063
Secondary antibody: Anti-Rabbit HRP Conjugated GE Healthcare
NA934V
(from Donkey)

Reagents stored in molecular biology lab

16% Paraformaldehyde Alfa Aesar	43368
10x PBS Sigma	P-4417
0.5M $K_4Fe(CN)_6.3H_2O$ Sigma	P9387
0.5M $K_3Fe(CN)_6$ Sigma	P8131
1M $MgCl_2$ Sigma	M2393
18.2MΩ/cm ultrapure water Elga	

do not substitute for alternative supplier. This product has been found to be lower in endotoxins levels than those from other suppliers.

Reagent Recipes:

Complete 2% (10%) FCS DMEM:

500 ml DMEM	
10 (50 ml) ml FCS	(2% (10%) final conc)
5 ml Pen/strep	(100 U Penicillin, 0.1 mg strep ml^{-1} final conc)
10 ml L-glutamine	(4 mM final conc)

4% FCS 2xMEM:

250 ml 2xMEM	
10 ml FCS	(4% final conc)
5 ml Pen/strep	(200 U Penicillin, 0.2 mg strep ml^{-1} final conc)
10 ml L-glutamine	(8 mM final conc)

4% Paraformaldehyde in PBS:

In the fume hood dilute 16% paraformaldehyde solution 1:4 in sterile PBS. Break the ampoule open with care and dispose of glass in a sharps bin.

0.2% Triton X-100 in PBS:

Disolve 100ul Triton X-100 in 50ml sterile PBS. Cut of end of pipette tip to dispense this viscous detergent.

X-Gal Liquid Staining Solution:

Stock solutions (prepare and store in mol biol lab) :

$K_3Fe(CN)_6$ 0.5M: dissolve 1.64g in 10 ml H_20

$K_4FE(CN)_6.3H_2O$ 0.5M: dissolve 2.112g in 10 ml H_20

$MgCl_2$ 1M: dissolve 2.033g $MgCl_2.6\ H_20$ in 10 ml H_20

[These solutions are stable at room temp for at least 6 months if protected from light.]

Per plate (make fresh – each plate requires 6 ml solution) – 9.73 ml H_20, 0.1 ml 0.5 M $K_3Fe(CN)_6$, 0.1 ml 0.5M $K_4FE(CN)_6$. $3H_2O$, 20 µl 1M $MgCl_2$, 50µl 50mg/ml X-Gal in DMF.
[Note: X-Gal concentration may be increased 2-3 fold for better plaque visualisation if required]

1.0 Equipment

Class II BioSafety Cabinet Mars	Scanlaf
CO_2 incubator Galaxy R	RS Biotech
37°C water bath SUB6	Grant
Microscope DMIL	Leica
6-well tissue culture plates	
Benchtop Centrifuge Allegra X-12R	Beckman Coulter
Disposable haemocytometer	
Multipette repeat pipettor Stream	Eppendorf
10 ml pipette tips	Eppendorf
1.5 ml microcentrifuge tubes (heat sterilised)	
10 µl filter tips	
200 µl filter tips	
1000 µl filter tips	
Vacuum aspirator	
Aspirator pipettes	
5, 10 and 25 ml serological pipettes	
Vortex	
1000mL waste bottle & lid (Duran) marked for Formaldehyde waste	

2.0 Method

2.1 Prepare a 6 well plate per virus with 1 x 10^6 CEF per well in 2 ml 10% FCS DMEM for use the next day or 0.5 x 10^6 CEF per well in 2 ml 10% FCS DMEM for use 2 days later.

2.2 Incubate (37°C, 5% CO_2) overnight.

2.3 Aspirate the 10% FCS DMEM using a 200 µl aspirating tip and replace with 1 ml of 2% FCS DMEM. Incubate (37°C, 5% CO_2) until required.

2.4 Label sufficient sterile, 1.5 ml microcentrifuge tubes for the following dilutions, in duplicate for each virus:

	Virus stock	10^{-2}	10^{-4}	10^{-6}	10^{-7}	10^{-8}
Virus (µl)	Stock	10	10	10	100	100
2% DMEM (µl)	-	990	990	990	900	900

2.5 Add the required volume of 2% FCS DMEM to each tube using the multipipettor.

2.6 Thaw the virus (es) to be titred and add 10 µl of the stock to the first tube of the series. Continue to prepare the dilution series as shown in the table above. **N.B**. **vortex every preparation of the new dilution for 3 seconds and change pipette tips for every dilution.**

2.7 Prior to addition of virus dilutions to wells, re-vortex those samples that will be added to the plates. Virus particles will settle of the tubes are not used immediately.

2.8 Add 100 µl of the appropriate viral dilutions to the relevant wells of the 6-well plate as shown below:

Series 1: 10^{-6}	Series 1: 10^{-7}	Series 1: 10^{-8}
Series 2:10^{-6}	Series 2:10^{-7}	Series 2: 10^{-8}

Ref at 5^{-5}	Ref at 10^{-6}	Ref at 5 x 10^{-6}
Ref at 5^{-5}	Ref at 10^{-6}	Ref at 5 x 10^{-6}

Once 100 µl of sample has been added, mix evenly in well by repeated movements left/right and forward/backwards. **DO NOT** swirl plates, this will lead to plaques concentrated around the sides of the wells.

2.9 Incubate at 37ºC (+/- 2ºC) + 5% CO_2 for 1 hour.

2.10 Proceed with either Agarose or CMC overlay:

Agarose overlay:

2.11 During the incubation, take the bottle of 2% LMP agarose (stored in the tissue culture lab) to melt (2-3 minutes on high power in the microwave in the mol. biol. lab). Transfer required amount of agarose to 50 ml Falcon tubes in the tissue culture lab biological safety cabinet. Pass the Falcon tubes through to the virus lab and place in the water bath at 37°C for at least 15 minutes.

2.12 Place the 4% FCS MEM in 37°C water bath in the virus lab.

2.13 Aspirate the culture medium from the wells (do not allow cells to dry out).

2.14 Pour 4% FCS MEM into an equal volume of 2% low melting point agarose in 50 ml Falcon tube *(note: add FCS MEM to the agarose to prevent agarose setting in the 50 ml Falcon tube as it is poured).*

2.15 Quickly pipette 2 ml per well of this mixture (to prevent the agarose solidifying).
2.16 Incubate for 2-4 days and count the plaques under fluorescent microscope.

CMC overlay:

2.17 Mix sufficient D2 media and CMC in a ratio 2/3 D2:1/3 CMC for 2 ml per well required.
2.18 Aspirate media containing virus using a 200 μl aspirating tip.
2.19 Replace with 2 ml D2/CMC overlay per well.
2.20 Incubate for 2-4 days and count the plaques as below:

3.0 GFP-expressing virus

3.1 Count the number of plaques in duplicate wells containing 50 - 100 plaques per well.

4.0 β-galactosidase-expressing virus:

4.1 Remove the fluid from the wells with the Vacusafe aspirator and 200 μl aspirating tips.
4.2 Fix the cells with 1 ml per well of paraformaldehyde (4% in PBS) for 5 min at room temperature.
4.3 Remove the fixative **with a pipette to the Formaldehyde waste bottle**.
4.4 Wash once with approximately 2 ml per well of PBS and remove using a pipette and place in formaldehyde waste bottle.
4.5 Add 1 ml X-Gal liquid staining solution per well. Leave for 1 hour.
4.6 Aspirate staining solution and wash cells with approx 2 ml per well PBS, then aspirate using Vacusafe pipetter/aspirator.
4.7 Plates may be inverted over a light background for counting blue plaques by eye (circle plaques with a marker pen on wells with between approximately 50 - 100 plaques for an accurate count)
4.8 If there is any uncertainty about whether a plaque is independent or a merge of two, this can be checked under a microscope (Note: plates may be photographed at this stage if required) Record results.
4.9 Dispose of plates as for normal virus contaminated waste.

5.0 Immunostaining

5.1 Remove the fluid from the wells with the Vacusafe aspirator
5.2 Fix the cells with approximately 1 ml per well of paraformaldehyde (4% in PBS) for 5 min at room temperature.
5.3 Remove the fixative **with a pipette to the formaldehyde waste bottle**.
5.4 Wash once with 2 ml per well of PBS. Again remove waste with a pipette to formaldehyde waste bottle.

5.5 Permeabilise cells with 0.2% Triton X-100 in PBS. Add 1ml per well for 5 min at room temperature. Aspirate waste
5.6 Wash cells twice with 2 ml per well PBS using Vacusafe aspirator.
5.7 Block with 1 ml per well PBS + 3% FCS and incubate for 1 hr at room temperature
5.8 Remove PBS + 3% FCS using Vacusafe aspirator.
5.9 Prepare 1ml per well of primary antibody diluted 1:1000 in PBS + 3% FCS
5.10 Add 1 ml of the primary antibody per well and incubate for 1 hr at room temperature.
5.11 Remove antibody solution and wash twice with approximately 2 ml of PBS per well. Remove using Vacusafe aspirator
5.12 Prepare the secondary HRP-conjugated antibody by diluting 1:300 in PBS + 3% FCS.
5.13 Add 1 ml of secondary antibody solution per well. Incubate for 45 minutes.
5.14 Remove the antibody solution and wash twice with approximately 2 ml of PBS per well. Remove using Vacusafe aspirator
5.15 Make up the DAB Liquid Chromagen developing solution: (allow 1ml per well) add one drop of Chromogen liquid to every 1 ml of DAB Liquid buffer solution that is required and mix well. (Always make up this solution fresh)
5.16 Add 1 ml of developing solution per well. Plaques will stain a distinct brown colour. Leave for ~10 min.
5.17 Discard solution into a glass bottle (marked DAB waste) containing one Pre-Sept tablet (leave bottle over night and discard contents with plenty of water down sink the next day).
5.18 Wash plates gently with approximately 2 ml tap water per well.
5.19 Allow plates to dry for half hour in air. Ideally leave upside down on a paper towel.
5.20 Count the number of plaques in duplicate wells containing 50 - 100 plaques per well.

8.0 Determination of Titre (pfu/ml)

8.1 Count the number of plaques in duplicate wells containing 50 - 100 spots per well.
8.2 Use the following formula to determine the titre in pfu/ml:

"*average number of spots*" x "*serial dilution*" x "*dilution factor*" = "*x*" pfu/ml

$$\text{e.g. } \frac{(36+40)}{2} = 38 \times (1\times10^{7}) \times 10 = 3.8 \times 10^{9} \text{ pfu/ml}$$

9.0 Database maintenance

9.1 Virus storage (s:Reagent storage info/virus storage/virus stock database)

Account name: user
Password: virus
Add new record and fill titre details.

9.2 MVA production chart: (s:Technical group meetings/vector core meetings/MVA production chart).
Add virus titre to relevant entry

10.0 Revision History

Version Number	What Changed	Who Changed it	Date changed
01	**First written**	**A.Turner**	
02	**Risk assessment referred to and CMC overlay option added**	**A.Turner**	
03	**Reference dilutions and dilution mixing clarified**	**S. Elias**	
04	**Changed to include FP9**	**Ali Turner**	
05	**FP9 removed to separate protocol. Counting using fluorescence microscope, X-gal staining and immunostaining merged to one protocol.**	**Ali Turner**	**23.08.10**
06	**Safety data added**	**S. Morris**	**19.04.11**

Appendix XVI

Primers used in the production of recombinant haemagglutinin constructs

Sequence identifier	Sequence (5'-3')
tPA_F	CACGTGTGATCAGATATCG
His_R	GGCACAGCAGATCTGAATT

Appendix XVII

Sequence of pCMV/R expression vector

gatctgctgtgccttctagttgccagccatctgttgtttgcccctcccccgtgccttccttgaccctggaaggtgc

cactcccactgtcctttcctaataaaatgaggaaattgcatcgcattgtctgagtaggtgtcattctattctgggg

ggtggggtggggcaggacagcaaggggaggattgggaagacaatagcaggcatgctggggatgcg

gtgggctctatgggtacccaggtgctgaagaattgacccggttcctcctgggccagaaagaagcaggcac

atccccttctctgtgacacaccctgtccacgcccctggttcttagttccagccccactcataggacactcatag

ctcaggagggctccgccttcaatcccacccgctaaagtacttggagcggtctctccctccctcatcagccca

ccaaaccaaacctagcctccaagagtgggaagaaattaaagcaagataggctattaagtgcagaggga

gagaaaatgcctccaacatgtgaggaagtaatgagagaaatcatagaattttaaggccatgatttaaggc

catcatggccttaatcttccgcttcctcgctcactgactcgctgcgctcggtcgttcggctgcggcgagcggta

tcagctcactcaaaggcggtaatacggttatccacagaatcaggggataacgcaggaaagaacatgtga

gcaaaaggccagcaaaaggccaggaaccgtaaaaaggccgcgttgctggcgtttttccataggctccgc

ccccctgacgagcatcacaaaaatcgacgctcaagtcagaggtggcgaaacccgacaggactataaa

gataccaggcgtttcccccctggaagctccctcgtgcgctctcctgttccgaccctgccgcttaccggatacct

gtccgcctttctcccttcgggaagcgtggcgctttctcatagctcacgctgtaggtatctcagttcggtgtaggtc

gttcgctccaagctgggctgtgtgcacgaacccccccgttcagcccgaccgctgcgccttatccggtaactat

cgtcttgagtccaacccggtaagacacgacttatcgccactggcagcagccactggtaacaggattagca

gagcgaggtatgtaggcggtgctacagagttcttgaagtggtggcctaactacggctacactagaagaac

agtatttggtatctgcgctctgctgaagccagttaccttcggaaaaagagttggtagctcttgatccggcaaa

caaaccaccgctggtagcggtggtttttttgtttgcaagcagcagattacgcgcagaaaaaaaggatctca

agaagatcctttgatcttttctacggggtctgacgctcagtggaacgaaaactcacgttaagggattttggtca

tgagattatcaaaaaggatcttcacctagatccttttaaattaaaaatgaagttttaaatcaatctaaagtatat

atgagtaaacttggtctgacagttaccaatgcttaatcagtgaggcacctatctcagcgatctgtctatttcgttc

atccatagttgcctgactcgggggggggggcgctgaggtctgcctcgtgaagaaggtgttgctgactcat

accaggcctgaatcgccccatcatccagccagaaagtgagggagccacggttgatgagagctttgttgta

ggtggaccagttggtgattttgaacttttgctttgccacggaacggtctgcgttgtcgggaagatgcgtgatctg

atccttcaactcagcaaaagttcgatttattcaacaaagccgccgtcccgtcaagtcagcgtaatgctctgcc

agtgttacaaccaattaaccaattctgattagaaaaactcatcgagcatcaaatgaaactgcaatttattcat

atcaggattatcaataccatatttttgaaaaagccgtttctgtaatgaaggagaaaactcaccgaggcagttc

cataggatggcaagatcctggtatcggtctgcgattccgactcgtccaacatcaatacaacctattaatttcc

cctcgtcaaaaataaggttatcaagtgagaaatcaccatgagtgacgactgaatccggtgagaatggcaa

aagcttatgcatttctttccagacttgttcaacaggccagccattacgctcgtcatcaaaatcactcgcatcaa

ccaaaccgttattcattcgtgattgcgcctgagcgagacgaaatacgcgatcgctgttaaaaggacaattac

aaacaggaatcgaatgcaaccggcgcaggaacactgccagcgcatcaacaatattttcacctgaatcag

gatattcttctaatacctggaatgctgttttcccggggatcgcagtggtgagtaaccatgcatcatcaggagta

cggataaaatgcttgatggtcggaagaggcataaattccgtcagccagtttagtctgaccatctcatctgtaa

catcattggcaacgctacctttgccatgtttcagaaacaactctggcgcatcgggcttcccatacaatcgata

gattgtcgcacctgattgcccgacattatcgcgagcccatttatacccatataaatcagcatccatgttggaat

ttaatcgcggcctcgagcaagacgtttcccgttgaatatggctcataacacccttgtattactgtttatgtaag

cagacagttttattgttcatgatgatatatttttatcttgtgcaatgtaacatcagagattttgagacacaacgtgg

ctttcccccccccccccattattgaagcatttatcagggttattgtctcatgagcggatacatatttgaatgtattta

gaaaaataaacaaatagggttccgcgcacatttccccgaaaagtgccacctgacgtctaagaaaccatt

attatcatgacattaacctataaaaataggcgtatcacgaggccctttcgtctcgcgcgtttcggtgatgacgg

tgaaaacctctgacacatgcagctcccggagacggtcacagcttgtctgtaagcggatgccgggagcag

acaagcccgtcagggcgcgtcagcgggtgttggcgggtgtcggggctggcttaactatgcggcatcagag

cagattgtactgagagtgcaccatatgcggtgtgaaataccgcacagatgcgtaaggagaaaataccgc

atcagattggctattggccattgcatacgttgtatccatatcataatatgtacatttatattggctcatgtccaaca

ttaccgccatgttgacattgattattgactagttattaatagtaatcaattacgggaacttccatagcccatatat

ggagttccgcgttacataacttacgggaatttccaaacctggctgaccgcccaacgacccccgcccattga

cgtcaataatgacgtatgttcccatagtaacgccaatagggaacttccattgacgtcaatgggtggagtattt
acggtaaactgcccacttgggaatttccaagtgtatcatatgccaagtacgccccctattgacgtcaatgac
gggaacttccataagcttgcattatgcccagtacatgaccttatgggaatttcctacttggcagtacatctacgt
attagtcatcgctattaccatggtgatgcggttttggcagtacatcaatgggcgtggatagcggtttgactcac
gggaacttccaagtctccaccccattgacgtcaatgggagtttgttttgactcaccaaaatcaacgggaattc
ccaaaatgtcgtaacaactccgccccattgacgcaaatgggcggtaggcgtgtacggtgggaggtctatat
aagcagagctcgtttagtgaaccgtcagatcgcctggagacgccatccacgctgttttgacctccatagaa
gacaccgggaccgatccagcctccatcggctcgcatctctccttcacgcgcccgccgccctacctgaggc
cgccatccacgccggttgagtcgcgttctgccgcctcccgcctgtggtgcctcctgaactgcgtccgccgtct
aggtaagtttaaagctcaggtcgagaccgggcctttgtccggcgctcccttggagcctacctagactcagcc
ggctctccacgctttgcctgaccctgcttgctcaactctagttaacggtggagggcagtgtagtctgagcagt
actcgttgctgccgcgcgcgccaccagacataatagctgacagactaacagactgttcctttccatgggtctt
ttctgcagtcaccgtcgtcgacacgtgtgatcagatatcgc

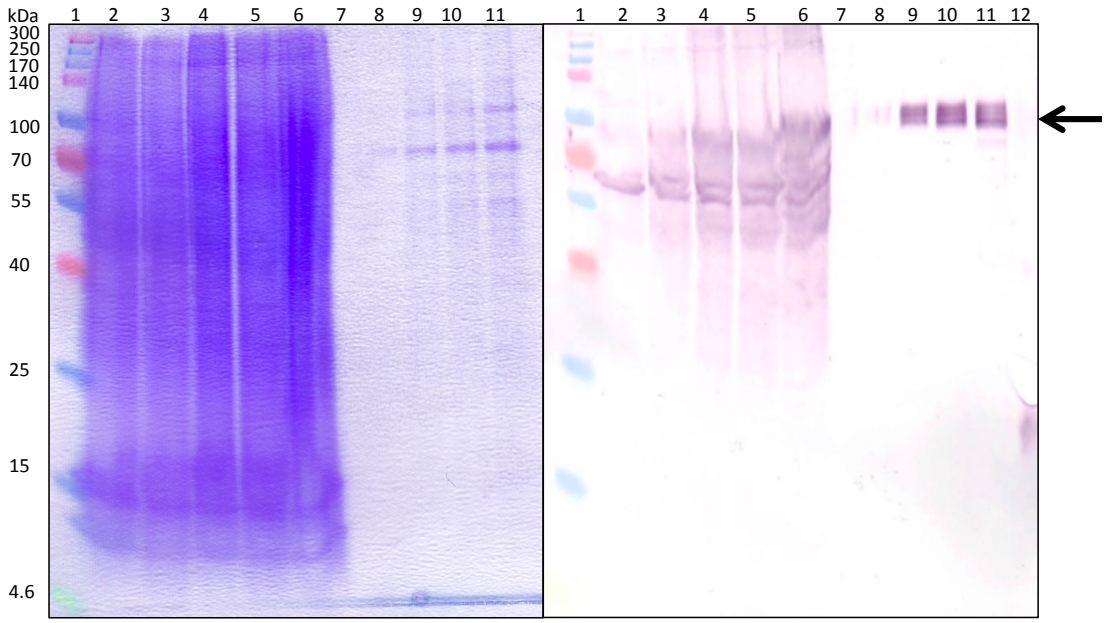
Appendix XVIII

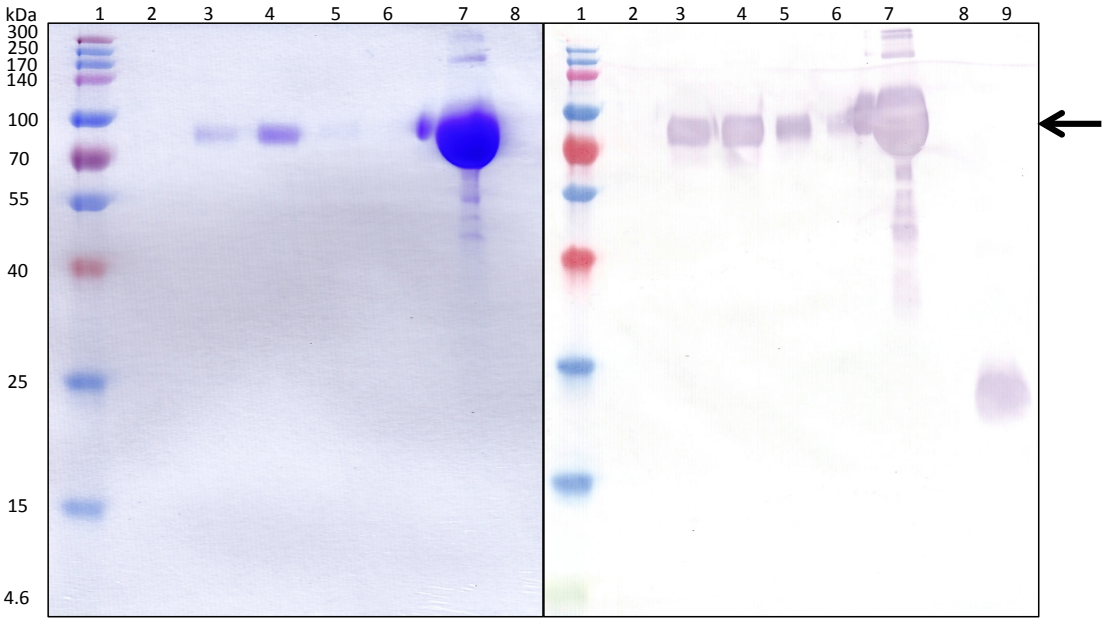
Protein expression and purification analysis

Cell pellet and supernatant samples were collected every 24 hours and examined for protein expression by reducing SDS-PAGE and Western blot using a monoclonal anti-his antibody for detection (top panel). Molecular mass in kilodaltons is shown to the left. The estimated or apparent molecular mass for each construct is indicated by an arrow. Lane 1 = molecular weight standard, lane 2 = cell pellet, 0h; lane 3 = cell pellet, 24h; lane 4 = cell pellet, 48h; lane 5 = cell pellet, 72h; lane 6 = cell pellet, 96h; lane 7 = cell supernatant, 0h; lane 8 = cell supernatant, 24h; lane 9 = cell supernatant, 48h; lane 10 = cell supernatant, 72h; lane 11 = cell supernatant, 96h; lane 12 = positive polyhistidine-tagged control.

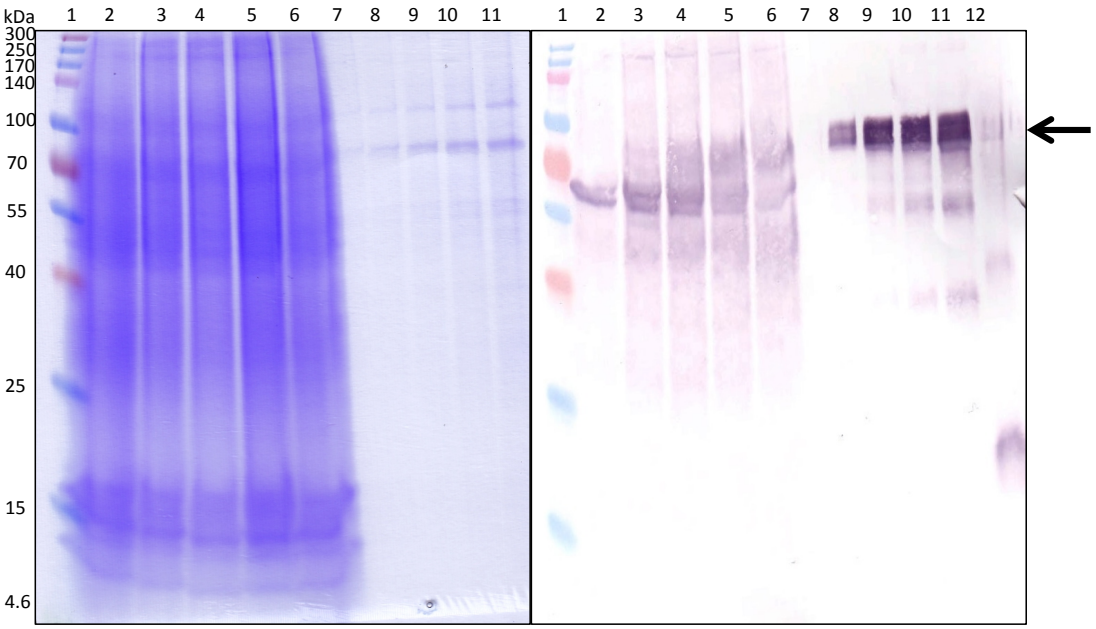
Eluted column fractions were examined for protein by reducing SDS-PAGE and Western blot using a monoclonal anti-his antibody for detection (bottom panel). Molecular mass in kilodaltons is shown to the left. The estimated or apparent molecular mass for each construct is indicated by an arrow. Lane 1 = molecular weight standard, lane 2 = first fraction; lane 3 = second fraction; lane 4 = third fraction; lane 5 = fourth fraction; lane 6 = fifth fraction; lane 7 = concentrated protein sample; lane 8 = Amicon Ultra centrifugal filter unit eluent; lane 9 = positive polyhistidine-tagged control.

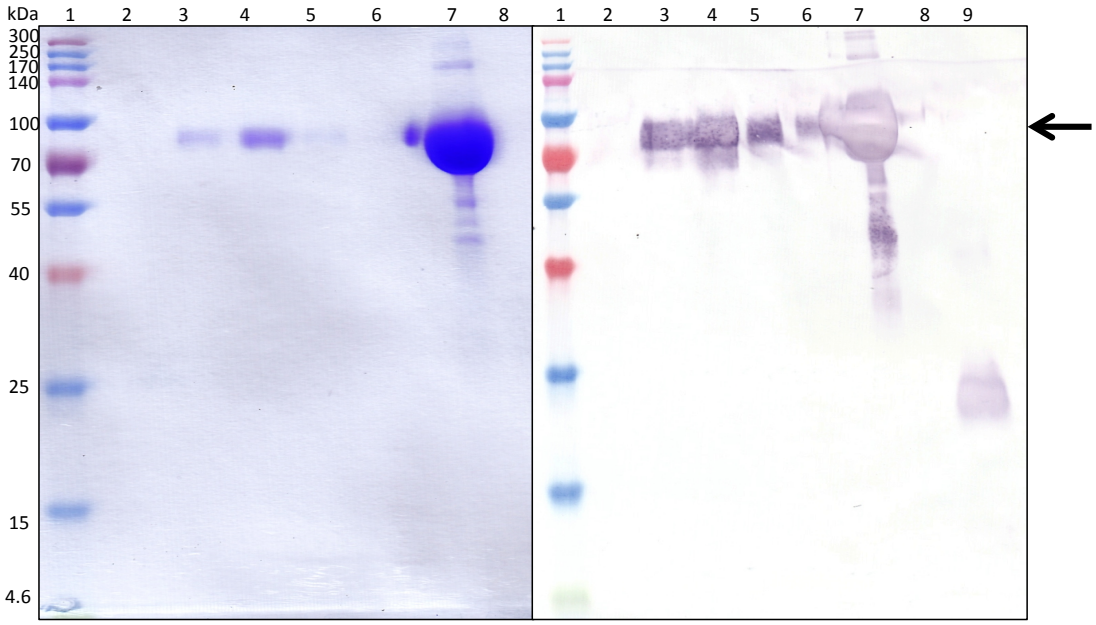
i. H1HA


kDa
1 2 3 4 5 6 7 8 9 10 11
1 2 3 4 5 6 7 8 9 10 11 12
300
250
170
140
100
70
55
40
25
15
4.6

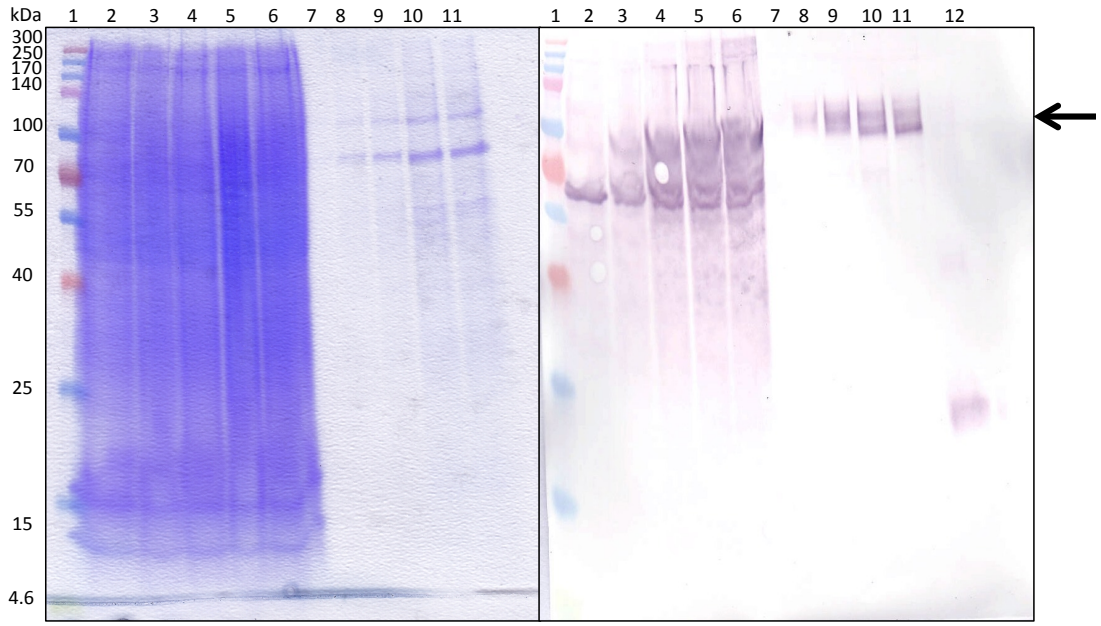

kDa
1 2 3 4 5 6 7 8
1 2 3 4 5 6 7 8 9
300
250
170
140
100
70
55
40
25
15
4.6

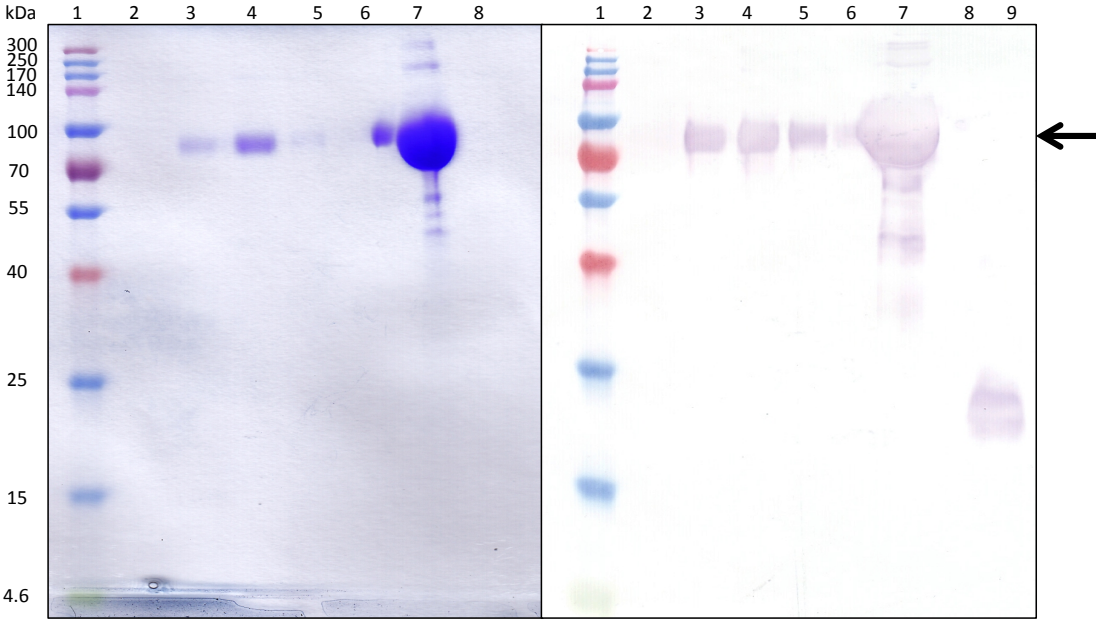
ii. H7HA


kDa
1 2 3 4 5 6 7 8 9 10 11
1 2 3 4 5 6 7 8 9 10 11 12
300
250
170
140
100
70
55
40
25
15
4.6

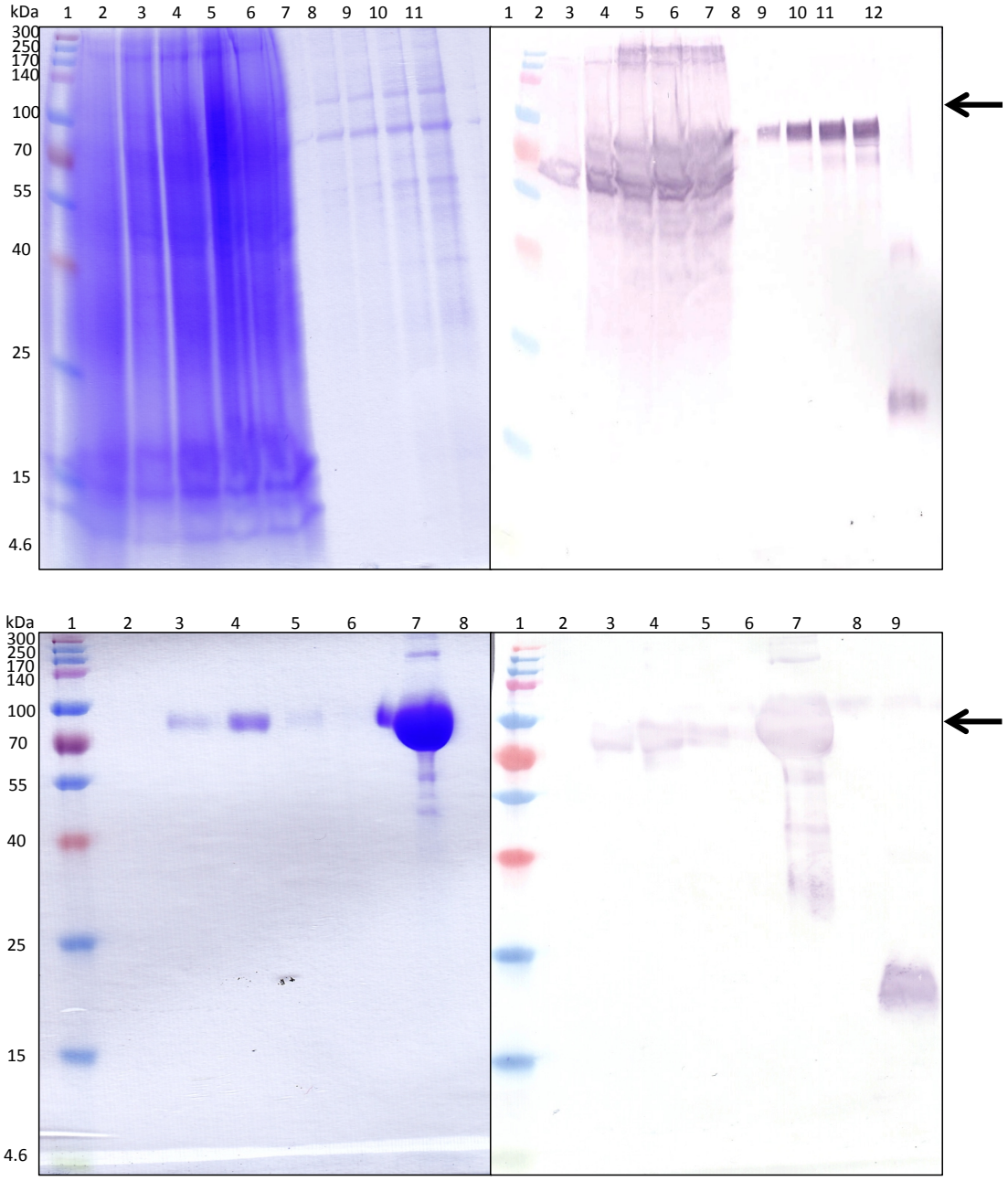

kDa
1 2 3 4 5 6 7 8
1 2 3 4 5 6 7 8 9
300
250
170
140
100
70
55
40
25
15
4.6

iii. cH9/H1

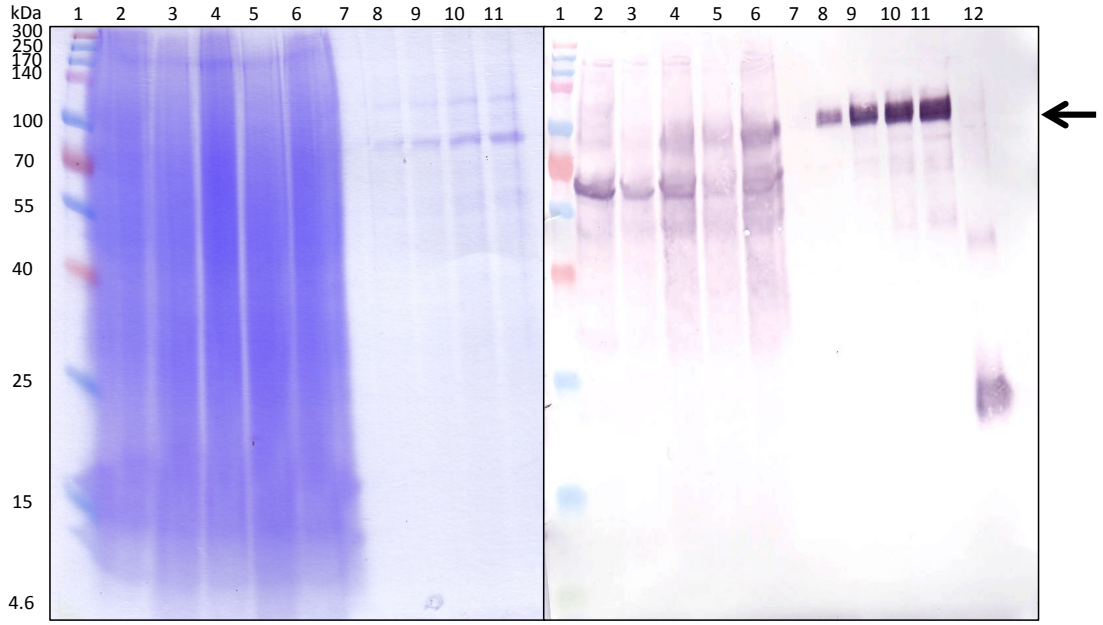

kDa
1 2 3 4 5 6 7 8 9 10 11
1 2 3 4 5 6 7 8 9 10 11 12
300
250
170
140
100
70
55
40
25
15
4.6

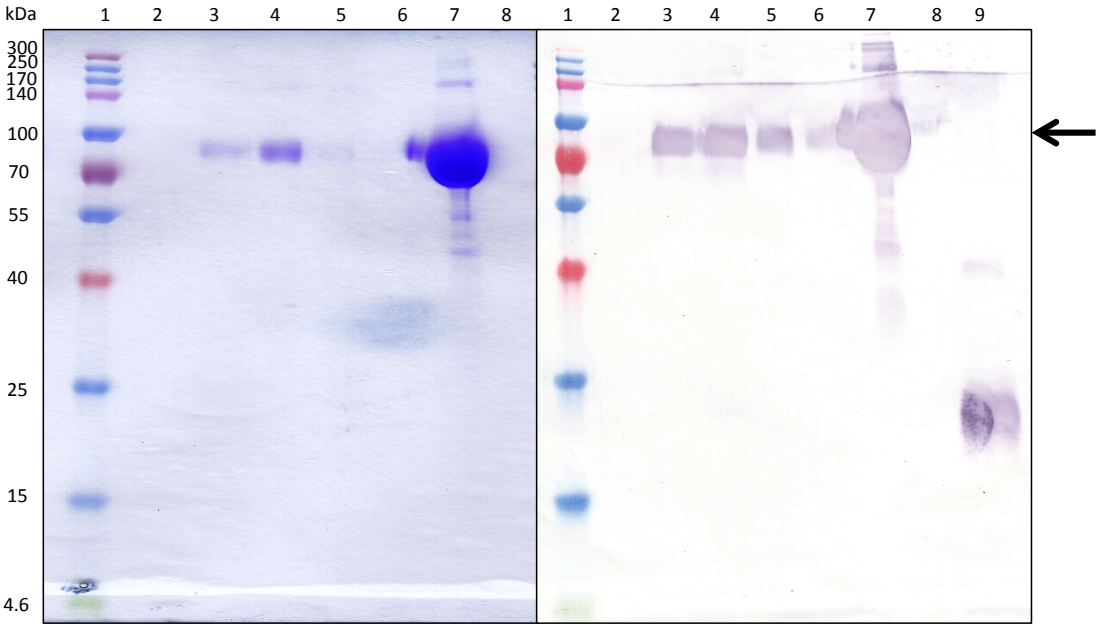

kDa
1 2 3 4 5 6 7 8
1 2 3 4 5 6 7 8 9
300
250
170
140
100
70
55
40
25
15
4.6

iv. cH16/H1

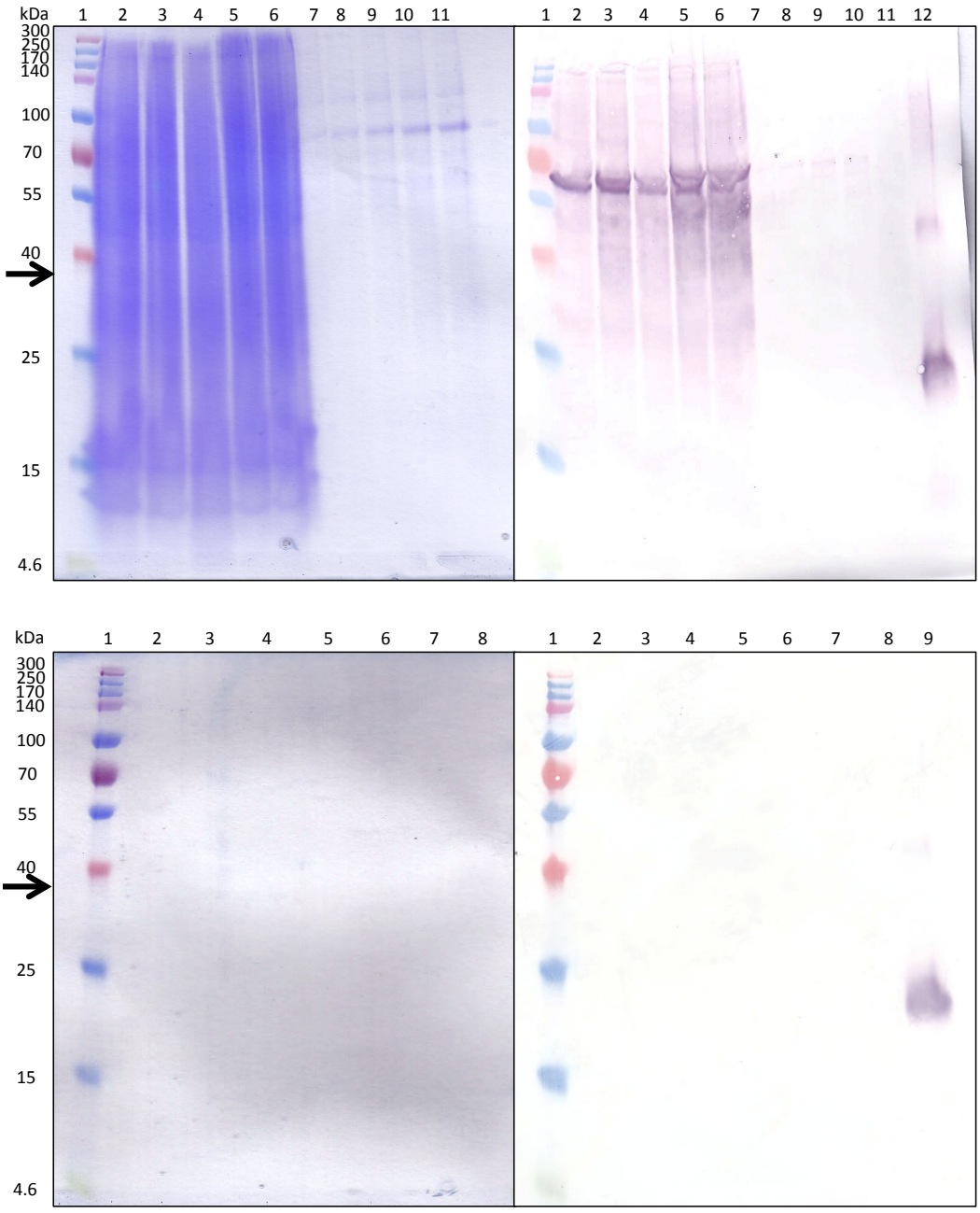

kDa
1 2 3 4 5 6 7 8 9 10 11
1 2 3 4 5 6 7 8 9 10 11 12
300
250
170
140
100
70
55
40
25
15
4.6
kDa
1 2 3 4 5 6 7 8
1 2 3 4 5 6 7 8 9
300
250
170
140
100
70
55
40
25
15
4.6

v. ΔStem-H1HA

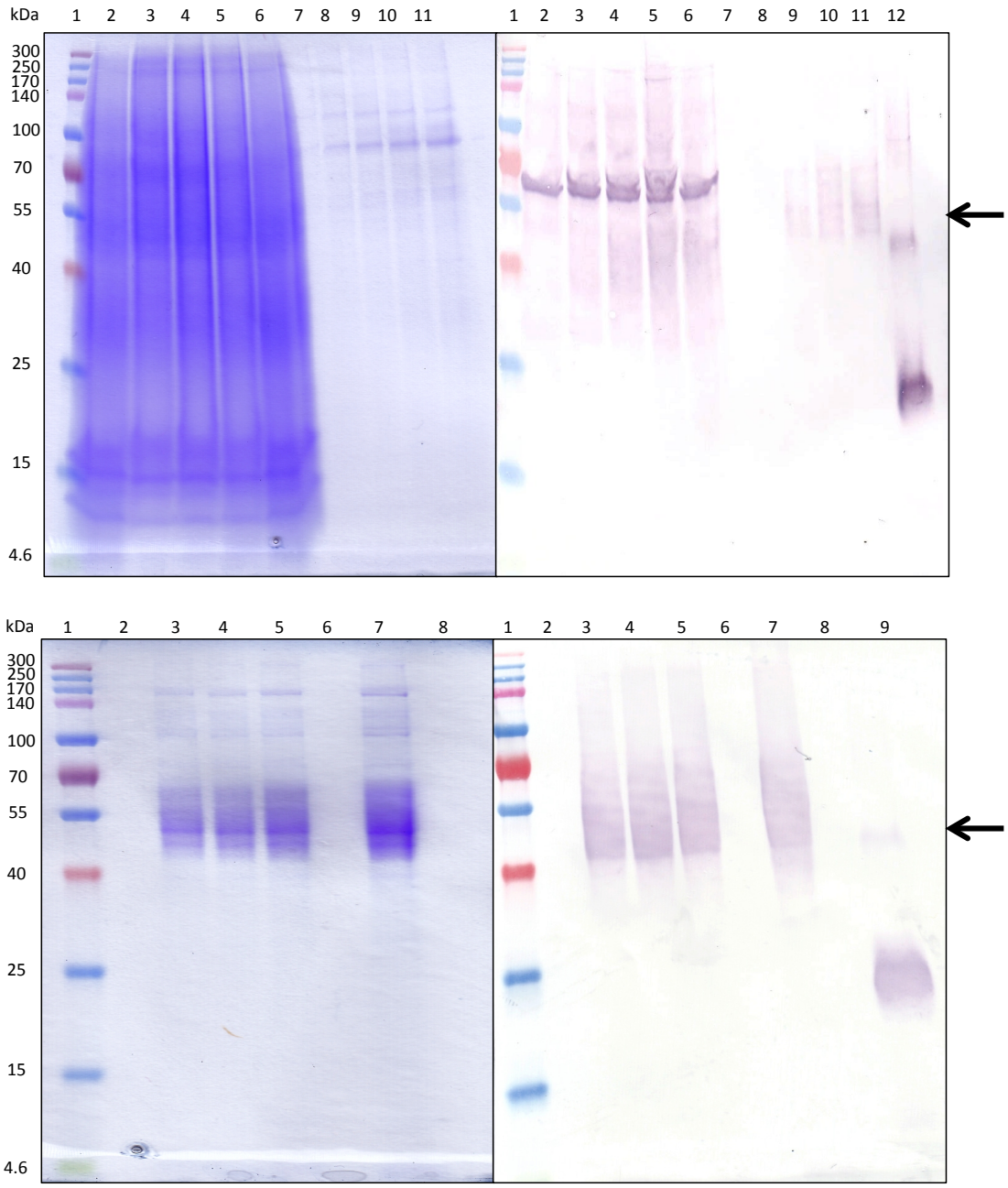

kDa
1 2 3 4 5 6 7 8 9 10 11
1 2 3 4 5 6 7 8 9 10 11 12
300
250
170
140
100
70
55
40
25
15
4.6


kDa
1 2 3 4 5 6 7 8
1 2 3 4 5 6 7 8 9
300
250
170
140
100
70
55
40
25
15
4.6

vi. Headless-H1HA



vii. H1HA-Stem



Appendix XIX

Primers used in the construction of T7 phage display library

Sequence identifier	Sequence (5'-3')
1-68 F	TAGTAGAATTCAATGAAGGCTATCCTGGTCGTG
1-68 R	CTACTAAAGCTTGTGCAGAGGGGCCAC
75-165 F	TAGTAGAATTCAGCCGGCTGGATCCTG
75-165 R	CTACTAAAGCTTCAGGTTCTTGTAGAAGCTCTTG
108-144 F	TAGTAGAATTCATACCCCGGCGACTTC
108-144 R	CTACTAAAGCTTGTCGTGGTTGGGCCAG
120-175 F	TAGTAGAATTCAGAGCAGCTGAGCAGCG
120-175 R	CTACTAAAGCTTGTAGCTGTTGCCCTTCTTGAC
182-220 F	TAGTAGAATTCATACATCAACGACAAGGGCAAAG
182-220 R	CTACTAAAGCTTGCTGCCCACGAACAC
197-286 F	TAGTAGAATTCACACCACCCTAGCACCAG
197-286 R	CTACTAAAGCTTGTCGCTGATGATGATGC
235-281 F	TAGTAGAATTCACCCAAAGTGCGGGAC
235-281 R	CTACTAAAGCTTGCCGCTGCCGG
239-335 F	TAGTAGAATTCAGACCAGGAAGGCCGG
239-335 R	CTACTAAAGCTTCAGGCCGGTGGCC
293-354 F	TAGTAGAATTCAAACACCACCTGTCAGACC
293-354 R	CTACTAAAGCTTGATAAAGCCGGCAATGG
302-356 F	TAGTAGAATTCAGCCATCAACACCAGCC
302-356 R	CTACTAAAGCTTGCCCTCGATAAAGCCG
341-356 F	TAGTAGAATTCAATCCAGAGCAGAGGCCTG
341-356 R	CTACTAAAGCTTGCCCTCGATAAAGCCG
394-489 F	TAGTAGAATTCAAACAAAGTGAACAGCGTGATC

394-489 R	CTACTAAAGCTTGTCGCACTTGTGGTAGAACTC
410-489 F	TAGTAGAATTCAGTGGGCAAAGAGTTCAACC
410-489 R	CTACTAAAGCTTGTCGCACTTGTGGTAGAACTC
T7 UP	GGAGCTGTCGTATTCCAGTC
T7 DOWN	AACCCCTCAAGACCCGTTTA

Appendix XX

Correlations between CD4$^+$ T cell populations and antibody responses following influenza vaccination

	TIV						TIV + MVA-NP+M1			
Population	Time point	Measurement	N	P value	r	Significance	P value	r	Significance
% of CD4$^+$ T cells	Day 21	Fold increase of anti-TIV antibodies	8	0.0714	0.8820	No	0.5240	-0.2515	No
% of CXCR5$^+$CD4$^+$ T cells	Day 21	Fold increase of anti-TIV antibodies	8	0.1966	-0.5328	No	0.1511	0.5714	No
% of CXCR3$^+$CCR6$^-$ CXCR5$^+$CD4$^+$ T cells	Day 21	Fold increase of anti-TIV antibodies	8	0.0576	-0.7143	No	0.0831	0.6667	No
% of CXCR3$^-$CCR6$^-$ CXCR5$^+$CD4$^+$ T cells	Day 21	Fold increase of anti-TIV antibodies	8	0.0458	0.7381	Yes	0.1323	-0.5952	No
% of CXCR3$^-$CCR6$^+$ CXCR5$^+$CD4$^+$ T cells	Day 21	Fold increase of anti-TIV antibodies	8	0.9768	-0.02381	No	0.4618	0.3095	No
% of PD-1^{++} CXCR3$^+$CCR6$^-$CXCR5$^+$CD4$^+$ T cells	Day 21	Fold increase of anti-TIV antibodies	8	0.9768	0.02381	No	0.2431	0.4762	No
% of PD-1^{++} CXCR3$^+$CCR6$^-$CXCR5$^+$CD4$^+$ T cells	Day 21	Fold increase of anti-TIV antibodies	8	0.8737	0.07186	No	0.2162	0.5000	No
% of PD-1^{++} CXCR3$^-$CCR6$^+$CXCR5$^+$CD4$^+$ T cells	Day 21	Fold increase of anti-TIV antibodies	8	0.8820	0.07143	No	0.7930	0.1190	No
% of CXCR3$^+$CCR6$^-$ CXCR5$^-$CD4$^+$ T cells	Day 21	Fold increase of anti-TIV antibodies	8	0.2162	-0.5000	No	0.3894	0.3571	No
% of CXCR3$^-$CCR6$^-$ CXCR5$^-$CD4$^+$ T cells	Day 21	Fold increase of anti-TIV antibodies	8	0.2431	0.4762	No	0.2675	-0.4524	No
% of CXCR3$^-$CCR6$^+$ CXCR5$^-$CD4$^+$ T cells	Day 21	Fold increase of anti-TIV antibodies	8	0.7575	-0.1091	No	0.5821	0.2381	No
% of PD-1^{++} CXCR3$^+$CCR6$^-$CXCR5$^-$CD4$^+$ T cells	Day 21	Fold increase of anti-TIV antibodies	8	0.3599	-0.3810	No	0.5008	0.2857	No
% of PD-1^{++} CXCR3$^-$CCR6$^+$CXCR5$^-$CD4$^+$ T cells	Day 21	Fold increase of anti-TIV antibodies	8	0.5821	-0.2381	No	0.9642	-0.01198	No
% of PD-1^{++} CXCR3$^-$CCR6$^+$CXCR5$^-$CD4$^+$ T cells	Day 21	Fold increase of anti-TIV antibodies	8	0.6191	-0.2143	No	0.3468	0.3832	No
% of CD45RO$^+$CXCR5$^+$CD4$^+$ T cells	Day 21	Fold increase of anti-TIV antibodies	8	0.2675	-0.4524	No	0.0999	0.6347	No
% of CXCR3$^+$CCR6$^-$ CD45RO$^+$CXCR5$^+$CD4$^+$ T cells	Day 21	Fold increase of anti-TIV antibodies	8	0.2162	-0.5000	No	0.0831	0.6667	No
% of CXCR3$^-$CCR6$^-$ CD45RO$^+$CXCR5$^+$CD4$^+$ T cells	Day 21	Fold increase of anti-TIV antibodies	8	0.4279	0.3333	No	0.1710	-0.5476	No
% of CXCR3$^-$CCR6$^+$ CD45RO$^+$CXCR5$^+$CD4$^+$ T cells	Day 21	Fold increase of anti-TIV antibodies	8	0.7520	0.1429	No	0.4618	0.3095	No
% of PD-1^{++} CXCR3$^+$CCR6$^-$CXCR5$^+$CD45RO$^+$CD4$^+$ T cells	Day 21	Fold increase of anti-TIV antibodies	8	1	0.0	No	0.2162	0.5000	No
% of PD-1^{++} CXCR3$^-$CCR6$^-$CXCR5$^+$CD45RO$^+$CD4$^+$ T cells	Day 21	Fold increase of anti-TIV antibodies	8	0.6085	0.2156	No	0.6191	0.2143	No
% of PD-1^{++} CXCR3$^-$CCR6$^+$CXCR5$^+$CD45RO$^+$CD4$^+$ T cells	Day 21	Fold increase of anti-TIV antibodies	8	0.6954	0.1677	No	0.9349	-0.04762	No
% of CXCR3$^+$CCR6$^-$ CD45RO$^+$CXCR5$^-$CD4$^+$ T cells	Day 21	Fold increase of anti-TIV antibodies	8	0.0467	-0.7186	Yes	0.2992	0.4286	No
% of CXCR3$^-$CCR6$^-$ CD45RO$^+$CXCR5$^-$CD4$^+$ T cells	Day 21	Fold increase of anti-TIV antibodies	8	0.2431	0.4762	No	0.1150	-0.6190	No
% of CXCR3$^-$CCR6$^+$ CD45RO$^+$CXCR5$^-$CD4$^+$ T cells	Day 21	Fold increase of anti-TIV antibodies	8	0.4704	0.2994	No	0.6191	0.2143	No
% of PD-1^{++} CXCR3$^+$CCR6$^-$CXCR5$^-$CD45RO$^+$CD4$^+$ T cells	Day 21	Fold increase of anti-TIV antibodies	8	0.5660	-0.2275	No	0.9349	-0.04762	No
% of PD-1^{++} CXCR3$^-$CCR6$^-$CXCR5$^-$CD45RO$^+$CD4$^+$ T cells	Day 21	Fold increase of anti-TIV antibodies	8	0.8820	0.07143	No	0.5008	0.2857	No
% of PD-1^{++} CXCR3$^-$CCR6$^+$CXCR5$^-$CD45RO$^+$CD4$^+$ T cells	Day 21	Fold increase of anti-TIV antibodies	8	0.8401	-0.09524	No	0.4279	0.3333	No

Appendix XXI

Sequence of Headless vaccine antigen

MKAILVVLLYTFATANADTLCIGYHANNSTDTVDTVLEKNVTVTHSVNLLEDK
HNGKLCGGGGCNTTCQTPKGAINTSLPFQNIHPITIGKCPKYVKSTKLRLAT
GLRNVPSIQSRGLFGAIAGFIEGGWTGMVDGWYGYHHQNEQGSGYAADL
KSTQNAIDEITNKVNSVIEKMNTQFTAVGKEFNHLEKRIENLNKKVDDGFLDI
WTYNAELLVLLENERTLDYHDSNVKNLYEKVRSQLKNNAKEIGNGCFEFYH
KCDNTCMESVKNGTYDYPKYSEEAKLNREEIDGVKLESTRIYQILAIYSTVAS
SLVLVVSLGAISFWMCSNGSLQCRICI

BIBLIOGRAPHY

1. Thucydides. The plague in Athens. Thucydides. The history of the Peloponnesian War. Translated by Thomas Hobbes. North Carolina medical journal 1980;41:230-2.

2. Potter CW. A history of influenza. Journal of applied microbiology 2001;91:572-9.

3. Taubenberger JK, Morens DM. Pandemic influenza--including a risk assessment of H5N1. Revue scientifique et technique 2009;28:187-202.

4. Ghendon Y. Introduction to pandemic influenza through history. European journal of epidemiology 1994;10:451-3.

5. Gatherer D. The 2009 H1N1 influenza outbreak in its historical context. Journal of clinical virology : the official publication of the Pan American Society for Clinical Virology 2009;45:174-8.

6. Hinsdale G. Early Records of Influenza Epidemics in America. Transactions of the American Climatological and Clinical Association American Climatological and Clinical Association 1919;35:92-105.

7. Molineux D. Dr. Molineux's Historical Account of the Late General Coughs and Colds; with Some Observations on Other Epidemick Distempers. Philosophical Transactions 1694;18:105-11.

8. Wilson JC. A Treatise on the Continued Fevers (1881): General Books LLC; 2009.

9. Hirsch A. Handbook of Geographical and Historical Pathology: London: New Sydenham Society; 1883.

10. Creighton C. A History of Epidemics in Britain....: From A.D. 664 to the great plague: F. Cass & Company; 1965.

11. Beveridge WI. The start of pandemics: site, season and spread. Developments in biological standardization 1977;39:443-4.

12. Influenza (Seasonal) Fact sheet No. 211. 2014. (Accessed 9th July, 2015, at http://www.who.int/mediacentre/factsheets/fs211/en/.)

13. Influenza Prevention: Information for Travelers. 2011. (Accessed 9th July, 2015, at http://www.cdc.gov/flu/travelers/travelersfacts.htm.)

14. Hope-Simpson RE. The role of season in the epidemiology of influenza. The Journal of hygiene 1981;86:35-47.

15. Moura FE. Influenza in the tropics. Current opinion in infectious diseases 2010;23:415-20.

16. Poehling KA, Edwards KM, Weinberg GA, et al. The underrecognized burden of influenza in young children. N Engl J Med 2006;355:31-40.

17. Ampofo K, Gesteland PH, Bender J, et al. Epidemiology, complications, and cost of hospitalization in children with laboratory-confirmed influenza infection. Pediatrics 2006;118:2409-17.

18. Coffin SE, Zaoutis TE, Rosenquist AB, et al. Incidence, complications, and risk factors for prolonged stay in children hospitalized with community-acquired influenza. Pediatrics 2007;119:740-8.

19. Zhou H, Thompson WW, Viboud CG, et al. Hospitalizations associated with influenza and respiratory syncytial virus in the United States, 1993-2008. Clinical infectious diseases : an official publication of the Infectious Diseases Society of America 2012;54:1427-36.

20. Thompson WW, Shay DK, Weintraub E, et al. Mortality associated with influenza and respiratory syncytial virus in the United States. JAMA 2003;289:179-86.

21. Thompson WW, Shay DK, Weintraub E, et al. Influenza-associated hospitalizations in the United States. Jama 2004;292:1333-40.

22. Neuzil KM, Reed GW, Mitchel EF, Simonsen L, Griffin MR. Impact of influenza on acute cardiopulmonary hospitalizations in pregnant women. American journal of epidemiology 1998;148:1094-102.

23. Nicoll A, Ciancio B, Tsolova S, Blank P, Yilmaz C. The scientific basis for offering seasonal influenza immunisation to risk groups in Europe. Euro surveillance : bulletin Europeen sur les maladies transmissibles = European communicable disease bulletin 2008;13.

24. Colquhoun AJ, Nicholson KG, Botha JL, Raymond NT. Effectiveness of influenza vaccine in reducing hospital admissions in people with diabetes. Epidemiology and infection 1997;119:335-41.

25. Rothberg MB, Haessler SD, Brown RB. Complications of viral influenza. The American journal of medicine 2008;121:258-64.

26. McNeil SA, Dodds LA, Fell DB, et al. Effect of respiratory hospitalization during pregnancy on infant outcomes. American journal of obstetrics and gynecology 2011;204:S54-7.

27. Harris JW. Influenza occurring in pregnant women: A statistical study of thirteen hundred and fifty cases. Journal of the American Medical Association 1919;72:978-80.

28. Molinari NA, Ortega-Sanchez IR, Messonnier ML, et al. The annual impact of seasonal influenza in the US: measuring disease burden and costs. Vaccine 2007;25:5086-96.

29. 7.6 million working days lost due to flu. 2010. (Accessed 9th July, 2015, at http://www.co-operative.coop/corporate/press/press-releases/pharmacy/76-million-working-days-lost-due-to-flu/ - 1.)

30. Cohen AL, McMorrow M, Walaza S, et al. Potential Impact of Co-Infections and Co-Morbidities Prevalent in Africa on Influenza Severity and Frequency: A Systematic Review. PloS one 2015;10:e0128580.

31. Simonsen L. The global impact of influenza on morbidity and mortality. Vaccine 1999;17 Suppl 1:S3-10.

32. Webster RG, Bean WJ, Gorman OT, Chambers TM, Kawaoka Y. Evolution and ecology of influenza A viruses. Microbiological reviews 1992;56:152-79.

33. Mehle A. Unusual influenza A viruses in bats. Viruses 2014;6:3438-49.

34. Short KR, Veldhuis Kroeze EJ, Reperant LA, Richard M, Kuiken T. Influenza virus and endothelial cells: a species specific relationship. Frontiers in microbiology 2014;5:653.

35. Fields BN, Knipe DM, Howley PM. Fields virology. Philadelphia: Wolters Kluwer Health/Lippincott Williams & Wilkins; 2013.

36. Types of Influenza Viruses. 2014. (Accessed 11th July, 2015, at http://www.cdc.gov/flu/about/viruses/types.htm.)

37. Schrauwen EJ, Fouchier RA. Host adaptation and transmission of influenza A viruses in mammals. Emerging microbes & infections 2014;3:e9.

38. de Jong JC, Claas EC, Osterhaus AD, Webster RG, Lim WL. A pandemic warning? Nature 1997;389:554.

39. Cumulative number of confirmed human cases for avian influenza A(H5N1) reported to WHO, 2003-2015. 2015. (Accessed 11th July, 2015, at

http://www.who.int/influenza/human_animal_interface/EN_GIP_20150623cumulativeNumberH5N1cases.pdf?ua=1.)

40. WHO RISK ASSESSMENT of Human infections with avian influenza A(H7N9) virus. 2015. (Accessed 11th July, 2015, at http://www.who.int/influenza/human_animal_interface/influenza_h7n9/RiskAssessment_H7N9_23Feb20115.pdf?ua=1.)

41. Influenza: the green book, chapter 19. 2015. (Accessed 17th July, 2015, at https://http://www.gov.uk/government/uploads/system/uploads/attachment_data/file/427809/Green_Book_Chapter_19_v9_0_May_2015_.PDF.)

42. Flu Plan Winter 2015/16. 2015. (Accessed 17th July, 2015, at https://http://www.gov.uk/government/uploads/system/uploads/attachment_data/file/418038/Flu_Plan_Winter_2015_to_2016.pdf.)

43. Vaccine Effectiveness - How Well Does the Flu Vaccine Work? 2013. (Accessed 17th July, 2015, at http://www.cdc.gov/flu/about/qa/vaccineeffect.htm.)

44. Cox NJ, Brammer TL, Regnery HL. Influenza: global surveillance for epidemic and pandemic variants. European journal of epidemiology 1994;10:467-70.

45. Brief history of the development of the Framework on Sharing influenza viruses and access to vaccines and other benefits. 2011. (Accessed 16th July, 2015, at http://www.who.int/influenza/pip/Framework_History_2011.pdf.)

46. Global Influenza Surveillance and Response System (GISRS). 2014. (Accessed 16th July, 2015, at http://www.who.int/influenza/gisrs_laboratory/en/.)

47. Pandemic influenza preparedness Framework for the sharing of influenza viruses and access to vaccines and other benefits. 2011. (Accessed 17th July, 2015, at http://www.who.int/influenza/resources/pip_framework/en/.)

48. Fry AM, Goswami D, Nahar K, et al. Effects of oseltamivir treatment of index patients with influenza on secondary household illness in an urban setting in Bangladesh: secondary analysis of a randomised, placebo-controlled trial. The Lancet Infectious diseases 2015;15:654-62.

49. Dobson J, Whitley RJ, Pocock S, Monto AS. Oseltamivir treatment for influenza in adults: a meta-analysis of randomised controlled trials. Lancet 2015;385:1729-37.

50. Jefferson T, Jones MA, Doshi P, et al. Neuraminidase inhibitors for preventing and treating influenza in healthy adults and children. The Cochrane database of systematic reviews 2014;4:CD008965.

51. Government responses on the Thirty Fifth to the Forty Fifth Reports from the Committee of Public Accounts: Session 2013-14. 2014. (Accessed 17th July, 2015, at https://http://www.gov.uk/government/uploads/system/uploads/attachment_data/file/302516/39796_Cm_8847_Accessible.pdf.)

52. Tong S, Li Y, Rivailler P, et al. A distinct lineage of influenza A virus from bats. Proceedings of the National Academy of Sciences of the United States of America 2012;109:4269-74.

53. Tong S, Zhu X, Li Y, et al. New world bats harbor diverse influenza A viruses. PLoS pathogens 2013;9:e1003657.

54. Wise HM, Foeglein A, Sun J, et al. A complicated message: Identification of a novel PB1-related protein translated from influenza A virus segment 2 mRNA. Journal of virology 2009;83:8021-31.

55. Chen W, Calvo PA, Malide D, et al. A novel influenza A virus mitochondrial protein that induces cell death. Nature medicine 2001;7:1306-12.

56. Jagger BW, Wise HM, Kash JC, et al. An overlapping protein-coding region in influenza A virus segment 3 modulates the host response. Science 2012;337:199-204.

57. Muramoto Y, Noda T, Kawakami E, Akkina R, Kawaoka Y. Identification of novel influenza A virus proteins translated from PA mRNA. Journal of virology 2013;87:2455-62.

58. Medina RA, Garcia-Sastre A. Influenza A viruses: new research developments. Nature reviews Microbiology 2011;9:590-603.

59. Selman M, Dankar SK, Forbes NE, Jia JJ, Brown EG. Adaptive mutation in influenza A virus non-structural gene is linked to host switching and induces a novel protein by alternative splicing. Emerging microbes & infections 2012;1:e42.

60. Clifford M, Twigg J, Upton C. Evidence for a novel gene associated with human influenza A viruses. Virology journal 2009;6:198.

61. Zhirnov OP, Poyarkov SV, Vorob'eva IV, Safonova OA, Malyshev NA, Klenk HD. Segment NS of influenza A virus contains an additional gene NSP

in positive-sense orientation. Doklady Biochemistry and biophysics 2007;414:127-33.

62. Wrigley NG. Electron microscopy of influenza virus. Br Med Bull 1979;35:35-8.

63. Wilson IA, Skehel JJ, Wiley DC. Structure of the haemagglutinin membrane glycoprotein of influenza virus at 3 A resolution. Nature 1981;289:366-73.

64. Gottschalk A. On the mechanism underlying initiation of influenza virus infection. Ergeb Mikrobiol Immunitatsforsch Exp Ther 1959;32:1-22.

65. Palese P, Tobita K, Ueda M, Compans RW. Characterization of temperature sensitive influenza virus mutants defective in neuraminidase. Virology 1974;61:397-410.

66. Lamb RA, Zebedee SL, Richardson CD. Influenza virus M2 protein is an integral membrane protein expressed on the infected-cell surface. Cell 1985;40:627-33.

67. Vasin AV, Temkina OA, Egorov VV, Klotchenko SA, Plotnikova MA, Kiselev OI. Molecular mechanisms enhancing the proteome of influenza A viruses: an overview of recently discovered proteins. Virus research 2014;185:53-63.

68. Bui M, Wills EG, Helenius A, Whittaker GR. Role of the influenza virus M1 protein in nuclear export of viral ribonucleoproteins. Journal of virology 2000;74:1781-6.

69. Cady SD, Luo W, Hu F, Hong M. Structure and function of the influenza A M2 proton channel. Biochemistry 2009;48:7356-64.

70. O'Neill RE, Talon J, Palese P. The influenza virus NEP (NS2 protein) mediates the nuclear export of viral ribonucleoproteins. The EMBO journal 1998;17:288-96.

71. Brunotte L, Flies J, Bolte H, Reuther P, Vreede F, Schwemmle M. The nuclear export protein of H5N1 influenza A viruses recruits Matrix 1 (M1) protein to the viral ribonucleoprotein to mediate nuclear export. The Journal of biological chemistry 2014;289:20067-77.

72. Hale BG, Randall RE, Ortin J, Jackson D. The multifunctional NS1 protein of influenza A viruses. The Journal of general virology 2008;89:2359-76.

73. Zamarin D, Ortigoza MB, Palese P. Influenza A virus PB1-F2 protein contributes to viral pathogenesis in mice. Journal of virology 2006;80:7976-83.

74. Yewdell JW, Ince WL. Virology. Frameshifting to PA-X influenza. Science 2012;337:164-5.

75. Hu J, Mo Y, Wang X, et al. PA-X decreases the pathogenicity of highly pathogenic H5N1 influenza A virus in avian species by inhibiting virus replication and host response. Journal of virology 2015;89:4126-42.

76. Rossman JS, Lamb RA. Influenza virus assembly and budding. Virology 2011;411:229-36.

77. Varki A. Essentials of glycobiology. Cold Spring Harbor, N.Y.: Cold Spring Harbor Laboratory Press; 2009.

78. Sieczkarski SB, Whittaker GR. Influenza virus can enter and infect cells in the absence of clathrin-mediated endocytosis. Journal of virology 2002;76:10455-64.

79. Chen C, Zhuang X. Epsin 1 is a cargo-specific adaptor for the clathrin-mediated endocytosis of the influenza virus. Proceedings of the National Academy of Sciences of the United States of America 2008;105:11790-5.

80. Wiley DC, Skehel JJ. The structure and function of the hemagglutinin membrane glycoprotein of influenza virus. Annual review of biochemistry 1987;56:365-94.

81. Pinto LH, Holsinger LJ, Lamb RA. Influenza virus M2 protein has ion channel activity. Cell 1992;69:517-28.

82. Bui M, Whittaker G, Helenius A. Effect of M1 protein and low pH on nuclear transport of influenza virus ribonucleoproteins. Journal of virology 1996;70:8391-401.

83. Chen BJ, Leser GP, Jackson D, Lamb RA. The influenza virus M2 protein cytoplasmic tail interacts with the M1 protein and influences virus assembly at the site of virus budding. Journal of virology 2008;82:10059-70.

84. Ali A, Avalos RT, Ponimaskin E, Nayak DP. Influenza virus assembly: effect of influenza virus glycoproteins on the membrane association of M1 protein. Journal of virology 2000;74:8709-19.

85. Huang RT, Rott R, Klenk HD. Influenza viruses cause hemolysis and fusion of cells. Virology 1981;110:243-7.

86. Connor RJ, Kawaoka Y, Webster RG, Paulson JC. Receptor specificity in human, avian, and equine H2 and H3 influenza virus isolates. Virology 1994;205:17-23.

87. Shinya K, Ebina M, Yamada S, Ono M, Kasai N, Kawaoka Y. Avian flu: influenza virus receptors in the human airway. Nature 2006;440:435-6.

88. Lakdawala SS, Jayaraman A, Halpin RA, et al. The soft palate is an important site of adaptation for transmissible influenza viruses. Nature 2015;526:122-5.

89. Ito T, Couceiro JN, Kelm S, et al. Molecular basis for the generation in pigs of influenza A viruses with pandemic potential. Journal of virology 1998;72:7367-73.

90. van Riel D, Munster VJ, de Wit E, et al. H5N1 Virus Attachment to Lower Respiratory Tract. Science 2006;312:399.

91. Doherty PC, Turner SJ, Webby RG, Thomas PG. Influenza and the challenge for immunology. Nature immunology 2006;7:449-55.

92. Hsieh YC, Wu TZ, Liu DP, et al. Influenza pandemics: past, present and future. Journal of the Formosan Medical Association = Taiwan yi zhi 2006;105:1-6.

93. Childs RA, Palma AS, Wharton S, et al. Receptor-binding specificity of pandemic influenza A (H1N1) 2009 virus determined by carbohydrate microarray. Nature biotechnology 2009;27:797-9.

94. Gu J, Xie Z, Gao Z, et al. H5N1 infection of the respiratory tract and beyond: a molecular pathology study. Lancet 2007;370:1137-45.

95. Rott R, Klenk HD, Nagai Y, Tashiro M. Influenza viruses, cell enzymes, and pathogenicity. American journal of respiratory and critical care medicine 1995;152:S16-9.

96. Webster RG, Laver WG, Air GM, Schild GC. Molecular mechanisms of variation in influenza viruses. Nature 1982;296:115-21.

97. Clinical Signs and Symptoms of Influenza. 2009. (Accessed 21st July, 2015, at http://www.cdc.gov/flu/professionals/acip/clinical.htm.)

98. Rello J, Pop-Vicas A. Clinical review: primary influenza viral pneumonia. Critical care 2009;13:235.

99. Rello J, Rodriguez A, Ibanez P, et al. Intensive care adult patients with severe respiratory failure caused by Influenza A (H1N1)v in Spain. Critical care 2009;13:R148.

100. Carter MJ. A rationale for using steroids in the treatment of severe cases of H5N1 avian influenza. Journal of medical microbiology 2007;56:875-83.

101. de Jong MD, Simmons CP, Thanh TT, et al. Fatal outcome of human influenza A (H5N1) is associated with high viral load and hypercytokinemia. Nature medicine 2006;12:1203-7.

102. Hayden FG, Fritz R, Lobo MC, Alvord W, Strober W, Straus SE. Local and systemic cytokine responses during experimental human influenza A virus infection. Relation to symptom formation and host defense. The Journal of clinical investigation 1998;101:643-9.

103. Kaiser L, Fritz RS, Straus SE, Gubareva L, Hayden FG. Symptom pathogenesis during acute influenza: interleukin-6 and other cytokine responses. Journal of medical virology 2001;64:262-8.

104. Akashi K, Hayashi S, Gondo H, et al. Involvement of interferon-gamma and macrophage colony-stimulating factor in pathogenesis of haemophagocytic lymphohistiocytosis in adults. British journal of haematology 1994;87:243-50.

105. Imashuku S, Hibi S, Fujiwara F, Todo S. Hyper-interleukin (IL)-6-naemia in haemophagocytic lymphohistiocytosis. British journal of haematology 1996;93:803-7.

106. Ioannidis I, Ye F, McNally B, Willette M, Flano E. Toll-like receptor expression and induction of type I and type III interferons in primary airway epithelial cells. Journal of virology 2013;87:3261-70.

107. Iwasaki A, Pillai PS. Innate immunity to influenza virus infection. Nature reviews Immunology 2014;14:315-28.

108. Marchant D, Singhera GK, Utokaparch S, et al. Toll-like receptor 4-mediated activation of p38 mitogen-activated protein kinase is a determinant of respiratory virus entry and tropism. Journal of virology 2010;84:11359-73.

109. Lee SM, Kok KH, Jaume M, et al. Toll-like receptor 10 is involved in induction of innate immune responses to influenza virus infection. Proceedings of the National Academy of Sciences of the United States of America 2014;111:3793-8.

110. Monsalvo AC, Batalle JP, Lopez MF, et al. Severe pandemic 2009 H1N1 influenza disease due to pathogenic immune complexes. Nature medicine 2011;17:195-9.

111. Le Goffic R, Pothlichet J, Vitour D, et al. Cutting Edge: Influenza A virus activates TLR3-dependent inflammatory and RIG-I-dependent antiviral responses in human lung epithelial cells. Journal of immunology 2007;178:3368-72.

112. Diebold SS, Kaisho T, Hemmi H, Akira S, Reis e Sousa C. Innate antiviral responses by means of TLR7-mediated recognition of single-stranded RNA. Science 2004;303:1529-31.

113. Lund JM, Alexopoulou L, Sato A, et al. Recognition of single-stranded RNA viruses by Toll-like receptor 7. Proceedings of the National Academy of Sciences of the United States of America 2004;101:5598-603.

114. Heil F, Hemmi H, Hochrein H, et al. Species-specific recognition of single-stranded RNA via toll-like receptor 7 and 8. Science 2004;303:1526-9.

115. Kadowaki N, Ho S, Antonenko S, et al. Subsets of human dendritic cell precursors express different toll-like receptors and respond to different microbial antigens. The Journal of experimental medicine 2001;194:863-9.

116. Alexopoulou L, Holt AC, Medzhitov R, Flavell RA. Recognition of double-stranded RNA and activation of NF-kappaB by Toll-like receptor 3. Nature 2001;413:732-8.

117. Wisskirchen C, Ludersdorfer TH, Muller DA, Moritz E, Pavlovic J. The cellular RNA helicase UAP56 is required for prevention of double-stranded RNA formation during influenza A virus infection. Journal of virology 2011;85:8646-55.

118. Schulz O, Diebold SS, Chen M, et al. Toll-like receptor 3 promotes cross-priming to virus-infected cells. Nature 2005;433:887-92.

119. Chuang T, Ulevitch RJ. Identification of hTLR10: a novel human Toll-like receptor preferentially expressed in immune cells. Biochimica et biophysica acta 2001;1518:157-61.

120. Takeuchi O, Akira S. Innate immunity to virus infection. Immunological reviews 2009;227:75-86.

121. Liu WC, Lin SC, Yu YL, Chu CL, Wu SC. Dendritic cell activation by recombinant hemagglutinin proteins of H1N1 and H5N1 influenza A viruses. Journal of virology 2010;84:12011-7.

122. Oosting M, Cheng SC, Bolscher JM, et al. Human TLR10 is an anti-inflammatory pattern-recognition receptor. Proceedings of the National Academy of Sciences of the United States of America 2014;111:E4478-84.

123. Rehwinkel J, Tan CP, Goubau D, et al. RIG-I detects viral genomic RNA during negative-strand RNA virus infection. Cell 2010;140:397-408.

124. Pichlmair A, Schulz O, Tan CP, et al. RIG-I-mediated antiviral responses to single-stranded RNA bearing 5'-phosphates. Science 2006;314:997-1001.

125. Hornung V, Ellegast J, Kim S, et al. 5'-Triphosphate RNA is the ligand for RIG-I. Science 2006;314:994-7.

126. Ichinohe T, Pang IK, Iwasaki A. Influenza virus activates inflammasomes via its intracellular M2 ion channel. Nature immunology 2010;11:404-10.

127. McAuley JL, Tate MD, MacKenzie-Kludas CJ, et al. Activation of the NLRP3 inflammasome by IAV virulence protein PB1-F2 contributes to severe pathophysiology and disease. PLoS pathogens 2013;9:e1003392.

128. Wang JP, Kurt-Jones EA, Finberg RW. Innate immunity to respiratory viruses. Cellular microbiology 2007;9:1641-6.

129. Moriwaki K, Chan FK. RIP3: a molecular switch for necrosis and inflammation. Genes & development 2013;27:1640-9.

130. Dinarello CA. Immunological and inflammatory functions of the interleukin-1 family. Annual review of immunology 2009;27:519-50.

131. Fesq H, Bacher M, Nain M, Gemsa D. Programmed cell death (apoptosis) in human monocytes infected by influenza A virus. Immunobiology 1994;190:175-82.

132. Julkunen I, Melen K, Nyqvist M, Pirhonen J, Sareneva T, Matikainen S. Inflammatory responses in influenza A virus infection. Vaccine 2000;19 Suppl 1:S32-7.

133. Julkunen I, Sareneva T, Pirhonen J, Ronni T, Melen K, Matikainen S. Molecular pathogenesis of influenza A virus infection and virus-induced regulation of cytokine gene expression. Cytokine & growth factor reviews 2001;12:171-80.

134. Sprenger H, Meyer RG, Kaufmann A, Bussfeld D, Rischkowsky E, Gemsa D. Selective induction of monocyte and not neutrophil-attracting chemokines after influenza A virus infection. The Journal of experimental medicine 1996;184:1191-6.

135. Ada GL, Jones PD. The immune response to influenza infection. Current topics in microbiology and immunology 1986;128:1-54.

136. Crotta S, Davidson S, Mahlakoiv T, et al. Type I and type III interferons drive redundant amplification loops to induce a transcriptional signature in influenza-infected airway epithelia. PLoS pathogens 2013;9:e1003773.

137. Lam WY, Yeung AC, Chan PK. Apoptosis, cytokine and chemokine induction by non-structural 1 (NS1) proteins encoded by different influenza subtypes. Virology journal 2011;8:554.

138. Platanias LC. Mechanisms of type-I- and type-II-interferon-mediated signalling. Nature reviews Immunology 2005;5:375-86.

139. Sadler AJ, Williams BR. Interferon-inducible antiviral effectors. Nature reviews Immunology 2008;8:559-68.

140. Nguyen KB, Salazar-Mather TP, Dalod MY, et al. Coordinated and distinct roles for IFN-alpha beta, IL-12, and IL-15 regulation of NK cell responses to viral infection. Journal of immunology 2002;169:4279-87.

141. Kolumam GA, Thomas S, Thompson LJ, Sprent J, Murali-Krishna K. Type I interferons act directly on CD8 T cells to allow clonal expansion and

memory formation in response to viral infection. The Journal of experimental medicine 2005;202:637-50.

142. Bauvois B, Nguyen J, Tang R, Billard C, Kolb JP. Types I and II interferons upregulate the costimulatory CD80 molecule in monocytes via interferon regulatory factor-1. Biochemical pharmacology 2009;78:514-22.

143. Montoya M, Schiavoni G, Mattei F, et al. Type I interferons produced by dendritic cells promote their phenotypic and functional activation. Blood 2002;99:3263-71.

144. Spadaro F, Lapenta C, Donati S, et al. IFN-alpha enhances cross-presentation in human dendritic cells by modulating antigen survival, endocytic routing, and processing. Blood 2012;119:1407-17.

145. Wijburg OL, DiNatale S, Vadolas J, van Rooijen N, Strugnell RA. Alveolar macrophages regulate the induction of primary cytotoxic T-lymphocyte responses during influenza virus infection. Journal of virology 1997;71:9450-7.

146. McGill J, Van Rooijen N, Legge KL. Protective influenza-specific CD8 T cell responses require interactions with dendritic cells in the lungs. The Journal of experimental medicine 2008;205:1635-46.

147. Mikhak Z, Strassner JP, Luster AD. Lung dendritic cells imprint T cell lung homing and promote lung immunity through the chemokine receptor CCR4. The Journal of experimental medicine 2013;210:1855-69.

148. Billiau A. Anti-inflammatory properties of Type I interferons. Antiviral research 2006;71:108-16.

149. Gonzalez-Navajas JM, Lee J, David M, Raz E. Immunomodulatory functions of type I interferons. Nature reviews Immunology 2012;12:125-35.

150. Guarda G, Braun M, Staehli F, et al. Type I interferon inhibits interleukin-1 production and inflammasome activation. Immunity 2011;34:213-23.

151. Arimori Y, Nakamura R, Yamada H, et al. Type I interferon limits influenza virus-induced acute lung injury by regulation of excessive inflammation in mice. Antiviral research 2013;99:230-7.

152. Waffarn EE, Baumgarth N. Protective B cell responses to flu--no fluke! Journal of immunology 2011;186:3823-9.

153. Randall TD. Bronchus-associated lymphoid tissue (BALT) structure and function. Advances in immunology 2010;107:187-241.

154. Rangel-Moreno J, Carragher DM, de la Luz Garcia-Hernandez M, et al. The development of inducible bronchus-associated lymphoid tissue depends on IL-17. Nature immunology 2011;12:639-46.

155. Jones PD, Ada GL. Influenza virus-specific antibody-secreting cells in the murine lung during primary influenza virus infection. Journal of virology 1986;60:614-9.

156. Miao H, Sangster MY, Livingstone AM, et al. Modeling the dynamics and migratory pathways of virus-specific antibody-secreting cell populations in primary influenza infection. PloS one 2014;9:e104781.

157. Potter CW, Oxford JS. Determinants of immunity to influenza infection in man. Br Med Bull 1979;35:69-75.

158. Jones PD, Ada GL. Persistence of influenza virus-specific antibody-secreting cells and B-cell memory after primary murine influenza virus infection. Cell Immunol 1987;109:53-64.

159. Hyland L, Sangster M, Sealy R, Coleclough C. Respiratory virus infection of mice provokes a permanent humoral immune response. Journal of virology 1994;68:6083-6.

160. Joo HM, He Y, Sangster MY. Broad dispersion and lung localization of virus-specific memory B cells induced by influenza pneumonia. Proceedings of the National Academy of Sciences of the United States of America 2008;105:3485-90.

161. Huang KY, Li CK, Clutterbuck E, et al. Virus-specific antibody secreting cell, memory B-cell, and sero-antibody responses in the human influenza challenge model. The Journal of infectious diseases 2014;209:1354-61.

162. Chu VT, Berek C. The establishment of the plasma cell survival niche in the bone marrow. Immunological reviews 2013;251:177-88.

163. Reynaud CA, Descatoire M, Dogan I, Huetz F, Weller S, Weill JC. IgM memory B cells: a mouse/human paradox. Cellular and molecular life sciences : CMLS 2012;69:1625-34.

164. Tamura S, Kurata T. Defense mechanisms against influenza virus infection in the respiratory tract mucosa. Japanese journal of infectious diseases 2004;57:236-47.

165. Burlington DB, Clements ML, Meiklejohn G, Phelan M, Murphy BR. Hemagglutinin-specific antibody responses in immunoglobulin G, A, and M isotypes as measured by enzyme-linked immunosorbent assay after primary or secondary infection of humans with influenza A virus. Infection and immunity 1983;41:540-5.

166. Jayasekera JP, Moseman EA, Carroll MC. Natural antibody and complement mediate neutralization of influenza virus in the absence of prior immunity. Journal of virology 2007;81:3487-94.

167. Mazanec MB, Coudret CL, Fletcher DR. Intracellular neutralization of influenza virus by immunoglobulin A anti-hemagglutinin monoclonal antibodies. Journal of virology 1995;69:1339-43.

168. Murphy BR, Nelson DL, Wright PF, Tierney EL, Phelan MA, Chanock RM. Secretory and systemic immunological response in children infected with live attenuated influenza A virus vaccines. Infection and immunity 1982;36:1102-8.

169. Yarchoan R, Barrow LA, Kurman C, Strober W, Nelson DL. Human peripheral blood mononuclear cells produce IgA anti-influenza virus antibody in a secondary in vitro antibody response. Journal of immunology 1985;135:1033-9.

170. Caton AJ, Brownlee GG, Yewdell JW, Gerhard W. The antigenic structure of the influenza virus A/PR/8/34 hemagglutinin (H1 subtype). Cell 1982;31:417-27.

171. Brand CM, Skehel JJ. Crystalline antigen from the influenza virus envelope. Nature: New biology 1972;238:145-7.

172. Eckert EA. Properties of an antigenic glycoprotein isolated from influenza virus hemagglutinin. Journal of virology 1973;11:183-92.

173. Jackson DC, Dopheide TA, Russell RJ, White DO, Ward CW. Antigenic determinants of influenza virus hemagglutinin. II. Antigenic reactivity of the isolated N-terminal cyanogen bromide peptide of A/Memphis/72 hemagglutinin heavy chain. Virology 1979;93:458-65.

174. Gerhard W, Yewdell J, Frankel ME, Webster R. Antigenic structure of influenza virus haemagglutinin defined by hybridoma antibodies. Nature 1981;290:713-7.

175. Brandenburg B, Koudstaal W, Goudsmit J, et al. Mechanisms of hemagglutinin targeted influenza virus neutralization. PloS one 2013;8:e80034.

176. Feng JQ, Mozdzanowska K, Gerhard W. Complement component C1q enhances the biological activity of influenza virus hemagglutinin-specific antibodies depending on their fine antigen specificity and heavy-chain isotype. Journal of virology 2002;76:1369-78.

177. Huber VC, Lynch JM, Bucher DJ, Le J, Metzger DW. Fc receptor-mediated phagocytosis makes a significant contribution to clearance of influenza virus infections. Journal of immunology 2001;166:7381-8.

178. Reber A, Katz J. Immunological assessment of influenza vaccines and immune correlates of protection. Expert review of vaccines 2013;12:519-36.

179. Hobson D, Curry RL, Beare AS, Ward-Gardner A. The role of serum haemagglutination-inhibiting antibody in protection against challenge infection with influenza A2 and B viruses. The Journal of hygiene 1972;70:767-77.

180. Johansson BE, Bucher DJ, Kilbourne ED. Purified influenza virus hemagglutinin and neuraminidase are equivalent in stimulation of antibody response but induce contrasting types of immunity to infection. Journal of virology 1989;63:1239-46.

181. Jegerlehner A, Schmitz N, Storni T, Bachmann MF. Influenza A vaccine based on the extracellular domain of M2: weak protection mediated

via antibody-dependent NK cell activity. Journal of immunology 2004;172:5598-605.

182. Hashimoto G, Wright PF, Karzon DT. Antibody-dependent cell-mediated cytotoxicity against influenza virus-infected cells. The Journal of infectious diseases 1983;148:785-94.

183. Webster RG, Reay PA, Laver WG. Protection against lethal influenza with neuraminidase. Virology 1988;164:230-7.

184. Treanor JJ, Tierney EL, Zebedee SL, Lamb RA, Murphy BR. Passively transferred monoclonal antibody to the M2 protein inhibits influenza A virus replication in mice. Journal of virology 1990;64:1375-7.

185. Carragher DM, Kaminski DA, Moquin A, Hartson L, Randall TD. A novel role for non-neutralizing antibodies against nucleoprotein in facilitating resistance to influenza virus. Journal of immunology 2008;181:4168-76.

186. LaMere MW, Lam HT, Moquin A, et al. Contributions of antinucleoprotein IgG to heterosubtypic immunity against influenza virus. Journal of immunology 2011;186:4331-9.

187. Gerhard W, Mozdzanowska K, Furchner M, Washko G, Maiese K. Role of the B-cell response in recovery of mice from primary influenza virus infection. Immunological reviews 1997;159:95-103.

188. Francis T, Jr. The current status of the control of influenza. Annals of internal medicine 1955;43:534-8.

189. Francis T, Jr. On the Doctrine of Original Antigenic Sin. Proceedings of the American Philosophical Society 1960;104:572-8.

190. Kim JH, Skountzou I, Compans R, Jacob J. Original antigenic sin responses to influenza viruses. Journal of immunology 2009;183:3294-301.

191. Doucett VP, Gerhard W, Owler K, Curry D, Brown L, Baumgarth N. Enumeration and characterization of virus-specific B cells by multicolor flow cytometry. Journal of immunological methods 2005;303:40-52.

192. Fazekas de St G, Webster RG. Disquisitions on Original Antigenic Sin. II. Proof in lower creatures. The Journal of experimental medicine 1966;124:347-61.

193. Zarnitsyna VI, Ellebedy AH, Davis C, Jacob J, Ahmed R, Antia R. Masking of antigenic epitopes by antibodies shapes the humoral immune response to influenza. Philosophical transactions of the Royal Society of London Series B, Biological sciences 2015;370.

194. Khurana S, Verma N, Yewdell JW, et al. MF59 adjuvant enhances diversity and affinity of antibody-mediated immune response to pandemic influenza vaccines. Science translational medicine 2011;3:85ra48.

195. Mastelic Gavillet B, Eberhardt CS, Auderset F, et al. MF59 Mediates Its B Cell Adjuvanticity by Promoting T Follicular Helper Cells and Thus Germinal Center Responses in Adult and Early Life. Journal of immunology 2015;194:4836-45.

196. Zhu J, Yamane H, Paul WE. Differentiation of effector CD4 T cell populations (*). Annual review of immunology 2010;28:445-89.

197. Murphy K. Janeway's Immunobiology. 8th ed2011.

198. Teijaro JR, Turner D, Pham Q, Wherry EJ, Lefrancois L, Farber DL. Cutting edge: Tissue-retentive lung memory CD4 T cells mediate optimal protection to respiratory virus infection. Journal of immunology 2011;187:5510-4.

199. Sathaliyawala T, Kubota M, Yudanin N, et al. Distribution and compartmentalization of human circulating and tissue-resident memory T cell subsets. Immunity 2013;38:187-97.

200. Brown DM, Roman E, Swain SL. CD4 T cell responses to influenza infection. Seminars in immunology 2004;16:171-7.

201. McKinstry KK, Strutt TM, Kuang Y, et al. Memory CD4+ T cells protect against influenza through multiple synergizing mechanisms. The Journal of clinical investigation 2012;122:2847-56.

202. Wilkinson TM, Li CK, Chui CS, et al. Preexisting influenza-specific CD4+ T cells correlate with disease protection against influenza challenge in humans. Nature medicine 2012;18:274-80.

203. Graham MB, Dalton DK, Giltinan D, Braciale VL, Stewart TA, Braciale TJ. Response to influenza infection in mice with a targeted disruption in the interferon gamma gene. The Journal of experimental medicine 1993;178:1725-32.

204. Leon B, Bradley JE, Lund FE, Randall TD, Ballesteros-Tato A. FoxP3+ regulatory T cells promote influenza-specific Tfh responses by controlling IL-2 availability. Nature communications 2014;5:3495.

205. Luthje K, Kallies A, Shimohakamada Y, et al. The development and fate of follicular helper T cells defined by an IL-21 reporter mouse. Nature immunology 2012;13:491-8.

206. Jegerlehner A, Maurer P, Bessa J, Hinton HJ, Kopf M, Bachmann MF. TLR9 signaling in B cells determines class switch recombination to IgG2a. Journal of immunology 2007;178:2415-20.

207. Duttagupta PA, Boesteanu AC, Katsikis PD. Costimulation signals for memory CD8+ T cells during viral infections. Critical reviews in immunology 2009;29:469-86.

208. Topham DJ, Tripp RA, Doherty PC. CD8+ T cells clear influenza virus by perforin or Fas-dependent processes. Journal of immunology 1997;159:5197-200.

209. Mosmann TR, Li L, Sad S. Functions of CD8 T-cell subsets secreting different cytokine patterns. Seminars in immunology 1997;9:87-92.

210. Locksley RM, Killeen N, Lenardo MJ. The TNF and TNF receptor superfamilies: integrating mammalian biology. Cell 2001;104:487-501.

211. Brehm MA, Daniels KA, Welsh RM. Rapid production of TNF-alpha following TCR engagement of naive CD8 T cells. Journal of immunology 2005;175:5043-9.

212. Suresh M, Lanier G, Large MK, et al. Role of lymphotoxin alpha in T-cell responses during an acute viral infection. Journal of virology 2002;76:3943-51.

213. Ahmed R, Gray D. Immunological memory and protective immunity: understanding their relation. Science 1996;272:54-60.

214. Kaech SM, Wherry EJ, Ahmed R. Effector and memory T-cell differentiation: implications for vaccine development. Nature reviews Immunology 2002;2:251-62.

215. van Gisbergen KP, Klarenbeek PL, Kragten NA, et al. The costimulatory molecule CD27 maintains clonally diverse CD8(+) T cell responses of low antigen affinity to protect against viral variants. Immunity 2011;35:97-108.

216. Bender BS, Croghan T, Zhang L, Small PA, Jr. Transgenic mice lacking class I major histocompatibility complex-restricted T cells have delayed viral clearance and increased mortality after influenza virus challenge. The Journal of experimental medicine 1992;175:1143-5.

217. Graham MB, Braciale TJ. Resistance to and recovery from lethal influenza virus infection in B lymphocyte-deficient mice. The Journal of experimental medicine 1997;186:2063-8.

218. Sridhar S, Begom S, Bermingham A, et al. Cellular immune correlates of protection against symptomatic pandemic influenza. Nature medicine 2013;19:1305-12.

219. McMichael AJ, Gotch FM, Noble GR, Beare PA. Cytotoxic T-cell immunity to influenza. N Engl J Med 1983;309:13-7.

220. Belz GT, Xie W, Doherty PC. Diversity of epitope and cytokine profiles for primary and secondary influenza a virus-specific CD8+ T cell responses. Journal of immunology 2001;166:4627-33.

221. Townsend AR, Rothbard J, Gotch FM, Bahadur G, Wraith D, McMichael AJ. The epitopes of influenza nucleoprotein recognized by cytotoxic T lymphocytes can be defined with short synthetic peptides. Cell 1986;44:959-68.

222. Belz GT, Xie W, Altman JD, Doherty PC. A previously unrecognized H-2D(b)-restricted peptide prominent in the primary influenza A virus-specific CD8(+) T-cell response is much less apparent following secondary challenge. Journal of virology 2000;74:3486-93.

223. Andreansky SS, Stambas J, Thomas PG, Xie W, Webby RJ, Doherty PC. Consequences of immunodominant epitope deletion for minor influenza virus-specific CD8+-T-cell responses. Journal of virology 2005;79:4329-39.

224. Crowe SR, Turner SJ, Miller SC, et al. Differential antigen presentation regulates the changing patterns of CD8+ T cell immunodominance in primary and secondary influenza virus infections. The Journal of experimental medicine 2003;198:399-410.

225. Lee JB, Oelke M, Ramachandra L, Canaday DH, Schneck JP. Decline of influenza-specific CD8+ T cell repertoire in healthy geriatric donors. Immunity & ageing : I & A 2011;8:6.

226. Nguyen HH, Zemlin M, Ivanov, II, et al. Heterosubtypic immunity to influenza A virus infection requires a properly diversified antibody repertoire. Journal of virology 2007;81:9331-8.

227. Schulman JL, Kilbourne ED. Induction of Partial Specific Heterotypic Immunity in Mice by a Single Infection with Influenza a Virus. Journal of bacteriology 1965;89:170-4.

228. Staeheli P, Haller O, Boll W, Lindenmann J, Weissmann C. Mx protein: constitutive expression in 3T3 cells transformed with cloned Mx cDNA confers selective resistance to influenza virus. Cell 1986;44:147-58.

229. Ibricevic A, Pekosz A, Walter MJ, et al. Influenza virus receptor specificity and cell tropism in mouse and human airway epithelial cells. Journal of virology 2006;80:7469-80.

230. Lu X, Tumpey TM, Morken T, Zaki SR, Cox NJ, Katz JM. A mouse model for the evaluation of pathogenesis and immunity to influenza A (H5N1) viruses isolated from humans. Journal of virology 1999;73:5903-11.

231. Belser JA, Lu X, Maines TR, et al. Pathogenesis of avian influenza (H7) virus infection in mice and ferrets: enhanced virulence of Eurasian H7N7 viruses isolated from humans. Journal of virology 2007;81:11139-47.

232. Driskell EA, Jones CA, Stallknecht DE, Howerth EW, Tompkins SM. Avian influenza virus isolates from wild birds replicate and cause disease in a mouse model of infection. Virology 2010;399:280-9.

233. Belser JA, Wadford DA, Pappas C, et al. Pathogenesis of pandemic influenza A (H1N1) and triple-reassortant swine influenza A (H1) viruses in mice. Journal of virology 2010;84:4194-203.

234. Watanabe H, Numata K, Ito T, Takagi K, Matsukawa A. Innate immune response in Th1- and Th2-dominant mouse strains. Shock 2004;22:460-6.

235. Jonas E. Salk WJM, JR., AND Thomas Francis, JR. A clinical,epidemiological and immunological evaluation of vaccination against epidemic influenza Am J Hy 1945;42:57-93.

236. Hannoun C. The evolving history of influenza viruses and influenza vaccines. Expert review of vaccines 2013;12:1085-94.

237. Francis T, Salk JE, Pearson HE, Brown PN. Protective Effect of Vaccination against Induced Influenza A. J Clin Invest 1945;24:536-46.

238. Salk JE, Pearson HE, Brown PN, Francis T. Protective Effect of Vaccination against Induced Influenza B. The Journal of clinical investigation 1945;24:547-53.

239. Davenport FM, Hennessy AV, Brandon FM, Webster RG, Barrett CD, Jr., Lease GO. Comparisons of Serologic and Febrile Responses in Humans to Vaccination with Influenza a Viruses or Their Hemagglutinins. The Journal of laboratory and clinical medicine 1964;63:5-13.

240. Gerdil C. The annual production cycle for influenza vaccine. Vaccine 2003;21:1776-9.

241. Cleeland R, Grunberg E, Prince HN. Inactivation of the hemagglutinins of type A influenza viruses by physical and chemical means: an aid to classification. Infection and immunity 1972;5:324-31.

242. Oxford JS, Potter CW, McLaren C, Hardy W. Inactivation of influenza and other viruses by a mixture of virucidal compounds. Applied microbiology 1971;21:606-10.

243. Wong SS, Webby RJ. Traditional and new influenza vaccines. Clinical microbiology reviews 2013;26:476-92.

244. Chan W, Zhou H, Kemble G, Jin H. The cold adapted and temperature sensitive influenza A/Ann Arbor/6/60 virus, the master donor virus for live attenuated influenza vaccines, has multiple defects in replication at the restrictive temperature. Virology 2008;380:304-11.

245. Jin H, Subbarao K. Live attenuated influenza vaccine. Current topics in microbiology and immunology 2014;386:181-204.

246. Ohmit SE, Petrie JG, Cross RT, Johnson E, Monto AS. Influenza hemagglutination-inhibition antibody titer as a correlate of vaccine-induced protection. The Journal of infectious diseases 2011;204:1879-85.

247. Belshe RB, Gruber WC, Mendelman PM, et al. Correlates of immune protection induced by live, attenuated, cold-adapted, trivalent, intranasal influenza virus vaccine. The Journal of infectious diseases 2000;181:1133-7.

248. Voordouw AC, Beyer WE, Smith DJ, Sturkenboom MC, Stricker BH. Evaluation of serological trials submitted for annual re-licensure of influenza

vaccines to regulatory authorities between 1992 and 2002. Vaccine 2009;28:392-7.

249. de Jong JC, Beyer WE, Palache AM, Rimmelzwaan GF, Osterhaus AD. Mismatch between the 1997/1998 influenza vaccine and the major epidemic A(H3N2) virus strain as the cause of an inadequate vaccine-induced antibody response to this strain in the elderly. Journal of medical virology 2000;61:94-9.

250. Pebody RG, Warburton F, Ellis J, et al. Low effectiveness of seasonal influenza vaccine in preventing laboratory-confirmed influenza in primary care in the United Kingdom: 2014/15 mid-season results. Euro surveillance : bulletin Europeen sur les maladies transmissibles = European communicable disease bulletin 2015;20:21025.

251. Webby RJ, Webster RG. Are we ready for pandemic influenza? Science 2003;302:1519-22.

252. Huber VC. Influenza vaccines: from whole virus preparations to recombinant protein technology. Expert review of vaccines 2014;13:31-42.

253. Maassab HF, Bryant ML. The development of live attenuated cold-adapted influenza virus vaccine for humans. Reviews in medical virology 1999;9:237-44.

254. Peiris JS, de Jong MD, Guan Y. Avian influenza virus (H5N1): a threat to human health. Clinical microbiology reviews 2007;20:243-67.

255. Genzel Y, Dietzsch C, Rapp E, Schwarzer J, Reichl U. MDCK and Vero cells for influenza virus vaccine production: a one-to-one comparison up to lab-scale bioreactor cultivation. Applied microbiology and biotechnology 2010;88:461-75.

256. Cox MM, Hollister JR. FluBlok, a next generation influenza vaccine manufactured in insect cells. Biologicals : journal of the International Association of Biological Standardization 2009;37:182-9.

257. Osterholm MT, Kelley NS, Sommer A, Belongia EA. Efficacy and effectiveness of influenza vaccines: a systematic review and meta-analysis. The Lancet Infectious diseases 2012;12:36-44.

258. Jefferson T, Rivetti A, Harnden A, Di Pietrantonj C, Demicheli V. Vaccines for preventing influenza in healthy children. The Cochrane database of systematic reviews 2008:CD004879.

259. Bodewes R, Fraaij PL, Geelhoed-Mieras MM, et al. Annual vaccination against influenza virus hampers development of virus-specific CD8(+) T cell immunity in children. Journal of virology 2011;85:11995-2000.

260. DiazGranados CA, Dunning AJ, Kimmel M, et al. Efficacy of high-dose versus standard-dose influenza vaccine in older adults. The New England journal of medicine 2014;371:635-45.

261. Tsai TF. Fluad(R)-MF59(R)-Adjuvanted Influenza Vaccine in Older Adults. Infection & chemotherapy 2013;45:159-74.

262. Waddington CS, Walker WT, Oeser C, et al. Safety and immunogenicity of AS03B adjuvanted split virion versus non-adjuvanted whole virion H1N1 influenza vaccine in UK children aged 6 months-12 years: open label, randomised, parallel group, multicentre study. Bmj 2010;340:c2649.

263. Miller E, Andrews N, Stellitano L, et al. Risk of narcolepsy in children and young people receiving AS03 adjuvanted pandemic A/H1N1 2009 influenza vaccine: retrospective analysis. Bmj 2013;346:f794.

264. Nohynek H, Jokinen J, Partinen M, et al. AS03 adjuvanted AH1N1 vaccine associated with an abrupt increase in the incidence of childhood narcolepsy in Finland. PloS one 2012;7:e33536.

265. Ahmed SS, Volkmuth W, Duca J, et al. Antibodies to influenza nucleoprotein cross-react with human hypocretin receptor 2. Science translational medicine 2015;7:294ra105.

266. Statement on narcolepsy and vaccination. 2011. (Accessed 27th December, 2015, at http://www.who.int/vaccine_safety/committee/topics/influenza/pandemic/h1n1_safety_assessing/narcolepsy_statement/en/.)

267. Khan KH. DNA vaccines: roles against diseases. Germs 2013;3:26-35.

268. Kim JH, Jacob J. DNA vaccines against influenza viruses. Current topics in microbiology and immunology 2009;333:197-210.

269. Ledgerwood JE, Wei CJ, Hu Z, et al. DNA priming and influenza vaccine immunogenicity: two phase 1 open label randomised clinical trials. The Lancet Infectious diseases 2011;11:916-24.

270. Lopez-Macias C. Virus-like particle (VLP)-based vaccines for pandemic influenza: performance of a VLP vaccine during the 2009 influenza pandemic. Human vaccines & immunotherapeutics 2012;8:411-4.

271. Lopez-Macias C, Ferat-Osorio E, Tenorio-Calvo A, et al. Safety and immunogenicity of a virus-like particle pandemic influenza A (H1N1) 2009 vaccine in a blinded, randomized, placebo-controlled trial of adults in Mexico. Vaccine 2011;29:7826-34.

272. Fries LF, Smith GE, Glenn GM. A Recombinant Viruslike Particle Influenza A (H7N9) Vaccine. New England Journal of Medicine 2013;369:2564-6.

273. Draper SJ, Heeney JL. Viruses as vaccine vectors for infectious diseases and cancer. Nature reviews Microbiology 2010;8:62-73.

274. Draper SJ, Moore AC, Goodman AL, et al. Effective induction of high-titer antibodies by viral vector vaccines. Nature medicine 2008;14:819-21.

275. Kopecky-Bromberg SA, Palese P. Recombinant vectors as influenza vaccines. Current topics in microbiology and immunology 2009;333:243-67.

276. Tripp RA, Tompkins SM. Virus-vectored influenza virus vaccines. Viruses 2014;6:3055-79.

277. Iwatsuki-Horimoto K, Horimoto T, Noda T, et al. The cytoplasmic tail of the influenza A virus M2 protein plays a role in viral assembly. Journal of virology 2006;80:5233-40.

278. Rossman JS, Jing X, Leser GP, Balannik V, Pinto LH, Lamb RA. Influenza virus m2 ion channel protein is necessary for filamentous virion formation. Journal of virology 2010;84:5078-88.

279. Fiers W, De Filette M, El Bakkouri K, et al. M2e-based universal influenza A vaccine. Vaccine 2009;27:6280-3.

280. El Bakkouri K, Descamps F, De Filette M, et al. Universal vaccine based on ectodomain of matrix protein 2 of influenza A: Fc receptors and alveolar macrophages mediate protection. Journal of immunology 2011;186:1022-31.

281. Zhong W, Reed C, Blair PJ, Katz JM, Hancock K, Influenza Serology Working G. Serum antibody response to matrix protein 2 following natural

infection with 2009 pandemic influenza A(H1N1) virus in humans. The Journal of infectious diseases 2014;209:986-94.

282. Neirynck S, Deroo T, Saelens X, Vanlandschoot P, Jou WM, Fiers W. A universal influenza A vaccine based on the extracellular domain of the M2 protein. Nature medicine 1999;5:1157-63.

283. Wolf AI, Mozdzanowska K, Williams KL, et al. Vaccination with M2e-based multiple antigenic peptides: characterization of the B cell response and protection efficacy in inbred and outbred mice. PloS one 2011;6:e28445.

284. Zhou C, Zhou L, Chen YH. Immunization with high epitope density of M2e derived from 2009 pandemic H1N1 elicits protective immunity in mice. Vaccine 2012;30:3463-9.

285. Heinen PP, Rijsewijk FA, de Boer-Luijtze EA, Bianchi AT. Vaccination of pigs with a DNA construct expressing an influenza virus M2-nucleoprotein fusion protein exacerbates disease after challenge with influenza A virus. The Journal of general virology 2002;83:1851-9.

286. Kitikoon P, Vincent AL, Janke BH, et al. Swine influenza matrix 2 (M2) protein contributes to protection against infection with different H1 swine influenza virus (SIV) isolates. Vaccine 2009;28:523-31.

287. Turley CB, Rupp RE, Johnson C, et al. Safety and immunogenicity of a recombinant M2e-flagellin influenza vaccine (STF2.4xM2e) in healthy adults. Vaccine 2011;29:5145-52.

288. Okuno Y, Isegawa Y, Sasao F, Ueda S. A common neutralizing epitope conserved between the hemagglutinins of influenza A virus H1 and H2 strains. Journal of virology 1993;67:2552-8.

289. Okuno Y, Matsumoto K, Isegawa Y, Ueda S. Protection against the mouse-adapted A/FM/1/47 strain of influenza A virus in mice by a monoclonal antibody with cross-neutralizing activity among H1 and H2 strains. Journal of virology 1994;68:517-20.

290. Corti D, Voss J, Gamblin SJ, et al. A neutralizing antibody selected from plasma cells that binds to group 1 and group 2 influenza A hemagglutinins. Science 2011;333:850-6.

291. Corti D, Suguitan AL, Jr., Pinna D, et al. Heterosubtypic neutralizing antibodies are produced by individuals immunized with a seasonal influenza vaccine. The Journal of clinical investigation 2010;120:1663-73.

292. Hancock K, Veguilla V, Lu X, et al. Cross-reactive antibody responses to the 2009 pandemic H1N1 influenza virus. N Engl J Med 2009;361:1945-52.

293. Ikonen N, Strengell M, Kinnunen L, et al. High frequency of cross-reacting antibodies against 2009 pandemic influenza A(H1N1) virus among the elderly in Finland. Euro surveillance : bulletin Europeen sur les maladies transmissibles = European communicable disease bulletin 2010;15.

294. Pica N, Hai R, Krammer F, et al. Hemagglutinin stalk antibodies elicited by the 2009 pandemic influenza virus as a mechanism for the extinction of seasonal H1N1 viruses. Proceedings of the National Academy of Sciences of the United States of America 2012;109:2573-8.

295. Wrammert J, Koutsonanos D, Li GM, et al. Broadly cross-reactive antibodies dominate the human B cell response against 2009 pandemic H1N1 influenza virus infection. The Journal of experimental medicine 2011;208:181-93.

296. Steel J, Lowen AC, Wang TT, et al. Influenza virus vaccine based on the conserved hemagglutinin stalk domain. MBio 2010;1.

297. Mallajosyula VV, Citron M, Ferrara F, et al. Influenza hemagglutinin stem-fragment immunogen elicits broadly neutralizing antibodies and confers heterologous protection. Proceedings of the National Academy of Sciences of the United States of America 2014;111:E2514-23.

298. Hai R, Krammer F, Tan GS, et al. Influenza viruses expressing chimeric hemagglutinins: globular head and stalk domains derived from different subtypes. Journal of virology 2012;86:5774-81.

299. Krammer F, Palese P. Influenza virus hemagglutinin stalk-based antibodies and vaccines. Current opinion in virology 2013;3:521-30.

300. Eggink D, Goff PH, Palese P. Guiding the immune response against influenza virus hemagglutinin toward the conserved stalk domain by hyperglycosylation of the globular head domain. Journal of virology 2014;88:699-704.

301. Bommakanti G, Citron MP, Hepler RW, et al. Design of an HA2-based Escherichia coli expressed influenza immunogen that protects mice from pathogenic challenge. Proceedings of the National Academy of Sciences of the United States of America 2010;107:13701-6.

302. Bommakanti G, Lu X, Citron MP, et al. Design of Escherichia coli-expressed stalk domain immunogens of H1N1 hemagglutinin that protect mice from lethal challenge. Journal of virology 2012;86:13434-44.

303. Lu Y, Welsh JP, Swartz JR. Production and stabilization of the trimeric influenza hemagglutinin stem domain for potentially broadly protective

influenza vaccines. Proceedings of the National Academy of Sciences of the United States of America 2014;111:125-30.

304. Krammer F, Margine I, Hai R, et al. H3 stalk-based chimeric hemagglutinin influenza virus constructs protect mice from H7N9 challenge. Journal of virology 2014;88:2340-3.

305. Krammer F, Pica N, Hai R, Margine I, Palese P. Chimeric hemagglutinin influenza virus vaccine constructs elicit broadly protective stalk-specific antibodies. Journal of virology 2013;87:6542-50.

306. Ulmer JB, Fu TM, Deck RR, et al. Protective CD4+ and CD8+ T cells against influenza virus induced by vaccination with nucleoprotein DNA. Journal of virology 1998;72:5648-53.

307. Epstein SL, Kong WP, Misplon JA, et al. Protection against multiple influenza A subtypes by vaccination with highly conserved nucleoprotein. Vaccine 2005;23:5404-10.

308. Huang B, Wang W, Li R, et al. Influenza A virus nucleoprotein derived from Escherichia coli or recombinant vaccinia (Tiantan) virus elicits robust cross-protection in mice. Virology journal 2012;9:322.

309. Wraith DC, Vessey AE, Askonas BA. Purified influenza virus nucleoprotein protects mice from lethal infection. The Journal of general virology 1987;68 (Pt 2):433-40.

310. Berthoud TK, Hamill M, Lillie PJ, et al. Potent CD8+ T-cell immunogenicity in humans of a novel heterosubtypic influenza A vaccine, MVA-NP+M1. Clinical infectious diseases : an official publication of the Infectious Diseases Society of America 2011;52:1-7.

311. Lillie PJ, Berthoud TK, Powell TJ, et al. Preliminary assessment of the efficacy of a T-cell-based influenza vaccine, MVA-NP+M1, in humans. Clinical infectious diseases : an official publication of the Infectious Diseases Society of America 2012;55:19-25.

312. Antrobus RD, Coughlan L, Berthoud TK, et al. Clinical assessment of a novel recombinant simian adenovirus ChAdOx1 as a vectored vaccine expressing conserved Influenza A antigens. Molecular therapy : the journal of the American Society of Gene Therapy 2014;22:668-74.

313. Lambe T, Carey JB, Li Y, et al. Immunity against heterosubtypic influenza virus induced by adenovirus and MVA expressing nucleoprotein and matrix protein-1. Scientific reports 2013;3:1443.

314. Guidance for Industry: Clinical Data Needed to Support the Licensure of Seasonal Inactivated Influenza Vaccines. 2007. (Accessed 3rd August, 2015, at http://www.fda.gov/BiologicsBloodVaccines/GuidanceComplianceRegulatoryInformation/Guidances/Vaccines/ucm074794.htm.)

315. Guideline on influenza vaccines. 2014. (Accessed 3rd August, 2015, at http://www.ema.europa.eu/docs/en_GB/document_library/Scientific_guideline/2014/07/WC500170300.pdf.)

316. Wood JM, Levandowski RA. The influenza vaccine licensing process. Vaccine 2003;21:1786-8.

317. Note for guidance on harmonization of requirements for influenza vaccines. 1997. (Accessed 21st June, 2015, at http://www.ema.europa.eu/docs/en_GB/document_library/Scientific_guideline/2009/09/WC500003945.pdf.)

318. Ovsyannikova IG, White SJ, Albrecht RA, Garcia-Sastre A, Poland GA. Turkey versus guinea pig red blood cells: hemagglutination differences alter hemagglutination inhibition responses against influenza A/H1N1. Viral immunology 2014;27:174-8.

319. Black S, Nicolay U, Vesikari T, et al. Hemagglutination inhibition antibody titers as a correlate of protection for inactivated influenza vaccines in children. The Pediatric infectious disease journal 2011;30:1081-5.

320. McElhaney JE, Xie D, Hager WD, et al. T cell responses are better correlates of vaccine protection in the elderly. Journal of immunology 2006;176:6333-9.

321. Forrest BD, Pride MW, Dunning AJ, et al. Correlation of cellular immune responses with protection against culture-confirmed influenza virus in young children. Clinical and vaccine immunology : CVI 2008;15:1042-53.

322. Barria MI, Garrido JL, Stein C, et al. Localized mucosal response to intranasal live attenuated influenza vaccine in adults. The Journal of infectious diseases 2013;207:115-24.

323. Boyce TG, Gruber WC, Coleman-Dockery SD, et al. Mucosal immune response to trivalent live attenuated intranasal influenza vaccine in children. Vaccine 1999;18:82-8.

324. Larocca C, Schlom J. Viral vector-based therapeutic cancer vaccines. Cancer journal 2011;17:359-71.

325. Ondondo BO. The influence of delivery vectors on HIV vaccine efficacy. Frontiers in microbiology 2014;5:439.

326. Reyes-Sandoval A, Berthoud T, Alder N, et al. Prime-boost immunization with adenoviral and modified vaccinia virus Ankara vectors

enhances the durability and polyfunctionality of protective malaria CD8+ T-cell responses. Infection and immunity 2010;78:145-53.

327. Viruses ICoTo, King AMQ, Adams MJ, Lefkowitz EJ, Carstens EB. Virus Taxonomy: Classification and Nomenclature of Viruses : Ninth Report of the International Committee on Taxonomy of Viruses: Academic Press; 2011.

328. Rowe WP, Huebner RJ, Gilmore LK, Parrott RH, Ward TG. Isolation of a cytopathogenic agent from human adenoids undergoing spontaneous degeneration in tissue culture. Proceedings of the Society for Experimental Biology and Medicine Society for Experimental Biology and Medicine 1953;84:570-3.

329. Adenoviruses: Symptoms. 2015. (Accessed 12th July, 2015, at http://www.cdc.gov/adenovirus/about/symptoms.html.)

330. Krilov LR. Adenovirus infections in the immunocompromised host. The Pediatric infectious disease journal 2005;24:555-6.

331. Adenovirus VIS. 2014. (Accessed 27th December, 2015, at http://www.cdc.gov/vaccines/hcp/vis/vis-statements/adenovirus.html.)

332. Zhang Y, Bergelson JM. Adenovirus receptors. Journal of virology 2005;79:12125-31.

333. Amalfitano A. Next-generation adenoviral vectors: new and improved. Gene therapy 1999;6:1643-5.

334. Marshall E. Gene therapy death prompts review of adenovirus vector. Science 1999;286:2244-5.

335. Tatsis N, Ertl HC. Adenoviruses as vaccine vectors. Molecular therapy : the journal of the American Society of Gene Therapy 2004;10:616-29.

336. Xiang ZQ, Yang Y, Wilson JM, Ertl HC. A replication-defective human adenovirus recombinant serves as a highly efficacious vaccine carrier. Virology 1996;219:220-7.

337. Mizuguchi H, Kay MA. A simple method for constructing E1- and E1/E4-deleted recombinant adenoviral vectors. Human gene therapy 1999;10:2013-7.

338. Gao GP, Yang Y, Wilson JM. Biology of adenovirus vectors with E1 and E4 deletions for liver-directed gene therapy. Journal of virology 1996;70:8934-43.

339. Zhong L, Granelli-Piperno A, Choi Y, Steinman RM. Recombinant adenovirus is an efficient and non-perturbing genetic vector for human dendritic cells. European journal of immunology 1999;29:964-72.

340. Worgall S, Busch A, Rivara M, et al. Modification to the capsid of the adenovirus vector that enhances dendritic cell infection and transgene-specific cellular immune responses. Journal of virology 2004;78:2572-80.

341. Morelli AE, Larregina AT, Ganster RW, et al. Recombinant adenovirus induces maturation of dendritic cells via an NF-kappaB-dependent pathway. Journal of virology 2000;74:9617-28.

342. Liu Q, Muruve DA. Molecular basis of the inflammatory response to adenovirus vectors. Gene therapy 2003;10:935-40.

343. Molinier-Frenkel V, Lengagne R, Gaden F, et al. Adenovirus hexon protein is a potent adjuvant for activation of a cellular immune response. Journal of virology 2002;76:127-35.

344. Gao W, Soloff AC, Lu X, et al. Protection of mice and poultry from lethal H5N1 avian influenza virus through adenovirus-based immunization. Journal of virology 2006;80:1959-64.

345. Lasaro MO, Ertl HCJ. New Insights on Adenovirus as Vaccine Vectors. Molecular Therapy: the Journal of the American Society of Gene Therapy 2009;17:1333-9.

346. Abbink P, Lemckert AA, Ewald BA, et al. Comparative seroprevalence and immunogenicity of six rare serotype recombinant adenovirus vaccine vectors from subgroups B and D. Journal of virology 2007;81:4654-63.

347. Kahl CA, Bonnell J, Hiriyanna S, et al. Potent immune responses and in vitro pro-inflammatory cytokine suppression by a novel adenovirus vaccine vector based on rare human serotype 28. Vaccine 2010;28:5691-702.

348. Farina SF, Gao GP, Xiang ZQ, et al. Replication-defective vector based on a chimpanzee adenovirus. Journal of virology 2001;75:11603-13.

349. Colloca S, Barnes E, Folgori A, et al. Vaccine vectors derived from a large collection of simian adenoviruses induce potent cellular immunity across multiple species. Science translational medicine 2012;4:115ra2.

350. Dicks MD, Guzman E, Spencer AJ, et al. The relative magnitude of transgene-specific adaptive immune responses induced by human and chimpanzee adenovirus vectors differs between laboratory animals and a target species. Vaccine 2015;33:1121-8.

351. Penaloza-MacMaster P, Provine NM, Ra J, et al. Alternative serotype adenovirus vaccine vectors elicit memory T cells with enhanced anamnestic capacity compared to Ad5 vectors. Journal of virology 2013;87:1373-84.

352. Tan WG, Jin HT, West EE, et al. Comparative analysis of simian immunodeficiency virus gag-specific effector and memory CD8+ T cells induced by different adenovirus vectors. Journal of virology 2013;87:1359-72.

353. Barnes E, Folgori A, Capone S, et al. Novel adenovirus-based vaccines induce broad and sustained T cell responses to HCV in man. Science translational medicine 2012;4:115ra1.

354. O'Hara GA, Duncan CJ, Ewer KJ, et al. Clinical assessment of a recombinant simian adenovirus ChAd63: a potent new vaccine vector. The Journal of infectious diseases 2012;205:772-81.

355. Tatsis N, Tesema L, Robinson ER, et al. Chimpanzee-origin adenovirus vectors as vaccine carriers. Gene therapy 2006;13:421-9.

356. Rampling T, Ewer K, Bowyer G, et al. A Monovalent Chimpanzee Adenovirus Ebola Vaccine - Preliminary Report. The New England journal of medicine 2015.

357. Mayr A, Munz E. [Changes in the vaccinia virus through continuing passages in chick embryo fibroblast cultures]. Zentralblatt fur Bakteriologie, Parasitenkunde, Infektionskrankheiten und Hygiene 1 Abt Medizinisch-hygienische Bakteriologie, Virusforschung und Parasitologie Originale 1964;195:24-35.

358. Stickl H, Hochstein-Mintzel V, Mayr A, Huber HC, Schafer H, Holzner A. [MVA vaccination against smallpox: clinical tests with an attenuated live vaccinia virus strain (MVA) (author's transl)]. Deutsche medizinische Wochenschrift 1974;99:2386-92.

359. Antoine G, Scheiflinger F, Dorner F, Falkner FG. The complete genomic sequence of the modified vaccinia Ankara strain: comparison with other orthopoxviruses. Virology 1998;244:365-96.

360. Drexler I, Heller K, Wahren B, Erfle V, Sutter G. Highly attenuated modified vaccinia virus Ankara replicates in baby hamster kidney cells, a potential host for virus propagation, but not in various human transformed and primary cells. The Journal of general virology 1998;79 (Pt 2):347-52.

361. Okeke MI, Nilssen O, Traavik T. Modified vaccinia virus Ankara multiplies in rat IEC-6 cells and limited production of mature virions occurs in other mammalian cell lines. The Journal of general virology 2006;87:21-7.

362. Zwilling J, Sliva K, Schwantes A, Schnierle B, Sutter G. Functional F11L and K1L genes in modified vaccinia virus Ankara restore virus-induced cell motility but not growth in human and murine cells. Virology 2010;404:231-9.

363. Sutter G, Wyatt LS, Foley PL, Bennink JR, Moss B. A recombinant vector derived from the host range-restricted and highly attenuated MVA strain of vaccinia virus stimulates protective immunity in mice to influenza virus. Vaccine 1994;12:1032-40.

364. Carroll MW, Overwijk WW, Chamberlain RS, Rosenberg SA, Moss B, Restifo NP. Highly attenuated modified vaccinia virus Ankara (MVA) as an effective recombinant vector: a murine tumor model. Vaccine 1997;15:387-94.

365. Cottingham MG, Andersen RF, Spencer AJ, et al. Recombination-mediated genetic engineering of a bacterial artificial chromosome clone of modified vaccinia virus Ankara (MVA). PloS one 2008;3:e1638.

366. Scheiflinger F, Falkner FG, Dorner F. Evaluation of the thymidine kinase (tk) locus as an insertion site in the highly attenuated vaccinia MVA strain. Archives of virology 1996;141:663-9.

367. Merchlinsky M, Moss B. Introduction of foreign DNA into the vaccinia virus genome by in vitro ligation: recombination-independent selectable cloning vectors. Virology 1992;190:522-6.

368. Orubu T, Alharbi NK, Lambe T, Gilbert SC, Cottingham MG. Expression and cellular immunogenicity of a transgenic antigen driven by endogenous poxviral early promoters at their authentic loci in MVA. PloS one 2012;7:e40167.

369. Oseroff C, Peters B, Pasquetto V, et al. Dissociation between epitope hierarchy and immunoprevalence in CD8 responses to vaccinia virus western reserve. Journal of immunology 2008;180:7193-202.

370. Tscharke DC, Karupiah G, Zhou J, et al. Identification of poxvirus CD8+ T cell determinants to enable rational design and characterization of smallpox vaccines. The Journal of experimental medicine 2005;201:95-104.

371. Tscharke DC, Woo WP, Sakala IG, et al. Poxvirus CD8+ T-cell determinants and cross-reactivity in BALB/c mice. Journal of virology 2006;80:6318-23.

372. Sette A, Grey H, Oseroff C, et al. Definition of epitopes and antigens recognized by vaccinia specific immune responses: their conservation in variola virus sequences, and use as a model system to study complex pathogens. Vaccine 2009;27 Suppl 6:G21-6.

373. Bronte V, Carroll MW, Goletz TJ, et al. Antigen expression by dendritic cells correlates with the therapeutic effectiveness of a model recombinant

poxvirus tumor vaccine. Proceedings of the National Academy of Sciences of the United States of America 1997;94:3183-8.

374. Mullarkey CE, Boyd A, van Laarhoven A, et al. Improved adjuvanting of seasonal influenza vaccines: preclinical studies of MVA-NP+M1 coadministration with inactivated influenza vaccine. European journal of immunology 2013;43:1940-52.

375. Gasteiger G, Kastenmuller W, Ljapoci R, Sutter G, Drexler I. Cross-priming of cytotoxic T cells dictates antigen requisites for modified vaccinia virus Ankara vector vaccines. Journal of virology 2007;81:11925-36.

376. Gorse GJ, Newman MJ, deCamp A, et al. DNA and modified vaccinia virus Ankara vaccines encoding multiple cytotoxic and helper T-lymphocyte epitopes of human immunodeficiency virus type 1 (HIV-1) are safe but weakly immunogenic in HIV-1-uninfected, vaccinia virus-naive adults. Clinical and vaccine immunology : CVI 2012;19:649-58.

377. Schliehe C, Bitzer A, van den Broek M, Groettrup M. Stable antigen is most effective for eliciting CD8+ T-cell responses after DNA vaccination and infection with recombinant vaccinia virus in vivo. Journal of virology 2012;86:9782-93.

378. Scriba TJ, Tameris M, Mansoor N, et al. Modified vaccinia Ankara-expressing Ag85A, a novel tuberculosis vaccine, is safe in adolescents and children, and induces polyfunctional CD4+ T cells. European journal of immunology 2010;40:279-90.

379. Sheehy SH, Duncan CJ, Elias SC, et al. Phase Ia clinical evaluation of the Plasmodium falciparum blood-stage antigen MSP1 in ChAd63 and MVA

vaccine vectors. Molecular therapy : the journal of the American Society of Gene Therapy 2011;19:2269-76.

380. Sheehy SH, Duncan CJ, Elias SC, et al. Phase Ia clinical evaluation of the safety and immunogenicity of the Plasmodium falciparum blood-stage antigen AMA1 in ChAd63 and MVA vaccine vectors. PloS one 2012;7:e31208.

381. Geiben-Lynn R, Greenland JR, Frimpong-Boateng K, Letvin NL. Kinetics of recombinant adenovirus type 5, vaccinia virus, modified vaccinia ankara virus, and DNA antigen expression in vivo and the induction of memory T-lymphocyte responses. Clinical and vaccine immunology : CVI 2008;15:691-6.

382. Jego G, Palucka AK, Blanck JP, Chalouni C, Pascual V, Banchereau J. Plasmacytoid dendritic cells induce plasma cell differentiation through type I interferon and interleukin 6. Immunity 2003;19:225-34.

383. Barouch DH, Yang ZY, Kong WP, et al. A human T-cell leukemia virus type 1 regulatory element enhances the immunogenicity of human immunodeficiency virus type 1 DNA vaccines in mice and nonhuman primates. Journal of virology 2005;79:8828-34.

384. Miura K, Orcutt AC, Muratova OV, Miller LH, Saul A, Long CA. Development and characterization of a standardized ELISA including a reference serum on each plate to detect antibodies induced by experimental malaria vaccines. Vaccine 2008;26:193-200.

385. Perkins DL, Lai MZ, Smith JA, Gefter ML. Identical peptides recognized by MHC class I- and II-restricted T cells. The Journal of experimental medicine 1989;170:279-89.

386. Wiley DC, Skehel JJ, Waterfield M. Evidence from studies with a cross-linking reagent that the haemagglutinin of influenza virus is a trimer. Virology 1977;79:446-8.

387. Matlin KS, Simons K. Reduced temperature prevents transfer of a membrane glycoprotein to the cell surface but does not prevent terminal glycosylation. Cell 1983;34:233-43.

388. Lazarowitz SG, Compans RW, Choppin PW. Influenza virus structural and nonstructural proteins in infected cells and their plasma membranes. Virology 1971;46:830-43.

389. Gething MJ, McCammon K, Sambrook J. Expression of wild-type and mutant forms of influenza hemagglutinin: the role of folding in intracellular transport. Cell 1986;46:939-50.

390. Copeland CS, Doms RW, Bolzau EM, Webster RG, Helenius A. Assembly of influenza hemagglutinin trimers and its role in intracellular transport. The Journal of cell biology 1986;103:1179-91.

391. Russ G, Bennink JR, Bachi T, Yewdell JW. Influenza virus hemagglutinin trimers and monomers maintain distinct biochemical modifications and intracellular distribution in brefeldin A-treated cells. Cell regulation 1991;2:549-63.

392. Yewdell JW, Yellen A, Bachi T. Monoclonal antibodies localize events in the folding, assembly, and intracellular transport of the influenza virus hemagglutinin glycoprotein. Cell 1988;52:843-52.

393. Rogers GN, Paulson JC, Daniels RS, Skehel JJ, Wilson IA, Wiley DC. Single amino acid substitutions in influenza haemagglutinin change receptor binding specificity. Nature 1983;304:76-8.

394. Rodriguez-Boulan E, Paskiet KT, Salas PJ, Bard E. Intracellular transport of influenza virus hemagglutinin to the apical surface of Madin-Darby canine kidney cells. The Journal of cell biology 1984;98:308-19.

395. McCauley J, Bye J, Elder K, et al. Influenza virus haemagglutinin signal sequence. FEBS Lett 1979;108:422-6.

396. Skehel JJ, Stevens DJ, Daniels RS, et al. A carbohydrate side chain on hemagglutinins of Hong Kong influenza viruses inhibits recognition by a monoclonal antibody. Proceedings of the National Academy of Sciences of the United States of America 1984;81:1779-83.

397. Ohuchi M, Ohuchi R, Feldmann A, Klenk HD. Regulation of receptor binding affinity of influenza virus hemagglutinin by its carbohydrate moiety. Journal of virology 1997;71:8377-84.

398. An Y, Rininger JA, Jarvis DL, et al. Comparative glycomics analysis of influenza Hemagglutinin (H5N1) produced in vaccine relevant cell platforms. J Proteome Res 2013;12:3707-20.

399. Magadan JG, Khurana S, Das SR, et al. Influenza A virus hemagglutinin trimerization completes monomer folding and antigenicity. Journal of virology 2013;87:9742-53.

400. Kong WP, Hood C, Yang ZY, et al. Protective immunity to lethal challenge of the 1918 pandemic influenza virus by vaccination. Proceedings of the National Academy of Sciences of the United States of America 2006;103:15987-91.

401. Stevens J, Corper AL, Basler CF, Taubenberger JK, Palese P, Wilson IA. Structure of the uncleaved human H1 hemagglutinin from the extinct 1918 influenza virus. Science 2004;303:1866-70.

402. Li S, Liu C, Klimov A, et al. Recombinant influenza A virus vaccines for the pathogenic human A/Hong Kong/97 (H5N1) viruses. The Journal of infectious diseases 1999;179:1132-8.

403. Winter G, Fields S, Brownlee GG. Nucleotide sequence of the haemagglutinin gene of a human influenza virus H1 subtype. Nature 1981;292:72-5.

404. Wei CJ, Boyington JC, McTamney PM, et al. Induction of broadly neutralizing H1N1 influenza antibodies by vaccination. Science 2010;329:1060-4.

405. Dereeper A, Guignon V, Blanc G, et al. Phylogeny.fr: robust phylogenetic analysis for the non-specialist. Nucleic Acids Res 2008;36:W465-9.

406. Felenstein J. PHYLIP - Phylogeny Inference Package (Version 3.2). Cladistics 1989;5:164-6.

407. Wang K, Holtz KM, Anderson K, Chubet R, Mahmoud W, Cox MM. Expression and purification of an influenza hemagglutinin--one step closer to a recombinant protein-based influenza vaccine. Vaccine 2006;24:2176-85.

408. Margine I, Palese P, Krammer F. Expression of functional recombinant hemagglutinin and neuraminidase proteins from the novel H7N9 influenza virus using the baculovirus expression system. Journal of visualized experiments : JoVE 2013:e51112.

409. Athmaram TN, Saraswat S, Santhosh SR, et al. Yeast expressed recombinant Hemagglutinin protein of novel H1N1 elicits neutralising antibodies in rabbits and mice. Virology journal 2011;8:524.

410. Kopera E, Dwornyk A, Kosson P, et al. Expression, purification and characterization of glycosylated influenza H5N1 hemagglutinin produced in Pichia pastoris. Acta biochimica Polonica 2014;61:597-602.

411. Dreyfus C, Ekiert DC, Wilson IA. Structure of a classical broadly neutralizing stem antibody in complex with a pandemic H2 influenza virus hemagglutinin. Journal of virology 2013;87:7149-54.

412. Magadan JG, Altman MO, Ince WL, et al. Biogenesis of influenza a virus hemagglutinin cross-protective stem epitopes. PLoS pathogens 2014;10:e1004204.

413. Krammer F, Margine I, Tan GS, Pica N, Krause JC, Palese P. A carboxy-terminal trimerization domain stabilizes conformational epitopes on the stalk domain of soluble recombinant hemagglutinin substrates. PloS one 2012;7:e43603.

414. Davis AR, Bos T, Ueda M, Nayak DP, Dowbenko D, Compans RW. Immune response to human influenza virus hemagglutinin expressed in Escherichia coli. Gene 1983;21:273-84.

415. Jabbar MA, Sivasubramanian N, Nayak DP. Influenza viral (A/WSN/33) hemagglutinin is expressed and glycosylated in the yeast Saccharomyces cerevisiae. Proceedings of the National Academy of Sciences of the United States of America 1985;82:2019-23.

416. Kuroda K, Hauser C, Rott R, Klenk HD, Doerfler W. Expression of the influenza virus haemagglutinin in insect cells by a baculovirus vector. The EMBO journal 1986;5:1359-65.

417. Singh I, Doms RW, Wagner KR, Helenius A. Intracellular transport of soluble and membrane-bound glycoproteins: folding, assembly and secretion of anchor-free influenza hemagglutinin. The EMBO journal 1990;9:631-9.

418. de Vries RP, de Vries E, Bosch BJ, de Groot RJ, Rottier PJ, de Haan CA. The influenza A virus hemagglutinin glycosylation state affects receptor-binding specificity. Virology 2010;403:17-25.

419. Wang CC, Chen JR, Tseng YC, et al. Glycans on influenza hemagglutinin affect receptor binding and immune response. Proceedings of the National Academy of Sciences of the United States of America 2009;106:18137-42.

420. Ohuchi M, Feldmann A, Ohuchi R, Klenk HD. Neuraminidase is essential for fowl plague virus hemagglutinin to show hemagglutinating activity. Virology 1995;212:77-83.

421. Wu MM, Grabe M, Adams S, Tsien RY, Moore HP, Machen TE. Mechanisms of pH regulation in the regulated secretory pathway. The Journal of biological chemistry 2001;276:33027-35.

422. Daniels RS, Douglas AR, Skehel JJ, Wiley DC. Analyses of the antigenicity of influenza haemagglutinin at the pH optimum for virus-mediated membrane fusion. The Journal of general virology 1983;64 (Pt 8):1657-62.

423. Thomson CA, Wang Y, Jackson LM, et al. Pandemic H1N1 Influenza Infection and Vaccination in Humans Induces Cross-Protective Antibodies that Target the Hemagglutinin Stem. Frontiers in immunology 2012;3:87.

424. Smith GP. Filamentous fusion phage: novel expression vectors that display cloned antigens on the virion surface. Science 1985;228:1315-7.

425. Scott JK, Smith GP. Searching for peptide ligands with an epitope library. Science 1990;249:386-90.

426. Bass S, Greene R, Wells JA. Hormone phage: an enrichment method for variant proteins with altered binding properties. Proteins 1990;8:309-14.

427. Desogus A, Burioni R, Ingianni A, Bugli F, Pompei R, Fadda G. Production and characterization of a human recombinant monoclonal Fab fragment specific for influenza A viruses. Clinical and diagnostic laboratory immunology 2003;10:680-5.

428. Asanuma H, Matsumoto-Takasaki A, Suzuki Y, et al. Influenza PR8 HA-specific Fab fragments produced by phage display methods. Biochemical and biophysical research communications 2008;366:445-9.

429. Zou P, Liu W, Wu F, Chen YH. Fine-epitope mapping of an antibody that binds the ectodomain of influenza matrix protein 2. FEMS immunology and medical microbiology 2008;53:79-84.

430. Lim AP, Chan CE, Wong SK, Chan AH, Ooi EE, Hanson BJ. Neutralizing human monoclonal antibody against H5N1 influenza HA selected from a Fab-phage display library. Virology journal 2008;5:130.

431. Luo W, Chen Y, Wang M, et al. Peptide mimics of a conserved H5N1 avian influenza virus neutralization site. The Biochemical journal 2009;419:133-9.

432. Sui J, Hwang WC, Perez S, et al. Structural and functional bases for broad-spectrum neutralization of avian and human influenza A viruses. Nature structural & molecular biology 2009;16:265-73.

433. Khurana S, Suguitan AL, Jr., Rivera Y, et al. Antigenic fingerprinting of H5N1 avian influenza using convalescent sera and monoclonal antibodies

reveals potential vaccine and diagnostic targets. PLoS medicine 2009;6:e1000049.

434. Yang J, Yoshida R, Kariya Y, et al. Characterization of human single-chain antibodies against highly pathogenic avian influenza H5N1 viruses: mimotope and neutralizing activity. Journal of biochemistry 2010;148:507-15.

435. Khurana S, Wu J, Verma N, et al. H5N1 virus-like particle vaccine elicits cross-reactive neutralizing antibodies that preferentially bind to the oligomeric form of influenza virus hemagglutinin in humans. Journal of virology 2011;85:10945-54.

436. Khurana S, Verma N, Talaat KR, Karron RA, Golding H. Immune response following H1N1pdm09 vaccination: differences in antibody repertoire and avidity in young adults and elderly populations stratified by age and gender. The Journal of infectious diseases 2012;205:610-20.

437. Khurana S, Loving CL, Manischewitz J, et al. Vaccine-induced anti-HA2 antibodies promote virus fusion and enhance influenza virus respiratory disease. Science translational medicine 2013;5:200ra114.

438. Domm W, Brewer M, Baker SF, et al. Use of bacteriophage particles displaying influenza virus hemagglutinin for the detection of hemagglutination-inhibition antibodies. Journal of virological methods 2014;197:47-50.

439. Russel M, Linderoth NA, Sali A. Filamentous phage assembly: variation on a protein export theme. Gene 1997;192:23-32.

440. Thie H, Schirrmann T, Paschke M, Dubel S, Hust M. SRP and Sec pathway leader peptides for antibody phage display and antibody fragment production in E. coli. New biotechnology 2008;25:49-54.

441. Barrett RW, Cwirla SE, Ackerman MS, Olson AM, Peters EA, Dower WJ. Selective enrichment and characterization of high affinity ligands from collections of random peptides on filamentous phage. Analytical biochemistry 1992;204:357-64.

442. Antrobus RD, Berthoud TK, Mullarkey CE, et al. Coadministration of seasonal influenza vaccine and MVA-NP+M1 simultaneously achieves potent humoral and cell-mediated responses. Molecular therapy : the journal of the American Society of Gene Therapy 2014;22:233-8.

443. Seddon AM, Curnow P, Booth PJ. Membrane proteins, lipids and detergents: not just a soap opera. Biochimica et biophysica acta 2004;1666:105-17.

444. Sui J, Sheehan J, Hwang WC, et al. Wide prevalence of heterosubtypic broadly neutralizing human anti-influenza A antibodies. Clinical infectious diseases : an official publication of the Infectious Diseases Society of America 2011;52:1003-9.

445. Ekiert DC, Bhabha G, Elsliger MA, et al. Antibody recognition of a highly conserved influenza virus epitope. Science 2009;324:246-51.

446. Ekiert DC, Friesen RH, Bhabha G, et al. A highly conserved neutralizing epitope on group 2 influenza A viruses. Science 2011;333:843-50.

447. Throsby M, van den Brink E, Jongeneelen M, et al. Heterosubtypic neutralizing monoclonal antibodies cross-protective against H5N1 and H1N1 recovered from human IgM+ memory B cells. PloS one 2008;3:e3942.

448. Kashyap AK, Steel J, Oner AF, et al. Combinatorial antibody libraries from survivors of the Turkish H5N1 avian influenza outbreak reveal virus

neutralization strategies. Proceedings of the National Academy of Sciences of the United States of America 2008;105:5986-91.

449. Friesen RH, Lee PS, Stoop EJ, et al. A common solution to group 2 influenza virus neutralization. Proceedings of the National Academy of Sciences of the United States of America 2014;111:445-50.

450. Wyrzucki A, Dreyfus C, Kohler I, Steck M, Wilson IA, Hangartner L. Alternative recognition of the conserved stem epitope in influenza A virus hemagglutinin by a VH3-30-encoded heterosubtypic antibody. Journal of virology 2014;88:7083-92.

451. Nakamura G, Chai N, Park S, et al. An in vivo human-plasmablast enrichment technique allows rapid identification of therapeutic influenza A antibodies. Cell host & microbe 2013;14:93-103.

452. Li GM, Chiu C, Wrammert J, et al. Pandemic H1N1 influenza vaccine induces a recall response in humans that favors broadly cross-reactive memory B cells. Proceedings of the National Academy of Sciences of the United States of America 2012;109:9047-52.

453. Miller MS, Tsibane T, Krammer F, et al. 1976 and 2009 H1N1 influenza virus vaccines boost anti-hemagglutinin stalk antibodies in humans. The Journal of infectious diseases 2013;207:98-105.

454. Tan GS, Lee PS, Hoffman RM, et al. Characterization of a broadly neutralizing monoclonal antibody that targets the fusion domain of group 2 influenza A virus hemagglutinin. Journal of virology 2014;88:13580-92.

455. Whittle JR, Wheatley AK, Wu L, et al. Flow cytometry reveals that H5N1 vaccination elicits cross-reactive stem-directed antibodies from multiple Ig heavy-chain lineages. Journal of virology 2014;88:4047-57.

456. To KK, Zhang AJ, Hung IF, et al. High titer and avidity of nonneutralizing antibodies against influenza vaccine antigen are associated with severe influenza. Clin Vaccine Immunol 2012;19:1012-8.

457. Galli G, Medini D, Borgogni E, et al. Adjuvanted H5N1 vaccine induces early CD4+ T cell response that predicts long-term persistence of protective antibody levels. Proceedings of the National Academy of Sciences of the United States of America 2009;106:3877-82.

458. Plotkin SA. Correlates of protection induced by vaccination. Clinical and vaccine immunology : CVI 2010;17:1055-65.

459. Miller JF, Mitchell GF. Cell to cell interaction in the immune response. I. Hemolysin-forming cells in neonatally thymectomized mice reconstituted with thymus or thoracic duct lymphocytes. The Journal of experimental medicine 1968;128:801-20.

460. Mitchell GF, Miller JF. Cell to cell interaction in the immune response. II. The source of hemolysin-forming cells in irradiated mice given bone marrow and thymus or thoracic duct lymphocytes. The Journal of experimental medicine 1968;128:821-37.

461. Nossal GJ, Cunningham A, Mitchell GF, Miller JF. Cell to cell interaction in the immune response. 3. Chromosomal marker analysis of single antibody-forming cells in reconstituted, irradiated, or thymectomized mice. The Journal of experimental medicine 1968;128:839-53.

462. Jacobson EB, Caporale LH, Thorbecke GJ. Effect of thymus cell injections on germinal center formation in lymphoid tissues of nude (thymusless) mice. Cellular immunology 1974;13:416-30.

463. Jacob J, Kelsoe G, Rajewsky K, Weiss U. Intraclonal generation of antibody mutants in germinal centres. Nature 1991;354:389-92.

464. Ho F, Lortan JE, MacLennan IC, Khan M. Distinct short-lived and long-lived antibody-producing cell populations. European journal of immunology 1986;16:1297-301.

465. Plotkin SA, Orenstein W, Offit PA. Vaccines. 6th ed2013.

466. Kopf M, Le Gros G, Coyle AJ, Kosco-Vilbois M, Brombacher F. Immune responses of IL-4, IL-5, IL-6 deficient mice. Immunological reviews 1995;148:45-69.

467. Grusby MJ. Stat4- and Stat6-deficient mice as models for manipulating T helper cell responses. Biochemical Society transactions 1997;25:359-60.

468. Schaerli P, Willimann K, Lang AB, Lipp M, Loetscher P, Moser B. CXC chemokine receptor 5 expression defines follicular homing T cells with B cell helper function. The Journal of experimental medicine 2000;192:1553-62.

469. Kim CH, Rott LS, Clark-Lewis I, Campbell DJ, Wu L, Butcher EC. Subspecialization of CXCR5+ T cells: B helper activity is focused in a germinal center-localized subset of CXCR5+ T cells. The Journal of experimental medicine 2001;193:1373-81.

470. Breitfeld D, Ohl L, Kremmer E, et al. Follicular B helper T cells express CXC chemokine receptor 5, localize to B cell follicles, and support immunoglobulin production. The Journal of experimental medicine 2000;192:1545-52.

471. Ansel KM, Ngo VN, Hyman PL, et al. A chemokine-driven positive feedback loop organizes lymphoid follicles. Nature 2000;406:309-14.

472. Chtanova T, Tangye SG, Newton R, et al. T follicular helper cells express a distinctive transcriptional profile, reflecting their role as non-Th1/Th2 effector cells that provide help for B cells. Journal of immunology 2004;173:68-78.

473. Rasheed AU, Rahn HP, Sallusto F, Lipp M, Muller G. Follicular B helper T cell activity is confined to CXCR5(hi)ICOS(hi) CD4 T cells and is independent of CD57 expression. European journal of immunology 2006;36:1892-903.

474. Haynes NM, Allen CD, Lesley R, Ansel KM, Killeen N, Cyster JG. Role of CXCR5 and CCR7 in follicular Th cell positioning and appearance of a programmed cell death gene-1high germinal center-associated subpopulation. Journal of immunology 2007;179:5099-108.

475. Nurieva RI, Chung Y, Martinez GJ, et al. Bcl6 mediates the development of T follicular helper cells. Science 2009;325:1001-5.

476. Yu D, Rao S, Tsai LM, et al. The transcriptional repressor Bcl-6 directs T follicular helper cell lineage commitment. Immunity 2009;31:457-68.

477. Johnston RJ, Poholek AC, DiToro D, et al. Bcl6 and Blimp-1 are reciprocal and antagonistic regulators of T follicular helper cell differentiation. Science 2009;325:1006-10.

478. Crotty S. Follicular helper CD4 T cells (TFH). Annual review of immunology 2011;29:621-63.

479. Odegard JM, Marks BR, DiPlacido LD, et al. ICOS-dependent extrafollicular helper T cells elicit IgG production via IL-21 in systemic autoimmunity. The Journal of experimental medicine 2008;205:2873-86.

480. Chang PP, Barral P, Fitch J, et al. Identification of Bcl-6-dependent follicular helper NKT cells that provide cognate help for B cell responses. Nature immunology 2012;13:35-43.

481. King IL, Fortier A, Tighe M, et al. Invariant natural killer T cells direct B cell responses to cognate lipid antigen in an IL-21-dependent manner. Nature immunology 2012;13:44-50.

482. Caccamo N, Battistini L, Bonneville M, et al. CXCR5 identifies a subset of Vgamma9Vdelta2 T cells which secrete IL-4 and IL-10 and help B cells for antibody production. Journal of immunology 2006;177:5290-5.

483. Weber JP, Fuhrmann F, Hutloff A. T-follicular helper cells survive as long-term memory cells. European journal of immunology 2012;42:1981-8.

484. Fairfax KC, Everts B, Amiel E, et al. IL-4-Secreting Secondary T Follicular Helper (Tfh) Cells Arise from Memory T Cells, Not Persisting Tfh Cells, through a B Cell-Dependent Mechanism. Journal of immunology 2015.

485. Glatman Zaretsky A, Taylor JJ, King IL, Marshall FA, Mohrs M, Pearce EJ. T follicular helper cells differentiate from Th2 cells in response to helminth antigens. The Journal of experimental medicine 2009;206:991-9.

486. Bauquet AT, Jin H, Paterson AM, et al. The costimulatory molecule ICOS regulates the expression of c-Maf and IL-21 in the development of follicular T helper cells and TH-17 cells. Nature immunology 2009;10:167-75.

487. Nurieva RI, Chung Y, Hwang D, et al. Generation of T follicular helper cells is mediated by interleukin-21 but independent of T helper 1, 2, or 17 cell lineages. Immunity 2008;29:138-49.

488. Hannet I, Erkeller-Yuksel F, Lydyard P, Deneys V, DeBruyere M. Developmental and maturational changes in human blood lymphocyte subpopulations. Immunology today 1992;13:215, 8.

489. Morita R, Schmitt N, Bentebibel SE, et al. Human blood CXCR5(+)CD4(+) T cells are counterparts of T follicular cells and contain specific subsets that differentially support antibody secretion. Immunity 2011;34:108-21.

490. Schmitt N, Bentebibel SE, Ueno H. Phenotype and functions of memory Tfh cells in human blood. Trends in immunology 2014;35:436-42.

491. Bentebibel SE, Lopez S, Obermoser G, et al. Induction of ICOS+CXCR3+CXCR5+ TH cells correlates with antibody responses to influenza vaccination. Science translational medicine 2013;5:176ra32.

492. Locci M, Havenar-Daughton C, Landais E, et al. Human circulating PD-1+CXCR3-CXCR5+ memory Tfh cells are highly functional and correlate with broadly neutralizing HIV antibody responses. Immunity 2013;39:758-69.

493. Klein F, Diskin R, Scheid JF, et al. Somatic mutations of the immunoglobulin framework are generally required for broad and potent HIV-1 neutralization. Cell 2013;153:126-38.

494. Liao HX, Lynch R, Zhou T, et al. Co-evolution of a broadly neutralizing HIV-1 antibody and founder virus. Nature 2013;496:469-76.

495. Lingwood D, McTamney PM, Yassine HM, et al. Structural and genetic basis for development of broadly neutralizing influenza antibodies. Nature 2012;489:566-70.

496. Spensieri F, Borgogni E, Zedda L, et al. Human circulating influenza-CD4+ ICOS1+IL-21+ T cells expand after vaccination, exert helper function,

and predict antibody responses. Proceedings of the National Academy of Sciences of the United States of America 2013;110:14330-5.

497. Ansel KM, McHeyzer-Williams LJ, Ngo VN, McHeyzer-Williams MG, Cyster JG. In vivo-activated CD4 T cells upregulate CXC chemokine receptor 5 and reprogram their response to lymphoid chemokines. The Journal of experimental medicine 1999;190:1123-34.

498. Agata Y, Kawasaki A, Nishimura H, et al. Expression of the PD-1 antigen on the surface of stimulated mouse T and B lymphocytes. International immunology 1996;8:765-72.

499. Hutloff A, Dittrich AM, Beier KC, et al. ICOS is an inducible T-cell co-stimulator structurally and functionally related to CD28. Nature 1999;397:263-6.

500. Herati RS, Reuter MA, Dolfi DV, et al. Circulating CXCR5+PD-1+ response predicts influenza vaccine antibody responses in young adults but not elderly adults. Journal of immunology 2014;193:3528-37.

501. Drillien R, Spehner D, Hanau D. Modified vaccinia virus Ankara induces moderate activation of human dendritic cells. The Journal of general virology 2004;85:2167-75.

502. Pappas L, Foglierini M, Piccoli L, et al. Rapid development of broadly influenza neutralizing antibodies through redundant mutations. Nature 2014;516:418-22.

503. Sasso EH, Johnson T, Kipps TJ. Expression of the immunoglobulin VH gene 51p1 is proportional to its germline gene copy number. The Journal of clinical investigation 1996;97:2074-80.

504. Johnson NP, Mueller J. Updating the accounts: global mortality of the 1918-1920 "Spanish" influenza pandemic. Bull Hist Med 2002;76:105-15.

505. Palache A. Seasonal influenza vaccine provision in 157 countries (2004-2009) and the potential influence of national public health policies. Vaccine 2011;29:9459-66.

506. Fiore AE, Uyeki TM, Broder K, et al. Prevention and control of influenza with vaccines: recommendations of the Advisory Committee on Immunization Practices (ACIP), 2010. MMWR Recomm Rep 2010;59:1-62.

507. Soema PC, Kompier R, Amorij JP, Kersten GF. Current and next generation influenza vaccines: formulation and production strategies. European journal of pharmaceutics and biopharmaceutics : official journal of Arbeitsgemeinschaft fur Pharmazeutische Verfahrenstechnik eV 2015.

508. Tewawong N, Suwannakarn K, Prachayangprecha S, et al. Molecular epidemiology and phylogenetic analyses of influenza B virus in Thailand during 2010 to 2014. PloS one 2015;10:e0116302.

509. DiazGranados CA, Denis M, Plotkin S. Seasonal influenza vaccine efficacy and its determinants in children and non-elderly adults: a systematic review with meta-analyses of controlled trials. Vaccine 2012;31:49-57.

510. Dowdle WR, Coleman MT, Mostow SR, Kaye HS, Schoenbaum SC. Inactivated influenza vaccines. 2. Laboratory indices of protection. Postgraduate medical journal 1973;49:159-63.

511. Masurel N, Laufer J. A one-year study of trivalent influenza vaccines in primed and unprimed volunteers: immunogenicity, clinical reactions and protection. The Journal of hygiene 1984;92:263-76.

512. Dreyfus C, Laursen NS, Kwaks T, et al. Highly conserved protective epitopes on influenza B viruses. Science 2012;337:1343-8.

513. Fu Y, Zhang Z, Sun J, Zhu Q. Isolation of broadly neutralizing antibodies from single human memory B cell against human influenza A viruses (TECH2P.922). The Journal of Immunology 2015;194:206.32.

514. Nachbagauer R, Wohlbold TJ, Hirsh A, et al. Induction of broadly reactive anti-hemagglutinin stalk antibodies by an H5N1 vaccine in humans. Journal of virology 2014;88:13260-8.

515. Margine I, Krammer F, Hai R, et al. Hemagglutinin stalk-based universal vaccine constructs protect against group 2 influenza A viruses. Journal of virology 2013;87:10435-46.

516. Krammer F, Hai R, Yondola M, et al. Assessment of influenza virus hemagglutinin stalk-based immunity in ferrets. Journal of virology 2014;88:3432-42.

517. Yassine HM, Boyington JC, McTamney PM, et al. Hemagglutinin-stem nanoparticles generate heterosubtypic influenza protection. Nature medicine 2015;21:1065-70.

518. Impagliazzo A, Milder F, Kuipers H, et al. A stable trimeric influenza hemagglutinin stem as a broadly protective immunogen. Science 2015.

519. Biswas S, Dicks MD, Long CA, et al. Transgene optimization, immunogenicity and in vitro efficacy of viral vectored vaccines expressing two alleles of Plasmodium falciparum AMA1. PloS one 2011;6:e20977.

520. Sliepen K, van Montfort T, Melchers M, Isik G, Sanders RW. Immunosilencing a highly immunogenic protein trimerization domain. The Journal of biological chemistry 2015;290:7436-42.

521. Su S, Chen J, Cao Z, et al. Detection of antibodies against Avian influenza virus subtypes H7 and H9 among veterinarians in Guangdong province, China. Journal of clinical microbiology 2013;51:4272-4.

522. Sanders RW, van Gils MJ, Derking R, et al. HIV-1 neutralizing antibodies induced by native-like envelope trimers. Science 2015.

523. DiLillo DJ, Tan GS, Palese P, Ravetch JV. Broadly neutralizing hemagglutinin stalk-specific antibodies require FcgammaR interactions for protection against influenza virus in vivo. Nature medicine 2014;20:143-51.

524. Francis T, Magill TP. Immunological Studies with the Virus of Influenza. The Journal of experimental medicine 1935;62:505-16.

525. Virelizier JL. Host defenses against influenza virus: the role of anti-hemagglutinin antibody. Journal of immunology 1975;115:434-9.

526. Francis T, Magill TP. The Incidence of Neutralizing Antibodies for Human Influenza Virus in the Serum of Human Individuals of Different Ages. The Journal of experimental medicine 1936;63:655-68.

527. Yap KL, Ada GL. Cytotoxic T cells specific for influenza virus-infected target cells. Immunology 1977;32:151-9.

528. Capone S, Reyes-Sandoval A, Naddeo M, et al. Immune responses against a liver-stage malaria antigen induced by simian adenoviral vector AdCh63 and MVA prime-boost immunisation in non-human primates. Vaccine 2010;29:256-65.

529. Draper SJ, Biswas S, Spencer AJ, et al. Enhancing blood-stage malaria subunit vaccine immunogenicity in rhesus macaques by combining adenovirus, poxvirus, and protein-in-adjuvant vaccines. Journal of immunology 2010;185:7583-95.

530. Boyd AC, Ruiz-Hernandez R, Peroval MY, et al. Towards a universal vaccine for avian influenza: protective efficacy of modified Vaccinia virus Ankara and Adenovirus vaccines expressing conserved influenza antigens in chickens challenged with low pathogenic avian influenza virus. Vaccine 2013;31:670-5.

531. Casimiro DR, Bett AJ, Fu TM, et al. Heterologous human immunodeficiency virus type 1 priming-boosting immunization strategies involving replication-defective adenovirus and poxvirus vaccine vectors. Journal of virology 2004;78:11434-8.

532. Draper SJ, Goodman AL, Biswas S, et al. Recombinant viral vaccines expressing merozoite surface protein-1 induce antibody- and T cell-mediated multistage protection against malaria. Cell host & microbe 2009;5:95-105.

533. Douglas AD, de Cassan SC, Dicks MD, Gilbert SC, Hill AV, Draper SJ. Tailoring subunit vaccine immunogenicity: maximizing antibody and T cell responses by using combinations of adenovirus, poxvirus and protein-adjuvant vaccines against Plasmodium falciparum MSP1. Vaccine 2010;28:7167-78.

534. Forbes EK, Biswas S, Collins KA, Gilbert SC, Hill AV, Draper SJ. Combining liver- and blood-stage malaria viral-vectored vaccines: investigating mechanisms of CD8+ T cell interference. Journal of immunology 2011;187:3738-50.

535. Kilbourn.Ed. FUTURE INFLUENZA VACCINES AND USE OF GENETIC RECOMBINANTS. Bulletin of the World Health Organization 1969;41:643-&.

536. Ura T, Okuda K, Shimada M. Developments in Viral Vector-Based Vaccines. Vaccines 2014;2:624.

537. Liu R, Moise L, Tassone R, et al. H7N9 T-cell epitopes that mimic human sequences are less immunogenic and may induce Treg-mediated tolerance. Human vaccines & immunotherapeutics 2015;11:2241-52.

538. Hill AV, Reyes-Sandoval A, O'Hara G, et al. Prime-boost vectored malaria vaccines: progress and prospects. Human vaccines 2010;6:78-83.

539. Temperton NJ, Hoschler K, Major D, et al. A sensitive retroviral pseudotype assay for influenza H5N1-neutralizing antibodies. Influenza and other respiratory viruses 2007;1:105-12.

540. Wang W, Anderson CM, De Feo CJ, et al. Cross-neutralizing antibodies to pandemic 2009 H1N1 and recent seasonal H1N1 influenza A strains influenced by a mutation in hemagglutinin subunit 2. PLoS pathogens 2011;7:e1002081.

541. Manz RA, Thiel A, Radbruch A. Lifetime of plasma cells in the bone marrow. Nature 1997;388:133-4.

542. Slifka MK, Antia R, Whitmire JK, Ahmed R. Humoral immunity due to long-lived plasma cells. Immunity 1998;8:363-72.

543. Shenoy GN, Chatterjee P, Kaw S, et al. Recruitment of memory B cells to lymph nodes remote from the site of immunization requires an inflammatory stimulus. Journal of immunology 2012;189:521-8.

544. Francis T, Jr. Vaccination against influenza. Bulletin of the World Health Organization 1953;8:725-41.

545. Davenport FM. Current knowledge of influenza vaccine. Jama 1962;182:11-3.

546. Monto AS, Ohmit SE, Petrie JG, et al. Comparative efficacy of inactivated and live attenuated influenza vaccines. The New England journal of medicine 2009;361:1260-7.

547. Ohmit SE, Victor JC, Rotthoff JR, et al. Prevention of antigenically drifted influenza by inactivated and live attenuated vaccines. The New England journal of medicine 2006;355:2513-22.

548. He XS, Holmes TH, Zhang C, et al. Cellular immune responses in children and adults receiving inactivated or live attenuated influenza vaccines. Journal of virology 2006;80:11756-66.

549. Wang TT, Tan GS, Hai R, et al. Broadly protective monoclonal antibodies against H3 influenza viruses following sequential immunization with different hemagglutinins. PLoS pathogens 2010;6:e1000796.

550. Tan GS, Krammer F, Eggink D, Kongchanagul A, Moran TM, Palese P. A pan-H1 anti-hemagglutinin monoclonal antibody with potent broad-spectrum efficacy in vivo. Journal of virology 2012;86:6179-88.

551. Breathnach CC, Clark HJ, Clark RC, Olsen CW, Townsend HG, Lunn DP. Immunization with recombinant modified vaccinia Ankara (rMVA) constructs encoding the HA or NP gene protects ponies from equine influenza virus challenge. Vaccine 2006;24:1180-90.

552. Wang W, Li R, Deng Y, et al. Protective Efficacy of the Conserved NP, PB1, and M1 Proteins as Immunogens in DNA- and Vaccinia Virus-Based Universal Influenza A Virus Vaccines in Mice. Clinical and vaccine immunology : CVI 2015;22:618-30.

553. Levi R, Arnon R. Synthetic recombinant influenza vaccine induces efficient long-term immunity and cross-strain protection. Vaccine 1996;14:85-92.

554. Sedegah M, Charoenvit Y, Minh L, et al. Reduced immunogenicity of DNA vaccine plasmids in mixtures. Gene therapy 2004;11:448-56.

555. Kastenmuller W, Gasteiger G, Gronau JH, et al. Cross-competition of CD8+ T cells shapes the immunodominance hierarchy during boost vaccination. The Journal of experimental medicine 2007;204:2187-98.

556. Kedl RM, Rees WA, Hildeman DA, et al. T cells compete for access to antigen-bearing antigen-presenting cells. The Journal of experimental medicine 2000;192:1105-13.

557. Baur K, Brinkmann K, Schweneker M, et al. Immediate-early expression of a recombinant antigen by modified vaccinia virus ankara breaks the immunodominance of strong vector-specific B8R antigen in acute and memory CD8 T-cell responses. Journal of virology 2010;84:8743-52.

558. Lindskog C, Ellstrom P, Olsen B, et al. European H16N3 gull influenza virus attaches to the human respiratory tract and eye. PloS one 2013;8:e60757.

559. Wohlbold TJ, Nachbagauer R, Margine I, Tan GS, Hirsh A, Krammer F. Vaccination with soluble headless hemagglutinin protects mice from challenge with divergent influenza viruses. Vaccine 2015;33:3314-21.